Life histories and population dynamics in variable environments

Samuel J L Gascoigne

Pembroke College

University of Oxford

A thesis submitted for the degree of

Doctor of Philosophy

Trinity 2024

Declaration of authorship

The work presented in this thesis is my own. In each of the chapters that form this dissertation, I have led or co-led the work - from conceptualization to writing. However, I have been extremely fortunate to be surrounded by an extensive group of collaborators that have elevated the science presented in this dissertation. In turn, here I provide a full list detailing all of the co-authors and their contributions toward the work presented in each chapter.

Chapter 1: General introduction

Author– Samuel J L Gascoigne

Chapter 2: Criteria for buffering in ecological modelling

Authors– Samuel J L Gascoigne, Maja Kajin & Roberto Salguero-Gómez

Contributions – SJLG conceived of this manuscript and wrote the first draft. All co-authors made major contributions to the final manuscript which has now been published in *Trends in Ecology & Evolution*.

Gascoigne, S. J. L., Kajin, M., & Salguero-Gómez, R. (2023a). Criteria for buffering in ecological modeling. *Trends in Ecology & Evolution*. https://doi.org/10.1016/j.tree.2023.11.006

Chapter 3: A unified framework to identify demographic buffering in natural populations

Authors– Gabriel Silva Santos, Samuel J L Gascoigne, André Tavares Corrêa Dias, Maja Kajin & Roberto Salguero-Gómez

Contributions – GSS developed the initial concept, performed the statistical analyses, and contributed to the first draft of the manuscript. SJLG developed the initial concept, contributed to the first draft and all other versions of the manuscript, and generated final figures. ATCD co-advised the project and contributed significantly to final versions of the manuscript. MK developed and managed the project, contributed to the first draft and all other versions of the manuscript, and generated final figures. RSG developed and managed the project and contributed to the first draft and all other versions of the manuscript. All authors made substantial contributions to editing the manuscript and further refining ideas and interpretations.

Chapter 4: Structured demographic buffering: A framework to explore the environment drivers and demographic mechanisms underlying demographic buffering

Authors– Samuel J L Gascoigne, Maja Kajin, Shripad D Tuljapurkar, Gabriel Silva Santos, Aldo Compagnoni, Ulrich K Steiner, Anna C Vinton, Harman Jaggi, Irem Sepil & Roberto Salguero-Gómez

Contributions – SJLG, IS and RSG conceived and managed the project. SJLG, MK, IS and RSG provided early idea development. SJLG, MK, GS, ST and RSG contributed to early methods development. SJLG coded the simulation, performed the analysis and wrote the first draft with contributions from IS and RSG. Later idea contributions and edits to the manuscript came from ST, AC, UKC, ACV and HJ. All authors contributed significantly to the final manuscript.

Chapter 5: Testing for efficacy in four measures of demographic buffering

Authors– Samuel J L Gascoigne, Maja Kajin, Irem Sepil & Roberto Salguero-Gómez

Contributions – SJLG conceived of this manuscript and wrote the first draft. All co-authors made major contributions to the final manuscript.

Chapter 6: Current perspectives and future directions in animal life history evolution

Authors– Samuel J L Gascoigne, Alice Rosen, Krish Sanghvi, Aldo Compagnoni, Ulrich K Steiner, Greta Bocedi, Roberto Salguero-Gómez & Irem Sepil

Contributions – SJLG conceived the initial ideas for this manuscript and wrote the first draft. SJLG and AR designed the figures which were subsequently built by AR. All authors contributed significantly to the ideas, structure and writing in this manuscript.

Chapter 7: Discussion

Author– Samuel J L Gascoigne

This thesis is lovingly dedicated to my parents

Paul and Tanya Gascoigne

for their support, their inspiration and for always saying - *this time next year.*

Acknowledgements

Wow, that went fast. This dissertation, and everything that has come out of my time as a DPhil student, represents the culmination of a great deal of support and inspiration from many people. This acknowledgements section represents a cross-section of all who pushed me, taught me, supported me and made these three and a half years the best I could have ever imagined. Consequently, this section is not exhaustive; however, I wish all who helped me get from October 2020 to March 2024 know I am extremely grateful and can't believe how lucky I have been.

First, I would like to thank my supervisors. Rob and Irem, thank you for everything. From inviting me to give my first talk to the SalGo team in 2019, to working tirelessly to get me across the pond during COVID, to putting up with me running around like a headless chicken for two and half years, you opened doors, kept me inspired and guided me to the finish line. Thank you for making this DPhil so formative, fun and motivating. I am very grateful for all the supervision, laughs and celebrations we have had along the way.

Second, I would like to thank the SalGo team and Fly lab. Thank you both for having and actively cultivating a sense of community – even during COVID. I would like to give a particular thank you to Maja, Anna, Connor, Erik and Krish. This dissertation is very different to what we initially set out to do – oh, the good ol' days of talking about insulin signalling. All of you have shaped my interests and this dissertation in so many ways. Thank you all very much.

Third, I would like to thank some of the other Oxford-folk who also helped me along the way. Andrew and Ming, thank you for always being there for an unnecessarily long coffee chat and waxing lyrical about anything and everything. You have both made my time in the department a joy. I would also like to thank Katrina. Of all the tips and tricks I have learned, your perspectives on the writing process and tips for writing efficiently and clearly take the biscuit. This dissertation would have been much harder to put together if not for your writing workshop – thank you very much. And lastly, I would like to thank Tim. Thank you for always letting us drop into your group meetings and bounce ideas off you at the pub. In addition to being a lot of fun, these chats also shaped how I view life history evolution in variable environments. Thank you all very much.

Fourth, I would like to thank my collaborators. At the beginning of the DPhil, Rob and Irem mentioned that it is always good to connect yourself with people that elevate your science. I can honestly say I have been beyond fortunate in this regard. Whilst this list is quite long, I would like to offer a particular thank you to Aldo, Uli and the members of Tulja lab (Tulja, Wenyun and Harman). All of you have elevated my science in rapid fashion. Thank you all so much for being so supportive and giving in your time and perspectives.

Fifth, I would like to thank some people on a more personal note. I would like to thank my siblings (David, Alex and Dani) for being incredibly motivating and supportive throughout the DPhil. I look up to all three of you. I love you all very much. Thank you

for being with me every step of the way – especially Alex. Alex, thank you for being my partner in crime for a whole year. We made a great team. I owe you all the JPs with jelly and tapioca pearls. I truly hope you look back on your time in Oxford fondly. I am very grateful for the time we had together. And Joe, thank you for always being there for me, even across an ocean. I am forever grateful I forgot that pencil on the first day of class - we've come so far. I would also like to thank Rob, Linda and Eddie. Thank you so much for opening your home to me in these final months. Thank you for all the support, kindness and memories. And now, Teri. I did a little inventory of all the writing in this dissertation and none of the chapters (from the General Introduction to the Discussion) were written when we met. Thank you so much for coming on this journey with me - especially the trials and tribulations that were Chapter 6. The memories we have made are the fondest I have from my time doing this DPhil. I am so excited to build many more together.

Sixth, I would like to thank my very loving grandparents. Granny, Grandad, Abueli and Vovo, thank you so much for supporting me on this journey from the beginning. For as long as I can remember, you have all encouraged me to pursue this dream - even when the going got tough. Thank you for always being supportive, interested and cheering me on through the finish line. You have all shaped me, my interests and how I have gone about this DPhil. So, as this DPhil comes a close, I hope I can relay how truly grateful I am for every part you have all played in getting me to this point. I love you all very much.

And last but most importantly, I would like to thank my parents. There is a reason this dissertation is dedicated to you. Without your love, support and example, this dissertation would never have been written. You are both my heroes, my role models and who I want to be when I grow up. Thank you for helping me achieve my dream and for always aiming to put the nest on the highest branch. Love you always. *Consilio et Animis*.

Abstract

Environmental variability has broad impacts on the population dynamics of species across the tree of life. Importantly, global climate change is projected to increase environmental variability in regions hosting the highest biodiversity. Therefore, understanding the life history strategies by which populations can evolve to accommodate the often negative effects of environmental variability is critical to understand how global climate change may impact populations across taxa. In this dissertation, I explore one strategy by which populations can accommodate the impacts of environmental variability – *i.e.*, demographic buffering. Specifically, I: (1) identify *criteria* for determining a buffering mechanism in ecological modelling, (2) demonstrate the utility of "new" perturbation approaches [*i.e.*, the summation of stochastic elasticities of variance $\left(\sum E^{\sigma^2}_{a_{ij}}\right)$ and self-second derivatives] when identifying demographic buffering, (3) analyse how environmental autocorrelation and variance impact demographic buffering (as measured by $\sum E^{\sigma^2}_{a_{ij}}$) and the demographic mechanisms that underly these effects, (4) test for *efficacy* across four measures of demographic buffering [*i.e.*, one correlational method (ρ), two methods using terms from Tuljapurkar's approximation (V_s and $V_s + V_c$) and $\sum E^{\sigma^2}_{a_{ij}}$] and (5) broadly review modern perspectives and suggest new directions regarding where future life history research may lead. Overall, I suggest that $\sum E^{\sigma^2}_{a_{ij}}$ is an effective measure of demographic buffering, and that environmental autocorrelation and variance influence $\sum E^{\sigma^2}_{a_{ij}}$ through population structure and demographic rate variance, respectively. Furthermore, I outline multiple avenues for future research to better understand how life histories evolve in variable environments.

Contents

Appendices

List of Figures

Life is the only game in which the object of the game is to learn the rules.

— Ashleigh Brilliant

My [algebraic] methods are really methods of working and thinking; this is why they have crept in everywhere anonymously.

— Emmy Noether

1

General introduction

Contents

1.1 Life histories: What are they and how do we study them?

The subject of life history theory is the *history of the life of organisms*. A life history is the sequence and timings of events in an individual's lifespan, governed by underlying demographic rates, that contribute to both individual fitness and broader population dynamics (Roff, 2002; Stearns, 1992). These events, from hereon called *life history traits*, are highly varied across the tree of life. For example, consider three species with highly dissimlar life histories: the orchid (*Orchis purperea*), the arctic tern (*Sterna paradisaea*) and the tardigrade (phylum Tardigrada). Starting with age at sexual maturity, the orchid takes 5-10 years to sexually mature (Rose, 1948), whilst the arctic tern and tardigrade take 4 years (Møller, 2006) and 28.2 days [at 20°C; Bingemer et al. (2016)], respectively. Regarding life expectancy, an established orchid is expected to survive over 60 years (Jacquemyn et al., 2010; Shefferson et al., 2020), the arctic tern 11-19 years (Petersen et al., 2020) and the tardigrade between two weeks and 200 days across its genera (Nagwani et al., 2022). This variance would continue for other life history traits (*e.g.*, generation time, net reproductive rate and degree of iteroparity) and the inclusion of other species across the tree of life. However, within this variance, patterns emerge.

Much of the canonical life history literature centers around patterns in life histories across and within species. From first principles, resources (*e.g.*, food, territory, mating availability) govern the parameter space of possible life histories (Stearns, 1989). Simply put, a realized life history is the product of two acts: resource acquisition and resource allocation (Van Noordwijk & De Jong, 1986). Organisms never have the luxury of infinite resources[1] and must invest their resources discretionarily amongst fitness components. These two facts constrain life histories and lead to intra-specific and inter-specific patterns of broad interest to evolutionary biologists and population ecologists. For example, life history trade-offs (*i.e.*, negative covariances amongst life history traits) are commonly found in species across biomes and trophic levels[2]. Well established examples of life history trade-offs include early *vs.* late-life reproduction (Green & Rothstein, 1991; Lemaître et al., 2015; Nussey et al., 2008), secondary sexual traits *vs.* immune response (Iglesias-Carrasco et al., 2016; Kilpimaa et al., 2004; Peters et al., 2004; Schroderus et al., 2010) and growth *vs.* defense (He et al., 2022; Karasov et al., 2017; McPeek, 2004). In addition, plastic responses in life history traits are often predictable across species - *e.g.*, poor environments during development leading to a later age at sexual maturity (Altmann & Alberts, 2005; Andrews, 1976; Rootes et al., 1991; Stearns, 1992). And finally, examined life histories across animals and plants vary across two main axes of variance – *i.e.*, the fast-slow continuum and reproductive schedule (Healy et al., 2019;

---

[1] Even an evergreen in a 24-hour lighthouse is limited by its lifespan and the underlying biochemistry that governs its photosynthetic rate.

[2] However, trade-offs are not always found (Chang et al., 2024; De Jong & Van Noordwijk, 1992; Metcalf, 2016; Van Noordwijk & De Jong, 1986).

Salguero-Gómez et al., 2016b)[3]. These insights are made possible as all life history traits, from *Escherichia coli* to the giant sequoia (*Sequoiadendron giganteum*), can be calculated using one toolbox – demographic methods.

The relationship between life histories and demography is an intimate one. To study life histories, demographic methods (*i.e.*, mathematical tools that use demographic rates for population and organism-level inferences) offer a robust solution. For example, let us imagine a discrete age-structured population where all individuals are assigned an age noted as x. The survivorship of this population (*i.e.*, the proportion of individuals that survive from age 0 to age x) can be expressed by the vector $\mathbf{l}_x$, and the per-capita reproductive rate of individuals of a given age x can be expressed as the vector $\mathbf{m}_x$. Using these two vectors, almost all of the fitness-related events (*e.g.*, net reproductive output) and timings (*e.g.*, age at sexual maturity) in an individual's lifespan can be calculated. Nevertheless, the link between life histories and demography goes beyond mathematical convenience.

Just as resources constrain life histories, so do their demographic rates. One example of this mathematical constraint is the Euler-Lotka equation (Eq. 1.1).

$$1 = \sum_{x=1}^{\omega} \lambda^{-x} \mathbf{l}_x \mathbf{m}_x \tag{1.1}$$

The Euler-Lotka equation is a characteristic equation constraining all possible age-based life histories by three inputs: survivorship ($\mathbf{l}_x$), per-capita reproduction ($\mathbf{m}_x$) and the asymptotic population growth rate (λ). Just as no organism has the luxury of accessing infinite resources, a population cannot have an $\mathbf{m}_x$ vector of all zeroes and a λ of 1; this combination of demographic rates is outside the parameter-space of possible age-based life histories.

To summarize, demographic methods are one of the primary tools for the quantification of life history traits and the study of life history evolution. Whilst some life history research uses non-demographic methods (see Chapter 6 for more details), this

---

[3] Also, this can be applied within species (Van De Walle et al., 2023).

dissertation will focus on the outputs and implications of demographic methods due to the generality of these tools and the generality of the research conducted herein.

1.2 Life histories in variable environments

The important events and their timings along an individual's lifespan are not static within a population. Instead, life histories vary across (Salguero-Gómez et al., 2016b; Healy et al., 2019) and within populations (Van De Walle et al., 2023) for a variety of reasons. Some of the reasons individual life histories may vary include spatial variance [*e.g.*, habitat (Benard & McCauley, 2008), resource availability (Grether et al., 2001; Komonen et al., 2004; Wilbur et al., 1974) and impacts of range expansion (Burton et al., 2010; Van Petegem et al., 2016; Urquhart-Cronish et al., 2024)]. Life histories may also differ due to chance[4]. However, this dissertation will focus on *temporal variance* – *i.e.*, the impacts of different environments across timesteps on population persistence.

Temporal variance, also known as environmental stochasticity within stochastic demography (Engen et al., 1998; Vinton et al., 2022), has broad impacts on life histories and population dynamics. To accommodate the often-negative impacts of environmental stochasticity, species have evolved various strategies in order to persist. For example, increased environmental stochasticity can lead to increased rates of dispersal (Jaggi et al., 2023) and dormancy (Gerber & Kokko, 2018; Gremer et al., 2012; Travis et al., 2021) despite both strategies incurring harsh costs to mortality and generation time, respectively[5]. Furthermore, changes in the degree of environmental stochasticity have further implications for phenotypic plasticity. If the temporal series is too unpredictable, populations may evolve a bet-hedging life history strategy (Bruijning et al., 2020; Grafen, 1999)[6]. Yet, if the temporal series is predictable, populations may evolve plastic mechanisms to track the environment with their fitness related traits (Orzack,

---

[4] For more on this, see recent work by Robin Snyder and Stephen Ellner parsing out the contribution from luck toward life history outcomes (Snyder & Ellner, 2018, 2022) and a recent synthesis in Hernández et al. (2024).

[5] This is elaborated on in Appendix B – see the phase diagram of life histories in variable environments.

[6] A bet-hedging life history strategy is defined by a collection of fitness traits that increases an individual's *geometric* mean fitness at the cost of an individual's *arithmetic* mean fitness (Bruijning et al., 2020; Grafen, 1999; Starrfelt & Kokko, 2012; Philippi & Seger, 1989).

1985; Vinton et al., 2022). In turn, there is a multitude of strategies to deal with environmental stochasticity, and the efficacy of each strategy is very much dependent on the timescale (Dupont et al., 2023; Orzack, 1985; Vinton et al., 2023), environmental driver (Vinton et al., 2022) and the observed reaction norm between the environment and fitness related traits (Acasuso-Rivero et al., 2019; Barraquand & Yoccoz, 2013; Bruijning et al., 2020). Nevertheless, environmental stochasticity's negative effect on population persistence is agnostic of time or taxa. Despite the potential for local positive effects on environmental stochasticity due to Jensen's inequality (Jensen, 1906), increased environmental stochasticity inevitably leads populations toward extinction (May, 1973). Moreover, the rationale for this negative effect is not linked to the multitude of strategies by which populations can persist, but instead due to the mathematics of geometric growth.

The impact of environmental stochasticity on population growth can be easily demonstrated by simulation. In Figure 1.1, populations with three different arithmetic mean population growth rates (λ_1) are projected into the future with differing levels of environmental stochasticity. By simulating populations across 500 timesteps, Figure 1.1 shows that (1) environmental stochasticity has a negative effect on population growth rate and (2) λ_1 does not accurately predict the growth of populations in a stochastic environment – the geometric mean population growth [also known as the stochastic population growth rate (λ_s)] does.

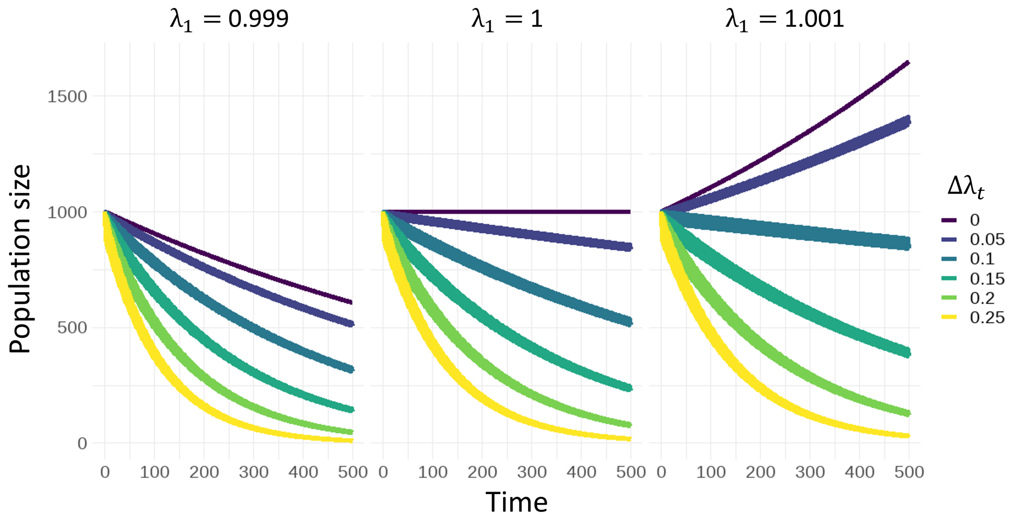

Figure 1.1: An illustration of how temporal variance perturbs population growth. Here, populations have arithmetic mean population growth rates (λ_1) of 0.999, 1 or 1.001 and are projected across 500 timesteps with varying degrees of environmental stochasticity ($\Delta\lambda_t$). Across these simulations, $\Delta\lambda_t$ corresponds to the two population growth rates used to simulation the population across timesteps. For example, if $\lambda_1 = 1$ and $\Delta\lambda_t = 0$, the population is continuously projected through a growth rate of 1 across all timesteps. However, if $\lambda_1 = 1$ and $\Delta\lambda_t = 0.2$, the population is alternatively projected through growth rates of 0.9 and 1.1 across the simulation (*i.e.*, $\lambda_t = 0.9$, $\lambda_{t+1} = 1.1$, $\lambda_{t+2} = 0.9$, $\lambda_{t+3} = 1.1$, *et cetera*).

The reason environmental stochasticity negatively impacts population growth rate is two-fold. First, the geometric mean (not the arithmetic mean) is necessary to calculate the expected growth rate of geometric systems. And second, variance perturbs growth in geometric systems (*e.g.*, discrete-time population models). Formally, the geometric mean is always less than or equal to arithmetic mean (known as the geometric mean – arithmetic mean inequality). And furthermore, the degree to which the geometric mean is less than the arithmetic mean can be approximated by the temporal variance of the system in question (*e.g.*, population growth rate),

$$G \approx \exp\left[\ln(\bar{X} - \frac{\sigma^2}{2\bar{X}^2})\right] \tag{1.2}$$

Here, the geometric mean (G) is approximated by taking the arithmetic mean ($\bar{X}$) and subtracting the impact of temporal variance (σ^2) dependent on the arithmetic mean (Jean & Helms, 1983). Specifically, for large values of $\bar{X}$ the impact of variance is minimized, whereas for low values of $\bar{X}$ the impact of variance is increased. Moreover, it is this penalization for temporal variance that bridges the gap between the simulation in Figure 1.1 and life histories in variable environments.

When discussing the growth of any geometric system, temporal variance reduces the expected growth of the system relative to the arithmetic mean[7]. Moreover, for populations that are critically endangered, this negative effect is especially pronounced. In life history theory, there is a vast literature discussing how populations can reduce this impact of environmental stochasticity on population growth (Bjørkvoll et al., 2012; Colchero et al., 2019; Gamelon et al., 2021; Hansen et al., 2019; Jelbert et al., 2019; Jenouvrier et al., 2022; McDonald et al., 2017; Sæther, 1997; Sæther et al., 2013; Tuljapurkar et al., 2009a; Vinton et al., 2023; Van De Walle et al., 2023). Furthermore, within population ecology, the ability of a population to accommodate the impact of environmental stochasticity on population growth is likened to the ability of some solutions to buffer the application of acids or bases and maintain their pH (Gascoigne et al., 2023a). Both scenarios involve the introduction of a disturbance (*i.e.*, environmental stochasticity, acidic/basic solution) and the stabilization of a metric of interest (*i.e.*, population growth rate, pH). In turn, the ability of a population to accommodate the impacts of environmental stochasticity is called demographic buffering – which is the focus of this dissertation.

1.3 Demographic buffering: From May to Pfister to the present

Researching the ability of a population to accommodate the negative impacts of environmental stochasticity on population growth (*i.e.*, demographic buffering) has been at the forefront of population ecology for decades. A series of developments detailed below, from Robert May to Catherine Pfister to present day research, lays the foundation for most current research in stochastic demography – and this dissertation in particular. In turn, this

---

[7] This impact is generalizable across geometric systems. For example, the study of financial markets (a geometric system of common interest) has led to a large literature on how best to deal with the impacts of temporal variation on investment decisions and portfolio structure (Korn, 1997; Lamberton & Lapeyre, 2011; Shreve, 2005).

section will briefly outline the major contributions in this field relating to demographic buffering – setting the scene for the work performed in this dissertation.

1.3.1 Robert May and unstructured systems

Variance perturbs geometric systems. As mentioned in the previous section, the growth rates of populations are perturbed proportional to the variance in population growth rates over time. However, a reduced population growth rate does not inherently lead to extinction. For example, if the stochastic population growth rate (λ_s – *i.e.*, the expected asymptotic growth of a population in variable environments) is greater than or equal to 1, the population will persist despite the impacts of variance in population growth rate. In turn, the existence of environmental stochasticity alone does not inherently implicate a population is destined to go extinct. However, the role environmental stochasticity in pushing populations toward extinction has been well defined, thanks to the work of Robert May.

One of the foundations of demographic buffering is a population's extinction threshold in relation to stochastic environments. In 1973, Robert May identified this limit in the context of density dependent populations[8] [Eq. 1.3, May (1973)].

$$\hat{n} = k_0 \left[1 - \frac{\sigma^2}{2k_0} \right] \tag{1.3}$$

Here, the expected number of individuals in a population ($\hat{n}$) can be calculated by taking the mean carrying capacity of the population (k_0) and subtracting the impact of temporal variance in carrying capacity (σ^2) dependent on k_0. Consequently, this equation defines an extinction threshold for populations in variable environments. Specifically, populations can persist as long as their carrying capacity is greater than half its temporal variance (*i.e.*, $k_0 > \frac{\sigma^2}{2}$)[9]. The importance of May's equation is in how it constrains life histories in variable environments. Just as resources (allocation *vs.* acquisition) and demographic rates (the Euler-Lotka equation, Eq. 1.1) constrain life histories, so does their temporal

---

[8] Note this work was primarily focused on communities and complexity which is still an open question in community ecology – see recent work in De Roos (2021).

[9] This can also be rewritten as an extinction threshold arising when the coefficient of variance in carrying capacity k_0 is greater than or equal to 2.

variance. However, there is a missing link between May's equation and life histories – which comes in the form of population structure.

In population ecology, structure refers to any form of heterogeneity that is deemed useful for formulating predictions. For example, population structure in some mammals implies differentiating individuals within the population by age and sex (*e.g.*, Childs et al., 2016; Jensen, 2000). Structure in some insects and reptiles requires differentiating individuals by stage and morph type (*e.g.*, Chi and Liu, 1985; Crouse et al., 1987). And, structure in some plants leads to differentiating individuals by size (*e.g.*, Merow et al., 2017; Rees and Ellner, 2009; Westerband and Horvitz, 2017). Whilst the traits may vary across species, incorporating structure allows for age/stage/size informed predictions. For example, structure is necessary to quantify life history traits such as: generation time, age at sexual maturity, reproductive dispersion, *et cetera*[10]. Therefore, structured population models are necessary for inquiries about life histories in variable environments. Unfortunately, this is where May's equation falls short. Equation 1.3 is an example of an unstructured population model as individuals are not differentiated by any trait. In other words, all individuals in a population are influenced by k_0 and σ^2 equally. In turn, new theory was required to link the negative impacts of environmental stochasticity to population dynamics in structured systems.

1.3.2 Filling the gap between unstructured and structured systems

After May's work in 1973, two new developments were required to link environmental stochasticity to structured populations. First, demographers needed to measure the *importance* associated with individual demographic rates (*i.e.*, the rates of survival, growth or reproduction associated with an individual age/stage/size). And second, the field needed to quantify how environmental stochasticity affects structured populations based on this measure of *importance*. These requirements were met, thanks to the development of matrix methods in demography.

---

[10] Thankfully, the methods to quantify life history traits informed by time (*e.g.*, generation time, age at sexual maturity) for stage or size structured population models are readily available due to age from stage decomposition methods (see Cochran and Ellner, 1992).

Matrix methods allow for the construction of structured population models called matrix population models (MPMs hereafter, Caswell, 2001). MPMs are square matrices[11] that project structured populations across discrete timesteps (*i.e.*, $t \rightarrow t + 1$). The size and structure of populations at time t ($\mathbf{n}_t$) and $t+1$ ($\mathbf{n}_{t+1}$) is dependent on the demographic rates that make up the individual terms of the MPM ($\mathbf{A}$)[12]. The demographic rates contained within the MPM are noted as a_{ij} quantifying the per-capita contributions of individuals in stage j (the j^{th} column in matrix $\mathbf{A}$) to stage i (the i^{th} row in matrix $\mathbf{A}$) across timesteps. Within MPMs, there are two main types: Leslie matrices and Lefkovitch matrices. A Leslie matrix is an MPM structured by age (Leslie, 1945), whilst the Lefkovitch matrix is structured by stage or size (Lefkovitch, 1965). In connection with May's work, both the Leslie and Lefkovitch matrices were being regularly applied to model structured populations across taxa – for good reason.

One of the primary reasons for the early application of MPMs is the ability to analytically derive key metrics for the population of interest. For example, some key metrics include:

1. The *population growth rate* (λ, the dominant eigenvalue of $\mathbf{A}$).
2. The *stable age/stage/size distribution* which represents the asymptotic proportion of individuals across stages ($\mathbf{w}$, the right eigenvector associated with the dominant eigenvalue of $\mathbf{A}$).
3. The *reproductive value* which represents the asymptotic contribution of a stage toward the generation of new offspring ($\mathbf{v}$, the left eigenvector associated with the dominant eigenvalue of $\mathbf{A}$)[13].

---

[11] Technically, matrix population models do not have to be square. Seasonal matrices can be non-square if individual stages are not present during all seasons (Caswell, 2001, p.346). Furthermore, MPMs can have greater than two dimensions if parameterized by multiple states (*e.g.*, Caswell, 2019a, 2020; Caswell and Salguero-Gómez, 2013; Childs et al., 2016; Roth and Caswell, 2016). However, these are minor points that do not affect the description noted above.

[12] Regarding notation, all non-scalar values (*e.g.*, vectors or matrices) are expressed in bold (*e.g.*, the MPM $\mathbf{A}$ and the population vector $\mathbf{n}_t$) whilst scalar values are expressed in plain text (*e.g.*, population growth rate λ).

[13] Prior to matrix methods, population metrics of interest (*e.g.*, λ, $\mathbf{w}$ and $\mathbf{v}$) were calculated iteratively using the Newton-Raphson algorithm [see Ebert (1999, p. 16) for more details].

This analytical toolkit laid the foundation for the new body of theory which connected environmental stochasticity with structured populations.

The two developments that linked environmental stochasticity with structured populations came in quick succession. First, Hal Caswell formalized a method to calculate the *importance* of individual demographic rates. In Caswell (1978), the *importance* of demographic rates is quantified as the partial derivative of the population growth rate with respect to individual demographic rates $\left(\frac{\partial\lambda}{\partial a_{ij}}\right)$. This measure came to be known as the sensitivities of population growth rate with respect to demographic rates. Whilst the mathematics for the formulation of sensitivities falls outside the scope of this dissertation (*i.e.*, perturbation theory and vector calculus), the quantification of sensitivity values is quite simple. For example, for any given element a_{ij} in matrix $\mathbf{A}$, its associated sensitivity value can be calculated as,

$$\frac{\partial\lambda}{\partial a_{ij}} = \frac{v_j w_i}{\langle \mathbf{v}, \mathbf{w} \rangle} = s_{ij}. \tag{1.4}$$

Here, the sensitivity of λ with respect to a_{ij} (s_{ij}) is calculated by the product of the reproductive value for the stage at time t (v_j) and the stable stage distribution at time $t + 1$ (w_i), divided by the scalar product of $\mathbf{v}$ and $\mathbf{w}$. And thanks to matrix multiplication, the sensitivity matrix ($\mathbf{S}$), which contains the sensitivity values associated with all demographic rates in $\mathbf{A}$, can be calculated as,

$$\mathbf{S} = \frac{\mathbf{v}\mathbf{w}^T}{\langle \mathbf{v}, \mathbf{w} \rangle}. \tag{1.5}$$

The second development in demographic methods involved an explicit connection of environmental stochasticity to structured populations. Through a series of works in the 1980s and 1990s, Shripad Tuljapurkar showed *how* to quantify the negative impact of environmental stochasticity on structured populations using sensitivities of population growth rate (Tuljapurkar, 1982, 1989, 1990). Using a small noise approximation (*i.e.*, a Taylor expansion relating the geometric mean to the arithmetic mean based on small variances in underlying parameters), the impact of environmental stochasticity on population growth can be directly connected to the difference between the stochastic population growth rate (λ_s) and the population growth rate associated with the mean environment (λ_1).

$$\log(\lambda_s) \approx \log(\lambda_1) - \frac{1}{2\lambda_1^2}\left[\sum_{ij} s_{ij}\,\mathrm{var}(a_{ij}) + \sum_{ij\neq kl} s_{ij}\,s_{kl}\,\mathrm{cov}(a_{ij}, a_{kl})\right] \tag{1.6}$$

This approximation, known as Tuljapurkar's approximation, shows how the impact of temporal variances [$\mathrm{var}(a_{ij})$] and covariances [$\mathrm{cov}(a_{ij}, a_{kl})$] in demographic rates on λ_s is dependent on sensitivities associated with the mean environment (s_{ij}) and the arithmetic mean population growth rate (λ_1)[14]. And, it is with this approximation that the paths of previous research converge on our modern perspective of *demographic buffering*.

Simply put, Tuljapurkar's approximation offers a mathematical approach to quantify demographic buffering. Any changes to the temporal variance, covariance or sensitivity values of the population that increase the summation contained in the square-brackets leads to a *less demographically buffered* population. On the other hand, any changes to values that reduce the summation contained in the square-brackets leads to a *more demographically buffered* population. In turn, Tuljapurkar's approximation is foundational for applied research within conservation biology (Morris & Doak, 2002), the evolution of phenotypic plasticity (Vinton et al., 2022) and demographic buffering in particular (Hilde et al., 2020).

1.3.3 From Catherine Pfister to the present

After the formulation of Tuljapurkar's approximation, the next frontier in stochastic demography was connecting theory to life histories. Up until the 1990s, stochastic demography was primarily focused on the implications of stochastic environments for population persistence; however, Tuljapurkar's approximation allowed a new line of inquiry. Tuljapurkar's approximation provides a potential link between demographic

---

[14] If Tuljapurkar's approximation looks similar to the geometric mean – arithmetic mean approximation (Eq. 2) and May's equation for density-dependent unstructured systems (Eq. 1.3), that is because they are similar. All three formulas show the negative effect of environmental stochasticity on a geometric process. In turn, all three formulas subtract the impact of variance proportional to the arithmetic mean (which is $\bar{X}$, k_0 and λ_1 for equations 1.2, 1.3 and 1.6 respectively). Furthermore, Tuljapurkar's approximation is structurally identical to equation 2 if both sides of the approximation are logged. In turn, Tuljapurkar's approximation can be simply viewed as a geometric mean – arithmetic mean approximation for structured systems.

buffering and life history theory as it explicitly incorporates the important timings and events in individual lifespans through their demographic rates. This link was first made in Pfister (1998).

In Pfister (1998), an explicit hypothesis was tested that eventually became known as the *demographic buffering hypothesis*. In summary, the hypothesis states that natural selection should generate a negative covariance between the temporal variance and importance of demographic rates in structured populations. This hypothesis builds off Tuljapurkar's approximation in two ways. First, the stochastic population growth rate (λ_s) can be inferred as a measure of fitness in variable environments, not just as an estimate of population growth[15]. And second, selection should act to increase the value of λ_s in structured populations. This second point can be achieved through two mechanisms – either through increases in λ_1[16] or by decreases in the negative effects of environmental stochasticity (*i.e.*, the square-brackets of equation 1.6). In turn, the demographic buffering hypothesis is explicitly connected to minimizing the contribution of environmental stochasticity on population growth through the covariance structure of demographic rate importance and variance.

To test the demographic buffering hypothesis, Pfister (1998) includes two analyses. The data for both analyses included 30 natural populations, representing species from brown algae to plants to animals, where each population had at least three temporally distinct MPMs. From these MPMs values of variance were calculated – specifically temporal variance and coefficient of variation. In addition, the sensitivity and elasticity values associated with the demographic rates were calculated[17]. The resulting analysis

---

[15] Nowadays, this is a fairly common interpretation (Cubaynes et al., 2022; Koons et al., 2009).

[16] Importantly, increases in λ_1 increase λ_s by both increasing the mean fitness/population growth rate in the mean environment *and* reducing the impacts of environmental stochasticity proportional to $\frac{1}{2\lambda_1^2}$.

[17] Just to clarify, the temporal coefficients of variation and elasticities associated with demographic rates were calculated because Tuljapurkar's approximation (Eq. 1.6) can be rewritten using *proportional* values. Just as variance (σ^2) is to the coefficient of variation $\left(\frac{\sigma}{\text{mean}}\right)$, sensitivities $\left(\frac{\partial\lambda}{\partial a_{ij}}\right)$ are to elasticities $\left(\frac{a_{ij}}{\lambda}\frac{\partial\lambda}{\partial a_{ij}}\right)$. The coefficient of variation represents the *proportional* variance of a sample relative to its mean. Elasticities represent the *proportional* sensitivity of λ to a demographic rate. Consequently, Tuljapurkar's approximation can be rewritten in terms of proportional values as $\log(\lambda_s) \approx \log(\lambda_1) - \frac{1}{2}\left[\sum_{ij} e_{ij}^2 \mathrm{CV}_{ij}^2 + \sum_{ij\neq kl} e_{ij} e_{kl} \left(\frac{\mathrm{cov}(a_{ij}, a_{kl})}{\bar{a}_{ij}\bar{a}_{kl}}\right)\right]$.

supported the demographic buffering hypothesis. Specifically, Spearman correlations between sensitivity ~ variance and elasticity ~ coefficient of variation indicated a broad negative relationship between the importance of demographic rates and their temporal variance across taxa. This support for the demographic buffering hypothesis formalized the connection between Tuljapurkar's approximation (as an estimate of demographic buffering) and life histories, laying the foundation for subsequent research into population dynamics and life histories in variable environments.

After Pfister (1998), multiple lines of research have re-evaluated and extended our understanding of demographic buffering in natural populations. A selection of these developments include:

1. **Reflections on correlation methods:** The results of Pfister (1998) hinge on the inferences drawn from Spearman and partial correlation of sensitivities/elasticities and variance/coefficients of variation (CV), respectively. However, given the constrained parameter space of demographic rates such as survival (between 0 and 1), correlation coefficients may be spurious. This was addressed in Morris and Doak (2004) where guidelines are laid out for the appropriate analysis of variance (*i.e.*, standardizing measures of variation with respect to maximum possible variance).

2. **Life histories as a buffering mechanism:** Tuljapurkar's approximation links structured population models with environmental stochasticity. However, this link does not implicitly extend to individual life history traits. The reason for this disconnect lies in Tuljapurkar's approximation being parameterized by demographic rates – which are not themselves life history traits. This gap between life history traits and environmental stochasticity remained until a collection of papers were published in quick succession in the early 2000s[18]. Morris et al. (2008) showed longevity, as a proxy for pace-of-life syndrome (Stearns, 1992), is positively correlated with a population's ability to buffer variable environments. Tuljapurkar

---

[18] Whilst no connection had been made between life history traits and environmental stochasticity, previous work had been performed to connect persistence strategies with variable environments [iteroparity: Orzack and Tuljapurkar (1989); diapause: Tuljapurkar and Istock (1993); migration: Wiener and Tuljapurkar (1994); biennialism: Klinkhamer and Jong (1983) and Roerdink (1988, 1989); homeostasis: Orzack (1985)].

et al. (2009a) showed generation time in addition to demographic dispersion, the spread of reproduction across a life history, buffers a population against variable environments. And lastly, Sæther et al. (2013) showed life history stages (ontogeny) matter when discussing buffering dynamics; simply put, perturbations by variable environments to early life stages often have disproportionate impacts on long term population dynamics when compared to perturbations to later life stages. Following these three papers, multiple comparative studies have been conducted to show the generality of these findings across taxa (McDonald et al., 2017; Paniw et al., 2018; Romeijn & Smallegange, 2022).

3. **New perturbation approaches:** A major development in the study of demographic buffering came with the creation of new perturbation approaches. In Tuljapurkar's approximation, the sensitivities represent the impact of a single demographic rate on the population growth rate of the mean MPM (*i.e.*, λ_1) – not the impacts of demographic rates on the stochastic population growth rate (*i.e.*¸ λ_s). This difference is non-trivial. Environmental stochasticity introduces non-linearity into the population model – meaning a change in temporal variance is not inherently proportional to the change in asymptotic dynamics. To deal with this non-linearity, two new developments in perturbation analysis were made. These new developments include *stochastic elasticities* [where the impacts of demographic rates on λ_s can be partitioned between the impact of their mean and their variance (Haridas & Tuljapurkar, 2005; Tuljapurkar et al., 2003)] and (2) *second derivatives* of population growth rate [where the curvilinear reaction norm of population growth rates with respect to demographic rates can be quantified, (Brodie et al., 1995; Caswell, 1996b; Shyu & Caswell, 2014)].

4. **Demographic lability:** One of the assumptions of demographic buffering is that the reaction norm between an environmental parameter (*e.g.*, precipitation and temperature) and population growth rate is concave (*i.e.*, ∩-shaped). At the extremes, this assumption is true by definition. For example, whilst we humans happily persist at 25°C, we are less equipped to persist at temperatures of -200°C

and +200°C. In turn, the reaction norm for human population growth rate with respect to temperature is *globally* concave; however, population's rarely experience this whole continuum. One of the developments after Pfister (1998), involved the recognition that populations can utilize *locally* convex reaction norms (*i.e.*, ∪-shaped) to persist in variable environments[19]. This phenomenon, known as *demographic lability* (Drake, 2005; Koons et al., 2009), has been identified in a variety of different species (McDonald et al., 2017) and now has a generalizable framework for its identification in structured population models (Le Coeur et al., 2022).

5. **Beyond the direct effects of temporal variance:** Variable environments impact structured populations in a variety of ways – temporal variance is just one such perturbation. Another impact comes in the form of perturbations to stage structure (*e.g.*, selective mortality events). Recently, there has been a rich framework developed to analyze these impacts, known as *transient dynamics*, using multiple analytical and numeric approaches (Caswell, 2007; Ezard et al., 2010; Stott et al., 2011, 2012). In addition, variable environments can also impact populations by the specific sequence of realized perturbations over time. To study these mechanisms, recent papers have incorporated environmental autocorrelation and lagged effects as discrete components of environmental stochasticity, separate to temporal variance (Cecco & Gouhier, 2018; Evers et al., 2023; Paniw et al., 2018; Tuljapurkar & Haridas, 2006).

These developments represent stepwise improvements in our understanding of population dynamics in variable environments. However, despite these improvements, the connection between demographic buffering and these developments remains unclear.

Currently, there are three open gaps in knowledge within the demographic buffering literature. First, how do we identify and quantify demographic buffering using the new perturbation approaches? Whilst previous work has used stochastic elasticities and

---

[19] The proof for the negative effect of concave reaction norms and the positive effect of convex reaction norms is based on Jensen's inequality (Jensen, 1906).

second derivatives (Morris et al., 2008; Caswell, 1996b; Shyu & Caswell, 2014), a formal connection between these two perturbation approaches and demographic buffering has not been defined. This remains a critical gap for the scaling of demographic buffering methods across the tree of life. Second, how does demographic buffering vary across multiple axes of environmental stochasticity (*e.g.*, temporal variance and autocorrelation)? This gap in knowledge is especially alarming because changes in environmental stochasticity is predicted to be a key threat to biodiversity in biodiversity hotspots (Bathiany et al., 2018). And third, how do the many measures of demographic buffering perform when used for conservation practices? Despite a vast literature on demographic buffering (Pfister, 1998; Hilde et al., 2020), there has been no formal test as to the efficacy of individual measures of demographic buffering to infer population responses to environmental stochasticity. Currently, all of these questions remain unanswered in the literature and are thus the subject of this dissertation.

1.4 Dissertation outline

In this dissertation, I connect recent developments in stochastic demography to the study of demographic buffering and life history evolution in six discrete chapters.

Chapter 2 defines what buffering actually means in ecological modelling. The concept of buffering is central to the topic of demographic buffering; however, the emergent property of buffering is rarely defined and often construed in different ways across ecology. In turn, this short chapter aims to define what buffering is in ecological modelling by laying out four simple criteria. I led this chapter and collaborated with Maja Kajin and Roberto Salguero-Gómez. This chapter has been published in *Trends in Ecology & Evolution* (Gascoigne et al., 2023a).

Chapter 3 demonstrates the utility of "new" perturbation approaches when identifying demographic buffering. Specifically, this chapter shows how stochastic elasticities and second derivatives of population growth rate can be used to identify demographic buffering at the population and demographic rate levels. I co-led this chapter with Gabriel Silva Santos and collaborated with André Tavares Corrêa Dias, Maja Kajin and Roberto Salguero-Gómez. This chapter is currently under review at *Ecology Letters*.

Chapter 4 builds on chapter 3 by analyzing demographic buffering in response to changes in environmental stochasticity. Whilst demographic buffering is intimately connected to the impacts of stochastic environments on population dynamics, we still do not know how different components of environmental stochasticity (*i.e.*, autocorrelation and variance) affect measures of demographic buffering. In turn, this chapter (1) identifies the impacts of environmental autocorrelation and variance on demographic buffering and (2) suggests demographic mechanisms that mediate these relationships. I led this chapter and collaborated with Maja Kajin, Shripad Tuljapurkar, Gabriel Silva Santos, Aldo Compagnoni, Ulrich Steiner, Anna Vinton, Harman Jaggi, Irem Sepil and Roberto Salguero-Gómez. This chapter is currently under review at *Ecology Letters*.

Chapter 5 builds on chapters 3 and 4 by aiming to identify the best method to measure demographic buffering. Over the course of the past 25 years, multiple methods have been used to assess demographic buffering. However, no previous study has compared these approaches for their efficacy to inform population dynamics. In turn, this chapter identifies four measures of demographic buffering and tests for the *efficacy* of each measure to inform population dynamics. I led this chapter and collaborated with Maja Kajin, Irem Sepil and Roberto Salguero-Gómez. This chapter is in preparation to be submitted to *Methods in Ecology & Evolution*.

Chapter 6 aims to reconnect chapters 2 through 5 to life history evolution. To do so, this chapter includes a broad review of modern perspectives in life history evolution and offers new perspectives on where future life history research may lead. I led this chapter and collaborated with Alice Rosen, Krish Sanghvi, Aldo Compagnoni, Ulrich Steiner, Greta Bocedi, Roberto Salguero-Gómez and Irem Sepil.

Chapter 7 provides a synthetic discussion of how Chapters 2 through 6 contribute to the literature on demographic buffering and our understanding of populations in variable environments. This synthesis is generated through (1) a brief synopsis of the primary findings across this dissertation, (2) a description of two take-home messages that directly interface with previous literature, (3) an outline of future research that can be undertaken following this dissertation and (4) my final thoughts on how this dissertation has contributed to the fields of life history theory and stochastic demography.

An inner process stands in need of outward criteria.

— Ludwig Wittgenstein

2

Criteria for buffering in ecological modelling

Contents

2.1 Preamble

Defining buffering is a problematic area across the field of ecology. Specifically with regard to demographic buffering, ideas often get conflated (*e.g.*, demographic buffering *vs*. the demographic buffering hypothesis) and blurred (*e.g.*, the interpretation of demographic buffering and demographic lability as different ends of the same continuum). However, these problems also arise outside the scope of demographic buffering.

Admittedly, early outlines of this dissertation were not going to include an argument for the definition of buffering for the ecological community. Usually, problems of definitions are dealt with by referencing a canonical text and moving on to the topic at hand[1]. However, this chapter was made necessary for two reasons. First, the connection between buffering in ecological modelling and chemistry has been a topic of conversation amongst our collaborators for a few years now; however, there was no text explicitly stating this narrative. And second, a paper came out in *Trends in Ecology & Evolution* (*i.e.*, Milles et al. (2023a)) that, in our view, obfuscates the notion of what a buffering mechanism actually means in the context of ecological systems.

In turn, we wrote this chapter[2] in response to Milles et al. (2023a)[3] to (1) relay a previously uncommunicated perspective on buffering in ecological modelling and (2) offer clarity for what *is* and *is not* a buffering mechanism.

2.2 Main text

Buffering is a key phenomenon at all levels of biological organization. From individuals to populations, communities and beyond, buffering mechanisms may enhance the persistence of ecological systems in a changing world. Milles et al. (2023a) synthesize and build on a large body of literature (Pfister, 1998; Morris et al., 2008; Hilde et al., 2020; Stott et al., 2011; Koons et al., 2009; Bruijning et al., 2020) by classifying buffering mechanisms into two categories: damping and repelling mechanisms. These categories make a timely contribution by combining predictions from stochastic systems [damping mechanisms that reduce variance in ecological dynamics (Pfister, 1998; Morris et al., 2008; Hilde et al., 2020)] and from disturbance ecology and transient dynamics [repelling mechanisms that resist or counteract population decline (Stott et al., 2011; Koons et al., 2009)]. Whilst damping and repelling mechanisms are helpful to understand ecological persistence, we still lack a useful definition of what a buffering mechanism actually is. In Milles et al. (2023a), a buffer mechanism "increases population persistence." However, we argue this definition is *necessary* but *not sufficient* to adequately characterize buffering mechanisms within an ecological system of interest. For example, when studying the buffering mechanisms of the wolf (*Canis lupus*) population in Yellowstone National Park, USA,

---

[1] Funnily enough, the canonical paper for demographic buffering is Pfister (1998) which at no point mentions the words buffer or buffering.

[2] Now published in *Trends in Ecology & Evolution* (Gascoigne et al., 2023a).

[3] To which they responded in Milles et al. (2023b).

legislation developed to reduce wolf culls should not count as a buffering mechanism – despite fitting the definition from Milles et al. (2023a). The reason legislation should not count as a buffering mechanism is that it acts extrinsically (not intrinsically) to the ecological system of interest (*i.e.*, the wolf population). Here, we propose a set of criteria – inspired by the birthplace of buffering (*i.e.*, chemistry) – that are *necessary* and *sufficient* for an ecological process to be considered a buffering mechanism.

In chemistry, buffering mechanisms are well defined. Chemists have used the term "buffer" for over 100 years to describe a solution's intrinsic ability to maintain its pH after being "perturbed" with a new solution. For example, let us imagine a solution of interest called go-juice. A sample of go-juice is an aqueous solution of a weak acid (HA, pH=4.5) and its conjugate base (A^-). These molecules reach equilibrium according to the following equation:

$$HA + H_2O \rightleftharpoons A^- + H_3O^+. \tag{2.1}$$

A chemist may be interested in how the pH of go-juice responds to the addition of a base. In turn, by adding 3mL of 0.5M sodium hydroxide (NaOH), which has a pH of 13.7, the pH of the disturbed solution now sits at 6.0. From these data, one can (1) calculate the buffering capacity (β, Equation 2.2) of the go-juice solution relative to the strength of the perturbation of 3mL of 0.5M NaOH and (2) identify the mechanisms by which the solution was able to buffer the perturbation – in this case by calculating the acid dissociation constant (Ka) of HA and understanding Le Chatelier's principle (Fig. 2.1A). These two inferences (*i.e.*, the estimation of buffering capacity and its mechanism(s)) represent the necessary conditions for a chemical buffer. We recommend that ecology should adopt these standards.

$$\beta = \frac{\text{moles of OH}^- \text{ per litre of go-juice}}{\text{final pH} - \text{initial pH}} \tag{2.2}$$

Taking inspiration from chemistry, we propose four criteria for an ecological process at the level of individuals, populations, communities, *etc.* to be considered a buffering mechanism. The candidate ecological process must:

1. Be perturbation specific. A system must be buffered against a perturbation (*e.g.*, frequency and intensity of heatwaves).
2. Be an intrinsic mechanism to the system of interest (*e.g.*, an individual, a population, a community).
3. Have a focal metric as a response variable (*e.g.*, thermal tolerance, extinction risk, species richness, stochastic population growth rate (λ_s) - see Fig. 2.1B).
4. Have a clear benchmark relative to either the absence of the mechanism, the unperturbed/previous state, or the degree of perturbation.

These four criteria represent an initial filter for a buffering mechanism to be subsequently classified as damping or repelling as per Milles et al. (2023a).

To illustrate the utility of these criteria, let us imagine two groups of ecologists independently examining the buffering mechanisms of reindeer (*Rangifer tarandus platyrhynchus*) populations in Svalbard, Norway. Upon completion of the research, both teams report different findings. The first team reports:

> *The reindeer population is buffered. Increased wolf culls buffer the population against environmental stochasticity.*

This report falls short of all proposed criteria as: (1) environmental stochasticity is not a specific perturbation, rather a combination of factors that influence the spatiotemporal variance of ecological dynamics (Vinton et al., 2022; Engen et al., 1998); (2) wolf culls are extrinsic, not intrinsic, to the reindeer population; (3) there is no focal metric; and (4) buffering is reported as binary (buffered/not buffered) instead of as a relative value. In contrast, the second team reports:

> *In response to increases in rain-on-snow events, the reindeer population exhibits shifts in its population structure. These shifts in population structure act as a damping buffering mechanism reducing variance in stochastic population growth rate (λ_s) by 30% relative to a population that does not exhibit these shifts in population structure.*

This report, inspired by Hansen et al. (2019), offers meaningful insight regarding how the reindeer population exhibits a damping buffering mechanism by following our proposed criteria: (1) the perturbation is specific to increases in rain-on-snow events; (2) the damping mechanism (*i.e.*, shifts in population structure) is intrinsic to the population of interest; (3) the team clearly defines λ_s as the response variable; and (4) the degree of buffering (*i.e.*, 30%) is relative to the absence of the mechanism.

Buffering mechanisms offer key insights to ecological systems across levels of biological organization. However, ecologists have not yet defined buffering in a generalizable manner that offers broad utility to the field. Here, we build on the damping-repelling framework from Milles et al. (2023a) by proposing four necessary criteria for an ecological process to make the grade of buffering mechanism. To close, we end with a caution. These new terms overlap with well-established concepts in the field of ecology. For instance, the parallelisms between damping and demographic buffering (Hilde et al., 2020; Gascoigne et al., 2023b; McDonald et al., 2017) and repelling and transient dynamics (Stott et al., 2011; Koons et al., 2009) may not prove advantageous to push the field forward.

2.3 Acknowledgments

We would like to thank O. Godoy, M. Qi, H. Jaggi and D. Gascoigne for valuable feedback. M.K. was supported by a Marie Curie Fellowship (MSCA MaxPersist #101032484) hosted by R.S-G. R.S-G. was supported by a NERC Independent Research Fellowship (#NE/M018458/1).

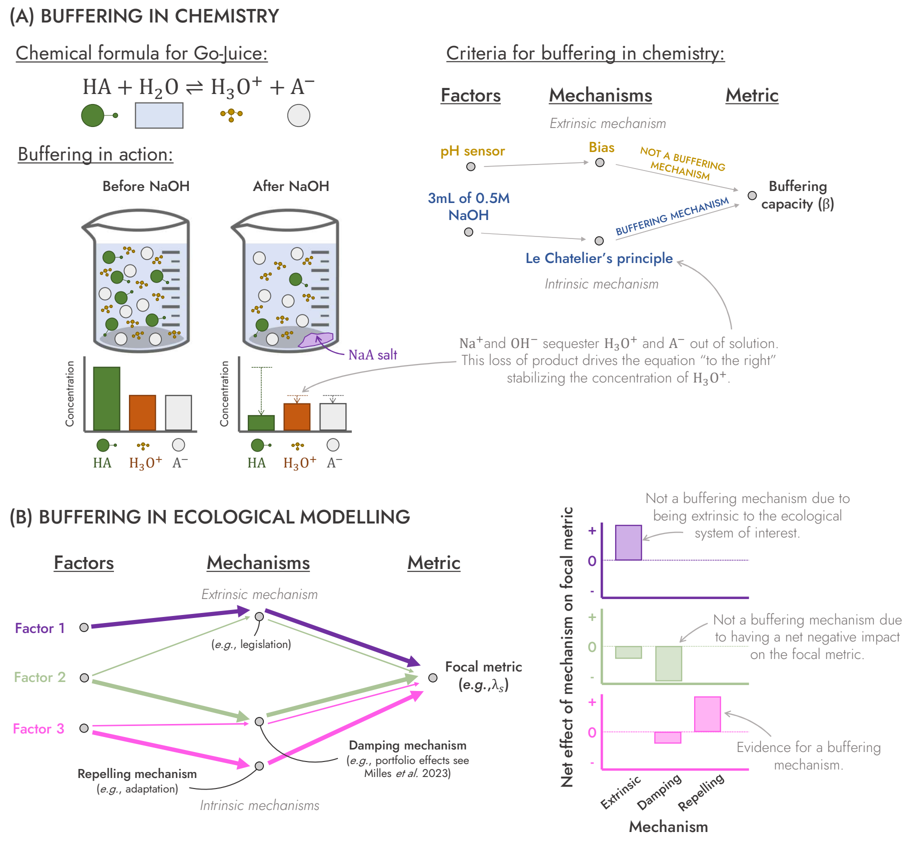

Figure 2.1: An illustration of buffering mechanisms from chemistry to ecology. (A) Buffering in chemistry has a clear definition: a solution's intrinsic ability to maintain its pH after being 'perturbed' with a new solution. To illustrate the translatability of this concept, we use our example of a made-up solution, go-juice, where buffering is shown by the stabilized concentration of H_3O^+ after the addition of 3mL of 0.5M NaOH. Here, both the pH meter and Le Chatelier's principle represent factors that may impact the measure of go-juice's buffering capacity (β). However, only Le Chatelier's principle makes the grade of buffering mechanism, because this principle refers to a mechanism intrinsic to the system (the chemical formula) while measurement error does not. (B) Here, we show how our proposed criteria for a buffering mechanism can be unambiguously identified in an ecological system. Following the same framework used in chemistry (A, top right), we illustrate how multiple factors can be tested for their degree of buffering in an ecological system. In our example, three candidate factors are shown to have varying effects, via different mechanisms, on a focal metric [here, stochastic population growth rate (λ_s)]. The strength of their impact is illustrated by the thickness of the arrows. On the right, we show the net effect of each mechanism as a function of each factor. Following our criteria, only one mechanism (the repelling mechanism in response to factor 3) can be considered as buffering the focal metric.

The data is the data. I mean, there it is for better or for worse. So, the idea is that you use a mathematical theory to paint the data blue. And if you paint the data blue, many times you can see things that you didn't see in the original data.

— Allen Tannenbaum

It may be very true that demographers know too much.

— Robert MacArthur (1960)

3

A unified framework to quantify demographic buffering in natural populations

Contents

3.1 Abstract

The Demographic Buffering Hypothesis (DBH) predicts that natural selection reduces the temporal fluctuations in demographic processes (such as survival, development, and reproduction), due to their negative impacts on population dynamics. However, a comprehensive approach that allows for the examination of demographic buffering

patterns across multiple species is still lacking. Here, we propose a three-step framework aimed at quantifying demographic buffering. Firstly, we categorize species along a continuum of variance based on the sums of stochastic elasticities. Secondly, we examine the linear selection gradients, followed by the examination of nonlinear selection gradients as the third step. With these three steps, our framework overcomes existing limitations of conventional approaches to quantify demographic buffering, allows for multi-species comparisons, and offers insight into the evolutionary forces that shape demographic buffering. We apply this framework to mammal species and discuss both the advantages and potential of our framework.

3.2 Introduction

Environmental stochasticity plays a pivotal role in shaping organisms' life histories (Bonsall & Klug, 2011). Nonetheless, how organisms will cope with the increasing variation in environmental conditions expected under climate change (Boyce et al., 2006; Morris et al., 2008) is one of the most intriguing questions in ecology and evolutionary biology (Sutherland et al., 2013). Evolutionary demography offers a wide array of explanations for the evolutionary processes that shape the diversity of demographic responses to environmental stochasticity (Charlesworth, 1994; Healy et al., 2019; Hilde et al., 2020; Pfister, 1998; Tuljapurkar et al., 2009a). The Demographic Buffering Hypothesis (*DBH*, hereafter) (Morris & Doak, 2004; Pélabon et al., 2020) is based on the fact that long-term stochastic population growth rate can be expressed in terms of the geometric mean of the annual population growth rates (Tuljapurkar, 1982). As the geometric mean of λ increases, so does the long-term stochastic population growth rate (λ_s, hereafter). However, it follows that variance in λ decreases λ_s (Morris & Doak, 2004; Tuljapurkar, 1982). In other words, temporal variation in λ negatively affects long-term population persistence. This theoretical context sets the stage for the DBH. The DBH stipulates that life histories are under selection pressure to minimise the negative impacts of environmental variation by constraining the temporal variance of those demographic processes (*e.g.*, survival, development, reproduction) to which population growth rate (*i.e.*, fitness) is most sensitive to (Gaillard & Yoccoz, 2003; Pfister, 1998). The demographic pattern operating the DBH, *i.e.*, demographic buffering, describes the selection-driven constraint on the temporal variance of the most impacting demographic processes for the population growth rate (Hilde et al., 2020; Morris & Doak, 2004; Pfister, 1998). Here, we focus on the latter - on the emerging pattern of demographic buffering in different animal life histories – rather than on the DBH itself.

A unified approach to unambiguously quantify demographic buffering is still missing. Indeed, identifying demographic buffering remains challenging (Doak et al., 2005; Morris & Doak, 2004) for at least three reasons. First is the different interpretation of results from correlational analyses (*e.g.*, as in Pfister, 1998). Some authors have used the correlation coefficient as an index to order species' life histories in a continuum ranging from buffered (Spearman's correlation $\rho < 0$ between the sensitivity of λ to demographic processes and their temporal variance) to labile ($\rho > 0$), regardless of the fit of the linear regression to more or less scattered data (McDonald et al., 2017). In contrast, other researchers interpret the absence of statistical support for demographic buffering as an alternative strategy where variance in demographic process(es) is favoured to track environmental conditions (the so-called Demographic Lability Hypothesis, *DLH* (*e.g.*, Koons et al., 2009; Reed and Slade, 2012; Jäkäläniemi et al., 2013; Hilde et al., 2020). However, the increased temporal variance is a necessary but not sufficient condition to constitute demographic lability – the increased temporal variance needs to lead to (often high) change in the demographic process mean value (Le Coeur et al., 2022).

The second obstacle to obtain generalisation across species' populations regarding demographic buffering is the hierarchical level at which this phenomenon is typically examined. Some studies base their investigations of demographic buffering on a characteristic drawn from *the entire population model* (*between-populations level*, hereafter) (McDonald et al., 2017; Reed & Slade, 2012). At the between-populations level, a life history is referred to as demographically buffered if the most important demographic process(es) has(ve) low temporal variance (Le Coeur et al., 2022; Hilde et al., 2020; Morris & Doak, 2004; Pfister, 1998). However, to understand how, why, and where demographic buffering occurs –or not– and how buffering patterns might be modified in response to the environment, it is essential to also consider the characteristics of the separate *components of population model* (*within-populations level*, hereafter). At the within-populations level, a given demographic process can be buffered against the environment, while another can be labile to it (Barraquand & Yoccoz, 2013; Jongejans et al., 2010; Koons et al., 2009). Thus far, studies have focused primarily on these two levels individually. However, here we argue that, to obtain a mechanistic understanding of how environmental stochasticity shapes life histories, both between- and within-populations levels need to be considered at the same time.

The third reason limiting a holistic understanding of demographic strategies in stochastic environments are the challenges inherent to examining their underlying mechanisms. Evidence for demographic buffering exists across some long-lived organisms with complex life cycles, (Doak et al., 2005; Gaillard & Yoccoz, 2003; McDonald et al., 2017; Pfister, 1998; Rotella et al., 2012), but also in short-lived species (Ferreira et al., 2013; Pfister, 1998; Reed & Slade, 2012). Importantly, these patterns of variation do not entirely inform how the life histories were shaped by natural selection. The beforementioned patterns of variation are represented by the *first-order* effects of perturbations in demographic processes on population growth rate (*i.e.*, elasticities). A first order effect informs us regarding the population growth rate's sensitivity to *variation in demographic processes*. While a second-order effect of perturbations in demographic processes reveals the population growth rate's sensitivity to *autocorrelation* (Tuljapurkar, 1990). Given so, integrating both, first and second-order effects of perturbations in demographic processes on the population growth rate, allows us to understand the behaviour of the fitness function at the vicinity of the local maxima and/or minima.

When the relationship between fitness and a demographic process is linear, the second-order derivatives of population growth rate with respect to demographic processes equal zero. In such cases, natural selection acts on the mean value of a demographic process (Shyu & Caswell, 2014). However, nonzero second derivatives indicate a nonlinear relationship between fitness and a demographic process (either concave if <0, or convex if >0) and thus provide additional and often overlooked characteristics of selection acting on demographic processes – not only their mean values, but also their variances and covariances (Brodie et al., 1995; Carslake et al., 2008; Shyu & Caswell, 2014).

The sign (*i.e.*, >0, =0, <0) of the self-second derivative of λ with respect to demographic processes determines the type of (non)linear selection acting on a demographic process. For instance, a negative self-second derivative for a given demographic process describes a concave form of selection, commonly referred to as the ∩-shaped selection (Caswell, 1996b, 2001; Shyu & Caswell, 2014). This form of selection reduces the temporal variance in said demographic process, thereby providing evidence of demographic buffering. Conversely, a demographic process yielding a positive self-second derivative identifies a convex, or ∪-shaped selection (Caswell, 1996b, 2001; Shyu & Caswell, 2014). Such a selection mechanism acts upon demographic processes amplifying their temporal variance, thus potentially evidencing demographic lability (Le Coeur et al., 2022; Koons et al., 2008). The evidence of lability is only potential, because to constitute demographic lability, the increased variance needs to shift the mean value of a demographic process. The shift in the mean value of a demographic process needs to outweigh the negative effect of variance in population growth rate.

The rich variation in demographic strategies across the tree of life is a result of evolutionary processes that have shaped variance in demographic processes through time. In this context, setting demographic buffering into the adaptive landscape context of linear and nonlinear selection enables us to identify and quantify the evolutionary processes that generate said demographic patterns. In this way, one will better understand how increased variability of environmental conditions might act on the existing – and shape novel – demographic strategies. However, we still lack a unified approach to constitute the signatures of demographic buffering.

Here, we present a framework that identifies and quantifies demographic buffering. Our framework provides a rich insight into the patterns of temporal variance in demographic processes affected by environmental stochasticity. This framework involves categorizing species or populations along a variance continuum based on the extent to which key demographic processes are buffered by natural selection, thereby limiting their temporal variability. The framework consists of four steps with a mix of well-known methods applied to stage-structured demographic information [*e.g.*, matrix population models (Caswell, 2001); integral projection models (Easterling et al., 2000; Ellner et al., 2016)]. First, we position species or populations on the aforementioned continuum to assess the cumulative effect of the variance in their key demographic processes on population growth rate at the between-populations level. Second, we investigate the presence of linear selection forces operating within the life cycle of each species or population at the within-populations level. Third, we explore the impact of non-linear selection forces acting within the life cycle of each species or population, also at the within-populations level. The combination of these three steps provides quantitative evidence for the occurrence of demographic buffering. Step four suggests the further necessary analyses to identify demographic lability.

To demonstrate the applicability of our framework, we apply it to 44 populations of 38 mammal species sourced from the COMADRE database (Salguero-Gómez et al., 2016a). We showcase how the framework can provide valuable insights into the patterns of demographic buffering across species. The framework offers novel, detailed insights into the selection pressures that act *within* species' life cycles, thus allowing for a thorough understanding of the evolutionary selection pressures that shape the patterns of demographic buffering across species. Beyond providing a quantitative, systematic toolset to quantify buffering through three steps, we have also offered a potential fourth step that briefly outlines how to evidence lability.

3.3 A unified framework to assess evidence of demographic buffering

The evidence for demographic buffering has been mainly assessed using Matrix Population Models (MPM; Pfister, 1998; Rotella et al., 2012). However, Integral Projection Models (IPM; Rodríguez-Caro et al., 2021; Wang et al., 2023) can be equally applied for identifying the demographic buffering signatures. Both MPMs and IPMs are stage-structured, discrete-time demographic models (Caswell, 2001; Ellner et al., 2016). For simplicity, here we focus on MPMs, but note that the same approaches are as equally applicable to IPMs (Doak et al., 2021; Griffith, 2017). Throughout this manuscript, we refer to demographic processes as both matrix entries a_{ij} (*i.e.*, upper-level parameters) and the vital rates that underline the matrix elements (*i.e.*, lower-level parameters), and note that their conversion is straightforward and described elsewhere (Franco & Silvertown, 2004). The framework operates on three steps.

The first step of our framework involves acquiring the relative impact of variation in demographic processes on the stochastic growth rate, λ_s, the so-called stochastic elasticities, $E^S_{a_{ij}}$ (Haridas & Tuljapurkar, 2005) (Fig. 3.1A). The sum of all stochastic elasticities ($\sum E^S_{a_{ij}}$), can be separated into two components to assess how temporal variance and mean values of each demographic process impact λ_s. The first component represents *the sum of stochastic elasticity of* λ_s *with respect to the variance* $\sum E^{\sigma^2}_{a_{ij}}$, and the second represents *the sum of stochastic elasticity of* λ_s *with respect to the mean* $\sum E^{\mu}_{a_{ij}}$, where $\sum E^S_{a_{ij}} = \sum E^{\sigma^2}_{a_{ij}} + \sum E^{\mu}_{a_{ij}}$ (Haridas & Tuljapurkar, 2005). Thus, the summation $\sum E^{\sigma^2}_{a_{ij}}$ quantifies the summed effect to which the stochastic population growth rate (λ_s) is influenced by changes in the variances of the demographic processes within the population matrix.

A higher sum of stochastic elasticity of λ_s with respect to the variance of demographic processes (*i.e.*, higher absolute value; $|\sum E^{\sigma^2}_{a_{ij}}|$) indicates that small changes in the variance of demographic processes would have a substantial impact on λ_s. In other words, the variance of that demographic process is not constrained by selection, indicating absence of demographic buffering. On the other hand, a lower (absolute) stochastic elasticity of λ_s with respect to the variance of a given demographic process suggests that λ_s is less sensitive to such perturbations, or, that variance in demographic processes is being constrained by natural selection, thus suggesting demographic buffering (Haridas & Tuljapurkar, 2005; Tuljapurkar et al., 2003) (Fig. 3.1A).

The first step of the framework thus features the between-populations level and places species or populations alongside a continuum. Species exhibiting unconstrained variance in demographic processes (*i.e.*, possibly not buffered, Fig. 3.1A, blue dots) are positioned on the left-hand side of the continuum. In contrast, species with constrained variance in demographic processes (*i.e.*, possibly buffered, Fig. 3.1A, yellow dots) are positioned on the right-hand side of the continuum. However, the left-hand side of the continuum does not necessarily imply evidence of demographic lability. This is so because demographic lability is defined as an increase in the *mean value* of a demographic process in response to improved environmental conditions (Le Coeur et al., 2022). By examining $\sum E^{\sigma^2}_{a_{ij}}$, we can visualize an increase or decrease of the contribution that *variance* of demographic processes has on the long-term population growth rate, while the mean value of a demographic process does not change.

Step 1 of our framework examines the impacts that environmental variation has on the long-term population growth rate, λ_s (Tuljapurkar et al., 2003). This means that the resulting variance continuum in this step of the framework is based on how λ_s was affected by variation in the key demographic parameter across all contiguous time periods. However, Haridas and Tuljapurkar (2005) explicitly acknowledge that covariances between demographic processes and serial correlations need to be investigated to diagnose buffering entirely. Our approach does not use covariances neither serial correlation, but rather focuses on the second derivatives of the population growth rate with respect to demographic processes and elucidates how selection is acting on variance (step 3, below).

Steps 2 and 3 of the framework are conducted at the within-populations level. Once species or populations are positioned along the variance continuum regarding the summed effect of variation on λ_s, (step 1), one needs to zoom into each life cycle separately, analysing the selection pressures acting on each one of the demographic processes composing the life cycle (*i.e.*, population model). In doing so, one can inspect the selection pressures that have generated the patterns found in step 1. Step 2 (Fig. 3.1B) requires obtaining the partial derivatives of the deterministic population growth rate, λ_1, relative to all matrix elements of the MPM of interest (*i.e.*, elasticities of λ_1 with respect to each demographic process in the MPM). Step 2 therefore informs on the impact that each of the demographic processes has on λ_1.

Finally, in step 3, one assesses the pattern of nonlinear selection by using the self-second derivatives of λ_1 with respect to each demographic process (Fig. 3.1C). This step reveals the potential nonlinear selection pressures on each of the demographic processes within a life cycle. This step is key to understanding the evolutionary processes (*i.e.*, types of nonlinear selection) that the demographic processes are subjected to. Without understanding the evolutionary processes operating on the demographic processes, the pattern observed in step 1 might be artefactual (*e.g.*, Lawler et al., 2009).

Steps 2 and 3 of the framework feature selection pressures that have been averaged over the contiguous time periods. This means that the resulting patterns are based on how λ_1 (obtained from averaging all sequential MPMs across the duration of the study) would be affected if a demographic process were perturbed. Therefore, steps 2 and 3 are based on different information when compared to step 1 and can thus complete our understanding of the role of selection pressures on shaping demographic patterns across multiple species.

Another important asset of step 3 includes the notion that the relative importance (elasticity) of demographic processes themselves changes with changing environment (Stearns, 1992). In other words, the extent to which λ_1 is sensitive to perturbations in a specific demographic process is *dynamic* (De Kroon et al., 2000). Thus, the self-second derivatives generate information on how the sensitivity (or elasticity) of λ_1 might change. If the sensitivity (or elasticity) of λ_1 can change, then it is important to know which demographic processes are most prone to trigger such a change. In the example of a hypothetical wolf species (Fig. 3.1), this means that if the reproduction of the third age-class individuals (matrix element $a_{1,3}$) decreased, the sensitivity of λ_1 to $a_{1,3}$ would increase (square with the largest black dot, Fig. 3.1C). Consequently, with increased environmental variability, the key demographic process might change from remaining in the fourth age class (matrix element $a_{4,4}$, Fig. 3.1B) to reproduction of the third age-class (matrix element $a_{1,3}$, Fig. 3.1C).

Combining the three steps of our framework allows for a quantitative identification of buffering. Steps 2 and 3 offer key insights as to *why* a given species or population is placed on either the buffered or the non-buffered end of the variance continuum. Clear evidence of demographic buffering consists of: (1) a species or population being positioned near the 0 end of the continuum (the right-hand side) in step 1; (2) this species' or populations' life cycle having one or more demographic processes with highest elasticity values in step 2; and (3) the same demographic process displaying the highest elasticity in step 2 with negative self-second derivative values in step 3. In this sense, Figure 3.1B shows that, for the chosen population of a hypothetical wolf species, the most important demographic process is remaining in the fourth stage (MPM element $a_{4,4}$), as this demographic process results in highest elasticity value (Fig. 3.1B yellow square). However, Fig. 3.1C reveals that $a_{4,4}$ is under little selection pressure for variance reduction. Thus, there is no clear evidence of buffering from the third step of the framework (*i.e.*, no concave selection forces).This way, the lack of concave selection forces on the key demographic process within wolf's life cycle explains why this species is placed on the left-hand side of the variance continuum (Fig. 3.1A).

Placing species on the non-buffered end of the continuum is a necessary but not sufficient condition for evidence demographic lability. It is key to highlight that demographic buffering and lability do not represent two extremes of the same continuum. The variance continuum allocates the species or populations from strongly buffered to non-buffered, but to test the for lability, a further step is needed.

Although not our primary goal here, we briefly introduce said step 4. To establish compelling evidence of lability, it is essential to fulfil several further criteria. First, sufficient data across various environments (over time or space) are required to construct reaction norms that depict how a demographic process responds to environmental changes (Morris et al., 2008; Koons et al., 2009) (Morris et al., 2008; Koons et al., 2009), which can be challenging in terms of sufficient and high-quality demographic and environmental data.

Second, non-linear relationships between demographic processes and the environment must be established based on the demographic process-environment reaction norms. Lastly, demographic processes where an increase in the mean value has a stronger positive impact on population growth rate than the detrimental effect of increased variance need to be identified. This latter condition is only achieved when the demographic process–environment reaction norm is convex (∪-shaped; Morris et al., 2008; Koons et al., 2009). Importantly, we note that more likely than previously thought (*e.g.*, Pfister, 1998), species do not exist as purely buffering or labile, but that within populations, some vital rates may be buffered, other labile, and others insensitive to the environment (*e.g.*, Doak et al., 2005). Deciphering generality in this likely complex pattern should attract much research attention going forward, in our opinion.

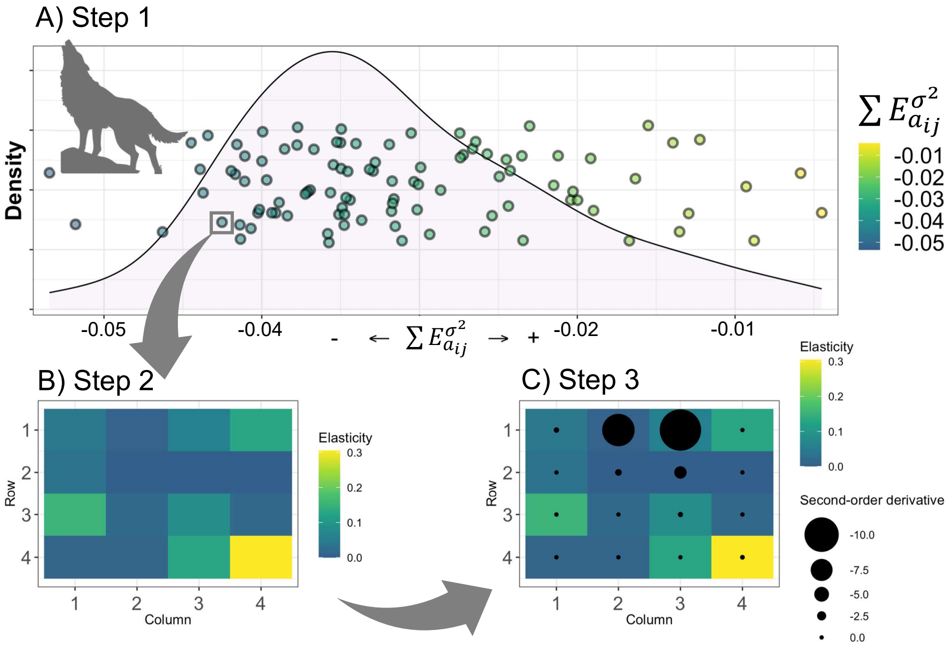

Figure 3.1: A three-step framework to assess evidence of demographic buffering. Step 1 - allocate species and/or populations on a variance continuum (A, dots representing 50 hypothetical species). The variance continuum operates at the between-populations level and is represented by partitioning the sum of all the stochastic elasticities ($\sum E_{a_{ij}}^{S}$) into two components: i) sums of stochastic elasticities with respect to the variance ($\sum E_{a_{ij}}^{\sigma^2}$), and ii) sums of stochastic elasticities with respect to the mean ($\sum E_{a_{ij}}^{\mu}$). The first step of our framework shows $\sum E_{a_{ij}}^{\sigma^2}$ forming a continuum where the right-hand side of the plot represents species (or populations) where a perturbation of variance in demographic processes results in weak or no impact on λ_s (yellow dots). The yellow-dotted species (or populations) can be classified as having potentially buffered life-cycles– based on all the demographic processes. The left-hand side of the graph represents species (or populations) where a perturbation of the variance in demographic processes results in strong impact on λ_s (blue dots). Thus, the blue-dotted species (or populations) can be classified as having potentially unbuffered life cycles – based on all the demographic processes. Step 2 - Access the linear selection pressures for individual species or populations at within-species level (B). Step 2 displays the elasticities of the deterministic population growth rate (λ_1) for a hypothetical population of wolf and reveals the linear selection gradients, and which demographic processes are the most influential for λ_1. Step 3 - Access the nonlinear selection pressures at the within-species level (C). In the third step self-second derivatives for the corresponding demographic processes from step 2 are displayed.

3.4 Demographic buffering in mammals: A case study using the unified framework

We demonstrate the performance of our framework using 44 MPMs from 38 mammal species. Mammals are of special interest here for two reasons: (1) mammalian life histories have been well studied (Bielby et al., 2007; Gillespie, 1977; Jones, 2011; Stearns, 1983); and (2) some of their populations have already been assessed in terms of buffering, particularly for primates (Campos et al., 2017; Morris et al., 2008, 2011; Reed & Slade, 2012; Rotella et al., 2012). Together, the well-studied life histories and previous information about the occurrence of buffering in mammals provide the necessary information to make accurate predictions and validate the performance of the proposed framework.

We used Matrix Population Models from 44 out of 139 studies with mammals available in the COMADRE database v.3.0.0 (Salguero-Gómez et al., 2016a). These 44 populations encompass 38 species from eight taxonomic orders. We included these MPMs in our analyses because they provide values of demographic processes (a_{ij}) for three or more contiguous time periods, thus allowing us to obtain the stochastic elasticity of each a_{ij}. Although we are aware that not all possible temporal variation in demographic processes may have been expressed within this period, we assumed three or more transitions are enough to provide sufficient variation for population comparison. At least three contiguous time periods - a common selection criteria in comparative studies of stochastic demography (Compagnoni et al., 2024) - also allowed to test and showcase our framework. Fortunately, several long-lived species, characterized by low variation in their demographic processes, were studied for a long time (*e.g.*, some primates in our dataset have been studied for over 20 years – Morris et al., 2011). We removed the populations where either only survival or only reproduction rates were reported because of the impossibility to calculate the stochastic growth rate. A detailed description of the analysed data and their original sources are available in the supplementary materials.

Homo sapiens was included in our analyses because it is the only mammalian species in which second-order derivatives have been applied (Caswell, 1996b). Therefore, *Homo sapiens* provides an ideal basis for comparisons among species. The data for *Homo sapiens* were gathered from 26 modern populations located in various cities, allowing us to construct a spatiotemporal variance. It is important to note that in this case, we are not working with true temporal variance but rather a variance that encompasses both spatial and temporal aspects.

For steps 2 and 3 of our framework, we utilized a subset of 16 populations (including *Homo sapiens*) whose population projection matrices (MPMs) were organized by age. We specifically selected these populations because their life cycles can be summarized by two main demographic processes: survival and contribution to recruitment of new individuals. The contribution to recruitment can be interpreted as either the mean reproductive output for each age class or an approximation thereof, depending on how the matrices are structured (Ebert, 1999). One advantage of using such matrices is that they encompass only two types of demographic processes, namely survival and recruitment, eliminating the need to account for multiple transitions between different life stages.

To perform the step 1 of our framework and obtain the $\sum E^{\sigma^2}_{a_{ij}}$ (and $\sum E^{\mu}_{a_{ij}}$), we followed Tuljapurkar et al. (2003) and Haridas and Tuljapurkar (2005). To perform step 2 of our framework, we calculated the deterministic elasticities of each demographic process extracted using the *popbio* package. All analyses were performed using R version 3.5.1 (R Core team, 2018). Finally, to perform the step 3 of our framework the self-second derivatives were adapted from *demogR* (Jones, 2007) following (Caswell, 1996b) and applied for the mean MPM.

3.4.1 Results

We ranked 44 populations from the 38 identified mammal species according to the cumulative impact of variation in demographic processes on λ_s using the step 1 of our framework (Fig. 3.2). Additional information (including standard deviations of the elasticity estimates and number of matrices available) is provided in the supplementary materials (Table 3.2). Most of the analysed orders were placed on the low-variance end of the variance continuum (Fig. 3.2). The smallest contributions of variation in demographic processes (*i.e.*, maximum value of $\sum E^{\sigma^2}_{a_{ij}}$, note that $\sum E^{\sigma^2}_{a_{ij}}$ ranges from 0 to -1), suggesting more buffered populations, were assigned to Primates: northern muriqui (*Brachyteles hyphoxantus*, $\sum E^{\sigma^2}_{a_{ij}} = -0.09 \times 10^{-4} \pm 0.12 \times 10^{-4}$) (mean ± standard deviation) (Fig. 3.2 silhouette a), mountain gorilla (*Gorilla beringhei*, $\sum E^{\sigma^2}_{a_{ij}} = -0.24 \times 10^{-4} \pm 0.08 \times 10^{-4}$) (Fig. 3.2 silhouette b), followed by the blue monkey (*Cercopithecus mitis*, $\sum E^{\sigma^2}_{a_{ij}} = -0.63 \times 10^{-4} \pm 0.06 \times 10^{-4}$ (Fig. 3.2 silhouette c). The first non-primate species placed near the low-variance end of the continuum was the Columbian ground squirrel (*Urocitellus columbianus*, Rodentia, $\sum E^{\sigma^2}_{a_{ij}} = -0.003 \pm 0.002$) (Fig. 3.2 silhouette d). The species with the highest contribution of variation in demographic processes placed at the high-variance end of the continuum was the stoat (*Mustela erminea*, Carnivora, $\sum E^{\sigma^2}_{a_{ij}} = -0.35 \pm 0.02$) (Fig. 3.2 silhouette e). All the 14 primate populations displayed potential evidence of buffering, occupying the right-hand side of the variance continuum, with the exception of the Patas monkey (*Erythrocebus patas*, Primates, $\sum E^{\sigma^2}_{a_{ij}} = -0.05 \pm 0.03$) (Fig. 3.2 silhouette f). The snowshoe hare (*Lepus americanus*, Lagomorpha, $\sum E^{\sigma^2}_{a_{ij}} = -0.29 \pm 0.16$) (Fig. 3.2 silhouette g) and the Bush rat (*Rattus fuscipes*, Rodentia, $\sum E^{\sigma^2}_{a_{ij}} = -0.25 \pm 0.03$) (Fig. 3.2 silhouette h) appear on the high-variance end of the continuum.

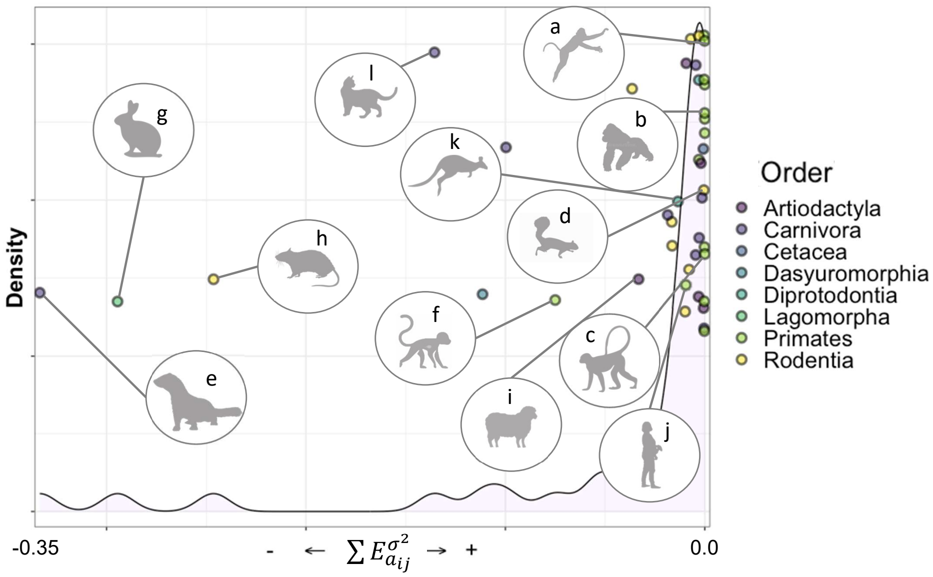

Figure 3.2: Results for step 1 of our framework showing the sum of stochastic elasticities with respect to the variance $\left(\sum E^{\sigma^2}_{a_{ij}}\right)$. The closer the $\sum E^{\sigma^2}_{a_{ij}}$ is to zero, the weaker the impact of variation in demographic processes on λ_s. The 44 populations from 38 species of mammals from the COMADRE database are ranked into the variance continuum from potentially buffered (right-hand side) to less buffered (left-hand side), since any variation in demographic processes would strongly impact λ_s. Colors represent different taxonomic orders with Primates occupying the right-hand side. Silhouettes: a) *Brachyteles hyphoxantus*, b) *Gorilla beringhei*, c) *Cercopithecus mitis*, d) *Urocitellus columbianus*, e) *Mustela erminea*, f) *Erythrocebus patas*, g) *Lepus americanus*, h) *Rattus fuscipes*, i) *Ovis aries*, j) *Homo sapiens*, k) *Macropus eugenii* and l) *Felis catus*. The y-axis represents the frequency of data points at each $\sum E^{\sigma^2}_{a_{ij}}$ value (depicted as a density function), but the jitter applied on the y-axis has no biological meaning.

As predicted for steps 2 and 3, we could not observe a clear pattern in support of buffering. This finding means that the demographic processes with the highest elasticity values failed to display strongly negative self-second derivatives (Fig. 3.3). Particularly for majority of primates - with the lack or minor temporal variation in demographic processes - demographic processes with high elasticities had positive values for the self-second derivatives (indicated by yellow squares with white dots in Fig. 3.3). Examples of primate species exhibiting high elasticities and positive values for the self-second derivatives and include northern muriqui (*Brachyteles hypoxanthus*), mountain gorilla (*Gorilla beringei*), white-faced capuchin monkey (*Cebus capucinus*), rhesus monkey (*Macaca mulatta*), blue monkey (*Cercopithecus mitis*), Verreaux's sifaka (*Propithecus* *verreauxi*) and olive baboon (*Papio cynocephalus*) (Fig. 3.3). This implies that the key demographic processes influencing λ_1 are not subject to selective pressure for reducing their temporal variability. However, even though the primates were positioned closer to the low-variance end of the continuum in step 1, the evidence from steps 2 and 3 does not support the occurrence of buffering in the most influential demographic processes.

The killer whale showed similar controversy between step 1 and steps 2-3 results as most primates. In step 1, the killer whale was positioned at the buffered end of the variance continuum (*Orcinus orca*, Cetacea, $\sum E^{\sigma^2}_{a_{ij}} = -0.70 \times 10^{-4} \pm 1.04 \times 10^{-5}$ (Fig. 3.2 silhouette not shown). However, steps 2 and 3 show that the three demographic processes in killer whale life cycle with highest elasticity values (matrix elements $a_{2,2}$, $a_{3,3}$ and $a_{4,4}$) are not under selection pressures for reducing their temporal variance, but the opposite (depicted by yellow and green squares with white dots, Fig. 3.3).

The only primate species exhibiting evidence of buffering in steps 2 and 3 was human. In human, demographic parameters representing survival from first to second age class (matrix element $a_{2,1}$) displayed high elasticities and negative self-second derivatives (depicted as yellow squares with black dots in Fig. 3.3). Evidence supporting buffering was also found in the Columbian ground squirrel (*Urocitellus columbianus*), where, similar to humans, survival from the first to the second age class (matrix element $a_{2,1}$) showed indications of selection acting to reduce $a_{2,1}$ variance. Accordingly, the Columbian ground squirrel was positioned close to the buffered end of the variance continuum in step 1. Hence, the Columbian ground squirrel was the sole species with consistent evidence of buffering across all three steps of the framework.

The Soay sheep (*Ovis aries*) was the species furthest from the buffered end of the variance continuum that enabled to perform steps 2 and 3. For the Soay sheep, remaining in the third age class (matrix element $a_{3,3}$) has the major influence on λ_1 and is under selection pressure to have its variance increased. The latter characteristics reveal potential conditions for lability even though the species is placed closer to the buffered end of the variance continuum.

Steps 2 and 3 illustrate the importance of examining buffering evidence on the within-populations level. These two steps of the framework identify the simultaneous acting of concave and convex selection on different demographic processes within a single life cycle. In polar bear (*Ursus maritimus*), the key demographic process (matrix element $a_{4,4}$) is under convex selection, as depicted by a yellow square with a white dot in Fig. 3.3. However, the demographic process with the second highest elasticity value (matrix element $a_{5,4}$) is under strong concave selection (depicted by a light green square with a black dot in Fig. 3.3).

By adding step 3 to the framework, another important information was accessed. The high absolute values of self-second derivatives (large dots, either black or white, Fig. 3.3) indicate where the sensitivity of λ_1 to demographic parameters is itself prone to environmental changes. For instance, if the value of $a_{5,4}$ for polar bear increased, the sensitivity of λ_1 to $a_{5,4}$ would decrease because the self-second derivative of $a_{5,4}$ is highly negative (depicted by the largest black dot in polar bear MPM). Vice versa holds for the $a_{4,4}$ demographic process, where an increase in the value of $a_{4,4}$ would increase λ_1's sensitivity to $a_{4,4}$, because the self-second derivative of $a_{5,4}$ is highly positive (depicted by the largest white dot in polar bear MPM). Thus, sensitivities (or equally elasticities) of demographic processes with high absolute values for self-second derivatives can easily change.

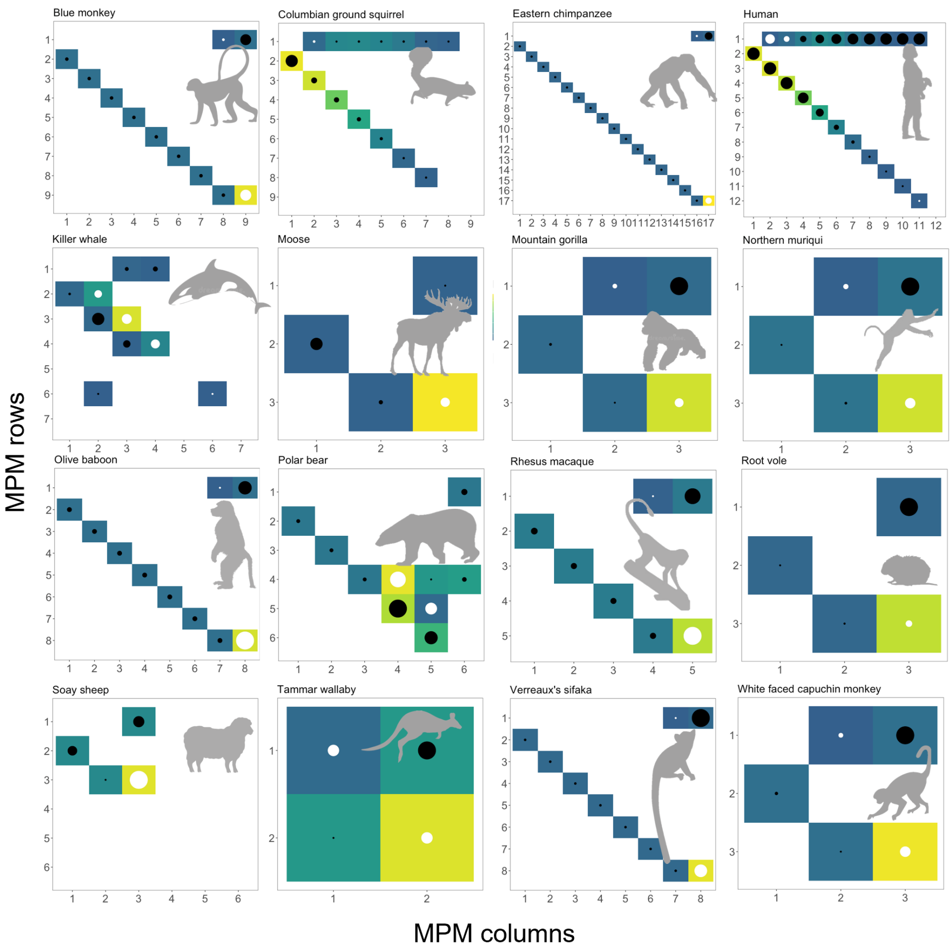

Figure 3.3: Results from steps 2 and 3 of the proposed framework. The 16 plots represent elasticity and self-second derivative values for age-structured animal MPMs. The color scale represents elasticity values for each demographic process in the MPM, where yellow represents high and blue low elasticity values. No color means elasticity=0. Since step 2 is a within-population level comparison, each plot has its own scale (see end of legend). The black dots represent negative self-second derivatives of λ_1 - thus concave selection - and the white dots represent positive self-second derivatives of λ_1 - thus convex selection. The dot sizes are scaled by the absolute value of self-second derivatives, where the smaller the dot, the closer a self-second derivative is to 0, indicting weak or no nonlinearity. Large dots indicate strong nonlinear selection forces. For the range of elasticity and self-second derivative values represented within each plot, see Table 3.1.

Table 3.1: Elasticity and self-second derivative values for 16 animal species.

Common name	Species	Elasticity (min, max)	Self-second derivative (min, max)
Blue monkey	*Cercopithecus mitis*	0.00, 0.52	-1.25, +1.27
Columbian ground squirrel	*Urocitellus columbianus*	0.00, 0.23	-1.48, +0.01
Eastern chimpanzee	*Pan troglodytes*	0.00, 0.60	-4.39, +2.59
Human	*Homo sapiens*	0.00, 0.18	-0.15, +0.08
Killer whale	*Orcinus orca*	0.00, 0.50	-5.72, +3.43
Moose	*Alces alces*	0.00, 0.55	-0.66, +0.36
Mountain gorilla	*Gorilla beringei*	0.00, 0.81	-1.46, +0.28
Northern muriqui	*Brachyteles hypoxanthus*	0.00, 0.72	-1.17, +0.35
Olive baboon	*Papio cynocephalus*	0.00, 0.54	-0.57, +1.13
Polar bear	*Ursus maritimus*	0.00, 0.26	-0.73, +0.54
Rhesus macaque	*Macaca mulatta*	0.00, 0.51	-0.54, +0.71
Root vole	*Microtus oeconomus*	0.00, 0.86	-2.54, +0.22
Soay sheep	*Ovis aries*	0.00, 0.56	-0.22, +0.40
Tammar wallaby	*Macropus eugenii*	0.00, 0.55	-0.64, +0.34
Verreaux's sifaka	*Propithecus verreauxi*	0.00, 0.66	-2.66, +1.21
White faced capuchin monkey	*Cebus capucinus*	0.00, 0.77	-1.03, +0.32

3.5 Discussion

In the Anthropocene, identifying and quantifying mechanisms of species responses to stochastic environments holds crucial importance. This importance is particularly tangible in the context of the unprecedented environmental changes and uncertainties that impact the dynamics and persistence of natural populations (Boyce et al., 2006). Correlational demographic analysis, whereby the importance of demographic processes and their temporal variability is examined (Pfister, 1998), has attempted to identify how species may buffer against the negative effects of environmental stochasticity. However, these widely used approaches have important limitations (see Introduction and Hilde et al., 2020). Our novel framework overcomes said limitations by providing a rigorous approach to quantify demographic buffering (Hilde et al., 2020; Pfister, 1998).

Evidencing demographic buffering is not straightforward. Indeed, through the analysis of stochastic population growth rate (λ_s) in our application of the framework to 44 populations of 38 species, we identify the highest density of natural populations near the buffered end of the variance continuum (step 1). However, we show that the same species then fail to exhibit signs of concave (∩-shaped) selection on the key demographic parameters when further analyses are performed averaging the variation across the duration of each study (steps 2 and 3). This finding confirms that placing the species near the buffered end of the variance continuum is *necessary* but not *sufficient* to diagnose demographic buffering. Indeed, buffering occurs when concave selection forces act on the key demographic parameter (Caswell, 1996b, 2001; Shyu & Caswell, 2014).

Combining the three steps into a unified framework is of utmost importance. In steps 2 and 3 of the framework, we find relatively limited overall evidence of buffering in the examination of our 16 (out of 38 in step 1) studied animal species. Step 3 of our framework reveals that the role of natural selection shaping temporal variation in demographic processes is more complex than expected. Indeed, demographic processes within our study populations are often under a mix of convex and concave selection. This mix of selection patterns was already suggested by Doak et al. (2005). Here, only two out of 16 mammal species revealed concave selection acting on the key demographic processes [the Columbian ground squirrel (*Urocitellus columbianus*) and humans (*Homo sapiens sapiens*)]. These two species were also placed near the buffered end of the variance continuum, therefore meeting all the necessary conditions to diagnose buffering. However, finding 12.5% (two out of 16) species that meet the criteria for demographic buffering is not in concordance with previous studies. Evidence of buffering has been reported across 22 ungulate species (Gaillard & Yoccoz, 2003). In the one ungulate we examined, the moose (*Alces alces*), we find only partial support for buffering in adult survival, since this species is placed near the buffered end of the variance continuum in step 1 but does not show concave selection pressures on adult survival in step 2/3, as would be necessary to confirm the occurrence of buffering.

Our overall findings reveal varying levels of support for the notion that adult survival in long-lived species tends to be buffered. Indeed, Gaillard et al. (1998) found that adult female survival varied considerably less than juvenile survival in large herbivores. This finding was also supported by further studies in ungulates and small rodents (Gaillard & Yoccoz, 2003), turtles (Heppell, 1998), vertebrates and plants (Pfister, 1998), and more recently across nine (out of 73) species of plants (McDonald et al., 2017).

When placing our study species along a variance continuum (step 1), primates tend to be located on the buffered end. However, most primates displayed convex

–instead of the expected concave– selection on adult survival. Similar results, where the key demographic process failed to display constrained temporal variability, have been reported for long-lived seabirds (Doherty et al., 2004). One explanation for the unexpected convex selection on adult survival involves trade-offs, as suggested by (Doak et al., 2005). When two demographic parameters are negatively correlated, the variance of population growth rate (λ) can be increased or decreased (Compagnoni et al., 2016; Evans & Holsinger, 2012). The well-established trade-off between survival and fecundity (Roff & Fairbairn, 2007; Stearns, 1992) might explain the observed deviation of our results. Because variation in primate recruitment is already constrained by physiological limitations (Campos et al., 2017), when adult survival and recruitment are engaged in a trade-off, this trade-off might lead to our unexpected result. Correlations among demographic processes inherently influence the biological limits of variance (Haridas & Tuljapurkar, 2005). This is because the magnitude of variation in a demographic process is constrained by other demographic processes that also exert an influence on it. Here, future studies may benefit from deeper insights via cross-second derivatives (Caswell, 1996b, 2001) to investigate correlations among demographic processes.

Examining the drivers of demographic buffering has become an important piece of the ecological and evolutionary puzzle of demography. As such, quantifying buffering can help us better predict population responses to environmental variability, climate change, and direct anthropogenic disturbances (Boyce et al., 2006; McDonald et al., 2017; Pfister, 1998; Vázquez et al., 2017). By setting demographic buffering into a broader and integrated framework, we hope to enhance comprehension and prediction of the implications of heightened environmental stochasticity on the evolution of life history traits. This understanding is crucial in mitigating the risk of extinction for the most vulnerable species.

3.6 Acknowledgements

This study was financed in part by the Coordenação de Aperfeiçoamento de Pessoal de Nível Superior - Brasil (CAPES) - Finance Code 001. GSS was supported by CAPES and CNPq (301343/2023-3). RS-G was supported by a NERC Independent Research Fellowship (NE/M018458/1). MK was supported by the European Commission through the Marie Skłodowska-Curie fellowship (MSCA MaxPersist #101032484) hosted by RSG.

3.7 Supplementary materials

Table 3.2: Metadata used in step 1 of our framework and the respective results presented in the main text, using COMADRE version 3.0.0.

Species author (COMADRE)	**Species**	**Common name**	**Order**	**# matrices**	λ_s	$\sum \mathbf{E}^{\sigma^2}_{\mathbf{a_{ij}}}$
Homo_sapiens_subsp._sapiens	*Homo sapiens sapiens*	Human	Primates	26	1.064	-3.132×10^{-3}
Alces_alces	*Alces alces*	Moose	Artiodactyla	14	1.205	-7.469×10^{-4}
Antechinus_agilis	*Antechinus agilis*	Agile antechinus	Dasyuromorphia	3	0.931	-1.123×10^{-1}
Bos_primigenius	*Bos primigenius*	Cattle	Artiodactyla	8	1.003	-3.743×10^{-3}
Brachyteles_hypoxanthus	*Brachyteles hypoxanthus*	Northern muriqui	Primates	25	1.051	-4.227×10^{-5}
Callospermophilus_lateralis	*Callospermophilus lateralis*	Golden-mantled ground squirrel	Rodentia	9	2.052	-6.429×10^{-2}
Cebus_capucinus	*Cebus capucinus*	White faced capuchin monkey	Primates	18	1.021	-1.761×10^{-4}
Cercopithecus_mitis	*Cercopithecus mitis*	Blue monkey	Primates	28	1.036	-4.287×10^{-5}
Cervus_canadensis_subsp._nelsoni	*Cervus canadensis*	Rocky Mountain elk	Artiodactyla	10	1.107	-8.814×10^{-3}
Eumetopias_jubatus	*Eumetopias jubatus*	Northern sea lion; Steller sea lion	Carnivora	4	0.904	-4.704×10^{-3}
Felis_catus	*Felis catus*	Feral cat	Carnivora	3	1.948	-1.370×10^{-1}
Gorilla_beringei	*Gorilla beringei*	Mountain gorilla	Primates	41	1.027	-5.222×10^{-5}
Hippocamelus_bisulcus	*Hippocamelus bisulcus*	Huemul deer	Artiodactyla	3	0.996	-1.937×10^{-3}
Leopardus_pardalis	*Leopardus pardalis*	Ocelot	Carnivora	4	1.086	-3.520×10^{-4}
Lepus_americanus	*Lepus americanus*	Snowshoe hare	Lagomorpha	5	0.812	-2.501×10^{-1}
Lycaon_pictus	*Lycaon pictus*	African wild dog	Carnivora	3	1.500	-9.781×10^{-2}
Macaca_mulatta_3	*Macaca mulatta*	Rhesus macaque	Primates	24	1.127	-3.977×10^{-4}
Macropus_eugenii	*Macropus eugenii*	Tammar wallaby	Diprotodontia	15	0.981	-1.389×10^{-2}
Marmota_flaviventris_2	*Marmota flaviventris*	Yellow-bellied marmot	Rodentia	8	0.890	-8.145×10^{-3}
Marmota_flaviventris_3	*Marmota flaviventris*	Yellow-bellied marmot	Rodentia	8	0.921	-6.662×10^{-3}
Microtus_oeconomus	*Microtus oeconomus*	Root vole	Rodentia	28	1.028	-7.665×10^{-4}
Mustela_erminea	*Mustela erminea*	Stoat	Carnivora	4	1.258	-3.089×10^{-1}
Orcinus_orca_2	*Orcinus orca*	Killer whale	Cetacea	50	0.999	-6.508×10^{-4}
Ovis_aries_2	*Ovis aries*	Soay sheep	Artiodactyla	6	1.099	-3.445×10^{-2}
Pan_troglodytes_subsp._schweinfurthii	*Pan troglodytes*	Eastern chimpanzee	Primates	45	0.982	-3.614×10^{-4}
Papio_cynocephalus	*Papio cynocephalus*	Olive baboon	Primates	37	1.054	-1.858×10^{-4}
Peromyscus_maniculatus_2	*Peromyscus maniculatus*	Deer mouse	Rodentia	4	1.107	-9.551×10^{-3}
Phascolarctos_cinereus_2	*Phascolarctos cinereus*	Koala	Diprotodontia	4	1.064	-2.658×10^{-3}
Phocarctos_hookeri	*Phocarctos hookeri*	New Zealand sea lion	Carnivora	16	1.023	-3.984×10^{-3}
Propithecus_verreauxi	*Propithecus verreauxi*	Verreaux's sifaka	Primates	24	0.986	-3.076×10^{-4}
Puma_concolor_8	*Puma concolor*	Cougar	Carnivora	15	1.115	-1.391×10^{-1}
Rattus_fuscipes	*Rattus fuscipes*	Bush rat	Rodentia	3	1.305	-2.500×10^{-1}
Spermophilus_armatus	*Urocitellus armatus*	Uinta ground squirrel	Rodentia	6	1.125	-1.533×10^{-2}
Spermophilus_armatus_2	*Urocitellus armatus*	Uinta ground squirrel	Rodentia	6	1.095	-2.017×10^{-2}
Spermophilus_columbianus	*Urocitellus columbianus*	Columbian ground squirrel	Rodentia	6	1.009	-4.323×10^{-2}
Spermophilus_columbianus_3	*Urocitellus columbianus*	Columbian ground squirrel	Rodentia	6	1.200	-3.669×10^{-3}
Ursus_americanus_subsp._floridanus	*Ursus americanus*	Florida black bear	Carnivora	4	1.020	-2.795×10^{-3}
Ursus_arctos_subsp._horribilis_5	*Ursus arctos*	Grizzly bear	Carnivora	7	1.026	-1.311×10^{-3}
Ursus_maritimus_2	*Ursus maritimus*	Polar bear	Carnivora	5	0.941	-1.686×10^{-2}
Brachyteles_hypoxanthus_2	*Brachyteles hypoxanthus*	Northern muriqui	Primates	25	1.111	3.193×10^{-6}
Cebus_capucinus_2	*Cebus capucinus*	White-faced capuchin monkey	Primates	22	1.059	-1.216×10^{-4}
Chlorocebus_aethiops_2	*Chlorocebus aethiops*	Vervet	Primates	8	1.187	-6.141×10^{-2}
Erythrocebus_patas	*Erythrocebus patas*	Patas monkey	Primates	9	1.128	-4.878×10^{-2}
Gorilla_beringei_subsp._beringei	*Gorilla beringei*	Mountain gorilla	Primates	41	1.053	-7.921×10^{-5}

Not only in research, but also in the everyday world of politics and economics, we would all be better off if more people realised that simple nonlinear systems do not necessarily possess simple dynamical properties.

— Robert May (1976)

4

Structured demographic buffering: A framework to explore the environmental drivers and demographic mechanisms underlying demographic buffering

Contents

4.1 Abstract

Environmental stochasticity is a key determinant of population viability. Decades of work exploring how environmental stochasticity influences population dynamics have highlighted the ability of some natural populations to limit the negative effects of environmental stochasticity, one of these strategies being demographic buffering. Whilst various methods exist to quantify demographic buffering, we still do not know which environment factors and demographic processes are most responsible for the demographic buffering observed in natural populations. Here, we introduce a framework to quantify the relative effects of three key drivers of demographic buffering: environment components (*e.g.*, temporal autocorrelation and variance), population structure, and demographic rates (*e.g.*, progression and fertility). Using Integral Projection Models, we explore how these drivers impact the demographic buffering abilities of three plant species with different life histories and demonstrate how our approach successfully characterises a population's capacity to demographically buffer against environmental stochasticity in a changing world.

4.2 Introduction

Understanding how populations minimise the negative effects of environmental stochasticity is central to ecology and evolution (Sutherland et al., 2013). A key prediction of life history theory is that increases in the temporal variance of demographic rates (*e.g.*, rates of progression, stasis, retrogression and fertility) lead to reductions in a population's stochastic growth rate (λ_s) (Tuljapurkar, 1982, 1989). In extreme cases, this demographic rate variance can lead to local extinction (Bull et al., 2007; Lennartsson & Oostermeijer, 2001; May, 1973; Melbourne & Hastings, 2008; Sæther et al., 1998).

Critically, environmental stochasticity, a key driver of demographic rate variance (Jongejans et al., 2010), is projected to change across the globe due to climate change (Bathiany et al., 2018; Cecco & Gouhier, 2018; Lewis & King, 2017; Masson-Delmotte et al., 2021; Shen et al., 2011; Urban, 2015). Therefore, understanding the environmental drivers and demographic mechanisms influencing the relationship between environmental stochasticity and population dynamics is both important and timely.

Three key considerations are needed to relate demographic rate variance to population dynamics. First, there are limits to the amount of variance that demographic rates can exhibit without driving a population to local extinction (Arthreya & Karlin, 1971; May, 1973). Second, the negative effects of demographic rate variance on population growth are exacerbated when the environmental drivers impact the demographic rate(s) of highest importance (*i.e.*, sensitivity) to λ_s. However, the negative effect of demographic rate variance on λ_s can be reduced (or increased) when demographic rates covary negatively (or positively) (Tuljapurkar, 1982, 1989), as demographic rates can compensate (amplify) for one another within a timestep. For example, demographic compensation may occur if instances of low adult survival happen concurrently with high adult reproduction, or vice versa (Sheth & Angert, 2018). Third, environment-demographic rate reaction norms can moderate the relationship between demographic rate variance and λ_s (Bruijning et al., 2020; King & Hadfield, 2019). Following Jensen's inequality (Jensen 1906), convex (∪-shaped) environment-demographic rate reaction norms result in a positive effect of demographic rate variance on λ_s, whereas concave (∩-shaped) reaction norms lead to a negative effect (Drake, 2005; Koons et al., 2009). These three key considerations regarding the impact of stochastic environments on population dynamics have produced key predictions in life history theory (Sæther et al., 2013; Tuljapurkar et al., 2009a), conservation biology (Foley, 1994; Higgins et al., 2000), and agriculture science (Lande et al., 1997; Mack, 2000). However, these three considerations alone do not allow us to quantify a population's ability to accommodate demographic rate variance; demographic buffering does.

Quantifying demographic buffering in natural populations has been a dynamic area of study in recent decades. The field has moved from regression-based approaches, where the deterministic elasticities (or sensitivities) of λ with respect to demographic rates are regressed against the coefficient of variation (or variance) of demographic rates (Pfister, 1998; Morris & Doak, 2004; Hilde et al., 2020), to a derivative-based approach that uses the summation of stochastic elasticities of variance, $\sum E^{\sigma^2}_{a_{ij}}$, as a measure of demographic buffering (Santos et al., 2023; Wang et al., 2023). This shift toward $\sum E^{\sigma^2}_{a_{ij}}$ offers a more holistic perspective on demographic buffering – taking the whole life history into account rather than individual elements (*i.e.*, demographic rates). Despite important insights (McDonald et al., 2017), the regression-based approach have important limitations, such as being confounded by the life cycle's complexity, the lack of standardized methods (Hilde et al., 2020), and difficulty in clear-cut interpretations (Santos et al., 2023).

Using the summation of stochastic elasticities of variance, one can explore the environmental drivers and demographic mechanisms behind demographic buffering. This insight is possible because $\sum E^{\sigma^2}_{a_{ij}}$ quantifies the proportional contribution of demographic rate variance to λ_s (Haridas & Tuljapurkar, 2005; Tuljapurkar et al., 2003) and, consequently, directly quantifies degree of demographic buffering. In practice, $\sum E^{\sigma^2}_{a_{ij}}$ is always negative. The reason $\sum E^{\sigma^2}_{a_{ij}}$ is negative stems from the impact of environmental stochasticity always reducing λ_s relative to the mean environment[1]. Whilst researchers have previously used $\sum E^{\sigma^2}_{a_{ij}}$ to quantify demographic buffering (Dalgleish et al., 2010; Morris et al., 2008), we still do not know how different environment components (*i.e.*, temporal autocorrelation and variance), population structure (*i.e.*, distribution of individuals in a population according to states, such as age, stage and/or size), and different demographic rates (*i.e.*, state-specific transition probabilities or reproductive contributions between time t and $t + 1$) impact $\sum E^{\sigma^2}_{a_{ij}}$.

---

[1] The negative impact of environmental stochasticity on population growth is equivalent to the geometric mean – arithmetic mean inequality (*i.e.*, the geometric mean for a set of random variables is always less than or equal to the set's arithmetic mean) but for a structured system. In this case, the geometric mean is λ_s which is always less than the population growth rate associated with the mean environment (λ_1) due to the negative impact of environmental stochasticity – which can be quantified as $\sum E^{\sigma^2}_{a_{ij}}$.

Here, we test the effects of the environment components, population structure and demographic rates on the ability of natural populations to remain demographically buffered. We use environment-explicit stochastic integral projection models (IPMs) (Easterling et al., 2000; Ellner et al., 2016) for three perennial plant species from the PADRINO database (Levin et al., 2022) to test two hypotheses. We expect that: (H1) environment autocorrelation and variance will have negative effects on $\sum E^{\sigma^2}_{a_{ij}}$. Specifically, as environments become more variable and positively autocorrelated, populations will become less buffered as predicted by Tuljapurkar (1982, 1989) small-noise approximation. (H2) Environmental autocorrelation and variance influence $\sum E^{\sigma^2}_{a_{ij}}$ via different demographic mechanisms. Specifically, we expect that: (H2a) environmental autocorrelation influences $\sum E^{\sigma^2}_{a_{ij}}$ via its impact on population structure (*i.e.*, the proportion of individuals in each size-class) across timesteps. We base this prediction on the fact that the impact of environmental autocorrelation on population dynamics can be quantified by the degree to which the sequence of environments shifts the population from its long-term mean stable state structure (Tuljapurkar & Haridas, 2006). Briefly, the rationale behind this expectation can be simplified by acknowledging that the commutative property of multiplication that applies to unstructured systems (*e.g.*, $2 \times 1 = 1 \times 2$) does not apply to structured systems (*e.g.*, $\mathbf{A} \times \mathbf{B} \neq \mathbf{B} \times \mathbf{A}$, where $\mathbf{A}$ and $\mathbf{B}$ are matrices of size $> 1 \times 1$). In turn, since the structure of the population is encoded into the population state distributions, we hypothesize that the impact of environmental autocorrelation on $\sum E^{\sigma^2}_{a_{ij}}$ is strongly mediated by population structure. Similarly, we expect (H2b) environment variance to influence $\sum E^{\sigma^2}_{a_{ij}}$ via the populations' underlying demographic rates. This prediction also follows Tuljapurkar's small-noise approximation (Tuljapurkar, 1982, 1989), where the impact of environment variance can be approximated by the summed product of the variance and sensitivities of individual demographic rates.

4.3 Methods

4.3.1 Stochastic integral projection models

To explore the drivers of demographic buffering, we used integral projection models (IPMs). IPMs are discrete time population models (*i.e.*, they project populations across well-defined intervals of time from t to $t+1$) that are structured with respect to a continuous variable (Easterling et al., 2000; Ellner et al., 2016). To investigate the environmental drivers and demographic mechanisms that impact degrees of demographic buffering in natural populations, we used environment explicit, parameter-stochastic IPMs for the temperate deciduous shrub *Berberis thunbergii* (Merow et al., 2017) and the tropical herbaceous perennials *Calathea crotalifera* (Westerband & Horvitz, 2017) and *Heliconia tortuosa* (Westerband & Horvitz, 2017), extracted from the PADRINO IPM database (Levin et al., 2022). The chosen model structure allows us to individually influence regression parameters that underpin the IPM subkernels (*i.e.*, the survival **P**- and fertility **F**-subkernels) based on the environment conditions to test our hypotheses.

We chose these three published IPMs to compare the roles of environmental parameters and λ_s on $\sum E^{\sigma^2}_{a_{ij}}$) to gain some generality. The *B. thunbergii* IPM uses five environmental parameters to build its kernels: mean temperature during warmest month, mean May precipitation, photosynthetically active radiation (PAR), soil nitrogen, and soil pH. The *C. crotalifera* and *H. tortuosa* IPMs use two environmental parameters to define their kernels: canopy openness and photosynthetic rate. The kernel structure and parameters used in vital rate regressions for *B. thunbergii*, *C. crotalifera* and *H. tortuosa* are detailed in Appendices A.1, A.2 and A.4, respectively. Furthermore, the models inhabit different domains of λ_s. The models of *B. thunbergii* and *H. torutosa* have values of $\lambda_s > 1$ (*B. thunbergii*: $\lambda_s = 1.378$; *H. tortuosa*: $\lambda_s = 1.367$), implying long-term population growth, *C. crotalifera* has a $\lambda_s < 1$ ($\lambda_s = 0.976$), describing long-term population decline (Fig. 4.1). This combination of environmental parameters and λ_s values across the three species offers a unique opportunity for the exploration of demographic buffering in variable environments. Since *C. crotalifera* and *H. torutosa* have the same environmental parameters and *B. thunbergii* and *H. tortuosa* have highly similar λ_s values, our study allows an exploration of demographic whilst mitigating the potential confounds of environmental parameters and λ_s. In turn, these three species are well suited to examine possible impacts of environmental parameters and λ_s on $\sum E^{\sigma^2}_{a_{ij}}$ across the autocorrelation – proportional variance parameter space.

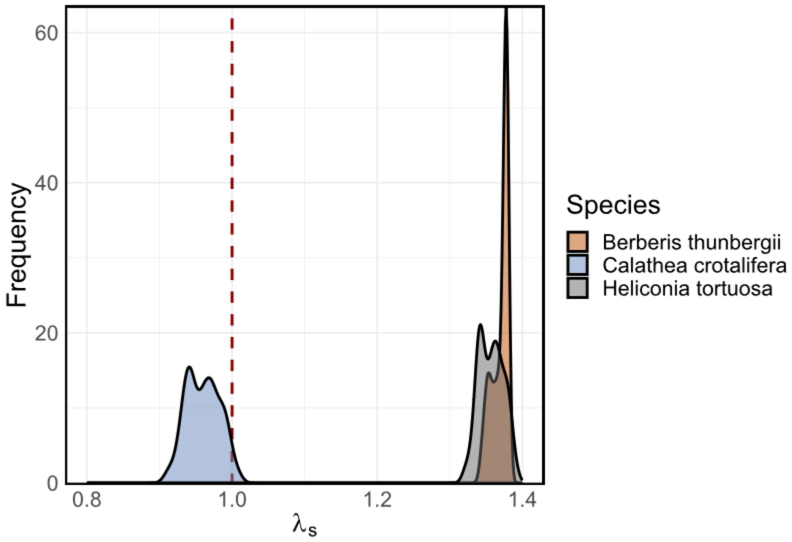

Figure 4.1: Distribution of λ_s from simulations across the environmental autocorrelation – variance parameter space. The red dashed line represents a population that stays stable when projected across time steps (*i.e.*, $\lambda_s = 1$). Values distributed to the left of the red dashed line represent populations who will asymptotically decline in number across time steps (*i.e.*, $\lambda_s < 1$), whilst values distributed to the right of the red dashed line represent populations that will asymptotically increase across time steps (*i.e.*, $\lambda_s > 1$).

4.3.2 Simulation methodology

To explore the roles of (H1) environmental drivers as well as (H2a) population structure and (H2b) demographic rates on demographic buffering, we simulated IPMs across the environmental autocorrelation – variance parameter space. In this simulation, all combinations of stochastic environmental parameters, with autocorrelation ranging from -0.8 to 0.8 and proportional variance ranging from 0.9 (10% less variance in the environment than the IPM in PADRINO) to 1.1 (10% more variance in the environment that the IPM in PADRINO) were generated for all environmental parameters. *B. thunbergii* had five environmental parameters, whilst *C. crotalifera* and *H. tortuosa* had two environment parameters (Fig. 4.2a,b). We used these sequences of environmental parameters to construct the time series of 1,000 IPM kernels from which we then estimated λ_s (Eq. 4.1, the geometric mean of changes in population size across timesteps). Specifically, to calculate λ_s: (1) a population of random structure was initialized, whereby the proportion of individuals of a given size class was generated from a uniform distribution ranging between the upper and lower limits of the IPMs (see Appendices A.1, A.2 and A.4), (2) the population was then multiplied through the series of 1,000 parameter-stochastic IPM kernels, and (3) population sizes from timestep 200 to 1,000 were used to calculate λ_s following the equation:

$$\lambda_s = \exp\left(E\left[\ln\left(\frac{N_{t+1}}{N_t}\right)\right]\right) \tag{4.1}$$

We omitted the first 200 projections from our calculation of λ_s to discard transient dynamics effects on short-term population size distributions (McDonald et al. 2016).

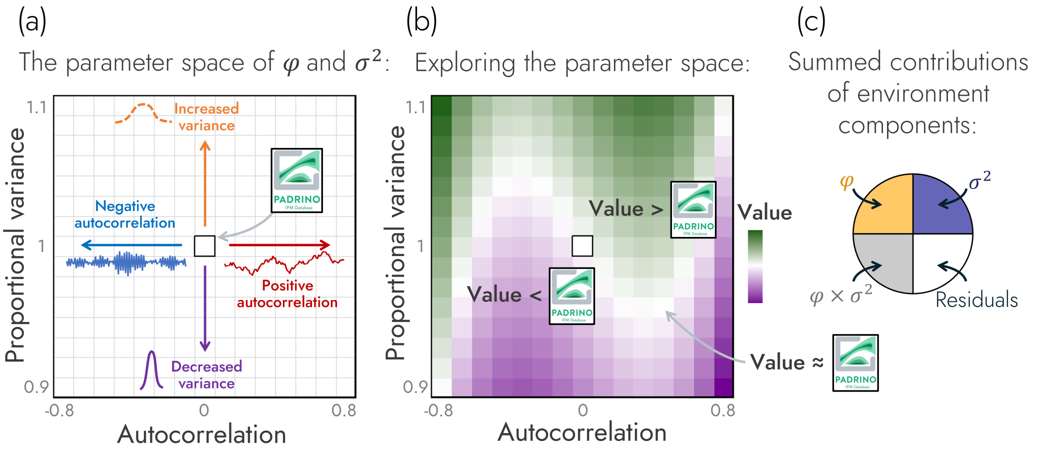

Figure 4.2: An overview of the simulation and analysis structure implemented to examine the impacts of climate drivers on natural populations. In our simulations, we explored how a population's measure of demographic buffering changes over the parameter space of possible environmental autocorrelation and variance values. (a) This space is visualized here across a 2D surface with environment autocorrelation on the x-axis and proportional variance on the y-axis. Environmental variance is noted as proportional variance which is defined as the relative increase (>1) or decrease (<1) in the variance of a climate driver is made relative to the climate driver's variance value stored in the PADRINO database. The middle of this landscape (*i.e.*, autocorrelation = 0 and proportional variance = 1) represents the population model stored in the PADRINO database. (b) The impact of environmental autocorrelation and variance on a response variable (*e.g.*, degree of demographic buffering or a measure of population structure) is shown projected as a third dimension across this landscape. Across this projection, values lower than those reported in the original PADRINO IPM model are coloured purple, values close to the PADRINO model are coloured white, and values greater than the PADRINO model are coloured green. (c) The most parsimonious model that predicts the response variable as a function of environmental autocorrelation and proportional variance was retained to calculate the summed linear and non-linear contribution of each predictor and the residuals towards the variance in the response variable.

4.3.3 Generating environmental time series

To explore the environmental drivers of demographic buffering (H1), we manipulated the temporal autocorrelation and variance of environmental variables in our environmentally explicit stochastic IPMs. Whilst the effects of variance of demographic rates and environmental variables on population dynamics are commonly researched in population ecology (Le Coeur et al., 2022; Drake, 2005; Jackson et al., 2022), temporal autocorrelation in environmental variables is much less explored despite temporal autocorrelation having broad impacts on population dynamics (Evers et al., 2023; Petchey, 2000; Petchey et al., 1997; Smallegange et al., 2014), life histories (Paniw et al., 2018; Vinton et al., 2023) and evolution (Vinton et al., 2022; Wieczynski et al., 2018). To fill this gap in knowledge, we used a first-order autoregressive function to generate the sequence of environment values used to build the series of IPM kernels. Here, φ represents the degree of autocorrelation across time steps whilst, ϵ_{t+1} represents white noise (*i.e.*, random draws from a normal distribution, $\epsilon \sim N(0, 1)$).

$$X_{t+1} = \varphi X_t + \epsilon_{t+1} \tag{4.2}$$

Subsequently, to coerce the autocorrelated series ($\mathbf{X}$) to realistic values for the vital rate regressions that build the IPMs (shown in Appendices A.1, A.2 and A.4), the final sequence of environment values was to a desired mean (μ) and variance (σ^2) of the simulated environment:

$$\text{environment} = \left[\frac{\sqrt{\sigma^2}\,[\mathbf{X} - \text{mean}(\mathbf{X})]}{\sqrt{\text{var}(\mathbf{X})}} \right] + \mu \tag{4.3}$$

As our objective is not to evaluate the effect of shifts in mean environment values on demographic buffering but rather to examine the impacts of variance and autocorrelation, μ values were kept constant across simulations, whilst σ^2 values varied across simulations. Since the environment variables across the three species have different variances ($\sigma^2_{init.}$), to standardize the increase/decrease in environment variance across parameters, we manipulated variances proportional to their variances coded in the PADRINO database ($\sigma^2_{prop.}$) (Levin et al., 2022).

$$\sigma^2 = \sigma^2_{init.}\,\sigma^2_{prop.} \tag{4.4}$$

Generating these environment time series subsequently creates a parameter space of environmental stochasticity with axes of temporal autocorrelation and proportional variance. It is worth noting that this parameter space does not represent a realized scenario in nature – as environmental variables do not vary (even proportionally) to the same degrees and conditions of positive and negative autocorrelation are not equally likely for our populations of interest. The purpose of this parameter space is to manipulate the degrees of environmental stochasticity across two-axes to inform how demographic buffering responds in a changing world.

4.3.4 Analysing the effects of environmental autocorrelation and variance

To explore the effects of environment components on each species' ability to remain demographically buffered (H1,2), we constructed a suite of linear models using autocorrelation and proportional variance as predictors whilst also including an autocorrelation × proportional variance as an interaction term. Furthermore, since the impact of autocorrelation and proportional variance on demographic buffering may be nonlinear, we also constructed models using the quadratic and cubic forms of proportional variance and autocorrelation as predictors. To select the most appropriate model to describe the data, we used model comparison based on AIC (see the supplementary methods for the full analysis pipeline and Tables S1-12 for a full AIC break down). After selecting the most parsimonious model, we calculated the proportion of variance in $\sum E^{\sigma^2}_{a_{ij}}$ that can be explained by the full model (R^2) along with the summed contributions of autocorrelation, proportional variance, autocorrelation × proportional variance and residuals (Fig. 4.1c). These contributions were calculated by taking the sum of squares associated with each predictor and dividing them by the total sum of squares associated with the selected model.

4.3.5 Perturbation analyses to quantify $\sum E^{\sigma^2}_{a_{ij}}$

To quantify the degree of demographic buffering across our simulations (testing H1,2), we calculated the summation of stochastic elasticities of variance of demographic rates with respect to λ_s. We estimated this variable, $\sum E^{\sigma^2}_{a_{ij}}$, numerically. Whilst the **K**-kernel of an IPM is defined as a continuous density function that projects a continuously structured population across discrete time steps, in practice we discretise the kernel into a matrix notated as **A** (Easterling et al., 2000; Ellner et al., 2016). Since **A** is composed of individual matrix elements (a_{ij}, representing both the survival-dependent changes of individuals from stage j to stage i and the per-capita contributions of individuals in stage j to stage i across timesteps) and our stochastic environment generates a temporal sequence of **A** matrices, we can quantify the temporal variance of each a_{ij} element in the series of **A** matrices [*i.e.*, var(a_{ij})]. In turn, we numerically calculate $\sum E^{\sigma^2}_{a_{ij}}$ by perturbing the temporal variance of each matrix element (a_{ij}) from our IPMs individually by 0.00001 proportionate (elasticity) to the unperturbed temporal variance of that matrix element[2]. After perturbation of the matrix element, we calculated a perturbed stochastic population growth rate associated with the perturbed element a_{ij} ($\lambda_s^{*a_{ij}}$). The summation of these weighted differences in λ_s and $\lambda_s^{*a_{ij}}$ yields $\sum E^{\sigma^2}_{a_{ij}}$.

$$\sum E^{\sigma^2}_{a_{ij}} = \sum \left[\frac{\mathrm{var}(a_{ij})}{\lambda_s} \times \frac{\lambda_s^{*a_{ij}} - \lambda_s}{0.00001 \times \mathrm{var}(a_{ij})} \right] \tag{4.5}$$

To calculate the impact of demographic rates on demographic buffering (H2b), we perturbed the subkernels that describe survival-dependent changes in size (**P**) and fertility (**F**) using the same method we used for the **K**-kernels. After calculating the subkernel-level elasticities of variance (Griffith, 2017), we subtracted the subkernel summed elasticities of demographic rates to calculate their relative contributions: **P** – **F** contribution. Positive (negative) values of **P** – **F** contribution indicate relative variance in rates of survival-dependent changes in size are more (less) impactful on λ_s than relative variance in rates of fertility.

4.3.6 Quantifying the impact of population structure on $\sum E^{\sigma^2}_{a_{ij}}$

To analyse how population structure influences demographic buffering (H2a), we used two numerical approaches. Whilst methods exist to *analytically* measure the impact of population structure on asymptotic properties of population dynamics (Tuljapurkar &

---

[2] It is worth noting that performing the perturbation at the level of demographic rate variances *vs.* standard deviations (as in Morris et al., 2008) does not affect the patterns as $\log(\sigma^2) = 2\log(\sigma)$.

Lee, 1997), currently there are no analytical approaches to quantify the degree to which multiple environment components influence $\sum E^{\sigma^2}_{a_{ij}}$ via population structure. In turn, we use two measures of population structure using a *regression-based approach* and an *estimate-based approach*. These approaches numerically link the impact of environmental autocorrelation and variance on $\sum E^{\sigma^2}_{a_{ij}}$ via population structure. Importantly, using these two approaches to investigate H2a allows us to cross-validate outputs (*i.e.*, the hypothesized result of environmental autocorrelation impacting $\sum E^{\sigma^2}_{a_{ij}}$ via shifts in population structure).

The *regression-based approach* involved examining deviances from stationary distributions. To do so, we first quantified the expected buffering value ($\sum E^{\sigma^2}_{a_{ij}}|$ASD) of individuals in the population. This expected buffering value is simply calculated as the weighted average of the buffering value associated with each stage ($\sum_j E^{\sigma^2}_{a_{ij}}$) and the proportion of individuals in that stage, relative to the population's average size distribution (ASD). To determine the population's average size distribution for a given environment, we iterated 1,000 randomly generated size distributions through the series of stochastic kernels and retained the mean of all size distributions across time steps 200 to 1,000. Burning in the first 200 timesteps mitigates the impact of transients on the ASD. After calculating the values of $\sum E^{\sigma^2}_{a_{ij}}|$ASD across the parameter space of environmental autocorrelation and variance, we quantified the degree to which variance in expected buffering values, deviated from variances in $\sum E^{\sigma^2}_{a_{ij}}$. To quantify these differences, we extracted the residuals from the $\sum E^{\sigma^2}_{a_{ij}}|\text{ASD} \sim \sum E^{\sigma^2}_{a_{ij}}$ regression where both $\sum E^{\sigma^2}_{a_{ij}}|$ASD and $\sum E^{\sigma^2}_{a_{ij}}$ are scaled (mean = 0, standard deviation = 1). Deviances of $\sum E^{\sigma^2}_{a_{ij}}|\text{ASD} \sim \sum E^{\sigma^2}_{a_{ij}}$ from a 1-to-1 line (*i.e.*, the existence of residuals from this regression) indicates shifts in population structure may be influencing $\sum E^{\sigma^2}_{a_{ij}}$. Subsequently, regressing these residuals against the environment components allows us to implicate an environment component – hypothesized to be environmental autocorrelation [H2a] – as driving the impact of population structure on $\sum E^{\sigma^2}_{a_{ij}}$.

The *estimate-based approach* involved calculating the mean of the distribution of demographic buffering across a life history, termed *mean buffered size*. Calculating mean buffered size allows us to explore if the degree of buffering across a life history is shifted towards smaller or larger sizes across the environmental autocorrelation – variance parameter space. To calculate this mean buffered size, we calculated the relative size [*i.e.*, 0 = smallest possible size (α) and 1 = maximum possible size (ω)] that corresponds to the centre of the distribution of $\sum E^{\sigma^2}_{a_{ij}}$ across the domain of sizes (Eq. 4.6). This calculation mirrors the method of calculating generation time as the mean age of reproductive individuals in the population (Ebert, 1999).

$$\text{mean buffered size} = \frac{1}{\omega}\left[\frac{\sum_j \left[j \sum_i E^{\sigma^2}_{a_{ij}}\right]}{\sum E^{\sigma^2}_{a_{ij}}} - \alpha\right] \tag{4.6}$$

After calculating the mean buffered size for each species across the environmental autocorrelation – variance parameter space, we regressed mean buffered size against the environment components to test our hypothesis that environmental autocorrelation influences $\sum E^{\sigma^2}_{a_{ij}}$ via shifts in population structure (H2a).

4.4 Results

4.4.1 Testing H1: Environmental variance is the primary driver of demographic buffering

Here we tested the hypothesis that environmental autocorrelation and variance have negative effects on demographic buffering as quantified via $\sum E^{\sigma^2}_{a_{ij}}$ (H1). To do so, we ran simulations of the *Berberis thunbergii*, *Calathea crotalifera* and *Heliconia tortuosa* IPMs across the domain of autocorrelation and proportional variance values and calculated $\sum E^{\sigma^2}_{a_{ij}}$. We found environmental variance to be the primary driver of variance in $\sum E^{\sigma^2}_{a_{ij}}$ (Fig. 4.3). The summed contributions of proportional variance accounted for 94% of the variance of $\sum E^{\sigma^2}_{a_{ij}}$ in *B. thunbergii* ($R^2 = 0.99$, Table S1, Fig. 4.3a), 85% of the variance of $\sum E^{\sigma^2}_{a_{ij}}$ in *C. crotalifera* ($R^2 = 0.89$, Table S2, Fig. 4.3b) and 83% of the variance of $\sum E^{\sigma^2}_{a_{ij}}$ in *H. tortuosa* ($R^2 = 0.89$, Table S3, Fig. 4.3c). Supporting our hypothesis, environment variance had a negative effect on $\sum E^{\sigma^2}_{a_{ij}}$ (see models for *B. thunbergii*, *C. crotalifera*, and *H. tortuosa* in Tables S1-3). However, we did not find evidence for a negative effect of environmental autocorrelation on $\sum E^{\sigma^2}_{a_{ij}}$. Instead, all species were best modelled when the quadratic and cubic forms of autocorrelation were used as predictors of $\sum E^{\sigma^2}_{a_{ij}}$ without the inclusion of a linear effect of autocorrelation. This finding indicates the impact of autocorrelation on $\sum E^{\sigma^2}_{a_{ij}}$ is non-linear across the environmental autocorrelation and variance parameter space.

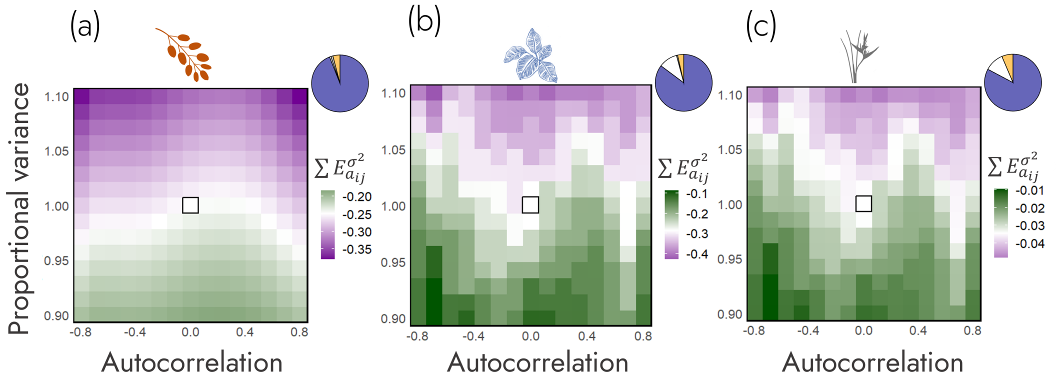

Figure 4.3: Environmental variance (σ^2) is the primary driver of demographic buffering. Across *Berberis thunbergii* (a), *Calathea crotalifera* (b) and *Heliconia tortuosa* (c), environmental variance (blue in pie-chart) explains the majority of variance in $\sum E^{\sigma^2}_{a_{ij}}$. Populations of all three species become relatively less buffered (lower values of $\sum E^{\sigma^2}_{a_{ij}}$, in purple) as proportional variance of environment components increase, whilst populations become relatively more buffered (higher values of $\sum E^{\sigma^2}_{a_{ij}}$, in green) as environmental variance decreases. This strong impact of proportional variance of environment components is summarized in the pie charts detailing the proportion of variance in $\sum E^{\sigma^2}_{a_{ij}}$ that can be explain by the environment components: environmental autocorrelation in orange, environmental variance in blue, environmental autocorrelation × variance interaction in grey (so small here it is not visible), and unexplained residuals in white. Since the pie charts are predominantly blue across all three species, variance in environment components is the primary driver of $\sum E^{\sigma^2}_{a_{ij}}$ across the environmental autocorrelation – variance parameter space.

4.4.2 Testing H2a: Temporal autocorrelation influences demographic buffering via population structure

We used two approaches to test the hypothesis that temporal autocorrelation influences demographic buffering via shifts in population structure (H2a). First, we used a measure of demographic buffering that accounts for population structure ($\sum E^{\sigma^2}_{a_{ij}}|\text{ASD}$) and regressed that against our normal measure of demographic buffering $\sum E^{\sigma^2}_{a_{ij}}$. Second, we measured the shifts in the distribution of buffering across the life history in response to environment components.

In our first approach, we regressed scaled values of $\sum E^{\sigma^2}_{a_{ij}}$ across all simulations against their respective $\sum E^{\sigma^2}_{a_{ij}}$ normalized by simulation specific stable size distribution ($\sum E^{\sigma^2}_{a_{ij}}|$ASD). Since both values are scaled to mean = 0 with standard deviation = 1, any deviation of $\sum E^{\sigma^2}_{a_{ij}}|\text{ASD} \sim \sum E^{\sigma^2}_{a_{ij}}$ from the 1-to-1 regression line indicates temporal shifts in population structure may impact demographic buffering. Interestingly, we found heterogeneity in the degree to which $\sum E^{\sigma^2}_{a_{ij}}|$ASD differed from $\sum E^{\sigma^2}_{a_{ij}}$ across species. Whilst *C. crotalifera* reported a 1-to-1 regression line between $\sum E^{\sigma^2}_{a_{ij}}|$ASD and $\sum E^{\sigma^2}_{a_{ij}}$ (R^2 = 1.000, Fig. 4.4d), *B. thunbergii* and *H. tortuosa* had residuals (*B. thunbergii*: R^2 = 0.9977, Fig. 4.4a; *H. tortuosa*: R^2 = 0.9995, Fig. 4.4g). These residuals indicate that population structure may influence $\sum E^{\sigma^2}_{a_{ij}}$, specifically in *B. thunbergii* and *H. tortuosa*.

To determine if environment autocorrelation is driving these residuals, we modelled the residuals of the $\sum E^{\sigma^2}_{a_{ij}}|\text{ASD} \sim \sum E^{\sigma^2}_{a_{ij}}$ regression against environmental autocorrelation and variance. Supporting our hypothesis (H2a), we found the residuals of the $\sum E^{\sigma^2}_{a_{ij}}|\text{ASD} \sim \sum E^{\sigma^2}_{a_{ij}}$ regression are mostly explained by environmental autocorrelation (Fig. 4.4b,e,h). In *B. thunbergii* and *H. tortuosa* (the species with the largest residuals from the $\sum E^{\sigma^2}_{a_{ij}}|\text{ASD} \sim \sum E^{\sigma^2}_{a_{ij}}$ regression), environmental autocorrelation accounted for 48% (R^2 = 0.56, Fig. 4.4b, Table S4) and 46% (R^2 = 0.84, Fig. 4.4h, Table S6) of the variance in residuals respectively; whilst environmental variance only accounted for 2% of the variance in residuals in both species. Regarding *C. crotalifera*, the largest contributor to variance in residuals was unexplained residual variance (56%, R^2 = 0.47, Fig. 4.4e, Table S5), followed by environmental autocorrelation (28%) and variance (16%).

In our second approach, we analysed the impact of environmental autocorrelation and variance on the distribution of demographic buffering across a life cycle. In turn, we calculated the centre of the distribution of demographic buffering across a life history: mean buffered size. Echoing the findings from the first line of enquiry, mean buffered size was best explained by changes in environmental autocorrelation – especially in *B. thunbergii* and *H. tortuosa*. Specifically, in *B. thunbergii*, 73% of the variance in mean buffered size was attributed to environmental autocorrelation whilst 17% was attributed to environmental variance ($R^2 = 0.91$, Fig. 4.4c, Table S7). Additionally, in *H. tortuosa*, 91% of the variance in mean buffered size was attributed to environmental autocorrelation with only 0.1% being attributed to changes in environment variance ($R^2 = 0.97$, Fig. 4.4i, Table S9). And finally, just as in the first line of enquiry, $\sum E_{a_{ij}}^{\sigma^2}$ in *C. crotalifera* is less exposed to impacts of shifts in population structure as the distribution of mean buffered size across the environmental autocorrelation – variance parameter space was mostly explained by residual variance (78%) rather than environmental autocorrelation (17%) or environmental variance (5%) ($R^2 = 0.26$, Fig. 4.4f, Table S8).

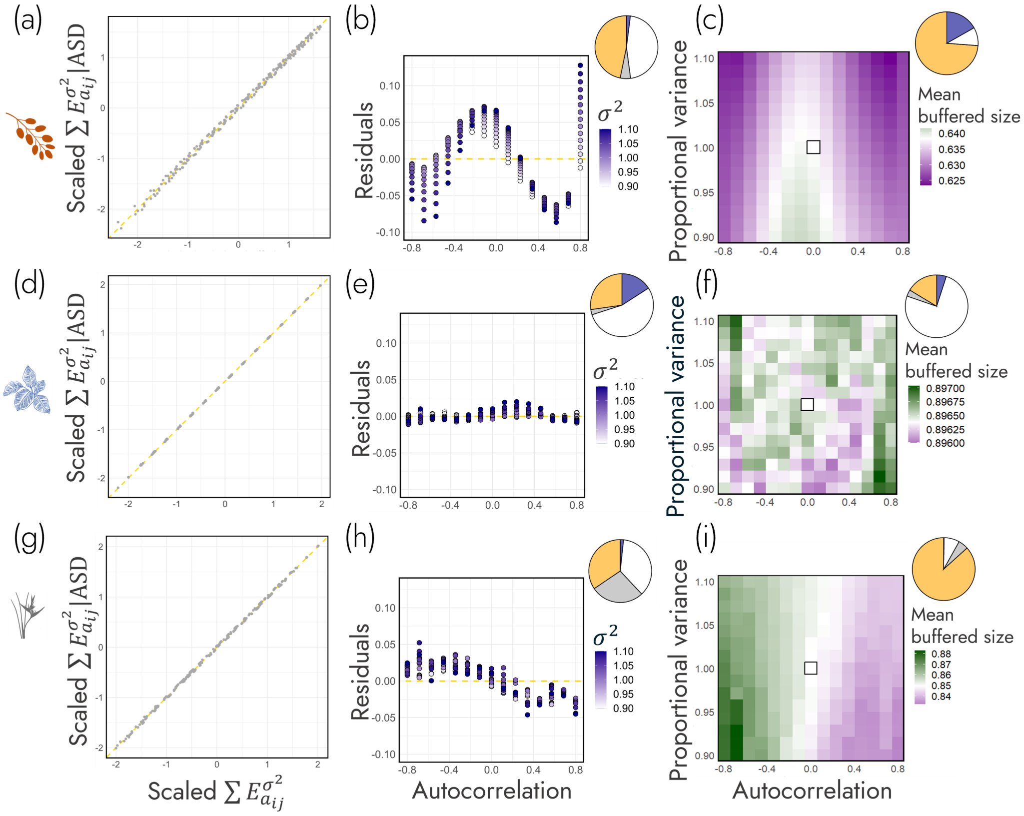

Figure 4.4: Environmental autocorrelation can influence demographic buffering ($\sum E_{a_{ij}}^{\sigma^2}$) via its impact on population structure. In addition, the degree to which environmental autocorrelation impacts $\sum E_{a_{ij}}^{\sigma^2}$ across *Berberis thunbergii* (a-c), *Calathea crotalifera* (d-f) and *Heliconia tortuosa* (g-i) is species-specific. The first column (a, d, g) shows the correlation between $\sum E_{a_{ij}}^{\sigma^2}$ and demographic buffering weighted by the average stage distribution ($\sum E_{a_{ij}}^{\sigma^2}$|ASD). Residuals from these regressions show the potential impact of population structure on $\sum E_{a_{ij}}^{\sigma^2}$. We then, in the second column (b, e, h), investigate these residuals as a function of the environmental autocorrelation (x-axis) and environmental variance (σ^2; purple). Lastly, in the third column (c, f, i), we quantify the impact of environmental autocorrelation and variance on the mean buffered size of the population. The pie charts at the top right-hand corner of panels in (b, e, h), and (c, f, i) detail the proportion of variance in the response variable that is explained by environmental autocorrelation (orange), environmental variance (blue), environmental autocorrelation × variance interaction (grey) and residuals (white). These pie charts show how environmental autocorrelation is the primary driver of shifts in $\sum E_{a_{ij}}^{\sigma^2}$ due to population.

4.4.3 Testing H2b: Demographic buffering is most sensitive to environmental variance's impact on rates of progression and fertility

To test the hypothesis that environmental variance impacts demographic buffering through vital rates (H2b), we ran the same perturbation analysis used to calculate $\sum E^{\sigma^2}_{a_{ij}}$ at the level of the sub-kernels: **P**-subkernel (survival-dependent changes in size) and the **F**-subkernel (fertility). By taking the difference of the subkernel elasticities of variance (*i.e.*, **P** – **F** contribution), we investigated (1) the role of underlying rates on demographic buffering and (2) the environment components that influence the **P** – **F** contribution across the environmental autocorrelation – variance parameter space.

First, we determined if the **P** – **F** contribution is a sufficient predictor of $\sum E^{\sigma^2}_{a_{ij}}$. The **P** – **F** contribution was highly predictive of $\sum E^{\sigma^2}_{a_{ij}}$ across all species (Fig. 4.5a). *B. thunbergii* had a negative relationship between **P** – **F** contribution and $\sum E^{\sigma^2}_{a_{ij}}$ ($r(223) = -0.968$, $p<0.001$), whilst *C. crotalifera* and *H. tortuosa* had positive relationships (*C. crotalifera*: $r(223) = 0.999$, $p<0.001$; *H. tortuosa*: $r(223) = 0.983$, $p<0.001$). These results indicate lower degrees of demographic buffering are associated with a greater impact of variance in rates of progression (*vs.* fertility) in *B. thunbergii*, but the opposite, a greater impact of variance in fertility (*vs.* progression) in *C. crotalifera* and *H. tortuosa*.

To test if variance in **P** – **F** contribution is most explained by environmental variance rather than autocorrelation (H2b), we regressed **P** – **F** contribution against the environment components. Across the three species, the **P** – **F** contribution was mostly explained by differences in degrees of environmental variance rather than autocorrelation across the environmental autocorrelation – variance parameter space (Fig.4.5b-d). Specifically, environmental variance explained 80%, 85% and 86% of the variance of **P** – **F** contribution in *B. thunbergii* ($R^2 = 0.99$, Fig. 4.5b, Table S10), *C. crotalifera* ($R^2 = 0.89$, Fig. 4.5c, Table S11) and *H. tortuosa* ($R^2 = 0.89$, Fig. 4.5d, Table S12), respectively. However, of the remaining variance, environmental autocorrelation explained 17%, 3% and 2% of the variance of **P** – **F** contribution, respectively.

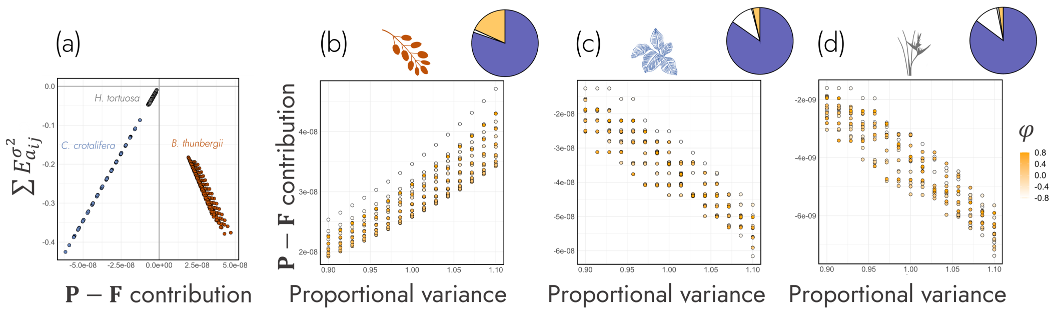

Figure 4.5: Environmental variance (σ^2) influences demographic buffering ($\sum E^{\sigma^2}_{a_{ij}}$) via the population's underlying demographic rates. (a) The relative contribution of progression (growth conditional on survival: **P**) and fertility (recruitment of new individuals from reproductive ones the previous year: **F**) on $\sum E^{\sigma^2}_{a_{ij}}$ (*i.e.*, **P**-**F** contribution). This approach was then applied to three plant species: (b) *Berberis thunbergii*, (c) *Calathea crotalifera*, and (d) *Heliconia tortuosa*). Dots are coloured by the degree of environmental autocorrelation (φ, yellow). The pie charts at the top right-hand corner of panels b-d detail the proportion of variance in **P**-**F** contribution that is explained by environmental autocorrelation (orange), environmental variance (blue), environmental autocorrelation × variance interaction (grey) and residuals (white). These pie charts show how environmental variance is the primary driver of shifts in the relative contributions of progression and fertility to $\sum E^{\sigma^2}_{a_{ij}}$.

4.5 Discussion

Environmental drivers and demographic mechanisms are key to quantify and predict a population's capacity for demographic buffering. Using three stochastic IPMs from the PADRINO database (Levin et al., 2022), we obtain partial support for the hypothesis that environmental autocorrelation and variance negatively impact a population's capacity to remain demographically buffered (H1). Interestingly, whilst environment variance negatively affects demographic buffering, there is a nonlinear effect of temporal autocorrelation on demographic buffering. Furthermore, even though environment autocorrelation and variance combine to make the environment time series, we show that their effects on demographic buffering are orthogonal dimensions of environmental stochasticity. Indeed, the effect of temporal autocorrelation on demographic buffering ($\sum E^{\sigma^2}_{a_{ij}}$) is mediated by population structure (H2a), whilst the effect of environmental variance on $\sum E^{\sigma^2}_{a_{ij}}$ is mediated by underlying demographic rates (H2b). Specifically, the influence of environmental variance on rates of progression *vs.* fertility is the greatest driver of differences in $\sum E^{\sigma^2}_{a_{ij}}$ across variable environments in the three examined species. This finding builds on multiple lines of evidence showing how different life histories can persist in variable environments via the differential variance of progression *vs.* fertility rates (Gaillard et al., 1998; Pfister, 1998).

Identifying the mechanisms that underpin the ability of natural populations to buffer against environmental stochasticity offers a powerful framework to explore a population's vulnerability to climate change. Current climatic forecasts predict changes in environmental stochasticity due to global climate change (Lewis & King, 2017; Masson-Delmotte et al., 2021; Shen et al., 2011). For example, periods of extreme variation in temperature and precipitation are expected to increase in the tropics and sub-tropics which host the highest biodiversity [temperature: Bathiany et al., 2018; precipitation: Trenberth, 2011]. Furthermore, extreme weather events are expected to become more common, leading to increased autocorrelation [*e.g.*, tropical cyclones: Knutson et al., 2010; fire frequency: Halofsky et al., 2020]. However, not all environmental components affect populations the same way (Hoffmann & Bridle, 2022; Vinton et al., 2022, 2023). The shape of demographic rates across a life history varies widely across the tree of life (Healy et al., 2019; Jones et al., 2014; Paniw et al., 2018; Salguero-Gómez et al., 2016b; Enríquez et al., 2022). Therefore, predicting the susceptibility of populations to environmental stochasticity, without a regard to the mechanism, overlooks key heterogeneity in the demographic processes necessary for accurate predictions. Our framework provides a promising avenue to incorporate this heterogeneity for informed analyses of the role of environmental stochasticity in a population's demographic buffering capacity.

Our results highlight an interesting, but often overlooked, role of population structure in demographic buffering. Whilst we find environment autocorrelation to primarily impact demographic buffering via shifts in population structure, there is also species-level heterogeneity in the strength and direction by which environment autocorrelation shifts population structure. Furthermore, our results indicate portions of the heterogeneity in $\sum E^{\sigma^2}_{a_{ij}}$ are explained by the interaction between environment autocorrelation and variance. One likely source of this heterogeneity is transient dynamics [*i.e.*, short-term, progressively weakening realizations of non-asymptotic population growth rate values resulting from a population not being at its stable-stage distribution (Stott et al., 2011)]. Whilst transient dynamics represent a suite of different stereotyped population dynamics (Capdevila et al., 2020b), only reactivity [the degree to which a population not at its stable-stage distribution increases/decreases relative to that same population projected from its stable-stage distribution (Neubert & Caswell, 1997)] has been linked to stochastic demography (McDonald et al., 2016). However, the link between reactivity, along with other transient dynamics, and demographic buffering remains unknown. Future work analysing which transient dynamics are increasing and decreasing levels of demographic buffering will finally integrate the analysis of transient dynamics with stochastic demography.

Historically, studies of life histories in stochastic environments have followed two branches: modelling and dimension reduction. Modelling life histories in stochastic environments, whereby analytic or numeric methods are used for demographic inference in individual populations, has progressively put to rest some key problems within life history theory [iteroparity: (Orzack & Tuljapurkar, 1989; Tuljapurkar et al., 2009a); diapause: (Tuljapurkar & Istock, 1993); migration: (Wiener & Tuljapurkar, 1994); biennialism: (Klinkhamer & Jong, 1983; Roerdink, 1988, 1989); homeostasis: (Orzack, 1985); lability: (Koons et al., 2009; Jongejans et al., 2010; Barraquand & Yoccoz, 2013); summarized in Caswell (2001)]. However, one of the limitations of a modelling approach is losing the realism captured within constraints, phylogenetic history or selection gradients that drive variance patterns in demographic rates.

From the empirical side, researchers have used dimension reduction techniques to unmask the patterns life histories exhibit in variable environments. Dimension reduction techniques, such as phylogenetically controlled principal component analyses (Revell, 2012), are especially useful as a life history is not a value nor an object; a life history strategy is an abstract concept that researchers probe with life history traits – such as: longevity, age at maturity, average body size, etc. To capture the signal of an individual life history strategy through the dimensionality, reducing the multidimensionality of life history metrics to its most important axes of variance (*i.e.*, principal components) has led to key discoveries (two-axes of life history variance: Salguero-Gómez et al., 2016b; Healy et al., 2019). Furthermore, this approach has been used to model life histories in stochastic environments (Paniw et al., 2018; Romeijn & Smallegange, 2022). However, this approach is limited to modelling only one component of a variable environment (*e.g.*, environmental autocorrelation or variance). This limitation is further emphasized by our results showing non-linearities between the effects of environment components on $\sum E^{\sigma^2}_{a_{ij}}$, thereby illustrating that the impact of an environment component on demographic process is context dependent.

Using our framework, researchers can stitch the modelling and dimension reduction approaches together. Our framework can be applied to any environmentally explicit structured population models: from physiologically structured population models (De Roos, 1997) to matrix population models (Caswell, 2001) to integral projection models (Easterling et al., 2000; Ellner et al., 2016), to dynamic energy budget models (Nisbet et al., 2000; Smallegange et al., 2017). By using open-access data [COMPADRE: (Salguero-Gómez et al., 2015); COMADRE: (Salguero-Gómez et al., 2016a); PADRINO: (Levin et al., 2022); AmP: (Marques et al., 2018)], researchers can explore the combined impact of autocorrelation and variance on $\sum E^{\sigma^2}_{a_{ij}}$ by interfacing the time series of a structured population models with stochastic matrices (Paniw et al. 2018). Once the landscape of $\sum E^{\sigma^2}_{a_{ij}}$ is mapped across environment autocorrelation and variance, the relative contributions of constraints, phylogeny and species-specific effects on $\sum E^{\sigma^2}_{a_{ij}}$ will be realized. This combined approach of modelling and dimension reduction offers generalization in a previously exception driven area of life history theory.

In conclusion, structure matters. Since Leslie (1945) and Lefkovitch (1965), demographers have explored how relatively simple structured population models can be used for biological inference. From transient dynamics (Capdevila et al., 2020b, 2022; Ezard et al., 2010; Hastings, 2001), to structured Lotka-Volterra models (De Roos, 2021; De Roos et al., 1990) to stability analysis (Cushing et al., 2003), researchers have generated a rich body of theory and evidence for the impact of population structure on demographic inferences. However, the impact of environmental structure, in the form of individual climate drivers (*e.g.*, temporal autocorrelation and variance), and their corresponding demographic mechanisms that mediate their effects are uncoupled. We argue they should be stitched together. Our framework exploring demographic buffering across the environmental autocorrelation – variance parameter space joins a recent push stitching the impacts of climate drivers (Vinton et al., 2022) with their respective demographic mechanisms (Le Coeur et al., 2022).

4.6 Acknowledgements

We thank Christina M. Hernández, for feedback on a previous version of this manuscript. M.K. was supported by a Marie Curie Fellowship (MSCA MaxPersist #101032484) hosted by R.S-G.; G.S.S. was supported by CNPq (#301343/2023-3); A.C was funded by the DFG (Deutsche Forschungsgemeinschaft #506492810). U.K.S was funded by the German Science Foundation (DFG Project #430170797). A.C.V. was supported by the National Science Foundation Postdoctoral Research Fellowship (#2010783) hosted by R.S-G. and I.S.; I.S. was supported by a Biotechnology and Biological Sciences Research Council (BBSRC) Fellowship (#BB/T008881/1), a Royal Society Dorothy Hodgkin Fellowship (#DHF/R1/211084), and a Wellcome Institutional Strategic Support Fund, University of Oxford (#BRR00060); R.S-G. was supported by a NERC Independent Research Fellowship (#NE/M018458/1).

4.7 Supplementary materials

4.7.1 Standardised analysis pipeline

To investigate the roles of environmental autocorrelation and variance on demographic buffering, we used a standardised analysis pipeline to reproducibly model the linear and non-linear impacts of environment components (*i.e.*, environmental autocorrelation and variance).

The standardised analysis pipeline has two phases. First, a suite of pre-defined statistical models were used to model the specified response variable (*e.g.*, **P**-**F** contribution). These models were classified as *a priori* (see below).

A priori models:

1. response variable ~ $\sigma^2 + \varphi + \sigma^2 \times \varphi$
2. response variable ~ $\sigma^2 + \varphi + \sigma^2 \times \varphi + \varphi^2$
3. response variable ~ $\sigma^2 + \varphi + \sigma^2 \times \varphi + \varphi^2 + \varphi^3$
4. response variable ~ $\sigma^2 + \varphi + \sigma^2 \times \varphi + \left(\sigma^2\right)^2$
5. response variable ~ $\sigma^2 + \varphi + \sigma^2 \times \varphi + \left(\sigma^2\right)^2 + \varphi^2$
6. response variable ~ $\sigma^2 + \varphi + \sigma^2 \times \varphi + \left(\sigma^2\right)^2 + \varphi^2 + \varphi^3$
7. response variable ~ $\sigma^2 + \varphi + \sigma^2 \times \varphi + \left(\sigma^2\right)^2 + \left(\sigma^2\right)^3$
8. response variable ~ $\sigma^2 + \varphi + \sigma^2 \times \varphi + \left(\sigma^2\right)^2 + \left(\sigma^2\right)^3 + \varphi^2$
9. response variable ~ $\sigma^2 + \varphi + \sigma^2 \times \varphi + \left(\sigma^2\right)^2 + \left(\sigma^2\right)^3 + \varphi^2 + \varphi^3$

We chose this list of statistical models as they (1) contain linear and linear-interaction terms of environmental autocorrelation (φ) and environmental variance (σ^2) (see the first three terms of each model), (2) they sequentially add combinations of environment autocorrelation and variance up to a cubic term and (3) simplifies the combination of possible models generate from 7 predictors (127 possible combinations).

After identifying the statistical model with the lowest AIC out of all of the *a priori* models, the model with the lowest AIC was passed through an ANOVA to estimate the significance of each of the predictors (α=0.05). If all of the predictors were significant (p<0.05), the *a priori* model with the lowest AIC was chosen[3]. However, if one or more of the predictors were not significant, further statistical models were constructed in the second phase of the pipeline.

In the second phase, all possible versions of the model selected in the first phase were constructed with the insignificant predictors knocked. For example, if *a priori* model 5 had the lowest AIC, but ($\sigma^2 \times \varphi$) and (φ^2) were insignificant, the following 3 post-hoc models would be constructed:

10. response variable $\sim \sigma^2 + \varphi + \left(\sigma^2\right)^2 + \varphi^2 \quad \left[\text{knock out } \sigma^2 \times \varphi\right]$
11. response variable $\sim \sigma^2 + \varphi + \sigma^2 \times \varphi + \left(\sigma^2\right)^2 \quad \left[\text{knock out } \varphi^2\right]$
12. response variable $\sim \sigma^2 + \varphi + \left(\sigma^2\right)^2 \quad \left[\text{knock out } \sigma^2 \times \varphi \text{ and } \varphi^2\right]$

After constructing the *post-hoc* models, AIC values were calculated and the model with the lowest AIC was selected.

---

[3] Here we are using p-values as a method to identify the impact of individual variables in the selected regressions and to potentially inform simpler models in the second phase. In turn, the selected regression after the first and second phases is solely due to AIC criterion – p-values are solely used to generate potentially simpler models for further AIC comparison.

4.7.2 Supplementary tables

Supplementary Table 1. Model selection to quantify the effects of environmental autocorrelation and variance on demographic buffering (DB) in *Berberis thunbergii*. This model selection corresponds to the data show in Figure 4.3a in the main text. Environmental autocorrelation is denoted as φ whilst environmental variance is denoted as σ^2.

Model type	Model number	Model	DF	AIC	Initial selection	Final selection
A priori	1	$DB \sim \sigma^2 + \varphi + \sigma^2 * \varphi$	5	-1333.377		
	2	$DB \sim \sigma^2 + \varphi + \sigma^2 * \varphi + \varphi^2$	6	-1566.159		
	3	$DB \sim \sigma^2 + \varphi + \sigma^2 * \varphi + \varphi^2 + \varphi^3$	7	-1681.584		
	4	$DB \sim \sigma^2 + \varphi + \sigma^2 * \varphi + (\sigma^2)^2$	6	-1349.455		
	5	$DB \sim \sigma^2 + \varphi + \sigma^2 * \varphi + (\sigma^2)^2 + \varphi^2$	7	-1619.828		
	6	$DB \sim \sigma^2 + \varphi + \sigma^2 * \varphi + (\sigma^2)^2 + \varphi^2 + \varphi^3$	8	-1783.319	**SELECTED**	
	7	$DB \sim \sigma^2 + \varphi + \sigma^2 * \varphi + (\sigma^2)^2 + (\sigma^2)^3$	7	-1347.510		
	8	$DB \sim \sigma^2 + \varphi + \sigma^2 * \varphi + (\sigma^2)^2 + (\sigma^2)^3 + \varphi^2$	8	-1618.012		
	9	$DB \sim \sigma^2 + \varphi + \sigma^2 * \varphi + (\sigma^2)^2 + (\sigma^2)^3 + \varphi^2 + \varphi^3$	9	-1781.704		
Post hoc	10	$DB \sim \sigma^2 + \sigma^2 * \varphi + (\sigma^2)^2 + \varphi^2 + \varphi^3$	7	-1785.317		**SELECTED**
Complete formula		$DB \sim -0.48626 + 1.242738 * [\sigma^2] + 0.026047 * [\sigma^2 * \varphi] - 1.003697 * [(\sigma^2)^2] - 0.045427 * [\varphi^2] - 0.050135 * [\varphi^3]$				

Supplementary Table 2. Model selection to quantify the effects of environmental autocorrelation and variance on demographic buffering (DB) in *Calathea crotalifera*. This model selection corresponds to the data show in Figure 4.3b in the main text. Environmental autocorrelation is denoted as φ whilst environmental variance is denoted as σ^2.

Model type	Model number	Model	DF	AIC	Initial selection	Final selection
A priori	1	$DB \sim \sigma^2 + \varphi + \sigma^2 * \varphi$	5	-925.2545		
	2	$DB \sim \sigma^2 + \varphi + \sigma^2 * \varphi + \varphi^2$	6	-953.4019		
	3	$DB \sim \sigma^2 + \varphi + \sigma^2 * \varphi + \varphi^2 + \varphi^3$	7	-980.3957		
	4	$DB \sim \sigma^2 + \varphi + \sigma^2 * \varphi + (\sigma^2)^2$	6	-927.4461		
	5	$DB \sim \sigma^2 + \varphi + \sigma^2 * \varphi + (\sigma^2)^2 + \varphi^2$	7	-956.2009		
	6	$DB \sim \sigma^2 + \varphi + \sigma^2 * \varphi + (\sigma^2)^2 + \varphi^2 + \varphi^3$	8	-983.8628	SELECTED	
	7	$DB \sim \sigma^2 + \varphi + \sigma^2 * \varphi + (\sigma^2)^2 + (\sigma^2)^3$	7	-925.4511		
	8	$DB \sim \sigma^2 + \varphi + \sigma^2 * \varphi + (\sigma^2)^2 + (\sigma^2)^3 + \varphi^2$	8	-954.2067		
	9	$DB \sim \sigma^2 + \varphi + \sigma^2 * \varphi + (\sigma^2)^2 + (\sigma^2)^3 + \varphi^2 + \varphi^3$	9	-981.8694		
Post hoc	10	$DB \sim \sigma^2 + \sigma^2 * \varphi + (\sigma^2)^2 + \varphi^2 + \varphi^3$	7	-985.6362		
	11	$DB \sim \varphi + \sigma^2 * \varphi + (\sigma^2)^2 + \varphi^2 + \varphi^3$	7	-984.4633		
	12	$DB \sim \sigma^2 + \varphi + (\sigma^2)^2 + \varphi^2 + \varphi^3$	7	-984.7991		
	13	$DB \sim \sigma^2 * \varphi + (\sigma^2)^2 + \varphi^2 + \varphi^3$	6	-986.2380		SELECTED
	14	$DB \sim \sigma^2 + (\sigma^2)^2 + \varphi^2 + \varphi^3$	6	-974.8492		
	15	$DB \sim \varphi + (\sigma^2)^2 + \varphi^2 + \varphi^3$	6	-985.4061		
	16	$DB \sim (\sigma^2)^2 + \varphi^2 + \varphi^3$	5	-975.5280		
Complete formula		$DB \sim 0.347261 + 0.032254 * [\sigma^2 * \varphi] - 0.603492 * [(\sigma^2)^2] + 0.049503 * [\varphi^2] - 0.108026 * [\varphi^3]$				

Supplementary Table 3. Model selection to quantify the effects of environmental autocorrelation and variance on demographic buffering (DB) in *Heliconia tortuosa*. This model selection corresponds to the data show in Figure 4.3c in the main text. Environmental autocorrelation is denoted as φ whilst environmental variance is denoted as σ^2.

Model type	Model number	Model	DF	AIC	Initial selection	Final selection
A priori	1	$DB \sim \sigma^2 + \varphi + \sigma^2 * \varphi$	5	-1891.832		
	2	$DB \sim \sigma^2 + \varphi + \sigma^2 * \varphi + \varphi^2$	6	-1913.937		
	3	$DB \sim \sigma^2 + \varphi + \sigma^2 * \varphi + \varphi^2 + \varphi^3$	7	-1930.921		
	4	$DB \sim \sigma^2 + \varphi + \sigma^2 * \varphi + (\sigma^2)^2$	6	-1895.561		
	5	$DB \sim \sigma^2 + \varphi + \sigma^2 * \varphi + (\sigma^2)^2 + \varphi^2$	7	-1918.323		
	6	$DB \sim \sigma^2 + \varphi + \sigma^2 * \varphi + (\sigma^2)^2 + \varphi^2 + \varphi^3$	8	-1935.878	**SELECTED**	
	7	$DB \sim \sigma^2 + \varphi + \sigma^2 * \varphi + (\sigma^2)^2 + (\sigma^2)^3$	7	-1893.568		
	8	$DB \sim \sigma^2 + \varphi + \sigma^2 * \varphi + (\sigma^2)^2 + (\sigma^2)^3 + \varphi^2$	8	-1916.330		
	9	$DB \sim \sigma^2 + \varphi + \sigma^2 * \varphi + (\sigma^2)^2 + (\sigma^2)^3 + \varphi^2 + \varphi^3$	9	-1933.886		
Post hoc	10	$DB \sim \sigma^2 + \sigma^2 * \varphi + (\sigma^2)^2 + \varphi^2 + \varphi^3$	7	-1937.869		
	11	$DB \sim \varphi + \sigma^2 * \varphi + (\sigma^2)^2 + \varphi^2 + \varphi^3$	7	-1935.573		
	12	$DB \sim \sigma^2 + \varphi + (\sigma^2)^2 + \varphi^2 + \varphi^3$	7	-1937.878		
	13	$DB \sim \sigma^2 * \varphi + (\sigma^2)^2 + \varphi^2 + \varphi^3$	6	-1937.564		
	14	$DB \sim \sigma^2 + (\sigma^2)^2 + \varphi^2 + \varphi^3$	6	-1939.586		**SELECTED**
	15	$DB \sim \varphi + (\sigma^2)^2 + \varphi^2 + \varphi^3$	6	-1937.573		
	16	$DB \sim (\sigma^2)^2 + \varphi^2 + \varphi^3$	5	-1939.284		
Complete formula		$DB \sim -0.0534906 + 0.1897105 * [\sigma^2] - 0.1655802 * [(\sigma^2)^2] + 0.0052008 * [\varphi^2] - 0.0091953 * [\varphi^3]$				

Supplementary Table 4. Model selection to quantify the effects of environmental autocorrelation and variance on the residuals of $\sum E_{a_{ij}}^{\sigma^2}$ and $\sum E_{a_{ij}}^{\sigma^2}$|ASD in *Berberis thunbergii*. This model selection corresponds to the data show in Figure 4.4b in the main text. Environmental autocorrelation is denoted as φ whilst environmental variance is denoted as σ^2.

Model type	Model number	Model	DF	AIC	Initial selection	Final selection
A priori	1	$residuals \sim \sigma^2 + \varphi + \sigma^2 * \varphi$	5	-741.7773		
	2	$residuals \sim \sigma^2 + \varphi + \sigma^2 * \varphi + \varphi^2$	6	-769.6791		
	3	$residuals \sim \sigma^2 + \varphi + \sigma^2 * \varphi + \varphi^2 + \varphi^3$	7	-890.4373		
	4	$residuals \sim \sigma^2 + \varphi + \sigma^2 * \varphi + (\sigma^2)^2$	6	-744.6596		
	5	$residuals \sim \sigma^2 + \varphi + \sigma^2 * \varphi + (\sigma^2)^2 + \varphi^2$	7	-773.2640		
	6	$residuals \sim \sigma^2 + \varphi + \sigma^2 * \varphi + (\sigma^2)^2 + \varphi^2 + \varphi^3$	8	-898.1634	**SELECTED**	**SELECTED***
	7	$residuals \sim \sigma^2 + \varphi + \sigma^2 * \varphi + (\sigma^2)^2 + (\sigma^2)^3$	7	-742.7117		
	8	$residuals \sim \sigma^2 + \varphi + \sigma^2 * \varphi + (\sigma^2)^2 + (\sigma^2)^3 + \varphi^2$	8	-771.3237		
	9	$residuals \sim \sigma^2 + \varphi + \sigma^2 * \varphi + (\sigma^2)^2 + (\sigma^2)^3 + \varphi^2 + \varphi^3$	9	-896.2684		
Complete formula		$residuals \sim -1.969071 + 3.965287 * [\sigma^2] - 0.512308 * [\varphi] + 0.364988 * [\sigma^2 * \varphi] - 1.970633 * [(\sigma^2)^2] - 0.074138 * [\varphi^2] + 0.299437 * [\varphi^3]$				

*Since all parameters were deemed significant (α<0.05), no *post hoc* selection was performed.

Supplementary Table 5. Model selection to quantify the effects of environmental autocorrelation and variance on the residuals of $\sum E_{a_{ij}}^{\sigma^2}$ and $\sum E_{a_{ij}}^{\sigma^2}$|ASD in *Calathea crotalifera*. This model selection corresponds to the data show in Figure 4.4e in the main text. Environmental autocorrelation is denoted as φ whilst environmental variance is denoted as σ^2.

Model type	Model number	Model	DF	AIC	Initial selection	Final selection
A priori	1	$residuals \sim \sigma^2 + \varphi + \sigma^2 * \varphi$	5	-1718.857		
	2	$residuals \sim \sigma^2 + \varphi + \sigma^2 * \varphi + \varphi^2$	6	-1756.217		
	3	$residuals \sim \sigma^2 + \varphi + \sigma^2 * \varphi + \varphi^2 + \varphi^3$	7	-1784.586		
	4	$residuals \sim \sigma^2 + \varphi + \sigma^2 * \varphi + (\sigma^2)^2$	6	-1759.530		
	5	$residuals \sim \sigma^2 + \varphi + \sigma^2 * \varphi + (\sigma^2)^2 + \varphi^2$	7	-1806.057		
	6	$residuals \sim \sigma^2 + \varphi + \sigma^2 * \varphi + (\sigma^2)^2 + \varphi^2 + \varphi^3$	8	-1843.012	**SELECTED**	**SELECTED***
	7	$residuals \sim \sigma^2 + \varphi + \sigma^2 * \varphi + (\sigma^2)^2 + (\sigma^2)^3$	7	-1757.962		
	8	$residuals \sim \sigma^2 + \varphi + \sigma^2 * \varphi + (\sigma^2)^2 + (\sigma^2)^3 + \varphi^2$	8	-1804.593		
	9	$residuals \sim \sigma^2 + \varphi + \sigma^2 * \varphi + (\sigma^2)^2 + (\sigma^2)^3 + \varphi^2 + \varphi^3$	9	-1841.650		
Complete formula	$residuals \sim 0.638800 - 1.276380 * [\sigma^2] - 0.019216 * [\varphi] + 0.029041 * [\sigma^2 * \varphi] + 0.637492 * [(\sigma^2)^2] - 0.009601 * [\varphi^2] - 0.018321 * [\varphi^3]$					

*Since all parameters were deemed significant (α<0.05), no *post hoc* selection was performed.

Supplementary Table 6. Model selection to quantify the effects of environmental autocorrelation and variance on the residuals of $\sum E_{a_{ij}}^{\sigma^2}$ and $\sum E_{a_{ij}}^{\sigma^2}|\text{ASD}$ in *Heliconia tortuosa*. This model selection corresponds to the data show in Figure 4.4h in the main text. Environmental autocorrelation is denoted as φ whilst environmental variance is denoted as σ^2.

Model type	Model number	Model	DF	AIC	Initial selection	Final selection
A priori	1	$residuals \sim \sigma^2 + \varphi + \sigma^2 * \varphi$	5	-1380.828		
	2	$residuals \sim \sigma^2 + \varphi + \sigma^2 * \varphi + \varphi^2$	6	-1386.508		
	3	$residuals \sim \sigma^2 + \varphi + \sigma^2 * \varphi + \varphi^2 + \varphi^3$	7	-1473.794		
	4	$residuals \sim \sigma^2 + \varphi + \sigma^2 * \varphi + (\sigma^2)^2$	6	-1392.269		
	5	$residuals \sim \sigma^2 + \varphi + \sigma^2 * \varphi + (\sigma^2)^2 + \varphi^2$	7	-1398.431		
	6	$residuals \sim \sigma^2 + \varphi + \sigma^2 * \varphi + (\sigma^2)^2 + \varphi^2 + \varphi^3$	8	-1492.824	**SELECTED**	
	7	$residuals \sim \sigma^2 + \varphi + \sigma^2 * \varphi + (\sigma^2)^2 + (\sigma^2)^3$	7	-1391.522		
	8	$residuals \sim \sigma^2 + \varphi + \sigma^2 * \varphi + (\sigma^2)^2 + (\sigma^2)^3 + \varphi^2$	8	-1397.730		
	9	$residuals \sim \sigma^2 + \varphi + \sigma^2 * \varphi + (\sigma^2)^2 + (\sigma^2)^3 + \varphi^2 + \varphi^3$	9	-1492.822		
Post hoc	10	$residuals \sim \sigma^2 + \sigma^2 * \varphi + (\sigma^2)^2 + \varphi^2 + \varphi^3$	7	-1493.981		**SELECTED**

Complete formula

$$residuals \sim -0.804339 + 1.592423 * [\sigma^2] - 0.065901 * [\sigma^2 * \varphi] - 0.782833 * [(\sigma^2)^2] - 0.009305 * [\varphi^2] + 0.066305 * [\varphi^3]$$

Supplementary Table 7. Model selection to quantify the effects of environmental autocorrelation and variance on the mean buffered size in *Berberis thunbergii*. This model selection corresponds to the data show in Figure 4.4c in the main text. Environmental autocorrelation is denoted as φ whilst environmental variance is denoted as σ^2.

Model type	Model number	Model	DF	AIC	Initial selection	Final selection
A priori	1	$mean\ buffered\ size{\sim}\sigma^2 + \varphi + \sigma^2 * \varphi$	5	-1808.928		
	2	$mean\ buffered\ size{\sim}\sigma^2 + \varphi + \sigma^2 * \varphi + \varphi^2$	6	-2170.820		
	3	$mean\ buffered\ size{\sim}\sigma^2 + \varphi + \sigma^2 * \varphi + \varphi^2 + \varphi^3$	7	-2291.923	**SELECTED**	**SELECTED**
	4	$mean\ buffered\ size{\sim}\sigma^2 + \varphi + \sigma^2 * \varphi + (\sigma^2)^2$	6	-1807.061		
	5	$mean\ buffered\ size{\sim}\sigma^2 + \varphi + \sigma^2 * \varphi + (\sigma^2)^2 + \varphi^2$	7	-2169.493		
	6	$mean\ buffered\ size{\sim}\sigma^2 + \varphi + \sigma^2 * \varphi + (\sigma^2)^2 + \varphi^2 + \varphi^3$	8	-2291.086		
	7	$mean\ buffered\ size{\sim}\sigma^2 + \varphi + \sigma^2 * \varphi + (\sigma^2)^2 + (\sigma^2)^3$	7	-1805.061		
	8	$mean\ buffered\ size{\sim}\sigma^2 + \varphi + \sigma^2 * \varphi + (\sigma^2)^2 + (\sigma^2)^3 + \varphi^2$	8	-2167.493		
	9	$mean\ buffered\ size{\sim}\sigma^2 + \varphi + \sigma^2 * \varphi + (\sigma^2)^2 + (\sigma^2)^3 + \varphi^2 + \varphi^3$	9	-2289.087		
Post hoc	10	$mean\ buffered\ size{\sim}\sigma^2 + \sigma^2 * \varphi + \varphi^2 + \varphi^3$	8	-2288.461		
	11	$mean\ buffered\ size{\sim}\sigma^2 + \varphi + \varphi^2 + \varphi^3$	8	-2290.699		
	12	$mean\ buffered\ size{\sim}\sigma^2 + \varphi^2 + \varphi^3$	7	-2144.997		
Complete formula		$mean\ buffered\ size{\sim}0.6679336 - 0.0313268 * [\sigma^2] - 0.0051673 * [\varphi] - 0.0019560 * [\sigma^2 * \varphi] - 0.0175639 * [\varphi^2] + 0.0133206 * [\varphi^3]$				

Supplementary Table 8. Model selection to quantify the effects of environmental autocorrelation and variance on the mean buffered size in *Calathea crotalifera*. This model selection corresponds to the data show in Figure 4.4f in the main text. Environmental autocorrelation is denoted as φ whilst environmental variance is denoted as σ^2.

Model type	Model number	Model	DF	AIC	Initial selection	Final selection
A priori	1	$mean\ buffered\ size \sim \sigma^2 + \varphi + \sigma^2 * \varphi$	5	-3226.940		
	2	$mean\ buffered\ size \sim \sigma^2 + \varphi + \sigma^2 * \varphi + \varphi^2$	6	-3241.007		
	3	$mean\ buffered\ size \sim \sigma^2 + \varphi + \sigma^2 * \varphi + \varphi^2 + \varphi^3$	7	-3261.367	**SELECTED**	**SELECTED**
	4	$mean\ buffered\ size \sim \sigma^2 + \varphi + \sigma^2 * \varphi + (\sigma^2)^2$	6	-3225.148		
	5	$mean\ buffered\ size \sim \sigma^2 + \varphi + \sigma^2 * \varphi + (\sigma^2)^2 + \varphi^2$	7	-3239.230		
	6	$mean\ buffered\ size \sim \sigma^2 + \varphi + \sigma^2 * \varphi + (\sigma^2)^2 + \varphi^2 + \varphi^3$	8	-3259.614		
	7	$mean\ buffered\ size \sim \sigma^2 + \varphi + \sigma^2 * \varphi + (\sigma^2)^2 + (\sigma^2)^3$	7	-3223.159		
	8	$mean\ buffered\ size \sim \sigma^2 + \varphi + \sigma^2 * \varphi + (\sigma^2)^2 + (\sigma^2)^3 + \varphi^2$	8	-3237.243		
	9	$mean\ buffered\ size \sim \sigma^2 + \varphi + \sigma^2 * \varphi + (\sigma^2)^2 + (\sigma^2)^3 + \varphi^2 + \varphi^3$	9	-3257.628		
Post hoc	10	$mean\ buffered\ size \sim \sigma^2 + \sigma^2 * \varphi + \varphi^2 + \varphi^3$	8	-3252.451		
	11	$mean\ buffered\ size \sim \sigma^2 + \varphi + \varphi^2 + \varphi^3$	8	-3249.336		
	12	$mean\ buffered\ size \sim \sigma^2 + \varphi^2 + \varphi^3$	7	-3241.391		
Complete formula		$mean\ buffered\ size \sim 0.8956762 + 0.0007139 * [\sigma^2] + 0.0009980 * [\varphi] - 0.0011847 * [\sigma^2 * \varphi] + 0.0002204 * [\varphi^2] + 0.0005852 * [\varphi^3]$				

Supplementary Table 9. Model selection to quantify the effects of environmental autocorrelation and variance on the mean buffered size in *Heliconia tortuosa*. This model selection corresponds to the data show in Figure 4.4i in the main text. Environmental autocorrelation is denoted as φ whilst environmental variance is denoted as σ^2.

Model type	Model number	Model	DF	AIC	Initial selection	Final selection
A priori	1	$mean\ buffered\ size{\sim}\sigma^2 + \varphi + \sigma^2 * \varphi$	5	-1971.458		
	2	$mean\ buffered\ size{\sim}\sigma^2 + \varphi + \sigma^2 * \varphi + \varphi^2$	6	-2090.884		
	3	$mean\ buffered\ size{\sim}\sigma^2 + \varphi + \sigma^2 * \varphi + \varphi^2 + \varphi^3$	7	-2119.626	**SELECTED**	**SELECTED***
	4	$mean\ buffered\ size{\sim}\sigma^2 + \varphi + \sigma^2 * \varphi + (\sigma^2)^2$	6	-1970.073		
	5	$mean\ buffered\ size{\sim}\sigma^2 + \varphi + \sigma^2 * \varphi + (\sigma^2)^2 + \varphi^2$	7	-2089.940		
	6	$mean\ buffered\ size{\sim}\sigma^2 + \varphi + \sigma^2 * \varphi + (\sigma^2)^2 + \varphi^2 + \varphi^3$	8	-2118.838		
	7	$mean\ buffered\ size{\sim}\sigma^2 + \varphi + \sigma^2 * \varphi + (\sigma^2)^2 + (\sigma^2)^3$	7	-1968.075		
	8	$mean\ buffered\ size{\sim}\sigma^2 + \varphi + \sigma^2 * \varphi + (\sigma^2)^2 + (\sigma^2)^3 + \varphi^2$	8	-2087.944		
	9	$mean\ buffered\ size{\sim}\sigma^2 + \varphi + \sigma^2 * \varphi + (\sigma^2)^2 + (\sigma^2)^3 + \varphi^2 + \varphi^3$	9	-2116.842		
Complete formula		$mean\ buffered\ size{\sim}0.8411429 + 0.0082338 * [\sigma^2] - 0.1178307 * [\varphi] + 0.0912694 * [\sigma^2 * \varphi] + 0.0088286 * [\varphi^2] + 0.0087587 * [\varphi^3]$				

*Since all parameters were deemed significant (α<0.05), no *post hoc* selection was performed.

Supplementary Table 10. Model selection to quantify the effects of environmental autocorrelation and variance on the **P-F** contribution in *Berberis thunbergii*. This model selection corresponds to the data show in Figure 4.5b in the main text. Environmental autocorrelation is denoted as φ whilst environmental variance is denoted as σ^2.

Model type	Model number	Model	DF	AIC	Initial selection	Final selection
A priori	1	$\mathbf{P-F}\ contribution \sim \sigma^2 + \varphi + \sigma^2 * \varphi$	5	-8282.140		
	2	$\mathbf{P-F}\ contribution \sim \sigma^2 + \varphi + \sigma^2 * \varphi + \varphi^2$	6	-8747.482		
	3	$\mathbf{P-F}\ contribution \sim \sigma^2 + \varphi + \sigma^2 * \varphi + \varphi^2 + \varphi^3$	7	-8783.395		
	4	$\mathbf{P-F}\ contribution \sim \sigma^2 + \varphi + \sigma^2 * \varphi + (\sigma^2)^2$	6	-8286.741		
	5	$\mathbf{P-F}\ contribution \sim \sigma^2 + \varphi + \sigma^2 * \varphi + (\sigma^2)^2 + \varphi^2$	7	-8804.515		
	6	$\mathbf{P-F}\ contribution \sim \sigma^2 + \varphi + \sigma^2 * \varphi + (\sigma^2)^2 + \varphi^2 + \varphi^3$	8	-8853.171	**SELECTED**	
	7	$\mathbf{P-F}\ contribution \sim \sigma^2 + \varphi + \sigma^2 * \varphi + (\sigma^2)^2 + (\sigma^2)^3$	7	-8284.763		
	8	$\mathbf{P-F}\ contribution \sim \sigma^2 + \varphi + \sigma^2 * \varphi + (\sigma^2)^2 + (\sigma^2)^3 + \varphi^2$	8	-8802.731		
	9	$\mathbf{P-F}\ contribution \sim \sigma^2 + \varphi + \sigma^2 * \varphi + (\sigma^2)^2 + (\sigma^2)^3 + \varphi^2 + \varphi^3$	9	-8851.442		
Post hoc	10	$\mathbf{P-F}\ contribution \sim \sigma^2 + \sigma^2 * \varphi + (\sigma^2)^2 + \varphi^2 + \varphi^3$	7	-8853.432		**SELECTED**
Complete formula		$\mathbf{P-F}\ contribution \sim [5.943e-08] - [1.541e-07] * [\sigma^2] - [4.113e-09] * [\sigma^2 * \varphi] + [1.208e-07] * [(\sigma^2)^2] + [1.038e-08] * [\varphi^2] + [3.724e-09] * [\varphi^3]$				

Supplementary Table 11. Model selection to quantify the effects of environmental autocorrelation and variance on the **P-F** contribution in *Calathea crotalifera*. This model selection corresponds to the data show in Figure 4.5c in the main text. Environmental autocorrelation is denoted as φ whilst environmental variance is denoted as σ^2.

Model type	Model number	Model	DF	AIC	Initial selection	Final selection
A priori	1	$\mathbf{P-F}\ \mathit{contribution} \sim \sigma^2 + \varphi + \sigma^2 * \varphi$	5	-8011.995		
	2	$\mathbf{P-F}\ \mathit{contribution} \sim \sigma^2 + \varphi + \sigma^2 * \varphi + \varphi^2$	6	-8040.051		
	3	$\mathbf{P-F}\ \mathit{contribution} \sim \sigma^2 + \varphi + \sigma^2 * \varphi + \varphi^2 + \varphi^3$	7	-8067.034		
	4	$\mathbf{P-F}\ \mathit{contribution} \sim \sigma^2 + \varphi + \sigma^2 * \varphi + (\sigma^2)^2$	6	-8014.190		
	5	$\mathbf{P-F}\ \mathit{contribution} \sim \sigma^2 + \varphi + \sigma^2 * \varphi + (\sigma^2)^2 + \varphi^2$	7	-8042.851		
	6	$\mathbf{P-F}\ \mathit{contribution} \sim \sigma^2 + \varphi + \sigma^2 * \varphi + (\sigma^2)^2 + \varphi^2 + \varphi^3$	8	-8070.503	**SELECTED**	
	7	$\mathbf{P-F}\ \mathit{contribution} \sim \sigma^2 + \varphi + \sigma^2 * \varphi + (\sigma^2)^2 + (\sigma^2)^3$	7	-8012.195		
	8	$\mathbf{P-F}\ \mathit{contribution} \sim \sigma^2 + \varphi + \sigma^2 * \varphi + (\sigma^2)^2 + (\sigma^2)^3 + \varphi^2$	8	-8040.857		
	9	$\mathbf{P-F}\ \mathit{contribution} \sim \sigma^2 + \varphi + \sigma^2 * \varphi + (\sigma^2)^2 + (\sigma^2)^3 + \varphi^2 + \varphi^3$	9	-8068.509		
Post hoc	10	$\mathbf{P-F}\ \mathit{contribution} \sim \sigma^2 + \sigma^2 * \varphi + (\sigma^2)^2 + \varphi^2 + \varphi^3$	7	-8072.276		
	11	$\mathbf{P-F}\ \mathit{contribution} \sim \varphi + \sigma^2 * \varphi + (\sigma^2)^2 + \varphi^2 + \varphi^3$	7	-8071.103		
	12	$\mathbf{P-F}\ \mathit{contribution} \sim \sigma^2 + \varphi + (\sigma^2)^2 + \varphi^2 + \varphi^3$	7	-8071.438		
	13	$\mathbf{P-F}\ \mathit{contribution} \sim \varphi + (\sigma^2)^2 + \varphi^2 + \varphi^3$	6	-8072.045		
	14	$\mathbf{P-F}\ \mathit{contribution} \sim \sigma^2 + (\sigma^2)^2 + \varphi^2 + \varphi^3$	6	-8061.454		
	15	$\mathbf{P-F}\ \mathit{contribution} \sim \sigma^2 * \varphi + (\sigma^2)^2 + \varphi^2 + \varphi^3$	6	-8072.878		**SELECTED**
	16	$\mathbf{P-F}\ \mathit{contribution} \sim (\sigma^2)^2 + \varphi^2 + \varphi^3$	5	-8062.133		
Complete formula		$\mathbf{P-F}\ \mathit{contribution} \sim [5.029e-08] - [8.739e-08] * [(\sigma^2)^2] + 4.676e-09 * [\sigma^2 * \varphi] + [7.155e-09] * [\varphi^2] - [1.564e-08] * [\varphi^3]$				

Supplementary Table 12. Model selection to quantify the effects of environmental autocorrelation and variance on the **P-F** contribution in *Heliconia tortuosa*. This model selection corresponds to the data show in Figure 4.5d in the main text. Environmental autocorrelation is denoted as φ whilst environmental variance is denoted as σ^2.

Model type	Model number	Model	DF	AIC	Initial selection	Final selection
A priori	1	$\mathbf{P-F}\ \mathit{contribution}{\sim}\sigma^2+\varphi+\sigma^2*\varphi$	5	-8958.788		
	2	$\mathbf{P-F}\ \mathit{contribution}{\sim}\sigma^2+\varphi+\sigma^2*\varphi+\varphi^2$	6	-8986.418		
	3	$\mathbf{P-F}\ \mathit{contribution}{\sim}\sigma^2+\varphi+\sigma^2*\varphi+\varphi^2+\varphi^3$	7	-9010.538		
	4	$\mathbf{P-F}\ \mathit{contribution}{\sim}\sigma^2+\varphi+\sigma^2*\varphi+(\sigma^2)^2$	6	-8962.007		
	5	$\mathbf{P-F}\ \mathit{contribution}{\sim}\sigma^2+\varphi+\sigma^2*\varphi+(\sigma^2)^2+\varphi^2$	7	-8990.381		
	6	$\mathbf{P-F}\ \mathit{contribution}{\sim}\sigma^2+\varphi+\sigma^2*\varphi+(\sigma^2)^2+\varphi^2+\varphi^3$	8	-9015.246	**SELECTED**	
	7	$\mathbf{P-F}\ \mathit{contribution}{\sim}\sigma^2+\varphi+\sigma^2*\varphi+(\sigma^2)^2+(\sigma^2)^3$	7	-8960.023		
	8	$\mathbf{P-F}\ \mathit{contribution}{\sim}\sigma^2+\varphi+\sigma^2*\varphi+(\sigma^2)^2+(\sigma^2)^3+\varphi^2$	8	-8988.399		
	9	$\mathbf{P-F}\ \mathit{contribution}{\sim}\sigma^2+\varphi+\sigma^2*\varphi+(\sigma^2)^2+(\sigma^2)^3+\varphi^2+\varphi^3$	9	-9013.267		
Post hoc	10	$\mathbf{P-F}\ \mathit{contribution}{\sim}\sigma^2+\sigma^2*\varphi+(\sigma^2)^2+\varphi^2+\varphi^3$	7	-9017.245		**SELECTED**
	11	$\mathbf{P-F}\ \mathit{contribution}{\sim}\varphi+\sigma^2*\varphi+(\sigma^2)^2+\varphi^2+\varphi^3$	7	-9015.157		
	12	$\mathbf{P-F}\ \mathit{contribution}{\sim}\sigma^2+\varphi+(\sigma^2)^2+\varphi^2+\varphi^3$	7	-9016.691		
	13	$\mathbf{P-F}\ \mathit{contribution}{\sim}\varphi+(\sigma^2)^2+\varphi^2+\varphi^3$	6	-9016.607		
	14	$\mathbf{P-F}\ \mathit{contribution}{\sim}\sigma^2+(\sigma^2)^2+\varphi^2+\varphi^3$	6	-8999.407		
	15	$\mathbf{P-F}\ \mathit{contribution}{\sim}\sigma^2*\varphi+(\sigma^2)^2+\varphi^2+\varphi^3$	6	-9017.155		
	16	$\mathbf{P-F}\ \mathit{contribution}{\sim}(\sigma^2)^2+\varphi^2+\varphi^3$	5	-8999.493		
Complete formula		$\mathbf{P-F}\ \mathit{contribution}{\sim}[5.029e-08]-[8.739e-08]*[(\sigma^2)^2]+4.676e-09*[\sigma^2*\varphi]+[7.155e-09]*[\varphi^2]-[1.564e-08]*[\varphi^3]$				

Assumptions are made, and most assumptions are wrong.

— Albert Einstein

If the flight velocity of pigs is one of the parameters in the model, the analysis will happily answer the question of what would happen if pigs could fly.

— Hal Caswell (2019b)

5

Testing for efficacy in four measures of demographic buffering

Contents

5.1 Abstract

Understanding population responses to variable environments is central to much of current research in population ecology and conservation biology. Environmental variability, a key component of global climate change, increases the extinction risk of species across the tree of life. Therefore, quantifying the sensitivity of populations to environmental variability is timely in the face of global climate change. A common approach to measure the impact of environmental variability on a population is by quantifying the population's capacity towards demographic buffering specifically, the population's ability to reduce the impact of environmental variability on its own growth rate. This line of work has, over the past 25 years, resulted in multiple, heterogeneous, methods to quantify demographic buffering. To date, we lack clarity on which method is most appropriate, and under what conditions. To identify the best method to quantify demographic buffering, we test four methods – one correlational method, two methods using terms from Tuljapurkar's approximation and the summation of stochastic elasticities of variance $\left(\sum E^{\sigma^2}_{a_{ij}}\right)$ – for their efficacy to inform conservation strategies. We compare and contrast these methods via three different tests to determine the efficacy of the methods across four integral projection models for plants representing different life history strategies. In the first test, we determine if the measures, structured by ontogeny, are similar or distinct by analyzing their covariance structure across the four species. In the second and third tests, we perform two counterfactual simulations to test if the measures offer insights about the populations' responses to variable environments that are better than chance. We find that the four methods significantly differ in their ability to identify and quantify demographic buffering. Furthermore, our simulations identify $\sum E^{\sigma^2}_{a_{ij}}$ as the most effective method to quantify demographic buffering. This work represents a clear example of *how* and *why* to test the metrics we infer from structured systems prior to their applications in systems of interest (*e.g.*, endangered populations). In addition, our finding that commonly used approaches to quantify demographic buffering are ineffective has broad implications for our current understanding of how natural populations are responding to climate change, and thus for effective conservation practices.

5.2 State of the art

Increased environmental variability is a key threat to natural populations in response to global climate change (Masson-Delmotte et al., 2021; Sutherland et al., 2013). From droughts to hurricanes, environmental variability takes a variety of forms across species (Raventós et al., 2021; Rodríguez-Caro et al., 2021). However, the net effect of environmental variability on population dynamics is broadly conserved across taxa: it often leads to a reduction in a population's stochastic population growth rate (λ_s; Tuljapurkar, 1982, 1989) and consequent increases in extinction risk (May, 1973). These effects are especially concerning as global climate change is projected to increase environmental variability in regions hosting the highest biodiversity (Bathiany et al., 2018). Therefore, understanding the sensitivity of populations to environmental variability and the strategies populations use to reduce this sensitivity is critical.

Demographic buffering is often used to quantify the impact of environmental variability on population dynamics. Demographic buffering quantifies the degree to which a population's combination of demographic rates (*e.g.*, survival, growth, reproduction) reduce the impact of environmental variability on λ_s. Similar to a chemical buffer on a solution's pH, a more demographically buffered population has a combination of demographic rates that reduce the population's sensitivity to environmental variability relative to a less demographically buffered population (Gascoigne et al., 2023a; Pfister, 1998). In turn, demographic buffering has been extensively used to infer both the sensitivity of populations to environmental variability (Hilde et al., 2020; Pfister, 1998) and the strategies populations use to reduce this sensitivity (McDonald et al., 2017). This understanding has led to a series of studies analysing the impact of climate variability on conservation measures (Colchero et al., 2021), population viability (Rodríguez-Caro et al., 2021), life histories (Morris et al., 2008) and many more topics across ecology and evolutionary biology (Gascoigne et al., 2023b; McDonald et al., 2017; Morris & Doak, 2004; Santos et al., 2023). However, researchers measure demographic buffering in numerous, different ways, as reviewed in Hilde et al. (2020).

Over the past 25 years, demographic buffering has taken a variety of mathematical forms and interpretations. Mathematically, demographic buffering has been calculated using multiple correlation and derivative based methods (Hilde et al., 2020; Santos et al., 2023). Furthermore, these measures of demographic buffering have been inferred as both a population's relationship to a variable environment (Rodríguez-Caro et al., 2021) and an evolved aspect of a population's life history (Li & Ramula, 2015; McDonald et al., 2017). Currently, we lack a comprehensive understanding of what is an *effective* measure of demographic buffering. We define "efficacy" as the ability of a measure of demographic buffering to infer a population's response to a variable environment. Unfortunately, previous research into demographic buffering often assumes the efficacy of their methods without testing this assumption. Furthermore, out of the suite of methods used to calculate demographic buffering, we do not know which measures are more effective than others. In turn, to fill this gap in knowledge, we aim to test for *efficacy* in measures of demographic buffering.

To test for efficacy in four measures of demographic buffering, we use four size-structured stochastic integral projection models (IPMs; Easterling et al., 2000). Using the PADRINO database (Levin et al., 2022), we simulate IPMs for four plant species with different life histories. Subsequently, we calculate four well-established measures of demographic buffering: one using a correlation method (Spearman's ρ, Pfister, 1998; McDonald et al., 2017), two methods using terms from Tuljapurkar's approximation (V_s and $V_s + V_c$, Tuljapurkar, 1989; Maldonado-Chaparro et al., 2018) and one method using summed stochastic elasticities of variance ($\sum E^{\sigma^2}_{a_{ij}}$, Haridas and Tuljapurkar, 2005; Tuljapurkar et al., 2003; Morris et al., 2008). We test the potential differential efficacy of these four measures of demographic buffering with three separate tests. In the first test, we analyzed the correlation structure of the four measures of demographic buffering structured along the ontogeny (*i.e.*, the size classes in each IPM) of the four species. Here, we hypothesized that (H1) different measures of demographic buffering would offer different values for the same populations as the methods are parameterized using dissimilar values (*e.g.*, stochastic *vs.* deterministic elasticities) and methods (*e.g.*, Spearman's ρ correlation *vs.* summed products). In the second test, we stabilized (*i.e.*, fixed values as constant through time) the demographic rates along the ontogeny, one size/stage increment at a time, and regressed the difference in stochastic population growth rate ($\Delta\lambda_s$) against the degree of buffering associated with each size class along the ontogeny. We hypothesized that (H2) there is a strong negative relationship between the degree of buffering along the ontogeny and $\Delta\lambda_s$ as we predicted stabilizing demographic rates to have the largest positive effect in the least buffered size classes. In the third test, we elucidate whether counterfactual simulations of the plant populations informed by their distributions of demographic buffering, along an ontogeny, yield improved population growth relative to chance. Specifically, we collectively stabilize the demographic rates of all size classes across a time series to varying degrees. The degree to which the size class specific demographic rates were stabilized was determined by the distributions of size class specific buffering, determined by each method (*i.e.*, ρ, V_s, $V_s + V_c$ and $\sum E^{\sigma^2}_{a_{ij}}$). To determine if these distributions offer improved information for demographic rate stabilization relative to chance, we also simulated the random stabilization of demographic rates along ontogeny as a control. We hypothesized that (H3) the stabilization of demographic rates informed by size-class specific demographic buffering distributions would yield a significantly higher $\Delta\lambda_s$ than a random stabilization of demographic rates.

5.3 Methodological approach

To test for efficacy in measures of demographic buffering, *i.e.* the ability of natural populations to minimise the expected negative effects of environmental stochasticity (Hilde et al., 2020; Rodríguez-Caro et al., 2021; Maldonado-Chaparro et al., 2018; Morris et al., 2008), we used four different measures of demographic buffering. Since these measures of demographic buffering are dependent on structured demographic models (*i.e.*, related to Tuljapurkar's approximation; Tuljapurkar, 1989), we used four environmentally explicit integral projection models (IPMs; Easterling et al., 2000) to test our hypotheses.

5.3.1 Environmentally explicit integral projection models

We used four integral projection models (IPMs) from the PADRINO IPM database (Levin et al., 2022) to test for efficacy in measures of demographic buffering. IPMs are discrete-time population models that project a population structured by a continuous trait (*e.g.*, height, mass) within a finite domain [*i.e.*, from the smallest trait value (α) to the largest one (ω)] across time steps. An environmentally explicit IPM can be written as,

$$n_{t+1}(z') = \int_{\alpha}^{\omega} K(z', z, \psi_t)\, n_t(z)\, dz. \tag{5.1}$$

Here, the distribution of the continuous trait at time t [$n_t(z)$] is projected through the so-called **K**-kernel [$K(z', z, \psi_t)$] to generate the distribution of the continuous trait at time $t+1$ [$n_{t+1}(z')$]. The **K**-kernel represents a continuous two-dimensional surface quantifying the survival and potential change in state values of individuals between t and $t + 1$, as well as the per-capita contributions of size z individuals at time t to the occurrence of size z' newly recruited individuals at time $t + 1$. In an environmentally explicit IPM, the **K**-kernel is a function of one or more time-dependent environment variables (ψ_t) (Ellner et al., 2016).

In our study, we simulated IPMs for four plant species with different life histories. Specifically, we used IPMs for one herbaceous perennial (*Berberis thunbergii*, Merow et al., 2017), two tropical perennials (*Calathea crotalifera* and *Heliconia tortuosa*, Westerband and Horvitz, 2017) and one biennial (*Carlina vulgaris*, Rees and Ellner, 2009). The parameter values and formulas used to construct these IPMs are detailed in Appendix A.

To simulate the IPMs, we used a mesh point integration method (Easterling et al., 2000; Ellner et al., 2016) which discretises the **K**-kernel into a matrix with $n \times n$ dimensions, where each bin (n) can be thought of as a small, discrete size class along the life cycle of the species. Since the discretised kernel mimics a matrix population model (MPM; Caswell, 2001), we will discuss our methods in the form of matrix notation where the matrix is represented as **A** with demographic rates a_{ij} referring to the survival-dependent changes in classes and reproductive contributions of individuals in stage j toward stage i (Caswell, 2001).

5.3.2 Tuljapurkar's approximation and measures of demographic buffering

The metrics used to quantify demographic buffering are derived from Tuljapurkar's approximation (Tuljapurkar, 1982, 1989, 1990). This approximation (Eq. 5.2) quantifies the degree to which the values of demographic rates across time contribute to its long-run stochastic population growth rate, λ_s.

$$\log(\lambda_s) \approx \log(\lambda_1) - \frac{1}{2}(V_s + V_c) \tag{5.2}$$

The approximation is calculated by subtracting the summed impact of *temporal variance* of these demographic rates (V_s, Eq. 5.3) and *within-time step covariance* between demographic rates (V_c, Eq. 5.4) from the logged population growth rate associated with arithmetic mean matrix - *i.e.*, the MPM constricted through element-by-element arithmetic means along the time series [$\log(\lambda_1)$].

$$V_s = \sum_{ij} e_{ij}^2 CV_{ij}^2 \tag{5.3}$$

$$V_c = \sum_{ij \neq kl} e_{ij}\, e_{kl} \left(\frac{\mathrm{cov}(a_{ij}, a_{kl})}{\bar{a}_{ij}\, \bar{a}_{kl}} \right) \tag{5.4}$$

Both V_s and V_c are calculated using the elasticities of λ_1 in response to demographic rates from the mean MPM (e_{ij})[1]. Additionally, V_s measures the impact of variance using the squared coefficient of variance of individual demographic rates (CV_{ij}^2), and V_c quantifies the impact of the covariances between demographic rates by dividing the within-time step covariance of demographic rates [$\mathrm{cov}(a_{ij}, a_{kl})$] by the product of their means ($\bar{a}_{ij}\, \bar{a}_{kl}$).

---

[1] Elasticities quantify the *proportional* contribution of underlying demographic rates to changes in population growth rate - *i.e.*, $e_{ij} = \frac{a_{ij}}{\lambda} \frac{\partial \lambda}{\partial a_{ij}}$

5.3.3 Four measures of demographic buffering

The first measure of demographic buffering is a correlation-based approach. As illustrated by Pfister (1998), one strategy by which a population can reduce V_s (Eq. 5.3) is by having a negative covariance between the elasticities of population growth rate associated with mean MPM (e_{ij}) and the temporal coefficient of variance values of said demographic rates (CV_{ij}). In turn, this first measure of demographic buffering (ρ) is a calculation of the covariance between e^2_{ij} and CV^2_{ij} [*i.e.*, $\text{cov}(e^2_{ij}, CV^2_{ij}) = \rho$]. A negative covariance in ρ would mean that the demographic rates that proportionally vary the most through time in a population in fact have the least impact on the overall performance of the population, as quantified by elasticities of λ_1, whilst the most important demographic rates would be proportionately stable over time. Out of all the possible measures of demographic buffering, this correlation-based approach is the most commonly used (Hilde et al., 2020).

The second and third measures of demographic buffering use the values directly from the second-term of Tuljapurkar's approximation. The second measure of demographic buffering quantifies the impact of temporal variance in demographic rates (V_s, Eq. 5.3). The third measure of demographic buffering sums the impact of demographic rate variance and within-timestep covariance ($V_s + V_c$, Eq. 5.3,5.4).

The fourth measure of demographic buffering uses the summation of stochastic elasticities of variance. The summation of stochastic elasticities of variance $\left(\sum E^{\sigma^2}_{a_{ij}}\right)$ represents the degree to which proportional increases in demographic rate variance negatively impacts λ_s. In turn, we can numerically represent $\sum E^{\sigma^2}_{a_{ij}}$ as,

$$\sum E^{\sigma^2}_{a_{ij}} = \sum \left[\frac{\text{var}(a_{ij})}{\lambda_s} \times \frac{\lambda_s^{*a_{ij}} - \lambda_s}{0.00001 \times \text{var}(a_{ij})} \right]. \qquad (5.5)$$

As *per* Haridas and Tuljapurkar (2005), we can rewrite Tuljapurkar's approximation (Eq. 5.2) as,

$$\log(\lambda_s) \approx \log(\lambda_1) + \frac{1}{2}\left(\sum E^{\sigma^2}_{a_{ij}}\right) \qquad (5.6)$$

Thus, we define the fourth measure of demographic buffering as $\sum E^{\sigma^2}_{a_{ij}}$.

5.3.4 Testing for efficacy in measures of demographic buffering

To test which measures of demographic buffering are most effective, and the degree to which they are effective, we ran three specific tests.

We tested H1, that the different measures of demographic buffering would offer different values for the same populations, in two steps. First, we quantified the degree of demographic buffering associated with each measure for all n size classes of the $n \times n$ discretised IPM kernel, one size class at a time. Second, we quantified the correlation of these values for all four species. If the measures of demographic buffering are distinct, different correlation patterns of the measures should emerge across the four examined species.

The second and third tests involved counterfactual simulations of the four species. Both simulations involved stabilizing the demographic rates of an individual size class (*i.e.*, j) toward their arithmetic mean across a simulated time series of 1,000 timesteps. This stabilization approach tests a key assumption of measures of demographic buffering: whether the degree to which a stage class is demographically buffered implicates the degree to which the whole population would benefit from the stabilization of demographic rates in said stage class. If a measure of demographic buffering is effective, we predict a positive relationship between the degree of stage specific demographic buffering and the degree to which the population benefits from the stabilization of demographic rates in each stage class along the life cycle of the species.

To test H2, that there is a strong negative relationship between the degree of buffering associated with an individual stage along an ontogeny and the improvement in population growth associated with the stabilization of demographic rates associated with said stage (*i.e.*, $\Delta\lambda_s$), we used a counterfactual approach. Specifically, we stabilized the demographic rates of each size class one at a time, whilst leaving the demographic rates of all other stages to vary through time. After running 1,000 simulations of the stabilized population time series, the mean stochastic population growth rate of the *stabilized* population was calculated. The difference between the stabilized stochastic population growth rate and the stochastic population growth rate of the non-stabilized population time series was calculated ($\Delta\lambda_s$). Subsequently, measures of $\Delta\lambda_s$ were regressed against each measure of stage-specific demographic buffering (*i.e.*, ρ, V_s, $V_s + V_c$ and $\sum E^{\sigma^2}_{a_{ij}}$). The degree to which $\Delta\lambda_s$ and the measures of stage-specific demographic buffering negatively covary corresponds to the efficacy of the individual measures of demographic buffering - *i.e.*, stabilizing demographic rates in the least buffered stages producing greater $\Delta\lambda_s$ values than more buffered stages. Negative covariances were assessed using Spearman's ρ correlations with significance attributed to $p < 0.05$.

To test H3, that the stabilization of demographic rates informed by size-class specific demographic buffering distributions would yield a significantly higher $\Delta\lambda_s$ than a random stabilization of demographic rates, we used another counterfactual approach. Specifically, we stabilized the demographic rates relative to their measures of stage-specific demographic buffering. In other words, if a stage class (j) was the least demographically buffered for a specific measure of demographic buffering (*e.g.*, $\sum E^{\sigma^2}_{a_{ij}}$), that stage class would be stabilized to its arithmetic mean. However, if a stage class were the most demographically buffered, the time series would resemble the non-stabilized population time series. For intermediate levels of demographic buffering, the population's time series of demographic rates was set to the weighted average of the stabilized and non-stabilized population time series, relative to the percentile the stage is demographically buffered (for more details, see supplementary methods). To test for efficacy, we used a permutation approach. Specifically, we simulated 10,000 random distributions of demographic buffering and stabilized the time series of demographic rates relative to these random distributions. This step resulted in a null distribution of how an ineffective measure of demographic buffering may stabilize the system. To test whether the measures of demographic buffering are effective, we identified the 95^{th} percentile within the null distribution and attributed efficacy to any measure that was consistently greater than the 95^{th} percentile across all four species.

5.4 Results

5.4.1 Test 1: Identify differences in the measures of demographic buffering across ontogeny

In the first test, we aimed to identify whether the four measures of demographic buffering offer similar or distinct inferences across the four examined species. For this step, we analysed the correlation structure of each measure of demographic buffering structured across ontogeny and found heterogeneity across the four demographic buffering metrics of our four species, thus supporting H1 (Fig. 5.1). These differences are demonstrated by the differences in correlation patterns across the four species. Interestingly, the only pairwise combination of demographic buffering measures that offered a highly stereotyped correlation structure was V_s and $V_s + V_c$. These results are also mirrored with a principal component analysis of the measures of demographic buffering across the four species (Fig. 5.2).

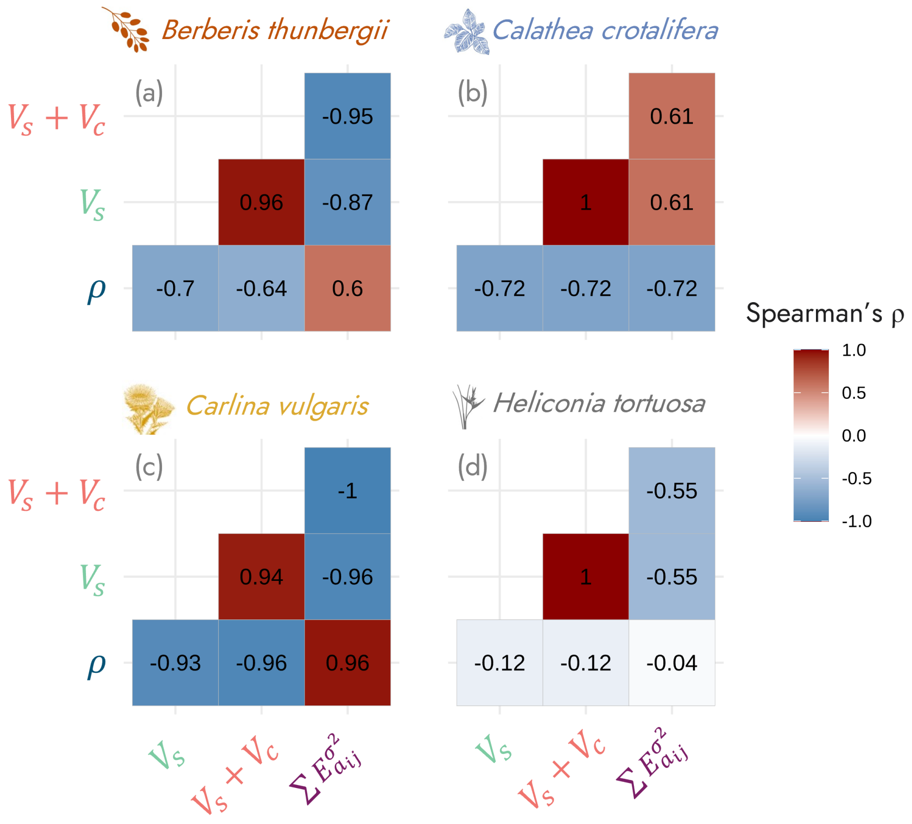

Figure 5.1: Heterogeneity in the measures of demographic buffering. Here, we show the correlation structure of four measures of demographic buffering structured across ontogeny for all four plant species. The four measures are: Spearman's ρ coefficient correlating elasticities and CV values associated with individual demographic rates, V_s which quantifies the impact of demographic rate variance on population growth using Tuljapurkar's approximation, $V_s + V_c$ which quantifies the impact of demographic rate variance and covariances on population growth using Tuljapurkar's approximation and the summed stochastic elasticities of variance ($\sum E^{\sigma^2}_{a_{ij}}$). The numbers in the centre of the cells represent the Spearman's ρ coefficient associated with pairwise combinations of the demographic buffering measures. Redder (bluer) tones correspond to more positive (negative) correlations.

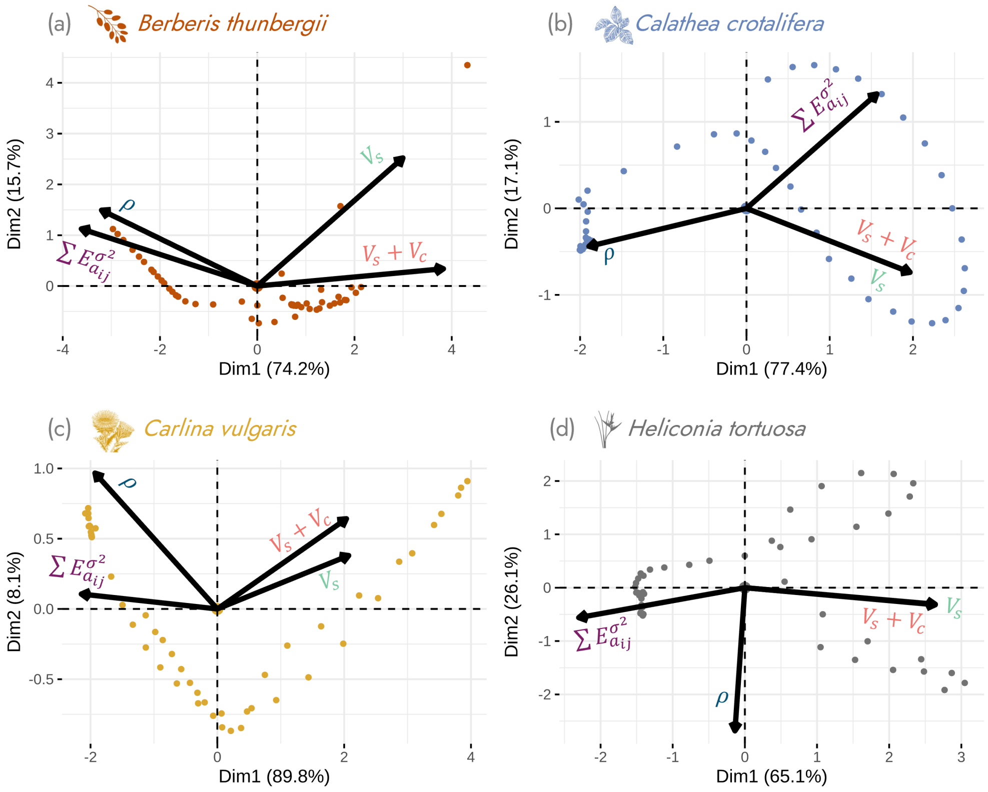

Figure 5.2: Heterogeneity in the measures of demographic buffering. Here we show the covariance structure, via a principal component analysis (PCA), of four different measures of demographic buffering, structured across ontogeny, for four species of plants. The four measures are: Spearman's ρ coefficient correlating elasticities and CV values associated with individual demographic rates, V_s which quantifies the impact of demographic rate variance on population growth using Tuljapurkar's approximation, $V_s + V_c$ which quantifies the impact of demographic rate variance and covariances on population growth using Tuljapurkar's approximation and the summed stochastic elasticities of variance ($\sum E^{\sigma^2}_{a_{ij}}$). Prior to running the PCA, all values were scaled and centred. The points represent buffering values associated with individual stages across the life history of each species. The arrows represent the covariance structure of each measure of demographic buffering. It is worth noting that the arrows for V_s and $V_s + V_c$ are almost perfectly overlapping in the plots for *Calathea crotalifera* and *Heliconia tortuosa*.

5.4.2 Test 2: Testing for efficacy by stabilizing demographic rates across individual stages

In the second test, we quantified the efficacy in each measure of demographic buffering. Specifically, we hypothesized (H2) that individual simulations of each species, where the demographic rates of each stage were stabilized (*i.e.*, re-parameterized to be constant through time) one stage at a a time, would lead to a negative relationship between the degree of buffering associated with a specific stage and $\Delta\lambda_s$. The rationale for this hypothesis is the stabilization of demographic rates in individual stages should have a larger positive effect in the least buffered stages than in more buffered stages. Of the four different methods for calculating demographic buffering, only $\sum E_{a_{ij}}^{\sigma^2}$ generated negative relationships between degree of buffering and $\Delta\lambda_s$ across the four species (Spearman's ρ, $p < 0.05$; Fig. 5.3). The other metrics (*i.e.*, ρ, V_s and $V_s + V_c$) only generated negative relationships between degree of buffering and $\Delta\lambda_s$ in *Berberis thunbergii* and *Carlina vulgaris* (Spearman's ρ, $p < 0.05$; Fig. 5.3). In turn, the second test indicates $\sum E_{a_{ij}}^{\sigma^2}$ is the only measure of demographic buffering that is predictably effective across all four species.

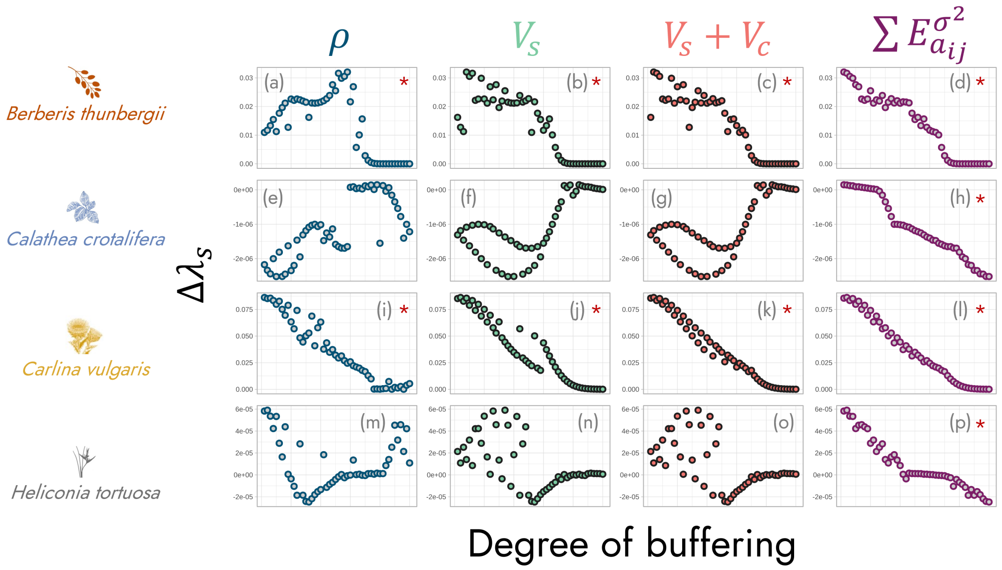

Figure 5.3: Stabilization of demographic rates across the life cycle of four examined species identifies $\sum E^{\sigma^2}_{a_{ij}}$ as an effective measure of demographic buffering. Here, the results from the simulations where demographic rates were stabilized for stages one at a time are shown – rows indicate species whilst columns represent the different measures of demographic buffering. The four measures are: Spearman's ρ coefficient correlating elasticities and CV values associated with individual demographic rates, V_s which quantifies the impact of demographic rate variance on population growth using Tuljapurkar's approximation, $V_s + V_c$ which quantifies the impact of demographic rate variance and covariances on population growth using Tuljapurkar's approximation and the summed stochastic elasticities of variance ($\sum E^{\sigma^2}_{a_{ij}}$). The x-axis of each graph represents the degree of buffering from least buffering (on the left) to the most buffered (on the right). The y-axis represents the change in stochastic population growth rate ($\Delta\lambda_s$) due to the stabilization of demographic rates in the associated life cycle stage. Significant negative relationships (assessed by Spearman's ρ, $p < 0.05$) are shown with red asterisks.

5.4.3 Test 3: Testing for efficacy by stabilizing demographic rates weighted by the distribution of demographic buffering across ontogeny

In the third test, we quantified the efficacy in each measure of demographic buffering. Specifically, we tested (H3) whether stabilizing demographic rates relative to the distribution of demographic buffering across ontogeny outperforms stabilization measures that were not informed by demographic buffering measures. From these simulations, we found that $\sum E^{\sigma^2}_{a_{ij}}$ is the only measure of demographic buffering that performs better than chance in improving the population's stochastic growth rate ($\Delta\lambda_s$) (Fig. 5.4). This findings is highlighted by all $\Delta\lambda_s$ values associated with $\sum E^{\sigma^2}_{a_{ij}}$ being greater than the 95^{th} percentile of the simulated null distribution.

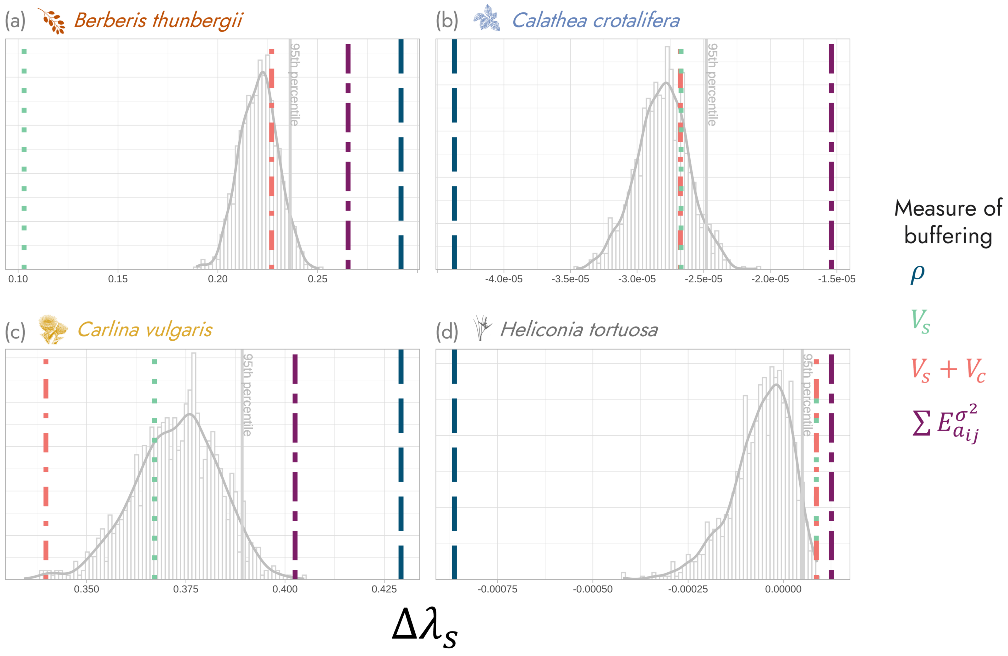

Figure 5.4: Stabilization of demographic rates weighted by the distribution of buffering across ontogeny indicates $\sum E_{a_{ij}}^{\sigma^2}$ is an effective measure of demographic buffering. Here, the results for simulations where demographic rate variances are stabilized relative to each measure of demographic buffering are shown. The four measures are: Spearman's ρ coefficient correlating elasticities and CV values associated with individual demographic rates, V_s which quantifies the impact of demographic rate variance on population growth using Tuljapurkar's approximation, $V_s + V_c$ which quantifies the impact of demographic rate variance and covariances on population growth using Tuljapurkar's approximation and the summed stochastic elasticities of variance ($\sum E_{a_{ij}}^{\sigma^2}$). The grey histograms represent the null distributions (*i.e.*, populations stabilized by a random buffering distribution), and the grey vertical line represents the 95th percentile of the null distribution. In this test, efficacy is attributed to a measure of demographic buffering that is consistently greater than the 95th percentile across all four species (*i.e.*, $\sum E_{a_{ij}}^{\sigma^2}$). The patterned vertical lines represent values of $\Delta\lambda_s$ for populations stabilized by the individual measures of demographic buffering.

5.5 Discussion

In this study, we aimed to test for efficacy across four measures of demographic buffering. To test for efficacy, we used four IPMs associated with plants with different life histories: a herbaceous perennial (*Berberis thunbergii*, Merow et al., 2017), two tropical perennials (*Calathea crotalifera* and *Heliconia tortuosa*, Westerband and Horvitz, 2017) and a biennial plant (*Carlina vulgaris*, Rees and Ellner, 2009). Collectively, our findings identify the summation of stochastic elasticities of variance $\left(\sum E^{\sigma^2}_{a_{ij}}\right)$ as the most effective measure of demographic buffering, over three other metrics: Spearman's ρ coefficient correlating elasticities and CV values associated with individual demographic rates, V_s which quantifies the impact of demographic rate variance on population growth using Tuljapurkar's approximation and $V_s + V_c$ which quantifies the impact of demographic rate variance and covariances on population growth using Tuljapurkar's approximation. The efficacy of $\sum E^{\sigma^2}_{a_{ij}}$ is supported by three independent tests. In test 1, the stage-based measures of demographic buffering were shown to have different correlation structures across the four species (Figs. 5.1,5.2). This disparity of results indicates the four measures are not measuring demographic buffering in the same manner. In tests 2 and 3, the measures of demographic buffering differed in their efficacy to infer a population's response to simulations of reduced demographic rate variance (Figs. 5.3,5.4). Specifically, only $\sum E^{\sigma^2}_{a_{ij}}$ was consistently effective across all four species in both tests 2 and 3.

Our findings have broad implications for past and future studies of demographic buffering. Previous studies have primarily focused on the correlation method (*i.e.*, ρ) for studies of individual populations (Hilde et al., 2020) or comparative approaches (McDonald et al., 2017) with few studies using $\sum E^{\sigma^2}_{a_{ij}}$ (but see Morris et al., 2008). This is problematic as tests 2 and 3 here show stage-based conservation measures based on the correlation approach to be ineffective – especially in contrast to $\sum E^{\sigma^2}_{a_{ij}}$. While previous work has shown the correlation-based approach to (1) have a phylogenetic signal across plant species (McDonald et al., 2017), (2) signal buffering versus labile strategies in variable environments (Li & Ramula, 2015) and (3) potentially be an axis of life history variation (Salguero-Gómez, 2021), we suggest these inferences might not extend to structured conservation measures of populations in variable environments. To fully connect our findings to previous literature, future work should focus on reanalysing results from broad comparative analyses (McDonald et al., 2017; Morris et al., 2008) using multiple measures - especially $\sum E^{\sigma^2}_{a_{ij}}$ - to test previous findings.

Whilst our findings offer new insights to the efficacy of the numerous existing demographic buffering measures, inferences drawn from these findings have important limitations. First, the degree to which the generality of these findings are constrained to certain life histories remains unknown. Whilst here we used species with different life history strategies (*i.e.*, one herbaceous perennial, two tropical perennials and one biennial), the extent to which these findings may apply to more unique life histories and different kingdoms (*e.g.*, eusocial insects, migratory megafauna or semelparous fish) is unknown and open to future research. Second, our results indicate that the measures of demographic buffering are in fact different and should, therefore, be treated as such. This is not to say that only $\sum E^{\sigma^2}_{a_{ij}}$ has a place in the buffering literature. For example, important research can – and has – been directed at other terms from Tuljapurkar's approximation to infer population responses to changes in environmental stochasticity (Compagnoni et al., 2016, 2021; Evers et al., 2023; Paniw et al., 2018). And third, our tests of efficacy of the various metrics of demographic buffering is stage specific, because structured populations often incur stage structured perturbations. For example, hunting and extreme events can perturb the demographic processes unevenly across a life cycle (Darimont & Child, 2014; Von Takach Dukai et al., 2018). However, whilst our approach is more in keeping with the ecological dynamics of structured populations, the theory around demographic buffering is often agnostic of stage specific perturbations (Hilde et al., 2020; Morris et al., 2008; Pfister, 1998; but see Gaillard et al., 1998). Therefore, the inefficacy of ρ, V_s and $V_s + V_c$ can only be attributed to stage explicit inferences of demographic buffering, not interpretations at the level of the whole population (Rodríguez-Caro et al., 2021) or across species (Pfister, 1998).

In the future, demographic buffering could be connected to two previously disparate corners of ecology and evolution. First, variance in demographic rates is not the sole driver of population extinction and persistence in variable environments (McDonald et al., 2016; Capdevila et al., 2020b; Hastings et al., 2018). Indeed, transient dynamics, temporary fluctuations in populations that decay over time due to progressive shifts toward a stable age/stage/size structure, are also at play (Stott et al., 2011, 2012; Tuljapurkar et al., 2023). Recent research has shown the transient portfolio of populations in response to disturbance to have broad impacts on population trajectories (Capdevila et al., 2020b; Jackson et al., 2019; McDonald et al., 2016; White et al., 2013; Ezard et al., 2010). Furthermore, the transient portfolio can be the mechanism by which the population is able to persist (Hansen et al., 2019) and be a key contributor to the variance of population growth rate overtime (Jelbert et al., 2019; McDonald et al., 2016). Unfortunately, previous papers focusing on demographic buffering have been agnostic to the transient dynamics in their populations of interest – thereby making this a key area for future work. Second, the link between demographic buffering and life history evolution is incomplete. The components that build all measures of demographic buffering are in some way connected to the sensitivities or elasticities of population growth rate (λ) in response to changes in demographic rates (Pfister, 1998; Hilde et al., 2020; Tuljapurkar, 1982). These sensitivities and elasticities are often used to infer ecological processes (*e.g.*, demographic buffering) but also selection gradients (Brodie et al., 1995; Caswell, 1978; Van Tienderen, 2000). Whilst previous work has implicated demographic buffering as a life history strategy (Jongejans et al., 2010; Koons et al., 2009; Rodríguez-Caro et al., 2021), there is no evidence for selection acting on any measure of demographic buffering in a natural population. In turn, future work must be aimed at filling this gap in knowledge.

In conclusion, we have shown: (1) the efficacy of $\sum E^{\sigma^2}_{a_{ij}}$ as a measure of demographic buffering, (2) how different measures of demographic buffering report different values for the same populations of interest and (3) the utility of counterfactual simulations to test for efficacy in metrics of interest. This work supports previous uses of $\sum E^{\sigma^2}_{a_{ij}}$ (Gascoigne et al., 2023b; Morris et al., 2008; Santos et al., 2023; Westerband & Horvitz, 2017) and opens new avenues of research to both confirm previous findings and extend ideas surrounding demographic buffering to other areas of ecology and evolution.

5.6 Acknowledgements

We would like to thank A. Compagnoni, H. Jaggi, W. Zuo, S. Tuljapurkar and members of the SalGo team for helpful discussions on the topics of demographic buffering and its associated methods. RS-G was supported by NERC grant #NE/X013766/1.

5.7 Supplementary methods

To perform the counterfactual simulations used in test 3, we stabilized the demographic rates associated with each stage (*i.e.*, where the demographic rate is a_{ij} and the focal stage is j) relative to the degree of buffering associated with each stage (DB_j). Note, here DB_j represents the degree of buffering associated with each measure of demographic buffering (*i.e.*, ρ, V_s, $V_s + V_c$ and $\sum E^{\sigma^2}_{a_{ij}}$) individually. The method by which we stabilized demographic rates is as follows.

First, we calculated the distribution of demographic buffering across ontogeny and scaled the values between 0 and 1. The scaled values (β_j) were calculated as:

$$\beta_j = \frac{DB_j - \min(DB_j)}{\max(DB_j) - \min(DB_j)}. \tag{5.7}$$

This scaling means that a β_j value of 0 is the least buffered stage whilst a β_j value of 1 is the most buffered stage[2].

Second, we used the original time series of demographic rates ($a_{ij,t}$) and the β_j distribution to generate a new series of demographic rates ($a^*_{ij,t}$) that are stabilized toward the mean demographic rate ($\bar{a}_{ij}$) proportional to β_j:

$$a^*_{ij,t} = \beta_j(a_{ij,t}) + (1 - \beta_j)(\bar{a}_{ij}). \tag{5.8}$$

In other words, if a stage class (j) were the least demographically buffered for a specific measure of demographic buffering (*e.g.*, $\sum E^{\sigma^2}_{a_{ij}}$), that stage class would be stabilized to its arithmetic mean. However, if a stage class were the most demographically buffered, the time series would resemble the non-stabilized population time series.

---

[2] It is worth noting that the relationship between the valued inferred from the measure of demographic buffering and degree of buffering varies across each measure. Specifically, ρ, V_s and $V_s + V_c$ have a negative relationship with degree of demographic buffering. However, $\sum E^{\sigma^2}_{a_{ij}}$ has a positive relationship with demographic buffering. In turn, all values were transformed to be both positive (as ρ and $\sum E^{\sigma^2}_{a_{ij}}$ can have negative values) and have a positive relationship with the inferred degree of demographic buffering.

> *It is clear that there is no classification of the Universe that is not arbitrary and full of conjectures. The reason for this is very simple: we do not know what kind of thing the universe is.*
>
> — Jorge Luis Borges, translated by Will Fitzgerald

> *The trick is to start with the specifics — a single wasp species or a biological process that doesn't seem especially significant — and to arrive at much more general interpretations of nature.*
>
> — Mary Jane West-Eberhard

6

Current perspectives and future directions in animal life history evolution

Contents

6.1 Abstract

A life history strategy represents the evolutionary answer to a species' ecological problems. From the fatally reproductive salmon *Salmo salar* to the seemingly immortal jellyfish *Turritopsis dohrnii*, different species have evolved vastly different answers to their ecological problems, generating the vast suite of life histories observed across the animal

kingdom. To explain this variation, life history theory has generated and tested specific hypotheses to describe this variance and define what drives it. Since Stearns (1992) and Roff (2002), multiple methodological approaches have been used to understand the eco-evolutionary processes that drive animal life history evolution. Specifically, insights from theoretical modelling, experiments, fieldwork and comparative studies have elucidated multiple mechanisms that drive variance in intra- and inter-specific life history outcomes. However, despite this progress, gaps in knowledge regarding how life histories evolve in a changing world still remain. Here, we review a selection of perspectives, developed over the past 20 years, that support much of life history research today. These perspectives include: (1) the two-axes framework (*i.e.*, the fast-slow continuum *vs.* reproductive schedule) to describe life history variation across taxa, (2) three different types of variance that impact life history evolution (*i.e.*, variance within time-steps, across time-steps and variance in life history outcomes) and (3) the utility of integrating ultimate and proximate modes of research to understand life history evolution. Subsequently, we suggest future directions that represent new frontiers in the study of animal life history evolution. These future directions are targeted at specific gaps in knowledge that offer timely insights for the broader ecology and evolutionary biology community - *i.e.*, (1) where does selection act in the construction of a life history strategy and (2) the problem of time in life history evolution. In summary, this review provides an integrative perspective, from physiological constraints to evolutionary pressures, regarding *how* life history strategies are studied and *why* life history research requires interdisciplinarity. The further discussion of current perspectives and future directions provides a cross-section of animal life history research today: where we are, how we got here and two research programs to improve our understanding of life history evolution in variable environments

6.2 Introduction

Life history theory describes the rich diversity of life history strategies that organisms use to pass their genes across generations. Specifically, a life history strategy is the sequence and timings of events along an organism's life course. These strategies are governed by underlying vital rates of survival, development and reproduction that collectively contributes to both individual fitness (Stearns, 1983; Charlesworth, 1994) and broader population dynamics (Roff, 2002; Stearns, 1992). Such events that constitute a life history strategy are referred to as life history traits (*e.g.*, generation time, mean lifespan, lifetime reproductive output).

Across the animal kingdom, there is large variation in life history strategies (Jones et al., 2014; Gaillard et al., 2005; Paniw et al., 2021). For instance, while the Greenland shark (*Somniosus microcephalus*) takes a protracted period of 150 years before reaching sexual maturity (Nielsen et al., 2016), the aphid *Rhopalosiphum prunifolia* completes its life cycle in just 4.7 days (at 25°C; Noda, 1960). As a futher example, the Chinook salmon (*Oncorhynchus tshawytscha*) populations take the perilous journey upstream to reproduce and immediately perish (Groot & Margolis, 1991) whilst the Great tit (*Parus major*), once reaching sexual maturity after one year, reproduces annually once (and sometimes twice) up until death (Verhulst et al., 1997). This broad heterogeneity in animal life histories has pushed researchers to explain: (1) these vast differences in life history strategies and (2) what drives the evolution of life history strategies in a changing world.

Animal life history research is highly interdisciplinary and can involve research methods focused at multiple levels of biological complexity. For example, life history research can involve:

1. Comparative demographic methods characterizing the major axes of variance in life history strategies (Healy et al., 2019; Salguero-Gómez et al., 2016b).
2. The quantification of life history trade-offs – *i.e.*, negative covariances between life history traits (Stearns, 1989; Zera & Harshman, 2001; Zera & Zhao, 2006).
3. Identifying the genetic, cellular and physiological pathways that initiate the timings associated with life history traits (*e.g.*, age at sexual maturity) (Jimenez, 2016).
4. Characterizing the sources of variation (*e.g.*, genetic, environmental, luck) in life history traits within a population (Careau et al., 2010).

All these research programmes, whilst operating within the interdisciplinary field of life history theory, test hypotheses using very different methods and are focused on different levels biological complexity. Hence, over the past decades, new findings in animal life history evolution have arisen from a variety of different approaches (Fig. 6.1).

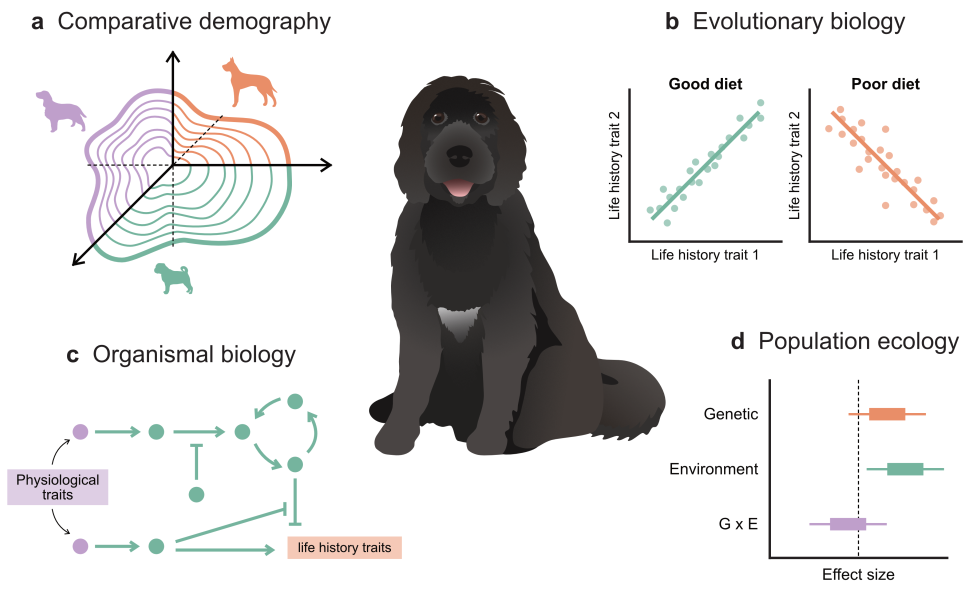

Figure 6.1: The many ways to study life histories. Here, we outline four distinct strategies to study the life histories of dogs. (a) Comparative demography may involve using dimension reduction methods [*e.g.*, phylogenetically controlled principal component analyses (Revell, 2009)] to identify the primary axes of dog life history variation. (b) Evolutionary biology may involve identifying the causes and constraints that lead to life history trait covariances (*e.g.*, how diet can alter the presence of trade-offs). (c) Organismal biology may involve studying the physiological pathways [*e.g.*, insulin/insulin-like growth factor signalling (Jimenez, 2016)] that mediate the generation of life history traits. (d) Population ecology may involve partitioning the variance in life history traits by their contributions from genes, the environment and their interaction.

Life history theory can greatly benefit from an integration of the different approaches researchers use to study animal life history evolution. To aid this integration, here we review current-perspectives and future directions in life history theory from across ecology and evolution. The current perspectives outlined in this paper represent step changes in thinking in life history research since Stearns (1992), Charnov (1993), Charlesworth (1994) and Roff (2002). Subsequently, we discuss future directions focused on understanding how life histories evolve in a changing world.

6.3 Current perspectives

Here, we outline a selection of current perspectives in animal life history research that have progressed significantly in the past 20 years. Whilst not exhaustive, these three sections act as a primer summarizing research programmes that have pushed the field of life history theory forward and bolster much of life history research today. These sections progressively zoom in, in terms of scale, on recent findings in life history research: from comparative approaches across species, to variance decomposition approaches within species to the drivers of individual life history traits.

6.3.1 Describing life histories across the animal kingdom

Ecologists have long been interested in answering the question, how and why do life history strategies differ? One of the first attempts to characterize life histories was Robert MacArthur and E. O. Wilson's r *vs.* K-continuum (MacArthur & Wilson, 1967). Built on the logistic growth equation $\left[\frac{dN}{dt} = rN\left(\frac{K-N}{K}\right)\right]$, the r *vs.* K-continuum differentiates life histories based on the term under strongest selection; notably, the r *vs.* K-continuum was also swiftly connected to the observation of survivorship curves that were also first formulated shortly after (Van Valen, 1973). Whilst generalizable across taxa, the r *vs.* K-continuum does not account for major life history traits and their tendency to covary. For example, generation time, mean life expectancy and age at sexual maturity vary greatly across the animal kingdom (from the aphid to the Greenland shark) and, furthermore, covary to a significant degree – to the degree of becoming a *syndrome*. As a consequence, another attempt to characterize life histories came when Stephen Stearns framed life history variation in terms of the fast-slow continuum (Stearns, 1983). Some life histories are *slow* (long generation time, higher mean lifespan and later age at sexual maturity) whilst others are *fast* (short generation time, lower mean life expectancy and earlier age at sexual maturity). Until recently, this fast-slow continuum was the primary method to explain the variation in life histories across the animal kingdom (Gaillard et al., 2005; Oli & Dobson, 2003).

Currently, animal life histories are characterized across two axes of life history variation. To empirically quantify the primary axes of life history variation in animals, Healy et al. (2019) used a body mass and phylogenetically corrected principal component analysis (PCA) of life history traits from 121 species. This PCA identified two axes that collectively explain 71% of the variance in life history traits. These axes include the fast-slow continuum and the distribution of age-specific reproduction and mortality – this follows (Salguero-Gómez et al., 2016b) finding a similar pattern in plants (also see Paniw et al., 2018; Gaillard et al., 2005; Oli and Dobson, 2003). Identifying these two axes of animal life history variation was immediately impactful for two reasons. First, this result shows that the distribution of demographic processes, such as survival and reproduction, is orthogonal to the fast-slow continuum. Therefore, selection for the evenness (*e.g.*, constant survival, iteroparity) or skew (*e.g.*, varied survival, semelparity) of demographic rates across a life history can arise in both slow and fast life histories. Second, this result connects directly to the Euler-Lotka equation ($1 = \sum_{x=1}^{\omega} \lambda^{-x} \mathbf{l}_x \mathbf{m}_x$), another fundamental equation in demography, which defines survivorship ($\mathbf{l}_x$) and reproduction ($\mathbf{m}_x$) as vectors that constrain the mathematical space of possible life histories.

After Healy et al. (2019), the two-axes framework for animal life histories has fostered new findings. Some examples include:

1. The sensitivity and resilience of a population to temporal autocorrelation and demographic disturbance is strongly correlated with pace-of-life syndrome (temporal autocorrelation: Paniw et al., 2018; demographic disturbance: Capdevila et al., 2022).

2. Both terrestrial and aquatic life histories inhabit the same two-axes of life history variation, but with key differences in their diversity (Capdevila et al., 2020a).

3. Populations can harbour high degrees of interindividual life history variation that differ across species whilst allowing for high intraspecific variation not described by the axes (Van De Walle et al., 2023; Hernández et al., 2024).

4. The two-axes framework aids in predicting the conservation status of various species in response to anthropogenic disturbance and climate change (Indo-Pacific fishes: Wang et al., 2020; chelonians and crocodilians: Rodríguez-Caro et al., 2023; the gray mouse lemur: Ozgul et al., 2023).

Whilst these findings have made new connections between life history theory and multiple areas of ecology, the two-axes framework is not without its flaws. The two-axes framework of animal life histories is data and, more specifically, model hungry. To perform the analysis, life history traits from across the animal kingdom must be derived. The life history traits are often derived from structured population models – many of which are stored in open-access databases (Jasilioniene et al., 2015; Levin et al., 2022; Marques et al., 2018; Salguero-Gómez et al., 2016a; Wilmoth et al., 2021; Bernard et al., 2023). Whilst these models sometimes contain errors (Che-Castaldo et al., 2020; Gascoigne et al., 2023c; Kendall et al., 2019), there has been a push for standardizing research practices around the dissemination of models (Gascoigne et al., 2023c; Simmonds & Jones, 2024). Thankfully, there has also been a recent push for standardizing the traits used within the two-axes framework (Stott et al., 2023). This standardization, across model construction, communication and the comparative inference drawn from them, represents a necessary next step for reproducibility in research using the two-axes framework (Salguero-Gómez, 2021).

6.3.2 Characterizing variance in life histories within populations

Life histories are not static. Yet, much of the canonical life history literature, from Pearl (1925) to Charlesworth (1994), and the comparative approaches detailed above have focused on the expression of *average* life histories in populations. Currently, the exploration of *variance* in life histories within a population is just as, if not more, exciting and relevant to understand life histories in a changing world.

Variance in life histories can take many different forms. Variance may arise by relatively complicated mechanisms such as strength of frequency dependence on demographic processes (Potter et al., 2023) or heterogeneity in parental care in a population (Møller & Thornhill, 1998). However, the emergent variance in life history strategies can be simply categorized into three types: variance within time-steps, variance across time-steps and variance in life history outcomes (*e.g.*, lifespan, reproductive output).

Variance within time-steps alludes to the heterogeneity within a population at time t. This heterogeneity, also called individual variability, may arise due to life history explicit factors. For example, individuals in a population may vary by genotype, sex, ontogenetically (*e.g.*, juvenile or adult), by a separate state (*e.g.*, dormancy or dispersal) or by strategy (*e.g.*, sneakers *vs.* guarders in *Onthophagus* beetles; Emlen, 1997). This heterogeneity is necessary to understand the relative fitness of individuals in a population. To quantify this relative fitness, researchers often use *reproductive value*: the discounted contribution of an individual to future offspring (for a thorough explanation, see: Barton and Etheridge, 2011 and Grafen, 2006). Using reproductive value, researchers can test hypotheses as to the evolution of life history strategies in structured populations [*e.g.*, senescence in age-structured populations (Newton & Rothery, 1997; Roper et al., 2021), the evolution of sociality (Roper et al., 2023), bet-hedging (Grafen, 1999) and parasitism (Andersson, 2017)].

Variance across time-steps, often called *environmental stochasticity*, refers to the difference in life history outcomes over time (*e.g.*, from time t to $t + 1$). To study life histories in response to environmental stochasticity, researchers often use the tools of stochastic demography (Tuljapurkar, 1990). This set of tools allows researchers to quantify the impact of variance across timesteps on life histories. Using these tools, researchers have identified the demographic mechanisms that drive the emergence of life history strategies (*e.g.*, *demographic buffering*: Pfister, 1998; Hilde et al., 2020) – some of whom were previously thought non-adaptive (*e.g.*, Jongejans et al., 2010; Koons et al., 2008, 2009; Tuljapurkar et al., 2009a).

Variance in life history outcomes is a relatively new area of study within life history evolution. Researchers in this field are interested in quantifying (1) the variance in life history outcomes and (2) what drives this variance. To quantify the variance in life history outcomes, researchers often use structured population models to calculate the expected variance in a life history outcome given a set of demographic processes. This variance is often referred to as *dynamic heterogeneity* (Tuljapurkar et al., 2009b) or *individual stochasticity* (Caswell, 2009), but confusion about definitions exists (Forsythe et al., 2021). Research into dynamic heterogeneity has uncoupled: genetic, environmental, gene by environment (*i.e.*, phenotypic plasticity) and demographic stochastic components and further provide quantitative estimates of dynamic (neutral) heterogeneity in life courses that can serve as null models (Snyder & Ellner, 2018, 2022; Steiner et al., 2021; Van Daalen & Caswell, 2017, 2020; Hernández et al., 2024).

Ideas about dynamic heterogeneity have been perceived with criticism (Cam et al., 2016) as deterministic perspectives are deeply rooted in our biological thinking – life history theory in particular. However, both empirical and theoretical research have illustrated how purely deterministic explanations fall short (Fay et al., 2022a; Snyder & Ellner, 2022; Enríquez et al., 2022). Individual stochasticity, even though neutral in itself, slows adaptation (Steiner & Tuljapurkar, 2012) and selective forces might act in favour of, against, or be close to neutral of the generating processes that drive the level of individual stochasticity (Steiner & Tuljapurkar, 2023). Such diversity is not surprising as increased variance in mortality and reproduction can increase individual stochasticity while reducing fixed heterogeneity but can also increase both components in some systems (Van Daalen & Caswell, 2020). Variance in reproduction associated to individual stochasticity is high within and between populations across species and such variance explains the variation in life history strategies amongst animals and plants to a similar if not larger degree than mean differences (Enríquez et al., 2022; Hernández et al., 2024).

6.3.3 Ultimate *vs.* proximate explanations of life history evolution

In the past, research into animal life history evolution has focused on ultimate (evolutionary) modes of research. Why has selection not resulted in the evolution of solely semelparous species (Cole's paradox: Cole, 1954)? What are the necessary conditions for dormancy/diapause/torpor to be the dominant strategy in a population (Tuljapurkar

& Istock, 1993; Tuomi et al., 2013)? This focus on ultimate rather than proximate (mechanistic) research questions arose due to a widely held sentiment that evolutionary biology was the ideal home for life history theory.

> The connection between genotype and phenotype has traditionally been provided by developmental biology and physiology, fields which have become increasingly molecular...... We cannot afford to wait until the molecular analysis of development and physiology has delivered a few mature summary statements relevant to individual variation in fitness, for that will take centuries – if it ever happens at all. We must make our own hypotheses and hope that the molecular connection will come at a later date.
>
> — Stearns (1992, p.10)

Thankfully, this "molecular connection" is now being well explored.

The molecular underpinnings of life history traits are central to life history research. Over the past 20 years, researchers have uncovered the molecular mechanisms of senescence – the deterioration of homeostasis and thus vital functions with age (López-Otín et al., 2013). From telomere shortening (Haussmann and Vleck, 2002; Henriques and Ferreira, 2012; but see Van De Crommenacker et al., 2022; Heidinger et al., 2012) to dysregulated physiological pathways (*e.g.*, hyperfunction theory: Blagosklonny, 2006, 2021), and from too much protein (Fanson et al., 2012) to differential resource allocation (Adler & Bonduriansky, 2014), researchers have identified many proximate explanations for senescence across the animal kingdom (López-Otín et al., 2013). Furthermore, mechanisms have also been fleshed out for the other side of life histories - fertility. All periods of reproduction, from pre-copulation to copulation to post-copulation to post-birth, contain candidate proximate mechanisms that influence the variation in life histories: including endogenous insulin/insulin-life growth factor signalling (IIS) (Lind et al., 2019; Regan et al., 2020; Sepil et al., 2020), target of rapamycin signalling (Alves et al., 2022), sperm traits (Ni et al., 2016; Sanghvi et al., 2024) and seminal fluid proteins (Hopkins et al., 2019; Sepil et al., 2020; Wigby et al., 2020) – just to name a few.

One takeaway from this plethora of proximate mechanisms is the lack of generality. For every life history trait, there is one or many physiological mechanisms that impact the generation of the life history trait phenotype. Whilst these mechanisms have offered a great deal of relevance to developmental biology (Davidson et al., 2023; Emlen & Nijhout, 2001; Kapali et al., 2022; McDonald et al., 2018; Shingleton et al., 2007; Simmons & Emlen, 2006) and evolutionary medicine (Stearns & Medzhitov, 2015), proximate mechanisms alone do not implicate the evolutionary drivers that shape life histories. To gain this generality, current research programs have linked the proximate with the ultimate to offer direct links between the two modes of research. Examples of this integrative approach to life history theory include:

1. Wolves in North America – In Cubaynes et al. (2022), the authors test the hypothesis that canine distemper virus (CDV) drives the latitudinal distribution of coat colour in the wolves of North America (*i.e.*, the increased frequency of black coats in higher latitudes). The authors use a combination of genetics and demographic models to show that CDV creates a selective pressure for disassortative mating, due to heterozygous advantage. In turn, Cubaynes et al. (2022) demonstrate how strength of selection on reproductive strategies can be moderated by genetically determined pathogen resistance.

2. *Drosophila melanogaster* and insulin across latitudes – In the lab, researchers have demonstrated the broad impacts of insulin/insulin-like growth factor signalling (IIS) on development (Parker & Shingleton, 2011; Shingleton et al., 2005, 2007), nutrient sensing (McDonald et al., 2021), environmental cues (Kapali et al., 2022; Regan et al., 2020; Snell-Rood & Moczek, 2012) and life histories (Giannakou & Partridge, 2007; Sepil et al., 2020) in *Drosophila melanogaster*. However, there was no evidence that these lab-based findings were related to the already known impacts of latitudinal clines on *Drosophila* life histories (James et al., 1997). To fill this gap in knowledge, Fabian et al. (2012) explored genome-wide patterns in latitudinal differentiation in *Drosophila melanogaster* across the east coast of North America. Interestingly, they found IIS associated genes (*e.g.*, *FOXO* and *InR*) that differentiated across the latitudinal cline. In turn, genome-wide tools of

natural populations are able to connect lab-based findings to real world life history phenomena.

3. Guppies in Trinidad – In Potter et al. (2023), the authors explore the possible mechanisms that maintain variance in male colouration in a population of guppies. The authors use a combination of a pedigree (spanning 10 generations), spatial data and demographic rates to show that variance in male colouration and the long discussed genetic mechanisms that underpin them (Houde, 1994; Hughes et al., 2005; Paris et al., 2022) are maintained via female preference for rarity. This female preference is adaptive due to an indirect benefit on the fitness of their "sexy sons." In turn Potter et al. (2023) show that female preference is sufficient to promote variance in genetically determined male secondary sexual signals – also see Kvalnes et al. (2022) for a similar, but density-dependent, case in barn owls.

These examples demonstrate how ultimate and proximate questions can be integrated to advance our understanding of life history evolution. Admittedly, these studies are built on great deals of hard-fought longitudinal data, making the scaling of this inference across taxa especially challenging. Thankfully, developments in the ways we model populations are making this obstacle progressively smaller (Bocedi et al., 2021; Coulson et al., 2021; Wilson et al., 2010).

6.4 Gaps in knowledge and recommended future directions

Here, we suggest future directions in animal life history evolution, each of which targets a specific gap in knowledge. We first describe the gap in knowledge and then outline research programs that may address these gaps and, possibly, offer new insights.

6.4.1 Where does selection act in the construction of a life history strategy?

There are two reasons why studying the evolution of life histories remains difficult.

First, defining fitness is problematic (Smith, 1983). In theory, fitness is easy to determine: the genetic contribution of an individual to successive generations relative to other individuals in the population. However, in the real world, fitness is harder to quantify. This difficulty is partly due to the multi-faceted nature of fitness. The fitness of an individual is determined by multiple components – *e.g.*, offspring number, offspring quality, parental care, social status. Each of these components combines to generate the sum total fitness we, as life history theorists, are interested in. Out of practicality, researchers often use life history traits as proxies of fitness (see Fig. 6.2). The basis for this approximate approach is in both ease and phenotypic correlations often being reasonable proxies for genetic correlations (see Cheverud's conjecture: Cheverud, 1988). Unfortunately, this approximation may lead to bias and misrepresent the fitness profile of individuals in a population (Pick, 2023).

The second reason why studying the evolution of life histories remains difficult is due to the complexity in modelling the evolution of life history strategies. Reverting back to the definition, a life history strategy is the sequence and timings of events in an individual's lifespan, governed by underlying vital rates, that contribute both to individual fitness and broader population dynamics. Of this series of events, researchers usually only capture a subset in a demographic model or a lab-based study. For example, demographic models rarely include mate choice mechanisms (despite their abundance: Westneat et al., 2000; Woodman et al., 2023), the impact of transgenerational effects (despite their abundance: Crean and Bonduriansky, 2014; Skinner, 2016) and behaviours that have direct impacts on individual fitness (*e.g.*, the Bogert effect: Bogert, 1949). All in all, this modelling constraint leaves the researcher with a dilemma: What events and timings are necessary to include when modelling a life history strategy? Is there such a thing as a model that is too complex, or not complex enough? Currently, researchers have not defined the criteria for the inclusion of a variable in a life history model; however, there are strong arguments against the inclusion of anything and everything (Borges, 1999; Caswell, 2019b, p.6).

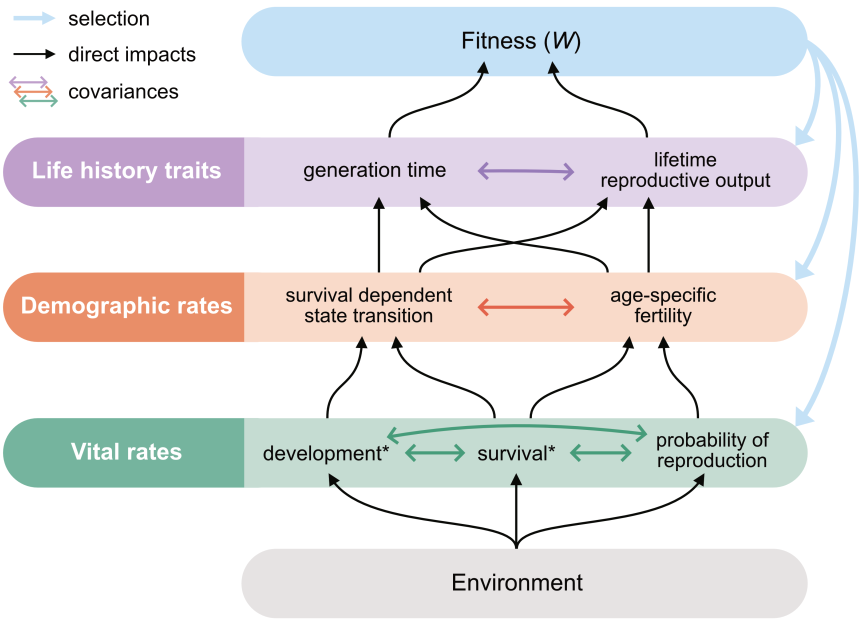

Figure 6.2: The complexities of life history evolution. Here, we show how the current toolbox of demographic methods reveal the inherent complexity of life history evolution. Life history traits, often used as proxies of fitness (W), have both direct (black arrows) and indirect (coloured arrows, *i.e.*, via covariances/trade-offs with other life history traits) impacts on fitness. Furthermore, life history traits themselves are constructed by underlying demographic rates and, at a deeper level, vital rates, which exhibit the same nested complexities of direct and indirect impacts on fitness. The blue arrows show that selection can act at all of these underlying levels. Below demographic rates and vital rates, environmental factors (*e.g.*, resource availability) can influence and constrain the realized vital rates, further complicating the expression of life history traits and their covariance structure (De Jong & Van Noordwijk, 1992; Metcalf, 2016; Van Noordwijk & De Jong, 1986).
* It is worth noting that in a life history solely structured by age, development and survival are identical. The partitioning of development and survival processes is useful in size or stage structured life histories.

To address these difficulties, we recommend two approaches. First, we recommend a trait-based approach as presented in Coulson (2021). In this approach, life histories can be viewed through one focal life history trait (*i.e.* body size) using for instance an integral projection model approach (Easterling et al., 2000; Ellner et al., 2016) or individual based modelling frameworks (Bocedi et al., 2021). Within this framework, a series of resource accrual traits are selected upon to optimize body size given a set of eco-evolutionary feedback loops. By using body size as the metric of interest, Coulson (2021) shows how perturbation analyses can be used to define the eco-evolutionary determinants of body size. This modelling approach (also see Coulson et al., 2021), whilst scalable, loses the complexities offered by previous demographic approaches. In turn, we also recommend a second approach which involves variance decomposition.

Both population ecologists and population geneticists have developed variance decomposition techniques to identify the drivers of system-wide behaviour through demographic rates or allele frequencies, respectively. These methods are life table response experiments (Caswell, 1996a, 2010; Hernández et al., 2023) and quantitative trait loci (QTL)/genome-wide association studies (GWAS) (*e.g.*, Ivanov et al., 2015). Whilst methods exist to knit together structured demographic models and genetic structure (De Vries & Caswell, 2019; Steiner et al., 2021), researchers currently do not have a tool to explore the genetic underpinnings of life history traits without a known link between a gene and a life history trait *a priori*. To build and test these models, we recommend using tractable model systems, such as *Drosophila melanogaster* and *Caenorhabditis elegans*, due to the readily available tools for GWAS/QTL studies and the easily modelled life history due to discrete ontogenetic stages. These models would thus represent ideal avenues for research programmes focussed on integrating ultimate and proximate understandings of life history evolution.

6.4.2 The issue of time in studying life histories

Currently, life history evolution has not addressed the problem of time. Specifically, time is relative. Here, we are not talking about how animals perceive time [this is a topic we will leave to other fields (Roberts, 2002; Zentall, 2005)]. Instead, we are discussing how time within the life history of an animal relates to the temporal pattern of events it senses in its environment.

Life histories and environments are temporally explicit processes. Whether we are discussing an age (*e.g.*, Holmes and York, 2003), stage (*e.g.*, Crouse et al., 1987) or size (*e.g.*, Bassar et al., 2015) structured life history, individuals change state (*i.e.*, growth, progression, shrinkage, retrogression), stay in the same state (*i.e.*, stasis), reproduce or die across timesteps t to $t + 1$. We note this would also work in the continuous case across *dt*. As a consequence of the temporal nature of life histories, many of the life history traits we derive are also temporally explicit (*e.g.*, generation time, age at sexual maturity, expected lifespan). In addition, environments are also temporally explicit. Whether we are discussing yearly (Hansen et al., 2019), monthly (Paniw et al., 2019), weekly (Wood et al., 2023) or even shorter timeframes (Jouvet et al., 2018), environment components are also structured across timesteps t to $t + 1$, or dt. We outline these obvious facts as it is the combination of the life history and environment timeframes where life history research gets messy (Tuljapurkar, 2023).

Previous research analysing the role of environment components has been agnostic as to the mismatched timeframes of life histories and environment regimes. In other words, researchers estimate the impacts of environment components on life histories across timesteps relevant to an environment component (Vinton et al., 2022), not the life history in question (but see Post, 2019; Park, 2019; Park and Post, 2022; Park and Wootton, 2021; Healy et al., 2013). This line of research is valuable from the point of view of conservation biologists as it is useful to estimate environment contributions toward broader population dynamics, however this does not allow us to interpret how life histories evolve. To illustrate this point, let us imagine two populations of interest, a mosquito population and an elephant population. Whilst El Niño and La Niña may have dramatic consequences on the size of the mosquito population at a certain point in time (Heft & Walton, 2008; Reisen et al., 2008), a timeframe of two to seven years is not small enough to fit within a life history of a mosquito. For the elephant, however, a two-to-seven-year timeframe is sufficient to disrupt life histories to the point of altering life history outcomes (Li & Ramula, 2015). To put the shoe on the other foot, daily predictable gusts of wind may have an impact on mosquito life history evolution (Endo & Eltahir, 2018; Wong & Jim, 2017) but likely does not impact the evolution of elephant life histories due to a timeframe disparity. In turn, whilst the impacts of environment regimes (agnostic of life history timeframes) on population dynamics is important, they do not necessarily inform the impacts of environment regimes on life history evolution.

To fill this gap in knowledge, we recommend accounting for generation time when analysing the impacts of environment components on life history evolution (Fig. 6.3a-d). We hypothesize that this standardization will demonstrate the degree to which life histories are able to accommodate environment components. We further hypothesize that this standardization will have important implications for the role of plastic/tracking *vs.* canalized/buffered strategies (Fig. 6.3e,f). Plastic strategies for life histories in variable environments have been discussed at length over the past twenty years (King & Hadfield, 2019; Koons et al., 2009; Snell-Rood, 2013; Sultan & Spencer, 2002; Vinton et al., 2022; West-Eberhard, 2003; Xue & Leibler, 2018), but, up until now, the impact of generation time has not been linked.

To test these hypotheses, we recommend a combination of comparative studies, theoretical modelling and experimental manipulations. Comparative analyses have brought great insights to animal life history evolution (Capdevila et al., 2020a, 2022; Healy et al., 2019). A reanalysis of some of these results, accounting for generation time, may yield findings indicating how well populations deal with the environments *they* experience across their life history (Fig. 6.3a-d). In addition, we recommend modelling approaches of stochastic environments built on underlying spectra (*e.g.*, 1/f noise: Halley, 1996; Halley and Inchausti, 2004) to test the degree to which life histories evolve plastic or canalized strategies based on how environments contribute to the evolution of phenotypic plasticity (Dupont et al., 2023; Hoffmann & Bridle, 2022; Vinton et al., 2022, 2023). And lastly, multiple model organisms represent candidate systmes to test the role of time in life history evolution. Some potential model systems *Callosobruchus maculatus* (see Lustenhouwer et al., 2023; Sanghvi et al., 2022; Bull and Bonsall, 2008), *Drosophila melanogaster* (see Kubrak et al., 2017; Long, 1970; Overgaard et al., 2011), *Caenorhabditis elegans* (see Dey et al., 2016) and *Escherichia coli* (see Jouvet et al., 2018).

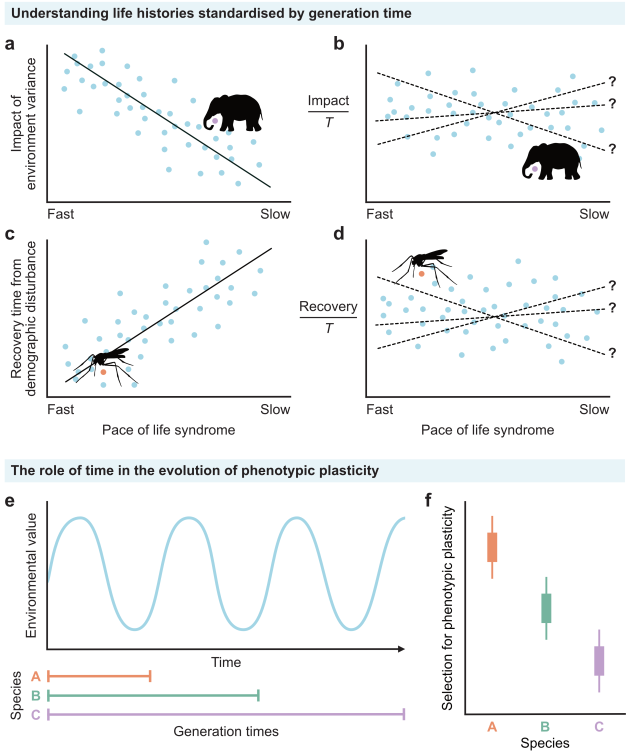

Figure 6.3: Accounting for time in both life histories and the environment in our understanding of life history evolution. Here, we show the impact of pace of life syndrome on inferences of life histories in variable environments. Previous research has shown broad relationships between the impact of environment variance [a, (Morris et al., 2008; Paniw et al., 2018)] and disturbance regimes [c, (Capdevila et al., 2022; Compagnoni et al., 2021)] across slow and fast life histories. Whilst informative for conservation purposes, this approach does not account for the timeframe within which life histories take place – a necessary consideration to understand life history evolution in variable environments. In turn, we propose a new line of research measuring the impact of environment variability (b) and disturbance regimes (d) accounting for generation time (T). This analysis would indicate the degree to which a life history is responsive or stable in environmental regimes *relative* to the life history's timeframe. Furthermore, this approach has broad implications connecting life histories in variable environments to the evolution of phenotypic plasticity. (e) Depending on the timeframe within which the life history takes place, individuals may be exposed to relatively stable average environment values across generations (species A) or relatively unstable average environment values across generations (species C) – from the same environment. The differences only arise due to differences in generation time. The implications of this mismatch in generation time is that species A may evolve plasticity mechanisms that allow it to *track* its environment, more so than species B and C, due to generation time (also see Dupont et al., 2023; Hoffmann and Bridle, 2022; Vinton et al., 2023).

6.5 Concluding remarks

Here, we offer a cross-section of the integrative field that is animal life history evolution. The current perspectives and future directions outlined in this manuscript are in no way exhaustive but are constructed as a resource to both review the current state-of-affairs in animal life history research and present frontiers for exploration. We fully expect the ideas relayed across this manuscript to develop, grow and maybe change as these frontiers are pushed – we leave this to the reader.

To close, we end with an important reminder. A life history is not a "thing"; one cannot physically grasp a life history. Instead, a life history strategy is an abstraction used to define the complex life course of individuals, from birth to death, in an evolutionary and ecological context. It is important for researchers to remember this abstraction when relaying their findings. Within life history theory, results are always context-dependent and subject to deserved scrutiny. However, through a push for generality, we progress to understanding the truths by which organisms make their way from t to $t + 1$.

6.6 Acknowledgements

We would like to thank various friends and colleagues who have helped us, sometimes inadvertently, develop the ideas we present in this manuscript. Specifically, we would like to thank T. Coulson, J. Deere, C. Bernard, M. Kajin, A. Vinton, J. H. Watson and many of the attendees from the 8^{th} meeting of the Evolutionary Demography Society in Paris, 2023.

I love it when a plan comes together.

— John "Hannibal" Smith

7

Discussion

Contents

7.1 Preamble

In this dissertation, I have studied the concept of demographic buffering – the means by which natural populations reduce the impact of environmental stochasticity on their population growth rate. This work has yielded:

1. A clarification on what buffering *actually* means in ecological modelling (Chapter

2).

2. A demonstration of how to use summed stochastic elasticities of variance $\sum E^{\sigma^2}_{a_{ij}}$ and second derivatives to quantify demographic buffering (Chapter 3).
3. A study that shows how demographic buffering is impacted by environmental variance and autocorrelation through distinct demographic mechanisms (Chapter 4).
4. A study that shows $\sum E^{\sigma^2}_{a_{ij}}$ to be an effective measure of demographic buffering (Chapter 5).
5. A review of the broad ideas surrounding animal life history evolution and where life history research may move in the future (Chapter 6).

Here, I will first provide a brief synopsis of the take-home messages of this doctoral dissertation. Second, I will identify two key ways in which this dissertation connects with the literature on demographic buffering – specifically with regard to the $\sum E^{\sigma^2}_{a_{ij}}$ and counterfactual approaches to nonlinear systems. And third, I will outline future directions for research into demographic buffering - not already discussed in Chapter 6.

7.2 Brief synopsis

This dissertation identifies the mechanisms that underly demographic buffering and introduces a method to quantify demographic buffering in structured populations. Across this dissertation, demographic buffering has been linked to two demographic mechanisms: demographic rates (Chp. 3, 4, 5) and population structure (Chp. 4, 5). Demographic rates and population structure hold up to the standard of buffering mechanisms as they fulfill the criteria laid out in Chapter 2. Specifically:

1. *With regard to being perturbation specific*, the impacts of demographic rates and population structure toward demographic buffering are specifically in response to environmental stochasticity.

2. *With regard to being an intrinsic mechanism*, both demographic rates and population structure are necessary for the projection of a structured populations across timesteps.

3. *With regard to having a focal metric*, the impacts of demographic rates and population structure on demographic buffering are quantified with respect to λ_s.

4. *With regard to having a benchmark*, the degree to which demographic rates and population structure buffer a population in a stochastic environment is quantified by the logged difference between the arithmetic mean population growth rate (λ_1) and the geometric mean population growth rate (λ_s).

In addition to identifying these mechanisms, this dissertation has broadly characterized $\sum E^{\sigma^2}_{a_{ij}}$ as a measure of demographic buffering (Chp. 3, 4, 5). For *between-population* level inferences of demographic buffering, $\sum E^{\sigma^2}_{a_{ij}}$ represents an effective tool for quantifying demographic buffering for interspecies comparisons (Chp. 3) as well as comparisons of the same population under different environmental scenarios (Chp. 4, 5). Furthermore, demographic buffering can also be explored at the *within-population* level (at the demographic rate level) by using first-order derivatives (*i.e.*, elasticities of population growth rate with respect to demographic rates) and second-order derivatives (*i.e.*, self-second derivatives of population growth rate with respect to demographic rates) (Chp. 3).

Regarding how $\sum E^{\sigma^2}_{a_{ij}}$ responds to stochastic environments, Chapter 4 shows how environmental variance and environmental autocorrelation impact $\sum E^{\sigma^2}_{a_{ij}}$ through distinct demographic mechanisms. Specifically, environment variance impacts $\sum E^{\sigma^2}_{a_{ij}}$ through demographic rate variance [as predicted from Tuljapurkar (1982, 1989, 1990)] and environmental autocorrelation impacts $\sum E^{\sigma^2}_{a_{ij}}$ through shifts in population structure [as predicted from Tuljapurkar and Haridas (2006)]. And, to confirm that $\sum E^{\sigma^2}_{a_{ij}}$ is an appropriate measure of demographic buffering, the efficacy of $\sum E^{\sigma^2}_{a_{ij}}$ as a measure of demographic buffering was also compared to other measures (*i.e.*, the Spearman's ρ correlation of elasticitites of λ and coefficient of variation values associated with individual demographic rates and two quantities derived from Tuljapurkar's approximation V_s, $V_s + V_c$) in Chapter 5, where$\sum E^{\sigma^2}_{a_{ij}}$ was identified as the most effective.

And finally, Chapter 6 synthesizes a large body of literature within life history theory and specifically outlined two major research programs that represent new frontiers for life history theorists which are intimately connected to the topic of demographic buffering[1] – *i.e.*, identifying where selection act in the construction of a life history strategy and the problem of time in life history evolution.

7.3 On the use of stochastic elasticities

One of the primary takeaways of this dissertation is the utility of the summation of stochastic elasticities of variance $\left(\sum E^{\sigma^2}_{a_{ij}}\right)$ for the study of demographic buffering. Chapters 3, 4 and 5 individually argue for why $\sum E^{\sigma^2}_{a_{ij}}$ is particularly useful for quantifying demographic buffering. However, two arguments for the utility of $\sum E^{\sigma^2}_{a_{ij}}$ remain unexplained – specifically regarding *definition* and the *number of demographic rates*. In turn, here I will outline these arguments, stemming from the literature and this dissertation, that $\sum E^{\sigma^2}_{a_{ij}}$ represents a useful measure of demographic buffering in structured populations.

7.3.1 Utility based on definition

Across this dissertation, demographic buffering has been defined as the ability of a population to accommodate the often negative impacts of environmental stochasticity on population growth rate (see page 7). Since population dynamics are governed by underlying demographic rates (*e.g.*, survival, growth, reproduction), demographic buffering is attributed to the collection of demographic rates that govern a population's dynamics, as it is the interaction of these rates that determine the sensitivity of a population to environmental stochasticity (Tuljapurkar et al., 2003).

The sensitivity of a population to environmental stochasticity is best expressed by Tuljapurkar's approximation [as detailed on pages 9 and 95, Tuljapurkar (1982, 1989,

---

[1] For an additional line of future research that bridges the gap between life history evolution and stochastic demography, see Appendix B.

1990)].

$$\log(\lambda_s) \approx \log(\lambda_1) - \frac{1}{2}\left[\sum_{ij} e_{ij}^2 \mathrm{CV}_{ij}^2 + \sum_{ij\neq kl} e_{ij} e_{kl} \left(\frac{\mathrm{cov}(a_{ij}, a_{kl})}{\bar{a}_{ij}\,\bar{a}_{kl}}\right)\right] \tag{7.1}$$

In addition to quantifying the impact of environmental stochasticity on population dynamics, Tuljapurkar's approximation also allows a quantification of demographic buffering based on this small-noise approximation – the summed quantity in the square brackets. In other words, the quantity in the square brackets of Tuljapurkar's approximation (Eq. 7.1) represents a mathematical approach to quantify the extent to which a population's demographic rates make it more or less sensitive to environmental stochasticity. And, since Tuljapurkar's approximation can be rewritten as,

$$\log(\lambda_s) \approx \log(\lambda_1) + \frac{1}{2}\left[\sum E_{a_{ij}}^{\sigma^2}\right], \tag{7.2}$$

$\sum E_{a_{ij}}^{\sigma^2}$ represents a measure of demographic buffering supported by both the definition of demographic buffering and Tuljapurkar's approximation. However, the most common method of quantifying demographic buffering is not directly supported in this way.

Across the literature, the most common method used to quantify demographic buffering is the correlation method (see Hilde et al., 2020). Specifically, most studies that measure demographic buffering use regressions of elasticities/sensitivities of population growth rate with respect to the coefficient of variation (CV)/variance (σ^2) of demographic rates through time (as per Pfister, 1998). Whilst the basis for the correlation method comes from Tuljapurkar's approximation[2], the output of the correlation method has no direct relationship to how the population will respond to environmental stochasticity. For example, imagine two populations (population A and population B) of the same species for whom the Spearman's ρ correlations between elasticities of population growth rate (λ) and demographic rate CV are measure. Let's say that the correlation method outputs Spearman's ρ coefficients of -0.7 and -0.1 for populations A and B, respectively. Given the logic of the correlation method, one can infer that both populations A and B are demographically buffered. However, from the infomation above alone one cannot infer that population A is less sensitive to environmental stochasticity than population B.

---

[2] As described on page 96.

This lack of inference is due to no direction connection between the correlation method and Tuljapurkar's approximation. On the other hand, if $\sum E^{\sigma^2}_{a_{ij}}$ is quantified for both populations A and B and the emerging estimates are -0.05 and -0.5, respectively, then one can infer that population A's demographic rates make population A 10 times less sensitive to environmental stochasticity than population B. In turn, $\sum E^{\sigma^2}_{a_{ij}}$ is a measure of demographic buffering that is intimately connected to Tuljapurkar's approximation (see the square brackets of Equations 7.1 and 7.2). Thus $\sum E^{\sigma^2}_{a_{ij}}$ first the definition of demographic buffering, whilst the correlation method (ρ) does not.

7.3.2 Utility across the number of demographic rates

The second argument for the utility of $\sum E^{\sigma^2}_{a_{ij}}$ as a measure of demographic buffering over other existing metrics is with respect to the number of demographic rates. The metric $\sum E^{\sigma^2}_{a_{ij}}$ is a measure of demographic buffering that is a agnostic to the number of demographic rates involved in the population model. In other words, whether the population is modelled by a time series of 2×2 matrix population models (Caswell, 2001) (*e.g.*, two discrete stages in the life cycle, say juveniles and adults) or an integral projection model (Easterling et al., 2000; Ellner et al., 2016) discretized into a $1,000 \times 1,000$ mesh, $\sum E^{\sigma^2}_{a_{ij}}$ is calculable and unbiased by the dimensionality of the population of interest (see values of $\sum E^{\sigma^2}_{a_{ij}}$ in Chapters 3 and 4). However, the same cannot be said for the correlation method.

The correlation method of demographic buffering often involves calculating the Spearman's ρ coefficient of elasticities/sensitivities of population growth rate with respect to CV/variance of demographic rates (Hilde et al., 2020; Pfister, 1998). Admittedly, previous work has shown that the correlation method can result in "spurious correlations" due to the finite domain of some demographic rates (Morris & Doak, 2004) – *e.g.*, since survival rates can only vary between 0 and 1, the maximum possible variance of a mean survival of 0.5 is far greater than that of a survival rate of 0.99[3]. However, the biases of

---

[3] Specifically, Morris and Doak (2004) recommend scaling the variances (σ^2) and coefficients of variance (CV) of demographic rates relative to their maximal possible of σ^2 and CV. In turn, the corrected $\sigma^2$and CV of survival values (p) can be calculated by dividing the raw σ^2 and CV values by $p(1-p)$ and $\sqrt{\frac{1-p}{p}}$, respectively.

the correlation method include more than the problems of variance – the Spearman's ρ coefficients themselves are a form of bias.

To illustrate how bias can arise from Spearman's ρ correlations, one can ask: What does the null distribution of the Spearman ρ coefficients look like? And, does the number of demographic rates impact the shape of this distribution? In reality, the number of demographic rates substantially transforms the shape of the null distribution of Spearman's ρ coefficients (Fig. 7.1). The reason for the impact of demographic rate number on Spearman's ρ correlation coefficients is simple. The number of demographic rates that project a population from time t to time $t + 1$ is finite. In turn, the number of combinations of rank-orders across demographic rates is also finite (*i.e.*, ranking demographic rates first to last across their elasticity and coefficients of variation). For example, if a population is modelled using three demographic rates [*e.g.*, (1) progression from the juvenile stage to the adult stage, (2) stasis within the adult stage and (3) adult reproduction of new juveniles], only four possible Spearman's ρ coefficients can be calculated (*i.e.*, -1, -0.5, 0.5 and 1; Fig. 7.1b). This particular scenario is especially problematic in studies that use both negative and positive values of Spearman's ρ as representations of demographic buffering and demographic lability, respectively (Hilde et al., 2020; McDonald et al., 2017). Therefore, the correlation method for determining demographic buffering is biased by the number of demographic rates analysed.

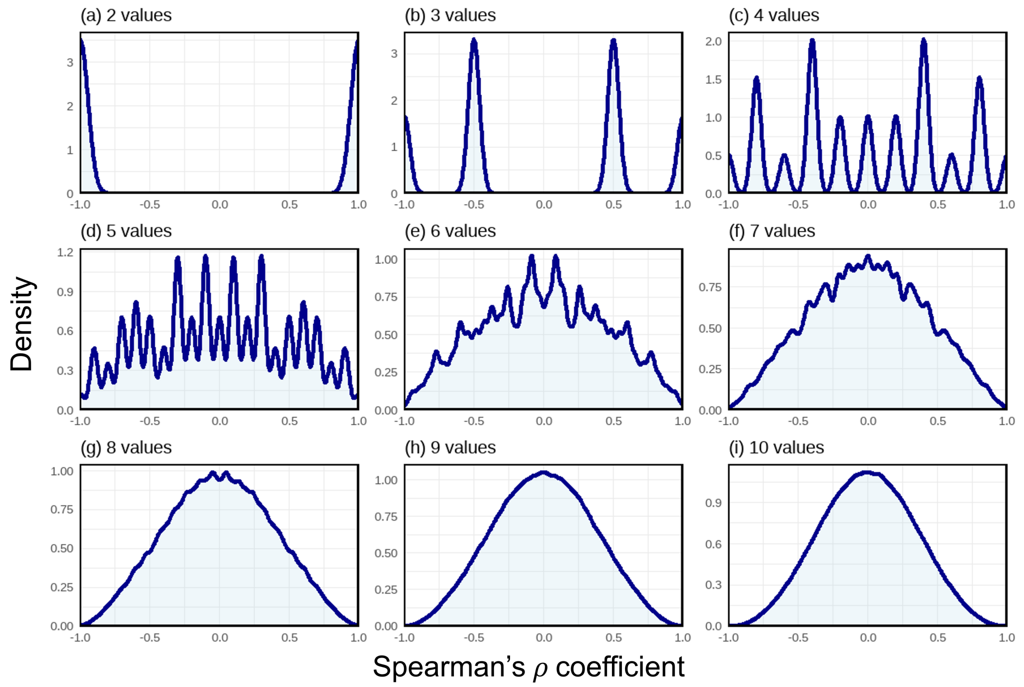

Figure 7.1: The number of demographic rates biases the null distribution of Spearman's ρ coefficient values. Above shows the null-distribution of Spearman's ρ coefficient values for sets ranging from 2 values (a) to 10 values (i). These null distributions were generated from 100,000 randomly generated rank-orders and then plotted using a density function.

To summarize, $\sum E_{a_{ij}}^{\sigma^2}$ represents an *unbiased* metric of demographic buffering as its values are unbiased by the number of demographic rates. However, the correlation method *is biased* as the null distribution of Spearman ρ coefficients (1) does not span the domain from -1 to 1 in a unimodal fashion (*e.g.*, Fig. 7.1a-d) and (2) shifts corresponding to the number of demographic rates analysed.

7.4 Counterfactual approaches to nonlinear systems

Across this dissertation, counterfactuals (*i.e.*, alternative representations of a real system) have been used to study demographic buffering. For example, in Chapter 4, environmental autocorrelation and variance were manipulated to illustrate the response of $\sum E_{a_{ij}}^{\sigma^2}$ (Fig. 4.3), mean buffered size (Fig. 4.4) and the contributions of demographic rates (Fig. 4.5) across these two axes. Furthermore, in Chapter 5, the demographic rates associated with individual stage classes and all stage classes were stabilized (*i.e.*, kept constant through time or scaled closer their mean values) to compare and contrast the efficacy of four alternative measures of demographic buffering (Figs. 5.3, 5.4). Admittedly, this counterfactual approach is not the only way these research questions could have been answered. A great deal of theory has been developed to show how populations respond to stochastic environments (Jaggi et al., 2023; Klinkhamer & Jong, 1983; Orzack, 1985; Orzack & Tuljapurkar, 1989; Roerdink, 1988, 1989; Tuljapurkar, 1982, 1989, 1990; Tuljapurkar et al., 2009a; Tuljapurkar & Haridas, 2006; Tuljapurkar & Istock, 1993; Wiener & Tuljapurkar, 1994). So, why did this dissertation not use analytic methods? The reason for this counterfactual approach is based on non-linearity of population responses to variable environments and the high dimensionality of integral projection models.

The research conducted within this dissertation is explicitly focused on a nonlinear system. Briefly put, the definition of a nonlinear system is the mapping of an input to an output where a proportional change in the input does not result in a proportional change in the output[4]. And, with respect to this dissertation, the response of populations to stochastic environments is an example of a non-linear system. When discussing environmental autocorrelation and variance (as in Chapter 4), proportional increases in autocorrelation, variance and their interaction do not lead to proportional changes in population dynamics. Whilst Tuljapurkar's approximation (Eq. 7.1, 7.2) linearizes the system to approximate these proportional contributions, the utility of Tuljapurkar's approximation breaks down as environmental stochasticity increases. Simply put, Tuljapurkar's approximation is a small noise approximation – *i.e.*, a Taylor expansion relating the geometric mean (λ_s) to the arithmetic mean (λ_1) based on small variances in underlying parameters (demographic rates, a_{ij}). In turn, to explore how populations respond to environmental stochasticity (Chapter 4) and test for efficacy (Chapter 5), new counterfactual methods were generated.

Counterfactual methods are common tools in stochastic demography. From perturbation analysis (Morris & Doak, 2002), process-based modelling (Bocedi et al., 2021; Lustenhouwer et al., 2023) to life history evolution (Travis et al., 2021), counterfactual methods are tools utilized across ecology and evolution to understand the response

---

[4] For a detailed explanation of how simple nonlinear systems lead to complex dynamics, see May (1976).

of nonlinear systems. These tools are often employed when analytical solutions are unknown, uninformative or intractable. For example, in Chapters 4 and 5, the following equation was used to calculate stochastic elasticities of variance:

$$\sum E^{\sigma^2}_{a_{ij}} = \sum \left[\frac{\mathrm{var}(a_{ij})}{\lambda_s} \times \frac{\lambda_s^{*a_{ij}} - \lambda_s}{0.00001 \times \mathrm{var}(a_{ij})} \right]. \tag{7.3}$$

This equation calculates $\sum E^{\sigma^2}_{a_{ij}}$ using a series of counterfactuals. In other words, $\sum E^{\sigma^2}_{a_{ij}}$ is calculated by:

1. Re-running a projection of the population in a stochastic environment where the variance of individual demographic rates is proportionally increased (by a factor of $0.00001 \times \mathrm{var}(a_{ij})$).
2. Calculating a new stochastic population growth rate arising from the perturbation ($\lambda_s^{*a_{ij}}$) and subtracting the stochastic population growth rate associated with the population (λ_s).
3. Summing all the differences proportional to the variance of the demographic rates divided by λ_s.

Yet, the calculation of $\sum E^{\sigma^2}_{a_{ij}}$ can be achieved analytically (as in Chapter 3, see Haridas and Tuljapurkar, 2005). So, why not use this approach in Chapters 4 and 5? The reason, we chose a counterfactual approach is due to the scale of the nonlinear system. In Chapter 3, low-dimensional MPMs were used with relatively low numbers of timesteps. However, in Chapters 4 and 5, populations represented high-dimensional IPMs that were projected across 1,000 timesteps. In turn, the eigen-decomposition of these systems was intractable – thereby supporting our counterfactual approach.

7.5 Future work

7.5.1 Connecting $\sum E^{\sigma^2}_{a_{ij}}$ to second derivatives of population growth rate

In Chapter 3, I outline a unified framework to quantify demographic buffering in natural populations. Specifically, within this framework, we show how demographic buffering *between populations* can be quantified using $\sum E^{\sigma^2}_{a_{ij}}$. And, we showed how demographic buffering within populations can be quantified using second derivatives of population growth rate. These two measures lend a new perspective on demographic buffering by explicitly stating the levels at which demographic buffering can take place – *i.e.*, *between vs. within populations*. However, across this dissertation, these two levels have not been connected. For example, the works in Chapters 4 and 5 are specifically focused on the *between population level* and $\sum E^{\sigma^2}_{a_{ij}}$, not the *within population level* and second derivatives. Interestingly, this dichotomy is not absolute and, thus, represents an exciting avenue of research that may bridge the gap between demographic buffering and demographic lability.

The literature on demographic buffering and demographic lability has often pitched these two demographic strategies against each other – as opposite sides of the same coin (Hilde et al., 2020; McDonald et al., 2017; Salguero-Gómez, 2021). However, this perspective overlooks a key difference between the two strategies. As discussed on page 7, demographic buffering is an environment – vital reaction norm *agnostic* metric. In other words, demographic buffering assumes a negative impact of environmental stochasticity on population growth rate (see page 15). On the other hand, demographic lability is an environment – vital rate reaction norm *informed* metric. Specifically, demographic lability can arise if the reaction norm between a fitness related trait (*e.g.*, demographic rate) and an environment parameter is ∪-shaped (*i.e.*, convex). Importantly, second derivatives of population growth rate explicitly measure the convexity/concavity of environment – vital rate reaction norms, not $\sum E^{\sigma^2}_{a_{ij}}$.

Recent work in demographic lability has generated a generalizable metric to quantify demographic lability in structured populations. Le Coeur et al. (2022) shows how to quantify the strength of convexity and concavity using second derivatives of population growth rate to generate a nonlinearity index (D). This nonlinearity index explicitly tests for demographic lability in structured populations. The work in this dissertation has aimed to do the same for demographic buffering. In turn, stitching together demographic buffering (as measured by $\sum E^{\sigma^2}_{a_{ij}}$) and demographic lability (as measured by the nonlinearity index

D) represents an exciting frontier in stochastic demography. Since these methods are distinct, we can test whether demographic buffering and demographic lability are in fact opposite sides of the same coin or whether buffering and lability can arise independently in structured populations.

7.5.2 Connecting demographic buffering to life history evolution

One of the weaknesses of the demographic buffering literature is with regard to causal evolutionary mechanisms. Whilst demographic buffering emerges in populations as an ecological response to stochastic environments (Pfister, 1998; Hilde et al., 2020), the evolutionary contribution towards the demographic buffering phenomenon represents a key gap in knowledge (although see Koons et al., 2009; Barraquand and Yoccoz, 2013). For example, whilst Chapter 4 clearly outlined how demographic rates and population structured mediate the impacts of environmental variance and autocorrelation, the question as to *why* these mechanisms exist remains unanswered. In other words, does demographic buffering arise as an evolved response of a population to a variable environment? Or, is demographic buffering the result of a constraint imposed by stochastic environments on structured populations?

To answer the question as to whether demographic buffering is an evolved response, high resolution longitudinal data is required. Specifically, natural or laboratory populations who have been exposed to changes in environmental stochasticity across generations would be necessary to answer this question. Some candidate natural populations for this study include the Soay Sheep (*Ovis aries*; Childs et al., 2011; Clutton-Brock and Pemberton, 2004; Coulson et al., 2001; Milner et al., 1999), Rum deer (*Cervus elaphus*; Nussey et al., 2008), Svalbard reindeer (*Rangifer tarandus platyrhynchus*; Hansen et al., 2019) or Dewy pines (*Drosophyllum lusitanicum*; Conquet et al., 2023). Some candidate laboratory populations include *Drosophila melanogaster* (James et al., 1997; Marshall & Sinclair, 2010), *Callosobruchus maculatus* (Bull & Bonsall, 2008) and *Escherichia coli* (Jouvet et al., 2018).

To test whether demographic buffering is an evolved response in structured populations, two analyses can be performed. The first analysis includes a moving window analysis (see Bahlai et al., 2021) where $\sum E^{\sigma^2}_{a_{ij}}$ is calculated across a timeline where environmental stochasticity also varies. Specifically, $\sum E^{\sigma^2}_{a_{ij}}$ would be calculated using discrete temporal bins (*e.g.*, 3 timesteps) starting from the beginning of the time series to the last timestep (ω) in increments of one timestep (*e.g.*, $\sum E^{\sigma^2}_{a_{ij}}$ would be calculated for timesteps 1 to 3, 2 to 4, 3 to 5, ..., $\omega - 3$ to $\omega - 1$, $\omega - 2$ to ω). If demographic buffering is an evolved response, we would first predict a cross-taxonomic pattern where degrees of demographic buffering are positively associated with degrees of environmental stochasticity. The second analysis includes a common garden experiment. After finding the cross-taxonomic pattern from natural and laboratory populations, common garden experiments can be performed on populations reared in either a stochastic or constant environment. The common garden experiment will be used to test whether the evolved increase in demographic buffering in the stochastic environment population confers a fitness advantage when compared to the constant environment population.

Admittedly, this line of research does not preclude the analysis of demographic lability in these systems. In turn, if the first line of proposed future work is accomplished (*i.e.*, connecting demographic buffering and lability using $\sum E^{\sigma^2}_{a_{ij}}$ and second derivatives), this second line of research could also be used to test under what circumstances do demographic buffering and demographic lability evolve.

7.5.3 Comparative demographic buffering in stochastic environments

One of the methodological limitations of the work performed in Chapters 4 and 5 is in regard to how stochasticity is included in the IPMs. Across these chapters, we used parameter-stochastic IPMs – *i.e.*, IPMs whose vital rate regression coefficients are functions of one or more environmental variables (see Appendix A). This IPM structure easily lends itself for simulation studies as the generation of a 1,000 kernel time series is relatively simple. However, most population models of structured populations in variable environments are not parameter-stochastic. Instead, most models are stochastic at the level of the **K**-kernel (for IPMs) or matrix (for MPMs). This difference is non-trivial for the scaling of Chapter 4 (*i.e.*, the study of demographic buffering across a parameter space of environmental autocorrelation and variance) across the tree of life.

Altering the environmental variance of a matrix-stochastic set of MPMs is relatively simple[5]. However, the difficulty lies in altering environmental autocorrelation. In chapter 4, environmental autocorrelation was implemented at the parameter level through a first order autoregressive function.

$$\mathbf{X}_{t+1} = \varphi \mathbf{X}_t + \epsilon_{t+1} \tag{7.4}$$

Here, φ represents the degree of autocorrelation across time steps whilst, ϵ_{t+1} represents white noise (*i.e.*, random draws from a normal distribution, $\epsilon \sim N(0, 1)$). However, this method is not possible for discrete states – *e.g.*, a matrix-stochastic set of MPMs.

Previous work testing the impact of discrete environmental autocorrelation on population dynamics has primarily focused on two-state scenarios – *i.e.*, good *vs.* bad environments (Paniw et al., 2018; Smallegange et al., 2014; Tuljapurkar & Haridas, 2006). The primary reason for the focus on two-state scenarios is due to the ease in implementing the environment in the form of a stochastic matrix **M**:

$$\mathbf{M} = \begin{bmatrix} p_g & p_b \\ 1 - p_g & 1 - p_b \end{bmatrix} \tag{7.5}$$

Here, the probabilities p_g and p_b represent the probabilities of transitioning to the good environment across timesteps from the good and bad environments, respectively. In addition to this simplicity, autocorrelation can be implemented with the parameterization of good *vs.* bad environment frequencies *a priori* (see Tuljapurkar and Haridas, 2006). However, this format has not been generalized to more than two states which poses a serious impediment to the scaling of Chapter 4 across the tree of life. In turn, future work must focus on building these methods.

---

[5] The rescaling of environmental variance in a set of MPMs can be achieved by rescaling MPMs within the set ($\mathbf{A}_x$) relative to their difference in population growth rate (λ_x) from the population growth rate associate with the mean matrix (λ_1). In other words, the rescaled value of $\mathbf{A}_x$ ($\mathbf{A}'_x$) can be calculated as $\mathbf{A}'_x = \mathbf{A}_x \left(\frac{\lambda_1 + \alpha(\lambda_x - \lambda_1)}{\lambda_x} \right)$ where α is the rescaling parameter. This rescaling approach is just as intuitive as how proportional variances were used in Chapter 4 - *i.e.*, if $\alpha = 0$: all matrices rescaled to λ_1; if $0 < \alpha < 1 = 0$: all matrices rescaled so the distribution of population growth rate values is closer to λ_1; if $\alpha = 1$: all matrices remain the same; and if $\alpha > 1$: all matrices are rescaled so the distribution of population growth rate values is further from λ_1.

A method to build stochastic matrices for more than two states

Here, I discuss a framework to build stochastic matrices for more than two states in order to scale the work in Chapter 4 across the tree of life.

First, to build these stochastic matrices, an assumption must be made about how heterogeneity is to be treated across the different states. For example, if a population has three associated MPMs (named A, B and C) across different environments:

- Should the differences between these MPMs be based on identity - *e.g.*, nominally by defining MPMs by their names A, B and C?
- Should the differences between these MPMs be based on their rank-order in population growth rate (λ) - *e.g.*, ordinally by ranking MPMs A, B and C by λ from lowest to highest?
- Or, should the differences between these MPMs be based on their absolute differences in population growth rate (λ) – *e.g.*, continuously by ranking MPMs A, B and C by their differences in raw λ values?

Admittedly, these distinctions are important but cannot be answered in this discussion. However, below I outline a potential mathematical formulation of stochastic matrices for states structured nominally, ordinally and continuously to hopefully scale these methods in the future.

For nominally structured states, the parameterization of the stochastic matrix is quite simple. In the nominal case, autocorrelation relates to the probability of being in the same state across timesteps. For example, an autocorrelation value of 1 means the environment sampled at time t and $t + 1$ must be the same. An autocorrelation value of 0 refers to white noise – *i.e.*, equal probabilities across all states. And, an autocorrelation value of -1 means the environment sampled at time t and $t + 1$ must be different. In turn, the nominal stochastic matrix for a population exposed to N states with an autocorrelation of φ can constructed with intermediary values ($\hat{p}_{ij}$) denoting the transitions from state j

to state *i* following this piece-wise equation:

$$\hat{p}_{ij} = \begin{cases} \frac{1+\varphi}{2} & i = j \\ \frac{1-\varphi}{2} & i \neq j \end{cases} \tag{7.6}$$

Admittedly, whilst this piecewise function obeys the rules for nominal autocorrelation described above, the piecewise function is incomplete as columns of the stochastic matrix ($\hat{\mathbf{p}}_j$) must sum to 1. In turn, to convert values of $\hat{p}_{ij}$ into the probabilities that makeup the stochastic matrix (p_{ij}), values of $\hat{p}_{ij}$ must be normalized by the sum of their column in the stochastic matrix – *i.e.*, $p_{ij} = \frac{\hat{p}_{ij}}{\sum \hat{\mathbf{p}}_j}$ (Fig. 7.2).

For ordinal stochastic matrices, the rank-order of the states must be considered. For example, if states are labelled on a Likert-like scale including:

- very bad
- bad
- okay
- good
- very good,

a positive autocorrelation should reflect an increased probability for the transition very good → good in comparison to very good → very bad. Likewise, a negative autocorrelation should reflect an increased probability for the transition very good → very bad in comparison to very good → good. In turn, the ordinal stochastic matrix can be parameterized following these rules:

- An autocorrelation of 1 means the probability of transitioning across N states (*e.g.*, very good → very bad) equals 0.
- An autocorrelation of 0 refers to white noise – *i.e.*, equal probabilities across all states.
- An autocorrelation of -1 means the probability of transitioning to and from the same state (*e.g.*, very good → very good) equals 0.

In turn, intermediary values of $\hat{p}_{ij}$ for an ordinal stochastic matrix with N states and autocorrelation φ can be calculated as:

$$\hat{p}_{ij} = \begin{cases} \frac{1+\varphi}{2} & i = j \\ \frac{\frac{-2\varphi|j-i|}{N-1}+\varphi+1}{2} & i \neq j \end{cases} \tag{7.7}$$

After the calculation of the intermediary $\hat{p}_{ij}$ values, the probabilities (p_{ij}) can be calculated through normalizing by the sum of the columns, as in the nominal matrix – *i.e.*, $p_{ij} = \frac{\hat{p}_{ij}}{\sum \hat{\mathbf{p}}_j}$ (Fig. 7.2).

And finally, the continuous stochastic matrix can be computed following the same rules of the ordinal matrix. The only difference between the ordinal and continuous matrices is in how the states are ordered through continuous values (*e.g.*, λ) rather than rank-order. In turn, intermediary values of $\hat{p}_{ij}$ for a continuous stochastic matrix with N states, a vector of associated population growth rate values $\boldsymbol{\lambda}$ and an autocorrelation φ can be calculated as:

$$\hat{p}_{ij} = \begin{cases} \frac{1+\varphi}{2} & i = j \\ \frac{\frac{-2\varphi|\lambda_j-\lambda_i|}{\max(\boldsymbol{\lambda})-\min(\boldsymbol{\lambda})}+\varphi+1}{2} & i \neq j \end{cases} \tag{7.8}$$

Subsequently, the intermediary values can be normalized as in the nominal and ordinal stochastic matrices – *i.e.*, $p_{ij} = \frac{\hat{p}_{ij}}{\sum \hat{\mathbf{p}}_j}$ (Fig. 7.2).

7.5.4 The role of transients in demographic buffering

The final avenue of future research in relation to my doctoral work on demographic buffering is in connection to transient dynamics. Transient dynamics are temporary fluctuations in populations that decay over time due to progressive shifts toward a stable age/stage/size structure. Across ecology, transient dynamics have been studied at the level of populations (Caswell, 2007; Ezard et al., 2010; Capdevila et al., 2020b), communities (Hastings, 2001; Hastings et al., 2018; Morozov et al., 2020), spatial ecology (Ovaskainen & Hanski, 2002) and whole ecosystems (Francis et al., 2021). This broad application of transient dynamics to ecosystem function is particularly useful when studying the stability and/or resilience of a system in response to a perturbation (Capdevila et al., 2020b). However, this perturbation rarely includes environmental stochasticity.

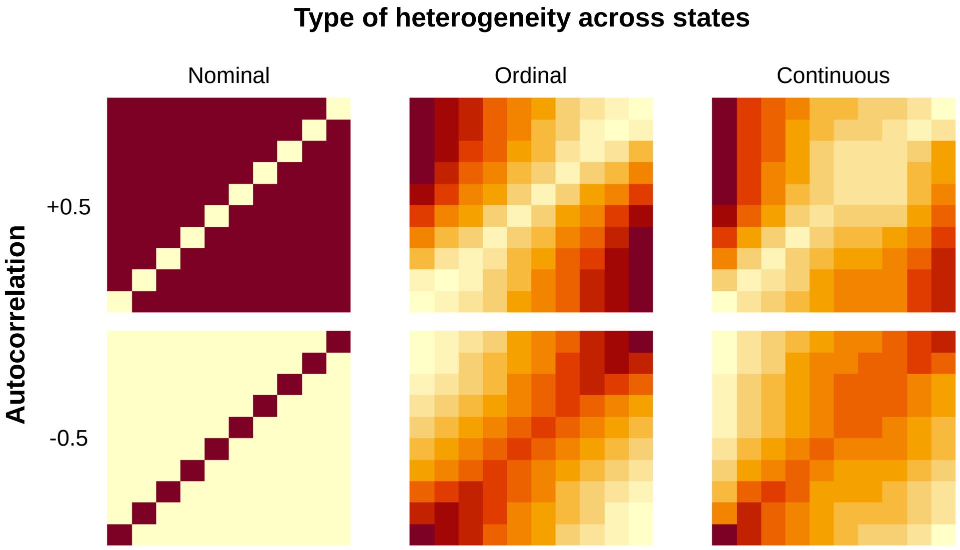

Figure 7.2: Nominal, ordinal and continuous approaches to constructing stochastic matrices. The above figure shows a proof of concept for the methods detailed above. Specifically, this figure visualizes six different stochastic matrices parameterized using the nominal, ordinal and continuous methods outlined above. The stochastic matrices represent transitions across 10 discrete states. The intensity of the red colouration corresponds to high probabilities whilst the pastel yellow corresponds to low probabilities. It is worth noting that the colour spectrum of each plot is unique to each matrix. To construct the continuous matrices, the following vector of λ values was used: 0.8, 0.9, 0.95, 1, 1.05, 1.08, 1.09, 1.1, 1.15, 1.2. Importantly, the uneven distribution of λ values drive the non-centrosymmetric structure of the continuous stochastic matrices. Since the nominal and ordinal matrices do not take these uneven intervals into account, both the nominal and ordinal matrices are centrosymmetric.

Across the literature, transient dynamics and stochastic demography remain disconnected. Despite vast bodies of literature in both camps (Capdevila et al., 2020b; Caswell, 2007; Doak et al., 2005; Engen et al., 1998; Grant & Benton, 2000; Hastings, 2001; Hilde et al., 2020; Koons et al., 2009; McDonald et al., 2016; Stott et al., 2011, 2012; White et al., 2013), the role of transient dynamics in population responses to environmental stochasticity remains unstudied (although see McDonald et al., 2016). This gap is made especially timely as recent work has shown that environmental stochasticity can be reframed as a series of environmental pulse disturbances, continuously shifting population structure about its asymptotic frequencies (Tuljapurkar et al., 2023). In turn, to bridge this gap between transient dynamics and demographic buffering, I detail a possible counterfactual approach to identify the role of transients in stochastic environments.

A method to quantify the role of transients in stochastic environments

Any stochastic environment can be represented as a temporal sequence of projection matrices (*i.e.*, $\mathbf{A}_t$). Tuljapurkar's approximation uses the temporal mean, variance and covariances of demographic rates within $\mathbf{A}_t$ to infer the role of demographic rate variance on population dynamics (Eq. 7.1, 7.2). However, this method explicitly uses the population structures that project through the environmental sequence $\mathbf{A}_t$.

The proposed method to quantify the role of transients dynamics in stochastic environments can be broken down into three steps. The first step of this method is to determine the stable age/stage/size distribution associated with $\mathbf{A}_t$ ($\hat{\mathbf{w}}$). This distribution can be measured analytically (Caswell, 2001) or simulated (as in Chapter 4 with mean buffered size). The second step of this method is to project a population vector ($\mathbf{n}_0$) through $\mathbf{A}_t$ and record the distance of each population vector ($\mathbf{n}_t$) from $\hat{\mathbf{w}}$ ($\mathbf{\Delta}_t$). Importantly, $\mathbf{\Delta}_t$ represents the relative (not absolute) distance between $\mathbf{n}_t$ and $\hat{\mathbf{w}}$. In turn, $\mathbf{\Delta}_t$ can be calculated as:

$$\mathbf{\Delta}_t = \frac{\mathbf{n}_t}{\sum \mathbf{n}_t} - \frac{\hat{\mathbf{w}}}{\sum \hat{\mathbf{w}}}. \tag{7.9}$$

The third step of this framework consists of reiterating the projection of $\mathbf{n}_0$ through $\mathbf{A}_t$ where the population structure at time t (*i.e.*, $\mathbf{n}_t$) is proportionally shifted closer to or further from $\hat{\mathbf{w}}$ based on the factor β to a new population structure $\mathbf{n}_t'$.

$$\mathbf{n}_t' = \left(\frac{\hat{\mathbf{w}}}{\sum \hat{\mathbf{w}}} + \beta \mathbf{\Delta}_t \right) \sum \mathbf{n}_t \tag{7.10}$$

In turn, $\mathbf{n}_t'$ represents a sequence of population vectors that have either been set proportional to $\hat{\mathbf{w}}$ (*i.e.*, $\beta = 0$), set proportionally closer to $\hat{\mathbf{w}}$ relative to $\mathbf{n}_t$ (*i.e.*, $0 < \beta < 1$), set proportional to $\mathbf{n}_t$ (*i.e.*, $\beta = 1$) or set proportionally further from $\hat{\mathbf{w}}$ than $\mathbf{n}_t$ (*i.e.*, $\beta > 1$). Therefore, calculating changes in long-run stochastic population growth rate (as in Chapter 5 with $\Delta\lambda_s$) in response to changes in β, represents a counterfactual approach to demonstrate the punitive or beneficial effects of transient dynamics in response to environmental stochasticity.

7.6 Concluding remark

This doctoral dissertation was driven by one focal research question: how do population dynamics and life histories respond to variable environments? The work within this dissertation has addressed one topic within this research question - *i.e.*, how to measure demographic buffering (defined as the means by which natural populations reduce the impact of environmental stochasticity on their population growth rate) and the mechanisms that underly this phenomenon. Identifying the metrics and mechanisms associated with demographic buffering has arisen from an integrative research program combining perturbation methods in structured populations (Tuljapurkar, 1982, 1990; Caswell, 1996b, 2001; Shyu & Caswell, 2014; Ellner et al., 2016) with open-access demographic data across the tree of life (Salguero-Gómez et al., 2015, 2016a; Jones et al., 2022; Levin et al., 2022). My work represents a step-wise change in our understanding of demographic buffering and outlines multiple lines of future research to progress this understanding even further. However, this work has not taken place in a vacuum. This dissertation builds on the shoulders of giants and, in particular, vast amounts of hard-fought demographic data. In other words, this dissertation has greatly benefited from a culture of open, reliable and transparent practices within ecology and evolutionary biology. Therefore, continuing and propagating this culture is imperative for (1) our future understanding of how population dynamics and life histories respond to variable environments and (2) the scientific community as a whole.

Appendices

All models are wrong, some are useful.

— George E. P. Box

Scientists generally agree that no theory is 100 percent correct. Thus, the real test of knowledge is not truth, but utility. Science gives us power. The more useful that power, the better the science.

— Yuval Noah Harari

A

IPM formulas, regressions and parameters

Contents

A.1 *Berberis thunbergii* IPM structure

Construction		**Model**	**Parameter**
Density-independent environmentally stochastic IPM		$n(z',t+1) = \int_{\alpha}^{\omega} K(z',z,\psi_t)n(z,t)dz$	$\alpha = 2$ $\omega = 25$ z = log(plant area)
		$\psi_t = \{T_t, P_t, PAR_t, N_t, pH_t\}$	ψ = an array containing climate values
***K*-kernel**		$K(z',z,\psi_t) = P(z',z,\psi_t) + F(z',z,\psi_t)$	
Sub-kernels	***P*-subkernel**	$P(z',z,\psi_t) = s(z,\psi_t) * g(z',z,\psi_t)$	
	***F*-subkernel**	$F(z',z,\psi_t) = f_s(z) * fl_p(z) * germ_p(\psi_t) * sdl_s(z')$	
Demographic functions	Survival	$\text{logit}(s(z,\psi_t)) = s_i + s_z * z + s_T * T_t + s_P * P_t + s_{PAR} * PAR_t + s_N * N_t + s_{pH} * pH_t$	s_i = -11.8 s_z = 1.05 s_T = 1.11 s_P = 0.22 s_{PAR} = -0.52 s_N = -0.1 s_{pH} = 0.11
	Growth	$g(z',z,\psi_t) = \text{dnorm}(z', g_\mu(z,\psi_t), g_{sd})$	g_{sd} = 1.48
		$g_\mu(z,\psi_t) = g_z * z + g_T * T_t + g_P * P_t + g_{PAR} * PAR_t + g_N * N_t + g_{pH} * pH_t$	g_z = 1.02 g_T = 0.65 g_P = 0.02 g_{PAR} = 0.59 g_N = -0.04 g_{pH} = 0.4
	Reproduction	$f_s(z) = \exp(seed_i + seed_z * z)$	$seed_i$ = -23.01 $seed_z$ = 1.32
		$\text{logit}(fl_p(z)) = fl_i + fl_z * z$	fl_i = -33.43 fl_z = 1.68
		$\text{logit}(germ_p(\psi_t)) = germ_i + germ_T * T_t + germ_P * P_t + germ_{PAR} * (PAR_t/0.018) + germ_{pH} * pH_t$	$germ_i$ = -11.8 $germ_T$ = 0.51 $germ_P$ = -0.02 $germ_{PAR}$ = -0.02 $germ_{pH}$ = 0.26
		$sdl_s(z') = \text{dnorm}(z', sdl_\mu, sdl_{sd})$	sdl_μ = 10.23 sdl_{sd} = 1.581
Environment values	Mean temperature in warmest month	$T \sim \text{N}(0, 1.5)$	
	Mean May precipitation	$P \sim \text{N}(0, 1.5)$	
	PAR	$PAR \sim \text{N}(0, 1.5)$	
	Soil Nitrogen	$N \sim \text{N}(0, 1.5)$	
	Soil pH	$pH \sim \text{N}(0, 1.5)$	

A.2 *Calathea crotalifera* IPM structure

Construction		**Model**	**Parameter**
Density-independent environmentally stochastic IPM		$n(z', t+1) = \int_{\alpha}^{\omega} K(z', z, \psi_t) n(z,t) dz$	$\alpha = 0.57$ $\omega = 11.9$ z = leaf area
		$\psi_t = \{j_t, A_t\}$	ψ = an array containing climate values
***K*-kernel**		$K(z', z, \psi_t) = P(z', z, j_t, A_t) + F(z', z, j_t)$	
Sub-kernels	***P*-kernel**	$P(z', z, j_t, A_t) = s(z, j_t) * g(z', z, j_t, A_t)$	
	***F*-kernel**	$F(z', z, j_t) = r_p(z, j_t) * r_o(z, j_t) * n_f * n_s * s_s(j_t) * sdl_s(j_t) * sdl_{size}(z', j_t)$	$n_f = 23$ $n_s = 3$
Demographic functions	Survival	$\text{logit}(s(z, \psi_t)) = s_i + s_z * z + s_j * j_t + s_{z*j} * z * j_t$	s_i = -2.74 $s_z = 0.95$ $s_j = 0.07$ s_{z*j} = -0.02
	Growth	$g(z', z, j_t, A_t) = \text{dnorm}(z', g_\mu(z, j_t, A_t), g_{sd})$	$g_{sd} = 1.53$
		$g_\mu(z, j_t, A_t) = g_i + g_z * z + g_j * j_t + g_A * A_t + g_{z*j} * z * j_t + g_{z*A} * z * A_t + g_{j*A} * j_t * A_t + g_{z*j*A} * z * j_t * A_t$	$g_i = 0.76$ $g_z = 0.9$ $g_j = 0.03$ $g_A = 0.006$ g_{z*j} = -0.001 $g_{z*A} = 0.00045$ g_{j*A} = -0.0052 $g_{z*j*A} = 0.00035$
	Reproduction	$\text{logit}(r_p(z, j_t)) = r_{p,i} + r_{p,z} * z + r_{p,j} * j_t + r_{p,z*j} * z * j_t$	$r_{p,i}$ = -13.23 $r_{p,z} = 1.401$ $r_{p,j}$ = -0.213 $r_{p,z*j} = 0.043$
		$r_o(z, j_t) = \exp(r_{o,i} + r_{o,z} * z + r_{o,j} * j_t + r_{o,z*j} * z * j_t)$	$r_{o,i}$ = -6.673 $r_{o,z} = 0.829$ $r_{o,j} = 0.067$ $r_{o,z*j}$ = -0.007
		$s_s(j_t < 6) = 0.29$ $s_s(j_t \geq 6) = 0.32$	
		$sdl_s(j_t < 6) = 0.14$ $sdl_s(j_t \geq 6) = 0.95$	
		$sdl_{size}(z', j_t < 6) = \text{dnorm}(z', 3.08, 0.54)$ $sdl_{size}(z', j_t \geq 6) = \text{dnorm}(z', 2.88, 1.4)$	
Environment values	Canopy openness*	$j \sim \text{N}(3, 1.4)$	
	Photosynthetic rate*	$A \sim \text{N}(6, 0.8)$	

* In Westerband and Horvitz (2017), canopy openness (*j*) and photosynthetic rate (*A*) were modelled as random samples from a sequence of values or draws from a uniform

distribution. Specifically canopy openness was realized at time t as random draws from the sequence $\{1,2,3,4,5\}$ whilst photosynthetic rate was realized at time t as random draws from a uniform distruction (*i.e.*, $A \sim \mathcal{U}(5,7)$). However, since our manipulation of the environment involves explicitly changing the temporal variance of a series, we coerced the distributions into normal distributions with the same mean and reported variance of the original sampling distributions reported in Westerband and Horvitz (2017).

A.3 *Carlina vulgaris* IPM structure

Construction		**Model**	**Parameter**
Density-independent environmentally stochastic IPM		$n(z',t+1) = \int_{\alpha}^{\omega} K(z',z,\psi_t)n(z,t)dz$	α = 1.5 ω = 5 z = log(longest leaf length) ψ_t = an array containing the parameters associated with environmentally stochastic demographic functions
K-kernel		$K(z',z,\psi_t) = P(z',z,\psi_t) + F(z',z,\psi_t)$	
Sub-kernels	***P***-subkernel	$P(z',z,\psi_t) = p_s(z,\psi_t) * [1 - p_f(z)] * g(z',z,\psi_t)$	
	F-subkernel	$F(z',z,\psi_t) = p_s(z,\psi_t) * p_f(z,\psi_t) * f_n(z) * f_d(z',\psi_t) * p_e$	p_e = 0.00095
Demographic functions	Size dynamics: Rosette growth and recruit size	$g(z',z,\psi_t) = \text{dnorm}\left(z', g_\mu(z,\psi_t), g_{sd}\right)$	g_{sd} = 0.29
		$g_\mu(z,\psi_t) = g_{i,t} + g_{z,t}(z)$ $f_{d,t} = \text{dnorm}\left(z', f_\mu, f_{sd}\right)$	$g_i, r_\mu \sim \text{MVN}(\boldsymbol{\mu}, \boldsymbol{\Sigma})$ $\boldsymbol{\mu} = (1.14, 3.16)$ $\boldsymbol{\Sigma} = \begin{pmatrix} 0.037 & 0.041 \\ 0.041 & 0.075 \end{pmatrix}$ $g_z \sim$ N(0.74, 0.13) f_{sd} = 0.5
	Probability of survival	$\text{logit}(p_s(z,\psi_t)) = s_i + s_z * z$	$s_i \sim$ N(-2.28, 1.16) $s_z \sim$ N(0.90, 0.41)
	Probability of flowering	$\text{logit}(fl_p(z,\psi_t)) = fl_i + fl_z * z$	$fl_i \sim$ N(-16.19, 1.03) fl_z = 3.88
	Seed production	$f_n(z) = \exp{(A + B * \text{z})}$	$A = 1, B = 2$

A.4 *Heliconia tortuosa* IPM structure

Construction		**Model**	**Parameter**
Density-independent environmentally stochastic IPM		$n(z', t+1) = \int_{\alpha}^{\omega} K(z', z, \psi_t) n(z, t) dz$	$\alpha = 0.78$ $\omega = 11.07$ z = leaf area
		$\psi_t = \{j_t, A_t\}$	ψ = an array containing climate values
***K*-kernel**		$K(z', z, \psi_t) = P(z', z, j_t, A_t) + F(z', z, j_t)$	
Sub-kernels	***P*-kernel**	$P(z', z, j_t, A_t) = s(z, j_t) * g(z', z, j_t, A_t)$	
	***F*-kernel**	$F(z', z, j_t) = r_p(z, j_t) * r_o(z, j_t) * n_f * n_s * s_s(j_t) * sdl_s(j_t) * sdl_{size}(z', j_t)$	$n_f = 37$ $n_s = 2.5$
Demographic functions	Survival	$\text{logit}(s(z, \psi_t)) = s_i + s_z * z + s_j * j_t + s_{z*j} * z * j_t$	s_i = -2.05 $s_z = 0.78$ s_j = -0.22 $s_{z*j} = 0.05$
	Growth	$g(z', z, j_t, A_t) = \text{dnorm}(z', g_{\mu}(z, j_t, A_t), g_{sd})$	$g_{sd} = 0.71$
		$g_{\mu}(z, j_t, A_t) = g_i + g_z * z + g_j * j_t + g_A * A_t + g_{z*j} * z * j_t + g_{z*A} * z * A_t + g_{j*A} * j_t * A_t + g_{z*j*A} * z * j_t * A_t$	$g_i = 2.6$ $g_z = 0.56$ g_j = -1.55 $g_A = 0.44$ $g_{z*j} = 0.18$ g_{z*A} = -0.034 $g_{j*A} = 0.014$ g_{z*j*A} = -0.0014
	Reproduction	$\text{logit}(r_p(z, j_t)) = r_{p,i} + r_{p,z} * z + r_{p,j} * j_t + r_{p,z*j} * z * j_t$	$r_{p,i}$ = -12.55 $r_{p,z} = 1.527$ $r_{p,j} = 0.154$ $r_{p,z*j}$ = -0.013
		$r_o(z, j_t) = \exp(r_{o,i} + r_{o,z} * z + r_{o,j} * j_t + r_{o,z*j} * z * j_t)$	$r_{o,i}$ = -1.009 $r_{o,z} = 0.157$ $r_{o,j}$ = -0.382 $r_{o,z*j} = 0.048$
		$s_s(j_t < 6) = 0.15$ $s_s(j_t \geq 6) = 0.2$	
		$sdl_s(j_t < 6) = 0.26$ $sdl_s(j_t \geq 6) = 0.33$	
		$sdl_{size}(z', j_t < 6) = \text{dnorm}(z', 2.73, 0.71)$ $sdl_{size}(z', j_t \geq 6) = \text{dnorm}(z', 2.34, 1.17)$	
Environment values	Canopy openness	$j \sim \text{N}(3, 1.4)$	
	Photosynthetic rate	$A \sim \text{N}(6.5, 0.8654937)$	

* In Westerband and Horvitz (2017), canopy openness (j) and photosynthetic rate (A) were modelled as random samples from a sequence of values or draws from a uniform

distribution. Specifically canopy openness was realized at time t as random draws from the sequence $\{1,2,3,4,5\}$ whilst photosynthetic rate was realized at time t as random draws from a uniform distruction (*i.e.*, $A \sim \mathcal{U}(5,8)$). However, since our manipulation of the environment involves explicitly changing the temporal variance of a series, we coerced the distributions into normal distributions with the same mean and reported variance of the original sampling distributions reported in Westerband and Horvitz (2017).

You can run, but if you can't run anymore, then you can hide. You can hide, but if you can't hide anymore, then you can fight. There is nothing after the fight, so you fight until there is nothing.

— Mark Greaney (2016)

B

A phase diagram of life histories in variable environments

The impact of variable environments on life histories is a key topic in life history evolution and population dynamics (Sutherland et al., 2013). The reason for this importance is, in addition to being interesting, global climate change is predicted to change environment variability [a key driver of variance in life history processes (Jackson et al., 2022)] across the globe – posing an imminent threat to biodiversity (Bathiany et al., 2018; Drake, 2005; Masson-Delmotte et al., 2021; Vasseur et al., 2014).

Much of our current understanding around life histories in variable environments is centred around Tuljapurkar's small noise approximation (Tuljapurkar, 1989, Eq. B.1).

$$\log(\lambda_s) \approx \log(\lambda_1) - \frac{\sigma^2 + \tau}{2\lambda_1^2} + \frac{\theta}{\lambda_1^2} \tag{B.1}$$

Here, the logarithmic long-run stochastic population growth rate [$\log(\lambda_s)$] can be approximated via the population growth rate associated with the mean environment (λ_1) with contributions from demographic rate variances (σ^2), covariances (τ) and temporal autocorrelation (θ). In studies of life histories in variable environments, $\log(\lambda_s)$ is often used as a measure of fitness associated with a specific life history strategy (Cubaynes et al., 2022). In turn, researchers have been interested in the ways by which life histories can optimize $\log(\lambda_s)$ given the terms on the right-hand side of the equation.

Over the course of the past decades, multiple studies have explored the impact of demographic rate variances (σ^2: Doak et al., 2005; Engen et al., 1998; Foley, 1994; McDonald et al., 2017; Morris et al., 2008; Morris and Doak, 2004; Pfister, 1998; Sæther, 1997; Sæther et al., 1998) with relatively less focus on demographic rate covariances (Compagnoni et al., 2016; Fay et al., 2022b) and environment autocorrelation (Evers et al., 2023; Gascoigne et al., 2023a; Tuljapurkar & Haridas, 2006). Similarly, despite a large body of literature, little focus is given to the relationship between the most important term in Tuljapurkar's approximation, $\log(\lambda_1)$, and the variance components. This represents a key gap in knowledge as the simplest way for a life history strategy to improve its associated fitness is through changes in its mean demographic rates, not variance components. And unfortunately, shifts in mean life history strategies cannot be neatly uncoupled from variances as they confound one another. Therefore, we argue life history theory would benefit from a new perspective to probe life history evolution in variable environments.

To build this new perspective, imagine a focal population of interest is being exposed to a novel perturbation (*e.g.*, predation, increased temperature, disease). In response to this perturbation, the focal population can canonically respond in three ways. These responses include: *fight*, *flight* and *hide*. Whilst differentially successful dependent on the type of perturbation, all of these responses represent possible strategies to deal with a novel perturbation.

This framework is useful as the same set of strategies can be utilized by populations in response to environmental variability. In response to the threat of environmental variability, populations can evolve life history strategies whereby they can (Fig. B.1a):

- persist (*fight*) via plasticity or adaptation to the variable environment.
- escape the environment (*flight*) via dispersal, migration or vagrancy.

- avoid the timestep (*hide*) via dormancy, torpor or hibernation.

These strategies are insightful as, in addition to being strategically distinct, their costs are broadly distinct as well (Fig. B.1a):

- *fighting* involves the cost of environmental variability outlined in Tuljapurkar's approximation (*i.e.*, variance in demographic rates).
- *flight* often involves a cost to demographic rates (*i.e.*, reduced survival or reproductive output).
- *hiding* involves a cost directly to fitness in the form of extending generation time.

From these costs we can build a visual representation of when and where each strategy should be selected for.

Here, we propose a phase diagram of life histories in variable environments (Fig. B.1b). Taking inspiration from the 150-year-old concept of phase diagrams in physics and chemistry, we show a framework whereby different combinations of costs associated with dispersal/migration/vagrancy and dormancy/torpor/hibernation can evolve and, as a strategy, invade the population. We hypothesize this phase diagram will look very different for life histories with different ecologies (*e.g.*, Fig. B.1c,d).

To test this phase diagram, we recommend a combination of theoretical modelling and experimental approaches. Modelling using two/multiple patch systems (Steiner et al., 2014; Sultan & Spencer, 2002) would allow a researcher to vary the cost of dispersal *a priori* – however we note the cost of dispersal can come in a variety of forms which should also be explicitly explored (Bonte et al., 2012). Furthermore, we recommend a modelling approach to explore a variety of life history archetypes to see how life histories shape the phase diagram (Takada et al., 2018). Analytical and individual-based eco-evolutionary models can be used to provide theoretical predictions on the evolution of, for example, dispersal *vs.* dormancy *vs.* *in situ* adaptation, under different combination of life histories, ecological conditions and relative costs of the different strategies (Gerber & Kokko, 2018; Travis et al., 2021; Vitalis et al., 2013).

Regarding experimental approaches, we recommend the use of insects with defined stages of development which also exhibit differential dispersal morphology [*e.g.*, the seed beetle *Callosobruchus maculatus* (Gascoigne et al., 2022; Sanghvi et al., 2021, 2022) with experimental evolution approaches (Lustenhouwer et al., 2023)]. In seed beetles, multiple patch systems can be constructed to moderate the cost of dispersal, and temperature during juvenile development can be used to moderate cost of dormancy (here defined as prolonged development time).

We acknowledge that the costs associated with the *fight*, *flight* and *hide* strategies are not mutually exclusive. For example, it is quite likely that a cost of dispersal on demographic rates leads to a shift in generation time. However, we offer this phase diagram of life histories in variable environments as both a hypothesis and a heuristic to start testing life history evolution beyond variance components.

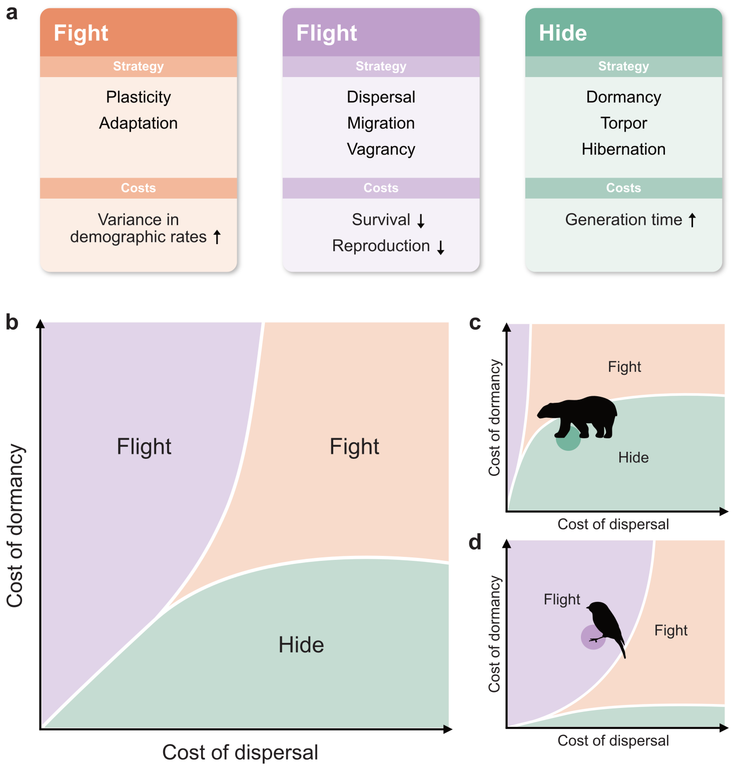

Figure B.1: A phase diagram of life histories in variable environments. Here, we illustrate how life history evolution in variable environments can be represented by three different competing strategies: *fighting* (persisting in the face of environmental variability), *flight* (escaping the immediate threat of environmental variability) and *hiding* (avoid a time-step through dormancy/hibernation/torpor to reduce the impact of environmental variability. (a) The costs of each strategy are broadly independent and can, thus, be viewed as in competition with one another. To visualize this competition, we construct a phase diagram (b, resembling phase diagrams from physics and chemistry). Here, the *fight*, *flight* and *hide* strategies emerge at different combinations of costs associated with the *flight* and *hide* strategies. We use dispersal and dormancy to represent the focal cost, but this could easily be migration/vagrancy or hibernation/torpor. We note that this space may look very different across species – shown by the polar bear (c) and the blue tit (d). The utility of this framework arises by the placing of a population on this phase diagram. To illustrate this, the polar is in the *hide* region – meaning the polar bear population could be successfully invaded by a life history strategy that has a relatively longer period of hibernation than the rest of the population. Likewise, the blue tit population in the *flight* region – meaning the blue tit population could be successfully invaded by a life history strategy that involves relatively more dispersal events across habitable patches than the rest of the population. We hypothesize that manipulating the costs along this space should predictably change the position of the population on the phase diagram.

> *It's the side projects that really take off. By side projects I mean the stuff that you thought was just messing around. Stuff that's just play. That's actually the good stuff. That's when the magic happens.*
>
> — Austin Kleon (2012)

C

Other works

The following publications and manuscripts have arisen from work performed during my DPhil:

- Salguero-Gómez, R., Jackson, J., & Gascoigne, S. J. L. (2021). Four key challenges in the open-data revolution. *Journal of Animal Ecology*, *90*, 2000–2004. https://doi.org/10.1111/1365-2656.13567
- Vinton, A. C., Gascoigne, S. J. L., Sepil, I., & Salguero-Gómez, R. (2022). Plasticity's role in adaptive evolution depends on environmental change components. *Trends in Ecology & Evolution*, *37*, 1067–1078. https://doi.org/10.1016/j.tree.2022.08.008
- Vinton, A. C., Gascoigne, S. J. L., Sepil, I., & Salguero-Gómez, R. (2023). The importance of spatial and temporal structure in determining the interplay between plasticity and evolution. *Trends in Ecology & Evolution*, *38*, 221–223. https://doi.org/10.1016/j.tree.2022.12.009
- Veit, W., Gascoigne, S. J. L., & Salguero-Gómez, R. (2023). Evolution, complexity, and life history theory. *Authorea*. https://doi.org/10.22541/au.167770655.

56360178/v1

- Bernard, C., Santos, G. S., Deere, J. A., Rodriguez-Caro, R., Capdevila, P., Kusch, E., Gascoigne, S. J. L., Jackson, J., & Salguero-Gómez, R. (2023). Mosaic - A unified trait database to complement structured population models. *Scientific Data*, *10*. https://doi.org/10.1038/s41597-023-02070-w

- Gascoigne, S. J. L., Rolph, S., Sankey, D., Nidadavolu, N., Pičman, A. S. S., Hernández, C. M., Philpott, M. E., Salam, A., Bernard, C., Fenollosa, E., Lee, Y. J., McLean, J., Perera, S. H. A., Spacey, O. G., Kajin, M., Vinton, A. C., Archer, C. R., Burns, J. H., Buss, D. L., … Salguero-Gómez, R. (2023c). A standard protocol to report discrete stage-structured demographic information. *Methods in Ecology & Evolution*. https://doi.org/10.1111/2041-210X.14164

- Wood, A., Gascoigne, S. J. L., Gambetta, G. A., Jeffers, E., & Coulson, T. (2023). Seasonal weather impacts wine quality in Bordeaux. *iScience*. https://doi.org/10.1016/j.isci.2023.107954

- Huang, Y., Wu, C., Huang, W., Liu, Y., Qi, M., Bai, J., Dong, Y., Gascoigne, S. J. L., Ciais, P., Peñuelas, J., & Salguero-Gómez, R. (2023). Climate change has desynchronized insect and vegetation phenologies across europe. *bioRxiv*. https://doi.org/10.1101/2023.12.11.571152

- Tuljapurkar, S., Jaggi, H., Gascoigne, S. J. L., Zuo, W., Kajin, M., & Salguero-Gómez, R. (2023). From disturbances to nonlinear fitness and back. *bioRxiv*. https://doi.org/10.1101/2023.10.20.563360

- Sanghvi, K., Vega-Trejo, R., Nakagawa, S., Gascoigne, S. J. L., Johnson, S. L., Salguero-Gómez, R., Pizzari, T., & Sepil, I. (2024). Meta-analysis shows no consistent evidence for senescence in ejaculate traits across animals. *Nature Communications*, *15*. https://doi.org/10.1038/s41467-024-44768-4

Received: 14 April 2021 | Accepted: 6 July 2021
DOI: 10.1111/1365-2656.13567

RESEARCH HIGHLIGHT

Journal of Animal Ecology BRITISH ECOLOGICAL SOCIETY

Four key challenges in the open-data revolution

Roberto Salguero-Gómez[1,2] | **John Jackson**[1] | **Samuel J. L. Gascoigne**[1]

[1]Department of Zoology, University of Oxford, Oxford, UK

[2]Max Planck Institute for Demographic Research, Rostock, Germany

Correspondence
Roberto Salguero-Gómez
Email: rob.salguero@zoo.ox.ac.uk

Funding information
Natural Environment Research Council, Grant/Award Number: NE/M018458/1

Handling Editor: Jennifer Gill

Abstract

In Focus: Culina, A., Adriaensen, F., Bailey, L. D., et al. (2021) Connecting the data landscape of long-term ecological studies: The SPI-Birds data hub. *Journal of Animal Ecology*, https://doi.org/10.1111/1365-2656.13388. Long-term, individual-based datasets have been at the core of many key discoveries in ecology, and calls for the collection, curation and release of these kinds of ecological data are contributing to a flourishing open-data revolution in ecology. Birds, in particular, have been the focus of international research for decades, resulting in a number of uniquely long-term studies, but accessing these datasets has been historically challenging. Culina et al. (2021) introduce an online repository of individual-level, long-term bird records with ancillary data (e.g. genetics), which will enable key ecological questions to be answered on a global scale. As well as these opportunities, however, we argue that the ongoing open-data revolution comes with four key challenges relating to the (1) harmonisation of, (2) biases in, (3) expertise in and (4) communication of, open ecological data. Here, we discuss these challenges and how key efforts such as those by Culina et al. are using FAIR (Findable, Accessible, Interoperable and Reproducible) principles to overcome them. The open-data revolution will undoubtedly reshape our understanding of ecology, but with it the ecological community has a responsibility to ensure this revolution is ethical and effective.

KEYWORDS
big data, demography, FAIR, individual-level data, interoperability, open access, ornithology, reproducible research

It has been over a decade since the publication of Clutton-Brock and Sheldon's (2010) review highlighting the importance of long-term, individual-based studies of animals for our understanding of ecology. The importance of these studies has in no way lessened. Key discoveries from long-term, individual-based studies in the last decade have been made on topics as broad as the evolution of sociality (Aplin et al., 2015; Firth et al., 2018), the role of climatic variation on intra-annual population dynamics (Paniw et al., 2019) and the role of individual differences in shaping ecological interactions (Griffiths et al., 2020). However, a new era in ecological research has emerged—the era of open data. Here, opportunities lie not only in the temporally rich insights made by one study but also in the broad patterns revealed by many. The recent publication in the *Journal of Animal Ecology* by Culina et al. (2021) introducing the SPI-birds data hub is an important contribution towards the ongoing momentum that is bringing ecology into this new era: one where data, tools, pipelines and expertise/advise are shared unconditionally and for free across the community.

Calls to arms to ecologists for a more biogeographically representative, longer-term, open-access body of biodiversity data are not new. However, these calls have become more prominent in recent years (Mills et al., 2015; Wilson, 2017). Recognition of the importance of open-access data and reproducible research pipelines in ecology has led multiple funding agencies (e.g. NERC, NSF, ARC) and journal publishers, including the British Ecological Society (2016), to 'strongly suggest' in the first instance, and later to mandatorily require for published research to be FAIR (Wilkinson et al., 2016): Findable, Accessible, Interoperable (i.e. data can interact with other data and workflows) and Reusable. Precipitated by this new research model, but also by ecologists' ethos regarding open access (Gallagher et al., 2020), volumes of ecologically relevant data are being amassed and subsequently released; these titanic efforts continue despite the glaring lack of funding support in most countries (Farley et al., 2018; Hampton et al., 2013).

Despite the great progress made in the last decade in open data in ecology, one should not get too comfortable. The open, big data landscape that is starting to emerge in ecology brings new challenges that may test more traditional ecological mindsets (Hampton et al., 2013). Here, we discuss four of these challenges, namely regarding (1) harmonisation, (2) biases, (3) expertise and (4) communication (Figure 1). For each, we provide examples of how and why the challenge arises and how the framework employed by Culina et al. (2021) navigates them using FAIR principles as a model for future efforts in the era of open data.

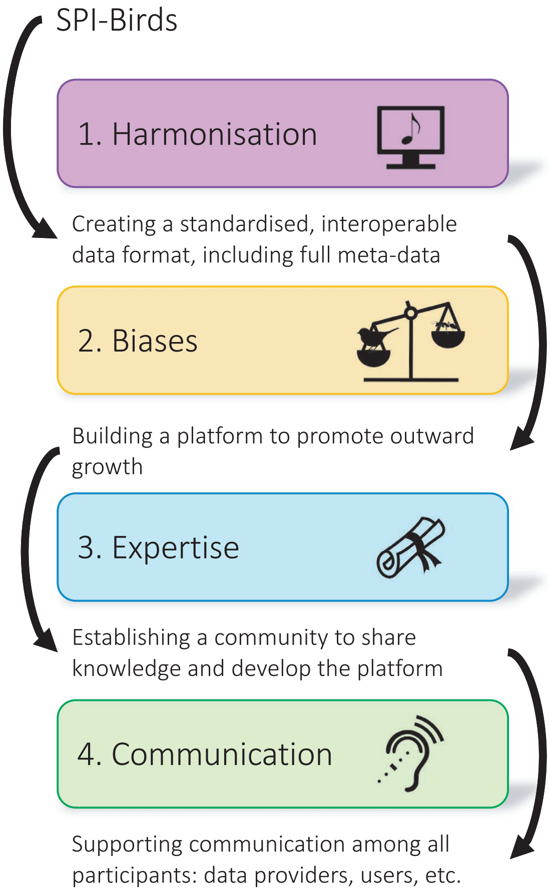

FIGURE 1 Four key challenges in the era of open data in ecology, and how the SPI-Birds database (Culina et al., 2021) has developed an effective platform to navigate these challenges

1 | CHALLENGE 1. HARMONISING OPEN DATA

Different datasets, even when collected strictly within the same sub-field of ecology (e.g. animal population ecology), can differ vastly. For instance, ornithologists refer to the term 'recruitment' as the age at which an individual first reproduces (J.D. Lebreton, pers. comm. 2015; B. Sheldon, pers. comm. 2021), whereas plant ecologists refer to it as the germination of a seedling (Harper, 1977). Thus, it is strongly advised to harmonise (i.e. standardise and homogenise) data from various sources, or databases that house data from different researchers and sub-disciplines, before the proposed analyses are conducted (Nadrowski et al., 2013) so that they are Interoperable and Reusable. Culina et al. (2021) navigate this through an interoperability pipeline and develop standardised formats for data such as the breeding season in the SPI-bird data hub (Figure 1). Furthermore, database curators invest significant efforts and time harmonising data and complementing them with metadata, as well as creating thesaurus to help users navigate their rich platforms (e.g. Garnier et al., 2017; Pey et al., 2014). However, sometimes the information detailed in the original sources, such as MSc/PhD thesis, grey reports, peer-review publications in different languages, does not allow for this task to be performed satisfactorily. When the harmonisation of data is incomplete, users of databases may benefit from the warnings and errors identified by database curators. For instance, in SPI-bird (Culina et al., 2021), there are *standard quality checks*, and warnings are explicitly noted as values that are uncommon or unusual, while 'likely errors' are flagged as seemingly impossible values. It is important to note that the ultimate responsibility to correctly conduct an analysis with open-access ecological databases remains with the user. Just because one *can* run an analysis with all the data at one's disposal, it does not mean one *should* do so.

2 | CHALLENGE 2. BIASES IN OPEN DATA

Naturally, the search for broad global patterns in ecology will only be as robust as the data that analyses are based on. Many global ecological datasets are taxonomically biased towards mammals and birds. In the case of long-term animal ecology datasets, a significant proportion of studies and databases are well represented primarily in areas of the planet with low biodiversity (Titley et al., 2017), or in areas that are actually least vulnerable to climate change (Paniw et al., 2021). Likewise, most terrestrial biodiversity is found in countries with low GDP, for which fewer data exist relative to countries with higher GDP. Like many initiatives, Culina et al. (2021) also display these geographic biases. Instead, the present study takes the approach of creating a framework and standards for the 'well-defined' community (primarily in northern Europe) that acts as a platform for global efforts (Figure 1).

We propose several ways that ecologists may navigate this challenge. As a minimum, ecologists using open-access data in ecology to search for global patterns must be aware of (and account for, where possible) geographic and taxonomic biases, contextualising findings rather than making blanket statements about findings occurring 'worldwide'. Likewise, phylogenetic approaches offer numerous tools to impute missing data following patterns of phylogenetic inertia—but one needs to be aware of which tools fit the job better (Gallagher et al., 2020). Finally, cross-matching algorithms to improve the overlap of interoperable databases can drastically increase the analytical power (Pennell et al., 2016). Ultimately however, greater international efforts are needed to increase the coverage of global biodiversity data in under-represented countries. In this regard, the application of conservation prioritisation in data-poor countries to expedite ecological data collection is a promising avenue of progress (El-Gabbas et al., 2020; Kujala et al., 2018). Furthermore, the development of lasting partnerships between researchers in high-income and low-income countries to build capacity is required to even biases in ecological data archiving (Donhauser & Shaw, 2019).

3 | CHALLENGE 3. EXPERTISE IN OPEN DATA

There is also a need to acquire the necessary expertise in the field to harness the full potential of the data. The multitude of records made available by, in this case, the SPI-Bird data hub contain great potential. However, the large volumes of data cannot be a substitute for the invaluable ornithological expertise of the researchers who collected the data, nor the quantitative skills of researchers used to analyse them. Unfortunately, this kind of expertise also tends to be geographically clustered in countries with high GDP and relatively low biodiversity. Culina et al.'s approach to this challenge is to nurture an active community in which researchers and data users are engaged with one another and building skills through workshops/meetings (Figure 1). In our experience, this approach is essential for the effective implementation of large-scale open-data platforms that overcome geographic and socio-political biases. At COMPADRE (Salguero-Gómez et al., 2015) and COMADRE (Salguero-Gomez et al., 2016), for instance, we have run workshops in three different languages and in four continents on over 30 occasions, and we have now adopted a strategy where we prioritise attendance of researchers from low-income countries.

4 | CHALLENGE 4. IMPROVING COMMUNICATION OF THE OPEN-DATA COMMUNITY

The era of big data in ecology is being support by a community composed of—at least—four different entities: data contributors, data curators, funding agencies and journals/societies. These entities risk failure of the whole enterprise if they do not adequately engage with each another. As such, communication and trust between them is critical. For instance, one of the main reasons that researchers may choose not to share data and contribute them to open-access databases is the risk of being scooped (Laine, 2017). This reticence to share data can prevail even though research has shown that researchers who publish second still end up getting a substantial portion of the recognition (Callaway, 2019). A way that open-data curators can support data contributors to overcome this initial concern is by offering an embargo period (something that we do in COMPADRE and COMADRE, but of which <1% of contributors request), or the possibility of making their data accessible (not open access) on the condition that they be offered co-authorship. SPI-Birds (Culina et al., 2021) partly follow the latter model, but with a minimal percentage of their total data (Figure 1). As a minimal requirement, SPI-Birds users must explicitly acknowledge any data owners and funding sources of the raw data (stored in meta-data). This not only improves communication in the community but also makes the raw data more findable in the future.

Database curators should make sure that credit be placed where it is due. Requesting that the original paper introducing a given database be cited when the database is used seems logical. However, what is even more logical—as well as fair and F.A.I.R.—is to request the individual contributing authors be cited too. This action to ensure appropriate accreditation may be hard to implement due to (1) the lack of database infrastructure to replicate a subset of citations in the final analysis and/or (2) the lack of space in journal prints to accommodate the potentially hundreds of the citations. For the former, some databases have already developed the functionality to provide database users with a citation summary of the data they have downloaded. For the latter, the move by many journals and societies from printed version to online only means that price-per-page is no longer a limitation to citation counts (Fox et al., 2016). In this way, data contributing researchers can benefit from other users utilising their data.

5 | FINAL REMARKS

Noah's ecological data ark is beginning to get crowded. However, ecologists, data curators, funding agencies, journals and ecological societies need to adapt their mindsets, infrastructures and approaches to fill this ark faster, with fewer biases, and more efficiently. A more coordinated effort between data contributors, curators, users, journals and societies will result in much-needed interoperability. Culina et al. (2021) is a testament to a new way of interaction, one that promotes FAIR principles to overcome these challenges and actively promotes international collaboration. Ultimately, the inherent value of SPI-Birds (Culina et al., 2021) will grow exponentially when considered in conjunction with, for instance, the long-term trends of insects on which birds depend (via InsectChange; Van Klink et al., 2021), human influence (via the Human Footprint Database; Venter et al., 2016) and climatic patterns (via CHELSA; Karger et al., 2017). The promise of big, open-access data in ecology is huge. We must endeavour, as a community, to deliver it.

ACKNOWLEDGEMENTS

We are grateful to the thousands of animal ecologists who routinely make their data open access and contribute them to open-access repositories, as well as the founding agencies, societies and journals that support open-access policies. Much of our own thinking regarding open access was drastically shaped by the generosity of M. Franco and J. Silvertown (founders of COMPADRE), who gave RSG their data for 100 plant demographic models without conditions. Without their gest, we would not have considered creating COMADRE and PADRINO, or setting them all open access. We have benefitted from conversations with P. Petraitis, S. Chamberlain, O. Jones, J. Che-Castaldo, D. Conde, A. Scheuerlein, D. Hodgson, T. Knight and many others. R.S.G. was supported by a NERC Independent Research Fellowship (NE/M018458/1).

CONFLICT OF INTEREST

The authors declare no conflicts of interest.

AUTHORS' CONTRIBUTIONS

R.S.-G. conceived the ideas and wrote the first version of the manuscript; J.J. created the figure; J.J. and S.J.L.G. contributed critically to the drafts and gave final approval for publication.

ORCID

Roberto Salguero-Gómez https://orcid.org/0000-0002-6085-4433
John Jackson https://orcid.org/0000-0002-4563-2840
Samuel J. L. Gascoigne https://orcid.org/0000-0002-2984-1810

REFERENCES

Aplin, L. M., Farine, D. R., Morand-Ferron, J., Cockburn, A., Thornton, A., & Sheldon, B. C. (2015). Experimentally induced innovations lead to persistent culture via conformity in wild birds. *Nature*, *518*, 538–541. https://doi.org/10.1038/nature13998

British Ecological Society. (2016). *Open data in the British Ecological Society*. Retrieved from https://www.britishecologicalsociety.org/open-data-in-the-british-ecological-society-journals/

Callaway, E. (2019). Scooped in science? Relax, credit will come your way. *Nature*, *575*(7784), 576–577. https://doi.org/10.1038/d41586-019-03648-4

Clutton-Brock, T., & Sheldon, B. C. (2010). Individuals and populations: The role of long-term, individual-based studies of animals in ecology and evolutionary biology. *Trends in Ecology & Evolution*, *25*, 562–573. https://doi.org/10.1016/j.tree.2010.08.002

Culina, A., Adriaensen, F., Bailey, L. D., Burgess, M. D., Charmantier, A., Cole, E. F., Eeva, T., Matthysen, E., Nater, C. R., Sheldon, B. C., Saether, B. E., Vriend, S. J. G., Zajkova, Z., Adamik, P., Aplin, L. M., Angulo, E., Artemyev, A., Barba, E., Barisic, S., … Visser, M. E. (2021). Connecting the data landscape of long-term ecological studies: The SPI-Birds data hub. *Journal of Animal Ecology*. https://doi.org/10.1111/1365-2656.13388

Donhauser, J., & Shaw, J. (2019). Knowledge transfer in theoretical ecology: Implications for incommensurability, voluntarism, and pluralism. *Studies in History and Philosophy of Science*, *77*, 11–20. https://doi.org/10.1016/j.shpsa.2018.06.011

El-Gabbas, A., Gilbert, F., & Dormann, C. F. (2020). Spatial conservation prioritisation in data-poor countries: A quantitative sensitivity analysis using multiple taxa. *BMC Ecology*, *20*, 35. https://doi.org/10.1186/s12898-020-00305-7

Farley, S. S., Dawson, A., Goring, S. J., & Williams, J. W. (2018). Situating ecology as a big-data science: Current advances, challenges, and solutions. *BioScience*, *68*, 563–576. https://doi.org/10.1093/biosci/biy068

Firth, J. A., Cole, E. F., Ioannou, C. C., Quinn, J. L., Aplin, L. M., Culina, A., McMahon, K., & Sheldon, B. C. (2018). Personality shapes pair bonding in a wild bird social system. *Nature Ecology & Evolution*, *2*, 1696–1699. https://doi.org/10.1038/s41559-018-0670-8

Fox, C. W., Paine, C. E. T., & Sauterey, B. (2016). Citations increase with manuscript length, author number, and references cited in ecology journals. *Ecology and Evolution*, *6*, 7717–7726. https://doi.org/10.1002/ece3.2505

Gallagher, R. V., Falster, D. S., Maitner, B. S., Salguero-Gomez, R., Vandvik, V., Pearse, W. D., Schneider, F. D., Kattge, J., Poelen, J. H., Madin, J. S., Ankenbrand, M. J., Penone, C., Feng, X., Adams, V. M., Alroy, J., Andrew, S. C., Balk, M. A., Bland, L. M., Boyle, B. L., … Enquist, B. J. (2020). Open Science principles for accelerating trait-based science across the Tree of Life (vol. 4, p. 294, 2019). *Nature Ecology & Evolution*, *4*, 662.

Garnier, E., Stahl, U., Laporte, M. A., Kattge, J., Mougenot, I., Kuhn, I., Laporte, B., Amiaud, B., Ahrestani, F. S., Bonisch, G., Bunker, D. E., Cornelissen, J. H. C., Diaz, S., Enquist, B. J., Gachet, S., Jaureguiberry, P., Kleyer, M., Lavorel, S., Maicher, L., … Klotz, S. (2017). Towards a thesaurus of plant characteristics: An ecological contribution. *Journal of Ecology*, *105*, 298–309. https://doi.org/10.1111/1365-2745.12698

Griffiths, J. I., Childs, D. Z., Bassar, R. D., Coulson, T., Reznick, D. N., & Rees, M. (2020). Individual differences determine the strength of interactions. *Proceedings of the National Academy of Sciences of the United States of America*, *117*, 17068–17073.

Hampton, S. E., Strasser, C. A., Tewksbury, J. J., Gram, W. K., Budden, A. E., Batcheller, A. L., Duke, C. S., & Porter, J. H. (2013). Big data and the future of ecology. *Frontiers in Ecology and the Environment*, *11*, 156–162. https://doi.org/10.1890/120103

Harper, J. L. (1977). *Population biology of plants*. Academic Press.

Karger, D. N., Conrad, O., Bohner, J., Kawohl, T., Kreft, H., Soria-Auza, R. W., Zimmermann, N. E., Linder, H. P., & Kessler, M. (2017). Data descriptor: Climatologies at high resolution for the earth's land surface areas. *Scientific Data*, *4*, 170122. https://doi.org/10.1038/sdata.2017.122

Kujala, H., Lahoz-Monfort, J. J., Elith, J., & Moilanen, A. (2018). Not all data are equal: Influence of data type and amount in spatial conservation prioritisation. *Methods in Ecology and Evolution*, *9*, 2249–2261. https://doi.org/10.1111/2041-210X.13084

Laine, H. (2017). Afraid of scooping – Case study on researchers strategies against fear of scooping in the context of open science. *Data Science Journal*, *16*, 29.

Mills, J. A., Teplitsky, C., Arroyo, B., Charmantier, A., Becker, P. H., Birkhead, T. R., Bize, P., Blumstein, D. T., Bonenfant, C., Boutin, S., Bushuev, A., Cam, E., Cockburn, A., Cote, S. D., Coulson, J. C., Daunt, F., Dingemanse, N. J., Doligez, B., Drummond, H., … Zedrosser, A.

(2015). Archiving primary data: Solutions for long-term studies. *Trends in Ecology & Evolution*, *30*, 581–589. https://doi.org/10.1016/j.tree.2015.07.006

Nadrowski, K., Ratcliffe, S., Bonisch, G., Bruelheide, H., Kattge, J., Liu, X. J., Maicher, L., Mi, X. C., Prilop, M., Seifarth, D., Welter, K., Windisch, S., & Wirth, C. (2013). Harmonizing, annotating and sharing data in biodiversityecosystem functioning research. *Methods in Ecology and Evolution*, *4*, 201–205. https://doi.org/10.1111/2041-210x.12009

Paniw, M., James, T. D., Ruth Archer, C., Römer, G., Levin, S., Compagnoni, A., Che-Castaldo, J., Bennett, J. M., Mooney, A., Childs, D. Z., Ozgul, A., Jones, O. R., Burns, J. H., Beckerman, A. P., Patwary, A., Sanchez-Gassen, N., Knight, T. M., & Salguero-Gómez, R. (2021). The myriad of complex demographic responses of terrestrial mammals to climate change and gaps of knowledge: A global analysis. *Journal of Animal Ecology*, *90*, 1398–1407. https://doi.org/10.1111/1365-2656.13467

Paniw, M., Maag, N., Cozzi, G., Clutton-Brock, T., & Ozgul, A. (2019). Life history responses of meerkats to seasonal changes in extreme environments. *Science*, *363*, 631–635. https://doi.org/10.1126/science.aau5905

Pennell, M. W., FitzJohn, R. G., & Cornwell, W. K. (2016). A simple approach for maximizing the overlap of phylogenetic and comparative data. *Methods in Ecology and Evolution*, *7*, 751–758. https://doi.org/10.1111/2041-210X.12517

Pey, B., Laporte, M. A., Nahmani, J., Auclerc, A., Capowiez, Y., Caro, G., Cluzeau, D., Cortet, J., Decaens, T., Dubs, F., Joimel, S., Guernion, M., Briard, C., Grumiaux, F., Laporte, B., Pasquet, A., Pelosi, C., Pernin, C., Ponge, J. F., ... Hedde, M. (2014). A Thesaurus for soil invertebrate trait-based approaches. *PLoS ONE*, *9*, e108985. https://doi.org/10.1371/journal.pone.0108985

Salguero-Gomez, R., Jones, O. R., Archer, C. R., Bein, C., de Buhr, H., Farack, C., Gottschalk, F., Hartmann, A., Henning, A., Hoppe, G., Romer, G., Ruoff, T., Sommer, V., Wille, J., Voigt, J., Zeh, S., Vieregg, D., Buckley, Y. M., Che-Castaldo, J., ... Vaupel, J. W. (2016). COMADRE: A global data base of animal demography. *Journal of Animal Ecology*, *85*, 371–384.

Salguero-Gómez, R., Jones, O. J., Archer, C. R., Buckley, Y. M., Che-Castaldo, J. P., Caswell, H., Hodgson, D. J., Scheuerlein, A., Conde, D. A., Brinks, E., Farack, C., Gottschalk, F., Hartmann, A., Henning, A., Hoppe, G., Römer, G., Runge, J., Ruoff, T., Wille, J., ... Vaupel, J. W. (2015). The COMPADRE Plant Matrix Database: An open online repository for plant demography. *Journal of Ecology*, *103*, 202–208.

Titley, M. A., Snaddon, J. L., & Turner, E. C. (2017). Scientific research on animal biodiversity is systematically biased towards vertebrates and temperate regions. *PLoS ONE*, *12*, e0189577. https://doi.org/10.1371/journal.pone.0189577

Van Klink, R., Bowler, D. E., Driessen, M. M., Ernest, S. K. M., Gentile, A., Gilbert, F., Gongalsky, K. B., Owen, J., Pe'er, G., Pe'er, I., Resh, V. H., Rochlin, I., Schuch, S., Swengel, A. E., Swengel, S. R., Valone, T. J., Vermeulen, R., Wepprich, T., Wiedmann, J. L., & Chase, J. M. (2021). InsectChange: A global database of temporal changes in insect and arachnid assemblages. *Ecology*, *102*, e03354.

Venter, O., Sanderson, E. W., Magrach, A., Allan, J. R., Beher, J., Jones, K. R., Possingham, H. P., Laurance, W. F., Wood, P., Fekete, B. M., Levy, M. A., & Watson, J. E. M. (2016). Sixteen years of change in the global terrestrial human footprint and implications for biodiversity conservation. *Nature Communications*, *7*, 11. https://doi.org/10.1038/ncomms12558

Wilkinson, M. D., Dumontier, M., Aalbersberg, I. J. J., Appleton, G., Axton, M., Baak, A., Blomberg, N., Boiten, J.-W., da Silva Santos, L. B., Bourne, P. E., Bouwman, J., Brookes, A. J., Clark, T., Crosas, M., Dillo, I., Dumon, O., Edmunds, S., Evelo, C. T., Finkers, R., ... Mons, B. (2016). Comment: The FAIR Guiding Principles for scientific data management and stewardship. *Scientific Data*, *3*, 160018. https://doi.org/10.1038/sdata.2016.18

Wilson, E. O. (2017). Biodiversity research requires more boots on the ground. *Nature Ecology & Evolution*, *1*, 1590–1591. https://doi.org/10.1038/s41559-017-0360-y

How to cite this article: Salguero-Gómez, R., Jackson, J., & Gascoigne, S. J. L. (2021). Four key challenges in the open-data revolution. *Journal of Animal Ecology*, 90, 2000–2004. https://doi.org/10.1111/1365-2656.13567

Trends in
Ecology & Evolution

CellPress
OPEN ACCESS

Opinion

Plasticity's role in adaptive evolution depends on environmental change components

Anna C. Vinton[1,*,@] Samuel J.L. Gascoigne,[1] Irem Sepil,[1] and Roberto Salguero-Gómez[1,2,3]

To forecast extinction risks of natural populations under climate change and direct human impacts, an integrative understanding of both phenotypic plasticity and adaptive evolution is essential. To date, the evidence for whether, when, and how much plasticity facilitates adaptive responses in changing environments is contradictory. We argue that explicitly considering three key environmental change components – rate of change, variance, and temporal autocorrelation – affords a unifying framework of the impact of plasticity on adaptive evolution. These environmental components each distinctively effect evolutionary and ecological processes underpinning population viability. Using this framework, we develop expectations regarding the interplay between plasticity and adaptive evolution in natural populations. This framework has the potential to improve predictions of population viability in a changing world.

Plasticity and adaptation in a changing world

Understanding, quantifying, and predicting the ability of organisms to adapt to changing environments is at the core of ecoevolutionary research [1–4]. In the face of unprecedented **environmental change** (see Glossary), natural populations, especially those with limited mobility/dispersal, can avoid extinction via **phenotypic plasticity** and/or **adaptive evolution** [4]. However, our understanding of the interplay between adaptive evolution and plasticity in changing environments remains limited [1,5–8]. This limitation is not trivial, for plasticity can itself evolve [9], be adaptive, or nonadaptive [10], and have differing effects on adaptive evolution [11,12].

For decades, researchers have theorised whether plasticity facilitates or hinders adaptive evolution [9,13]; the evidence is contradictory, and general patterns have yet to emerge [5,10,11,14,15]. The primary conflicting hypotheses for whether plasticity facilitates or hinders adaptive evolution are:

- (H1) Plasticity weakens directional selection by masking genotypic variation (e.g., **Bogert effect** [16]), thus slowing the rate of genetic change [5,17–19].
- (H2) Plasticity facilitates evolution by allowing the population to persist under environmental change long enough for genetic change to occur [20–22] (e.g., **plasticity-first hypothesis** [22] or **Baldwin effect** [20]).

This debate remains unresolved. Despite cases where theoretical predictions agree with empirical findings [5,10,11,14,15,23], we lack a general framework to establish the context-dependence of plasticity's impact alongside climate change. Here, we introduce an environmentally explicit framework that allows for the development and testing of hypotheses regarding when and how plasticity interacts with evolution. We highlight three environmental change components: **rate of mean change**, **environmental variability**, and **temporal autocorrelation**. These environmental

Highlights

Global biodiversity is jeopardised by unprecedented environmental change, the hallmark of the Anthropocene. To estimate the extinction risks of species, understanding how individuals and populations respond to changing environments is crucial.

Adaptive evolution and phenotypic plasticity are two key mechanisms by which natural populations avoid extinction in the face of environmental change. However, the relative roles and interplay between the two are still unresolved.

Whether plasticity hinders (H1) or facilitates (H2) adaptive evolution has been ardently researched, but without cross-study standardization of how changing environments impact whether (H1) or (H2) is more likely over time.

We propose an integrative framework based on how key environmental components influence the 'building blocks' of ecoevolutionary responses to examine when plasticity aids or hinders adaptive evolution. We synthesise key microevolutionary and ecological processes regarding how natural populations respond to environmental change.

Studies may benefit from this framework to deepen our understanding of how plasticity influences adaptive evolution by reframing H1 and H2 in the context of environmental change, and will thus increase our ability to forecast extinction risks in the Anthropocene.

[1]Department of Biology, University of Oxford, Oxford, OX1 3SZ, UK
[2]Centre for Biodiversity and Conservation Science, University of Queensland, St Lucia 4071, QLD, Australia
[3]Evolutionary Demography Laboratory, Max Plank Institute for Demographic Research, Rostock 18057, Germany

components distinctly impact evolutionary and ecological processes as mechanisms of population response [24–26] and are widely documented consequences of climate change [27–29]. Consequently, there is an urgent need to integrate the effects of environmental change in a generalizable way. This will allow ecologists and evolutionary biologists to better contextualise, mechanistically understand, predict, and compare their findings.

Moving optimum theory links environmental change to the resulting evolutionary responses according to changes in phenotypic traits. When a population is confronted with an environment that changes directionally, there is a **critical rate of change** that must be matched by change in the mean phenotype of the population. That is, the mean phenotype must remain close to the theoretical **phenotypic optimum**. In this context, a **phenotypic lag** between the mean phenotype and the optimum phenotype may emerge which, if too large, increases extinction risk [30,31]. Evolutionary processes (e.g., selection, genetic variation) and ecological processes (e.g., life history, within-generation plasticity, and population dynamics) together influence how far a population can lag and persist. Thus, the contribution of plasticity to population persistence and adaptation is largely determined by this phenotypic lag.

We argue that H1 and H2 are not mutually exclusive. Rather, plasticity may facilitate or hinder adaptive evolution depending on the properties of environmental change. To assess the impact of plasticity on adaptive evolution, we specify the links among the type of environmental change, plasticity, and adaptive evolution. Thus, we utilise theoretical and experimental work to:

(i) Assess how three key components of environmental change (rate of mean change, variability, and temporal autocorrelation) each alter the evolutionary and ecological mechanisms behind phenotypic tracking of a moving optimum.
(ii) Introduce a unified framework of testable hypotheses detailing how those three components of environmental change can influence the relative benefit of plasticity to adaptive evolution.

Mechanisms of evolutionary response to changing environments: interactions between environmental change and genetic variation, heritability, and selection

To understand the role of plasticity in adaptive evolution, one needs to consider how different environmental components impact the mechanisms of evolutionary tracking in the absence of plasticity. For adaptive evolution to occur, natural selection must act on variation in a heritable trait. The genetic architecture of a trait under selection will, in part, determine the potential for adaptive evolution and ecoevolutionary dynamics [32]. Most traits that mediate population dynamics are determined by multiple genes, each of which typically has a small effect (quantitative traits) [32,33]. One way to assess whether or not a quantitative trait may evolve is via the **breeder's equation**, which equates the change in a trait to the selection differential times its narrow-sense heritability. Heritability is a function of both genetic variation [34,35] and the environment in which that variation is expressed [36]. The contributions of environmental change/variation to phenotypic and genetic variation are often relegated to an error term that absorbs unmeasured uncertainties in quantitative genetic models ([37], but see [38]). In the following sections, we discuss literature that addresses how rate of mean change, variability, and temporal autocorrelation in the environment each influence heritability, genetic variation, and selection. By considering the environmental impacts on these evolutionary mechanisms, we aim to understand the ability of genetic change to track a fitness optimum in changing environments. This understanding informs the importance of plastic responses in decreasing phenotypic lag.

*Correspondence:
Anna.Vinton@biology.ox.ac.uk
(A.C. Vinton).
Twitter: @TheoreticalAnna

Impact of the rate of environmental change on underlying genetics

When the rate of environmental change is too slow, selection is weak and can be ineffective in part due to a small **lag load** [39,40]. As the rate of environmental change increases, selection strengthens, and the population can track the moving optimum with a consistent phenotypic lag [41]. In this range of environmental change, additive genetic variance and heritability can also increase [39,42]. In this case, up to a certain intermediate rate of environmental change, genetic variation and evolutionary potential may be expected to increase. This can occur simply due to higher additive genetic variance and thus an increase in standing variation available to selection. However, phenotypic lag can become too large for the rate of selection to follow if the environment, and thus the trait optimum, changes too quickly [39,41,43]. Here, the phenotypic lag increases, which can lead to decreased fitness and eventually local extinction [44]. As such, the mean time to extinction in a natural population decreases as the rate of environmental change increases beyond the optimal rate [39]. Thus, the rate of environmental change in evolutionary experiments and theory is key to assess the potential benefit of plasticity on adaptive evolution.

Impact of environmental variation and temporal autocorrelation on underlying genetics

Moderate environmental variation can optimise selection, and ultimately evolutionary tracking [45,46] (but see [2]). In contrast, the ability of populations to evolutionarily track a shifting adaptive peak can increase with greater temporal autocorrelation [25]. Moreover, theoretical work predicts that positively autocorrelated environmental fluctuations can increase additive genetic variance and its ability to reduce genetic load. This increase in genetic variance allows the mean phenotype to track a changing environment more closely [25]. Thus, evolutionary potential may be higher in temporally autocorrelated environments than in uncorrelated environments.

The evolutionary effects of environmental variability and autocorrelation are often framed in terms of increasing frequencies of novel and unfavourable environments [47]. Greater environmental variability and lower temporal autocorrelation expose individuals to environments that are novel and often unfavourable, and their impact on evolutionary response is mixed depending on other factors at play [47]. In addition, a direct consequence of higher variability and higher autocorrelation is that populations spend less time in **temporal refugia** [29], which reduces fitness.

Conversely, theoretical and empirical research have shown that exposure to unfavourable environments can also lead to increased additive genetic variance, thereby increasing the evolutionary potential of a trait [47]. This increase in additive genetic variance can occur when selection is ineffective at removing mutations that are maladaptive only in rare environments [47,48]. Moreover, novel environments can reveal cryptic, or previously unexpressed genetic variation [12]. Thus, exposure to novel, and unfavourable environments could increase genetic variation and therefore heritability.

Determining the magnitude and frequency that genetic variance increases in response to **environmental novelty** and harshness is non-trivial, as the opposite effect can also occur [47,49–51]. The effect of environmental novelty and harshness depends on the system-specific evolutionary history, and interaction between environmental and genetic effect [47]. For example, both environmental novelty and harshness can decrease additive genetic variance if an unfavourable condition prevents individuals from expressing the underlying genetically determined benefits from a trait [51]. In such cases, selection could favour the regulation of gene expression such that alleles are not expressed in an unfavourable environment. This lack of expression in

Glossary

Adaptive evolution: genetic changes in a population that confer directional changes in a fitness-related trait. The direction of trait evolution is determined by the new phenotypic optimum, whilst the magnitude of change results from the strength of selection (genetic variation and heritability).

Baldwin effect: a novel state of a trait that emerges/changes via plastic mechanisms that is subsequently reinforced by genetic mechanisms that stabilise the trait across generations. This line of thinking has been used to describe a range of traits, from developmental variation in house finches to multicellularity [81].

Bogert effect: the effect of plasticity in masking genetic variation from selection. Common examples include thermoregulatory behaviours in ectotherms.

Breeder's equation: an equation that quantifies the expected difference in mean trait value as the product of the narrow sense heritability, or the proportion of trait variation attributed to additive genetic effects (h^2) and the selection differential the trait is exposed to $(S) : \Delta Z = h^2 S$.

Critical rate of change: the maximum rate of environmental change the population can handle. Exceeding this limit inevitably results in a population decline towards extinction.

Demographic buffering: a strategy where populations have negative covariance of a vital rate's impact on population growth rate and its variance over time.

Environmental change: a shift in abiotic factors (e.g., temperature and precipitation) and/or biotic factors (e.g., predation risk and community structure) that shifts the phenotypic optimum of a trait.

Environmental novelty: the degree to which biotic and abiotic factors differ between present and past. This novelty can be quantified by the distance the phenotypic optimum has moved relative to the optimum in the previous environmental state.

Environmental variability: the variance of an environmental variable (e.g., temperature and precipitation) value over time.

Lag load: the distance between the average fitness of a population and its local adaptive peak. The greater the lag load, the higher the selective pressure.

unfavourable environments may occur through decreasing the heritability of traits underpinned by associated alleles [47]. Here, heritability could decrease when additive genetic effects determine a trait such as body size. If unfavourable conditions decrease growth rate, this decrease can lead to a reduction in the additive genetic variance.

In turn, depending on the mechanisms at play, evolutionary tracking may be either facilitated or hindered in environments with an increasing rate of change, variation, and/or autocorrelation. Whether or not a population is likely to successfully track a moving environmental optimum will in part determine the necessity of plasticity to help bridge this gap. Thus, the impact of the environmental change variables on evolutionary tracking should be considered when addressing H1-2.

Mechanisms of ecological response to changing environments: interactions between environmental change and life history, plasticity, and population dynamics

Environmental change impacts on population size and life history

The importance of phenotypic plasticity in adaptive evolution depends on changes in population size, which influences the likelihood of local extinctions [52,53]. Such impacts of population size depend on **life history strategies**; for example, long-lived species can persist longer at small population sizes than short-lived species, whose populations can collapse quickly [54,55]. Furthermore, these strategies can determine the rate of trait evolution [8]. It is therefore vital to consider the impact of different environmental components on population dynamics and life history to understand the impact of the type of environmental change on the interplay between plasticity and adaptive evolution.

Higher rates of mean environmental change typically lead to decreases in population size [56]. This finding suggests that local extinction will increase as the rate of climate warming exceeds the rate of adaptive responses. However, population size can increase in some species under higher rates of environmental change. For instance, bird species adapted to drier climates can utilise agricultural land and colonise drier habitats under climate change [57]. Demographic theories can help to explain such contradictory empirical cases: for instance, differences in life history and population structure (e.g., size, age) can translate a rate of change in a trait (e.g., reproduction) into different outcomes of population growth rate.

The interplay between increasing environmental variability and population size has now been intensively studied both theoretically and empirically [58]. It is usually assumed that a more variable environment is detrimental for populations. However, recent syntheses show that the effect of environmental variability can have both positive and negative effects on population growth rates [2,59]. For example, disparities in population size responses to environmental variability are influenced by differences in the magnitude of density dependence [60]. Density dependence varies between systems due to species-specific physiology or life history [60,61]. Such differences cause further disparities in **transient dynamics** of population trends [62]. Further, nonlinear relationships between environmental states and **vital rates** across st/age classes within populations ('**reaction norms**') can induce varying **demographic buffering** capabilities across populations and species [63,64]. Variation in degrees of demographic buffering via plasticity of vital rates, can contribute to the observed inconsistencies in comparative analyses of population dynamics in variable environments [65].

Temporal autocorrelation in the environment has gained much attention in population biology and climate change research [29,66]. Here too, the emerging message is that autocorrelated

Life history strategies: the age-specific schedules of vital rates (see below) and associated phenotypes (e.g., morphology, behaviour, offspring investment) that determine the fitness of individuals and viability of populations.
Moving optimum theory: a body of work showing that, at any point in time, there is a phenotypic optimum that maximises the fitness of individuals. This optimum can change over time due to biotic and abiotic factors. In turn, populations track the moving optimum, at a certain lag, via plasticity and/or adaptive evolution.
Phenotypic lag: a gap between the moving phenotypic optimum and the population mean trait.
Phenotypic optimum: the phenotype that maximises fitness at a point in time.
Phenotypic plasticity: environmentally induced changes in an individual's phenotype without changes in its genetic makeup. These changes can be adaptive, or nonadaptive (have a neutral or negative impact).
Plasticity-first hypothesis: genetically-based variation in plasticity among individuals in a population responds to selection in a novel environment. This initial variation in plasticity allows for the population to persist when it would not have been able to do so if it were plastic and then to respond to selection.
Rate of mean change: the direction and magnitude of differences in average environmental values (e.g., temperature and precipitation) over time.
Reaction norms: the effect of an environmental factor on the value of a trait.
Temporal autocorrelation: the correlation of terms in series separated by a time interval. High autocorrelation refers to a case where successive values are highly correlated, a negative autocorrelation indicates an inverse relationship between two variables, and no autocorrelation refers to a case where successive values are uncorrelated.
Temporal refugia: a period in which the degree/number/duration of perturbations in the environment that negatively affect fitness is reduced, allowing for intermittent rescues in population size and structure.
Transient dynamics: short-term fluctuations in population size/structure that arise due to both (i) perturbations in the structure and/or size of the population and (ii) probabilistic events (e.g., survival and reproduction) as the

environments can have positive [67,68] or negative [68] impacts on population size and extinction risk, depending on life history strategies [69] and phylogenetic history [70]. For example, annual plant populations have lower extinction risks than perennial populations when the environment is positively temporally autocorrelated [68]. In some cases, long stretches of adverse conditions caused by positive environmental autocorrelation can exacerbate extinction risk [66]. One example is when highly positively autocorrelated fluctuations cause multiple generations to experience negative growth [12]. Conversely, highly autocorrelated environments could allow for an increasing population size, as populations may be better able to track the optimum trait value [44]. And lastly, simulations of density-independent stage-structured populations suggest that pace-of-life and degree of iteroparity positively correlate with a population's sensitivity to environmental autocorrelation [70].

population approaches a stationary equilibrium.
Vital rate: a demographic process (e.g., survival, growth, reproduction). Vital rate values typically vary across the structured life cycle of an organism (e.g., age, stage, size).

Environmental change impacts on role of within-generational plasticity

While selective pressures tend to decrease phenotypic lag, so can plasticity [30,71] (but see [10]). However, the impact of plasticity on lag size is complex, for plasticity itself can evolve [72], has different forms depending on the life history strategies [72,73], and level of biological organisation [74,75]. Even within these levels, there is disagreement about how different environments alter the ability of plasticity to affect lag in populations of different sizes [75]. How we judge the efficacy of plasticity to affect population dynamics depends on assumptions about plasticity's inherent costs and limitations [76] and how they interact with the three environmental parameters (Figure 1).

Increasing rates of environmental change have been theorised to decrease the benefit of plasticity when the environment becomes extreme. However, much of this work utilised a categorical framework such as 'abrupt' and 'gradual', as opposed to a continuous measure [26]. A key implicit assumption in moving optimum theory is that plasticity can buffer decreases in population size, but incurs some energetic cost [37,77]. This cost depends on the type of trait (e.g., morphology, phenology, physiology, behaviour) and the rate of environmental change [75]. Moreover, the trade-off between the ability of plasticity to buffer environmental changes and its costs can be impacted by correlations between trait values as well as the slopes of their respective reaction norms. In turn, these trait covariances and reaction norms can influence the interplay between selection on mean trait values, and changes in plasticity [78]. The cost of plasticity thus adjusts the critical limit of environmental change, producing a complex interaction between rate of environmental change and net benefit of plasticity [30].

Environmental variability also impacts the ability of plasticity to benefit population size. Although plasticity can mitigate the detrimental effects of environmental variability in some cases, individual-based simulations have shown that the magnitude of environmental fluctuations has surprisingly limited effects on population persistence [79]. This has also been shown in herbivory defence traits of wild radish populations, cementing the idea that although plasticity often correlates with environmental variation, the interplay between environmental variation and plasticity is non-trivial [80,81].

Environmental temporal autocorrelation seems to have a more apparent effect on the benefit of plasticity to population persistence than environmental variability. The theoretical and empirical literature suggests that unreliable environmental cues decrease the ability of plasticity to reduce extinction risk [12,76,82]. In addition, we note that epigenetic modifications can relay a predictive adaptive response to the next generation(s), which is likely to be advantageous in highly predictable environments [83], warranting further study. More predictable fluctuations select for increased plasticity, suggesting that plasticity has a beneficial role for tracking moving optima [84]. Moreover, less predictable environments have been hypothesised to decrease – and even reverse – the potential beneficial role of plasticity on population growth rate [12].

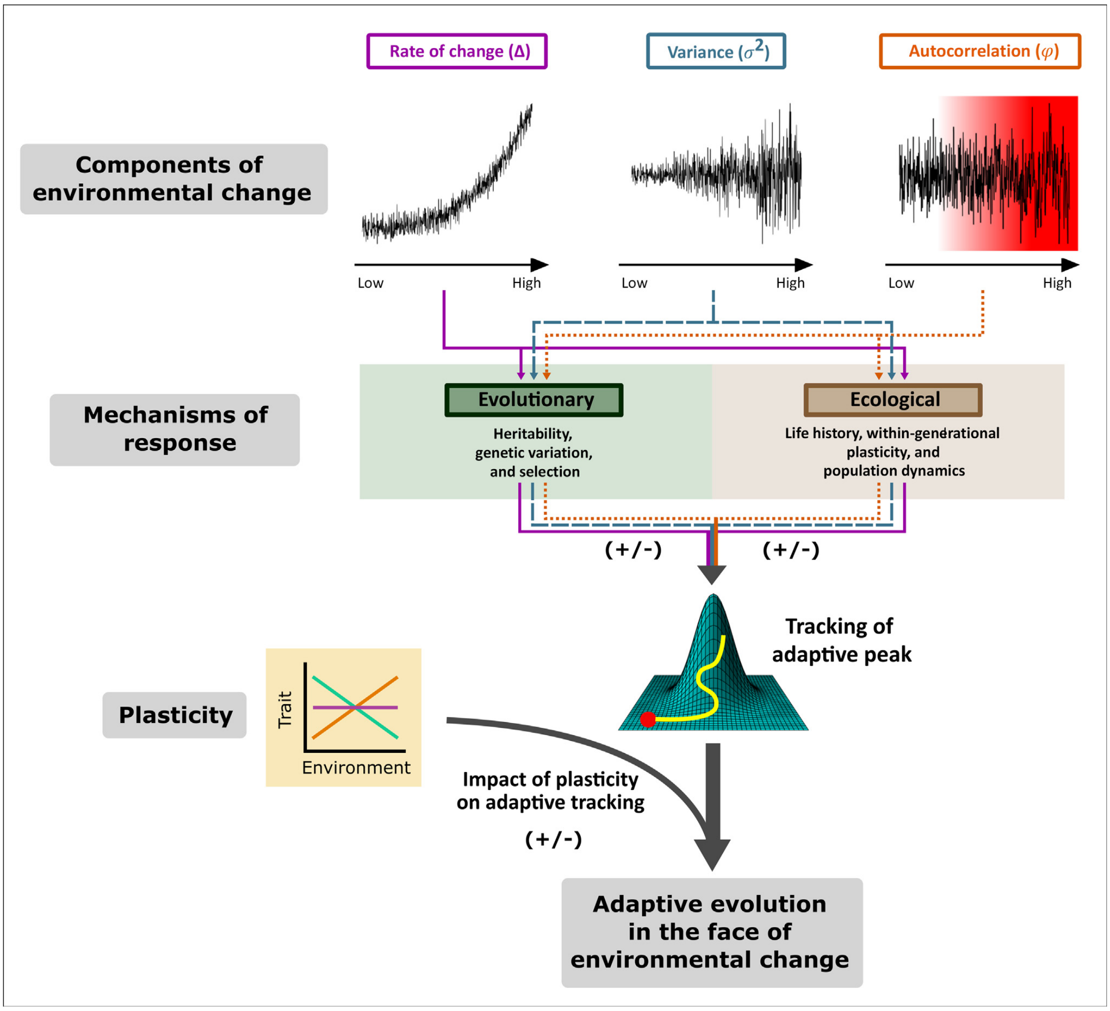

Trends in Ecology & Evolution

Figure 1. Framework to assess the environment-dependent impact of phenotypic plasticity on adaptive evolution. First, the three key environmental change components (rate of change, variance, and autocorrelation) each influence the two broad categories of mechanisms through which natural populations respond to changing environments: evolutionary and/or ecological processes. Evolutionary processes include heritability, genetic variation, and natural selection. Ecological processes encompass demographic dynamics driven by fluctuations in population size, within-generational plasticity, and life history. At the core of our conceptual framework, all of these mechanisms influence whether and how well a population can track the fitness peak, which moves through trait space as the environment changes. Plasticity enters the framework by impacting a populations' ability to adaptively track the fitness peak. Decomposing environmental change into key components in this fashion allows us to contextualise the magnitude and direction of plasticity's impact on population persistence and adaptive evolution via mechanistic links.

Synthesis: when does plasticity help or hinder adaptive evolution?

Climate change is predicted to lead to changes in the rate, variation, and autocorrelation of environmental variables. Moving optimum theory provides a mechanistic approach to develop hypotheses about the impact of plasticity on adaptive evolution in changing environments. In this context, H1 and H2 cannot be tested without controlling for the types of environmental change. The facilitative role that plasticity might play for adaptive evolution in the face of environmental change depends on *how* the environment is changing. Each of the three environmental components (Figure 1) influences the two broad categories of ecoevolutionary response mechanisms, as discussed in earlier sections. The interaction between environmental change components and response mechanisms produces a rich breadth of hypotheses (Box 1). Empirical and theoretical tests of these hypotheses will form a more integrative understanding of adaptive responses to a changing world.

Box 1. Hypotheses regarding the benefit of plasticity on adaptive evolution in response to increasing mean rate of environmental change

Each of these hypotheses utilises moving optimum theory to infer how the relationship between phenotypic lag and adaptive tracking can be moderated by phenotypic plasticity alongside an increasing rate of mean environmental change (Figure I).

Hypothesis A[i]

The benefit of plasticity increases with rising rates of environmental change, eventually plateauing. Selection is weak when environmental change is slow, and phenotypic lag is small. Population growth is consequently high, and heritability of fitness-related traits is also high. In this scenario, plasticity adds little to adaptive tracking, thus the costs of plasticity outweigh the benefits in decreasing the phenotypic lag. Conversely, when the mean environment changes too fast for adaptive evolution to track, and phenotypic lag is high, plasticity helps the population ‘catch up’ with the moving optimum by allowing the population to increase in size, and thus maintain the genetic diversity.

Hypothesis A[ii]

The benefit of plasticity decreases with increasing rates of environmental change. Contrary to Hypothesis A[i], when selection is weak, lag load can increase. In this scenario, plasticity can bring the phenotypic mean close to the selection peak at a low rate of environmental change. Conversely, as rate of mean environmental change increases, the limits of plasticity set by its costs (i.e., physiological toll and masking of genetic diversity [76,81]) may result in a limited role of plasticity for adaptive tracking. If population size is small at high rates of environmental change, plasticity can increase the chance of extinction due to drift by shifting the phenotypic average and thus shading the genetic variation from selection. This results in the maintenance of maladapted individuals and further decreases the population size. Moreover, a high rate of environmental change can limit the efficacy of plasticity given the low predictability of the future environment.

Hypothesis A[iii]

The benefit of plasticity is maximised at an intermediate rate of environmental change, above (following A[i]) and below (following A[ii]) which its benefit decreases.

To test these hypotheses, we must first shift our thinking regarding the rate of environmental change from a categorical to a continuous framework. For example, increases in temperature and salinity can be simulated experimentally and considered using multiple rates of change [26]. Ideally, the trait or vital rate of interest should be assessed at the individual level within and across generations to estimate plasticity and evolution. The amount of plasticity and genetic change can then be compared across the different environmental levels. Ectotherms such as fruit flies (e.g., *Drosophila melanogaster*), phytoplankton (e.g., *Microcystis aeruginosa*), or nematodes (e.g., *Caenorhabditis elegans*) pose ideal systems to study these effects, given their short generation time and the ease in modifying their environment in a laboratory setting [85–87]. Moreover, given their small size, organism such as these allow for research into less studied levels of organization: populations and communities [26,81].

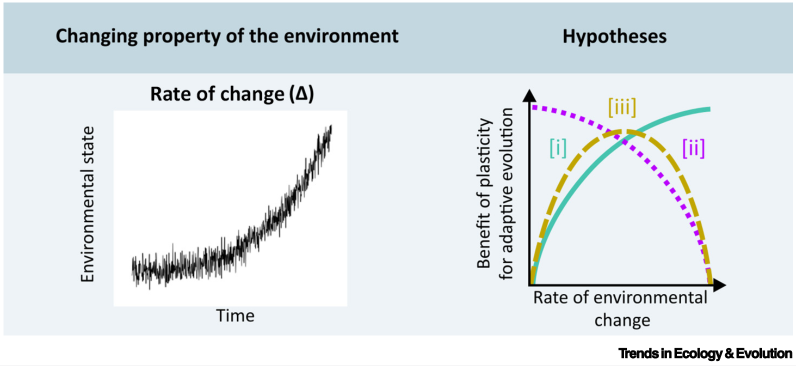

Figure I. Hypotheses for the relationship between the mean rate of environmental change and benefit of plasticity for adaptive evolution. The left side of the panel depicts an increasing rate of environmental change over time. The right side shows the graphical Hypotheses [i–iii], which describe [i] increase, [ii] decrease, and [iii] intermediate suboptimal benefit of plasticity for adaptive evolution across an increasing rate of environmental change.

Here, we leverage the mechanisms of evolutionary response that we have discussed to suggest a baseline of testable hypotheses for how the facilitative role of plasticity may change as environmental parameters change (see Boxes 1–3 and the figures therein). Our primary goal is to call attention to how plasticity's contribution to adaptive evolution depends on environmental context. Contradictory hypotheses abound; we contend that these in fact present focal targets for future empirical validation.

Box 2. Hypotheses regarding the benefit of plasticity on adaptive evolution in response to increasing environmental variation

As in Box 1, each of these hypotheses utilises moving optimum theory, here determining the impact of increasing environmental variation on plasticity's role in adaptive evolution (Figure I).

Hypothesis B[i]

The benefit of plasticity to adaptive evolution increases with increasing environmental variation. As the environment becomes more variable, plastic responses can dampen detrimental effects of unpredictable fluctuations, thereby preventing extinction [71,72,75]. Buffering can afford the population more time to reach its adaptive peak via adaptive evolution. This benefit would eventually cross a point of diminishing returns, as when the environment becomes too variable, the costs of plastic responses may outweigh their benefits. This decrease in the benefit of plasticity is in part due to the lack of predictability in the temporal environment. Moreover, in a highly variable environment with a stationary mean, evolution may be nonadaptive [2,88], and thus plasticity may allow the genotypic mean to remain near the environmental mean amidst the environmental variability.

Hypothesis B[ii]

The benefit of plasticity to adaptive evolution decreases with increasing environmental variation. In an environment with low variation, plasticity works together with evolution to fix advantageous traits for the new environment. As the environment becomes more variable, plastic responses may drive a disconnect between phenotypic selection and genotypic selection, ultimately making the genetic variation in the population maladapted to future environmental conditions. In other words, plasticity might help a population more flexibly explore the fitness landscape, therefore avoiding being stuck in a valley or a local peak, and instead finding a global peak when the environment is moderately variable. If the environment is too variable, however, 'peak-searching' can be disrupted even with plasticity because the landscape itself shifts quickly.

Hypothesis B[iii]

The benefit of plasticity to evolution is highest in low and high environmental variability. The ability of the trait mean in the population to reach the peak of fitness landscapes via adaptive evolution may be optimal at an intermediate level of environmental variance. In this case, the facilitative role of plasticity would be low at an intermediate level of environmental variance if it masks genetic variance of the population from selection, or shifts the phenotypic average.

As in Box 1, more experimental and theoretical work would help address the mechanisms underlying Hypothesis B[i]–[iii]. For instance, the impact of temperature variation on the grass *Brachypodium distachyon* is being studied using greenhouse experimental settings [89]. Systems like this, where researchers are already quantifying plastic traits and the impact of environmental variability, are ideal to test these hypotheses. Moreover, although controlled greenhouse and laboratory studies are necessary to improve understanding of plasticity's impact on adaptive evolution, they may obscure potential costs of plasticity [81]. Thus, studies that increase in realism from greenhouses to the field are necessary, and model grass species pose ideal candidates for work at both scales [90].

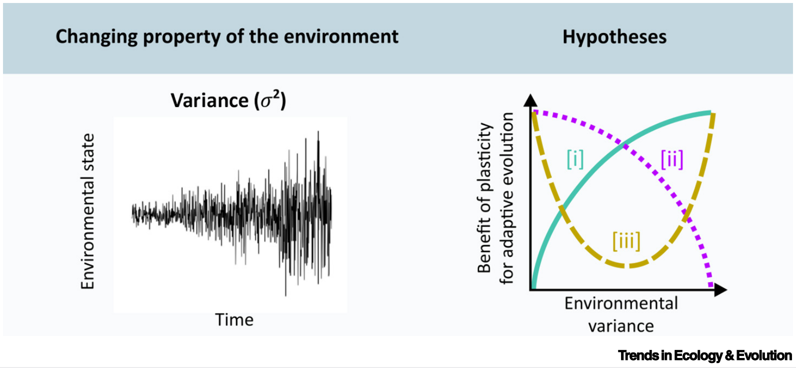

Figure I. Hypotheses for the relationship between the amount of environmental variation and benefit of plasticity for adaptive evolution. The left side of the panel depicts an increase in environmental variation over time. The right side of the panel shows Hypotheses [i–iii], which describe an [i] increasing, [ii] decrease, or [iii] intermediate optimal in benefit of plasticity for adaptive evolution with increasing environmental variance.

Box 3. Hypotheses regarding the benefit of plasticity on adaptive evolution in response to increasing environmental temporal autocorrelations

As in Boxes 1 and 2, we construct hypotheses regarding the impact of environmental autocorrelation on the potential benefit of plasticity for adaptive evolution, and adaptive tracking (Figure I).

Hypothesis C[i]

The benefit of plasticity to adaptive evolution increases with increasing temporal autocorrelation. Higher autocorrelation in the environment corresponds to higher reliability of temporal cues and thus higher predictability of future environmental states [82]. Therefore, plastic responses may more accurately track moving selection targets, and aid adaptive tracking. In addition, adaptive evolution may be less likely to occur in isolation in highly autocorrelated environments.

Hypothesis C[ii]:

The benefit of plasticity to adaptive evolution decreases with increasing temporal autocorrelation. Autocorrelation can occur at various temporal lags [29] and the length of the lag can be out of sync with the pace of life history (e.g., generation time) of the focal species. In such case greater environmental autocorrelation might lead to the population existing in unfavourable conditions for long periods of time. If the populations stay in unfavourable conditions for extended periods, it can see a reduction in genetic variation and increase in extinction risk. Thus, the ability for plasticity to help adaptively track optima may decrease.

To test hypotheses C[i]–[ii], different levels of temporal autocorrelation must be generated. The impacts of temporal autocorrelation on life history, population dynamics, and plasticity have been studied [66,70,82]. However, to test hypotheses C[i]–[ii], controlled studies across generations need to be conducted to assess a variety of autocorrelation scenarios on intragenerational and intergenerational adaptation. In addition to systems recommended in Boxes 1 and 2, marine invertebrate systems such as *Bugula neritina,* which are likely to be impacted by varying temporal autocorrelation [91], would pose an ideal system to test these hypotheses. To test hypotheses C[i]–[ii], we also need theoretical models parameterised to estimate the changing impacts of temporal autocorrelation, in addition to experimental studies in controlled environments.

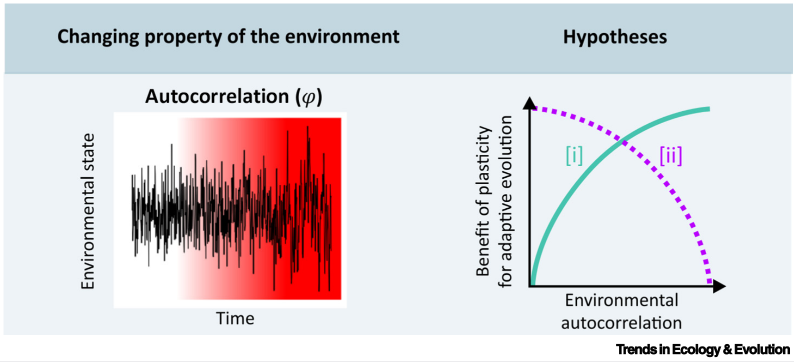

Figure I. Hypotheses for the relationship between temporal autocorrelation and benefit of plasticity for adaptive evolution. The left side of the panel depicts an increasing temporal autocorrelation in the environmental state over time. The right side of the panel shows Hypotheses [i–ii], which describe an [i] increase or [ii] decrease in the benefit of plasticity for adaptive evolution with increasing temporal autocorrelation.

Concluding remarks

A growing number of studies have tested the predictions generated from H1 and H2 (e.g., the Baldwin effect, plasticity-first hypothesis, and Bogert effect) [5,10,22,92]. Yet, as far as we know, no study to date has systematically compared and contrasted, theoretically or experimentally, how these predictions differ across the three parameters of environmental change (rate of change, variation, autocorrelation) (see Outstanding questions). Here, we pose a framework yielding testable hypotheses to encourage both experimental and theoretical research that takes into account simultaneous variation in plasticity and genetics in response to changing

Outstanding questions

How can the effect of plasticity on evolution be quantified? We suggest that manipulating the rate of mean change, variability, or autocorrelation with appropriate controls could elucidate the interplay between plasticity and selection. Importantly, focusing on how these environmental drivers impact heritability, selection, genetic variability, within-generational plasticity, life history, or population size can clarify the mechanism of influence on plasticity's impact on adaptive evolution. To test these hypotheses, one must first define the types of environmental change that may be experimentally manipulated, the genetic mechanisms that affect the trait(s) of interest (see section 'Mechanisms of evolutionary response to changing environments: interactions between environmental change and genetic variation, heritability, and selection'), and type of plasticity in the population (see section 'Mechanisms of ecological response to changing environments: interactions between environmental change and life history, plasticity, and population dynamics'). Specifically, progress must be made to further understanding of related mechanisms such as epigenetic changes, the role of cryptic genetic variation, as well as the prevalence of costs of plasticity.

Which hypotheses (Boxes 1–3) of the potential role of plasticity are most robust and accurate? This question cannot yet be answered, for the hypotheses we have put forth, which are stimulated by both ecoevolutionary theory and evidence, are thus far untested regarding their relative prevalence or accuracy. Thus, the need for experimental data, both in the laboratory and in natural settings, is vital to increase our understanding of the relative prevalence of each prediction. Moreover, new information about the mechanisms underlying ecological and evolutionary responses to different types of environmental change will raise new questions regarding when plasticity's potential role in adaptive responses might be greatest.

Can knowledge about the context-dependent role of plasticity in adaptive evolution aid in land management and determine conservation priorities? We suggest that simultaneously estimating environments. We argue that autocorrelation, the least understood facet of environmental change in regard to the interplay between plasticity and evolution, deserves further exploration, in tandem with rate of change and variation. Specifically, the scientific community will gain key insights from scaling laboratory experiments with autocorrelation treatments to natural environments. Thus, we recommend a special focus be placed here, given expected increases in autocorrelation (with local variation) in both marine and terrestrial systems due to climate change.

the environmental change components reviewed in this article and measuring both the evolutionary and phenotypic plastic responses in the relevant system can unlock new insights into the ability of populations to persist under climate change.

Phenotypic and genotypic data from natural populations exposed to changing environmental regimes are becoming increasingly common. These data allow direct assessment of genetic and plastic adaptive processes over time and under different environmental scenarios. Therefore, the time is ripe to reassess our understanding of the relative roles of phenotypic evolution by selection and plasticity. Here, we have introduced an integrative framework that delineates hypotheses for when and how much plasticity might facilitate adaptive evolution and persistence under realistic types of environmental change. With more explicit theories and field measurements of how the rate of change, variability, and temporal autocorrelation of the environment impact the mechanisms of evolutionary responses (see Outstanding questions), we may reach a deeper understanding of species responses in the Anthropocene.

Acknowledgments

We thank S. Stearns, M. Paniw, O. Jones, and C. Desjonquères for feedback on earlier versions of this manuscript. We thank J. Park for feedback on this manuscript and figure preparation. We also thank the Biology Fly laboratory at the University of Oxford for their helpful discussion. A.C.V. was supported by the National Science Foundation Postdoctoral Research Fellowship in Biology under Grant No. (2010783), hosted by R.S.G. I.S. was supported by a Biotechnology and Biological Sciences Research Council (BBSRC) Fellowship (BB/T008881/1) and a Wellcome Institutional Strategic Support Fund, University of Oxford (BRR00060). R.S.G. was supported by an NERC Independently Research Fellowship (NE/M018458/1).

Declaration of interests

No interests are declared.

References

1. Gibert, P. *et al.* (2019) Phenotypic plasticity, global change, and the speed of adaptive evolution. *Curr. Opin. Insect Sci.* 35, 34–40
2. Vinton, A.C. and Vasseur, D.A. (2020) Evolutionary tracking is determined by differential selection on demographic rates and density dependence. *Ecol. Evol.* 10, 5725–5736
3. Bell, G. and Gonzalez, A. (2009) Evolutionary rescue can prevent extinction following environmental change. *Ecol. Lett.* 12, 942–948
4. Merilä, J. and Hendry, A.P. (2014) Climate change, adaptation, and phenotypic plasticity: the problem and the evidence. *Evol. Appl.* 7, 1–14
5. Ancel, L.W. (2000) Undermining the Baldwin expediting effect: does phenotypic plasticity accelerate evolution? *Theor. Popul. Biol.* 58, 307–319
6. Ghalambor, C.K. *et al.* (2015) Non-adaptive plasticity potentiates rapid adaptive evolution of gene expression in nature. *Nature* 525, 372–375
7. van Gestel, J. and Weissing, F.J. (2018) Is plasticity caused by single genes? *Nature* 555, E19–E20
8. Schmid, M. *et al.* (2022) A tradeoff between robustness to environmental fluctuations and speed of evolution. *Am. Nat.* 200, E16–E35
9. Sommer, R.J. (2020) Phenotypic plasticity: from theory and genetics to current and future challenges. *Genetics* 215, 1–13
10. Ghalambor, C.K. *et al.* (2007) Adaptive versus non-adaptive phenotypic plasticity and the potential for contemporary adaptation in new environments. *Funct. Ecol.* 21, 394–407
11. Levis, N.A. and Pfennig, D.W. (2019) Plasticity-led evolution: evaluating the key prediction of frequency-dependent adaptation. *Proc. R. Soc. B Biol. Sci.* 286, 20182754
12. Ashander, J. *et al.* (2016) Predicting evolutionary rescue via evolving plasticity in stochastic environments. *Proc. R. Soc. B Biol. Sci.* 283, 20161690
13. Stearns, S.C. (1989) The evolutionary significance of phenotypic plasticity. *BioScience* 39, 436–445
14. Gunderson, A.R. and Stillman, J.H. (2015) Plasticity in thermal tolerance has limited potential to buffer ectotherms from global warming. *Proc. R. Soc. B Biol. Sci.* 282, 20150401
15. Johansson, D. *et al.* (2017) Reciprocal transplants support a plasticity-first scenario during colonisation of a large hyposaline basin by a marine macro alga. *BMC Ecol.* 17, 14
16. Bogert, C.M. (1949) Thermoregulation in reptiles, a factor in evolution. *Evolution* 3, 195–211
17. Wright, S. (1990) Evolution in mendelian populations. *Bull. Math. Biol.* 52, 241–295
18. Anderson, R.W. (1995) Learning and evolution: a quantitative genetics approach. *J. Theor. Biol.* 175, 89–101
19. Huey, R.B. *et al.* (2003) Behavioral drive versus behavioral inertia in evolution: a null model approach. *Am. Nat.* 161, 357–366
20. Baldwin, J.M. (1896) A new factor in evolution. *Am. Nat.* 30, 441–451
21. Gibert, J.-M. (2017) The flexible stem hypothesis: evidence from genetic data. *Dev. Genes Evol.* 227, 297–307
22. Levis, N.A. and Pfennig, D.W. (2016) Evaluating 'plasticity-first' evolution in nature: key criteria and empirical approaches. *Trends Ecol. Evol.* 31, 563–574
23. Villellas, J. *et al.* (2021) Phenotypic plasticity masks range-wide genetic differentiation for vegetative but not reproductive traits in a short-lived plant. *Ecol. Lett.* 24, 2378–2393
24. Vasseur, D.A. *et al.* (2014) Increased temperature variation poses a greater risk to species than climate warming. *Proc. R. Soc. B Biol. Sci.* 281, 20132612

25. Ruokolainen, L. *et al.* (2009) Ecological and evolutionary dynamics under coloured environmental variation. *Trends Ecol. Evol.* 24, 555–563
26. Pinek, L. *et al.* (2020) Rate of environmental change across scales in ecology. *Biol. Rev.* 95, 1798–1811
27. Meehl, G.A. and Tebaldi, C. (2004) More intense, more frequent, and longer lasting heat waves in the 21st century. *Science* 305, 994–997
28. Rummukainen, M. (2012) Changes in climate and weather extremes in the 21st century. *WIREs Clim. Change* 3, 115–129
29. Di Cecco, G.J. and Gouhier, T.C. (2018) Increased spatial and temporal autocorrelation of temperature under climate change. *Sci. Rep.* 8, 14850
30. Kopp, M. and Matuszewski, S. (2014) Rapid evolution of quantitative traits: theoretical perspectives. *Evol. Appl.* 7, 169–191
31. Chevin, L.-M. *et al.* (2013) Phenotypic plasticity and evolutionary demographic responses to climate change: taking theory out to the field. *Funct. Ecol.* 27, 967–979
32. Yamamichi, M. (2022) How does genetic architecture affect eco-evolutionary dynamics? A theoretical perspective. *Philos. Trans. R. Soc. B Biol. Sci.* 377, 20200504
33. Hill, W.G. (2010) Understanding and using quantitative genetic variation. *Philos. Trans. R. Soc. B Biol. Sci.* 365, 73–85
34. Young, A.I. (2019) Solving the missing heritability problem. *PLoS Genet.* 15, e1008222
35. Zuk, O. *et al.* (2012) The mystery of missing heritability: genetic interactions create phantom heritability. *Proc. Natl. Acad. Sci.* 109, 1193–1198
36. Boyer, S. *et al.* (2021) Adaptation is influenced by the complexity of environmental change during evolution in a dynamic environment. *PLoS Genet.* 17, e1009314
37. Ørsted, M. *et al.* (2019) Strong impact of thermal environment on the quantitative genetic basis of a key stress tolerance trait. *Heredity* 122, 315–325
38. Wood, C.W. and Brodie III, E.D. (2016) Evolutionary response when selection and genetic variation covary across environments. *Ecol. Lett.* 19, 1189–1200
39. Burger, R. and Lynch, M. (1995) Evolution and extinction in a changing environment: a quantitative-genetic analysis. *Evolution* 49, 151–163
40. Guzella, T.S. *et al.* (2018) Slower environmental change hinders adaptation from standing genetic variation. *PLoS Genet.* 14, e1007731
41. Lynch, M. and Lande, R. (1993) Evolution and extinction in response to environmental change. In *Biotic Interactions and Global Change* (Kareiva, P.M. *et al.*, eds), pp. 234–250, Sinauer Associates
42. Bürger, R. (1999) Evolution of genetic variability and the advantage of sex and recombination in changing environments. *Genetics* 153, 1055–1069
43. Gomulkiewicz, R. and Houle, D. (2009) Demographic and genetic constraints on evolution. *Am. Nat.* 174, E218–E229
44. Lande, R. and Shannon, S. (1996) The role of genetic variation in adaptation and population persistence in a changing environment. *Evolution* 50, 434–437
45. Abdul-Rahman, F. *et al.* (2021) Fluctuating environments maintain genetic diversity through neutral fitness effects and balancing selection. *Mol. Biol. Evol.* 38, 4362–4375
46. Bruijning, M. *et al.* (2020) The evolution of variance control. *Trends Ecol. Evol.* 35, 22–33
47. Hoffmann, A.A. and Merilä, J. (1999) Heritable variation and evolution under favourable and unfavourable conditions. *Trends Ecol. Evol.* 14, 96–101
48. Kawecki, T.J. *et al.* (1997) Mutational collapse of fitness in marginal habitats and the evolution of ecological specialisation. *J. Evol. Biol.* 10, 407–429
49. Wilson, A.J. *et al.* (2006) Environmental coupling of selection and heritability limits evolution. *PLoS Biol.* 4, e216
50. Gaitán-Espitia, J.D. *et al.* (2017) Geographical gradients in selection can reveal genetic constraints for evolutionary responses to ocean acidification. *Biol. Lett.* 13, 20160784
51. Gebhardt-Henrich, S.G. and Van Noordwijk, A.J. (1991) Nestling growth in the Great Tit I. Heritability estimates under different environmental conditions. *J. Evol. Biol.* 4, 341–362
52. O'Grady, J.J. *et al.* (2004) What are the best correlates of predicted extinction risk? *Biol. Conserv.* 118, 513–520
53. Clements, C.F. *et al.* (2019) Early warning signals of recovery in complex systems. *Nat. Commun.* 10, 1681
54. Wright, J. *et al.* (2019) Life-history evolution under fluctuating density-dependent selection and the adaptive alignment of pace-of-life syndromes. *Biol. Rev.* 94, 230–247
55. Reynolds, J. (2003) Life histories and extinction risk. In *Macroecology* (Blackburn, T.M. and Gaston, K.J., eds), pp. 195–217, Blackwell Publishing
56. Spooner, F.E.B. *et al.* (2018) Rapid warming is associated with population decline among terrestrial birds and mammals globally. *Glob. Change Biol.* 24, 4521–4531
57. Frishkoff, L.O. *et al.* (2016) Climate change and habitat conversion favour the same species. *Ecol. Lett.* 19, 1081–1090
58. Boyce, M.S. *et al.* (2006) Demography in an increasingly variable world. *Trends Ecol. Evol.* 21, 141–148
59. Lawson, C.R. *et al.* (2015) Environmental variation and population responses to global change. *Ecol. Lett.* 18, 724–736
60. Turchin, P. (2013) *Complex Population Dynamics: A Theoretical/Empirical Synthesis (MPB-35)*, Princeton University Press
61. Fauteux, D. *et al.* (2021) Climate variability and density-dependent population dynamics: Lessons from a simple High Arctic ecosystem. *Proc. Natl. Acad. Sci.* 118, e2106635118
62. Salguero-Gomez, R. and Gamelon, M. (2021) *Demographic Methods across the Tree of Life*, Oxford University Press
63. Hilde, C.H. *et al.* (2020) The demographic buffering hypothesis: evidence and challenges. *Trends Ecol. Evol.* 35, 523–538
64. Gamelon, M. *et al.* (2021) Effects of pulsed resources on the dynamics of seed consumer populations: a comparative demographic study in wild boar. *Ecosphere* 12
65. McDonald, J.L. *et al.* (2017) Divergent demographic strategies of plants in variable environments. *Nat. Ecol. Evol.* 1, 0029
66. Postuma, M. *et al.* (2020) The effect of temporal environmental autocorrelation on eco-evolutionary dynamics across life histories. *Ecosphere* 11, e03029
67. Roy, M. *et al.* (2005) Temporal autocorrelation can enhance the persistence and abundance of metapopulations comprised of coupled sinks. *Am. Nat.* 166, 246–261
68. Heino, M. and Sabadell, M. (2003) Influence of coloured noise on the extinction risk in structured population models. *Biol. Conserv.* 110, 315–325
69. Ratikainen, I.I. and Kokko, H. (2019) The coevolution of lifespan and reversible plasticity. *Nat. Commun.* 10, 538
70. Paniw, M. *et al.* (2018) Interactive life-history traits predict sensitivity of plants and animals to temporal autocorrelation. *Ecol. Lett.* 21, 275–286
71. de Villemereuil, P. *et al.* (2020) Fluctuating optimum and temporally variable selection on breeding date in birds and mammals. *Proc. Natl. Acad. Sci.* 117, 31969–31978
72. Fox, R.J. *et al.* (2019) Beyond buying time: the role of plasticity in phenotypic adaptation to rapid environmental change. *Philos. Trans. R. Soc. B Biol. Sci.* 374, 20180174
73. Bailey, N.W. *et al.* (2018) Indirect genetic effects in behavioral ecology: does behavior play a special role in evolution? *Behav. Ecol.* 29, 1–11
74. Forsman, A. (2015) Rethinking phenotypic plasticity and its consequences for individuals, populations and species. *Heredity* 115, 276–284
75. Wennersten, L. and Forsman, A. (2012) Population-level consequences of polymorphism, plasticity and randomized phenotype switching: a review of predictions. *Biol. Rev.* 87, 756–767
76. DeWitt, T.J. *et al.* (1998) Costs and limits of phenotypic plasticity. *Trends Ecol. Evol.* 13, 77–81
77. Van Buskirk, J. and Steiner, U.K. (2009) The fitness costs of developmental canalization and plasticity. *J. Evol. Biol.* 22, 852–860
78. Mitchell, D.J. and Houslay, T.M. (2020) Context-dependent trait covariances: how plasticity shapes behavioral syndromes. *Behav. Ecol.* 32, 25–29
79. Scheiner, S.M. *et al.* (2020) The genetics of phenotypic plasticity. XVII. Response to climate change. *Evol. Appl.* 13, 388–399
80. Karban, R. and Nagasaka, K. (2004) Are defenses of wild radish populations well matched with variability and predictablity of herbivory? *Evol. Ecol.* 18, 283–301

81. Pfennig, D.W. (2021) In *Phenotypic Plasticity & Evolution | Causes, Consequences, Controversies* (Pfennig, D.W., ed.), CRC Press
82. Reed, T.E. *et al.* (2010) Phenotypic plasticity and population viability: the importance of environmental predictability. *Proc. R. Soc. B Biol. Sci.* 277, 3391–3400
83. Duncan, E.J. *et al.* (2014) Epigenetics, plasticity, and evolution: how do we link epigenetic change to phenotype? *J. Exp. Zoolog. B Mol. Dev. Evol.* 322, 208–220
84. Leung, C. *et al.* (2020) Reduced phenotypic plasticity evolves in less predictable environments. *Ecol. Lett.* 23, 1664–1672
85. Jørgensen, L.B. *et al.* (2019) How to assess *Drosophila* heat tolerance: unifying static and dynamic tolerance assays to predict heat distribution limits. *Funct. Ecol.* 33, 629–642
86. Glauser, D.A. (2022) Temperature sensing and context-dependent thermal behavior in nematodes. *Curr. Opin. Neurobiol.* 73, 102525
87. Layden, T.J. *et al.* (2022) Thermal acclimation influences the growth and toxin production of freshwater cyanobacteria. *Limnol. Oceanogr. Lett.* 7, 34–42
88. Higgins, K. and Lynch, M. (2001) Metapopulation extinction caused by mutation accumulation. *Proc. Natl. Acad. Sci.* 98, 2928–2933
89. Nunes, T.D.G. *et al.* (2022) Quantitative effects of environmental variation on stomatal anatomy and gas exchange in a grass model. *Quant. Plant Biol.* 3
90. Scholthof, K.-B.G. *et al.* (2018) Brachypodium: a monocot grass model genus for plant biology. *Plant Cell* 30, 1673–1694
91. Marshall, D.J. (2021) Temperature-mediated variation in selection on offspring size: a multi-cohort field study. *Funct. Ecol.* 35, 2219–2228
92. Perry, B.W. *et al.* (2018) Evolution: plasticity versus selection, or plasticity and selection? *Curr. Biol.* 28, R1104–R1106

Trends in
Ecology & Evolution
CellPress

Letter

The importance of spatial and temporal structure in determining the interplay between plasticity and evolution

Anna C. Vinton[1,*,@],
Samuel J.L. Gascoigne,[1]
Irem Sepil,[1] and
Roberto Salguero-Gómez[1,2,3]

Hoffmann and Bridle [1] describe two processes that the framework introduced by Vinton *et al.* [2] did not explicitly consider. These two processes, reversibility of plastic responses and time lags in sensitivity of responses to the environment, can affect how plasticity impacts evolution. These processes are easily incorporated into our framework by adding stage structure and lagged environmental drivers. In Vinton *et al.* [2], when discussing the costs of plasticity, we primarily focused on energetic impacts on fitness, and the role of environmental predictability. Hoffmann and Bridle [1] are correct that differential impacts of plasticity across an individual's lifetime might determine its response to different types of environmental change.

In Vinton *et al.* [2], we took a quantitative genetic approach whereby an individual's phenotypic trait can be decomposed into a genetic and environmental component. Environmental drivers impact the environmental component of the phenotype [3]. For example, the presence of predators may induce the development of armour in *Daphnia* [4]. Morphological traits such as armour that develop early in life are irreversible. Such irreversible plasticity could impact population dynamics and evolution if there is a cost of having armour in a predator-free environment, a cost to not having it in a predator-rich environment, and/or the presence of predators fluctuates with time. Thus, the expression of armour remains constant at all ages greater than the age at which it was produced. In contrast, other traits are reversible. For instance, in *Drosophila melanogaster*, individuals can reversibly adjust the fluidity of their membranes in response to temperature change [5]. Such phenotypically plastic reversibility is most likely to impact evolution for long-lived species, or species which experience high intragenerational environmental variation.

Both the reversibility of plasticity and temporal lag between the environmental cue and the plastic response become especially relevant for individuals experiencing high temporal variation, especially in environments with low temporal autocorrelation. For example, *Daphnia* exposed to predator cues produce offspring that develop spines even if the offspring does not experience these cues. Thus, parental and developmental cues can contradict each other and the adaptive anticipatory effects prove maladaptive. Environmental lags such as these are straightforward to incorporate into the framework in Vinton *et al.* [2]. To do so, one must identify the pertinent environmental drivers from previous time steps and link their effects on phenotypic transitions going forward [6].

Furthermore, spatial structure can impact the effect of plasticity on fitness [7]. If the environment is locally heterogeneous, the organism might experience multiple environments during its lifespan – in this context plasticity will be beneficial. In contrast, if the environment is locally homogeneous, individuals may only experience a single type of environment within their home range. Here, there is less opportunity to modify their phenotype.

The reversibility and time lags of plasticity can be incorporated into our framework introduced in Vinton *et al.* [2] via an explicit temporal component. This component accounts for the stage of individuals, as well as other issues that we did not include in depth, such as how the cost of plasticity may be related to the life stage in which it occurs (Figure 1). To incorporate these drivers, we recommend two relevant widely used methods: structured population and individual-based models (IBMs). Structured population models such as integral projection models (IPMs) have the advantage that they quantify all possible transitions between phenotypic traits, even if these transitions are unlikely. These models can also be analysed with the tool box of linear algebra. Specifically, trade-offs of plasticity within lifecycle stages, or related to a quantitative trait such as body size, can be incorporated to assess the impact of plasticity on population growth rate and evolution [3]. Similarly, spatial structure can also be incorporated [8]. Performing integrated sensitivity analysis would allow us to assess how important specific stages or traits are to population dynamics and evolution while explicitly incorporating lagged trade-offs. The data to construct a model necessary for such analysis are best obtained via experimental manipulations – or via simulations. In addition to the data recommended in Vinton *et al.* [2], experimental work will be necessary to parameterise the stages at which individuals are most sensitive to environmental change, as well as at the stages where phenotypic plasticity occurs [9].

A limitation of IPMs is that they become computationally demanding when the number of phenotypic traits being tracked becomes large. IBMs may be more appropriate in such cases. A limitation of IBMs, however, is that they only iterate forward a sample of all possible phenotypic transitions, such that each run of the model will produce a different outcome, thus limiting reproducibility. Nonetheless, the algorithms defining IBMs are similar to those used in structured population models. This similarity means that, for low dimensional stage models, insights gained from IPMs and IBMs are equivalent [10].

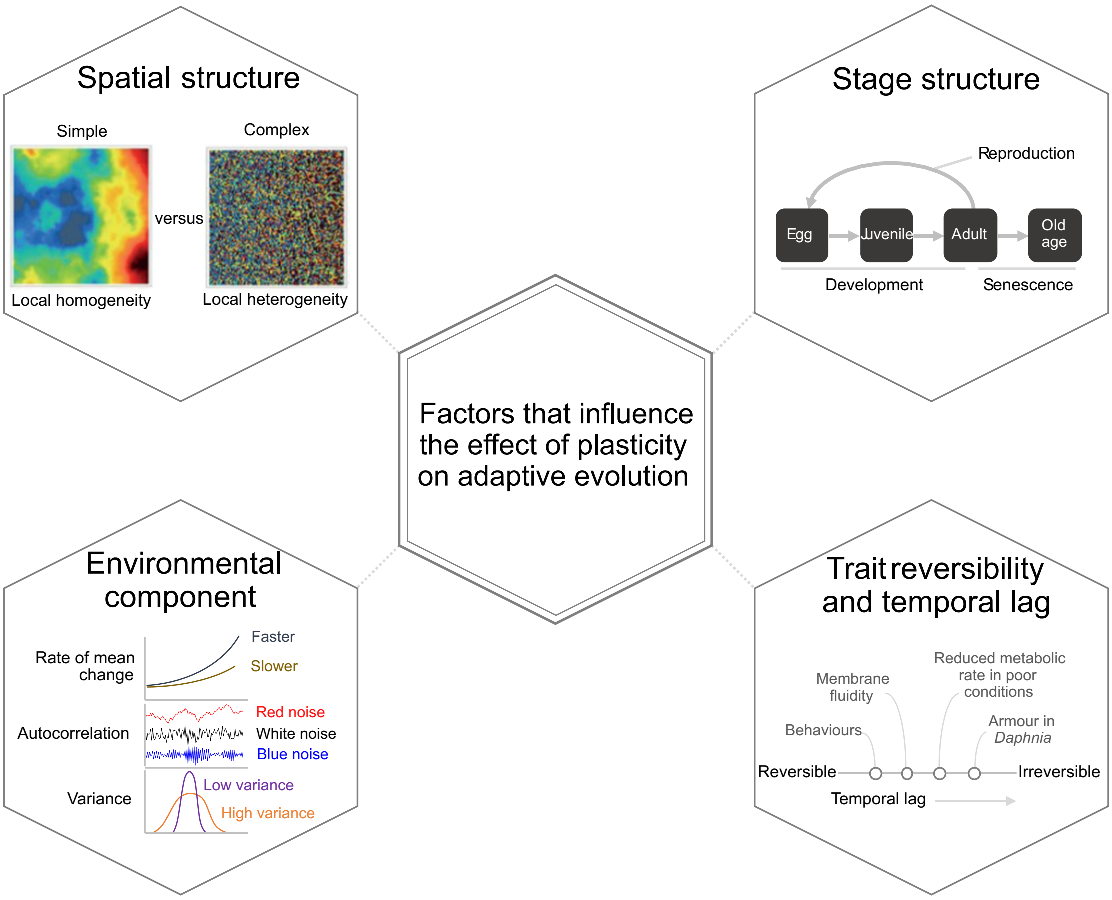

Trends in Ecology & Evolution

Figure 1. Factors that impact the cost of plasticity on individual fitness. In addition to the components discussed in Vinton *et al.* [2], here we explicitly include the importance of the reversibility and temporal lag of plasticity, spatial structure and stage structure in the impact of plasticity on adaptive evolution. Spatial complexity (top left) depicts the importance of the scale of spatial variability within an individual's home range. Stage structure (top right) depicts the importance of the stage (e.g., age or body size) in the potential benefit of plasticity. Trait reversibility and temporal lag (bottom right) refer to the potential impact of whether plasticity can be reversed, and the time lag between when an individual is sensitive to an environment, and when the plasticity is manifested. Lastly, environmental component (bottom left) refers to the different types of temporal change discussed in Vinton *et al.* [2], changes in the environmental mean, variation, and temporal autocorrelation.

The flexibility of the proposed modelling approaches has been vastly increased in recent years. For instance, IPMs have been expanded to examine the role of plasticity on population growth rate, phenotypic traits, life history traits, and ecoevolutionary dynamics [3]. An example includes the role of plasticity in great tit (*Parus major*) in hatching date, coupled with shifts in temperature [11]. Although reversibility and environmentally lagged variables have not been explicitly incorporated into these approaches, it is a simple step to do so. The conditions under which these processes impact the role of plasticity in adaptive evolution have yet to be investigated, and there will likely be parameter space in which factors such as reversibility and lag time are more or less impactful. We pose the utilisation of the aforementioned well-developed approaches to theoretically and empirically explore the impact of these processes. Ultimately a spatiotemporal framework will lend the ability to connect hypotheses drawn from Vinton *et al.* [2] to real-world systems.

Acknowledgments

We thank Tim Coulson for his expertise and feedback in developing and writing this manuscript. A. C.V. was supported by the National Science Foundation Postdoctoral Research Fellowship in Biology under Grant No. (2010783). I.S. was supported by a Biotechnology and Biological Sciences Research Council (BBSRC) Fellowship (BB/T008881/1) and a Welcome Institutional Strategic Support Fund, University of Oxford (BRR00060). R.S-G. was supported by a NERC Independently Research Fellowship (NE/M018458/1).

[1]Department of Biology, University of Oxford, Oxford OX1 3SZ, UK
[2]Centre for Biodiversity and Conservation Science, University of Queensland, St Lucia 4071, QLD, Australia
[3]Evolutionary Demography Laboratory, Max Planck Institute for Demographic Research, Rostock 18057, Germany

*Correspondence:
Anna.Vinton@biology.ox.ac.uk (A.C. Vinton).
@Twitter: @TheoreticalAnna

https://doi.org/10.1016/j.tree.2022.12.009

References

1. Hoffmann, A.A. and Bridle, J. (2023) Plasticity and the costs of incorrect responses. *Trends Ecol. Evol.* 38, 219–220
2. Vinton, A.C. *et al.* (2022) Plasticity's role in adaptive evolution depends on environmental change components. *Trends Ecol. Evol.* 37, 1067–1078
3. Coulson, T. *et al.* (2017) Modeling adaptive and nonadaptive responses of populations to environmental change. *Am. Nat.* 190, 313–336
4. Diel, P. *et al.* (2020) Knowing the enemy: inducible defences in freshwater zooplankton. *Diversity* 12, 147
5. Cooper, B.S. *et al.* (2014) Thermal adaptation of cellular membranes in natural populations of *Drosophila melanogaster*. *Funct. Ecol.* 28, 886–894
6. Evers, S.M. *et al.* (2021) Lagged and dormant season climate better predict plant vital rates than climate during the growing season. *Glob. Change Biol.* 27, 1927–1941
7. Bridle, J. and Hoffmann , A.A. (2022) Understanding the biology of species' ranges: when and how does evolution change the rules of ecological engagement? *Philos. Trans. R. Soc. B Biol. Sci.* 377, 20210027
8. Jongejans, E. *et al.* (2011) Importance of individual and environmental variation for invasive species spread: a spatial integral projection model. *Ecology* 92, 86–97
9. Coulson, T. *et al.* (2021) Predicting evolution over multiple generations in deteriorating environments using evolutionarily explicit Integral Projection Models. *Evol. Appl.* 14, 2490–2501
10. Ellner, S.P. *et al.* (2016) *Data-driven Modelling of Structured Populations. A Practical Guide to the Integral Projection Model*, Springer
11. Simmonds, E.G. *et al.* (2020) Phenological asynchrony: a ticking time-bomb for seemingly stable populations? *Ecol. Lett.* 23, 1766–1775

Evolution, Complexity, and Life History Theory

Walter Veit[1,2,3], Samuel J L Gascoigne[3], and Rob Salguero-Gómez[3]

[1]Department of Philosophy, University of Bristol
[2]Munich Center for Mathematical Philosophy, LMU
[3]Department of Biology, University of Oxford

March 1, 2023

Please cite as: Veit, W., Gascoigne, S.J.L, and Salguero-Gómez, R. (2022). Evolution, Complexity, and Life History Theory. Preprint. [Add Link]

Check www.walterveit.com for citation details once published

Evolution, Complexity, and Life History Theory

Walter Veit[1,2,3,*], Samuel J. L. Gascoigne[3], and Roberto Salguero-Gómez[3,4,5]

[1]Department of Philosophy, University of Bristol
[2]Munich Center for Mathematical Philosophy, LMU
[3]Department of Biology, University of Oxford
[4]Centre for Biodiversity and Conservation, University of Queensland
[5]Evolutionary Demography Laboratory, Max Planck Institute for Demographic Research

*Contact email corresponding author: wrwveit@gmail.com

Abstract

In this paper, we revisit the long-standing debate of whether there is a pattern in the evolution of organisms towards greater complexity, and how this hypothesis could be tested using an interdisciplinary lens. We argue that this debate remains alive today due to the lack of a quantitative measure of complexity that is related to the teleonomic (*i.e.* goal-directed) nature of living systems. Further, we argue that such a biological measure of complexity can indeed be found in the vast literature produced within life history theory. We propose that an ideal method to quantify this complexity lays within life history strategies (*i.e.,* schedules of survival and reproduction across an organism's life cycle), as it is precisely these strategies that are under selection to optimise the organism's fitness. In this context, we set an agenda for future steps: (1) how this complexity can be measured mathematically, and (2) how we can engage in a comparative analysis of this complexity across species to investigate the evolutionary forces driving increases or for that matter decreases in teleonomic complexity.

Keywords: biological complexity; evolutionary trends; fitness; goal directedness; life history theory; life history complexity; optimality; teleonomy.

Index

---

1 Introduction

In a 1991 paper in this journal, Daniel McShea criticised the longstanding conviction among evolutionists, ever since Darwin (1859), that the complexity of species increases over evolutionary time, in addition to the closely related idea of progressive evolution (see Levit and Olsson 2006). Aiming to question these ideas, McShea argued that there is almost no empirical evidence supporting this belief in a kind of directionality of evolution and that biologists may simply be misled by their own biased presuppositions. Further, he suggested that research should shift from more theoretical model-building work to empirical inquiries into actual increases in complexity offering several avenues for future research. Unfortunately, such a shift has not yet taken place. Rather, it seems that the interest among evolutionary biologists in the notions of complexity and progress has been waning for at least three decades, with the exception of their own work (McShea 1996a,b, 2021; McShea and Brandon 2010). Despite the scepticism advocated by McShea, however, it appears that biologists (as opposed to philosophers of biology) have nevertheless remained convinced in the consensus idea of an increase in complexity through evolutionary time.

The goal of this programmatic paper is to argue that McShea may have been incorrect in attributing this belief to mere cultural or perceptual biases among biologists. While we agree with his call for more empirical research, we do not share his dismissal of theoretical model-building work to understand complexity. Our core argument in this paper is that the natural phenomenon driving most of these ideas and intuitions regarding the directedness of evolution towards complexity is not any kind of complexity, but a special kind of complexity, distinct to the study of living systems, that has been increasing ever since the origin of life. We argue that this debate remains unresolved because of the lack of a distinctive biological measure of complexity that is related to the *teleonomic* nature of living systems.

Importantly, we use Pittendrigh's (1958) definition of the term 'teleonomic', as an evolutionary replacement of pre-Darwinian teleological explanations, *i.e.* that life is to be explained in terms of its purpose (often associated with a designer) rather than the mechanisms that gave rise to it. The concepts of goals, purposes, functions, and the like were revolutionized in the light of Darwin's theory of evolution by natural selection that explained them in causal terms. For instance, the goal of an organism is the maximization of fitness - not because that is true for any living system, but because natural selection has selected for such individuals in the past, which gives us predictive power to theorize about individuals in the present. Thus, as we use 'teleonomic' in this article, we define 'teleonomic' as the goal-directedness of living systems towards fitness-maximization. While the term teleonomic is also relevant for discussions of the 'functions' of traits, that is not the focus of this article, which is also why measures of functional complexity do not successfully capture the goal-directness of organisms (see McShea 2000 for an overview of this literature). By using this teleonomic lens, we conceptualize teleonomic complexity in terms of how complex the strategies are that organisms have evolved in order to achieve this goal. Some of these strategies are recognizably more complex and our goal here is to emphasize the need to measure and study this complexity.

Furthermore, we argue that such a biological measure of complexity is already available within the rich arsenal of metrics provided by life history theory and comparative demography. It is only in assessing the complexity of life history strategies that we are provided with a teleonomic measure of complexity that assesses the degree of complexity within evolved life history strategies in the pursuit of the goal of fitness-maximization. In addition, we conclude by outlining two directions for future research, one concerning how this complexity can be measured mathematically, and the other for how we can engage in a comparative analysis of this complexity across species to gain key insights toward understanding the evolution of organismal complexity.

Article Outline

This programmatic paper is structured as follows. In Section 2, we outline the debate on the evolution of complexity and argue that we should not be interested in any kind of complexity when it comes to the evaluation of progressive views of evolution without considering teleonomic complexity. In Section 3, we discuss how to measure teleonomic complexity, one must turn to life history theory. Finally, Section 4 outlines avenues for further research into the evolution of complexity.

2 Complexity and Evolution

We agree with McShea (1991) in that discussions of biological complexity have been present among a long row of evolutionists dating back to Darwin[1], Lamarck (1984), Cope (1871), Spencer (1890), Huxley (1953), Rensch (1960), Simpson (1961), and that these discussions have been of particular importance in the investigation of macro-evolutionary trends in paleobiology (Eble 2005; Jablonski 2005; Lowery & Fraass 2019). Despite some critiques of the idea, the last century saw great confidence in the idea that evolution increases complexity:

> [I]ncreasing complexity is still the conventional wisdom. Clear statements that complexity increases can be found in the work of Stebbins (1969), Denbigh (1975), Papentin (1980), Saunders and Ho (1976; 1981), Wake et al. (1986), Bonner (1988), and others. And lately the new thermodynamic school of thought has added its voice to the chorus: Wicken (1979; 1987), Brooks and Wiley (1988), and Maze and Scagel (1983) have all argued that complexity ought to and does increase in evolution. In my own experience, the consensus extends well beyond evolutionary biology and professional scientists. People seem to know that complexity increases as surely as they know that evolution has occurred.
>
> – Daniel McShea (1991, p. 303)

Much of the writing on biological complexity has unsurprisingly focused on the evolution and explosion of multicellular life and body-plans in the Cambrian. And yet, despite this conventional impression and the search for evidence for this thesis, very little evidence either in favour or against the hypothesis has been obtained. As McShea (1991) notes, few have actually empirically investigated whether complexity increases with evolutionary time. Yet, there have been many attempts at developing adaptive rationales for why an increase in complexity is beneficial and ought to be expected.

Biologists have long confidently maintained that 'organismal' or 'biological complexity' will increase throughout evolutionary history. Indeed, this is an idea that, as McShea (1991) points out, "extends well beyond evolutionary biology and professional scientists. People seem to know that complexity increases as surely as they know that evolution has occurred" (p. 304). This strange attraction to the idea that complexity inevitably increases with evolutionary time may be especially perplexing since it sits uncomfortably close to older vitalist and teleological views of

---

[1] Though as McShea (1991) notes, Darwin only discussed his views on marcoevolutionary trajectories toward complexity in his Notebook E, not in his *Origin* (see Darwin 1987, p. 422).

progressive evolution or as it is sometimes called 'orthogenesis' (Ruse 2019). It is thus unsurprising that McShea (1996b) has been critical of attempts to revive Herbert Spencer's ideas of progressive evolution and the adaptive rationales of complexity and mind (Godfrey-Smith 1996), though also noting that the idea of progressive evolution remains "essentially the conventional wisdom even today" (p. 469). While we do not agree that the idea of progressive evolution is conventional wisdom today (or for that matter, even in 1991), the seeming increase in complexity in organisms such as during the Cambrian explosion (Valentine et al. 1994) has certainly come to inspire a lot of speculation (e.g., Carroll 2001; Zhang et al. 2014). If there is no evidence for an increase in complexity over evolutionary time-scales, however, there would appear to be little point in offering an adaptive explanation for a phenomena that may merely be a myth - perhaps as other critics of the idea alongside McShea (1991), such as Williams (1966), Lewontin (1968), Hinegardner and Engelberg (1983) hint at, a remainder of earlier hierarchical views of the biological world with humans placed on top that biologists have largely abandoned, though remain popular among the public.

McShea (1991) highlights how both empirical and theoretical studies have lacked rigor. For instance, most studies and perspectives miss concise discussions of what complexity actually means. Admittedly, while the concept has long puzzled philosophers and scientists alike, it seems reasonably clear that complexity is a *phenomenon* in nature. Complexity is as our folk understanding of the term rightly suggests opposed to the idea of simplicity, but this understanding does not give us much purchase on making the notion precise. Parts of nature can be readily placed on a continuum from simplicity to complexity. A frog catching a fly is more complex than a stone washed up at a beach. So one might be hopeful that we could develop a straightforward and unified measure of complexity to capture this phenomena in nature - a way of ranking systems on a single scale of complexity. Yet, attempts to operationalize complexity have resisted consensus.

We believe that part of the challenge here has been especially due to attempts to provide biologically neutral measures of complexity that could in principle be applied to any non-biological system. These neutral measures miss out on what we think has driven most advocates of the view that natural selection would select for greater complexity. For example, McShea (1991) repeatedly emphasizes that it is *morphological complexity*, rather than genetic complexity or ecosystem complexity, that he is interested in. And as he makes clear, the way this complexity should be measured has largely been inspired by researchers in information theory whose operationalizations of complexity could be applied to living and non-living systems alike.However, we argue the complexity that matters for biological systems should be informed by the drivers of evolutionary change; a teleonomic measure of complexity that assesses how the complexity of different strategies organisms have evolved to achieve their goal of fitness maximization.

One rough-and-ready measure of biological complexity in terms of heterogeneity is found, as Godfrey-Smith notes, in Bonner's 1988 book *The Evolution of Complexity*, where he measures complexity as a function of distinctive cell types in a multicellular organism, a move typical in discussions on cell-differentiation, division of labour, and the evolution of multicellularity (see Márquez-Zacarías et al. 2021). While this measure certainly is closer to the kind of teleonomic complexity we are interested in, it is only a proximate measure at best since it makes no reference to the complex trade-offs organisms undergo in the pursuit of fitness maximization. Furthermore, this definition in terms of heterogeneity lacks scale. For example, a patch of one cell is less complex than a patch of three cells. But, what if they can be differentiated? How does a patch of five cells of the same type compare to a patch of two cells of different types? The definition falls under the weight of its own constraints - in turn lacks scale. This shortcoming emphasizes the necessity of scalability in a measure of biological complexity. The metric must be exhaustive in the parameter space it can describe. In turn, the biological complexity of an *Escherichia coli*, a gopher and a giant squid from the depths must exist at some point in the same parameter space quantifying biological complexity.

In explaining ideas about biological complexity, many have drawn on Shannon's (1948) information theory published in "A Mathematical Theory of Communication", sometimes referred to as 'Shannon information' or 'Shannon entropy'. Following Godfrey-Smith (1996), Shannon information can be calculated as follows: for any system that has an exhaustive number of possible states, there is a probability of being in that state *i* denoted as P_i, "then the complexity or disorder of the system is measured as: $\mathrm{E} = -\sum P_i \log_2 (P_i)$" (p. 28). If there are few possible states or most of the probability space is exhausted by a few options, entropy or thermodynamic probability is low, *i.e.* there is little uncertainty. If there are many alternative states with similar likelihoods, however, then uncertainty is high and the system is more complex. The higher the entropy, the higher the (potential) informational content of the states. Here, both organisms and environments can be understood as complex or simple the number and probability of their possible states. However, what these measures are lacking is a link to the 'goal' of biological systems, *i.e.* fitness. While these measures of entropy are certainly useful to capture uncertainty, variability, changeability, heterogeneity, and disorder of systems (Godfrey-Smith 1996), we are skeptical that it captures the kind of complexity that is important to living systems (Smith 1975). This skepticism is so because, as mentioned above, they do not recognize the complex strategic trade-offs organisms undergo to maximize their fitness. Indeed, in the measure of entropy there is no connection to the biological notion of reproduction and survival, the building blocks of organismal fitness.

Finally, to understand teleonomic complexity, we have to understand the population rather than the individual, which is neglected in many such measures of biological complexity. As van Groenendael et al. (1994) note, “Variation in life history traits among individuals within populations is ubiquitous in both plants and animals” (p. 2410). Nevertheless, the fact that life history strategies can be very complex also makes them very difficult to study. As such, we are happy to take up the task McShea (1991) has left to the discipline: “I leave it to others to discover the extent to which my remarks apply in other complexity domains” (p. 305). Why does the teleonomic complexity of species increase over evolutionary time? As we shall argue in the next section, the means for this task are to be found in life history theory as *the theory* of organismal strategies we find in nature.

3 Life History Theory and Teleonomic Complexity

Life history theory originated out of the study of the trade-offs between survival and reproduction. Some of these were very simple mathematical models (e.g. Leslie and Lefkovitch matrix population models: Leslie 1945; Lefkovitch 1965), while others were quite complex to understand the schedules of survival and reproduction can impact fitness (see especially Stearns 1992; Roff 1992). As Veit (2023) puts it: “To understand a species’ teleonomic strategy is to understand their species-specific trade-offs between costly investments of resources into development, fecundity, and survival, with fitness providing an ultimate ‘common currency’ for this economic decision problem, or ‘game’ against nature” (p. 13). Trade-offs are universal and so the so-called Darwinian demon cannot evolve. Because of the myriad factors that have to be traded off against each other, it is no surprise that Morbeck et al. (1997) has nicely described life history theory as providing us with “a means of addressing the integration of many layers of complexity of organisms and their worlds” (p. xi). It is here that we find ourselves provided with the theoretical means to understand teleonomic complexity.

While Lewontin criticized adaptationism for not being able to deal with trade-offs and treating organisms as mere robotic bundles of traits (Lewontin 1985; see also Gould and Lewontin 1979), life-history theory offers an adaptationist framework to make sense of just such trade-offs. These trade-offs can be seen as the result of natural selection shaping traits such that a life history agent is able to pursue their goal of maximizing fitness:

> In life-history theory, [...] numerous aspects of an organism’s life-cycle, such as the timing of reproduction or the length of its immature phase, can be understood by treating the organism as if it were an agent trying to maximize its expected number of offspring-or some other appropriate fitness measure-and had devised a strategy for achieving that goal.
>
> – Samir Okasha (2018, p. 10)

As evolution gives rise to more complex life history strategies, it is easy to see why many early evolutionists were convinced of the idea of progressive evolution. With fitness-maximization being both the teleonomic 'goal' and cause of organisms, life histories allow us to study the varying degrees of complexity organisms use to achieve this goal (e.g., from the relatively simple and fatally semelparous salmon to the relatively complex immortal jellyfish, *Turritopsis dohrnii*, that can reproduce sexually and asexually aswell as switch back and forth between sexual mature and sexually immature stages). We, therefore, think that our notion of teleonomic complexity offers an elegant way of explaining the connection between complexity and 'progress' that has often been made in this debate without necessarily having to explain it away as a mere cognitive bias.

Interestingly, such a teleonomic perspective does not have to imply that increases in complexity are inevitable. Indeed, because increases in complexity are typically associated with costs there is also an evolutionary drive towards simplicity, i.e. organisms developing less complex strategies. Two excellent examples that make this obvious are annualism and dwarfism.

While most animals typically reproduce over multiple reproductive cycles, many plants such as annual weeds are *annualists*, i.e. their life cycle involves only a single breeding season before the individual dies (Hautekèete, Piquot & Van Dijk 2001; Friedman 2020). On the other side, we find *perenniality*, i.e. life cycles lasting more than one year. Should we expect natural selection to inevitably move species towards perenniality? When chance of survival is low it makes sense for species to evolve very short life cycles and invest everything in one of few reproductive cycles. Natural selection thus often makes life history strategies less complex by moving from complex trade-offs towards investing everything in one breeding season (Bena et al. 1998; Fox 1990). Furthermore, species often switch quite rapidly (in evolutionary terms) from one strategy to the other or for that matter back again, suggesting that there is a lot of evolutionary pressure on the costs of more complex life history strategies (Friedman 2020). Similarly, we can find dwarfism in many species, i.e. individuals or species becoming significantly smaller in response to selection. Examples include the pygmy marmoset, *Callithrix pygmaea* (Montgomery & Mundy 2013), which stands in opposition to the common observation that animal size increases over time (Alroy 1998). The selective pressures that lead to dwarfism are manifold, though the most often discussed factor is related to the isolation of breeding populations to islands (Foster 1964). As we hope to have thus made clear, we should not expect some general explanation that can explain changes in life course complexity across all of life. Our explanations will have to be more fine-grained than that. Steiner and Tuljapurkar (2022), for instance, have recently shown using life history data that much of the non-environmental and non-genetic variability of phenontypes in a population cannot simply be categorized as neutral in respect to evolution, or for that matter selected for or against. The variability of life courses within even a single population remains a major puzzle within the field (see also Flatt 2020) and we hope that the development of our framework will help us move closer towards an understanding of how and why life history strategies change over evolutionary time. Thus, let us now turn to how this complexity can be understood in the context of life history theory.

Life History Strategies and Complexity

A life history strategy is the eco-evolutionary equivalent of a bar of soap in the bathtub; the firmer you try to grip its definition, the more the blighter lurches further from grasp. From parental care (Klug & Bonsall 2010) to dispersal (Bonte & Dahirel 2016), a plethora of phenotypes are required to fully characterise life histories across the tree of life. Simply put, a life history strategy is not a physical characteristic of a population one can extract and manipulate. In turn, when we discuss a life history strategy we must require our discourse to be general across form, temporal and spatial scales. Life histories are combinations of life history traits, and the latter refer to key moments along the life cycle of a species (e.g., age at maturity, frequency of reproduction, rate of development and generation time; Stearns 1992).

With this in mind, we propose we define a life history strategy as the time points and actions across an individual's lifespan that allow the population to persist in the face of ecological perturbations. Using this definition, let us build the archetype of a life history strategy – in its simplest form:

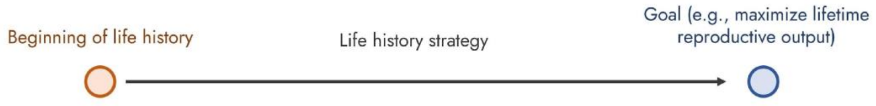

Figure 1: The goal of life history strategies

All life history strategies are defined by a schedule starting from the start of a life history (*e.g.*, birth, fission, cloning). This beginning is followed by a life history strategy that directs the individual towards a goal (*e.g.*, maximizing lifetime reproductive output or inclusive fitness).

Now that we have built our archetypal life history strategy, let us explore life history complexity. We can define life history complexity as being informed by two components of the aforementioned life history strategy. Firstly, life history complexity is informed by the number of paths individuals of the same population can take from the beginning of their life history to their goal - a term known as individual heterogeneity in life history theory (Tuljapurkar et al. 2008, Vindenes & Langangen 2015). Secondly, life history complexity is informed by the relative contribution of each of the paths toward the goal. For example, here are two life history strategies with different levels of life history complexity due to the number of possible paths.

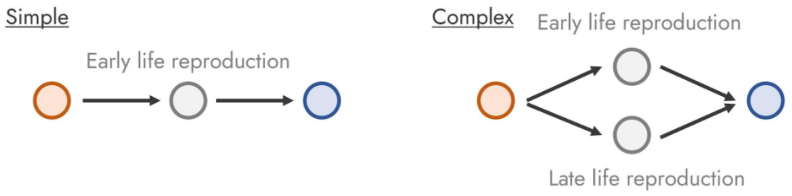

Figure 2: Complex and simple life history strategies

Furthermore, here are two life history strategies that differ in their complexity based on the evenness in importance of paths for individuals to reach their goal.

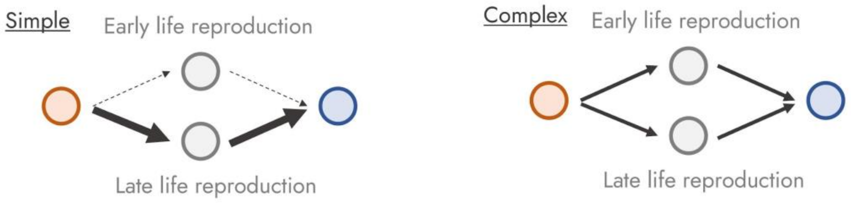

Figure 3: Complex and simple life history strategies

In short, by analysing the number and importance of paths in a life history, we are able to (even if only relatively) create a framework for life history complexity that is both based on the necessary properties of a life history strategy - shown in the archetypal example – and scalable across modes of life history research (e.g., from demography to behavioural ecology to developmental biology).

While we will not go into the mathematical measurement of this complexity in this paper here, we will nevertheless note that it will be straightforward to calculate this complexity by drawing on available matrix population models - a discrete time stage/age structured mathematical model where survival, growth and reproduction values are coerced into matrix form - of different species' demographic data to assess their life history strategies. As Van Groenendael et al. (1994) have argued, matrix models have shown themselves to be extraordinarily useful for the mathematical analysis of complex life history strategies (see also van Groenendael et al. 1988), which is why we believe it will provide the ideal resource to measure life history complexity.

4 Conclusion and Further Directions

Our goal in this paper was to introduce a set of conceptual ideas on how to assess a distinctive kind of biological complexity unique to living systems that we have called *teleonomic complexity*. In his seminal paper, McShea (1991) assumed that we should think of ideas about the evolution of complexity as being about morphological complexity. Yet, we have argued that the seemingly progressive evolution views of these authors can be naturalized in a less problematic sense in terms of an increase in teleonomic complexity without thereby invoking the idea of orthogenesis. As we hope to have made clear here, the apparent belief of many evolutionists in progress towards greater complexity can in principle be naturalized in a Darwinian way by restating this thesis as one about an increase in teleonomic complexity. That is, over evolutionary time, more complex life history strategies will emerge and it is this teleonomic complexity that we should be interested in.

That this complexity should be measured through the lens of life history theory was the second argument of our paper. All species have evolved life history strategies to achieve their teleonomic goals of maximizing their genetic representation in the next generation. These fitness differences can be mapped out in different ways to assess the diversity of life and one important dimension along which we can assess this diversity is of course complexity. Some life history strategies are more complex than others and natural selection is leading to an ever-growing exploration of more complex life history strategies (Giménez et al. 2004; Sebert-Cuvillier et al. 2007; Higgins et al. 2015). We are, of course, not endorsing the simplistic orthogenesis view that evolution leads to perfection and greater complexity as an end in itself. However, complex design solutions to the problems animals, plants, and other organisms face do not come out of nowhere. Their history is one from successively more complex strategies upon which more complex strategies can come to be explored. Natural selection provides an entirely unproblematic kind of progress if it is defined in a teleonomic manner, since we can expect it to come up with new and more 'ingenious' strategies that make sense of the apparent directness of evolution. We have thus argued against the suggestion by McShea that biologists may have fallen victim to their own cultural and perceptual biases forces *scala naturae* thinking into our view of life.

Nevertheless, while we have offered an explication of the idea of teleonomic complexity here, it remains a difficult problem to show how we can measure this complexity in practice. Acknowledging the difficulty of this task, we are currently working on a follow-up paper, where we will draw on graph theory to demonstrate how life history complexity can be mathematically measured such that others could engage in the same kinds of analyses to us of the same or other data sets. This task, however, will be left for another paper.

While we have argued that McShea depicts theoretical work unfairly, he was certainly right that there is a need for more empirical work to fill out what has largely remained a data and inference vacuum. We are carefully optimistic that teleonomic complexity can be expected to increase over evolutionary time, yet we acknowledge the need to provide further evidence for this view both in virtue of theoretical models and empirical studies. In another paper, we will apply our new life history complexity measure to the COMADRE (Salguero-Gómez et al. 2016) and COMPADRE (Salguero-Gómez et al. 2015) databases offering matrix population models of hundreds of animal and plants species to offer a comparative analysis of the complexity of life history strategies across a broad range of taxa.

Finally, we hope that our programmatic paper will raise interest in the teleonomic complexity of different species, which should not be confused with other notions such as morphological or functional complexity. It is our hope that both biologists and philosophers will contribute to its investigations and in order to understand under which conditions life history strategies become more complex or for that matter become more simple.

Funding

This article is part of a project that has received funding from the European Research Council (ERC) under the European Union's Horizon 2020 research and innovation program (grant agreement number 101018533).

References

Alroy, J. 1998. Cope's rule and the dynamics of body mass evolution in North American fossil mammals. Science 280: 731– 734.

Bena, G., Lejeune, B., Prosperi, J. M., & Olivieri, I. (1998). Molecular phylogenetic approach for studying life-history evolution: the ambiguous example of the genus Medicago L. Proceedings of the Royal Society of London. Series B: Biological Sciences, 265(1401), 1141-1151.

Bonner, J. T. (1988). The Evolution of Complexity. Princeton, NJ: Princeton University Press.

Bonte, D., & Dahirel, M. (2017). Dispersal: a central and independent trait in life history. Oikos, 126(4), 472-479.

Brooks, D. and E. Wiley (1988). Evolution as Entropy, 2nd edition. University of Chicago Press, Chicago.

Carroll, S. B. (2001). Chance and necessity: the evolution of morphological complexity and diversity. Nature, 409(6823), 1102-1109.

Cope, E. (1871). The Method of Creation of Organic Forms. Proceedings of the American Philosophical Society 12, 229–263.

Darwin, C. (1987). Notebook E. In P.H. Barrett et al. (Ed.), Charles Darwin's Notebooks. Ithaca, NY: Cornell University Press.

Darwin, C. (1859). On the origin of species by means of natural selection, or preservation of favoured races in the struggle for life. London: John Murray.

Eble, G.J. (2005). Morphological modularity and macroevolution: conceptual and empirical aspects. In: Callebaut W, Rasskin-Gutman D (eds) Modularity: understanding the development and evolution of complex natural systems. MIT Press, Cambridge.

Flatt, T. (2020) Life-history evolution and the genetics of fitness components in Drosophila melanogaster. Genetics, 214(1), 3 – 48.

Foster, J.B. 1964. Evolution of mammals on islands. Nature 202: 234–235.

Fox, G. A. (1990). Perennation and the persistence of annual life histories. The American Naturalist, 135(6), 829-840.

Friedman, J. (2020). The evolution of annual and perennial plant life histories: ecological correlates and genetic mechanisms. Annual Review of Ecology, Evolution, and Systematics, 51, 461-481.

Giménez, Klaus Anger, L., & Torres, G. (2004). Linking life history traits in successive phases of a complex life cycle: effects of larval biomass on early juvenile development in an estuarine crab, Chasmagnathus granulata. Oikos, 104(3), 570-580.

Denbigh, K. (1975). A Non-Conserved Function for Organized Systems. In L. Kubat and J. Zeman (Eds.), Entropy and Information in Science and Philosophy, pp. 83–92. American Elsevier, New York.

Godfrey-Smith, P. (1996). Complexity and the Function of Mind in Nature. Cambridge: Cambridge University Press.

Gould, S. J. and R. C. Lewontin (1979). The spandrels of San Marco and the Panglossian paradigm: a critique of the adaptationist programme. Proceedings of The Royal Society of London. Series B. Biological Sciences 205 (1161), 581–598.

Griffiths, P. E. and J. Matthewson (2018). Evolution, dysfunction, and disease: A reappraisal. The British Journal for the Philosophy of Science 69(2), 301–327.

Hautekèete, N. C., Piquot, Y., & Van Dijk, H. (2001). Investment in survival and reproduction along a semelparity–iteroparity gradient in the Beta species complex. Journal of Evolutionary Biology, 14(5), 795-804.

Higgins, R. M., Diogo, H., & Isidro, E. J. (2015). Modelling growth in fish with complex life histories. Reviews in Fish Biology and Fisheries, 25, 449-462.

Hinegardner, R. and J. Engelberg (1983). Biological complexity. Journal of Theoretical Biology 104(1), 7–20.

Huxley, J. (1953). Evolution in Action. New York: Harper and Brothers.

Jablonski, D. (2005). Mass extinctions and macroevolution. Paleobiology, 31(S2), 192-210.

Klug, H., & Bonsall, M. B. (2010). Life history and the evolution of parental care. Evolution, 64(3), 823-835.

Lamarck, J. (1984). Zoological Philosophy. Chicago: University of Chicago Press. H. Elliot, Trans.

Lefkovitch, L. P. (1965). The Study of Population Growth in Organisms Grouped by Stages. Biometrics, 21(1), 1–18.

Leslie, P. H. (1945). On the Use of Matrices in Certain Population. Biometrika, 33(3), 183–212.

Levit, G. S., & Olsson, L. (2006). "Evolution on rails": mechanisms and levels of orthogenesis. Ann Hist Philos Biol, 11, 99-138.

Lewontin, R. (1968). Evolution. In D. Sills (Ed.), International Encyclopedia of the Social Sciences, Volume 5, pp. 202–210. The MacMillan Company and The Free Press.

Lewontin, R. C. (1985). The organism as the subject and object of evolution. In R. Levins and R. C. Lewontin (Eds.), The Dialectical Biologist. Cambridge, MA: Harvard University Press.

Lowery, C. M., & Fraass, A. J. (2019). Morphospace expansion paces taxonomic diversification after end Cretaceous mass extinction. Nature Ecology & Evolution, 3(6), 900-904.

Márquez-Zacarías, P., R. M. Pineau, M. Gomez, A. Veliz-Cuba, D. Murrugarra, W. C. Ratcliff, and K. J. Niklas (2021). Evolution of Cellular Differentiation: From Hypotheses to Models. Trends in Ecology & Evolution 36(1), 49–60.

Maze, J. and R. Scagel (1983). A different view of plant morphology and the evolution of form. Systematic botany, 469–472.

McNamara, J. M. and A. I. Houston (1996). State-dependent life histories. Nature 380(6571), 215–221.

McShea, D. W. (1991). Complexity and evolution: what everybody knows. Biology & Philosophy 6(3), 303–324.

McShea, D. W. (1996a). Perspective metazoan complexity and evolution: is there a trend? Evolution 50(2), 477–492.

McShea, D. W. (1996b). Unpredictability! and the Function of Mind in Nature. Adaptive Behavior 4(3-4), 466–470.

McShea, D. W. (2000). Functional complexity in organisms: parts as proxies. Biology & Philosophy, 15(5), 641.

McShea, D. W. (2021). Evolution of complexity. Evolutionary Developmental Biology: A Reference Guide, 169–179.

McShea, D. W. and R. N. Brandon (2010). Biology's first law: the tendency for diversity and complexity to increase in evolutionary systems. University of Chicago Press.

Montgomery, S. H., & Mundy, N. I. (2013). Parallel episodes of phyletic dwarfism in callitrichid and cheirogaleid primates. Journal of evolutionary biology, 26(4), 810-819.

Morbeck, M., A. Galloway, and A. Zihlman (1997). The Evolving Female: A Life-History Perspective. Princeton, NJ: Princeton University Press.

Okasha, S. (2018). Agents and Goals in Evolution. Oxford: Oxford University Press.

Papentin, F. (1980). On order and complexity. I. General considerations. Journal of Theoretical Biology 87(3), 421–456.

Pittendrigh, C. S. (1958). Adaptation, natural selection, and behavior. In A. Roe and G. G. Simpson (Eds.), Behavior and Evolution. New Haven: Yale University Press.

Rensch, B. (1960). Evolution above the Species Level. New York: Columbia University Press.

Roff, D. A. (1992). Evolution of Life Histories: Theory and Analysis. New York: Chapman and Hall.

Roff, D. A. (2002). Life History Evolution. New York: W. H. Freeman.

Ruse, M. (2019). The Darwinian Revolution. Cambridge University Press.

Salguero-Gómez, R., Jones, O. R., Archer, C. R., Bein, C., de Buhr, H., Farack, C., ... & Vaupel, J. W. (2016). COMADRE: a global data base of animal demography. Journal of Animal Ecology, 85(2), 371-384.

Salguero-Gómez, R., Jones, O. R., Archer, C. R., Buckley, Y. M., Che-Castaldo, J., Caswell, H., ... & Vaupel, J. W. (2015). The compadre Plant Matrix Database: an open online repository for plant demography. Journal of Ecology, 103(1), 202-218.

Saunders, P. T. and M.-W. Ho (1976). On the increase in complexity in evolution. Journal of Theoretical Biology 63(2), 375–384.

Saunders, P. T. and M.-W. Ho (1981). On the increase in complexity in evolution II. The relativity of complexity and the principle of minimum increase. Journal of Theoretical Biology 90(4), 515–530.

Sebert-Cuvillier, E., Paccaut, F., Chabrerie, O., Endels, P., Goubet, O., & Decocq, G. (2007). Local population dynamics of an invasive tree species with a complex life-history cycle: a stochastic matrix model. ecological modelling, 201(2), 127-143.

Shannon, C. E. (1948). A mathematical theory of communication. The Bell system technical journal 27(3), 379–423.

Simpson, G. (1961). Principles of Animal Taxonomy. New York: Columbia University Press.

Smith, C. J. (1975). Problems with entropy in biology. Biosystems, 7(2), 259-265.

Spencer, H. (1890). First Principles, 5th edition. London: Williams and Norgate.

Stearns, S. C. (1992). The Evolution of Life Histories. Oxford: Oxford University Press.

Stebbins, G. (1969). The Basis of Progressive Evolution. University of North Carolina Press, Chapel Hill.

Steiner, U. K., & Tuljapurkar, S. (2022). Adaption, neutrality and life-course diversity. Ecology Letters.

Tuljapurkar, S., Steiner, U. K., & Orzack, S. H. (2009). Dynamic heterogeneity in life histories. Ecology letters, 12(1), 93-106.

Valentine, J., Collins, A., & Meyer, C. (1994). Morphological complexity increase in metazoans. Paleobiology, 20(2), 131-142.

van Groenendael, J., H. de Kroon, and H. Caswell (1988). Projection matrices in population biology. Trends in ecology & evolution 3(10), 264–269.

Van Groenendael, J., H. De Kroon, S. Kalisz, and S. Tuljapurkar (1994). Loop analysis: evaluating life history pathways in population projection matrices. Ecology 75(8), 2410–2415.

Veit, W. (2022). Health, Consciousness, and the Evolution of Subjects. Synthese. https://doi.org/10.1007/s11229-022-03998-z

Vindenes, Y., & Langangen, Ø. (2015). Individual heterogeneity in life histories and eco-evolutionary dynamics. Ecology letters, 18(5), 417-432.

Wake, D., E. Connor, A. de Ricqles, J. Dzik, D. Fisher, S. Gould, M. LaBarbera, D. Meeter, V. Mosbrugger, W.-E. Reif, R. Rieger, A. Seilacher, and G. Wagner (1986). Directions in the History of Life. In D. Raup and D. Jablonski (Eds.), Patterns and Processes in the History of Life, pp. 47–67. Springer-Verlag, Berlin.

Wicken, J. (1987). Evolution, Thermodynamics, and Information. Oxford University Press, Oxford.

Wicken, J. S. (1979). The generation of complexity in evolution: A thermodynamic and information-theoretical discussion. Journal of Theoretical Biology 77(3), 349–365.

Williams, G. C. (1966). Natural selection, the costs of reproduction, and a refinement of Lack's principle. The American Naturalist 100(916), 687– 690.

Zhang, X., Shu, D., Han, J., Zhang, Z., Liu, J., & Fu, D. (2014). Triggers for the Cambrian explosion: hypotheses and problems. Gondwana Research, 25(3), 896-909.

www.nature.com/scientificdata

scientific **data**

OPEN

DATA DESCRIPTOR

MOSAIC - A Unified Trait Database to Complement Structured Population Models

Connor Bernard[1]✉, Gabriel Silva Santos[1,2,3], Jacques A. Deere[1,4], Roberto Rodriguez-Caro[1,5], Pol Capdevila[1,6], Erik Kusch[7,8], Samuel J. L. Gascoigne[1], John Jackson[1] & Roberto Salguero-Gómez[1,9,10]

Despite exponential growth in ecological data availability, broader interoperability amongst datasets is needed to unlock the potential of open access. Our understanding of the interface of demography and functional traits is well-positioned to benefit from such interoperability. Here, we introduce MOSAIC, an open-access trait database that unlocks the demographic potential stored in the COMADRE, COMPADRE, and PADRINO open-access databases. MOSAIC data were digitised and curated through a combination of existing datasets and new trait records sourced from primary literature. In its first release, MOSAIC (v. 1.0.0) includes 14 trait fields for 300 animal and plant species: biomass, height, growth determination, regeneration, sexual dimorphism, mating system, hermaphrodism, sequential hermaphrodism, dispersal capacity, type of dispersal, mode of dispersal, dispersal classes, volancy, and aquatic habitat dependency. MOSAIC includes species-level phylogenies for 1,359 species and population-specific climate data. We identify how database integration can improve our understanding of traits well-quantified in existing repositories and those that are poorly quantified (*e.g.*, growth determination, modularity). MOSAIC highlights emerging challenges associated with standardising databases and demographic measures.

Background & Summary

The ecological sciences have recently joined the open data revolution[1–3]. As a result of initiatives promoting open data, total species distribution records measure in the hundreds of millions[4,5]. Functional trait data exist for tens of thousands of species across the globe[6–8]. Global distributed networks, remote sensing, and other ecological sensor data networks are feeding information into the open data space, and we are experiencing a rapid increase in the number of ecological databases. The growth of open data is reflected in state-of-the-art climate models (*e.g.*, ERA-5 [https://www.ecmwf.int/en/forecasts/dataset/ecmwf-reanalysis-v5]) becoming available at fine spatial and temporal resolutions suitable for biological analyses[9,10], the growth of behavioural trait datasets[11], and large population datasets (Living Planet Data, successor to the Global Population Dynamics Database [http://livingplanetindex.org/data_portal]; Human Mortality Database;[12] Human Fertility Database;[13] AnAge Database;[14] DATLife [Max Plank Institute of Demographic Research 2022; https://datlife.org/]). Data access and scaling has extended to biological complexity at the ecological community ecology level (BioTime;[15] Web of Life;[16] metaCommunity Ecology: Species, Traits, Environment and Space (CESTES[17]); Environmental Data Initiative [https://environmentaldatainitiative.org/]). The growth of records in ecology datasets and complementary

[1]Department of Biology, University of Oxford, 11a Mansfield Rd, OX13SZ, Oxford, United Kingdom. [2]Department of Ecology, Rio de Janeiro State University, 20550-900, Rio de Janeiro, Brazil. [3]National Institute of the Atlantic Forest (INMA), 29650-000, Santa Teresa, Espírito Santo, Brazil. [4]Department of Evolutionary and Population Biology, Institute for Biodiversity and Ecosystem Dynamics, University of Amsterdam, 1012 WX, Amsterdam, Netherlands. [5]Departamento de Biología Aplicada, Universidad Miguel Hernández. Av. Universidad, s/n, 03202, Elche (Alicante), Spain. [6]School of Biological Sciences, University of Bristol, 24 Tyndall Ave, Bristol, BS8 1TQ, United Kingdom. [7]Center for Biodiversity Dynamics in a Changing World (BIOCHANGE), Arhus University, Aarhus, Denmark. [8]Section for Ecoinformatics & Biodiversity, Department of Biology, Arhus University, Aarhus, Denmark. [9]Centre for Biodiversity and Conservation Science, University of Queensland, St. Lucia, QLD, Australia. [10]Evolutionary Demography Laboratory, Max Plank Institute for Demographic Research, Rostock, Germany. ✉e-mail: connor.bernard@biology.ox.ac.uk

environmental datasets is enabling us to test ecological theory at larger and more complex scales. In line with the expansion of open access data practices, however, there is a need to improve and coordinate data standards to guide the systematic collection and management of data across different trait collection programmes[18–20].

Despite the increased availability of biological data, synthesizing datasets for analysis is hampered by the lack of complementarity between databases. The rise of data sharing and proliferation of databases can encourage a fragmented and decentralized information landscape unless there is active coordination. Interoperable data systems reflect continuity in the format of data types and structure to allow compatibility across computers and software. Converting datasets into interoperable formats may require the transformation of constituent data types into standardized spatial, temporal, and measurement scales, accounting for known differences/biases in methods[21]. The need to improve interoperability across datasets is demonstrated by the widescale emergence of data harmonization initiatives across fields of ecology[22–24]. In the past decade, dozens of initiatives have taken shape to both centralize data from existing datasets and to improve data interoperability: standardising units, scales, and terminology for comparative purposes[25,26]. Unifying data formats and streamlining their integration unlocks the potential for existing datasets to answer questions that cut across levels of biological complexity. Linking together levels of biological complexity is critical for identifying how phenomena emerge and transmit across different levels of biological organisation, upscaling and downscaling through biological systems. For example, the critical linkages between genetics and biochemistry[27], biochemistry and physiology[28], and physiology and demography[29,30] have benefitted from dataset integration.

The limitations of global-scale datasets are shifting away from data availability and toward data interoperability. For functional traits, momentum toward data integration is evidenced by recent database initiatives[31] and global networks that, like the Open Trait Network (https://opentraits.org/), aim to standardize and integrate trait data across taxa[18]. Despite major improvements in the consolidation and accessibility of trait data, there is not yet a single-source centralized database spanning behaviour, physiology, habitat, and other trait data for a wide range of species. Existing databases are often linked by taxonomy (*e.g.*, FishBase[32], CoralTraits[33], MammalBase[34], AmphiBio[35]); trait type (*e.g.*, Tree of Sex[36], TreeBase[37], Xylum Functional Traits[38]); data type (*e.g.*, GBIF (https://www.gbif.org/), MOL[39], TetraDensity[40]); or a combination of the taxonomies and traits (WooDiv[41], CarniDiet[42]). A number of other databases take a more general approach in their thematic scope, but are still constrained to a limited set of traits and taxonomy (*e.g.*, Amniote[43], Pantheria[44], BIEN[7,45], TRY[23]). MOSAIC offers a platform that integrates databases in the remit of species with structured population models across their ecological traits.

Here, we introduce MOSAIC, a centralized database of trait data across the Tree of Life. MOSAIC is an open-access database that complements the existing demographic data available in the COMPADRE Plant Matrix Database[46], COMADRE Animal Matrix Database[47], and the new PADRINO IPM Database[48]. MOSAIC v. 1.0.0 includes 14 frequently used traits that encompass morphological, reproductive, dispersal, and habitat type attributes for some 300 species of animals and plants. Additional traits will be added in the future (see *Future Direction, below*). MOSAIC allows users to integrate structured population data to probe larger questions through the collection, curation, and complementarity of relevant contextual data.

Methods

Scope and coverage of MOSAIC. The MOSAIC database (v. 1.0.0) includes 14 key trait records across 300 species (Fig. 1). MOSAIC is designed to provide complementary data for analysis in connection with structured population models: matrix population models (MPMs[49]), where state variables are discrete (*e.g.*, age[50], ontogeny/development[51], discrete classes of size[52]), and integral projection models (IPMs[53]), where the state variables are continuous (*e.g.*, size[54], mass[55], parasite load[56]). The traits included in MOSAIC 1.0.0 were identified as a set of physical, physiological, geographic, and behavioural attributes of most immediate relevance to demographic research (see Table 1; more information at https://mosaicdatabase.web.ox.ac.uk). Traits were also selected in consideration of the lack of standardized and centralized databases for certain traits (*e.g.*, volancy, modularity, and growth indeterminacy; see Fig. 2 for trait variance and taxonomic structure of select traits excluded from existing databases). Importantly, we note that MOSAIC is not a general dataset for analysis of functional traits, as this is available through other extensive repositories (*e.g.*, TRY[23], BIEN[7,45]). Instead, the focus of MOSAIC is on providing taxonomic coverage to species with open-access structured population models available in the COMADRE[47], COMPADRE[46], and PADRINO[48] databases (See Figs. 3, 4 for spatial scope and taxonomic scope with respect to structured population databases, respectively). MOSAIC provides a much-needed interoperability between existing databases that are relevant to demography. By doing so, MOSAIC helps to fill critical data needs of population ecologists and functional trait ecologists (see Fig. 5 for relevant covariance structure).

Data sources. MOSAIC is both a *meta*-database (a database of databases) and a database in its own right, containing new trait records from primary literature (Fig. 1). The MOSAIC database contains records centralized from existing datasets where functional traits relevant to population ecologists can be openly accessed and redistributed (*e.g.*, BIEN[7,45]). Licensing terms of these databases are included in the supplement (Appendix S1: Database Licensing Terms for Constituent Databases of MOSAIC). The records reflected in the MOSAIC database do not encompass the entirety of the source databases but are instead partial facsimiles of those databases that reflect records relevant to demographic databases (COMADRE, COMPADRE, PADRINO). MOSAIC has three major components: (1) trait records sourced from existing databases (22%); (2) trait records newly procured through searching the primary literature (71%); and (3) trait record markers indicating the presence of records in non-open-access database (7%). MOSAIC trait markers exist for one of two reasons: the database containing the records of interest does not allow records to be accessed or limits redistribution rights behind individual registration and/or specific use applications; or records in other databases contain multiple records for a species, which do not currently fit within the data structure of version 1.0.0 of MOSAIC (see *Future Targets for MOSAIC*).

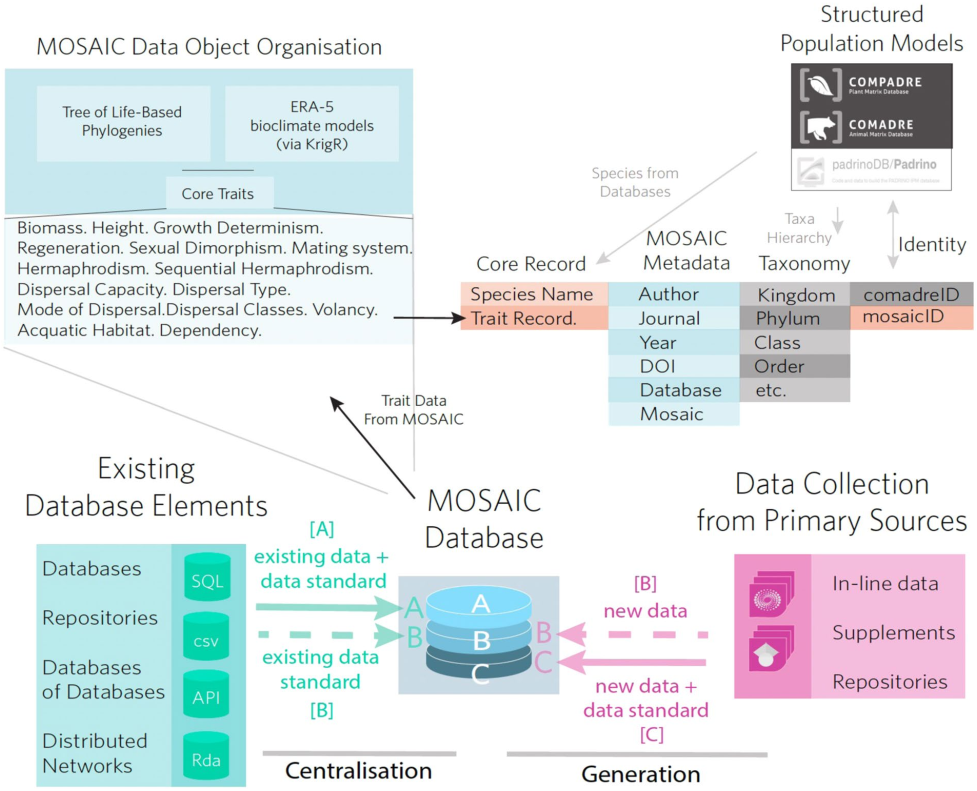

Fig. 1 Structure of the MOSAIC database (v1.0.0). The MOSAIC database comprises a combination of existing trait records centralised from data servers, databases, and datasets and new records collected from the primary literature by the MOSAIC team. Existing records are labelled, MOSAIC-A, in the mosaic metadata attribute field and include provenance in the metadata. New data records that adhere to existing data standards and that fit into the remit of an existing database (*i.e.*, a data gap filled by the MOSAIC team) are labelled MOSAIC-B. New records that do not have an existing data standard or for which there is not an existing database are labelled MOSAIC-C.

In addition to identifying whether a trait record is new, the “MOSAIC” attribute field also identifies whether the attribute field (*i.e.*, trait name) is part of an existing database. For example, the MOSAIC field might indicate that a record for specific leaf area is new for a specific species, and also that the attribute is part of databases such as TRY[23] or BIEN[7,45]. By contrast, a new species record for volancy would indicate that there are currently no databases that systematically collect data on volancy attributes and therefore that all volancy records in the MOSAIC database are new.

Organisation of sources in MOSAIC. The MOSAIC attribute field is a factorial variable with three levels: MOSAIC-A, MOSAIC-B, and MOSAIC-C. The first of these levels, MOSAIC-A (Fig. 1), labels only records that reflect existing databases (*i.e.*, provenance of an existing data acquisition service); the second, MOSAIC-B, labels new records collected by the MOSAIC team that are in a trait field within the scope of an existing database initiative (*e.g.*, specific leaf area in BIEN); and the third, MOSAIC-C, labels new records collected by the MOSAIC team on traits for which there is not currently a database initiative centralising records. If a datum has been adopted from another dataset or database, then the relevant source is referenced in the *Database* attribute column. Note that this value will be “NA” for all MOSAIC-C records, logically. Over time, data sharing will move records in MOSAIC-B to MOSAIC-A as the MOSAIC-B traits are assimilated in the database networks that specialize on an existing trait (*i.e.*, data feedback; see Fig. 1).

Sources and provenance of records. Because of existing limitations on data access, some datasets cannot be transferred into MOSAIC. Where data exist outside of the MOSAIC platform, but have restricted access, the MOSAIC database directs users toward the appropriate database on a trait and taxa-specific level (see `meta-MOSAIC`). The *MOSAIC User Guide* (Appendix S2) explains differences between data gaps that are yet to be

Aspect	Variable	Description	Units
Taxonomy	1 *Species Author*	Taxonomic species name as used by the author(s) in the publication. When more than one study exists for the same species, these are given sequential numeric suffixes (e.g. Ursus_americanus, Ursus_americanus_2, etc.)	NA
(Parallels COM(P) ADRE)	2 *Species Accepted*	Currently accepted taxonomic name according to the Catalogue of Life (www.catalogueoflife.org). See the Supplementary Online Material S3 for an R script to check accepted and synonym names from SpeciesAuthor above	NA
	3 *Common Name*	English common name of SpeciesAccepted	NA
	4 *Family*	Taxonomic family of study species	NA
	5 *Order*	Taxonomic order of study species	NA
	6 *Class*	Taxonomic class of study species	NA
	7 *Phylum*	Taxonomic phylum of study species	NA
	8 *Kingdom*	Taxonomic Kingdom of study species	NA
Species information General	9 *Organism type*	General plant/algae type, based mainly on architectural organisation. The species was assigned to one of these possible values using the description of plant growth type provided by the author and other external sources (e.g. other publications)	Categorical/ Factorial
	10 *DicotMonocot*	Whether species is a dicot or monocot	Categorical/Factorial
	11 *AngioGymno*	Whether species is an angiosperm or a gymnosperm	Categorical/Factorial
Source information	12 *Authors*	Surname (family name) of all author	NA
	13 *Journal*	The document from which data were sourced.	NA
	14 *YearPublication*	Year of publication	NA
	15 *DOI*	Digital Object Identifier number	NA
Traits	01 *Biomass*	Mean mass of an individual/whole-organism. (Plants) Plant mass is measured as aboveground dry mass. See “Further information” for additional information on belowground biomass.	Grams
	02 Height	(Plants) Mean height of the whole organism/whole individual from surface (i.e. substrate) to tallest vertical extremity. (Animals) Mean ventro-dorsal length. (i.e. for terrestrial quadrupeds, vertical distance from the ground to the top of the shoulder. For marine bony fishes, from the top of the high point of the dorsal fin to the base of the ventral ridge or ventral fin, whichever is a longer distance perpendicular to the anterior-posterior axis.)	Centimetres
	03 Growth Determination	Whether a species exhibits growth determinacy or not.	Categorical/Factorial
	04 Regeneration	Capacity for an individual to regenerate any substantial part of its body, including autotomy. Autotomy is defined as “The voluntary severance by an animal of a part of its body (commonly one of its own limbs), usually to escape capture by a predator that has seized that part. The part then regrows.”	Categorical/Factorial
	05 Sexual Dimorphism	An indicator of whether sexual dimorphism is exhibited in the species. Sexual dimorphism is defined as “the occurrence of morphological differences (other than primary sexual characters) that distinguish males from females of a species of organism.” (Oxford Dictionaries of Ecology and Zoology)	Categorical/Factorial
	06 Mating System	System of mating; the organisation of sexual interactions of individuals within populations based on sex.	Categorical/Factorial
	07 Hermaphrodism	Indicator of whether a species exhibits hermaphrodism or monoeicieosity. Hermaphrodism is defined as: “An individual that possesses both male and female sex organs; i.e. it is bisexual.” (Oxford Dictionary of Zoology). Monoeciousness is defined as: “Applied to an organism in which separate male and female organs occur on the same individual (e.g. to a plant which bears male and female reproductive structures in the same flower or separate male and female flowers on the same plant, or to a hermaphrodite animal). Some authors restrict the term botanically to plants with separate male and female flowers; plants which bear male and female reproductive organs in the same flower are then called hermaphrodite.”	Categorical/Factorial
	08 Sequential Hermaphrodism	Indicator of whether a species is protogynous or protandrous.	Categorical/Factorial
	09 Dispersal Capacity	An indicator for whether or not a species exhibits dispersal behaviour or at any stage in its life cycle. Where dispersing, a categorical description of whether dispersal is natal or breeding or otherwise. Dispersal is defined as “The tendency of an organism to move away, either from its birth site (natal dispersal) or breeding site (breeding dispersal): the opposite of philopatry.” (Oxford Dictionary of Zoology).	Categorical/Factorial
	10 Type of Dispersal	An indication of whether dispersal is a passive (requires assistance) or active (no assistance) event. See DispClasses for more information	Categorical/Factorial
	11 Mode of Dispersal	An indicator of the mode of dispersal of the species (plant and animal specific terminology). (*e.g.*, phoretic dispersal in *Daphnia magna*).	Categorical/Factorial
	12 Dispersal Classes	Age- or stage-classes of the species that are capable of dispersal.	Categorical/Factorial
	13 Volancy	An indicator of whether a species is volant or non-volant (i.e., able to fly or not).	Categorical/Factorial
	14 Aquatic Habitat Dependency	An indicator of whether a species is dependent on water or not. (e.g., limnic, lentic, lotic)	Categorical/Factorial

Table 1. Variable names and meaning contained in the MOSAIC Database, organised into seven general trait domains. A more detailed description can be found in the MOSAIC user guide found at: https://mosaicdatabase.web.ox.ac.uk/.

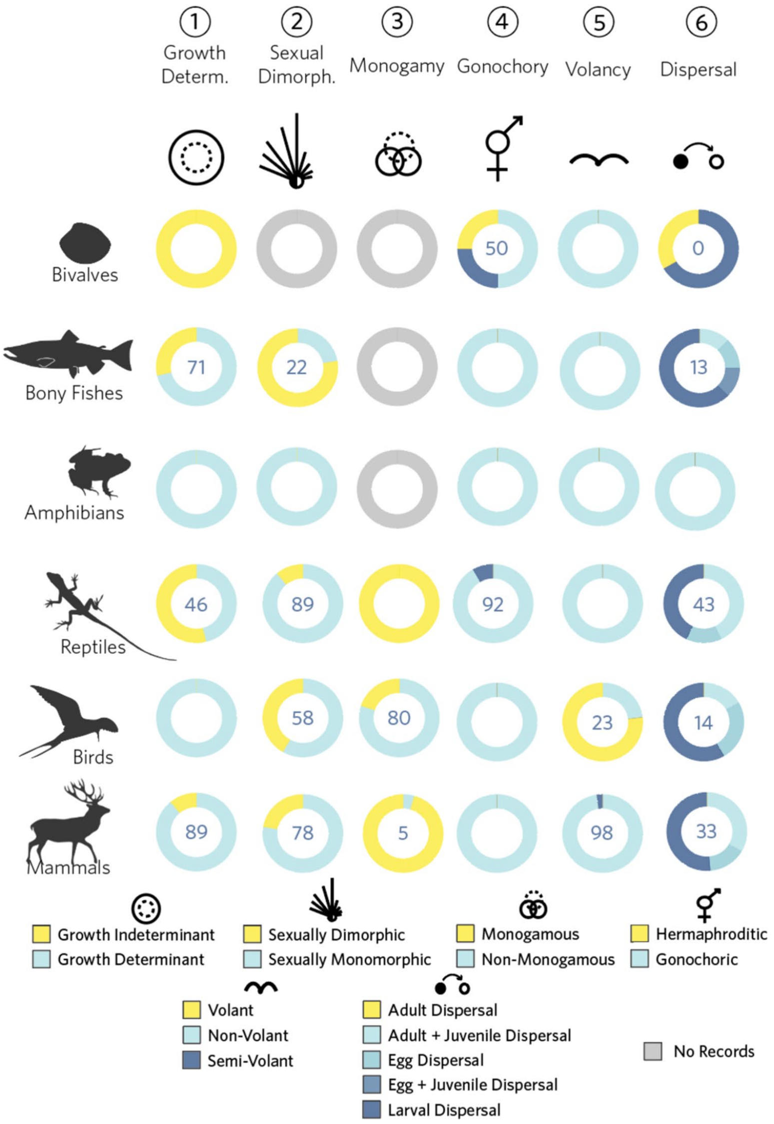

Fig. 2 Trait fields in the MOSAIC database (v1.0.0). The MOSAIC database contains a combination of continuous and discrete trait fields. Six of the 14 trait fields are illustrated here for animals, and organised by trait level (all discrete fields) and taxonomic classification. Trait distributions vary strongly by trait and taxonomy. Observed variation in trait values by taxonomic group is a prerequisite condition to their potential value toward explaining reported variation in vital rates and resulting demographic properties across the Tree of Life. Species included in the MOSAIC database are limited to those for which stage-structured population data exist in the COMADRE, COMPADRE, and PADRINO databases.

reviewed and those that are true gaps (*e.g.*, volancy/flight capability of plants). Data were obtained through searching peer-reviewed records and PhD dissertations of ISI Web of Science, Scopus, and Google Scholar using key words pertinent to the species name and trait field in question (see Appendix S3 for a list of keywords queried). The archives of data repositories, including the Figshare digital repository[57] (https://figshare.com/articles/dataset/MOSAIC_trait_database/21035857; see Appendix S3 for a complete list of repositories reviewed – to be maintained hereafter on the MOSAIC portal) and journal archives that have a high occurrence of data

(a) COMADRE

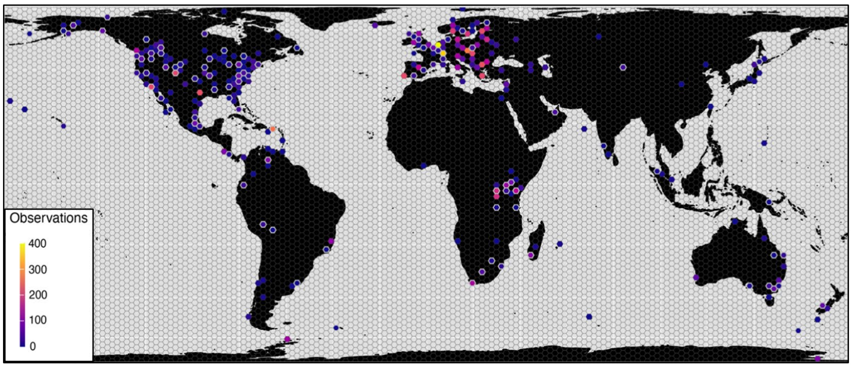

(b) COMPADRE

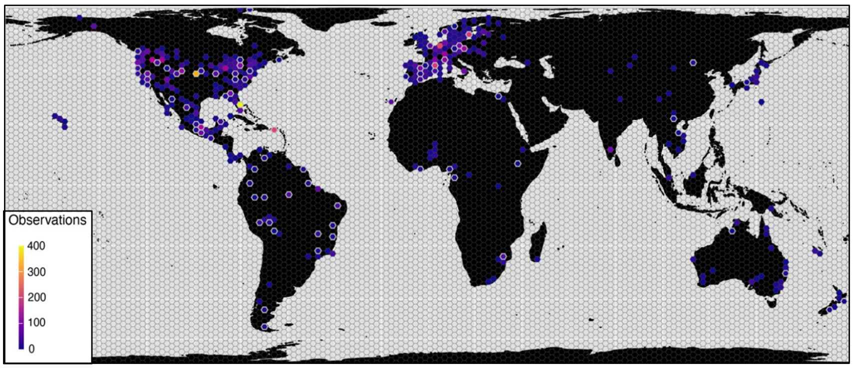

Fig. 3 The spatial distribution of MOSAIC (v1.0.0) records relative to the (a) COMADRE and (b) COMPADRE databases. The COMADRE and COMPADRE dataset include animal and plant demographic data, respectively, on all continents except Antarctica, with a substantial bias to North America and Central Europe. MOSAIC introduces trait records that include models in all major geographies of COMADRE and COMPADRE. The map shows the density of matrix population models globally (color graded by density per area in *ca*. 150 km^2 hexagonal cells). Cells bordered by white represent localities of population models for which there are trait records included in the first release of the MOSAIC trait database. Species prioritised in v1.0.0 of MOSAIC did not include the PADRINO dataset, so no distribution figure is shown for integral projection models.

publishing, including *Nature Scientific Data*, *Methods in Ecology and Evolution*, and *Journal of Ecology* were carefully reviewed. MOSAIC also reflects a review of data from data aggregating servers, such as the open traits network (https://opentraits.org/), the ecological data wiki (https://ecologicaldata.org/), environmental data initiative (https://environmentaldatainitiative.org/), and databases that aggregate other databases (*e.g.*, BIEN[7,45] and TRY[23]). The complete set of key words used in this review is detailed in a supplement to the *User Guide* (Appendix S3). A current list of databases reviewed in the development of MOSAIC is included in Appendix S4. Suggested data sources and key terms can be submitted through the MOSAIC data portal.

metaMOSAIC: licensed data, access limitations, and restricted redistribution of existing records and databases. Not all datasets permit open use, dissemination, and redistribution of their trait data. Where limitations on the data collation and redistribution apply, there may be application procedures, registration, and other actions necessary for an individual to obtain access to specific trait records for analysis (*e.g., TRY*). MOSAIC centralizes the metadata for datasets that do not allow data to be redistributed to help navigate to relevant data resources outside the scope of open access. Records in limited access databases can be searched in MOSAIC by taxonomic group and by trait. MOSAIC links researchers to application materials for requesting access to those limited-access databases. The data access of licensed or non-open-access databases is stored in a data object called `metaMOSAIC` that is an extension of the MOSAIC database. Thus, the MOSAIC dataset provides data where it is accessible and `metaMOSAIC` guides researchers to where data exist with registration. When searching fields in the MOSAIC database, the `metaMOSAIC` adjunct dataset indicates if data are available

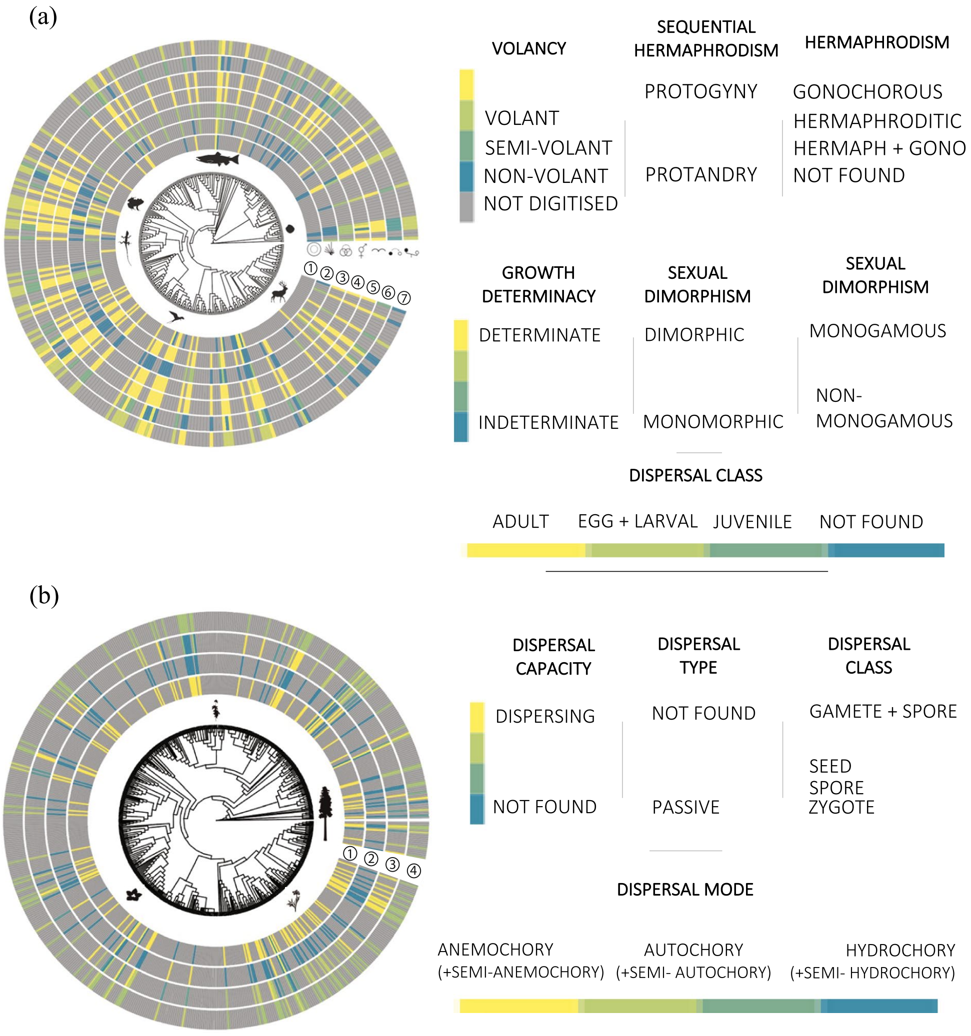

Fig. 4 Phylogenetic mapping of traits included in MOSAIC (v1.0.0). (**a**) Phylogenetic distribution of seven major traits for animals: (1) growth determination; (2) sexual dimorphism; (3) monogamy; (4) gonochory; (5) volancy; (6) dispersal; and (7) biomass. (**b**) Phylogenetic distribution of four traits in plants: (1) dispersal capability; (2) dispersal type; (3) dispersal mode; and (4) dispersal class. Figures developed in R using the ggtree package.

in these ancillary sources (see *User Guide* in Appendix S2 for more information) and provide links to pertinent sources and data through the provider. `metaMOSAIC` is part of the main database object accessible through the MOSAIC portal.

Database updates. The MOSAIC database will be updated as new data are added to the COMADRE, COMPADRE, and PADRINO databases. Updates of the MOSAIC database will account for newly discovered data sources and new literature that adds to or changes the species-level traits in the database, as well as correct errors from earlier versions. New MOSAIC versions will be released periodically with a notice published on the website, in the data object metadata, the mosaic GitHub page (https://github.com/mosaicdatabase), and through updates in associated packages in conformance with standard semantic versioning (a three-part version code reflecting major, minor, and patch updates, in respective positions). Updates will be published to the mosaic

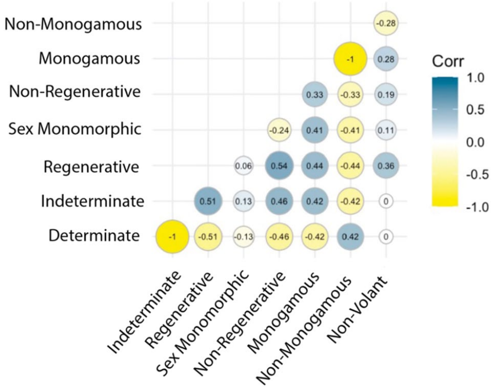

Fig. 5 Trait covariance in the MOSAIC database (v1.0.0). Some traits exhibit high correlation in the MOSAIC database, such as between growth determination and between growth regeneration. Trait associations are expected to occur in the MOSAIC dataset and may reflect widespread constraints or statistical anomalies, particularly when dealing with small samples or specific taxonomic subgroups. Trait covariation can be symptomatic of biomechanical constraints (*e.g*., flight and biomass), major growth characteristics (*e.g*., modularity and growth determination), or other past or presently compelled associations (*e.g*., height and vessel density).

portal (https://mosaicdatabase.web.ox.ac.uk), social media (Twitter: @mosaicdatabase), and GitHub (https://github.com/mosaicdatabase). The MOSAIC portal includes a location for submission of recommendations for additions or suggested changes to the database.

Future targets of MOSAIC. *Versioning*. MOSAIC database updates and version history will be posted to the MOSAIC portal in the future.

Taxonomic scope. Future versions of MOSAIC are scheduled for expansion to include 50 core traits across some 1,500 species (the current entirety of COMPADRE, COMADRE, and PADRINO; *MOSAIC target traits*; see *User Guide* [Appendix S2]). The MOSAIC core traits list will guide the future roll-out of attributes gathered and stewarded by the MOSAIC team, but additional trait suggestions can be submitted through the online portal.

Interspecific variation. Future versions of the MOSAIC database will adopt a file structure that will accommodate multiple records per species. Once records for COMADRE, COMPADRE, and PADRINO are fully populated across the MOSAIC traits with mean, pooled, or other representative quantities (*e.g*., mean leaf size for all plants or adult bodymass of animals), secondary records will be added. Existing trait databases may contain multiple records per species (see, for example, structure of COMADRE[47], COMPADRE[46], BIEN[7,45], TRY[23]), although some databases host a single record per species' trait, such as age and growth rate for animals in AnAge[14]. To facilitate research into intra-specific trait variation[58–60], MOSAIC provides provenance of records, whether records were subject to selection or merger (means or pooling), and fields that identify whether multiple records are known to exist. Where records for a given species were isolated from existing databases, mean values are often retrieved, and the database sourcing additional data is noted in the database under the attributed field ("Additional Trait Data Available" field).

citMOSAIC: Citizen science. In addition to `metaMosaic`, which guides users to licenced data not reported in the MOSAIC database, MOSAIC plans to roll out a database of identical structure to MOSAIC that gathers information from citizen science datasets. Like MOSAIC, citMOSAIC will have three components (citMOSAIC-A, citMOSAIC-B, citMOSAIC-C), reflecting the same relationship of databases and fields to MOSAIC. citMOSAIC will be kept independent of the main MOSAIC database to avoid conflation of peer reviewed literature and PhD dissertations from citizen science data. Where appropriate to use datasets together, the metadata, query functionality, and design of citMOSAIC will mirror that of MOSAIC to promote interoperation of databases. citMOSAIC will be downloadable from the MOSAIC portal website.

Data Records

The current version of MOSAIC (v. 1.0.0) is deposited as series of flat data files (comma separated values and text files) in Figshare (https://figshare.com/articles/dataset/MOSAIC_trait_database/21035857). The data in this paper and complete database are also published on the MOSAIC website https://mosaicdatabase.web.ox.ac.uk and associated GitHub repository https://github.com/mosaicdatabase/mosaicdatabase. All data is open access without restrictions on access.

The MOSAIC database can be downloaded directly into R as a series of flat tabular data (comma separated values and text files) on Figshare (https://figshare.com/articles/dataset/MOSAIC_trait_database/21035857) and, optionally, as an S4 object (see *Usage Notes—Accessing MOSAIC*). Future versions of the MOSAIC datasets with any corrections and new data records will be updated to the GitHub page (github.com/mosaicdatabase/mosaic-database) linked with the direct download in R and updated to Figshare. Data use and redistribution is covered by a Creative Commons CC-BY license, with unrestricted use and modification with attribution, consistent with MOSAIC's constituent databases (Appendix S1).

Description of the individual trait fields are included in Table 1. Detailed discussion of each data field, units, precision, and cautionary notes included in the MOSAIC *User Guide* (Appendix S2). In its first version (v. 1.0.0), MOSAIC data has 41% density coverage across 14 core trait fields of approximately 300 species. MOSAIC provides 100% density of climate data for all species in COMADRE, COMPADRE, and PADRINO for which there are GPS locations (86% of all records across the databases). 71.9% of species in COMADRE, COMPADRE, and PADRINO had records in the Online Tree of Life phylogeny included in MOSAIC. Data completeness varies greatly amongst trait fields, as does the sourcing of data from primary and secondary datasets (Fig. 2).

Across formats, each tabular row or vector element represents a single species. Columns are representative of attributes or metadata associated with attributes. Unique identifiers associated with the matrix population models and integral population models in COM(P)ADRE and PADRINO databases, respectively, to link demographic models with trait records. In the current MOSAIC version (v. 1.0.0), only one record per species is released, but future versions will incorporate multiple records per species.

Technical Validation

The technical validity of records in the MOSAIC database is based on three levels of review. First, all records in MOSAIC, regardless of whether they are collected from primary or secondary data sources, are obtained from either peer reviewed journals or scholarly equivalent documents (*e.g.*, PhD dissertation). Second, all data sources in MOSAIC were reviewed to ensure that they are reasonably representative of the trait record for the species (e.g., screened for sample size, geography relative to the pertinent population record(s), and methods suitable to the trait). Third, MOSAIC will be periodically reviewed, added to, and amended, additive to any revisions that might come about through the feedback portal. As a result, MOSAIC will be adaptively managed to ensure that all records are of suitably high-quality and grounded in peer-reviewed data. MOSAIC also contains metadata for all records, ensuring provenance to original records and secondary standardisation.

Peer-reviewed data. All data in MOSAIC are either published in a peer reviewed academic journal, PhD dissertation, or other peer reviewed source (e.g., Oxford Bibliographies). Unique identifiers for the publications that source the data is provided for every record. Prior to the review of the record by the MOSAIC team, all trait records were technically scrutinized and reviewed by more than one subject area expert. In addition to peer review of the publication record, many MOSAIC records are sourced from existing databases that impose technical standards beyond those imposed by the initial publication and have technically assessed the quality of underlying data.

Record review and selection. The MOSAIC team evaluated whether records were consistent across the literature. Where multiple records were identified containing different numeric values for a continuous trait, the MOSAIC team selected a focal record based on: (1) sample size, (2) geographic extent, (3) geographic proximity to the site, and (4) method of measurement. If multiple records were identified for factorial traits that were in conflict with one another, then those records were excluded from the initial release of MOSAIC v.1.0.0. Only unanimously consistent factorial trait values were included in the first version of MOSAIC. At least two members of the MOSAIC team assessed records in every case to ensure that there was agreement in the sourcing of the data.

Quality checks. The MOSAIC team reviewed the data for any outliers. In addition to reviewing for general anomalies from the data variance structure, as part of the data collection protocol, the MOSAIC team screened data for bounds applicable to each trait (see *User Guide*, Appendix S2). These value bounds ensured that all reported data were within the range of biologically realistic values as an additional safeguard against spurious values. Beyond confirming the general data structural integrity, the MOSAIC team compared the overlay of records in COMADRE, COMPADRE, and PADRINO with the source data for MOSAIC to ensure congruence of the data transferred from source databases. All automated data overlays were manually checked for their integrity against source data.

Ongoing development & growth. The MOSAIC database will continue to grow and, in the future, will accommodate multiple trait records per species. This trait record redundancy will provide another level of protection against spurious records, in addition to providing quantification of trait variance. Future database development plans include a schedule to incorporate GPS coordinates to formalize the distance between each trait record and the corresponding population records.

Metadata. The MOSAIC database contains the source data for each trait record, including (1) Author(s), (2) Year of Publication, (3) Journal of Publication, (4) DOI/ISBN of the publication, and (5) Inclusion in other databases. Future versions of the database may contain additional metadata for the trait data.

Usage Notes

Accessing MOSAIC. A guide for downloading the MOSAIC database can be accessed in the Supplementary Material (Appendix S2). The MOSAIC database is open access and can be downloaded into R as a csv using the below line of code:

`read.csv("https://raw.githubusercontent.com/mosaicdatabase/mosaicdatabase/main/MOSAIC_v1.0.0.csv")`

The MOSAIC database is a comma separated value (csv) format that is publicly archived under a CC-BY-4.0 license accessible from Figshare (https://figshare.com/articles/dataset/MOSAIC_trait_database/21035857), GitHub (https://github.com/mosaicdatabase/mosaicdatabase), and the MOSAIC portal (https://mosaicdatabase.web.ox.ac.uk). Phylogenetic data is formatted for use and manipulation using the open-source R-package ape (Analyses of Phylogenetics and Evolution; Schliep & Paradis 2019) which can be installed by CRAN.

Mosaic *User Guide*, *Vignette*, and *Data Collection Protocols* are all included in the Supplemental materials (Appendix S2, S3, and S5). The *User Guide* specifies the classifications, precision, and data types for each trait field. The MOSAIC *User Guide* details the metadata on the structure of data for each trait (*e.g.*, species, genus, mosaic index). An updated list of the databases that are directly or indirectly addressed by the MOSAIC database is maintained on the MOSAIC portal.

Field values. MOSAIC records contain one of three values: "NA," "NDY," or a trait value that can be numeric, factorial, or a character string, as discussed further in the User Guide. NAs apply to fields that have been reviewed and which do not apply to the species of interest. For example, plants do not have flight capacity, and thus NAs apply to them for this trait. Likewise, height and canopy size are key morphological dimension of plants that may not transfer meaningfully to most vertebrates, where adult biomass is a more relevant[61,62] and oftentimes used trait. By contrast, NDYs represent "Not Digitized Yet", indicating fields/species that have not been reviewed for potential records. All other values will reflect the units described in the User Guide.

Database navigation. The *User Guide* contains detailed information on navigating the MOSAIC R data object. The primary MOSAIC object contains species-specific attribute values for 14 traits. Climate data and phylogeny are independent files accessible in the same locations described above (csv and phylo formatted, respective). Climate is an independent file because it is based solely on model-specific coordinates (and therefore has multiple values per species). Phylogeny is an independent file because it is a phylo object (a special kind of list object in R accessed through ape) and therefore is not in a format amenable to species-specific csv summary.

The primary MOSAIC file contains 14 fields and can be queried through S3 syntax. Rows represent species and are included in the column titled: `species_accepted`. Columns represent attributes that are either the trait value or trait metadata. The base format for accessing data is: `mosaic$trait.name`. In the aforementioned syntax, the `trait.name` should reflect one trait (*e.g.*, volancy). Metadata can be accessed with the syntax: `mosaic$trait.name_metadata`, where metadata is replaced by the name of the metadata field (e.g., journal, doi, author). Species names are specified in conformance with the Catalogue of Life (www.catalogueoflife.org), also consistent with the COMPADRE, COMADRE, and PADRINO databases. The *User Guide* provides specific guidelines for querying fields within the data object in R and for negotiating the dataset in finer detail (Appendix S2).

Error reporting. Users can submit errors for correction by email to: mosaicdatabase@biology.ox.ac.uk. The MOSAIC portal also has an *Error Report* page for reporting potentially erroneous records, or to query additional questions (https://mosaicdatabase.web.ox.ac.uk/suggested-additions-error-reporting; but see also FAQ: https://mosaicdatabase.web.ox.ac.uk/frequently-asked-questions). Potential errors can be reported anonymously or with contact information (*e.g.*, name, email). Decisions on reported errors will be disclosed on the Error Report page (https://mosaicdatabase.web.ox.ac.uk/suggested-additions-error-reporting) and to the reporting party if contact information is included in the request.

Recommended records. Users can submit records by email to: mosaicdatabase@biology.ox.ac.uk. The MOSAIC portal also has a *Recommended Records* page (https://mosaicdatabase.web.ox.ac.uk/suggestion-additions) for reporting suggested records that are not included in the MOSAIC database. Recommendations can be made with or without contact information. Contact information will be used exclusively for clarifying questions and updating the commenter when records are included. MOSAIC will report decisions on the *Recommendations Incorporated* page (https://mosaicdatabase.web.ox.ac.uk/suggestion-additions). Users may also request new data fields to be prioritized in future rollouts. Given the realities of limiting resources, The MOSAIC team will do their best to include the requested records in future versions.

Cautionary notes. Records in the MOSAIC database are gathered and standardized under the protocols detailed in the *User Guide* (Appendix S2; also available through the MOSAIC portal). Users should be attentive to the precision, levels, and context of data in MOSAIC when used for analysis. For those records in the dataset that come from multiple individuals, we present them as statistical components (*e.g.*, minimum, maximum, or mean trait values). Functional traits in MOSAIC may be estimated from populations studied in COMADRE, COMPADRE, PADRINO, or other databases (Table S4). The potential temporal and spatial mismatch between databases that are linked in an analysis merits close attention[63]. The studies in the MOSAIC database also include research conducted by different investigators using independent tools, technologies, sample designs, and study methods. The influence of research methods and instruments on the error values in the dataset may require additional consideration for potential bias, noise, and imprecision. Where more than one life history trait value exists for a given species, MOSAIC users will need to determine whether averaging or selective filtering to one study is most appropriate in view of the specifics of the given research question. In certain cases, trait values for a species might only be available for a single st/age and therefore may not provide a complete picture of the trait variation amongst st/ages. Users are encouraged to be cautious when contextualising the scope of representation of the values in the database and their analyses.

Representation, variance, and Bias in MOSAIC v1.0.0. MOSAIC has the potential to help identify macroecological patterns and guide targeted experimental studies that can mechanistically examine the causes and correlates of demographic variability. MOSAIC leverages thousands of animal and plant species housed in

COMPADRE, COMADRE, and PADRINO and offers promise for evaluating general hypotheses and identifying novel ones from newly discovered patterns. Despite the inductive value and generality of macroecological inference[64–66], caution is required in inferring process and cause from trait-demographic patterns using MOSAIC. MOSAIC is a starting point and contextualising instrument, not a stand-alone tool for inferring how traits determine demography and/or how demographic processes may shape traits. In its version 1.0.0, MOSAIC contains a high degree of variance in trait values known to shape demographic outcomes across major taxonomic groups. For example, determinant growth is present for 0% of Amphibians and Birds and 100% of Bivalves, while volancy is present for 0% in Reptiles, Amphibians, and Bony Fish and 77% in Birds (Fig. 2). Animal adult biomass and plant height follow lognormal trait distributions (see Appendix S5). 11% of mammals are indeterminate growers *vs*. 54% of reptiles and 0% birds, and 95% of mammals are monogamous compared to 100% of reptiles and 20% of birds in MOSAIC. Recent studies have examined how different vital rates are explained by functional traits[67–70]. However, understanding how trait variation across taxa translates to demographically influential properties remains underdeveloped.

MOSAIC's initial release (v1.0.0) includes records for all major regions of the globe for which we have structured population models (Fig. 3). Nevertheless, species trait values are not necessarily gathered from the same localities as population models (see *future directions* for more information on systematising spatial mismatch). This is an important consideration for users of MOSAIC (and more generally of trait-based approaches) wishing to bring together functional traits and demographic rates, as traits and vital rates are known to vary considerably within the same species across spatial scales[71–73]. Moreover, while there is at least one trait for each of these locations, the data density remains variable. Thus, records are not necessarily representative of the global spread or the full spatial scope of MOSAIC. For example, the highest complete coverage for MOSAIC traits is concentrated toward localities with the with the longest-term demographic models (see COMPADRE locations associated with MOSAIC records).

Phylogenetically, the initial release of MOSAIC is somewhat limited. Version 1.0.0 covers 300 of the 1,400 species currently available in COMPADRE, COMADRE and PADRINO. However, MOSAIC trait data are well distributed across clades (Fig. 4). While there is not a highly skewed phylogenetic concentration with respect to the existing structured population models or clustering of records into small groups across the Tree of Life, phylogenetic density of MOSAIC records remains low. Therefore, information from the MOSAIC database may be limited for a given genus or order and, as such, should be approached with caution. In future versions of MOSAIC, the phylogenetic bias is expected to diminish with more samples and stronger phylogenetic representation.

Covariance across traits is also an important source of confound in existing analyses linking traits and vital rates. Positive and negative correlations across traits that have independent influences on vital rates can create apparent associations of demographic properties with traits, spuriously functionalising non-functional traits[74]. Disentangling the relevance of key axes of trait variation for their demographic influences demands a clear quantification of the direction and strength networks of trait associations, trade-offs, and demographic consequences. Population biologists seek to understand not only how individual traits relate to different aspects of demographic performance (*e.g*., population growth rate, risk of quasi-extinction, *etc*.), but also understanding how trait syndromes shape those demographic outcomes. MOSAIC presents a highly varied covariance structure in trait values for the examined 300 species. For example, without *a priori* expectation, indeterminate growth and regeneration traits show strong correlation ($r = 0.51$; Fig. 5), which could influence each other's effects on vital rates. The same could be argued for the correlation between volancy and reproductive strategy ($r = 0.28$ with monogamy; Fig. 5).

The MOSAIC database can be used as a platform to showcase the lack of overlap between trait and vital rate data for the same species. This picture calls for a more systematic way address global biases in ecological data quantification/collection. Even where we have complete information about species in the COMADRE, COMPADRE, and PADRINO databases, we are subject to the constraints and biases of those datasets, such as spatial bias toward high-GDP countries and the phylogenetic bias toward temperate regional perennial plants[75,76]. The compounding of error and density across datasets highlights the need to prioritize stronger representation of functional traits linked with demography. The standardized framework of MOSAIC is an ideal platform to work from to achieve this goal.

In view of potential biases introduced by low sampling density and the patchiness of cover in traits, users of the database are advised to consult the literature about the representativeness and congruency between MOSAIC data and related trait diversity within clades. Users need to be mindful of the scope of the questions that they are setting out to answer and to be aware of the influence of sample sizes and coherency or heterogeneity of traits across different taxonomic levels.

Extensions and relevance. *From databases to data networks.* Broad aperture digitisation efforts (*e.g*., BIEN[7,45] and TRY[23]) have helped resolve many answers to demographic questions. Examples include whether there are trait spectra and key trade-off patterns amongst functional traits and whether these are correlated with particular environments and life history strategies[77–79], Trait-based ecology and Trait Driver Theory[80] are indebted to such opportunity-driven research programmes. More generally, however, the trait-based ecology paradigm has failed to support clear answers to many research questions of central interest to demographers[29,81]. This limited reach of the functional trait programme coincides with a dearth of species-specific overlap across the range of functional traits that are collected by the functional trait databases.

The proliferation of databases and open data initiatives over the last two decades[82] evidences an interest in improving both data access and data usability[18,83,84]. While existing databases standardize trait fields, collate records, and link associated metadata, existing databases often store data for simple, quantitative traits. Relatively few ecological trait databases store diverse data types (such as rate arrays, population time series, physiological rates at different structural levels, and habitat shape files) that may be associated with multidimensional, ecological study systems (but see CESTES[17], GFBio[85], DarwinCore[86]).

The digitisation and standardisation of *existing* data and their integration with complementary, new data presents a growing set of challenges and opportunities in ecology[87]. Efforts to gap-fill records can leverage the value of existing datasets while expediting the schedule for specific research outcomes. As trait datasets grow, the importance of targeted, gap-filling initiatives to address bias and to capitalize on existing data will also increase[88]. The value of existing records is further enhanced through improvements in the interoperability of datasets. Much of this work is done manually, at a high cost, and with little support from funding agencies[87], and yet it has been effective at facilitating research and creating new value for old data. In recent years, initiatives have sought to improve the interoperability of datasets by guiding prospective data structure or retroactively harmonising existing datasets. These include programmes that develop universal standards to improve global interoperability (such as DarwinCore[86] and Frictionless [https://frictionlessdata.io/]data standards) or that contain guidelines for data metastructure (such as the FAIR principles (findability, accessibility, interoperability, and reusability, *sensu* Wilkinson *et al*., 2016) and the OpenTraits framework[18]). These initiatives address emerging and scaling challenges of ecoinformatics, such as the protocols by which we share data, search data, and preserve provenance in data storage structures. These protocols will be essential in centralising datasets as diverse as government monitoring datasets (*e.g*., those stored in U.S. Data clearing houses [https://www.data.gov; https://www.dataone.org/]; National Biodiversity Atlas [https://nbnatlas.org/]); centralized monitoring and experimental networks (*e.g*., LTER and NEON), raw or reanalyzed remote sensing datasets (*e.g*., Landsat data, NASA EarthData datasets, ERA-5 data), and private datasets (https://www.natureserve.org/) that will demand versatile and navigationally efficient data structures.

Population ecology has benefitted from widespread open-access databases but requires further dataset integration to answer its central questions. Understanding whether and how some morphological or physiological traits predict demographic outcomes and why others fail to do so is of central interest to questions in physiological, population, and community ecology[29,69,89,90]. Population ecologists routinely use data that are distributed across a wide range of databases. Comparative and macroecological researchers use phylogenies[91–93], adult body-mass[61,94–96], and high-resolution, global climate information[97–99] to answer relevant biological, evolutionary and ecological questions and to contextualize their findings. Population ecologists frequently examine a subset of physiological, morphological, and behavioural attributes associated with demographic outcomes (*i.e*., functional traits[100]). The trait-based research programme seeks to, among other aims[6], identify the intrinsic and extrinsic regulators of vital rates and the causes of variation and constraints on possible trait values[65,66]. Not all traits predict demographic outcomes and functional traits may exercize influence on only a few demographic pathways[68,101]. The answers to these questions rely on the existence of vital rate and trait data, the overlap of which has been limited in the absence of targeted attention. For instance, of the hundreds of thousands of records available across thousands of plant species in TRY[23] and over 345 plant species in COMPADRE[46], Adler *et al*. (2014) report functional trait-vital rate relationships for only 222 plant species due to their limited data overlap.

Ecological data are complex and their structures will need consistent rules to link datasets together. It will be important for future datasets to adopt database designs that render large, thematically, and structurally diverse data to be readily locatable and usable without expert knowledge. Here, we show one such example in the scope of comparative research, using thematic groups and a strategy of achieving adequate record breadth before revisiting depth of records for specific species. The need for open access data, integrated workflows, and interoperable data systems is increasing with the scaling of data collection through use of robotics and technologies. The gaps in existing data systems, interoperability, and data acquisition can be filled strategically for specific applications, offering targeted and efficient dataset development. With data interoperability guiding the structure of new datasets, the modular development of area-specific datasets will enable more generalized use over time and help meet the aims of existing database initiatives.

Code availability

Convenience functions for navigating the MOSAIC database are included in the supplemental material (S5) and on the MOSAIC website https://mosaicdatabase.web.ox.ac.uk and associated GitHub repository https://github.com/mosaicdatabase/Rmosaic. All code is open access without restrictions on access.

Received: 26 June 2022; Accepted: 14 March 2023;

References

1. Reichman, O. J., Jones, M. B. & Schildhauer, M. P. Challenges and opportunities of open data in ecology. *Science (80-.).* **331**, 703–705 (2011).
2. Marx, V. The big challenges of big data. *Nature* **498**, 255–260 (2013).
3. Farley, S. S., Dawson, A., Goring, S. J. & Williams, J. W. Situating ecology as a big-data science: Current advances, challenges, and solutions. *Bioscience* **68**, 563–576 (2018).
4. Maldonado, C. *et al*. Estimating species diversity and distribution in the era of Big Data: To what extent can we trust public databases? *Glob. Ecol. Biogeogr.* **24**, 973–984 (2015).
5. Troia, M. J. & McManamay, R. A. Filling in the GAPS: evaluating completeness and coverage of open-access biodiversity databases in the United States. *Ecol. Evol.* **6**, 4654–4669 (2016).
6. Díaz, S. *et al*. The global spectrum of plant form and function. *Nature* **529**, 167–171 (2016).
7. Maitner, B. S. *et al*. The bien r package: A tool to access the Botanical Information and Ecology Network (BIEN) database. *Methods Ecol. Evol.* **9**, 373–379 (2018).
8. Enquist, B. J. *et al*. The commonness of rarity: Global and future distribution of rarity across land plants. *Sci. Adv.* **5**, 1–14 (2019).
9. Davy, R. & Kusch, E. Reconciling high resolution climate datasets using KrigR. *Environ. Res. Lett.* (2021).
10. Hersbach, H. *et al*. The ERA5 global reanalysis. *Q. J. R. Meteorol. Soc.* **146**, 1999–2049 (2020).

11. Rowcliffe, J. M., Jansen, P. A., Kays, R., Kranstauber, B. & Carbone, C. Wildlife speed cameras: measuring animal travel speed and day range using camera traps. *Remote Sens. Ecol. Conserv.* **2**, 84–94 (2016).
12. Wilmoth, J. R., Andreev, K., Jdanov, D. & Glei, D. A. Methods Protocol for the Human Mortality. *Database. Database* **2007**, 1–80 (2007).
13. Jasilioniene, A. *et al. Methods Protocol for the Human Fertility Database. Max Planck Institute for Demographic Research* (2015).
14. De Magalhães, J. P. & Costa, J. A database of vertebrate longevity records and their relation to other life-history traits. *J. Evol. Biol.* **22**, 1770–1774 (2009).
15. Dornelas, M. *et al.* BioTIME: A database of biodiversity time series for the Anthropocene. *Glob. Ecol. Biogeogr.* **27**, 760–786 (2018).
16. Fortuna, M. A., Ortega, R. & Bascompote, J. The web of life. *arXiv* https://doi.org/10.4324/9780203410134 (2014).
17. Jeliazkov, A. *et al.* A global database for metacommunity ecology, integrating species, traits, environment and space. *Sci. Data* **7**, 1–15 (2020).
18. Gallagher, R. V. *et al.* Open Science principles for accelerating trait-based science across the Tree of Life. *Nat. Ecol. Evol.* **4**, 294–303 (2020).
19. Kissling, W. D. *et al.* Towards global data products of Essential Biodiversity Variables on species traits. *Nat. Ecol. Evol.* **2**, 1531–1540 (2018).
20. Wilkinson, M. D. *et al.* Comment: The FAIR Guiding Principles for scientific data management and stewardship. *Sci. Data* **3**, 1–9 (2016).
21. Nadrowski, K. *et al.* Harmonizing, annotating and sharing data in biodiversity-ecosystem functioning research. *Methods Ecol. Evol.* **4**, 201–205 (2013).
22. Culina, A. *et al.* Navigating the unfolding open data landscape in ecology and evolution. *Nat. Ecol. Evol.* **2**, 420–426 (2018).
23. Kattge, J. *et al.* TRY plant trait database – enhanced coverage and open access. *Glob. Chang. Biol.* **26**, 119–188 (2020).
24. Schneider, F. D. *et al.* Towards an ecological trait-data standard. *Methods Ecol. Evol.* **10**, 2006–2019 (2019).
25. Edwards, J. L., Lane, M. A. & Nielsen, E. S. Interoperability of biodiversity databases: Biodiversity information on every desktop. *Science (80-.).* **289**, 2312–2314 (2000).
26. Maurer, S. M., Firestone, R. B. & Scriver, C. R. Science's neglected legacy: Large, sophisticated databases cannot be left to chance and improvisation. *Nature* **405**, 117–120 (2000).
27. Consortium, E. P. An integrated encyclopedia of DNA elements in the human genome. *Nature* **489**, 57–74 (2012).
28. Vitousek, M. N., Johnson, M. A. & Husak, J. F. Illuminating endocrine evolution: The power and potential of large-scale comparative analyses. *Integr. Comp. Biol.* **58**, 712–719 (2018).
29. Laughlin, D. C., Gremer, J. R., Adler, P. B., Mitchell, R. M. & Moore, M. M. The Net Effect of Functional Traits on Fitness. *Trends Ecol. Evol.* **35**, 1037–1047 (2020).
30. Swenson, N. G. *et al.* A reframing of trait–demographic rate analyses for ecology and evolutionary biology. *Int. J. Plant Sci.* **181**, 33–43 (2020).
31. Guerrero-Ramírez, N. R. *et al.* Global root traits (GRooT) database. *Glob. Ecol. Biogeogr.* **30**, 25–37 (2021).
32. Froese, R. & Pauly, D. FishBase. (2010).
33. Madin, J. S. *et al.* The Coral Trait Database, a curated database of trait information for coral species from the global oceans. *Sci. data* **4**, 170174 (2016).
34. Lintulaakso, K. MammalBase—database of recent mammals. (2013).
35. Oliveira, B. F., São-Pedro, V. A., Santos-Barrera, G., Penone, C. & Costa, G. C. AmphiBIO, a global database for amphibian ecological traits. *Sci. Data* **4**, 1–7 (2017).
36. Ashman, T. L. *et al.* Tree of Sex: A database of sexual systems. *Sci. Data* **1**, 1–8 (2014).
37. Boettiger, C. & Temple Lang, D. Treebase: An R package for discovery, access and manipulation of online phylogenies. *Methods Ecol. Evol.* **3**, 1060–1066 (2012).
38. Borghetti, M., Gentilesca, T., Colangelo, M., Ripullone, F. & Rita, A. Xylem Functional Traits as Indicators of Health in Mediterranean Forests. *Curr. For. Reports* **6**, 220–236 (2020).
39. Jetz, W., Thomas, G. H., Joy, J. B., Hartmann, K. & Mooers, A. O. The global diversity of birds in space and time. *Nature* **491**, 444–448 (2012).
40. Santini, L., Isaac, N. J. B. & Ficetola, G. F. TetraDENSITY: A database of population density estimates in terrestrial vertebrates. *Glob. Ecol. Biogeogr.* **27**, 787–791 (2018).
41. Monnet, A. C. *et al.* WOODIV, a database of occurrences, functional traits, and phylogenetic data for all Euro-Mediterranean trees. *Sci. Data* **8**, 1–11 (2021).
42. Middleton, O., Svensson, H., Scharlemann, J. P. W., Faurby, S. & Sandom, C. CarniDIET 1.0: A database of terrestrial carnivorous mammal diets. *Glob. Ecol. Biogeogr.* **30**, 1175–1182 (2021).
43. Myhrvold, N. P. *et al.* An amniote life-history database to perform comparative analyses with birds, mammals, and reptiles. *Ecology* **96**, (2015).
44. Jones, K. E. *et al.* PanTHERIA: a species-level database of life history, ecology, and geography of extant and recently extinct mammals. *Ecology* **90**, 2648–2648 (2009).
45. Enquist, B. J., Condit, R., Peet, R. K., Schildhauer, M. & Thiers, B. The Botanical Information and Ecology Network (BIEN): Cyberinfrastructure for an integrated botanical information network to investigate the ecological impacts of global climate change on plant biodiversity. *PeerJ Prepr.* (2016).
46. Salguero-Gómez, R. *et al.* The compadre Plant Matrix Database: An open online repository for plant demography. *J. Ecol.* https://doi.org/10.1111/1365-2745.12334 (2015).
47. Salguero-Gómez, R. *et al.* COMADRE: A global data base of animal demography. *J. Anim. Ecol.* https://doi.org/10.1111/1365-2656.12482 (2016).
48. Levin, S. C. *et al.* Rpadrino: an R package to access and use PADRINO, an open access database of Integral Projection Models. *bioRxiv* (2022).
49. Caswell, H. *Matrix population models*. (Sinauer, 2001).
50. Morris, W. F. *et al.* Longevity can buffer plant and animal populations against chnaging climatic variability. *Ecology* **89**, 19–25 (2008).
51. Smallegange, I. M., Deere, J. A. & Coulson, T. Correlative changes in life-history variables in response to environmental change in a model organism. *Am. Nat.* **183**, 784–797 (2014).
52. Crouse, D. T., Crowder, L. B. & Caswell, H. A stage-based population model for loggerhead sea turtles and implications for conservation. *Ecology* **68**, 1412–1423 (1987).
53. Easterling, M. R., Ellner, S. P. & Dixon, P. M. Size-specific sensitivity: Applying a new structured population model. *Ecology* **81**, 694–708 (2000).
54. Jongejans, E., Shea, K., Skarpaas, O., Kelly, D. & Ellner, S. P. Importance of individual and environmental variation for invasive species spread: A spatial integral projection model. *Ecology* **92**, 86–97 (2011).
55. Ozgul, A. *et al.* Coupled dynamics of body mass and population growth in response to environmental change. *Nature* **466**, 482–485 (2010).
56. Metcalf, C. J. E., Graham, A. L., Martinez-Bakker, M. & Childs, D. Z. Opportunities and challenges of Integral Projection Models for modelling host-parasite dynamics. *J. Anim. Ecol.* **85**, 343–355 (2016).

57. Bernard, C. *et al*. MOSAIC trait database. *figshare* https://doi.org/10.6084/m9.figshare.21035857.v1 (2022).
58. Messier, J., McGill, B. J. & Lechowicz, M. J. How do traits vary across ecological scales? A case for trait-based ecology. *Ecol. Lett.* **13**, 838–848 (2010).
59. Siefert, A. *et al*. A global meta-analysis of the relative extent of intraspecific trait variation in plant communities. *Ecol. Lett.* **18**, 1406–1419 (2015).
60. Albert, C. H. Intraspecific trait variability matters. *J. Veg. Sci.* **26**, 7–8 (2015).
61. Capdevila, P. *et al*. Longevity, body dimension and reproductive mode drive differences in aquatic versus terrestrial life-history strategies. *Funct. Ecol.* **34**, 1613–1625 (2020).
62. Gaillard, J.-M., Festa-Bianchet, M. & Yoccoz, N. G. Population dynamics of large herbivores: variable recruitment with constant adult survival. *Trends Ecol. Evol.* **13**, 249–251 (1998).
63. Csergő, A. M. *et al*. Less favourable climates constrain demographic strategies in plants. *Ecol. Lett.* **20**, 969–980 (2017).
64. McGill, B. & Collins, C. A unified theory for macroecology based on spatial patterns of abundance. *Evol. Ecol. Res.* **5**, 469–492 (2003).
65. Salguero-Gómez, R., Violle, C., Gimenez, O. & Childs, D. Delivering the promises of trait-based approaches to the needs of demographic approaches, and vice versa. *Funct. Ecol.* **32**, 1424–1435 (2018).
66. Buckley, Y. M. & Puy, J. The macroecology of plant populations from local to global scales. *New Phytol.* **233**, 1038–1050 (2022).
67. Carmona, C. P., de Bello, F., Azcárate, F. M., Mason, N. W. H. & Peco, B. Trait hierarchies and intraspecific variability drive competitive interactions in Mediterranean annual plants. *J. Ecol.* **107**, 2078–2089 (2019).
68. Pistón, N. *et al*. Multidimensional ecological analyses demonstrate how interactions between functional traits shape fitness and life history strategies. *J. Ecol.* **107**, 2317–2328 (2019).
69. Adler, P. B. *et al*. Functional traits explain variation in plant life history strategies. *Proc. Natl. Acad. Sci. USA* **111**, 10019 (2014).
70. Poorter, L. *et al*. Are functional traits good predictors of demographic rates? Evidence from five neotropical forests. *Ecology* **89**, 1908–1920 (2008).
71. Violle, C. *et al*. The return of the variance: Intraspecific variability in community ecology. *Trends Ecol. Evol.* **27**, 244–252 (2012).
72. Albert, C. H. *et al*. Intraspecific functional variability: Extent, structure and sources of variation. *J. Ecol.* **98**, 604–613 (2010).
73. Bolnick, D. I. *et al*. Why intraspecific trait variation matters in community ecology. *Trends Ecol. Evol.* **26**, 183–192 (2011).
74. McElreath, R. *Statistical rethinking: A Bayesian course with examples in R and Stan*. (Chapman and Hall/CRC, 2020).
75. Kendall, B. E. *et al*. Persistent problems in the construction of matrix population models. *Ecol. Modell.* **406**, 33–43 (2019).
76. Römer, G., Dahlgren, J. P., Salguero-Gómez, R., Stott, I. M. & Jones, O. R. Plant demographic knowledge is biased towards short-term studies of temperate-region herbaceous perennials. *bioRxiv* 1–46 (2021).
77. Reich, P. B. *et al*. The evolution of plant functional variation: Traits, spectra, and strategies. *Int. J. Plant Sci.* **164**, (2003).
78. Laughlin, D. C. Rugged fitness landscapes and Darwinian demons in trait-based ecology. *New Phytol.* **217**, 501–503 (2018).
79. Wilkes, M. A. *et al*. Trait-based ecology at large scales: Assessing functional trait correlations, phylogenetic constraints and spatial variability using open data. *Glob. Chang. Biol.* **26**, 7255–7267 (2020).
80. Enquist, B. J. *et al*. Scaling from traits to ecosystems: developing a general trait driver theory via integrating trait-based and metabolic scaling theories. in *Advances in ecological research* 249–318 (2015).
81. Bellier, E., Kéry, M. & Schaub, M. Relationships between vital rates and ecological traits in an avian community. *J. Anim. Ecol.* **87**, 1172–1181 (2018).
82. Cheruvelil, K. S. & Soranno, P. A. Data-intensive ecological research is catalyzed by open science and team science. *Bioscience* **68**, 813–822 (2018).
83. Whitlock, M. C. Data archiving in ecology and evolution: Best practices. *Trends Ecol. Evol.* **26**, 61–65 (2011).
84. Michener, W. K. Meta-information concepts for ecological data management. *Ecol. Inform.* **1**, 3–7 (2006).
85. Diepenbroek, M. *et al*. Towards an Integrated Biodiversity and Ecological Research Data Management and Archiving Platform: The…. *Inform. 2014 – Big Data Komplexität meistern. GI-Edition Lect. Notes Informatics – Proc. 232* 1711–1721 (2014).
86. Wieczorek, J. *et al*. Darwin core: An evolving community-developed biodiversity data standard. *PLoS One* **7**, (2012).
87. Salguero-Gómez, R., Jackson, J. & Gascoigne, S. J. L. Four key challenges in the open-data revolution. *J. Anim. Ecol.* **90**, 2000–2004 (2021).
88. Conde, D. A. *et al*. Data gaps and opportunities for comparative and conservation biology. *Proc. Natl. Acad. Sci. USA* **116**, 9658–9664 (2019).
89. Chalmandrier, L. *et al*. Linking functional traits and demography to model species-rich communities. *Nat. Commun.* **12**, (2021).
90. Yang, J., Cao, M. & Swenson, N. G. Why Functional Traits Do Not Predict Tree Demographic Rates. *Trends Ecol. Evol.* **33**, 326–336 (2018).
91. Levin, S. C., Crandall, R. M., Pokoski, T., Stein, C. & Knight, T. M. Phylogenetic and functional distinctiveness explain alien plant population responses to competition: Phylogeny and traits explain dominance. *Proc. R. Soc. B Biol. Sci.* **287**, (2020).
92. Daskalova, G. N., Myers-Smith, I. H. & Godlee, J. L. Rare and common vertebrates span a wide spectrum of population trends. *Nat. Commun.* **11**, 1–13 (2020).
93. Roper, M., Capdevila, P. & Salguero-Gómez, R. Senescence: Why and where selection gradients might not decline with age. *Proc. R. Soc. B Biol. Sci.* **288**, (2021).
94. Healy, K. *et al*. Ecology and mode-of-life explain lifespan variation in birds and mammals. *Proc. R. Soc. B Biol. Sci.* **281**, (2014).
95. Terry, J. C. D., O'Sullivan, J. D. & Rossberg, A. G. No pervasive relationship between species size and local abundance trends. *Nat. Ecol. Evol.* **6**, 140–144 (2022).
96. Williams, N. F., McRae, L., Freeman, R., Capdevila, P. & Clements, C. F. Scaling the extinction vortex: Body size as a predictor of population dynamics close to extinction events. *Ecol. Evol.* **11**, 7069–7079 (2021).
97. Daskalova, G. N., Bowler, D., Myers-Smith, I. H. & Dornelas, M. Representation of global change drivers across biodiversity datasets. *EcoEvoRxiv* 1–36 (2021).
98. Paniw, M., Maag, N., Cozzi, G., Clutton-Brock, T. & Ozgul, A. Life history responses of meerkats to seasonal changes in extreme environments. *Science (80-.).* **363**, 631–635 (2019).
99. Stenseth, N. C. & Mysterud, A. Climate, changing phenology, and other life history traits: Nonlinearity and match-mismatch to the environment. *Proc. Natl. Acad. Sci. USA* **99**, 13379–13381 (2002).
100. Violle, C. *et al*. Let the concept of trait be functional! *Oikos* **116**, 882–892 (2007).
101. Salguero-Gómez, R. & Laughlin, D. C. Not all traits are functional: the Panglossian paradigm. *Authorea*, https://doi.org/10.22541/au.163940711.10447233/v1 (2021).

Acknowledgements

We thank Mark Roper, Sara Middleton, Etienne Cousin, and Thomas Marrien for their contributions to discussion at the beginning of the project, Jessica Hass and Lauren Hinchcliffe for collecting data for the project, John Park for his contributions to the conception of citMOSAIC, and Sam Levin for valuable comments on the Rmosaic package. This work was supported by a NERC IRF (NE/M018458/1) to RS-G. RCRC acknowledges postdoctoral support from the Regional Valencian Government and the European Social Fund (APOSTD/2020/090).

Author contributions

C.B. and R.S.G. conceived the ideas; C.B., R.S.G., G.S.S., J.D. and P.C. designed the methodology; C.B., G.S.S., J.D., P.C. and S.J.L.G. integrated databases; C.B., G.S.S., and J.D. collected primary records data; E.K. led the climate data acquisition and analysis of geospatial data; and C.B. led the writing of the manuscript with assistance from J.J. All authors contributed critically to the drafts and gave final approval for publication.

Competing interests

The authors declare no competing interests.

Additional information

Supplementary information The online version contains supplementary material available at https://doi.org/10.1038/s41597-023-02070-w.

Correspondence and requests for materials should be addressed to C.B.

Reprints and permissions information is available at www.nature.com/reprints.

Publisher's note Springer Nature remains neutral with regard to jurisdictional claims in published maps and institutional affiliations.

Received: 14 February 2023 | Accepted: 18 May 2023

DOI: 10.1111/2041-210X.14164

Methods in Ecology and Evolution

RESEARCH ARTICLE

A standard protocol to report discrete stage-structured demographic information

Samuel J. L. Gascoigne[1] | **Simon Rolph[2]** | **Daisy Sankey[1]** | **Nagalakshmi Nidadavolu[1]** | **Adrian S. Stell Pičman[1,3]** | **Christina M. Hernández[4]** | **Matthew E. R. Philpott[1]** | **Aiyla Salam[1]** | **Connor Bernard[1]** | **Erola Fenollosa[1]** | **Young Jun Lee[1]** | **Jessica McLean[1]** | **Shathuki Hetti Achchige Perera[1]** | **Oliver G. Spacey[1]** | **Maja Kajin[1,3]** | **Anna C. Vinton[1]** | **C. Ruth Archer[5]** | **Jean H. Burns[6]** | **Danielle L. Buss[7,8]** | **Hal Caswell[9]** | **Judy P. Che-Castaldo[10]** | **Dylan Z. Childs[2]** | **Pol Capdevila[11]** | **Aldo Compagnoni[1,12,13]** | **Elizabeth Crone[14]** | **Thomas H. G. Ezard[15]** | **Dave Hodgson[8]** | **Tiffany M. Knight[12,13,16]** | **Owen R. Jones[17]** | **Eelke Jongejans[18,19]** | **Jenni McDonald[20,21]** | **Brigitte Tenhumberg[22]** | **Chelsea C. Thomas[23]** | **Andrew J. Tyre[24,25]** | **Satu Ramula[26]** | **Iain Stott[27]** | **Raymond L. Tremblay[28,29,30]** | **Phil Wilson[8]** | **James W. Vaupel[31,‡]** | **Roberto Salguero-Gómez[1,32,33]**

[1]Department of Biology, University of Oxford, Oxford, UK; [2]Department of Animal & Plant Sciences, University of Sheffield, Sheffield, UK; [3]Department of Biology, University of Ljubljana, Ljubljana, Slovenia; [4]Department of Ecology and Evolutionary Biology, Cornell University, Ithaca, New York, USA; [5]Institute of Evolutionary Ecology and Conservation Genomics, University of Ulm, Ulm, Germany; [6]Department of Biology, Case Western Reserve University, Cleveland, Ohio, USA; [7]Department of Archaeology, University of Cambridge, Cambridge, UK; [8]College of Life and Environmental Sciences, University of Exeter, Penryn, UK; [9]Institute for Biodiversity and Ecosystem Dynamics, University of Amsterdam, Amsterdam, The Netherlands; [10]Branch of Species Status Assessment Science Support, U.S. Fish and Wildlife Service, Washington, DC, USA; [11]School of Biological Sciences, University of Bristol, Bristol, UK; [12]Institute of Biology, Martin Luther University Halle-Wittenburg, Halle (Saale), Germany; [13]German Centre for Integrative Biodiversity Research (iDiv) Halle-Jena-Leipzig, Leipzig, Germany; [14]Department of Biology, Tufts University, Medford, Massachusetts, USA; [15]School of Ocean and Earth Science, University of Southampton, Southampton, UK; [16]Department of Community Ecology, Helmholtz Centre for Environmental Research-UFZ, Halle (Saale), Germany; [17]Department of Biology, University of Southern Denmark, Odense, Denmark; [18]Animal Ecology and Physiology, Radboud University, Nijmegen, The Netherlands; [19]NIOO-KNAW, Animal Ecology, Wageningen, The Netherlands; [20]Veterinary Department, Cats Protection, National Cat Centre, Haywards Heath, UK; [21]Bristol Veterinary School, University of Bristol, Bristol, UK; [22]School of Biological Sciences and Department of Mathematics, University of Nebraska, Lincoln, Nebraska, USA; [23]Alexander Center for Applied Population Biology, Conservation & Science Department, Chicago, Illinois, USA; [24]School of Natural Resources, University of Nebraska-Lincoln, Lincoln, Nebraska, USA; [25]Global Resistance Management Team, Bayer U.S. – Crop Science, Chesterfield, Missouri, USA; [26]Department of Biology, University of Turku, Turku, Finland; [27]School of Life Sciences, University of Lincoln, Lincoln, UK; [28]Department of Biology, University of Puerto Rico, San Juan, Puerto Rico, USA; [29]Center for Applied Tropical Ecology and Conservation, University of Puerto Rico, San Juan, Puerto Rico, USA; [30]Department of Biology, University of Puerto Rico-Humacao, Puerto Rico, USA; [31]Interdisciplinary Centre on Population Dynamics, University of Southern Denmark, Odense, Denmark; [32]Centre for Biodiversity and Conservation Science, University of Queensland, St Lucia, Queensland, Australia and [33]Evolutionary Demography Laboratory, Max Planck Institute for Demographic Research, Rostock, Germany

Correspondence
Samuel J. L. Gascoigne
Email: samuel.gascoigne@pmb.ox.ac.uk

Roberto Salguero-Gómez
Email: rob.salguero@biology.ox.ac.uk

Funding information
Maria Zambrano Next Generation

Abstract

1. Stage-based demographic methods, such as matrix population models (MPMs), are powerful tools used to address a broad range of fundamental questions in ecology, evolutionary biology and conservation science. Accordingly, MPMs now exist for over 3000 species worldwide. These data are being digitised as

---

‡Unfortunately, our dear friend and colleague passed before the submission of this paper.

EU Fellowship; Natural Environment Research Council, Grant/Award Number: NE/L007770/1, NE/M018458/1 and NE/N006798/1; NSF, Grant/Award Number: DEB-1933497; NSF Advances in Bioinformatics Development Award, Grant/Award Number: DBI-1661342; European Research Council, Grant/Award Number: 788195

Handling Editor: Res Altwegg

an ongoing process and periodically released into two large open-access online repositories: the COMPADRE Plant Matrix Database and the COMADRE Animal Matrix Database. During the last decade, data archiving and curation of COMPADRE and COMADRE, and subsequent comparative research, have revealed pronounced variation in how MPMs are parameterized and reported.

2. Here, we summarise current issues related to the parameterisation and reporting of MPMs that arise most frequently and outline how they affect MPM construction, analysis, and interpretation. To quantify variation in how MPMs are reported, we present results from a survey identifying key aspects of MPMs that are frequently unreported in manuscripts. We then screen COMPADRE and COMADRE to quantify how often key pieces of information are omitted from manuscripts using MPMs.
3. Over 80% of surveyed researchers ($n=60$) state a clear benefit to adopting more standardised methodologies for reporting MPMs. Furthermore, over 85% of the 300 MPMs assessed from COMPADRE and COMADRE omitted one or more elements that are key to their accurate interpretation. Based on these insights, we identify fundamental issues that can arise from MPM construction and communication and provide suggestions to improve clarity, reproducibility and future research utilising MPMs and their required metadata. To fortify reproducibility and empower researchers to take full advantage of their demographic data, we introduce a standardised protocol to present MPMs in publications. This standard is linked to www.compadre-db.org, so that authors wishing to archive their MPMs can do so prior to submission of publications, following examples from other open-access repositories such as DRYAD, Figshare and Zenodo.
4. Combining and standardising MPMs parameterized from populations around the globe and across the tree of life opens up powerful research opportunities in evolutionary biology, ecology and conservation research. However, this potential can only be fully realised by adopting standardised methods to ensure reproducibility.

KEYWORDS
comparative demography, matrix population models, open access, reproducibility

1 | INTRODUCTION

Population ecology has come of age. The development of theories, experimental approaches and statistical methodologies have resulted in the publication of demographic information for an increasingly representative sample of the world's biodiversity (De Magalhães & Costa, 2009; Levin et al., 2022; Salguero-Gómez et al., 2015, 2016). These data span the taxonomic tree from microbes (Jouvet et al., 2018) to macro-vertebrates (Fujiwara & Caswell, 2001), and cover virtually all continents and biomes—though with important taxonomic biases (Conde et al., 2019; Römer et al., 2021). The potential of this impressive and rapidly increasing amount of information is starting to be realised. Indeed, through combining these demographic models, researchers have identified functional traits that explain variation in plant life history strategies (Adler et al., 2014; also see Bernard et al., 2023), short-term (transient) characteristics that drive the demographic dynamics of plant populations in variable environments (McDonald et al., 2016), and ways in which life history strategies allow species to persist alongside a changing climate (Jelbert et al., 2019; Paniw et al., 2019).

One of the most widely used tools for describing and analysing species' complex life histories is the matrix population model (MPM, hereafter). Briefly, in an MPM, individuals of a population are classified by discrete stages and/or ages (st/age hereafter) according to some biological (Caswell, 2001, p. 31) or statistical/sampling criteria (Salguero-Gómez & Plotkin, 2010). These individuals are followed in discrete time steps, typically adjusted by the generation time of the species. Indeed, time steps can vary from 12 to 24 h as in nematode worms *Caenorhabditis elegans* and aphids *Myzus periscae* (Bruijning et al., 2019; Li et al., 2014), to monthly/annual periods in mammals and plants (Coulson et al., 2001; Ferreira et al., 2016), all the way to 50 years in slow-growing red woods (Namkoong & Roberds, 1974).

From these data, researchers estimate losses through mortality, transition probabilities among st/ages and their per-capita a/sexual contributions via reproduction (Nordstrom et al., 2021; Omeyer et al., 2021).

A single MPM can be used to calculate a vast repertoire of biologically meaningful outputs. These outputs include proxies for the performance and viability of populations, such as deterministic (λ) or stochastic population growth rates (λ_s) (Doak et al., 2005), quasi-extinction risk (Davis, 2022), population response to perturbations of underlying vital rates such as survival or reproduction (Caswell, 2001, p. 206), transient dynamics (Capdevila et al., 2020; Ezard et al., 2010; Stott et al., 2011) and life history traits, such as rates of senescence (Baudisch et al., 2013), degree of iteroparity (Salguero-Gómez et al., 2017) and age at maturity (Caswell, 2001, p. 124). This wealth of demographic inference highlights why many advances in demography and life history theory utilise MPMs (Franco & Silvertown, 1996; Pfister, 1998; Sæther et al., 2013; Tuljapurkar, 1989).

MPMs for plants and animals have been archived, error-checked, complemented with additional information (e.g. GPS coordinates, IUCN conservation status), and released open-access in the COMPADRE Plant Matrix Database (Salguero-Gómez et al., 2015) and the COMADRE Animal Matrix Database (Salguero-Gómez et al., 2016). In the latest data release, COMPADRE v. 6.22.5 [COMADRE v. 4.21.8] contains 8851 [3317] MPMs from 760 [415] unique species published in 643 [395] studies. At the time of writing, a further 1307 species are pending digitization in the COMPADRE network, at a rate of 4.5 new works containing MPMs being screened, digitised, and quality checked every week (S. Gascoigne, pers. obs.). However, one of the challenges of the digitization process is the tremendous variation in how data are collected, presented and used to parameterize MPMs.

Data standardisation improves reproducibility and promotes data sharing across research disciplines (Reichman et al., 2011). Data standardisation, and the associated detailed metadata, is therefore key for research to be replicated, validated, openly discussed and ultimately for science to advance (Powers & Hampton, 2019; Reichman et al., 2011; Salguero-Gómez et al., 2021). Examples of these standards include reporting sample size and variance of estimates and detailing the full list of original sources of data (Gerstner et al., 2017). In this context, standards can be used as checklist items to improve publications quality and reproducibility and to aid the peer-review process (Reichman et al., 2011). Furthermore, meta-analyses (Gurevitch et al., 2018) and phylogenetic comparative analyses (Healy et al., 2019; Salguero-Gómez et al., 2017), which offer valuable opportunities to examine general patterns and identify gaps in knowledge, rely on data conforming to certain standards.

MPMs are being adapted, extended and applied beyond their original, species-specific context in comparative demography. However, not all MPMs are built and reported equally. The current presentation of MPMs in COMPADRE and COMADRE may give the false impression that all MPMs are published in a homogeneous format, despite differences in how and why the MPMs are produced (Caswell, 2001). This impression may have emerged from the amount of verification the COMADRE and COMPADRE digitisation team does behind the scenes (e.g. validating model outputs, author correspondence for additional information). While verification is an inevitable aspect of database curation, most of our efforts are spent communicating with authors rather than digitising data. Our goal here is to (i) present the current standard of MPM communication in the literature, (ii) identify common issues in MPM communication and their impacts, (iii) suggest ways to support the clear communication of MPM data and metadata, (iv) highlight advantages for authors and the scientific community at large and (v) introduce a standard method for sharing MPM data and metadata.

2 | MPM COMMUNICATION: CURRENT STATE OF AFFAIRS

To present the current practices in MPM data and metadata communication, with the ultimate goal to evaluate the need for standardised data and metadata reporting, we performed a survey of researchers and screened a subset of papers that have been used to generate MPMs stored in COMPADRE and COMADRE.

2.1 | A survey on matrix communication

We surveyed expert population ecologists, who we identified as having published peer-reviewed papers that include MPMs, regarding our current ability to communicate MPM data and metadata for reproducibility purposes. Specifically, we asked how well peer-reviewed publications relay the attributes of MPMs necessary for reproducibility. Additionally, we asked if researchers thought a standardised method of matrix communication is 'necessary for the coherent communication of MPMs in the literature' (the full list of 11 questions can be found in Supporting Information). The survey was distributed using Google Forms. We identified 1390 potential participants based on the criterion of being the lead and/or corresponding author from a publication containing at least one MPM. Over 50% of corresponding email addresses were outdated and not contacted further. Of the remaining approximately 650 researchers, that were contacted, 60 participants completed the survey. As expected, researchers report a great deal of heterogeneity in components of MPM communication (Figure 1). The best communicated attributes according to these survey participants are trait names (i.e. the phenotype by which the MPM was structured—stage/age/size classes), census duration and projection interval while the worst communicated attributes are life cycle graphs, formulae defining the vital rates and population vectors (i.e. number/frequency of individuals in each st/age). Importantly, 83% of survey participants agreed that the discipline needs a standardised method for MPM communication.

2.2 | A screen of papers in COMPADRE and COMADRE

To quantify how well MPM data and metadata are communicated in peer-reviewed publications, we screened 300 randomly

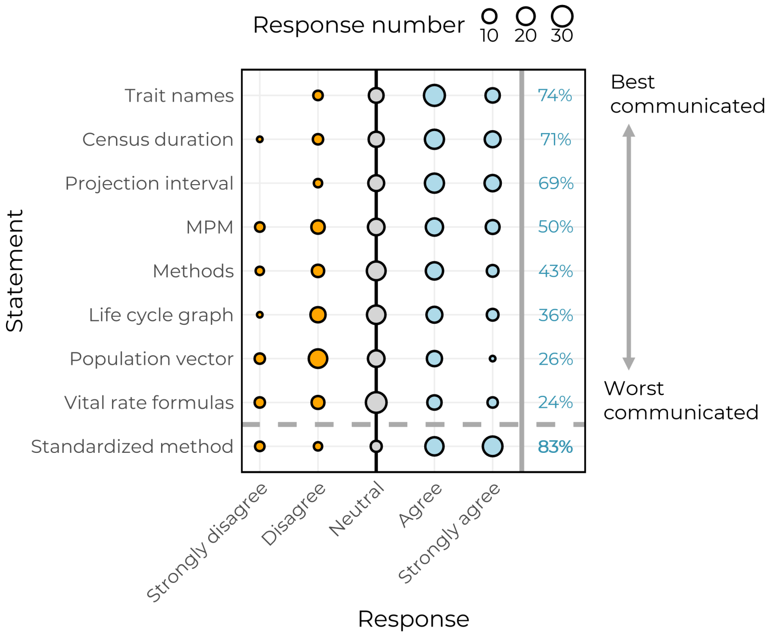

FIGURE 1 Survey results from experts in population ecology that participated ($n=60$). Participants ranked their confidence in the appropriate communication of components of matrix population models (MPMs) in peer-reviewed papers. Each component of MPM communication on the y-axis represents a statement shown in the survey (see SOM for the full survey). For all statements above the dashed line, participants were asked if that attribute (e.g. projection interval) is sufficiently well-reported in peer-reviewed publications. The statement 'standardised method' indicates participants' response to whether the field of population ecology would benefit from a standardised method of MPM reporting. The size of the dots indicates the number of respondents with that response and are coloured (i.e. orange = disagreement; grey = neutral; blue = agreement). For ease, percent agreement (i.e. the percentage of participants that either agreed or strongly agreed with the statement) is shown on the right-hand side of the plot.

sampled papers containing MPMs already digitised in COMPADRE and COMADRE (150 papers each). Across the different key attributes of MPMs that we examined, there was considerable variation in how reliably authors provided the data and metadata necessary for digitising, archiving, and performing comparative analysis (Figure 2). For instance, the generic location of the examined population (i.e. province/city/landmark; COMPADRE: 95.1%, COMADRE: 86.2% of papers reported it), the fully parameterized MPM (93.3%, 88.9%), and the census date (89.6%, 77.7%) were frequently explicitly stated in the papers, while latitude-longitude of the examined population (52.4%, 39.9%), its life-cycle diagram (44.5%, 40.1%), and population vector (i.e. st/age distribution of individuals at time *t*) (33.2%, 32.6%) were not. Interestingly, plant studies using MPMs (COMPADRE) contain overall more explicit data and metadata than animal studies (COMADRE; Figure 2). Furthermore, we used this information to categorise the quality of each of the examined 300 papers according to their reproducibility—defined as their inclusion of components of MPM communication (Figure 3). The distribution of component communication across kingdoms is similar. Crucially, only 13.9% of papers in COMADRE and 15.8% of papers in COMPADRE contain all the information necessary for comparative analyses and accurate projections (Figure 3). Thus, approximately 85% of papers require emailing authors to request undisclosed information.

3 | COMMON ISSUES IN MATRIX CONSTRUCTION

Here, we identify key issues in the parameterization of MPMs to illustrate the impact of methodology on demographic inference. To do so, we draw from the findings from the previous section and our experience curating COMPADRE and COMADRE. We outline the following issues for two reasons: (i) to advise demographers in how to identify them in the literature and (ii) to prevent these issues persisting in future publications. We note that a comprehensive list was recently made available by Kendall et al. (2019, see also Che-Castaldo et al., 2020). Here, we add to these previous papers by outlining steps for researchers to avoid/mitigate these issues in their own research. A summary of these issues, from occurrence to impact, is detailed in Figure S1.

3.1 | Census type, timing and frequency

MPMs are discrete-time demographic models parameterized by the tracking of individuals across censuses. Thus, the type (e.g. longitudinal, cross-sectional), timing and frequency of sampling needs to be carefully planned. These criteria are particularly important as census

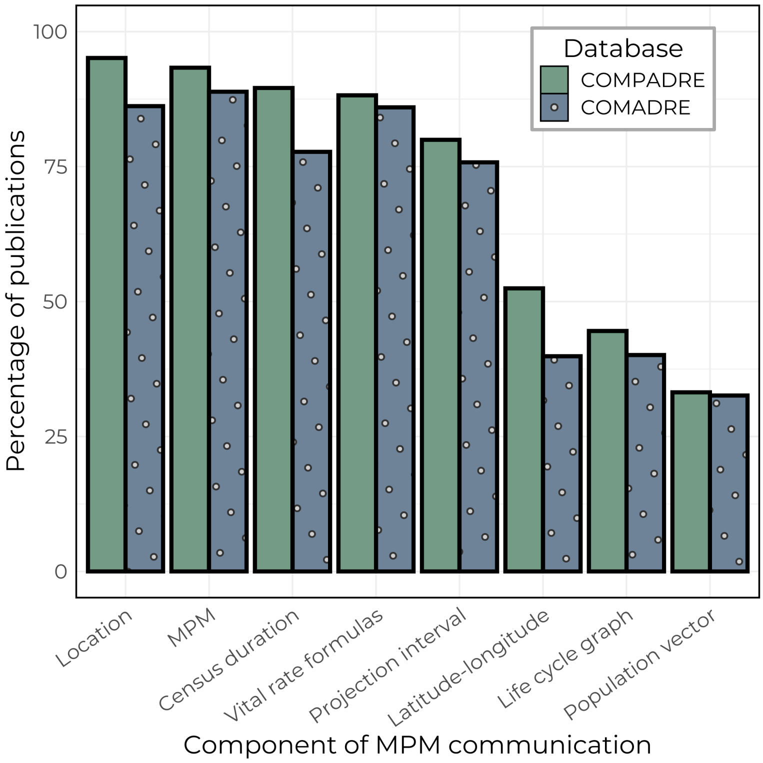

FIGURE 2 Both plant and animal MPM papers show similar patterns as to which presented components of MPM are communicated. The *y*-axis indicates the percentage of peer-reviewed publications in COMPADRE and COMADRE that contain a given attribute necessary for the clear communication of MPM information and its reproducibility from a random subset of 150 papers of the 643 total papers from COMPADRE and 150 out of the 395 total papers from COMADRE (300 papers total). The attributes are: Location: province/city/landmark; MPM: was the MPM included in the manuscript; Census duration: start and end dates for data collection; Vital rate formulas: decomposition of matrix elements into their underlying components (i.e. contributions from survival, growth, and reproduction); Projection interval: the time period between observations; Latitude-longitude: spatial coordinates; Life cycle graph: the visual representation of demographic transitions and a/sexual per-capita contributions; Population vector: st/age distribution of individuals at time *t* associated with reported MPMs.

type directly affects matrix construction, and census timing and frequency can inadvertently influence demographic outputs (Emery & Gross, 2005).

Typically, an MPM comes in two forms regarding the spread of reproduction between censuses: birth-flow or birth-pulse (see Caswell, 2001, p. 22). The distinction is based on whether reproduction occurs continuously (i.e. birth-flow) or in a narrow temporal window (i.e. birth-pulse). Birth-pulse MPMs are further categorised into pre- versus post-reproductive census. Although both pre- and post-reproductive censuses often lead to similar demographic inference (see Cooch et al., 2003), their difference lies in when populations are censused relative to the position of the narrow reproductive window. In the former, populations are censused immediately before a reproductive window, while post-reproductive censuses follow on from a reproductive window. A pre-reproductive census requires the inclusion of offspring survival in reproductive matrix elements, while a post-reproductive census requires the inclusion of parent survival in reproductive matrix elements. We often encounter mistakes in the accommodation of offspring or parent survival in reproductive matrix elements (see also Kendall et al., 2019). A key step in matrix construction that can prevent the incorrect accommodation of survival is drawing the life cycle graph (as *per* Ebert, 1999, p. 61) with respect to census timing (demonstrated in Ellner et al., 2016, p. 13), as well as explicitly detailing the census type used to parameterize the MPM. However, sometimes drawing the life cycle graph may be unfeasible or uninformative. For example, the graph for an age classified model with 100 age classes is too large to draw and too redundant to be useful; but, they can be simplified with a dashed line if multiple adjacent classes have the same demographic rates (e.g. Ebert, 1999, p. 2). Models with many stages and highly connected transitions are not feasible to draw the life cycle graph (e.g. the graph for *Calathea ovandensis* in Neubert and Caswell (2000)). But even in complex situations (e.g. the series of seasonal graphs for the emperor penguin in Jenouvrier et al. (2010)) the graph may be helpful in organising the structure of the model.

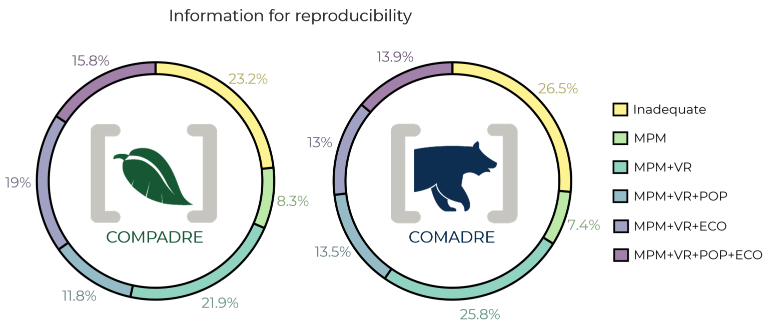

FIGURE 3 Across plant and animal MPM papers, most publications do not contain sufficient information for reproducibility. Proportion of papers in COMPADRE and COMADRE grouped by their open-access information in peer-review publications regarding matrix population model (MPM) data and metadata. Following the same scheme as in Figure 2, papers were ranked into six groups from 'inadequate' to 'MPM + VR + POP+ECO' (i.e. fully reproducible). 'Inadequate' refers to papers missing the MPM and/or projection interval (i.e. an MPM specific time interval necessary for projection), without which most demographic outputs cannot be calculated. 'MPM': paper contains the MPM and projection interval but no vital rate formulas describing the matrix elements. 'MPM + VR': contains all of the information for 'MPM' along with vital rate formulas for the matrix elements. 'MPM + VR + POP': contains all of the information for 'MPM + VR' along with the population vector. 'MPM + VR + ECO': contains all of the information for 'MPM + VR' along with latitude-longitude coordinates and census duration of the examined population. 'MPM + VR + POP + ECO': contains all of the information for 'MPM + VR' along with population vector/ distribution, latitude-longitude coordinates and census duration.

Census timing and frequency affects model construction, making a constructed MPM impractical for demographic inference if the life history of the examined organism is not considered. Consider a researcher comparing the demographic processes of fruit flies and fruit trees. The researcher first notices that there are four discrete stages to the fruit flies' life history: three juvenile stages encompassing the development from egg to instar to pupae, and one adult stage where individuals disperse and reproduce. Since development from egg to adult takes ~10 days in this species, the researcher decides to perform the census every 10 days for both the fruit fly and the fruit trees over a 3-month period. However, because neither mortality nor reproduction occur across such a short census in the fruit tree population, the resulting fruit tree MPM, when projected forward, will persist forever, neither increasing nor declining. This same issue would occur the other way around. If 5-year intervals were deemed sufficient for the fruit trees, then individually measured fruit flies would never survive across time steps. A solution to this problem exists, using periodic matrix models to include periods much shorter or longer than other periods. For example, Hunter and Caswell (2005) analysed the Sooty Shearwater *Puffinus griseus* including two harvesting periods of several weeks in duration and then an annual interval for the species, with a lifespan of decades. Smith et al. (2005) and Shyu et al. (2013) used periodic seasonal models to accommodate life cycles in which some stages are only present for part of the annual cycle. The approach (Caswell, 2001, section 13.1) is powerful and general.

3.2 | Unrealistic stage-specific survival

Issues in parameterising stage-specific survival, whilst easy to diagnose, can result in an array of unnatural life histories. Transition and survival probabilities are bounded between 0 (i.e. the event never happens) and 1 (i.e. always occurs). As such, the stage-specific survival of an MPM, the summed nonreproductive elements in a given column of the MPM $\mathbf{A}$ must not exceed 1. When it does, individuals in that stage have an unrealistic chance of surviving >100%, resulting in an incorrect representation of the organism's life history. Stage-specific survival values >1 typically arise due to rounding errors, typos, inclusion of unstated a/sexual reproductive events. As such, it is generally advised to omit these MPMs in comparative analysis (Jones et al., 2014). Unstated a/sexual reproductive events occur when a given element $a_{i,j}$ in the MPM $\mathbf{A}$ contains both survival-dependent processes, such as growth/shrinkage, but also fertility, and these have not been reported separately. Ideally, authors would carefully identify whether various vital rates are being confounded with survival-dependent demographic processes in each MPM element. For the comparative demographer using COMPADRE and COMADRE, we recommend either avoiding MPM models where stage-specific survival >1 or altering the model so that the stage-specific survival is fixed to a maximum of 1 (e.g. Buckley et al., 2010).

In many published MPMs, some life stages have an estimated survival probability of 1 or an incomplete life cycle, likely the result of small sample size or rare event along the life history of the species. Perfect survival (i.e. mortality = 0) is unlikely to be accurate, and may need to be estimated or imputed (Johnson et al., 2018). A reproducible approach to infer realistic survival and transition values was recently proposed by Tremblay et al. (2021), using a Bayesian approach to estimate parameter values using priors in addition to the observed data to obtain posterior MPMs. An advantage of this approach is that the confidence intervals of the parameters that represent probabilities (i.e. stasis, transition, survival) are obtained from a beta distribution. This advantage of using a Bayesian inferred multinomial Dirichlet distribution for estimating the mean values is that the researchers can infer variance and skew of the posterior distributions to further inform MPM construction and demographic inference (e.g. Tremblay et al., 2009a, 2009b). And finally, since sample size can be a key driver of unrealistic stage-specific survival, sample size and uncertainty (e.g. confidence interval, standard deviation) must be reported to (1) relay the precision of the estimated survival value to your audience and (2) for accurate inclusion of survival values in meta-analyses and comparative methods.

3.3 | Incorrectly parameterizing fertility

Fertility often presents a challenge to constructing accurate MPMs. This challenge is partly due to the ambiguity of the term 'fertility'. The issue arises when the per-capita contributions of reproductive adults to new recruits (e.g. eggs, neonates, seeds, etc.) do not represent the links over the full projection interval of the study. Remember that the entry $a_{i,j}$ in an MPM is the (expected) number of stage i individuals at $t+1$ per stage j individual at time t. If stage i is some kind of 'newborn' individual, then $a_{i,j}$ must include all the processes between time t and time $t+1$ (Caswell, 2001, p. 61). Reproductive output, in turn, is a composite demographic process of the number of offspring produced in a reproductive event and the relevant survival that will penalise how many new offspring will *actually* make it to the next observation. Failure to accommodate this vital rate decomposition can result in the introduction of a one-timestep lag into the organism's life cycle, as newly created offspring spend a projection interval 'in limbo' before their onward transitions. The best-known example is in the classic model of teasel *Dipsacus sylvestris* by Werner and Caswell (1977), in which flowering plants at time t were described as producing seeds at time $t+1$, which only germinated to seedlings at time $t+2$. The issue was discussed and corrected in Caswell (2001). Furthermore, this issue has been reported, for instance, in reproductive structures such as seeds that do not actually undergo a permanent seed bank. An MPM with this issue will typically (Kendall et al., 2019), but not always (Nguyen et al., 2019), underestimate the asymptotic population growth rate, λ. Naturally the challenge will then be in estimating the relative importance of the seed bank and the lifespan on nongerminated seeds. The effect of incorrectly parameterizing fertility on λ is greatest in cases of extreme growth, such as invasive species, or extreme decline, such as critically endangered species (Rueda-Cediel et al., 2018). Furthermore, this issue can also cause overestimation of the transient envelope (see Ezard et al., 2010). Thus, we recommend reporting the fertility vital rate formulas with the associated MPMs and clearly identifying the values of these underlying vital rates (as in Box 1).

3.4 | Indirectly calculating vital rates

Estimating vital rates often involves combinations of direct and indirect measurements. Direct measurement empirically derives vital rates from individual-based data where identified individuals are censused multiple times, as in cohort life table studies, mark-recapture methods and many quadrat studies of marked plants. However, vital rates can be hard to observe in species with high offspring production, complex phenology and/or small population sizes (Beissinger & Westphal, 1998). Consequently, recruitment estimates are often supplemented into MPMs from controlled conditions; examples include the laboratory (Jouvet et al., 2018), greenhouse (Gontijo & Carvalho, 2020), zoo (Clubb et al., 2009) and botanic garden (Jiménez-Valdés et al., 2010). Since some MPM methods require a full life cycle to obtain key metrics (e.g. transient metrics: Stott et al., 2011), external study sites or literature sources are often used to parameterize components of the MPM to 'close the loop' in incomplete life cycles (Omeyer et al., 2021). However, captive populations may not represent wild population dynamics (Clubb & Mason, 2003), particularly in regards to survival (Che-Castaldo et al., 2021) or reproduction (Clubb et al., 2009).

Another method to indirectly estimate vital rates involves using ex-situ methods to obtain upper and lower bounds on recruitment (or other vital rates) and explore the parameter space within those bounds. The approach was introduced by Caswell et al. (1998) in a study of the effects of bycatch mortality on the harbour porpoise. Age-specific survival and fertility schedules were selected from other species with similar life cycles, re-scaled to match the longevity of the harbour porpoise, and used to produce uncertainty distributions for population growth and the effects of the measured bycatch. Reporting the distribution and associated parameters provide a measure of uncertainty from which to inform the construction of an MPM (Tenhumberg et al., 2008). Furthermore, the use of hierarchical models to estimate missing values and borrowing strength from other populations or species may improve parameter estimation (James et al., 2021; Tremblay & McCarthy, 2014).

And lastly, integrated population models represent a valuable framework for indirectly estimating the demographic rates and population dynamics (size and structure) by combining data sources, particularly combining longitudinal individual data with population census data (Plard et al., 2019; Schaub & Kéry, 2021). Integrated population models allow for the construction of population models (including MPMs) by (1) combining data sources, (2) defining a life history a priori (this is often some form of stage-structured population model) and (3) quantifying the maximum likelihood of demographic rates encoded in the life history given the data sources. Integrated population models are particularly useful when uncertainty around data acquisition is known (e.g. in capture-mark-recapture studies) (Riecke et al., 2019).

3.5 | Population vector

An estimate of the structure of the population, classified by age or stage, is a useful piece of information when available, but it will only sometimes be available. Current population structure provides a logical starting point for projections of short-term and long-term population viability (Werner & Peacock, 2019). Furthermore, using the population vector (i.e. abundance and stage distribution) for projections helps to account for the effects of transient dynamics, which measure the

BOX 1 Example presentation of a hypothetical three-stage plant matrix population model (MPM) using a clear and explicit presentation of data applicable to most MPM construction techniques.

(A) Matrix type

A simple deterministic density-independent matrix.*

*This free text field allows for the brief description of matrix type. If the matrix is structured by one variable the matrix is simple. If not, the matrix is considered general (e.g. age x stage). Deterministic refers to if the demographic rates that build the MPM are held constant (deterministic) or drawn from a distribution (stochastic). Density-independent versus density-dependent indicates if the demographic rates are or are not influenced by population density.

(B) Life cycle diagram

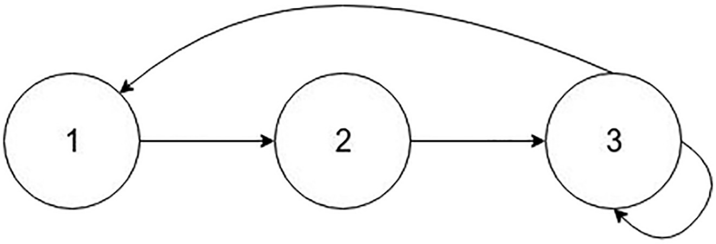

(C) Census description

Census attribute	Example
Census duration	May 2021 to May 2022
Location (latitude–longitude)	Sheffield, UK (53°24′41.5″N 1°30′02.3″W)
Projection interval	1 year
Mode of reproduction	Birth-pulse (taking place in June and July)
Census type	Pre-reproductive census

(D) Stage names and classification

Stage number	Stage name	Classifying criteria
1	Seedling	A recently germinated individual that has fewer than four leaves and has not developed the radial rosette structure. The leaves are less than three centimetres in length
2	Rosette	An individual with a pronounced radial morphology in leaf structure. The leaves are between three and six centimetres in length
3	Adult plant	An individual with a pronounced radial morphology and has the ability to produce flowers. The leaves are greater than six centimetres in length

(E) Vital rate definitions

Vital rate	Definition	Data source
S_{ij}	Probability of survival from class j to class i	Field site
N_s	Number of seeds per fruit	Field site
N_{fx}	Number of fruits produced by an individual in size category x	Field site
P_{rx}	Probability of reproduction of an adult in category x	Field site
P_s	Probability of seed germination and seedling survival across the projection interval	Greenhouse

BOX 1 (Continues)

(F) Vital rate values

Vital rate	Estimate*	Standard error**	Sample size (individuals)***
S_{21}	0.400	0.100	80
S_{32}	0.850	0.050	160
S_{33}	0.900	0.020	160
N_s	1000	150	80
N_{f3}	2.000	300	80
P_{r3}	0.300	0.040	200
P_s	0.005	0.001	500

*If these estimates are dependent on population size (i.e. density-dependence) or in response to an environment variable (i.e. environmental stochasticity), the estimate should be communicated as a function (e.g. $S_{33} \sim 0.9 + \beta_{\text{precipitation}} \times 0.01$ where $\beta_{\text{precipitation}} \sim N(5, 1)$). Furthermore, if this is a point estimate, researchers should indicate if the values represent mean or median values.

**This measure of uncertainty may also be the estimate's standard deviation, variance or a confidence/credible interval at the discretion of the researcher.

***Indicate if the unit of measurement/replication is at the level of individual organisms or at the level of groups (e.g. cohorts, colonies, families).

(G) MPM formula (May 2021 to May 2022)

0	0	$N_s \times N_{f3} \times P_{r3} \times P_s$
S_{21}	0	0
0	S_{32}	S_{33}

(H) Population vector (May 2021)

Stage	Number	95% Confidence interval*
1	1350	1150–1550
2	550	530–570
3	300	290–310

*This measure of uncertainty may also be the estimate's standard deviation, variance or a confidence/credible interval at the discretion of the researcher.

effect of nonstationary population structure on near-term population growth rates (Capdevila et al., 2020). Reported population stage or age vectors reflect two key components: the actual population structure at the census in time *t* and the methodological choices. This second component is critical to accurately represent the studied population.

Across the development and curation of COMPADRE and COMADRE, we have noticed two sources of error that affect population vector estimation. The first error is a detection bias, where researchers identify certain st/ages with a higher rate of detection over more cryptic stages (e.g. adult plants versus seed banks). The second error is the misappropriation of methods used to quantify demographic rates as a basis for estimating stage abundance. This second error stems from a misunderstanding of the difference between estimating *rates* and the estimation of *numbers*. To measure demographic rates, researchers sometimes increase the sampling effort of certain st/age classes over other st/age classes during a census. This differential sampling effort across st/ages is particularly common when st/age classes have survival probabilities close to its limits (i.e. 0 and 1). For instance, in tree demography, there are typically only a few very large individuals per area examined. Thus, oftentimes researchers supplement the sample size of this category by sampling outside of the predefined area (Jones & Hubbell, 2006). However, many types of demographic rate estimation do not provide any information on numbers and structure. Cohort life tables, that follow a cohort of individuals as they age, are blind to the structure of the population in which the cohort develops. Indeed, there may be no such population (e.g. the entire history of laboratory cohort-based demography going back to Pearl in the 1920s (Pearl et al., 1927)). Mark-recapture estimation of rates from longitudinal data draws all its inference from the marked individuals and makes no inferences about the number and structure of the unmarked. The literature on mark-recapture methods for estimating rates recognises that estimating population numbers is thus much more difficult than estimating rates (Lebreton et al., 1992) and requires different mark-recapture models (e.g. the inclusion of trap happiness/shyness in vital rate estimation). Therefore, if projection from an actual structure is desired, that initial condition may be more appropriately measured in a separate census, rather than extracted from the measurements of rates that inform the MPM.

3.6 | Omitting cryptic life stages

The identification and estimation of vital rates in cryptic stages poses a challenge in population ecology. Cryptic stages represent points along an organism's life cycle that are somewhat hidden from or overlooked by population ecologists when building population models (Doak et al., 2002). A life stage could be cryptic because it is logistically challenging to observe or observable but indistinguishable from a similar seeming class (Nguyen et al., 2019). In plants, cryptic stages can emerge from seed banks for plants, such as orchids, where the seeds are too small to be identified in the field (Paniw et al., 2017) or some herbaceous perennials (e.g. *Astragulus scaphoides*) where prolonged periods of vegetative dormancy can allow individuals to stay underground for one or more growing seasons (Gremer & Sala, 2013). Additionally, animals can exhibit cryptic stages by undergoing diapause or delays in development due to adverse environment conditions (*Aedes albopictus*: Jia et al., 2016). Pelagic seabirds (albatrosses, petrels, penguins) often spend pre-reproductive stages, sometimes of many years durations, at sea, completely cryptic until returning to the breeding colony as adults. Sophisticated multistate mark-recapture methods can provide estimates of parameters for these parts of the life cycle (e.g. Jenouvrier et al. (2018), using the multievent algorithm of Choquet et al. (2009)). Omitting a cryptic life stage can reduce the biological realism of an MPM and alter the number of stages in the MPM, which can further impact demographic outputs (Salguero-Gómez & Plotkin, 2010; Tenhumberg et al., 2009). In some cases, cryptic life stages will only be identified via a multidisciplinary approach including field and laboratory methods, coupled with Bayesian frameworks to integrate data and prior knowledge (e.g. Paniw et al., 2017).

3.7 | One-sex versus two-sex models

Much of demography focuses on females, under the assumptions that fertility is determined by females without limitation by males (see Caswell, 2001, p. 568). Such models may include males (e.g. Hunter et al., 2010), but if reproduction is determined by female rates (i.e. are female-dominant), males represent a set of stages that do not contribute to population growth. Most existing animal MPMs are female-based and female-dominant (Salguero-Gómez et al., 2016) because, given sampling biases towards mammals and birds (Conde et al., 2019), it is oftentimes not feasible, or necessary for the research question, to track male reproductive interactions (Archer et al., 2022). These studies typically assume a 1:1 sex ratio, sex-congruent vital rates and that reproduction is not male-limited (Compagnoni et al., 2017; Miller & Compagnoni, 2022). While one-sex models are common in animal MPMs (currently 77% in COMADRE v. 4.21.8), care must be taken to not make assumptions about sex-ratio dependent dynamics within these systems (Archer et al., 2022) Indeed, these assumptions may not be met when any of the following are true: there is a bias in sex ratio (Archer et al., 2022), there is reproductive skew (Sky et al., 2022), or a high sensitivity of population dynamics in response to mating choice (Veran & Beissinger, 2009). Furthermore, sex-dependent detectability can further confound estimates of sex-ratio and their associated impacts on vital rates if not taken into account. Two-sex models that do not assume dominance by one sex are nonlinear and require specification of a mating function that describes fertility as a function of male and female abundance (Caswell, 2001). Defining such mating functions is generally difficult or impossible, except in the particularly easy case of strict monogamy (Jenouvrier et al., 2010).

Reporting sex ratios can greatly expand the scope of a study (Shyu & Caswell, 2016a, 2016b); for example evaluating the impact of sex ratio and the Allee effect (Boukal & Berec, 2002). Unfortunately, this reporting is rarely done in work archived in COMPADRE and COMADRE. Moreover, if there are differences in vital rate values between sexes, such as survival, growth, and/or reproductive output, a one-sex MPM may neglect important processes (Archer et al., 2022; Caswell, 2001, p. 568). In plants, reporting two-sex dynamics is even more rare (0.2% in COMPADRE v. 6.22.5). However, this low percentage likely reflects the rarity of dioecy or other mating systems with two or more sexes in plants (Käfer et al., 2017) and the commonness of polygamous mating systems which makes male-limited reproduction rare (see Compagnoni et al., 2017; Miller & Compagnoni, 2022).

3.8 | Irreducibility and ergodicity

The property of irreducibility has implications for the eigenvalue spectrum of a matrix, and hence biologically relevant outputs (e.g. population growth rates, stable stage structures). These implications are well known in the literature on MPMs (Caswell, 2001). An irreducible matrix is one in which the life cycle graph is completely connected; that is, there exists a direct or indirect path from any stage to any other stage. It is sometimes asserted that reducible MPMs are somehow invalid; they are not. There are (at least) four situations in which reducible matrices naturally occur.

1. Life cycles with post-reproductive stages. The post-reproductive stages can make no contribution to the potentially reproductive stages (e.g. MPMs for humans, orcas).
2. Two-sex models with dominance by one sex (usually females, but could be male). In a female-dominant model, all reproduction is credited to females. Males are produced by females, but make no contribution to the female part of the life cycle (e.g. Hunter et al. (2010) for polar bears).
3. Spatial models in which dispersal is one-directional, as in river systems or oceanic currents.
4. Age × stage-classified models (Caswell, 2009; Caswell & Salguero-Gómez, 2013). In these models, reproduction produces (by definition) individuals in age class 1, but the model includes all

combinations of age and stage, including impossible combinations of age class 1 and stages that do not exist at age 1.

Reducibility may or may not be easy to spot from the life cycle graph, but it can be tested numerically. The matrix ***A*** is irreducible if and only if the matrix $(\boldsymbol{I}+\boldsymbol{A})^{s-1}$ is positive (Caswell, 2001). Irreducibility, together with primitivity, is a sufficient condition for ergodicity, guaranteeing that the population will converge to the same stable structure regardless of the initial condition. A reducible matrix may not have this property; clearly, for example, a population started with only post-reproductive individuals will not converge to the same structure as one started with some pre-reproductive individuals. With regard to ergodicity, it is also known that an MPM is ergodic if and only if all entries of its dominant left eigenvector (***v***) are positive (Stott et al., 2010). In short, despite appropriate model structure and correct parameterisation, demographic data may lead to reducible and/or nonergodic matrices.

4 | FULL REPRESENTATION OF AN MPM IN PUBLICATIONS

In this section, we justify the need for clear presentation of MPMs in the scientific literature, suggest where to archive MPMs open-access, and discuss how these two actions benefit the original authors, publishing journal, readers, comparative demographers, meta-analysts and the discipline at large. A table containing corresponding data to include when publishing MPMs along with a rationale for inclusion and examples of good practice can be found in Table S1.

4.1 | Partitioning demographic processes

It is important to define what each matrix element in an MPM represents. Various demographic processes can overlap into the same matrix element in an MPM, particularly in species with a fast and/or plastic lifecycle relative to the MPM projection interval. For example, the value in an MPM that represents the link between large individuals at time t and smaller individuals at time $t+1$ might correspond to sexual reproduction, clonal reproduction, fission, retrogression, or a composite of multiple processes. The mathematical derivations of key life history traits (e.g. generation time, life expectancy, rate of senescence, degree of iteroparity) require that these processes be clearly separated (Jones et al., 2022). This is critical for the family of analyses based on Markov chains; the matrix ***U*** defines the transient state transitions in an absorbing Markov chain (Caswell, 2011, 2013). By reporting the underlying demographic rate structure in a life cycle diagram and its consequent full matrix population model ***A***, one can separate matrices into survival-dependent processes (e.g. progression/growth, retrogression/shrinkage, fission, fusion, stasis) in the submatrix ***U***, sexual reproduction in the submatrix ***F*** and clonal reproduction in the submatrix ***C*** (Figure 4). Importantly, both ***F*** and ***C*** submatrix elements must incorporate survival according to census type (i.e. pre-/post-reproductive census).

Reporting the matrix ***A*** as well as the submatrices ***U***, ***F*** and ***C*** lends two key benefits: (1) explicitly indicates how the values in ***A*** are generated from underlying vital rates; and (2) the submatrices can be used to calculate a vast plethora of demographic measures that cannot be calculated from ***A*** alone, such as longevity (mean and variance), occupancy times (means and variances), lifetime reproductive output (means and variances), net reproductive rate, generation time and entropy (Keyfitz entropy (Keyfitz, 1968) and Demetrius' entropy (Demetrius, 1992)) just to name a few.

4.2 | Attribution of secondary data sources

Secondary data sources are critical for reproducibility. These data sources provide information and support for methodologies used in MPM construction. In some cases, MPMs simply use secondary data to complete the life cycle, whereas others are constructed purely from secondary sources (see Table S1). Secondary sources include

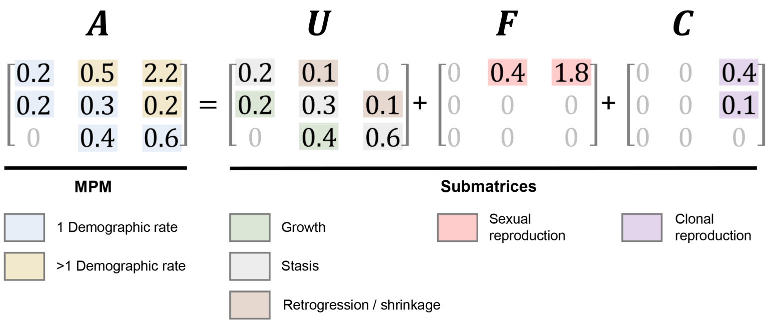

$$\begin{bmatrix}0.2 & 0.5 & 2.2\\0.2 & 0.3 & 0.2\\0 & 0.4 & 0.6\end{bmatrix}=\begin{bmatrix}0.2 & 0.1 & 0\\0.2 & 0.3 & 0.1\\0 & 0.4 & 0.6\end{bmatrix}+\begin{bmatrix}0 & 0.4 & 1.8\\0 & 0 & 0\\0 & 0 & 0\end{bmatrix}+\begin{bmatrix}0 & 0 & 0.4\\0 & 0 & 0.1\\0 & 0 & 0\end{bmatrix}$$

FIGURE 4 Decomposing an MPM into its submatrices allows for the isolation for otherwise masked vital rates. Matrix ***A*** represents the MPM. Since individual transitions can be represented by multiple demographic rates (e.g. retrogression, sexual reproduction and clonal reproduction), decomposing ***A*** into its ***U***, ***F*** and ***C*** submatrices allows for targeted demographic inference about what demographic transitions are driving the dynamics of the population.

previous studies, data from databases, simulations, indirect observations and theoretical estimates. The use of secondary data sources may mean that the final MPM does not accurately represent vital rate trade-offs, and so should be recognised in the methods section of the publication or its Supporting Information. Sufficient communication of secondary sources includes the source of the data, whether a point estimate, confidence interval, or distribution was integrated with the primary data source as well as the rationale for their inclusion. For example, Omeyer et al. (2021) presents a table of data sources used in construction of the MPM. If these secondary sources are not recognised in tandem with the MPM, the inferred demographic processes, however realistic they may be, may not pass peer review nor uptake by the scientific community. In turn, clear communication of these secondary sources is highly recommended.

4.3 | Archival of information in COMPADRE and COMADRE

We propose that the COMPADRE and COMADRE matrix databases provide the most appropriate way of archiving and accessing MPMs. While we recognise that there are other ecological database repositories (e.g. dryad: https://datadryad.org/; figshare: https://figshare.com; zenodo: https://zenodo.org), the open access COMPADRE and COMADRE databases (https://compadre-db.org/Contribute) provide a dedicated data archival platform, specifically for MPMs, allowing direct contributions from researchers as well as digitization of published MPMs by our data validation teams. The web-based data entry portal provides a structured data curation process (i.e. from screening, to standardisation, to validation) that can accommodate MPMs of different dimensions and for diverse life histories. On entry, MPMs are complemented with relevant biogeographic variables and details on census methodology in COMPADRE and COMADRE. Details of the original publication, including DOI and citation functionality (see https://compadre-db.org/Education/article/obtaining-references), are stored alongside each MPM to ensure that their contribution towards any future publication is recognised. All data are archived long-term through Oxford Open Access and Bodleian Library support.

Other recent enhancements to COMPADRE and COMADRE will further aid the research community. Previously, the databases were only accessible via download of an R-object file which contained all matrices in that version of the database. The database is now accessible via a queryable website (https://compadre-db.org/QueryDatabase) that allows users to find and download individual matrices. We also strive to empower researchers and educators with teaching materials (https://compadre-db.org/Education) and the production of new R-packages (Jones et al., 2022) for ease and scalability of MPM-related research. Along with these materials, all details of the database structure and workflow are open-access (https://jonesor.github.io/CompadreGuides/user-guide.html). These improvements to the databases and their interface structure have been directly targeted to equip demographers with more tools to conduct research with and train students on MPMs along with increasing database transparency to ensure best research practices.

5 | A STANDARD PROTOCOL FOR REPORTING MPMS

Here, we introduce a proposed checklist for how to report an MPM in publications (Box 1). We recommend using the checklist when designing data collection as well as when writing up the MPM for publication. We recommend using this template as Supporting Information for published MPMs as it allows for the clear communication of model construction in addition to ease in integrating published MPMs into the COMPADRE and COMADRE databases.

6 | THE THEORY DOES NOT STAND STILL: NONLINEARITY, ENVIRONMENT-DEPENDENCE AND MULTISTATE MODELS

MPMs have become a predominant approach in the toolbox of population ecologists partly due to their simplicity of construction and analysis. But the theory underlying matrix-based demography does not stand still, and in the last 20 years it has enlarged dramatically. These new methods produce models whose structure does not fit into the frameworks for reporting that seemed so comprehensive in the past. These recent advances in MPM theory and methods, enable researchers to link population dynamics and demography to environmental conditions and multiple individual traits (e.g. sex and age (Childs et al., 2016); age and kinship (Caswell, 2019b, 2020)) rather than a single trait. These advances also offer benefits for the study of population responses to extreme climate (Jenouvrier et al., 2022), as well as more nuanced investigations of comparative and evolutionary demography (Childs et al., 2016). In turn, in this section, we overview some exciting areas of structured demography that can open novel research questions for the modern demographer and list some of the challenges they pose for communication and reporting.

6.1 | Nonlinear dynamics

Nonlinear MPMs are those in which entries of the projection matrix depend on the population state (numbers and structure) and may be frequency- or density-dependent. Frequency-dependent nonlinearities depend only on the relative abundance of stages; they occur in two-sex models in which mating depends on the relative abundance of males and females, and in population genetic models where dynamics depend on the relative abundance of genotypes (de Vries & Caswell, 2019). Density-dependent models depend on the abundance and structure of the population; recent examples include Pardini et al. (2009) and Shyu et al. (2013) for analyses of control strategies for garlic mustard *Alliaria petiolata* and de Vries et al. (2020) for laboratory studies of pesticide resistance in *Tribolium*.

The analysis of nonlinear MPMs focuses on demographic outcomes different from those of linear models; equilibria, attractors, bifurcations, oscillations and stability (see Caswell, 2001, Chapters 16 and 17, and Cushing et al., 2003 for the most detailed analysis yet). However, what makes these models problematic for the current status of COMPADRE and COMADRE is that the unit of the model is not a matrix, but rather a matrix *function*, in which the entries of the projection matrix are functions of the state of the population. Sensitivity analyses are available to study pretty much any demographic outcome in response to any parameter (Caswell, 2019a), but reporting the functions that define the MPM is not at all standardised.

6.2 | Environment-dependence

A similar problem arises in environment-dependent MPMs. In such models, some or all of the demographic rates are functions of some aspects of the environment; for example, polar bears as functions of statistics of Arctic sea ice (Regehr et al., 2010), sifaka as functions of rainfall (Lawler et al., 2009), the emperor penguin as a function of seasonal sea ice patterns in the Antarctic (Jenouvrier et al., 2012) and the North Atlantic right whale as functions of time and of trends in time (Fujiwara & Caswell, 2001). As with nonlinear MPMs, the model is not a matrix, but a function that maps from the environmental variable(s) to the entries in the matrix. Protocols for reporting such functions are not yet available but are important to develop.

6.3 | Multistate models

An exciting emerging area of demographic research is the construction and analysis of multistate MPMs, in which individuals are classified by more than one state variable. This includes age and stage (Caswell & Salguero-Gómez, 2013), stage and spatial location (Hunter & Caswell, 2005), stage and genotype (de Vries & Caswell, 2019), stage and infection status (Klepac & Caswell, 2011), age and unmeasured heterogeneity (Hartemink et al., 2017), and stage-specific incidence of disease (Caswell & Van Daalen, 2021). A detailed presentation of the methods is given in (Caswell et al., 2018) and the extension to more than two state axes (so-called hyperstate matrices) is given in (Roth & Caswell, 2016). The incorporation of additional states enables researchers to tease apart various sources of individual heterogeneity, the variance of life history outcomes for individuals from the same population model, and to ask deeper comparative and evolutionary questions. For example, maternal age has a strong impact on vital rates in monogonont rotifers (Bock et al., 2019). Applying vec-permutation methods (Caswell, 2012) to build multistate MPMs has allowed researchers to quantify the population-level impacts of the observed maternal age effect and to investigate the evolutionary processes that can lead to this type of senescence in rotifers (Hernández et al., 2020). Multidimensional MPMs and Markov chain approaches have been particularly important in the study of 'luck' in life histories, which explores why some individuals live long and prosper, while others do not (Snyder & Ellner, 2018). In studies of 'luck', variance among individuals for a life history outcome is partitioned into contributions from between-group and within-group variation (e.g. Snyder & Ellner, 2018; van Daalen & Caswell, 2017). Examples of sources of individual heterogeneity include maternal age (van Daalen et al., 2022), birth-year environment (Snyder & Ellner, 2022), and genetic variation (Steiner et al., 2021). The within-group variation is called individual stochasticity or 'luck' and arises from the fact that vital rates are probabilistic processes.

These models pose a challenge for reporting because the MPM consists not of a single matrix, but of four sets of matrices. Consider an age × stage-classified model. It is composed of a set of matrices giving transitions among stages for each age class, a set of matrices ***D*** giving age transitions for each stage, a set of matrices ***F*** giving stage-specific fertility for each age, and a set of matrices ***H*** that allocate newborn offspring to the appropriate ages. These are assembled into block structured transition and fertility matrices from which all the usual demographic outcomes can be calculated and related to both age and stage (e.g. see Caswell and Salguero-Gómez (2013) for an analysis of selection gradients for both age and size).

7 | DISCUSSION

Demographic research has come a long way since the introduction of age-based (Leslie, 1945) and stage-based matrix models (Lefkovitch, 1965). Advances in this field have been fuelled partly by clear communication of methods and associated code. We aim to continue this expansion with MPM communication.

As the depth and breadth of the literature continues to expand, we are starting to build a comprehensive picture of demography across the spectrum of life (Adler et al., 2014; Healy et al., 2019; Salguero-Gómez et al., 2017). Through the work of the COMPADRE and COMADRE databases, we have come to appreciate the utility and opportunities of a standardised way of compiling MPMs. Indeed, a significant portion of the time (>50%) we spend curating these databases is actually not on digitising, error-checking, and complementing data, but on contacting authors for clarification and request of missing data and metadata. Through this arduous process, we have identified valuable—yet typically missing—information in MPMs. Whilst the missing data highlighted here as being particularly important primarily reflects the interests and perspectives of comparative demographers, including the data outlined in the standardised method would benefit demography as a whole.

This paper intends to act as a useful reference for authors, editors, reviewers, managers/conservationists and comparative demographers. Furthermore, we hope this manuscript will promote a constructive discussion on the purpose, construction and presentation of stage-based demographic information. Box 1 contains a comprehensive example of the key information we believe should be incorporated into the publication of any MPM. Should the methods suggested here be adopted, there will be clear benefits for the growth of the COMPADRE and COMADRE demographic databases; however, we believe these benefits extend beyond COMPADRE and COMADRE users towards the whole field of population ecology and fields that use MPMs for their own inference (e.g. conservation biology and biodiversity monitoring). A greater level of detail and transparency when describing how and why an MPM is produced will result in greater accuracy, accessibility, reproducibility and citability—this has clear benefits to the field as a whole and to individual researchers. In addition, greater consistency and transparency facilitates peer review, and indeed, these guidelines may offer a tool that can be cited by associate editors and peer-reviewers who may frequently advocate some (or all) of the steps suggested herein. Furthermore, adoption of the steps suggested here may increase confidence in the results presented and facilitate learning/uptake of MPMs by early career researchers.

Finally, we close with a caution. We have used the term 'accurate' at points throughout this paper, applied to MPMs, but we must acknowledge that there is no such thing as an accurate model, be it an MPM or any other type. A model is a series of choices, choices of aspects that are included and aspects that are neglected. Model selection techniques such as AIC (Anderson & Burnham, 2002) make these choices explicit and measure their support in terms of likelihood. But even without using the explicit statistical method, the message is clear. Choices of i-state variables, of projection intervals, of types of time variation, of functional dependence on a chosen set of environmental factors and so forth, all of these are inaccurate. The point is not to seek for accuracy: it is to be clear about communicating the choices you made in constructing the model, the analyses you chose to apply and the interpretation of the results. An 'accurate' model of an ecological system, experimental or observational, would be as complicated as the real system. That does not end well (Borges, 1999).

AUTHOR CONTRIBUTIONS

This paper was conceptualised at a workshop hosted by Jenni McDonald, Danielle L. Buss and Dave Hodgson. Subsequently, Samuel J. L. Gascoigne, Simon Rolph, Christina M. Hernández and Roberto Salguero-Gómez generated the first draft of the manuscript with ideas contributed from all authors. Samuel J. L. Gascoigne conducted the survey. Samuel J. L. Gascoigne, Daisy Sankey, Nagalakshmi Nidadavolu and Adrian S. Stell Pičman conducted the screen of papers from COMPADRE and COMADRE. All authors contributed ideas in drafts of the manuscript.

ACKNOWLEDGEMENTS

We thank the hundreds of population ecologists who have contributed open-access matrix population models ready for fully reproducible research, and those who have, throughout the last 15 years, answered our emails asking for additional data and metadata. We also thank Chloé R. Nater and one anonymous reviewer for their helpful comments. Conversations leading to this manuscript were initiated during a workshop held at the University of Exeter Cornwall campus with support of NERC grant (NE/N006798/1) to Jenni McDonald and Dave Hodgson. We acknowledge the support of the Evolutionary Demography Laboratory at the Max Planck Institute for Demographic Research (MPIDR) in the development of the COMPADRE Plant Matrix Database and COMADRE Animal Matrix Database, and the maintenance of COMPADRE & COMADRE through the distributed network of digitising nodes including MPIDR, University of Oxford, University of Exeter, Southampton University, Trinity College Dublin, Lincoln Park Zoo, University of Southern Denmark and iDiv. Roberto Salguero-Gómez was supported by a NERC Independent Research Fellowship (NE/M018458/1). Christina M. Hernández was supported by a US-NSF grant (DEB-1933497). Pol Capdevila was supported by a Maria Zambrano Next Generation EU Fellowship. Judy P. Che-Castaldo, Owen R. Jones, Roberto Salguero-Gómez and Chelsea C. Thomas were supported by an NSF Advances in Bioinformatics Development Award (#DBI-1661342). Danielle L. Buss was funded by NERC Discovery Science grant NE/L007770/1. Tiffany M. Knight was supported by the Helmholtz Association and the Alexander von Humboldt foundation. Hal Caswell was supported by the European Research Council, Advanced Grant 788195. Lastly, this paper is in memoriam of our dear friend and colleague James W. Vaupel, who sadly passed before the submission of this manuscript. His multiple contributions to demography will no doubt outlive multiple Bristlecone pine generation times.

CONFLICT OF INTEREST STATEMENT

The authors declare no conflict of interest.

PEER REVIEW

The peer review history for this article is available at https://www.webofscience.com/api/gateway/wos/peer-review/10.1111/2041-210X.14164.

DATA AVAILABILITY STATEMENT

The code used in this paper can be found at Zenodo (Gascoigne, 2023, https://zenodo.org/record/7967075) and on GitHub at https://github.com/SamuelGascoigne/Standard_MPM_Protocol.

ORCID

Samuel J. L. Gascoigne https://orcid.org/0000-0002-2984-1810
Simon Rolph https://orcid.org/0000-0001-6755-9456
Christina M. Hernández https://orcid.org/0000-0002-7188-8217
Connor Bernard https://orcid.org/0000-0003-2175-5712
Erola Fenollosa https://orcid.org/0000-0002-6189-2124
Oliver G. Spacey https://orcid.org/0000-0002-0280-8201
Maja Kajin https://orcid.org/0000-0001-9996-5897
Anna C. Vinton https://orcid.org/0000-0002-8279-1736
C. Ruth Archer https://orcid.org/0000-0003-2501-425X
Jean H. Burns https://orcid.org/0000-0001-6140-9094
Danielle L. Buss https://orcid.org/0000-0001-5362-240X
Hal Caswell https://orcid.org/0000-0003-4394-6894
Judy P. Che-Castaldo https://orcid.org/0000-0002-9118-9202
Dylan Z. Childs https://orcid.org/0000-0002-0675-4933
Pol Capdevila https://orcid.org/0000-0002-2842-4302

Aldo Compagnoni https://orcid.org/0000-0001-8302-7492
Elizabeth Crone https://orcid.org/0000-0002-5287-221X
Thomas H. G. Ezard https://orcid.org/0000-0001-8305-6605
Dave Hodgson https://orcid.org/0000-0003-4220-2076
Tiffany M. Knight https://orcid.org/0000-0003-0318-1567
Owen R. Jones https://orcid.org/0000-0001-5720-4686
Eelke Jongejans https://orcid.org/0000-0003-1148-7419
Jenni McDonald https://orcid.org/0000-0002-5050-750X
Brigitte Tenhumberg https://orcid.org/0000-0003-3801-3192
Andrew J. Tyre https://orcid.org/0000-0001-9736-641X
Satu Ramula https://orcid.org/0000-0001-7795-0352
Iain Stott https://orcid.org/0000-0002-1399-3596
Raymond L. Tremblay https://orcid.org/0000-0002-8588-4372
James W. Vaupel https://orcid.org/0000-0003-0783-3905
Roberto Salguero-Gómez https://orcid.org/0000-0002-6085-4433

REFERENCES

Adler, P. B., Salguero-Gómez, R., Compagnoni, A., Hsu, J. S., Ray-Mukherjee, J., Mbeau-Ache, C., & Franco, M. (2014). Functional traits explain variation in plant life history strategies. *Proceedings of the National Academy of Sciences of the United States of America*, *111*(27), 10019. https://doi.org/10.1073/pnas.1410430111

Anderson, D. R., & Burnham, K. P. (2002). Avoiding pitfalls when using information-theoretic methods. *The Journal of Wildlife Management*, *66*(3), 912–918.

Archer, C. R., Paniw, M., Vega-Trejo, R., & Sepil, I. (2022). A sex skew in life-history research: The problem of missing males. *Proceedings of the Royal Society B: Biological Sciences*, *289*. https://doi.org/10.1098/rspb.2022.1117

Baudisch, A., Salguero-Gómez, R., Jones, O. R., Wrycza, T., Mbeau-Ache, C., Franco, M., & Colchero, F. (2013). The pace and shape of senescence in angiosperms. *Journal of Ecology*, *101*(3), 596–606. https://doi.org/10.1111/1365-2745.12084

Beissinger, S. R., & Westphal, M. I. (1998). On the use of demographic models of population viability in endangered species management. *The Journal of Wildlife Management*, *62*(3), 821. https://doi.org/10.2307/3802534

Bernard, C., Santos, G. S., Deere, J. A., Rodriguez-Caro, R., Capdevila, P., Kusch, E., Gascoigne, S. J. L., Jackson, J., & Salguero-Gómez, R. (2023). MOSAIC: A unified trait database to complement structured population models. *Scientific Data*, *10*(335). https://doi.org/10.1038/s41597-023-02070-w

Bock, M. J., Jarvis, G. C., Corey, E. L., Stone, E. E., & Gribble, K. E. (2019). Maternal age alters offspring lifespan, fitness, and lifespan extension under caloric restriction. *Scientific Reports*, *9*(1), 1–16. https://doi.org/10.1038/s41598-019-40011-z

Borges, J. L. (1999). On exactitude in science. In J. L. Borges (Ed.), *Collected fictions*, translated by Andrew Hurley. Penguin Random House. Originally published as Del Rigor en la Ciencia, in Borges, J. L. (1954), *Historia Universal de la Infamia*.

Boukal, D. S., & Berec, L. (2002). Single-species models of the Allee effect: Extinction boundaries, sex ratios and mate encounters. *Journal of the Torrey Botanical Society*, *218*, 375–394. https://doi.org/10.1006/yjtbi.3084

Bruijning, M., Jongejans, E., & Turcotte, M. M. (2019). Demographic responses underlying eco-evolutionary dynamics as revealed with inverse modelling. *Journal of Animal Ecology*, *88*(5), 768–779. https://doi.org/10.1111/1365-2656.12966

Buckley, Y. M., Ramula, S., Blomberg, S. P., Burns, J. H., Crone, E. E., Ehrlén, J., Knight, T. M., Pichancourt, J. B., Quested, H., & Wardle, G. M. (2010). Causes and consequences of variation in plant population growth rate: A synthesis of matrix population models in a phylogenetic context. *Ecology Letters*, *13*(9), 1182–1197. https://doi.org/10.1111/j.1461-0248.2010.01506.x

Capdevila, P., Stott, I., Beger, M., & Salguero-Gómez, R. (2020). Towards a comparative framework of demographic resilience. *Trends in Ecology & Evolution*, *35*(9), 776–786. https://doi.org/10.1016/j.tree.2020.05.001

Caswell, H. (2001). *Matrix population models: Construction, analysis, and interpretation* (2nd ed.). Sinauer.

Caswell, H. (2009). Stage, age and individual stochasticity in demography. *Oikos*, *118*(12), 1763–1782. https://doi.org/10.1111/j.1600-0706.2009.17620.x

Caswell, H. (2011). Beyond R0: Demographic models for variability of lifetime reproductive output. *PLoS ONE*, *6*(6), e20809. https://doi.org/10.1371/journal.pone.0020809

Caswell, H. (2012). Matrix models and sensitivity analysis of populations classified by age and stage: A vec-permutation matrix approach. *Theoretical Ecology*, *5*(3), 403–417. https://doi.org/10.1007/s12080-011-0132-2

Caswell, H. (2013). Sensitivity analysis of discrete Markov chains via matrix calculus. *Linear Algebra and its Applications*, *438*(4), 1727–1745. https://doi.org/10.1016/j.laa.2011.07.046

Caswell, H. (2019a). *Sensitivity analysis: Matrix methods in demography and ecology*. Springer Nature.

Caswell, H. (2019b). The formal demography of kinship: A matrix formulation. *Demographic Research*, *41*(24), 679–712. https://doi.org/10.4054/DemRes.2019.41.24

Caswell, H. (2020). The formal demography of kinship II: Multistate models, parity, and sibship. *Demographic Research*, *42*(38), 109–114. https://doi.org/10.4054/DemRes.2020.42.38

Caswell, H., Brault, S., Read, A. J., & Smith, T. D. (1998). Harbor porpoise and fisheries: An uncertainty analysis of incidental mortality. *Ecological Applications*, *8*(4), 1226. https://doi.org/10.2307/2640975

Caswell, H., de Vries, C., Hartemink, N., Roth, G., & van Daalen, S. F. (2018). Age × stage-classified demographic analysis: A comprehensive approach. *Ecological Monographs*, *88*(4), 560–584. https://doi.org/10.1002/ecm.1306

Caswell, H., & Salguero-Gómez, R. (2013). Age, stage and senescence in plants. *Journal of Ecology*, *101*(3), 585–595. https://doi.org/10.1111/1365-2745.12088

Caswell, H., & Van Daalen, S. (2021). Healthy longevity from incidence-based models: More kinds of health than stars in the sky. *Demographic Research*, *45*(December), 397–452. https://doi.org/10.4054/DEMRES.2021.45.13

Che-Castaldo, J., Havercamp, K., Watanuki, K., Matsuzawa, T., Hirata, S., & Ross, S. R. (2021). Comparative survival analyses among captive chimpanzees (*Pan troglodytes*) in America and Japan. *PeerJ*, *9*, 1–21. https://doi.org/10.7717/peerj.11913

Che-Castaldo, J., Jones, O. R., Kendall, B. E., Burns, J. H., Childs, D. Z., Ezard, T. H. G., Hernandez-Yanez, H., Hodgson, D. J., Jongejans, E., Knight, T., Merow, C., Ramula, S., Stott, I., Vindenes, Y., Vindenes, Y., Yokomizo, H., & Salguero-Gómez, R. (2020). Comments to 'Persistent problems in the construction of matrix population models'. *Ecological Modelling*, *416*, 1–3. https://doi.org/10.1016/j.ecolmodel.2019.108913

Childs, D. Z., Sheldon, B. C., & Rees, M. (2016). The evolution of labile traits in sex- and age-structured populations. *Journal of Animal Ecology*, *85*(2), 329–342. https://doi.org/10.1111/1365-2656.12483

Choquet, R., Rouan, L., & Pradel, R. (2009). Program E-SURGE: A software for fitting multievent models. In D. L. Thomson, E. G. Cooch, & M. J. Conroy (Eds.), *Modeling demographic processes in marked populations* (pp. 845–865). Springer. https://doi.org/10.1007/978-0-387-78151-8

Clubb, R., Rowcliffe, M., Lee, P., Mar, K. U., Moss, C., & Mason, G. J. (2009). Fecundity and population viability in female zoo elephants: Problems and possible solutions. *Animal Welfare*, *18*(3), 237–247.

Clubb, R., & Mason, G. (2003). Capitivity effects on wide-range carnivores. *Nature*, *425*(6957), 473–474.

Compagnoni, A., Steigman, K., & Miller, T. E. X. (2017). Can't live with them, can't live without them? Balancing mating and competition in two-sex populations. *Proceedings of the Royal Society B: Biological Sciences*, *284*(1865), 2–11. https://doi.org/10.1098/rspb.2017.1999

Conde, D. A., Staerk, J., Colchero, F., da Silva, R., Schöley, J., Baden, H. M., Jouvet, L., Fa, J. E., Syed, H., Jongejans, E., Meiri, S., Gaillard, J. M., Chamberlain, S., Wilcken, J., Jones, O. R., Dahlgren, J. P., Steiner, U. K., Bland, L. M., Gomez-Mestre, I., … Vaupel, J. W. (2019). Data gaps and opportunities for comparative and conservation biology. *Proceedings of the National Academy of Sciences of the United States of America*, *116*(19), 9658–9664. https://doi.org/10.1073/pnas.1816367116

Cooch, E. G., Gauthier, G., & Rockwell, R. F. (2003). Apparent differences in stochastic growth rates based on timing of census: A cautionary note. *Ecological Modelling*, *159*(2–3), 133–143. https://doi.org/10.1016/S0304-3800(02)00292-2

Coulson, T., Catchpole, E. A., Albon, S. D., Morgan, B. J. T., Pemberton, J. M., Clutton-Brock, T. H., Crawley, M. J., & Grenfell, B. T. (2001). Age, sex, density, winter weather, and population crashes in Soay sheep. *Science*, *292*(5521), 1528–1531. https://doi.org/10.1126/science.292.5521.1528

Cushing, J. M., Constantino, R. F., Dennis, B., Desharnais, R., & Henson, S. M. (2003). *Chaos in ecology: Experimental nonlinear dynamics*. Elsevier.

Davis, K. J. (2022). Managed culls mean extinction for a marine mammal population when combined with extreme climate impacts. *Ecological Modelling*, *473*(November 2021), 110122. https://doi.org/10.1016/j.ecolmodel.2022.110122

De Magalhães, J. P., & Costa, J. (2009). A database of vertebrate longevity records and their relation to other life-history traits. *Journal of Evolutionary Biology*, *22*(8), 1770–1774. https://doi.org/10.1111/j.1420-9101.2009.01783.x

de Vries, C., & Caswell, H. (2019). Selection in two-sex stage-structured populations: Genetics, demography, and polymorphism. *Theoretical Population Biology*, *130*, 160–169. https://doi.org/10.1016/j.tpb.2019.07.012

de Vries, C., Desharnais, R. A., & Caswell, H. (2020). A matrix model for density-dependent selection in stage-classified populations, with application to pesticide resistance in *Tribolium*. *Ecological Modelling*, *416*(November 2018), 108875. https://doi.org/10.1016/j.ecolmodel.2019.108875

Demetrius, L. (1992). Growth rate, population entropy, and evolutionary dynamics. *Theoretical Population Biology*, *41*(2), 208–236. https://doi.org/10.1016/0040-5809(92)90044-T

Doak, D. F., Morris, W. F., Pfister, C., Kendall, B. E., & Bruna, E. M. (2005). Correctly estimating how environmental stochasticity influences fitness and population growth. *The American Naturalist*, *166*(1), E14–E21. https://doi.org/10.1086/430642

Doak, D. F., Thomson, D., & Jules, E. S. (2002). Population viability analysis for plants: Understanding the demographic consequences of seed banks for population health. In S. R. Beissinger & D. R. McCullough (Eds.), *Population viability analysis* (pp. 312–337). University of Chicago Press.

Ebert, T. A. (1999). Populations methods in demography. *Methods & Demography*, *January 1999*, 2.

Ellner, S. P., Childs, D. Z., & Rees, M. (2016). *Data-driven modelling of structured populations*.

Emery, S. M., & Gross, K. L. (2005). Effects of timing of prescribed fire on the demography of an invasive plant, spotted knapweed *Centaurea maculosa*. *Journal of Applied Ecology*, *42*(1), 60–69. https://doi.org/10.1111/j.1365-2664.2004.00990.x

Ezard, T. H. G., Bullock, J. M., Dalgleish, H. J., Millon, A., Pelletier, F., Ozgul, A., & Koons, D. N. (2010). Matrix models for a changeable world: The importance of transient dynamics in population management. *Journal of Applied Ecology*, *47*(3), 515–523. https://doi.org/10.1111/j.1365-2664.2010.01801.x

Ferreira, M. S., Kajin, M., Cerqueira, R., & Vieira, M. V. (2016). Marsupial population dynamics in a tropical rainforest: Intraspecific competition and nonlinear effect of rainfall. *Journal of Mammalogy*, *97*(1), 121–127. https://doi.org/10.1093/jmammal/gyv161

Franco, M., & Silvertown, J. (1996). Life history variation in plants: An exploration of the fast-slow continuum hypothesis. *Philosophical Transactions of the Royal Society, B: Biological Sciences*, *351*(1345), 1341–1348. https://doi.org/10.1098/rstb.1996.0117

Fujiwara, M., & Caswell, H. (2001). Demography of the endangered North Atlantic right whale. *Nature*, *414*(6863), 537–541. https://doi.org/10.1038/35107054

Gascoigne, S. (2023). SamuelGascoigne/Standard_MPM_Protocol: Initial release (1.0.0). *Zenodo*, https://doi.org/10.5281/zenodo.7967075

Gerstner, K., Moreno-Mateos, D., Gurevitch, J., Beckmann, M., Kambach, S., Jones, H. P., & Seppelt, R. (2017). Will your paper be used in a meta-analysis? Make the reach of your research broader and longer lasting. *Methods in Ecology and Evolution*, *8*(6), 777–784. https://doi.org/10.1111/2041-210X.12758

Gontijo, L. M., & Carvalho, R. M. R. (2020). Using life stage-structured matrix models to determine natural enemy:pest release ratios for augmentative biological control. *Journal of Applied Entomology*, *144*(5), 364–372. https://doi.org/10.1111/jen.12734

Gremer, J. R., & Sala, A. (2013). It is risky out there: The costs of emergence and the benefits of prolonged dormancy. *Oecologia*, *172*(4), 937–947. https://doi.org/10.1007/s00442-012-2557-8

Gurevitch, J., Koricheva, J., Nakagawa, S., & Stewart, G. (2018). Meta-analysis and the science of research synthesis. *Nature*, *555*(7695), 175–182. https://doi.org/10.1038/nature25753

Hartemink, N., Missov, T. I., & Caswell, H. (2017). Stochasticity, heterogeneity, and variance in longevity in human populations. *Theoretical Population Biology*, *114*, 107–116. https://doi.org/10.1016/j.tpb.2017.01.001

Healy, K., Ezard, T. H. G., Jones, O. R., Salguero-Gómez, R., & Buckley, Y. M. (2019). Animal life history is shaped by the pace of life and the distribution of age-specific mortality and reproduction. *Nature Ecology and Evolution*, *3*(8), 1217–1224. https://doi.org/10.1038/s41559-019-0938-7

Hernández, C. M., van Daalen, S. F., Caswell, H., Neubert, M. G., & Gribble, K. E. (2020). A Demographic and Evolutionary Analysis of Maternal Effect Senescence. *Proceedings of the National Academy of Sciences of the United States of America*, *117*(28), 16431–16437. https://doi.org/10.1073/pnas.1919988117

Hunter, C. M., & Caswell, H. (2005). Selective harvest of sooty shearwater chicks: Effects on population dynamics and sustainability. *Journal of Animal Ecology*, *74*(4), 589–600. https://doi.org/10.1111/j.1365-2656.2005.00929.x

Hunter, C. M., Caswell, H., Runge, M. C., Regehr, E. V., Amstrup, S. C., & Stirling, I. (2010). Climate change threatens polar bear populations: A stochastic demographic analysis. *Ecology*, *91*(10), 2883–2897. https://doi.org/10.1890/09-1641.1

James, T. D., Salguero-Gómez, R., Jones, O. R., Childs, D. Z., & Beckerman, A. P. (2021). Bridging gaps in demographic analysis with phylogenetic imputation. *Conservation Biology*, *35*(4), 1210–1221. https://doi.org/10.1111/cobi.13658

Jelbert, K., Buss, D., McDonald, J., Townley, S., Franco, M., Stott, I., Jones, O., Salguero-Gómez, R., Buckley, Y., Knight, T., Silk, M., Sargent, F., Rolph, S., Wilson, P., & Hodgson, D. (2019). Demographic amplification is a predictor of invasiveness among plants. *Nature Communications*, *10*(1). https://doi.org/10.1038/s41467-019-13556-w

Jenouvrier, S., Aubry, L. M., Barbraud, C., Weimerskirch, H., & Caswell, H. (2018). Interacting effects of unobserved heterogeneity and individual stochasticity in the life history of the southern fulmar. *Journal of Animal Ecology*, *87*(1), 212–222. https://doi.org/10.1111/1365-2656.12752

Jenouvrier, S., Caswell, H., Barbraud, C., & Weimerskirch, H. (2010). Mating behavior, population growth, and the operational sex ratio: A periodic two-sex model approach. *The American Naturalist*, *175*(6), 739–752. https://doi.org/10.1086/652436

Jenouvrier, S., Holland, M., Stroeve, J., Barbraud, C., Weimerskirch, H., Serreze, M., & Caswell, H. (2012). Effects of climate change on an emperor penguin population: Analysis of coupled demographic and climate models. *Global Change Biology*, *18*(9), 2756–2770. https://doi.org/10.1111/j.1365-2486.2012.02744.x

Jenouvrier, S., Long, M. C., Coste, C. F. D., Holland, M., Gamelon, M., Yoccoz, N. G., & Sæther, B. E. (2022). Detecting climate signals in populations across life histories. *Global Change Biology*, *28*(7), 2236–2258. https://doi.org/10.1111/gcb.16041

Jia, P., Lu, L., Chen, X., Chen, J., Guo, L., Yu, X., & Liu, Q. (2016). A climate-driven mechanistic population model of *Aedes albopictus* with diapause. *Parasites & Vectors*, *9*(1), 1–15. https://doi.org/10.1186/s13071-016-1448-y

Jiménez-Valdés, M., Godínez-Alvarez, H., Caballero, J., & Lira, R. (2010). Population dynamics of Agave marmorata Roezl. Under two contrasting management systems in Central Mexico. *Economic Botany*, *64*(2), 149–160. https://doi.org/10.1007/s12231-010-9117-0

Johnson, D. J., Needham, J., Xu, C., Massoud, E. C., Davies, S. J., Anderson-Teixeira, K. J., Bunyavejchewin, S., Chambers, J. Q., Chang-Yang, C. H., Chiang, J. M., Chuyong, G. B., Condit, R., Cordell, S., Fletcher, C., Giardina, C. P., Giambelluca, T. W., Gunatilleke, N., Gunatilleke, S., Hsieh, C. F., … McMahon, S. M. (2018). Climate sensitive size-dependent survival in tropical trees. *Nature Ecology and Evolution*, *2*(9), 1436–1442. https://doi.org/10.1038/s41559-018-0626-z

Jones, F. A., & Hubbell, S. P. (2006). Demographic spatial genetic structure of the Neotropical tree, *Jacaranda copaia*. *Molecular Ecology*, *15*(11), 3205–3217. https://doi.org/10.1111/j.1365-294X.2006.03023.x

Jones, O. R., Barks, P., Stott, I., James, T. D., Levin, S., Petry, W. K., Capdevila, P., Che-Castaldo, J., Jackson, J., Römer, G., Schuette, C., Thomas, C. C., & Salguero-Gómez, R. (2022). Rcompadre and Rage—Two R packages to facilitate the use of the COMPADRE and COMADRE databases and calculation of life-history traits from matrix population models. *Methods in Ecology and Evolution*, *13*(4), 770–781. https://doi.org/10.1111/2041-210X.13792

Jones, O. R., Scheuerlein, A., Salguero-Gómez, R., Camarda, C. G., Schaible, R., Casper, B. B., Dahlgren, J. P., Ehrlén, J., García, M. B., Menges, E. S., Quintana-Ascencio, P. F., Caswell, H., Baudisch, A., & Vaupel, J. W. (2014). Diversity of ageing across the tree of life. *Nature*, *505*(7482), 169–173. https://doi.org/10.1038/nature12789

Jouvet, L., Rodríguez-Rojas, A., & Steiner, U. K. (2018). Demographic variability and heterogeneity among individuals within and among clonal bacteria strains. *Oikos*, *127*(5), 728–737. https://doi.org/10.1111/oik.04292

Käfer, J., Marais, G. A. B., & Pannell, J. R. (2017). On the rarity of dioecy in flowering plants. *Molecular Ecology*, *26*(5), 1225–1241. https://doi.org/10.1111/mec.14020

Kendall, B. E., Fujiwara, M., Diaz-Lopez, J., Schneider, S., Voigt, J., & Wiesner, S. (2019). Persistent problems in the construction of matrix population models. *Ecological Modelling*, *406*(March), 33–43. https://doi.org/10.1016/j.ecolmodel.2019.03.011

Keyfitz, N. (1968). Changing vital rates and age distributions. *Population Studies*, *22*(2), 235–251. https://doi.org/10.1080/00324728.1968.10405537

Klepac, P., & Caswell, H. (2011). The stage-structured epidemic: Linking disease and demography with a multi-state matrix approach model. *Theoretical Ecology*, *4*(3), 301–319. https://doi.org/10.1007/s12080-010-0079-8

Lawler, R. R., Caswell, H., Richard, A. F., Ratsirarson, J., Dewar, R. E., & Schwartz, M. (2009). Demography of Verreaux's sifaka in a stochastic rainfall environment. *Oecologia*, *161*(3), 491–504. https://doi.org/10.1007/s00442-009-1382-1

Lebreton, J. D., Burnham, K. P., Clobert, J., & Anderson, D. R. (1992). Modeling survival and testing biological hypotheses using marked animals: A unified approach with case studies. *Ecological Monographs*, *62*(1), 67–118. https://doi.org/10.2307/2937171

Lefkovitch, L. P. (1965). The study of population growth in organisms grouped by stages. *Biometrics*, *21*(1), 1–18.

Leslie, P. H. (1945). On the use of matrices in certain population. *Biometrika*, *33*(3), 183–212.

Levin, S. C., Evers, S., Potter, T., Guerrero, M. P., Childs, D. Z., Compagnoni, A., Knight, T. M., & Salguero-Gómez, R. (2022). Rpadrino: An R package to access and use PADRINO, an open access database of Integral Projection Models. *Methods in Ecology and Evolution*, *2022*(May), 1–7. https://doi.org/10.1111/2041-210x.13910

Li, W. H., Ju, Y. R., Liao, C. M., & Liao, V. H. C. (2014). Assessment of selenium toxicity on the life cycle of *Caenorhabditis elegans*. *Ecotoxicology*, *23*(7), 1245–1253. https://doi.org/10.1007/s10646-014-1267-x

McDonald, J. L., Stott, I., Townley, S., & Hodgson, D. J. (2016). Transients drive the demographic dynamics of plant populations in variable environments. *Journal of Ecology*, *104*(2), 306–314. https://doi.org/10.1111/1365-2745.12528

Miller, T. E. X., & Compagnoni, A. (2022). Two-sex demography, sexual niche differentiation, and the geographic range limits of Texas bluegrass (*Poa arachnifera*). *The American Naturalist*, *200*(1), 17–38. https://doi.org/10.1086/719668

Namkoong, G., & Roberds, J. H. (1974). Extinction probabilities and the changing age structure of redwood forests. *The American Naturalist*, *108*(961), 355–368.

Neubert, M. G., & Caswell, H. (2000). Demography and dispersal: Calculation and sensitivity analysis of invasion speed for structured populations. *Ecology*, *81*(6), 1613–1628. https://doi.org/10.1890/0012-9658(2000)081[1613:DADCAS]2.0.CO;2

Nguyen, V., Buckley, Y. M., Salguero-Gómez, R., & Wardle, G. M. (2019). Consequences of neglecting cryptic life stages from demographic models. *Ecological Modelling*, *408*(July), 108723. https://doi.org/10.1016/j.ecolmodel.2019.108723

Nordstrom, S. W., Dykstra, A. B., & Wagenius, S. (2021). Fires slow population declines of a long-lived prairie plant through multiple vital rates. *Oecologia*, *196*(3), 679–691. https://doi.org/10.1007/s00442-021-04955-2

Omeyer, L. C. M., Stokes, K. L., Beton, D., Çiçek, B. A., Davey, S., Fuller, W. J., Godley, B. J., Sherley, R. B., Snape, R. T. E., & Broderick, A. C. (2021). Investigating differences in population recovery rates of two sympatrically nesting sea turtle species. *Animal Conservation*, *24*, 832–846. https://doi.org/10.1111/acv.12689

Paniw, M., Maag, N., Cozzi, G., Clutton-Brock, T., & Ozgul, A. (2019). Life history responses of meerkats to seasonal changes in extreme environments. *Science*, *363*(6427), 631–635. https://doi.org/10.1126/science.aau5905

Paniw, M., Quintana-Ascencio, P. F., Ojeda, F., & Salguero-Gómez, R. (2017). Accounting for uncertainty in dormant life stages in stochastic demographic models. *Oikos*, *126*(6), 900–909. https://doi.org/10.1111/oik.03696

Pardini, E. A., Drake, J. M., Chase, J. M., & Knight, T. M. (2009). Complex population dynamics and control of the invasive biennial *Alliaria petiolata* (Garlic mustard). *Ecological Applications*, *19*(2), 387–397. https://doi.org/10.1890/08-0845.1

Pearl, R., Miner, J. R., & Parker, S. L. (1927). Experimental studies on the duration of life. XI. Density of population and life duration in *Drosophila*. *The American Naturalist*, *61*, 289–318. https://doi.org/10.1086/280154

Pfister, C. A. (1998). Patterns of variance in stage-structured populations: Evolutionary predictions and ecological implications. *Proceedings of the National Academy of Sciences of the United States of America*, *95*(1), 213–218. https://doi.org/10.1073/pnas.95.1.213

Plard, F., Fay, R., Kéry, M., Cohas, A., & Schaub, M. (2019). Integrated population models: Powerful methods to embed individual processes in population dynamics models. *Ecology*, *100*(6), 1–15. https://doi.org/10.1002/ecy.2715

Powers, S. M., & Hampton, S. E. (2019). Open science, reproducibility, and transparency in ecology. *Ecological Applications*, *29*(1), 1–8. https://doi.org/10.1002/eap.1822

Regehr, E. V., Hunter, C. M., Caswell, H., Amstrup, S. C., & Stirling, I. (2010). Survival and breeding of polar bears in the southern Beaufort Sea in relation to sea ice. *Journal of Animal Ecology*, *79*(1), 117–127. https://doi.org/10.1111/j.1365-2656.2009.01603.x

Reichman, O. J., Jones, M. B., & Schildhauer, M. P. (2011). Challenges and opportunities of open data in ecology. *Science*, *331*(6018), 703–705. https://doi.org/10.1126/science.1197962

Riecke, T. V., Williams, P. J., Behnke, T. L., Gibson, D., Leach, A. G., Sedinger, B. S., Street, P. A., & Sedinger, J. S. (2019). Integrated population models: Model assumptions and inference. *Methods in Ecology and Evolution*, *10*(7), 1072–1082. https://doi.org/10.1111/2041-210X.13195

Römer, G., Dahlgren, J. P., Salguero-Gómez, R., Stott, I. M., & Jones, O. R. (2021). Plant demographic knowledge is biased towards short-term studies of temperate-region herbaceous perennials. *BioRxiv*, 1–46. https://doi.org/10.1101/2021.04.25.441327

Roth, G., & Caswell, H. (2016). Hyperstate matrix models: Extending demographic state spaces to higher dimensions. *Methods in Ecology and Evolution*, *7*(12), 1438–1450. https://doi.org/10.1111/2041-210X.12622

Rueda-Cediel, P., Anderson, K. E., Regan, T. J., & Regan, H. M. (2018). Effects of uncertainty and variability on population declines and IUCN Red List classifications. *Conservation Biology*, *32*(4), 916–925. https://doi.org/10.1111/cobi.13081

Sæther, B. E., Coulson, T., Grøtan, V., Engen, S., Altwegg, R., Armitage, K. B., Barbraud, C., Becker, P. H., Blumstein, D. T., Dobson, F. S., Festa-Bianchet, M., Gaillard, J.-M., Jenkins, A., Jones, C., Nicoll, M. A. C., Norris, K., Oli, M. K., Ozgul, A., & Weimerskirch, H. (2013). How life history influences population dynamics in fluctuating environments. *The American Naturalist*, *182*(6), 743–759. https://doi.org/10.1086/673497

Salguero-Gómez, R., Jackson, J., & Gascoigne, S. J. L. (2021). Four key challenges in the open-data revolution. *Journal of Animal Ecology*, *90*(9), 2000–2004. https://doi.org/10.1111/1365-2656.13567

Salguero-Gómez, R., Jones, O. R., Archer, C. R., Bein, C., de Buhr, H., Farack, C., Gottschalk, F., Hartmann, A., Henning, A., Hoppe, G., Römer, G., Ruoff, T., Sommer, V., Wille, J., Voigt, J., Zeh, S., Vieregg, D., Buckley, Y. M., Che-Castaldo, J., … Vaupel, J. W. (2016). COMADRE: A global data base of animal demography. *Journal of Animal Ecology*, *85*, 371–384. https://doi.org/10.1111/1365-2656.12482

Salguero-Gómez, R., Jones, O. R., Archer, C. R., Buckley, Y. M., Che-Castaldo, J., Caswell, H., Hodgson, D., Scheuerlein, A., Conde, D. A., Brinks, E., de Buhr, H., Farack, C., Gottschalk, F., Hartmann, A., Henning, A., Hoppe, G., Römer, G., Runge, J., Ruoff, T., … Vaupel, J. W. (2015). The COMPADRE Plant Matrix Database: An open online repository for plant demography. *Journal of Ecology*, *103*, 202–218. https://doi.org/10.1111/1365-2745.12334

Salguero-Gómez, R., Jones, O. R., Blomberg, S. P., Hodgson, D. J., Zuidema, P. A., & Kroon, H. D. (2017). Erratum: Fast–slow continuum and reproductive strategies structure plant life-history variation worldwide (Proc Natl Acad Sci USA (2015) 113 (230–235)). *Proceedings of the National Academy of Sciences of the United States of America*, *114*(45), E9753. https://doi.org/10.1073/pnas.1717717114

Salguero-Gómez, R., & Plotkin, J. B. (2010). Matrix dimensions bias demographic inferences: Implications for comparative plant demography. *The American Naturalist*, *176*(6), 710–722. https://doi.org/10.1086/657044

Schaub, M., & Kéry, M. (2021). *Integrated population models: Theory and ecological applications with R and JAGS*. Academic Press.

Shyu, E., & Caswell, H. (2016a). A demographic model for sex ratio evolution and the effects of sex-biased offspring costs. *Ecology and Evolution*, *6*(5), 1470–1492. https://doi.org/10.1002/ece3.1902

Shyu, E., & Caswell, H. (2016b). Frequency-dependent two-sex models: A new approach to sex ratio evolution with multiple maternal conditions. *Ecology and Evolution*, *6*(19), 6855–6879. https://doi.org/10.1002/ece3.2202

Shyu, E., Pardini, E. A., Knight, T. M., & Caswell, H. (2013). A seasonal, density-dependent model for the management of an invasive weed. *Ecological Applications*, *23*(8), 1893–1905. https://doi.org/10.1890/12-1712.1

Sky, N. H., Jackson, J., Chege, G., Gaymer, J., Kimiti, D., Mutisya, S., Nakito, S., & Shultz, S. (2022). Female reproductive skew exacerbates the extinction risk from poaching in the eastern black rhino. *Proceedings of the Royal Society B: Biological Sciences*, *289*(1972), 20220075. https://doi.org/10.1098/rspb.2022.0075

Smith, M., Caswell, H., & Mettler-Cherry, P. (2005). Stochastic flood and precipitation regimes and the population dynamics of a threatened floodplain plant. *Ecological Applications*, *15*(3), 1036–1052. https://doi.org/10.1890/04-0434

Snyder, R. E., & Ellner, S. P. (2018). Pluck or luck: Does trait variation or chance drive variation in lifetime reproductive success? *The American Naturalist*, *191*(4), E90–E107. https://doi.org/10.1086/696125

Snyder, R. E., & Ellner, S. P. (2022). Snared in an evil time: How age-dependent environmental and demographic variability contribute to variance in lifetime outcomes. *The American Naturalist*, *200*(3), E124–E140. https://doi.org/10.1086/720411

Steiner, U. K., Tuljapurkar, S., & Roach, D. A. (2021). Quantifying the effect of genetic, environmental and individual demographic stochastic variability for population dynamics in *Plantago lanceolata*. *Scientific Reports*, *11*(1), 1–11. https://doi.org/10.1038/s41598-021-02468-9

Stott, I., Townley, S., Carslake, D., & Hodgson, D. J. (2010). On reducibility and ergodicity of population projection matrix models. *Methods in Ecology and Evolution*, *1*(3), 242–252.

Stott, I., Townley, S., & Hodgson, D. J. (2011). A framework for studying transient dynamics of population projection matrix models. *Ecology Letters*, *14*(9), 959–970. https://doi.org/10.1111/j.1461-0248.2011.01659.x

Tenhumberg, B., Louda, S. M., Eckberg, J. O., & Takahashi, M. (2008). Monte Carlo analysis of parameter uncertainty in matrix models for the weed *Cirsium vulgare*. *Journal of Applied Ecology*, *45*(2), 438–447. https://doi.org/10.1111/j.1365-2664.2007.01427.x

Tenhumberg, B., Tyre, A. J., & Rebarber, R. (2009). Model complexity affects transient population dynamics following a dispersal event: A case study with pea aphids. *Ecology*, *90*(7), 1878–1890. https://doi.org/10.1890/08-1665.1

Tremblay, R. L., & McCarthy, M. A. (2014). Bayesian estimates of transition probabilities in seven small lithophytic orchid populations: Maximizing data availability from many small samples. *PLoS ONE*, *9*(7), 1–12. https://doi.org/10.1371/journal.pone.0102859

Tremblay, R. L., Perez, M.-E., Larcombe, M., Brown, A., Quarmby, J., Bickerton, D., French, G., & Bould, A. (2009a). Dormancy in *Caladenia*: A Bayesian approach to evaluating latency. *Australian Journal of Botany*, *57*(4), 340–350. https://doi.org/10.1071/BT08163

Tremblay, R. L., Perez, M.-E., Larcombe, M., Brown, A., Quarmby, J., Bickerton, D., French, G., & Bould, A. (2009b). Population dynamics of *Caladenia*: Bayesian estimates of transition and extinction probabilities. *Australian Journal of Botany*, *57*(4), 351–360. https://doi.org/10.1071/BT08167

Tremblay, R. L., Tyre, A. J., Pérez, M. E., & Ackerman, J. D. (2021). Population projections from holey matrices: Using prior information to estimate rare transition events. *Ecological Modelling*, *447*(August 2020), 109526. https://doi.org/10.1016/j.ecolmodel.2021.109526

Tuljapurkar, S. (1989). An uncertain life: Demography in random environments in population analysis but it ignores variation in population vital rates. *Theoretical Population Biology* (English Edition), *294*, 227–294.

van Daalen, S. F., & Caswell, H. (2017). Lifetime reproductive output: Individual stochasticity, variance, and sensitivity analysis. *Theoretical Ecology*, *10*(3), 355–374. https://doi.org/10.1007/s12080-017-0335-2

van Daalen, S. F., Hernández, C. M., Caswell, H., Neubert, M. G., & Gribble, K. E. (2022). The contributions of maternal age heterogeneity to variance in lifetime reproductive output. *The American Naturalist*, *199*(5), 603–616. https://doi.org/10.1086/718716

Veran, S., & Beissinger, S. R. (2009). Demographic origins of skewed operational and adult sex ratios: Perturbation analyses of two-sex models. *Ecology Letters*, *12*(2), 129–143. https://doi.org/10.1111/j.1461-0248.2008.01268.x

Werner, P. A., & Caswell, H. (1977). Population growth rates and age versus stage-distribution models for teasel (*Dipsacus sylvestris* Huds.). *Ecology*, *58*(5), 1103–1111. https://doi.org/10.2307/1936930

Werner, P. A., & Peacock, S. J. (2019). Savanna canopy trees under fire: Long-term persistence and transient dynamics from a stage-based matrix population model. *Ecosphere*, *10*(5). https://doi.org/10.1002/ecs2.2706

SUPPORTING INFORMATION

Additional supporting information can be found online in the Supporting Information section at the end of this article.

Data S1: A survey on matrix communication.

How to cite this article: Gascoigne, S. J. L., Rolph, S., Sankey, D., Nidadavolu, N., Stell Pičman, A. S., Hernández, C. M., Philpott, M. E. R., Salam, A., Bernard, C., Fenollosa, E., Lee, Y. J., McLean, J., Hetti Achchige Perera, S., Spacey, O. G., Kajin, M., Vinton, A. C., Archer, C. R., Burns, J. H., Buss, D. L. … Salguero-Gómez, R. (2023). A standard protocol to report discrete stage-structured demographic information. *Methods in Ecology and Evolution*, *14*, 2065–2083. https://doi.org/10.1111/2041-210X.14164 iScience

CellPress
OPEN ACCESS

Article

Seasonal weather impacts wine quality in Bordeaux

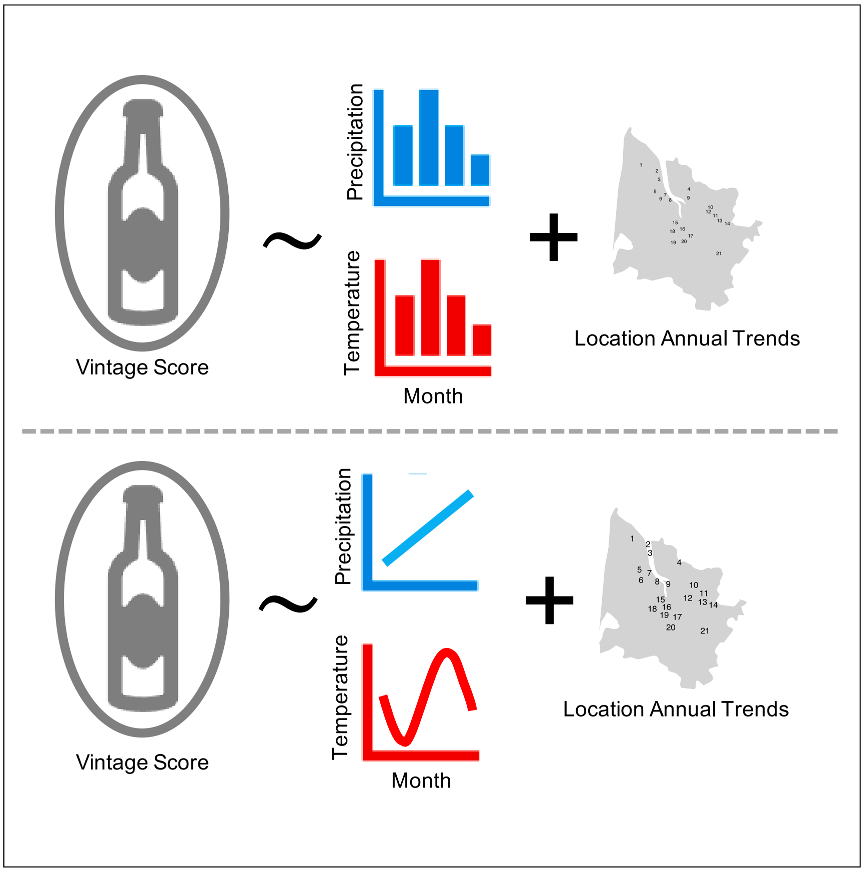

Andrew Wood, Samuel J.L. Gascoigne, Gregory A. Gambetta, Elizabeth S. Jeffers, Tim Coulson

wood_and@hotmail.com

Highlights

Wine quality measured through critics scores varies across space and time

Weather at multiple points during the year impacts wine quality in Bordeaux

Climate shifts suggest wine quality may improve with future predicted climate

Wood et al., iScience *26*, 107954
October 20, 2023
https://doi.org/10.1016/j.isci.2023.107954

iScience

CellPress
OPEN ACCESS

Article

Seasonal weather impacts wine quality in Bordeaux

Andrew Wood,[1,3,*] Samuel J.L. Gascoigne,[1] Gregory A. Gambetta,[2] Elizabeth S. Jeffers,[1] and Tim Coulson[1]

SUMMARY

Critics judge quality based upon subjective characteristics of wine. These judgments are converted by critics into quantitative scores, which allow for comparison of vintages. This paper uses high resolution discrete and continuous time-based weather estimates at both a local and regional level to determine the role of weather conditions on producing high quality Bordeaux vintages, as determined by critics scores. By using discrete-time weather variables across local AOCs, this study reveals climate-quality relationships across the whole year, including previously ignored season effects. By using continuous time weather variables, we reinforce the evidence for these local effects by finding higher quality wine is made in years with higher rainfall, warmer temperatures; and earlier, shorter seasons. We propose management impacts of our results and suggest that as the climate continues to change, the quality of Bordeaux wines may continue to improve.

INTRODUCTION

Climate change is globally impacting agricultural produce, both in terms of yield and quality.[1,2] Despite these expected effects, the link between climate change and agricultural produce quality has not been widely explored. Wine (*Vitis vinifera*) presents the ideal system to study this relationship as wine price is governed primarily by quality,[3] which is dependent on weather during the vine's growing season.[4] Additionally, wine quality in Bordeaux (France) has been measured by many independent experts over time, meaning that there exists a multi-critic regional and local longitudinal dataset for quality.[5–11] With the availability of high-resolution weather data we can now use this information to examine how weather influences quality on both a regional and local scale.

Local variation in the quality of wine was first acknowledged with the introduction of wine rating systems. The Bordeaux Grand Cru system was created in 1855 to classify individual vineyards into one of five categories based on price and perceptions of quality. This Grand Cru classification system has been expanded such that there now exists 14 defined categories of wines in Bordeaux, with other wines simply being categorized as unclassified via this method.[11] A series of geographical protections were introduced in 1936, referred to as *appellations d'origine contrôlée*, or AOCs. Acting on the local scale, they create individualities for wines, with each AOC having distinct viticultural characteristics and vinicultural identities.[12] Such identities can link an AOC to perceived quality, with some becoming more famous than others. Regional and local disparities can be explored by comparing scores for the whole of Bordeaux to individual wine scores linked to an AOC. Consequently, each individual wine is wrapped in its own historic quality ratings which have the potential to shift perceptions of the current and future wines. Such perceptions must be considered in any attempt to understand quality.

Some studies have directly examined quality using tasting scores.[13–15] In Bordeaux these tasting scores traditionally take the form of a *primeur* score. These scores are bestowed by wine critics at tastings approximately 10 months after harvest and just after blending. While these wines are not mature and often highly tannic,[11] this scoring system provides a direct standardized measurement of quality and allows for an ascertainment of the quality of the wine before it fully ages. Other critics, mainly wine merchants, rate Bordeaux as a whole region, giving an overall classification as to whether or not a year is good or not. Due to this two-scale rating system, there exists the potential to compare regional tasting scores to local tasting scores.

Weather conditions have also been demonstrated to have an impact on the wine quality. Most famously, Ashenfelter's (1995) Bordeaux equation[6–8] suggested that the average price of wine in Bordeaux is a linear function of winter precipitation and summer temperature. Other models have used monthly weather, demonstrating that finer resolution weather data and local chateau characteristics[6,16] can contribute to explaining price variation in Bordeaux wines. These local effects have been examined using this same price-based approach by Lecocq and Visser (2006) using local weather stations.[17] The models in Lecoq and Visser (2006) found similar results at both regional and local scales and thus suggested that in most cases regional and local weather records are interchangeable.

Tasting scores have been correlated with single-year metrics of weather such as annual mean temperature and precipitation[7,9,18] in wine-growing regions from Australia[14] to California.[13] Consensus from the Bordeaux equation, price modeling and current quality scores suggest that higher temperature and lower precipitation leads to higher quality grapes.[5,7,11] Ashenfelter and Jones (2013) suggest that: critics scores "reflect qualitatively the same weather factors that have been documented to be determinants of wine quality."[6] Multiple studies have shown

---

[1] Department of Biology, University of Oxford, 11a Mansfield Road, Oxford OX1 3SZ, UK
[2] EGFV, Bordeaux Sciences Agro, INRAE, Université de Bordeaux, ISVV, Villenave d'Ornon, France
[3] Lead contact
*Correspondence: wood_and@hotmail.com
https://doi.org/10.1016/j.isci.2023.107954

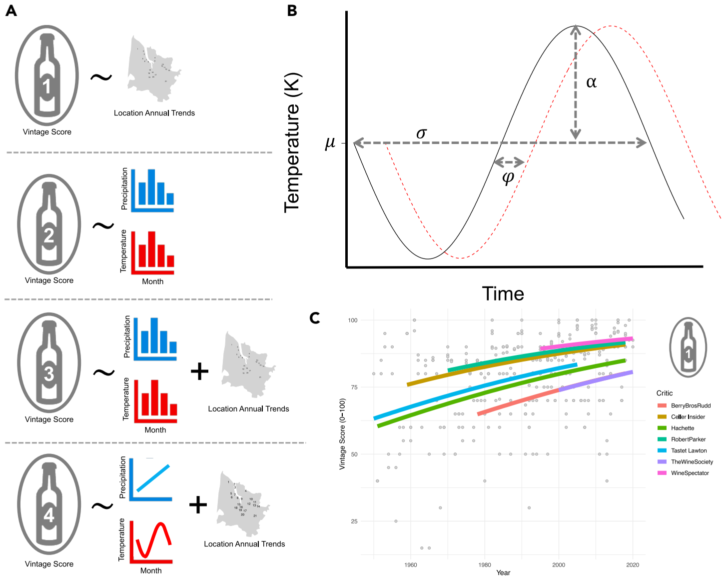

Figure 1. Methods panel plot

(A) Summary of the generalized linear models run to analyze the relationship between wine critics scores and the weather, controlling for location annual trends (location and year interactions). In each row the number on the bottle refer to the model number, and tilde means "is a function of".

(B) Depiction of sine wave with depiction of parameters fitted. μm is the mean temperature, α the amplitude, σ the wavelength, and φ the phase shift.

(C) Mean critics scores (scaled from 0 to 100) over time for Bordeaux as a whole with colored lines showing the GLM fitted.

that a higher number of warm days during flowering and at the onset of berry ripening (spring and summer) and lower precipitation during berry maturation (autumn) leads to higher quality.[5,19,20] But other conflicting studies have shown impacts outside of this time frame, with weather affecting quality across the year. Notably, the Bordeaux equation suggests that primarily winter precipitation and summer temperature is important. But Vittorio and Ginsburgh (1996) use the number of days of hail in April as well as temperature and precipitation during June to September.[16] Jones and Storchman (2001) look at phenological stages and find that four different weather aspects (evapotranspiration; total rainfall; and the number of days with temperatures more than 25°C and 30°C) all have an effect on the price of the final wine.[11] Baciocco et al. (2014) suggest that low rainfall and high heat accumulation over the year lead to higher ranked wines.[10] Bonada et al. (2020) claim that rainfall during winter dormancy impacts quality.[21] Alongside such varying insights in the literature comes a finding of a reduction in quality with high temperatures.[18,20] Other evidence also links spring frosts to changes in quality.[22] Overall, these findings suggests the potential for regional differences in climate change to potentially impact wine quality.[23] Thus, it is important to understand which features of the weather are affecting wine quality and when, in order to determine the precise impacts of climate change on a viticulturally relevant spatial resolution.

In this study, we explore the link between weather and critic quality scores, using weather and quality scores for Bordeaux wines, at both regional and local levels. We use discrete time models with time steps such that the impact of temperature and precipitation on wine quality scores across the year can be ascertained. We then use continuous time models which explore the weather across the whole year as single functions for rainfall and temperature. In turn, we aim to give greater understanding as to when wine quality is most susceptible to changes in temperature and precipitation, and how we can examine such changes.

RESULTS

Between 1950 and 2020 there was a general increase in quality scores for wine quality in the Bordeaux region. The maximal annual mean score was 98.67 points (1961), and the minimum was 32.5 (recorded in 1965). A generalized linear model was fitted to determine the location annual trends, as per model 1 in the model summary figure (Figure 1A). In this GLM, the overall critic score for Bordeaux is predicted by the year, controlling for critic. Year fitted as a continuous variable in the model was found to be statistically significant (coef = 0.0195, χ (1) = 4.4528, $p < 0.05$, $R^2 = 0.27$), meaning there is a general increase in critics' quality score over time (Table S3).

Quality scores were also examined on a local scale. The maximal mean critics score was 99 points (recorded once in 2019) and the minimum was 28 (recorded once in 2006). Critics showed high correlation between ratings (Figure S2). A binomial GLM was fitted, again as per model 1

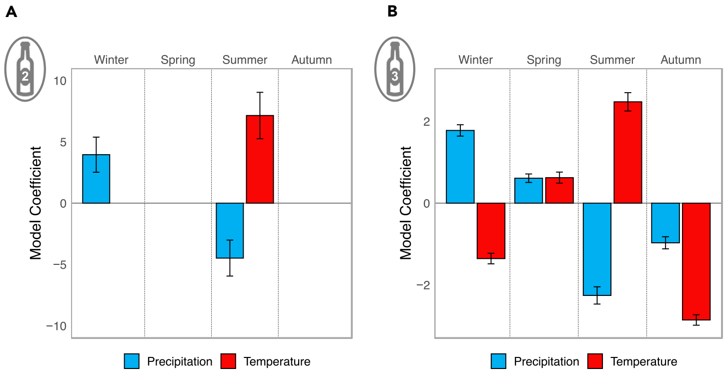

Figure 2. Weather variable model coefficients

(A and B) Weather variable model coefficients for generalized linear models (GLMs) fitted to explain (A) mean critic score for the whole of Bordeaux and (B) mean critic score controlling for AOC, Grand Cru status, and year. Bar presence signifies coefficient had a p value of less than 0.05 with standard error bars.

on the model summary figure (Figure 1A). It reported no significant coefficients for Year nor Year:AOC interactions. This suggests that, for the time period, there is no local increase in quality over time (for test statistics see Table S4).

Discrete time model

Generalized linear models were also built to explore the relationship between grouped monthly weather variables and the mean overall Bordeaux general score, controlling for the yearly trend of improvements ($R^2 = 0.61$; Table S5), as per model 2 in the model summary figure (Figure 1A). As weather has been normalized, only the sign (positive or negative) and the relative size of the coefficients are important. The largest significant ($p < 0.05$) coefficient in the model is the positive coefficient for summer temperatures (coef = −4.48, F (1,59) = 122.1716, p = 0.0004), followed by the negative coefficient for summer precipitation (coef = 7.14, F (1,59) = 114.0373, $p < 0.05$), and then the positive coefficient for winter precipitation (coef = 3.95, F (1,59) = 164.4203, df = 3, $p < 0.05$), as shown in Figure 2A. Models were found to fit well from visual inspection of residual plots (see Figure S3). According to this model, changes in temperature and precipitation at other times of year would not change the overall Bordeaux scores, excluding stochastic extreme weather events.

A generalized linear model was also run on the local (AOC) scale, as per model 3 on the wine model summary figure (Figure 1A). Model 3 examines the relationship between grouped monthly weather variables and individual wine scores, controlling for year increases, AOC, and Grand Cru status (n = 4521, $R^2 = 0.35$; for full details see Table S6). All weather terms were found to be significant, with coefficients shown graphically in Figure 3. Again, temperature and rainfall have been normalized for comparison purposes, and so exact coefficients are without real-world meaning. The largest coefficient is the negative term for temperature in autumn, followed by the positive coefficient for summer temperature, the positive term and the third largest impact is the negative coefficient for precipitation in summer. Models fitted well from visual inspection of plots (Figure S4). The variation in the coefficients shows the heterozygosity of the impacts, with positive and negative impacts occurring across the year. The coefficients appear to be in a wave formation, with both temperature and precipitation increasing and decreasing in a cyclical manner.

Results for models using parameters from continuous time weather models

Cumulative precipitation increases linearly with increasing month (Figure S5). Over time there exists a generalized trend of increasing precipitation with increasing year (year coef = 0.0000318, F(1,6185) = 1676.8, $p < 0.05$, for full results see Table S7). When mean critic scores are modeled against cumulative precipitation controlling for AOC and year, as per model option 4 in Figure 1A, a positive correlation is found (coef = 1779.8, F(1,6171) = 28.1, n = 4521, $p < 0.05$, $R^2 = 0.29$, Table S8). This suggests that higher whole year cumulative rainfall is beneficial for the production of higher quality wines.

Mean monthly temperatures have minima at around 3 to 4 months after September, in December and January. Peaks occur between 9- and 10-month past September—in June and July (Figure S6), increasing and decreasing in a wave pattern. Sine curves were fitted across each of the mean monthly temperatures and fitted the data well (mean R^2 is 0.95 and standard deviation of R^2 is 0.02, Table S9). μm and α were found to be the most variable terms, with means of 8.01 and 286.72 and standard errors of 0.79 and 0.65 (Table S9). σ and φ were found to have means of 0.52 and 3.07 and standard errors of 0.02 and 0.23 (Table S9). This suggests that mean temperature and temperature extremes can vary more than the timings of when seasons change.

Mean precipitation and the sine parameters of quality were used together as explanatory variables in a GLM, as per model 4 in Figure 1A. All factors, namely: mean precipitation (MeanPrecip), mean temperature (μ; C), amplitude (α; A), periodicity (σ, omega), and curve shift (φ; phi) were found to have significant ($p < 0.05$) positive coefficients (see Table S10 for test statistics). The marginal effects from this model can be

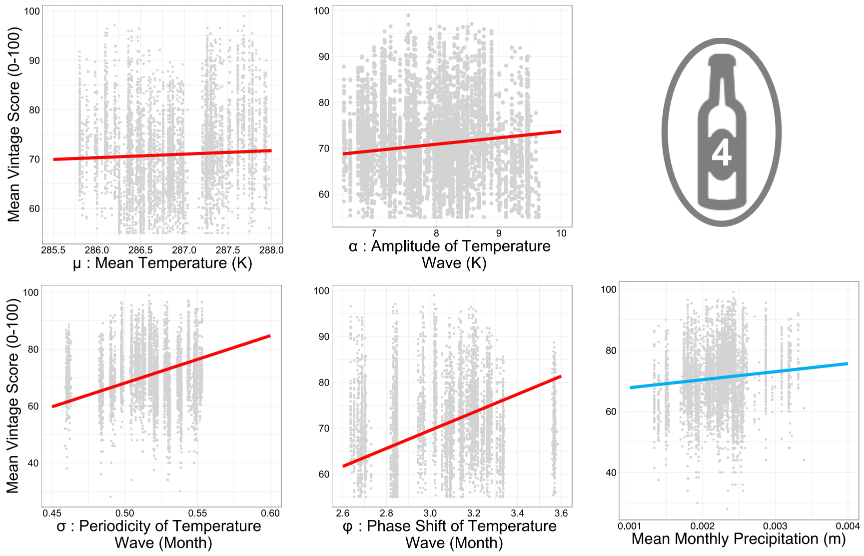

Figure 3. Model effects plots

Model effects plot showing the vintage score against the sine wave parameters and mean monthly precipitation, with the slope of the line being the coefficients of each parameter.

seen plotted in Figure 3. These results suggest that the greater the extremes in temperature (higher amplitude), the shorter and earlier the season (decrease in wavelength and positive temperature phase shift), and the larger the mean temperature and mean monthly precipitation, the higher the mean critic score of the wine.

DISCUSSION

All of the models suggest that weather is an important factor in the determination of wine quality. Taken as a whole, the models suggest that weather impacts the quality of wine over the course of the year, with importance varying between seasons and aspects of seasonal weather. This paper includes a new method of examining the weather-wine linkage, using continuous time rather than discrete time periods. It concludes that different aspects of temperature and precipitation are important to quality throughout the year, with high quality requiring periods of both high and low temperature and precipitation. Exploring weather as a continuous series, we find that higher quality wine is made in years with greater temperature extremes; earlier, shorter seasons; and potentially a higher mean temperature.

At a regional scale, quality can be seen to have increased over the last several decades (Figure 1C). The cause of such a trend cannot be distinguished statistically on such a scale. Multiple factors all act in concert to improve wine critics scores, namely: climate change, increasing technology, increased positivity in critics reviews, and increased matching of wines consumer pref. [4,28,29]. This increase in technology and consequential changes in wine characteristics since the 1960s have been described as the "Peynaudization" of Bordeaux wines.[30] Controlling for such trends therefore allows for greater exploration of the impact of individual aspects of wine quality scores. At a local scale, no increase in trend can be seen to exist, and thus no universal increase in quality can be detected (Table S4). This may be due to the shorter time duration, variation in wine making techniques, or potentially even that the regional trends reflect critic regional sentiment rather than specific wines and thus no actualized trend exists.

The overall Bordeaux generalized linear model (model 2 in Figure 1A) suggests the traditional view of high winter precipitation, high summer temperatures and low precipitation in the summer and autumn lead to high quality grapes (Figure 2A). This combination of precipitation and sunshine has previously been termed the "Bordeaux Equation,"[7,8] and has shaped the global understanding of grapevines.[29,31] However, the weather location we used to examine these regional scores is in the city center of Bordeaux. This is an urban area not related to viticulture. This suggests that general regional weather has some effect, but that this is not the whole story.

Like the Bordeaux equation, our overall models also advocate for the impact of out of growing season effects too, corroborating statistically with findings from Bonada et al. (2020) that an increase water availability during the dormancy phase (in our case from precipitation and in their case due to irrigation) leads to an increase in quality.[21] During winter the grapevines are experiencing dormancy, and a negative temperature coefficient here suggests a cooling period is required for high quality wine. The models also concur with previous findings that rainfall during the winter leads to higher quality,[17,21] with agricultural suggestions that this may be due to lower soil salinity.[32] It has been suggested that more rain in the winter could lead to a better water balance during the growing season, however, it has previously been shown that in Bordeaux only 3 of the last 70 years have started the growing season not at full water soil capacity.[2] Flowering, fruit set, and potentially the onset of berry ripening (depending on the year) all occur in summer, with hotter and drier weather again being suggested to make high quality wine in this time period, potentially due to lower promotion of major grape diseases.[7,19]

The individual AOC model (model 3 in Figure 1A) suggests a more complex view of the relationship and quality. While the same relationships between weather and quality are there during the summer and autumn for temperature and precipitation, additional effects are also present (Figure 2B). These are the negative effects of temperature in winter and autumn and precipitation in autumn, as well as the positive effect in temperature and precipitation in spring. The higher number of significant time periods suggests that weather impacts occur right across the year, with impacts of weather on quality score potentially varying due to the phenological stage of the grapevine.[5] As well as the dormancy effects, higher precipitation and higher temperatures in spring advocate for wetter and warmer weather for bud and leaf burst. Finally, cooler and drier weather is best for ripening in autumn and the optimal harvest to make a high-quality vintage. There is also an element of susceptibility suggested, with the impacts of water deficit on wine quality having greater impact on wine quality during the winter and summer months, and wine quality being more susceptible to temperatures in summer and autumn.

Combined, the two normalized weather models (models 2 and 3) suggest a difference between the regional and local levels. They suggest that heterogeneity at the local (AOC) level is being masked when only examining the regional level. They therefore suggest that, in order to improve the viticultural understanding and hence relevance of such modeling approaches, more local scale weather effects should be considered.

While these discrete-time suggestions are useful independently, they do not inform about time sequences of weather, which is exactly how it occurs. To explore this more fully, weather was treated as a continuous time variable. When examined in continuous time, monthly precipitation was found to be erratic and thus suited a cumulative approach, with increases being added and forming a linear accumulation. The fact that such an accumulation is well approximated by a linear model suggests an almost constant aseasonal pattern of precipitation, with the slope of this linear accumulation being the mean monthly precipitation. Conceptually, examining this mean monthly precipitation allows us to consider whether a whole year is wet or dry, rather than just the segments set out in the discrete GLMs. The significant precipitation term suggests that, even controlling for temperature, year, location, and class, a positive relationship exists between mean monthly precipitation and wine quality (Table S10). Wetter years appear to lead to higher quality wines. Coupled with the discrete time models (Figure 2), this model therefore suggests that this high rainfall should optimally occur post-harvest and pre-growth, during the dormancy period.

Temperature is not linear, rather it fluctuates according to seasonality and thus can be well approximated with a sine curve. Each of the parameters of the sine curve informs aspects of a temperature regime over the course of a year. In the GLM exploring the impact of temperature and precipitation parameters on mean quality score (again controlling for year, class, and AOC), the coefficients of each of the terms are found to be positive (Table S10). This suggests that, aside from being wetter, years that make higher quality wine are characterized by greater temperature extremes, with a higher mean temperature, and earlier, shorter seasons. While the increase in mean temperature concurs with previous research,[7,20] more extreme weather suggests colder winters and hotter summers give higher quality. Earlier seasons suggests that consistently warmer weather during early phenological stages is also beneficial. Warmer weather means lower risk of frost, suggesting that damage to crops extends beyond losses and into quality.[22,33] Warmer weather also potentially suggests that higher metabolic rates and higher photosynthetic rates lead to higher quality grapes. Shorter seasons suggest that the cooling of temperatures toward the end of the growing season may positively impact the ripening of grapes. With increases in both mean and extreme temperatures predicted across France,[34] and changes in timing and length of growing season also predicted across growing regions,[35] this leads to the potential suggestion that wine in Bordeaux may continue to improve over time.

Among these trends there still exists the question of the local versus regional disparities. The differences between the local and regional models in both their model coefficients and statistical significances suggest the impacts from the local scale are being masked when examined at the regional scale. This may be because of the individual differences in weather, or due to disparities in the wine making in each of the AOCs. For each of the models that are built, the Grand Cru classification system suggests significant differences between the classification levels, and similarly AOC level differences appear to exist (see Tables S6–S10). However, one potential source of variation in these data may be bias in expert opinion.[36–40] Statistically, it is impossible with these data to fully disentangle wine bias from perceived quality. Future studies where the data for wine quality is both linked to local weather and also rated in a double-blind fashion, will be necessary to capture the degree to which expert bias informs or weakens our predictions.

We suggest that such variation in quality classification between regions has masked local variation in impacts of weather on quality across the year. While we accept that biases exist within wine, both for a specific locale or classification, we have also demonstrated a significant shared understanding of quality.

There are clear management implications of these findings, which result from trying to optimize the environment for vine growth and fruit composition. Our models suggest that water regime is critical in determining higher quality wines. Specifically, to increase wine quality, ideal conditions include high water abundance during the winter months and low water abundance in the summer, coupled with high temperatures. Climate change in Bordeaux will likely lead to more extreme weather, with variation depending on the location.[41] While some places will be in drought, others will encounter less total rainfall punctuated with short heavy rain events.[41] For red wine production we suggest that if irrigation were to be considered, it would be best to target the water regimes highlighted in this work: a well-replenished soil water profile over the winter months followed by moderate to severe water deficits during the summer months (depending on yield and wine style considerations). In cases where heavy rainfall could be an issue in summer, increased drainage, erosion control, or, at an extreme, rainfall covers could be necessary. With regard to temperature management, summer management strategies which promote localized higher temperatures are suggested (especially during the ripening period). This can be achieved by increasing defoliation around the berries to reduce shading, but caution is warranted to guard against exposing fruit to temperature extremes. Finally, we agree with common practices of avoiding frost damage by raising temperatures around the vines during the spring months. With predicted phenological and weather changes leading to hotter and earlier summers, our results suggest that average Bordeaux quality scores may continue to increase.

This paper has explored the impact of weather on wine, seeking to determine the optimal growing conditions for high quality Bordeaux vintages. It explores the infamous Bordeaux equation, finding that the equation works well for explaining regional patterns, but that for individual AOCs the weather impacts occur over the course of the year. Exploring this weather sequentially, this paper finds that higher quality wine is made in years with greater temperature extremes; earlier, shorter seasons; and a higher mean temperature. This all suggests that as climate change increases, the wine quality may continue to get better.

Limitations of the study

We appreciate that the study was only conducted using ratings for Bordeaux chateaus, and that the corresponding limitations are therefore that we can only control for the winery at the winery level. We cannot control for the winemaker changing, or any potential changes in the exact plots used to make the wines. Finally, it is statistically impossible to tell the difference over time between improvements in wine due to climate and winemaker (and hence this trend has been removed from dataset). Despite these limitations, we have shown a robust trend within the dataset concerning the impact of seasonal weather on the quality of wines.

STAR★METHODS

Detailed methods are provided in the online version of this paper and include the following:

- KEY RESOURCES TABLE
- RESOURCE AVAILABILITY
  - Lead contact
  - Materials availability
  - Data and code availability
- METHOD DETAILS
  - Weather data
  - Quality data
- QUANTIFICATION AND STATISTICAL ANALYSIS
  - Generalized linear models

SUPPLEMENTAL INFORMATION

Supplemental information can be found online at https://doi.org/10.1016/j.isci.2023.107954.

ACKNOWLEDGMENTS

The authors would like to thank the data providers and F. Lovell-Read for her help with sine curves, C. Bernard for his support and T. Taberer for her proof-reading. This work was supported by funding from the Biotechnology and Biological Sciences Research Council (BBSRC) [grant number BB/M011224/1].

AUTHOR CONTRIBUTIONS

A.W. and S.G. conceived the main ideas and initial methodology; all authors contributed improvements to ideas and the methodology; A.W. collected the data and A.W. and S.G. analyzed the data; A.W. led the writing of the manuscript, with edits from all authors. All authors contributed critically to the drafts and gave final approval for publication.

DECLARATION OF INTERESTS

We declare no conflicts of interest.

INCLUSION AND DIVERSITY

We support inclusive, diverse, and equitable conduct of research.

Received: May 18, 2023
Revised: June 26, 2023
Accepted: September 13, 2023
Published: October 11, 2023

REFERENCES

1. Lobell, D.B., Field, C.B., Cahill, K.N., and Bonfils, C. (2006). Impacts of future climate change on California perennial crop yields: Model projections with climate and crop uncertainties. Agric. For. Meteorol. *141*, 208–218. https://doi.org/10.1016/j.agrformet.2006.10.006.
2. van Leeuwen, C., and Darriet, P. (2016). The Impact of Climate Change on Viticulture and Wine Quality. J. Wine Econ. *11*, 150–167. https://doi.org/10.1017/jwe.2015.21.
3. Roucher, A., Aristodemou, L., and Tietze, F. (2022). Predicting wine prices based on the weather: Bordeaux vineyards in a changing climate. Front. Environ. Sci. *10*, 2266. https://doi.org/10.3389/FENVS.2022.1020867.
4. van Leeuwen, C., Friant, P., Choné, X., Tregoat, O., Koundouras, S., and Dubourdieu, D. (2004). Influence of Climate, Soil, and Cultivar on Terroir. Am. J. Enol. Vitic. *55*, 207–217.
5. Jones, G.V., and Davis, R.E. (2000). Climate Influences on Grapevine Phenology, Grape Composition, and Wine Production and Quality for Bordeaux, France. Am. J. Enol. Vitic. *51*, 249–261.
6. Ashenfelter, O., and Jones, G.v. (2013). The Demand for Expert Opinion: Bordeaux Wine. J. Wine Econ. *8*, 285–293. https://doi.org/10.1017/JWE.2013.22.
7. Ashenfelter, O., Ashmore, D., and Lalonde, R. (1995). Bordeaux Wine Vintage Quality and the Weather. Chance *8*, 7–14. https://doi.org/10.1080/09332480.1995.10542468.
8. Ashenfelter, O. (2008). Predicting the Quality and Prices of Bordeaux Wine. Econ. J. *118*, F174–F184. https://doi.org/10.1111/J.1468-0297.2008.02148.X.
9. Almaraz, P. (2015). Bordeaux wine quality and climate fluctuations during the last century. Clim. Res. *64*, 187–199. https://doi.org/10.2307/24897566.
10. Baciocco, K.A., Davis, R.E., and Jones, G.V. (2014). Climate and Bordeaux wine quality: identifying the key factors that differentiate vintages based on consensus rankings. J. Wine Res. *25*, 75–90. https://doi.org/10.1080/09571264.2014.888649.
11. Jones, G., and Storchmann, K.H. (2001). Wine market prices and investment under uncertainty: an econometric model for Bordeaux Crus Classés. Agric. Econ. *26*, 115–133. https://doi.org/10.1016/S0169-5150(00)00102-X.
12. Martin, G.J., Mazure, M., Jouitteau, C., Martin, Y.-L., Aguile, L., and Allain, P. (1999). Characterization of the Geographic Origin of Bordeaux Wines by a Combined Use of Isotopic and Trace Element Measurements. Am. J. Enol. Vitic. *50*, 409–417.
13. Ramirez, C.D. (2008). Wine Quality, Wine Prices, and the Weather: Is Napa "Different"? J. Wine Econ. *3*, 114–131. https://doi.org/10.1017/S1931436100001164.
14. Soar, C.J., Sadras, V.O., and Petrie, P.R. (2008). Climate drivers of red wine quality in four contrasting Australian wine regions. Aust. J. Grape Wine Res. *14*, 78–90. https://doi.org/10.1111/J.1755-0238.2008.00011.X.
15. Corsi, A., and Ashenfelter, O. (2019). Predicting Italian Wine Quality from Weather Data and Expert Ratings. J. Wine Econ. *14*, 234–251. https://doi.org/10.1017/JWE.2019.41.
16. di Vittorio, A., and Ginsburgh, V. (1996). Red wines of Medoc vintages from 1949 to 1989 at Christie's auctions. J. Soc. Stat. Paris *137*, 19–49.
17. Lecocq, S., and Visser, M. (2006). Spatial Variations in Weather Conditions and Wine Prices in Bordeaux. J. Wine Econ. *1*, 114–124. https://doi.org/10.1017/S1931436100000158.
18. Webb, L., Whetton, P., and Barlow, E. (2008). Modelling the relationship between climate, winegrape price and winegrape quality in Australia. Clim. Res. *36*, 89–98. https://doi.org/10.3354/cr00739.
19. Byron, R.P., and Ashenfelter, O. (1995). Predicting the Quality of an Unborn Grange. Econ. Rec. *71*, 40–53. https://doi.org/10.1111/J.1475-4932.1995.TB01870.X.
20. Gambetta, G.A., and Kurtural, S.K. (2021). Global warming and wine quality: are we close to the tipping point? OENO One *55*, 353–361. https://doi.org/10.20870/OENO-ONE.2021.55.3.4774.
21. Bonada, M., Edwards, E.J., McCarthy, M.G., Sepúlveda, G., and Petrie, P.R. (2020). Impact of low rainfall during dormancy on vine productivity and development. Aust. J. Grape Wine Res. *26*, 325–342. https://doi.org/10.1111/AJGW.12445.
22. Nemani, R.R., White, M.A., Cayan, D.R., Jones, G.v., Running, S.W., Coughlan, J.C., and Peterson, D.L. (2001). Asymmetric warming over coastal California and its impact on the premium wine industry. Clim. Res. *19*, 25–34. https://doi.org/10.3354/CR019025.
23. Jones, G.V., White, M.A., Cooper, O.R., and Storchmann, K. (2005). Climate change and global wine quality. Clim. Change *73*, 319–343. https://doi.org/10.1007/s10584-005-4704-2.
24. Wickham, H., Averick, M., Bryan, J., Chang, W., McGowan, L., François, R., Grolemund, G., Hayes, A., Henry, L., Hester, J., et al. (2019). Welcome to the {tidyverse. J. Open Source Softw. *4*, 1686. https://doi.org/10.21105/joss.01686.
25. Muñoz Sabater, J. (2019). ERA5-Land hourly data from 1981 to present. Copernicus Climate Change Service (C3S) Climate Data Store (CDS). https://doi.org/10.24381/cds.e2161bac.
26. Kusch, E., and Davy, R. (2022). KrigR—a tool for downloading and statistically downscaling climate reanalysis data. Environ. Res. Lett. *17*, 024005. https://doi.org/10.1088/1748-9326/ac48b3.
27. Wijnimport, B. (2022). BordOverview. https://www.bordoverview.com/.
28. Rodó, X., and Comín, F.A. (2000). Links between large-scale anomalies, rainfall and wine quality in the Iberian Peninsula during the last three decades. Global Change Biol. *6*, 267–273. https://doi.org/10.1046/J.1365-2486.2000.00299.X.
29. Dalu, J.D., Baldi, M., Marta, A.D., Orlandini, S., Maracchi, G., Dalu, G., Grifoni, D., and Mancini, M. (2013). Mediterranean climate patterns and wine quality in North and Central Italy. Int. J. Biometeorol. *57*, 729–742. https://doi.org/10.1007/S00484-012-0600-4/FIGURES/15.
30. Styles, O. (2004). Emile Peynaud Dies at 92 (Decanter).
31. Grifoni, D., Mancini, M., Maracchi, G., Orlandini, S., and Zipoli, G. (2006). Analysis of Italian Wine Quality Using Freely Available Meteorological Information. Am. J. Enol. Vitic. *57*, 339–346.
32. Isidoro, D., and Grattan, S.R. (2011). Predicting soil salinity in response to different irrigation practices, soil types and rainfall scenarios. Irrigat. Sci. *29*, 197–211. https://doi.org/10.1007/S00271-010-0223-7/FIGURES/8.
33. Jones, J.E., Wilson, S.J., Lee, G., and Smith, A.M. (2010). Effect of frost damage and pruning on current crop and return crop of Pinot Noir *38*, 209–216. https://doi.org/10.1080/01140671.2010.498402.
34. Machard, A., Inard, C., Alessandrini, J.M., Pelé, C., and Ribéron, J. (2020). A Methodology for Assembling Future Weather Files Including Heatwaves for Building Thermal Simulations from the European Coordinated Regional Downscaling Experiment (EURO-CORDEX) Climate Data. Energies *13*, 3424. https://doi.org/10.3390/EN13133424.
35. Ivits, E., Cherlet, M., Tóth, G., Sommer, S., Mehl, W., Vogt, J., and Micale, F. (2012). Combining satellite derived phenology with climate data for climate change impact assessment. Global Planet. Change *88*, 85–97. https://doi.org/10.1016/J.GLOPLACHA.2012.03.010.
36. Cliff, M.A., and King, M.C. (2007). The evaluation of judges at wine competitions: the application of Eggshell plots. J. Wine Res. *8*, 75–80. https://doi.org/10.1080/09571269708718104.
37. Cao, J., and Stokes, L. (2010). Evaluation of Wine Judge Performance through Three Characteristics: Bias, Discrimination, and Variation. J. Wine Econ. *5*, 132–142. https://doi.org/10.1017/S1931436100001413.
38. Castriota, S., Curzi, D., and Delmastro, M. (2013). Tasters' bias in wine guides' quality evaluations *20*, 1174–1177. https://doi.org/10.1080/13504851.2013.797552.
39. Livat, F., and Vaillant, N.G. (2006). Expert opinion and brand reputation: An analysis from a French Cuban cigars guidebook. Appl. Econ. Lett. *13*, 97–100. https://doi.org/10.1080/13504850500390564.
40. Reuter, J. (2009). Does Advertising Bias Product Reviews? An Analysis of Wine Ratings. J. Wine Econ. *4*, 125–151. https://doi.org/10.1017/S1931436100000766.
41. Drappier, J., Thibon, C., Rabot, A., and Geny-Denis, L. (2017). Relationship between wine composition and temperature: Impact on Bordeaux wine typicity in the context of global warming—Review *59*, 14–30. https://doi.org/10.1080/10408398.2017.1355776.

STAR★METHODS

KEY RESOURCES TABLE

REAGENT or RESOURCE	SOURCE	IDENTIFIER
Deposited data		
ERA-5 Land Hourly Weather Data	https://doi.org/10.24381/cds.e2161bac	
BordOverview Wine Database	https://www.bordoverview.com/	
Software and algorithms		
RStudio		
tidyverse packages		
Krigr package		

RESOURCE AVAILABILITY

Lead contact

Further information and requests for resources and reagents should be directed to and will be fulfilled by the lead contact, Andrew Wood (wood_and@hotmail.com).

Materials availability

This study did not generate new unique reagents.

Data and code availability

This paper analyses existing, publicly available data. All data is publicly available at locations referenced within the text. Wine data is available here: https://www.bordoverview.com/ and climate data from: https://cds.climate.copernicus.eu/cdsapp#!/dataset/10.24381/cds.68d2bb30?tab=overview as documented in the reference list and the key resources table. Any additional information required to reanalyse the data reported in this paper is available from the lead contact upon request.

METHOD DETAILS

This study is an analysis of the linkage between two key weather variables: temperature and precipitation, and the critic scores at a regional and local (AOC) level for the Bordeaux region. As in previous approaches,[7,23] analysis of the relationship between weather variables and wine quality scores are based upon the assumption that beneficial weather influences will lead to higher wine quality. The quality-weather interaction methodology can be split into two approaches. Both approaches fit critics scores against weather using a generalized linear model (GLM), but each uses different quantifications of weather as variables. The first approach uses the mean temperature and precipitation during discrete time-steps as the variables; the second approach uses the parameters of functions fitted to the temperature and precipitation data as the variables in statistical models of quality. All data extraction and analysis were undertaken in R version 4.2, using the *tidyverse*[24] and *baseR* packages.

Weather data

Historical weather data were extracted from the ERA-5 land reanalysis weather dataset[25] for each Bordeaux AOC region and central Bordeaux on a monthly time-step using the *Krigr* package[26] (see Table S1 for AOCs and their locations). ERA-5 land is a high temporal and spatial resolution interpolated dataset which is available on a 0.1° grid at time scales varying from hourly to monthly since January 1950.[25] Temperature and precipitation data were extracted on a monthly time-step for a 1km radius from the latitude and longitude point given per AOC for a period of January 1950 to December 2020. Temperature was measured in Kelvin (K), and precipitation in meters (m), both SI units for their respective measures. A growing season was defined as running from 1st November to 31st October, with harvest occurring at the end of the year. This aligns with standard growing season measurements (May-October) but extends them to include the overwintering effects (November-May).

Monthly weather variables were expectedly found to be strongly autocorrelated (Appendix 6), and thus unable to be used individually for building GLMs. Accordingly, months were grouped into autocorrelated groups, which could be roughly thought of as seasons. These groups were determined by those consecutive months by which the inter-month temperature or precipitation Pearson correlation coefficient was above 0.4. Winter was defined as being November and December, Spring as January to May, Summer as June to August, and Autumn as September and October.

A second way of dealing with this temporal autocorrelation is to describe temporal variation in the weather data to a continuous function. Precipitation is erratic, and hence to examine it in a continuous fashion, cumulative precipitation was used. The cumulative monthly precipitation was modeled linearly using a GLM, meaning that the cumulative precipitation can be approximated using the mean monthly precipitation.

Monthly mean temperature across the year were also described using a sine curve, as in Figure 1B. Non-linear least squares used to fit the data to the following equation:

$$\alpha \sin(\sigma M + \varphi) + \mu$$

Where M is the number of months since October, and $\alpha, \sigma, \varphi,$ and μ are parameters to be fitted. Figure 1B shows how each parameter relates to a part of the sine curve. Starting values for parameters were chosen based upon a fixed periodicity for σ and φ $(\sigma = \frac{2\pi}{12}, \varphi = 3)$. σ was chosen because of the annual cycle, hence division by twelve, and φ was chosen as October is 3 months after the approximate peak annual temperature. α and μ were fitted using the maximum, minimum and mean values of the temperature data per site and year using the equations: $\alpha = (\max(t) - \min(t))/2$; $\mu = \text{mean}(t)$.

Quality data

Annual quality scores were collected on two scales, regional and local. Regional critic scores are based on the opinions of how Bordeaux performed as a whole, with individual variation largely ignored and general trends suggested.[20] Local scores are based on individual wines, which are tasted *en primeur* and then rated based upon this premature wine.[27] For each, publicly available wine critic, scores were transformed into a standardized 0–100 scale. Whole region scores were available for the period of 1950–2020 and were drawn from several sources,[9,20] with additional data drawn from online vintage charts (see Table S2). Regional primeur critics scores for the period 2014–2020 were compiled by Bolomey Wijnimport[27] and consist of published ratings from major wine experts from France, UK, US, the Netherlands and Germany. All publications were tested for correlation between their scores, and 14 wine publications were chosen based on having a Pearson Correlation Coefficient of more than 0.4 with at least 3 other selected publications. This cut-off was chosen as a liberal threshold for the inclusion of publications in our analysis. The chosen cut-off means that at least 16% of the variance in critics scores can be attributed to a shared understanding of quality across 3 other publications. These scores were standardized within publications such that each was on a 0 to 100 scale. If wines were rated by more than one publication (78% wines) mean standardized scores were taken.

QUANTIFICATION AND STATISTICAL ANALYSIS

Generalized linear models

Generalised linear models (GLMs) were used to explore the relationship between weather and quality. A summary diagram of the models fitted can be found in Figure 1A. In the diagram, the number in the bottle refers to the model number, and tildes mean "is a function of". GLMs were chosen because they are a flexible modeling approach which does not require any particular error structure or variance.

As per model 1 in the summary diagram (Figure 1A), mean quality scores over time were investigated using a GLM with a binomial distribution and logit link, controlling for the critic. This was due to the bounded nature of the scoring system (0–100) and decreasing variation in quality scores over time. This allows for a comparison of longer-term regional versus local trends over time. At a regional scale, the yearly trend interacted with region to determine the differential baseline trend over time.

For both the regional (model 2, Figure 1A) and local (model 3, Figure 1A) level scores, a GLM with a Gaussian distribution was fitted between the mean of the annual critic scores and the normalized temperature and precipitation during each weather grouping, controlling for year and, in model 3, the AOC and Grand Cru status of the vineyard. Normality of residuals was checked visually using a qqplot and residuals vs. fitted plot. The seasonal means of temperature and precipitation were normalized by subtracting the mean of the weather group and dividing by the standard deviation (Standard Score normalisation). This means that the GLM examined the proportional positive or negative impact of each of the variables on quality, rather than the absolute value. In normalizing such environmental data, comparisons could be made between the variables and therefore the relative contributions of each can be ascertained. The year was controlled for by adding it as a continuous variable, and, in the AOC model, the locality was also controlled for by adding it as a factor.

GLMs were also built to compare the mean vintage score with weather treated as a continuous function (model 4, Figure 1A). This model utilized an additive Gaussian GLM to examine how each of these variables explained the variance within the mean critic scores, controlling for AOC, year, and class. These models were run for both temperature and precipitation separately and then together. We also ran a GLM without year as an explanatory variable due to covariance.

Climate change has desynchronized insect and vegetation phenologies across Europe

by

Yanru Huang[1,2,3], Chaoyang Wu[2,4*], Wenjiang Huang[1,2*], Yang Liu[5], Man Qi[3], Jie Bai[1,2], Yingying Dong[1,2], Samuel J L Gascoigne[3], Philippe Ciais[6], Josep Peñuelas[7,8], Roberto Salguero-Gómez[3*]

[1] State Key Laboratory of Remote Sensing Science, Aerospace Information Research Institute, Chinese Academy of Sciences, Beijing 100094, China
[2] University of Chinese Academy of Sciences, Beijing 100049, China
[3] Department of Biology, University of Oxford, Oxford OX1 3SZ, UK
[4] The Key Laboratory of Land Surface Pattern and Simulation, Institute of Geographical Sciences and Natural Resources Research, Chinese Academy of Sciences, Beijing, China
[5] State Key Laboratory of Information Engineering in Surveying, Mapping and Remote Sensing, Wuhan University, Wuhan 430079, China
[6] Laboratoire des Sciences du Climat et de l'Environnement, IPSL-LSCE CEA CNRS UVSQ, 91191, Gif sur, Yvette, France
[7] CSIC, Global Ecology Unit CREAF-CSIC-UAB, Bellaterra, Barcelona 08193, Catalonia, Spain
[8] CREAF, Cerdanyola del Valles, Barcelona 08193, Catalonia, Spain

Keywords: climate change, environmental sensitivity, insect citizen science, phenological mismatch, vegetation phenology, voltinism.

***Email:** wucy@igsnrr.ac.cn, huangwj@aircas.ac.cn, rob.salguero@biology.ox.ac.uk

Summary

Climate change is drastically affecting the phenologies of species worldwide, including shifts in development[1–3]. The potential impact of climate change on the synchronicity of plant-insect phenology is particularly concerning since the stability of pollination networks and food chains depends on their tight temporal dependencies[4–6]. Furthermore, the recently reported "insect armageddon"[7] makes it urgent to establish trends and identify primary drivers of plant-insect phenological synchrony. Here, coupling high-resolution remote sensing and citizen science data across Europe over 34 years, we examine the differences in occurrence dates of 1,584 herbivorous insects across four orders and the corresponding dates of leaf unfolding. We find that 61.2% of the vegetation and insect phenologies have become highly asynchronous, with vegetation phenology advancing four-fold faster than insect phenology. These trends were modulated by insects' life-cycles and taxonomic order. A primary driver of this phenological mismatch is the higher sensitivity of vegetation phenology than insect phenology to climate, which has prevented insects from matching the pace of plant phenological advance in the growing season. Our analyses provide a unique continental overview and underlying mechanisms of the asynchronicity between vegetation and insect phenologies, thus enhancing our ability to predict and manage its potential cascading ecological effects.

Main

The timing of events during the life cycle of an organism (e.g., maturation, reproduction, and dispersal) is fundamental to its persistence[8]. Species phenologies are key to the maintenance of entire communities[9] and their ecosystem services[10]. Important phenological shifts, however, have been reported worldwide in recent decades[11]. For example, global warming has advanced the date of laying of great tits (*Parus major*) by more than two weeks in the last six decades[12], and the start of the growing season on the Qinghai-Tibetan Plateau has advanced by nearly 10 days in the last two decades[13].

Phenological shifts due to climate change are thought to optimise species fitness, or at least to reduce the negative impacts of a changing environment[14]. Not all phenological shifts, however, are equal, nor do they have the same consequences. The direction and intensity of phenological shifts vary considerably across taxa[15], locations[16], and environments[17]. Importantly, species within a community can have different phenological shifts in response to the same climatic driver, thereby disrupting food webs[18]. Climate change consequently has the potential to impede the temporal and spatial synchrony of biological interactions, ultimately leading to trophic collapse[19].

The phenological synchrony between vegetation and insects at a given location ensures the match between the supply and demand of resources. This temporal match is crucial to maintain the flow of energy in food chains, which ultimately support viable populations and biodiversity[20]. Insect feeding is tightly linked to specific stages of vegetation development because this relationship ensures that insects obtain the required resources[21]. Phenological asynchrony emerges when the phenologies of co-existing vegetation and insects shift at different rates and/or in different directions[22]. The ecological consequences of this phenomenon can be devastating, including mismatches in food-pollinator interactions[23] or the decline in insect biodiversity[24,25]. Indeed, 17-50% of pollinators are projected to experience interruptions in food supply due to phenological mismatches under the on-going gradual warming[26]. Eighty-four percent of crops cultivated in Europe directly depend on insect-mediated pollination for their yield[27], so a potential mismatch between the phenologies of vegetation and insects poses an important threat to the stability of both ecosystems and livelihoods.

The impacts of climate change on the synchrony of vegetation and insect phenologies have been debated for decades. Some studies suggest that climate change has negative impacts on the synchrony of vegetation and insect phenologies[28,29], but others propose that some species may adapt to climate change and maintain the temporal synchrony of their biological events[21,30]. Approaches to examine this mismatch have predominantly used manipulative experiments and ground-based observations[31,32]. However, we still lack a generalized view about how climate change affects phenological synchrony across large scales and diverse taxa, because findings remain specific to species, geography, and experiment[33]. Remote-sensing studies have verified the widespread advance of vegetation phenology in spring and its delay in autumn in recent decades[34]. The main controversy is about insect phenology, which is characterized by greater complexity and dynamism than vegetation phenology. This complexity challenges our efforts to monitor insect phenology. Fortunately, data from citizen scientists provide a valuable resource for the extensive, long-term, and multispecies insect monitoring[35]. Integrating data from multiple sources can finally allow a comprehensive assessment of the synchrony between vegetation and insect phenologies.

Here, we investigate the trends and driving factors of phenological (a)synchronies between vegetation and insects across Europe from 1982 to 2015, supported by high-resolution remotely sensed data and citizen science. Specifically, (1) we quantify the rate and direction of shifts in vegetation phenology, insect phenology, and their differences (vegetation-insect phenological difference, VID) at both continental and regional scales across Europe. We test four hypotheses about the trends of changes in VID (Figure 1). (2) We next evaluate whether the rate and direction of changes in VID differs amongst insect orders (Hemiptera, Hymenoptera, Coleoptera, and Lepidoptera) and life-cycle voltinism (i.e., number of generations produced per year), and how these differences manifest themselves across latitudinal gradients. Finally, (3) we analyze the differences in the sensitivity of vegetation and insect phenologies to changes in environmental factors. We identify the likely environmental factors driving the asynchrony in VID by combining these analyses with the trends of climate change.

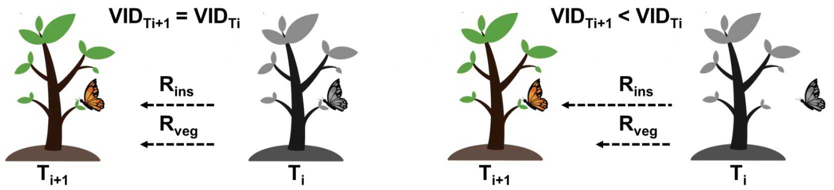

(H1) Stable phenology

(H2) Synchronizing phenology

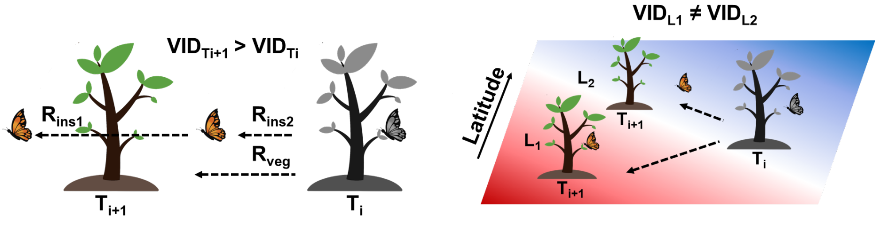

(H3) Asynchronizing phenology

(H4) Mixed phenology

Figure 1. We test four hypotheses regarding how climate change may have shaped vegetation-insect phenological differences (VID) across Europe in recent decades. **H1 - stable phenology**: the rate of advance (R_{veg} and R_{ins}) does not differ significantly between vegetation phenology (leaf-unfolding date, LUD) and insect phenology (insect occurrence date, IOD), so the change between the initial state VID_{Ti} (grey tree and grey butterfly) and VID_{Ti} (coloured tree and butterfly) would not be large. **H2 - synchronising phenology**: the peak of the phenology of insects starts after the peak of the phenology of vegetation, but both synchronise so that VID_{Ti+1}

$< VID_{Ti}$, because $R_{veg} < R_{ins}$. **H3 - asynchronising phenology**: VID_{Ti+1} is larger than VID_{Ti} , with two potential scenarios: ① $R_{veg} > R_{ins1}$, and ② $R_{veg} < R_{ins2}$. **H4 - mixed phenology**: the spatial trends of VID differs latitudinally due to the spatial heterogeneity of climate change. For example, location L_1 and location L_2 would initially have the same VID at time T_i, but VID_{L1} and VID_{L2} would differ significantly at time T_{i+1}. Both LUD and IOD advance as climate change progresses. The background colour in panel H4 represents the spatial heterogeneity of the climatic factors.

Phenological asynchrony between vegetation and insects has intensified

To establish trends and identify putative mechanisms in the phenological (a)synchronisation between vegetation and insects in Europe, we acquired 34 years of insect occurrence date (IOD) data for 1,584 species of herbivorous insects, observed by citizen scientists, and extracted the leaf-unfolding date of vegetation (LUD) at the corresponding spatiotemporal locations using remote sensing data (Figure S1). Using a quantile-regression model, we found that vegetation phenology LUD in Europe advanced by 12 days during 1982-2015 (-0.37 d/y ± 0.006 S.E.; Table S1), consistent with the estimate of vegetation phenology in spring in northern Europe[36]. In contrast, while insect phenology IOD also significantly advanced during the same period, it did so at a pace four-fold slower (-0.09 d/y ± 0.007) than the vegetation (Wilcoxon V = 199622, $P<0.001$) (Figure 2c). This lag in the advance of insect phenology relative to vegetation suggests a potential decoupling in trophic interactions[37]. Of the 1,807 insect phenological patterns, 79.6% had an increase in VID (with 61.2% being significant, $P<0.05$), only 20.4% exhibited a decrease in VID (with 7.4% significant, $P<0.05$), indicating an exacerbation of phenological asynchrony (H3 scenario ① in Figure 1) at a rate of nearly three days per decade (0.28 d/y ± 0.009; Figure 2d).

The regional rate of change in VID differed significantly between low latitudes (L_1: ≤55°N) (-0.02 d/y ± 0.004) and high latitudes (L_2: >55°N) (0.38 d/y ± 0.007) (Wilcoxon W = 1191, $P<0.001$) (Figure 2a, b, Table S2). The expected increase in VID was 0.03 d/y ± 0.001 for each degree increase in latitude. This pattern was attributed to the increased difference in the rates (R) of change of LUD and IOD between the high latitudes (R_{LUD} = -0.42 d/y ± 0.005, R_{IOD} = 0.02 d/y ± 0.003) and low latitudes (R_{LUD} = -0.19 d/y ± 0.005, R_{IOD} = -0.16 d/y ± 0.004). Our analysis also found that VID intensified phenological asynchrony along the latitudinal gradient, consistent with previous observations[5,17], as illustrated in panel H4 in Figure 1.

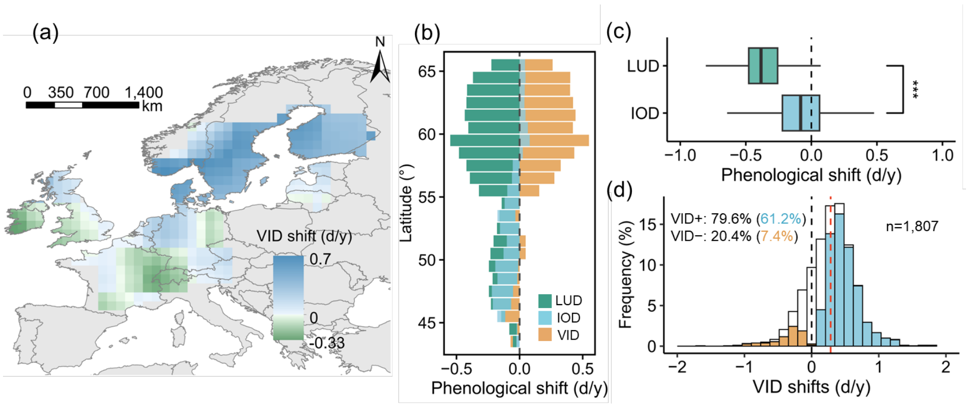

Figure 2. Synchronisation changes between the European leaf-unfolding date (LUD) of vegetation and the insect occurrence date (IOD) (1982-2015). (a) Spatial distribution of the rate of the shift in the vegetation-insect phenological difference (VID) at the regional scale using the moving window algorithm, with green and blue corresponding to synchronous and asynchronous matches in phenology, respectively. (b) Regional trends of LUD (green), IOD (blue), and VID (orange) with phenological shifts as a function of latitude. IOD shifts from advanced to slightly delayed, and LUD trends to increasingly advance as latitude increases. (c) Continental trends of phenological shifts in LUD and IOD, indicating how the phenology of vegetation advances more rapidly than the phenology of insects; ***, *P*<0.001, by a Wilcoxon signed-rank test. (d) The continental trend indicates that the VID of more species patterns is becoming asynchronous, where blue and orange indicate significant asynchronicity (VID+) and synchronicity (VID−), respectively, with white indicating no significant change. The red dashed vertical line represents the mean rate of shift in VID.

Rate of shift in the vegetation-insects phenological difference varies with taxonomic order and degree of voltinism

The shifts in VID across Europe in the last three decades indicated a strong specificity of insect order (Kruskal-Wallis $\chi^2(3)$ =158.26, *P*<0.001) (Figure 3a, Table S3). For example, the rate of shift of VID during the study period was fastest for Lepidoptera (e.g., butterflies and moths), at 0.34 d/y ± 0.01. This order was followed by Hemiptera (true bugs), with a shift in VID of 0.16 d/y ± 0.05, and by Hymenoptera (e.g., bees), with a shift of 0.15 d/y ± 0.04. In contrast, the rate of shift was slower for Coleoptera (beetles), at only 0.04 d/y ± 0.03. These findings suggested that Coleoptera adjusted their IOD ($R_{IOD} = -0.27$ d/y ± 0.02) most rapidly to match the changes in vegetation phenology, leading to fewer phenological patterns with significant VID shifts (27.72% $P<0.05$). Conversely, the phenology of Lepidoptera, with a slower rate of adaptation ($R_{IOD} = -0.04$ d/y ± 0.01), increasingly differed from vegetation phenology (78.23% $P<0.05$), consistent with recent findings for the mean changes in flight day amongst insect orders in Europe[6].

Further analyses identified significant differences in the rate of variation of VID for each insect order along the latitudinal gradient (L_1 low and L_2 high) (Figure 3c), thus supporting the mixed phenology hypothesis (Figure 1, H4). Differences in the rates of phenological change along the latitudinal gradient were nonetheless significant only between Lepidoptera and Coleoptera (Wilcoxon W = 76233, $P=0.025$) (Table S3). Specifically, Lepidoptera had a mean difference in rate of VID variation between low (L_1) and high (L_2) latitudes of 0.49 d/y ± 0.01, significantly higher than the difference for Coleoptera (0.38 d/y ± 0.05). This finding suggests that Coleoptera may adapt faster than Lepidoptera to environmental changes along latitudinal gradients, consistent with estimates for Danish beetles and butterflies[38].

Life-cycle voltinism was a key moderator of how insect phenology responded to climate change (Figure 3b, Table S4). Indeed, VID changed faster in univoltine (1 generation/yr) than multivoltine insects (>1 generation/yr; univoltine generation $R_u = 0.29 \pm 0.01$, first generation $R_{m1} = 0.19 \pm 0.03$; Wilcoxon W = 229365, $P<0.001$). This pattern is consistent with the findings of the phenological analysis of 130 lepidopteran species (including 39 multivoltine species) in the UK[3], in that univoltine insects in our study advanced their phenologies less (-0.09 d/y ± 0.01) than did the first generation of multivoltine insects (-0.15 d/y ± 0.02). This finding suggests that multivoltine insects may adapt more quickly than univoltine insects to climate change, possibly because more generations have more chances to adjust their life history strategies[39]. Of the 223 species of multivoltine insects in our data set with sufficient records (>400 records for each generation), 70.4% had lower rates of shifts in VID for the first voltine pattern compared to the second (second generation $R_{m2} = 0.38 \pm 0.03$, Wilcoxon V = 5977, $P<0.001$).

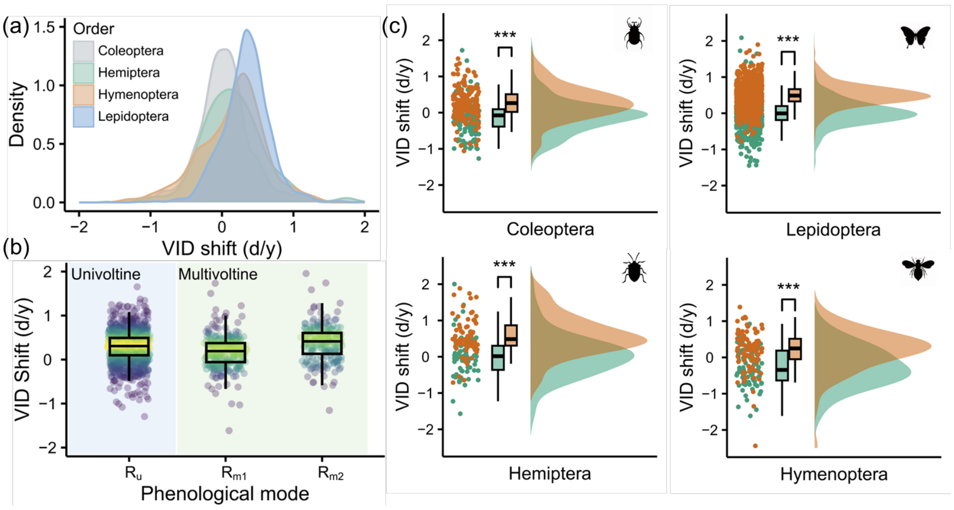

Figure 3. Shift in vegetation-insect phenological difference (VID) across insect orders and levels of life-cycle voltinism (i.e., number of generations/year), with beetles and multivoltine first-generation insects being more capable of tracking shifts in vegetation phenology. (a) Probability density curves of VID shifts across four insect orders. (b) VID shifts in univoltine insects (R_u) and multivoltine insects (first generation (R_{m1}), second generation (R_{m2})). The colours represent the density of data, with yellow and blue indicating high and low densities, respectively. (c) Differences in VID shifts along a latitudinal gradient in Europe for the four

insect orders, distinguishing between low (green: $L_1 \leq 55°N$) and high (orange: $L_2 > 55°N$) latitudes. ***, $P<0.001$ by a Wilcoxon signed-rank test.

Vegetation phenology is more sensitive than insect phenology to climate

The variation in VID could be attributed to the different directions and magnitudes of responses of vegetation and insect phenologies to the same environmental factors. We used statistical methods including partial correlation analysis, ridge regressions, and random forests (See Methods), to identify the likely environmental drivers of the phenological mismatch. The results of these analyses indicate that the average absolute sensitivity (|PC|, the partial correlation coefficient, and |RC|, the ridge regression coefficient) to environmental factors was generally higher for LUD than IOD, with six of the eight environmental factors differing highly significantly ($P<0.001$) (Figure 4a, b). This finding is consistent with long-term phenological studies in the northern Eurasian continent[18], suggesting that the vegetation, as primary producers, was more adjustable than insects to environmental conditions. We obtained consistent outcomes for both PC and RC (Spearman $\rho>0.73$, $P<0.001$): VID tended to synchronize ($PC_{LUD-IOD}$ and $RC_{LUD-IOD} >0$) with each unit increase in monthly evapotranspiration (ET), precipitation (PRE), wind speed (WIND), and soil-moisture content (SM). Conversely, VID shifted towards asynchrony ($PC_{LUD-IOD}$ and $RC_{LUD-IOD} < 0$) (Figure 4c) for each unit increase in monthly soil humidity (HU), solar radiation (RAD), air temperature (TEM), and soil temperature (ST). The analysis of the trends of environmental factors over 34 years (Figure S2) found that the overall increases in RAD, TEM, and ST, and the decreases in ET and WIND likely led to the intensification of the asynchronous VID in Europe. The thermal indicators (TEM and ST) had the largest average impact on LUD ($FI_{ST} = 0.16 \pm 0.002$, $FI_{TEM} = 0.16 \pm 0.002$) and IOD ($FI_{ST} = 0.13 \pm 0.001$, $FI_{TEM} = 0.15 \pm 0.001$) (Figure 4c). These findings are in agreement with recent research elucidating the key influence of temperature on vegetation and insect phenologies[16,40].

At the regional scale, the spatial differences of sensitivity of LUD and IOD to environmental factors, and trends of changes in environmental factors, collectively lead to an asynchronous intensification of VID along the latitudinal gradient. A total of 69% of VID values across Europe indicated a trend towards asynchrony ($R_{VID} > 0$; VID+), whereas only 31% showed a trend towards synchrony ($R_{VID} < 0$; VID−; Figure 2a). Further analyses identified a significant difference ($P<0.05$) in $RC_{LUD\text{-}IOD}$ between the VID+ and VID− regions (Figure S3). An analysis of the annual effect of environmental factors found that the increases in ST and HU, and the decrease in WIND, led to a stronger phenological asynchrony in the VID+ regions compared to the VID− regions (Figures 4e-g; S4). The environmental sensitivities of LUD and IOD generally varied significantly along the latitudinal gradient (Figure S5), representing the differences in environmental adaptability between populations at high and low latitudes[41].

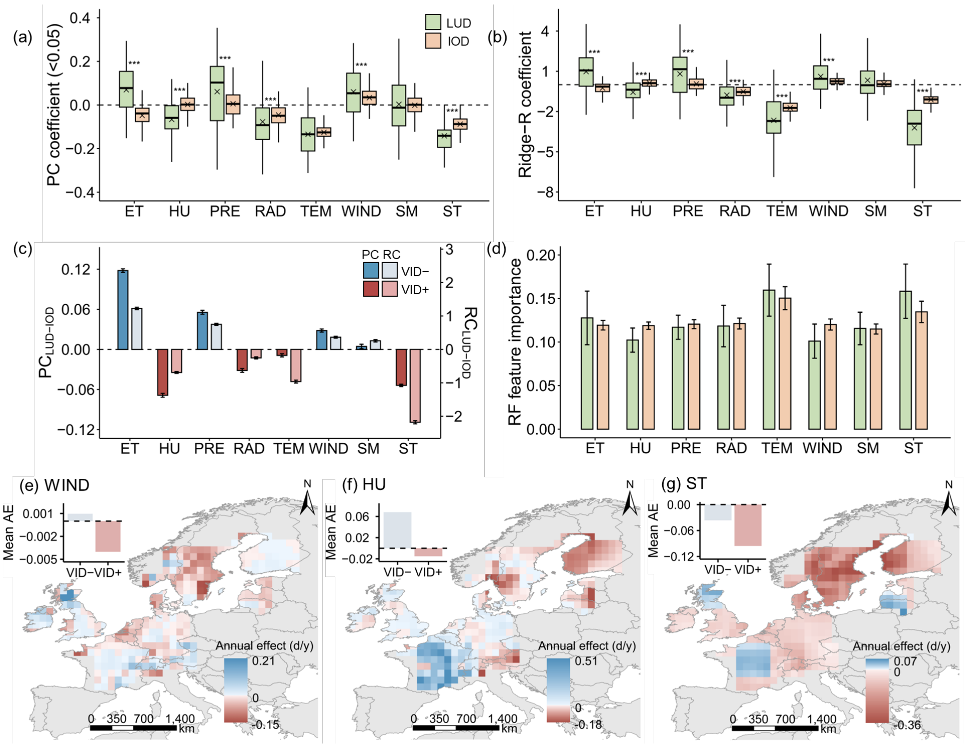

Figure 4. The asynchrony of the vegetation-insect phenological difference (VID) across Europe we report here has been primarily driven by the sensitivities of the leaf-unfolding date (LUD) and the insect occurrence date (IOD) to environmental factors. (a and b) LUD has a higher absolute sensitivity than IOD to environmental factors. (a) The partial correlation coefficient (PC) (only PC with $P<0.05$ were retained). (b) The ridge regression (Ridge-R) coefficients (RC); green refers to LUD, whereas orange refers to IOD. ***, $P<0.001$; **, $0.001\leq P<0.01$; *, $0.01\leq P<0.05$ by a Wilcoxon signed-rank test. (c) VID tends to synchronise with each unit increase in monthly evapotranspiration (ET), precipitation (PRE), average wind speed (WIND), and soil-moisture content (SM). VID shifts towards asynchrony for each unit increase in monthly relative humidity (HU), solar radiation (RAD), average temperature (TEM), and soil temperature (ST). Error bars represent ± S.E.; blue indicates VID tending towards synchrony (VID−: $PC_{LUD\text{-}IOD}$ and $RC_{LUD\text{-}IOD}$ >0), and red indicates VID tending towards

asynchrony (VID+: $PC_{LUD\text{-}IOD}$ and $RC_{LUD\text{-}IOD} < 0$). (d) The thermal indicators (TEM and ST) are most important for LUD and IOD. Random forest (RF) feature importance, indicating the relative importance of each factor for LUD and IOD, with a collective sum of 1; error bars represent ± S.D. (e-g) WIND, HU, and ST are key drivers of the significantly greater phenological asynchrony in the VID+ than the VID− regions. The annual effect (AE) estimates the yearly impact of the environmental factors on VID, calculated as $RC_{LUD\text{-}IOD} \times R_{ENV}$ (annual rate of change of the environmental factors; Figure S4).

3. Discussion

The extent and direction of changes in phenological synchrony are the outcome of intricate interactions between the life history strategies of plants and insects, their physiological characteristics, and external environmental stressors[30,37,42]. Here, we examined shifts in the phenology of 1,584 herbivorous insect species and the corresponding vegetation phenologies across Europe between 1982 and 2015, and found that the phenological synchrony between European vegetation and insects has gradually become more misaligned. This pattern was mostly attributed to more pronounced phenological advances for vegetation than insects, so maintaining the historical synchrony between insect and vegetation phenologies is likely to prove challenging going forward[37]. Notably, we found strong taxa- and life-cycle-specific effects on phenological shifts that are also in agreement with a study conducted in Ireland[43]. Finally, we found that the phenological mismatch across Europe was mostly due to increases in monthly radiation and air and soil temperatures, and decreases in evapotranspiration and wind speed.

One of the pivotal causes of the progressive misalignment between vegetation and insect phenologies was their different responses to external environmental conditions. Our study found that this asynchrony was not uniformly distributed but had distinct geographical patterns. Areas at higher latitudes have experienced a more pronounced decoupling of vegetation-insect phenological synchrony in recent decades. We found that this phenological asynchrony was not only associated with the pace and magnitude of climate change in these regions, but was also associated with the spatial variations in the sensitivities of vegetation and insect phenologies to different climatic factors, a finding in agreement with other reports in other regions across the world[15,44]. European vegetation has generally become more sensitive to environmental fluctuations compared to insects in the last 34 years. The phenological mismatch between vegetation and insects may continue to worsen over time, because climatic predictions project a future scenario of continued increases in global temperatures. Multispatial and temporal-scale analyses, such as ours, are imperative for understanding and forecasting this phenomenon due to the disparities across geographical regions and biological taxa[45].

Open-access data sets containing data from the long-term monitoring of vegetation and insect phenologies have fortunately become more available. Such integrated data will aid in deepening our understanding of the interactive dynamics between vegetation and insects under climate change[46]. Approaching the analytical outcomes of these data sets with caution, however, is crucial due to inevitable taxonomic and biogeographical sampling biases[47].

The phenological misalignment between vegetation and insects could have profound implications for food webs, ecosystem functions, and ecosystem services[9]. Vegetation-insect asynchrony may potentially strongly affect population structure, adaptability, and species niches[25,49,50]. We must identify the potential physiological and ecological mechanisms underlying the different phenological responses of vegetation and insects to enhance our ability to predict and mitigate the impacts of phenological asynchrony[45]. Future research should focus on the complex interactions within interspecific phenological networks and the potential impacts of both biotic and abiotic factors on phenological changes[24,51]. It should also pay close attention to high-latitude areas, where phenological changes are more pronounced[22], as we found, which will aid in deepening our understanding of the unique patterns and consequences of phenological asynchrony in regions experiencing intensified climate change. These large-scale, integrative approaches will provide a robust scientific basis for ecological conservation, the management of resources, and the development of policies.

Methods

Satellite-derived data for spring vegetation phenology. The satellite-derived leaf unfolding date (LUD) was determined using the Normalized Difference Vegetation Index (NDVI). We thus accessed the GIMMS NDVI3g data set (http://poles.tpdc.ac.cn/en/data/), a product derived from the Advanced Very High-Resolution Radiometer (AVHRR)[52]. This data set has a temporal resolution of 15 days and a spatial resolution of 8 km^2. We focused on pixels of vegetation in the temperate terrestrial ecosystems of Northern Hemisphere (>30°N) for 1982-2015, where the dynamics of vegetation phenology were strongly seasonal. We excluded pixels with an annual mean NDVI < 0.1 to reduce the effect of sparse vegetation[53]. We identified pixels with a continuous daily average temperature <0 °C for at least five days as the snow-contaminated phase and replaced them with the NDVI of the nearest snow-free date[54] to minimise the impact of snow. We then smoothed the curves of daily NDVI time series using the Savitzky-Golay method[55] to reduce the effect of noise from atmospheric disturbance. Finally, we extracted the average LUD using three methods to ensure the robustness of the results: (1) the dynamic-threshold method[56], (2) the piecewise logistic function method[57], and (3) the modified double-logistic function method[58] (see details below).

The dynamic threshold method determines the threshold of LUD using the proportion of the smoothed NDVI annual time series as:

$$NDVI_{ratio} = \frac{NDVI_i - NDVI_{\min}}{NDVI_{\max} - NDVI_{\min}}$$

where $NDVI_i$ is the NDVI on the i-th day of a year (DOY), $NDVI_{\max}$ and $NDVI_{\min}$ are the annual peak and minimum NDVI values, respectively, and LUD is the date whenspring $NDVI_{ratio}$ first increases to 0.5.

The piecewise-logistic function method divides the smoothed curve of the NDVI time series into two periods, before and after the annual peak (α). This method then fits the daily curve using the piecewise logistic function:

$$NDVI_i = \begin{cases} \dfrac{c_1}{1+e^{a_1+b_1 t}} + d_1, i \le \alpha \\ \dfrac{c_2}{1+e^{a_2+b_2 t}} + d_2, i < \alpha \end{cases}$$

where a and b are fitting parameters, with a as the initial rate of increase in NDVI and b as the rate of change of NDVI with time, c is the amplitude of the change of NDVI change (i.e., the difference between the peak and background values), and d is the NDVI background value.

Finally, the modified double-logistic function method fits a smoothed curves of the NDVI time series using a double-logistic function:

$$NDVI_i = \alpha_1 + \frac{\alpha_2}{1+e^{-\partial_1(t-\beta_1)}} - \frac{\alpha_3}{1+e^{-\partial_2(t-\beta_2)}}$$

where α_1 is the background NDVI, α_2 is the difference between the summer peak NDVI and the spring minimum NDVI, and α_3 is the difference between the summer peak NDVI and the autumnal minimum NDVI. ∂_1 and ∂_2 are the curvatures of the ascending and descending phases, respectively, and β_1 and β_2 are the average DOYs of vegetation greening and senescence, respectively.

Records of occurrence of herbivorous insects across Europe. We used records of the occurrence of herbivorous insects from crowdsourced data sets to calculate insect phenology due to the limitations of precise spatial and temporal coverage and species representation of phenological records for herbivorous insects. We searched the Global Biodiversity Information Facility (GBIF, https://www.gbif.org/) for all occurrences of species of four insect orders

(Hemiptera, Hymenoptera, Coleoptera, and Lepidoptera) across Europe (Lon -11° to 35°, Lat 34° to 71°) for 1982-2015. This search found a total of 2,937 insect species. We next excluded insects that primarily depended on predation, parasitism, or saprophagy during any stage of their life cycles. We also removed duplicate entries and records with inaccurate coordinates (uncertainty > 1 km^2). The final database retained ≥8 million observations.

Classification of insect phenological patterns. We classified the complex life histories of insects based on their degree of voltinism (i.e., the number of generations in one year). Variation in voltinism in insects can thus produce either unimodal or multimodal phenological patterns and is linked to important ecological processes such as population dynamics and community interactions[59]. The timing and peak period of occurrence of insect larvae and their adults may differ considerably[60]. These different developmental stages have distinct nutritional requirements and ecological effects, e.g. the herbivory of larvae and the pollinating behaviour of adults[61,62]. We removed records of occurrence with life-stage labels of egg, larval, or pupal stages (<1%) from our data set due to the lack of data to support modelling. We thus focused our modelling only on the mean date of occurrence of adults.

We calculated the probability density of species records for each DOY (Day of the year) to obtain the annual fluctuations of insect population and subsequently smoothed the probability-density curve using Gaussian filters[63] and Savitzky-Golay filters to reduce noise. We next used the find_peaks function from the "scipy" Python package to determine whether a species had multimodal phenology (i.e., more than one population peak). We then refined the phenological patterns following a thorough comparison with both scientific and grey literature[6]. We found that 295 species had multimodal patterns of distribution (Figure S6). We also used the K-Means algorithm to classify the records of the occurrences of these species:

$$J(p, IOD) = \sum_{i=1}^{k} \sum_{(x \in p_i)} \left\| IOD_x - IOD_i \right\|^2$$

where k is the number of phenological patterns (number of clusters), IOD_i is the mean date of the occurrence of insects for phenological pattern p_i, and $\left\| IOD_x - IOD_i \right\|^2$ is the squared Euclidean distance between each insect occurrence date (IOD_x) and the mean observed date (IOD_i) of each group of phenological patterns. The K-Means algorithm was thus used to find the optimal phenological classification that minimises the mean squared error (MSE) of the objective function $J(p, IOD)$[64]. We calculated k-means for $k = 2$ to the maximum number of peaks to determine the optimal number of patterns. We recorded the silhouette coefficient (SC)[65] for each k. The number of clusters with the maximum SC was considered as the best number of patterns k_{opt}. We removed outliers with residuals >3 S.D. during the clustering and removed phenological patterns with fewer than 400 records due to the uncertainty of the crowdsourced data in our data set. Finally, we identified 1,807 phenological patterns encompassing a total of 1,584 species (Figure S1).

Spatiotemporal differences in the analysis of vegetation-insect phenology. We evaluated the overall trend of variation in vegetation phenology, insect phenology, and their differences (VID) over time and geographical locations. We applied a quantile-regression model to each of the 1,807 phenological patterns to ensure the robustness of our estimation results:

$$Q_\tau(Y_x | year, Lat, Lon) = \alpha + \beta_1 \times year + \beta_2 \times Lat + \beta_3 \times Lon + \beta_4 \times (Lat \times Lon)$$

where, Q_τ is the τ quantile, with $\tau = 0.5$ set as the median. Y_x is the response variable corresponding to observation record x (leaf unfolding date, LUD_x; insects occurrence date, IOD_x; or vegetation-insect difference, VID_x). In this equation α is the intercept, and β_1, β_2,

β_3 and β_4 are the coefficients for the year, latitude (Lat), longitude (Lon), and interaction term, respectively. We defined the rate of change of Y_x relative to the predictor variables as the absolute value of β_i; this rate of change was positive when the absolute value of the response variable increased between 1980 and 2015 and negative when it decreased.

We divided the phenological patterns into areas at high (>55°N) and low (≤55°N) latitudes for separate quantile-regression models. We calculated the trends of the four insect orders separately to avoid the dominance of Lepidoptera species (>70%) and to determine whether the changes in VID had significant geographical patterns, while also considering the limitations of spatial data. We also conducted spatial statistics to obtain local trends. We thus divided Europe into 5×5° geographical grids based on a grid analysis and used a moving-window algorithm[6,41]. Briefly, the algorithm moved by 1-4° in longitude or latitude, and the quantile-regression models of the phenological patterns for LUD, IOD, and VID were constructed grid-by-grid. We then averaged the results for the rate of change based on the 1×1° grid unit to minimise the variations in sampling public data across regions. We only retained the results from a single geographical grid that had at least 10 insect species, and each phenological pattern had a record of no less than 10 years[66], to ensure the reliability and representativeness of the data.

Analysis of the impact of environmental factors on vegetation and insect phenologies

Data acquisition. We incorporated two comprehensive data sets to obtain long-term environmental data from 1982 to 2015 across Europe for elucidating the influence of environmental factors on the vegetation and insect phenologies (Table S5).

The E-OBS data set, a daily gridded data set of terrestrial observations for Europe, is based on the network of stations of the European Climate Assessment & Dataset (ECA&D) project[67].

This data set aggregates many types of data directly from the European National Meteorological and Hydrological Services. Its comprehensive nature makes it an indispensable data set for monitoring the climate across Europe[68]. We obtained meteorological data from the E-OBS 27.0e data set (accessible at https://www.ecad.eu/download/ensembles/download.php) on average air temperature (TEM), precipitation (PRE), average wind speed (WIND), average relative humidity (HU), and global solar radiation (RAD). These data, with a spatial resolution of 0.1×0.1°, were further processed to deduce monthly averages.

We incorporated soil parameters into our assessment in recognition of the pivotal interplay between soil and both vegetation growth and insect activity, most notably in the realms of nutrient cycling and habitat provisioning[69], using the ECMWF Reanalysis v5 (ERA5)-Land reanalysis data set[70]. ERA5, unlike its predecessor, offers a consistent portrayal of the evolution of terrestrial variables over several decades, but at a heightened resolution. Specifically, we extracted data from the monthly ERA5-Land data set (accessible at https://cds.climate.copernicus.eu/#!/home) on soil temperature (ST) and soil-moisture content (SM). We also obtained evapotranspiration (ET) metrics from the data set, where negative values indicate evaporation and positive values indicate condensation, due to the integral role of transpiration in maintaining vegetation health and its consequential potential microclimatic impacts on insect populations[71].

Analytical strategy. We used a partial correlation analysis[72] to separately identify the effects of the environmental factors on the vegetation and insect phenologies for understanding the underlying causes of changes in VID (TEM, PRE, WIND, HU, RAD, SM, ST, and ET in Figure 4). Environmental factors usually affect biological phenology in the months before its onset. Considering the variation in the times of insect observation, the environmental factors were detrended and standardized using linear regression to remove the multiyear trend[73]. The optimal preseason length was defined as the period during which phenology (IOD or LUD) and the environmental factors had the highest absolute correlation for each species, with the search extending up to six months before the average time of the phenology[4]. We then conducted a partial correlation analysis using the "pingouin" Python package, calculating the partial correlation coefficient (PC) and significance for each environmental factor with phenology, while controlling for other variables.

We used ridge regression (Ridge-R)[75] and the random-forest method (RF)[76] from the "sklearn" Python package to assess the contribution of the environmental factors to the shift in VID, minimising the influence of collinearity. Phenology (IOD or LUD) was the response variable, with environmental factors with optimal preseason times as the predictive variables. The regression coefficient (RC) in Ridge-R was used to assess environmental sensitivity, representing the number of days the phenology advanced or delayed per unit standardised change in the environmental factor. The feature importance in the RF method was evaluated by measuring the decrease in impurity (MSE) each time a feature was split[75]. We similarly used the moving-window algorithm to conduct the three methods at the regional scale to understand the spatial patterns of the impacts of the environmental factors on the variation of VID.

Author Contributions

C.W. proposed the original idea. R.S-G. and W.H. designed the research framework. Y.H. processed all data, derived models, generated figures, and drafted the manuscript. R.S.-G. guided its execution. All authors contributed to the writing of this study.

Acknowledgments

C.W., W.H., and Y.D. were supported by National Key R&D Program of China (2023YFB3906200) and National Natural Science Foundation of China (42125101, 42071320). Y.H. was supported by the China Scholarship Council (202204910383). R.S.-G. was supported by NERC Pushing the Frontiers (NE/X013766/1).

References

1. Horton, K. G. *et al.* Phenology of nocturnal avian migration has shifted at the continental scale. *Nat. Clim. Chang.* 10, 63–68 (2020).
2. Möhl, P., von Büren, R. S. & Hiltbrunner, E. Growth of alpine grassland will start and stop earlier under climate warming. *Nat Commun* 13, 7398 (2022).
3. Macgregor, C. J. *et al.* Climate-induced phenology shifts linked to range expansions in species with multiple reproductive cycles per year. *Nat Commun* 10, 4455 (2019).
4. Høye, T. T., Post, E., Schmidt, N. M., Trøjelsgaard, K. & Forchhammer, M. C. Shorter flowering seasons and declining abundance of flower visitors in a warmer Arctic. *Nature Clim Change* 3, 759–763 (2013).
5. Burgess, M. D. *et al.* Tritrophic phenological match–mismatch in space and time. *Nat Ecol Evol* 2, 970–975 (2018).
6. Duchenne, F. *et al.* Phenological shifts alter the seasonal structure of pollinator assemblages in Europe. *Nat Ecol Evol* 4, 115–121 (2020).
7. Blüthgen, N., Dicks, L. V., Forister, M. L., Outhwaite, C. L. & Slade, E. M. Insect declines in the Anthropocene. *Nat Rev Earth Environ* 1–4 (2023) doi:10.1038/s43017-023-00478-x.
8. Iler, A. M., CaraDonna, P. J., Forrest, J. R. K. & Post, E. Demographic Consequences of Phenological Shifts in Response to Climate Change. *Annual Review of Ecology, Evolution, and Systematics* 52, 221–245 (2021).

9. Visser, M. E. & Gienapp, P. Evolutionary and demographic consequences of phenological mismatches. *Nat Ecol Evol* 3, 879–885 (2019).

10. Beard, K. H., Kelsey, K. C., Leffler, A. J. & Welker, J. M. The Missing Angle: Ecosystem Consequences of Phenological Mismatch. *Trends in Ecology & Evolution* 34, 885–888 (2019).

11. Peñuelas, J. & Filella, I. Responses to a Warming World. *Science* 294, 793–795 (2001).

12. Cole, E. F., Regan, C. E. & Sheldon, B. C. Spatial variation in avian phenological response to climate change linked to tree health. *Nat. Clim. Chang.* 11, 872–878 (2021).

13. Shen, M. *et al.* Plant phenology changes and drivers on the Qinghai–Tibetan Plateau. *Nat Rev Earth Environ* 3, 633–651 (2022).

14. Singer, M. C. & Parmesan, C. Phenological asynchrony between herbivorous insects and their hosts: signal of climate change or pre-existing adaptive strategy? *Philosophical Transactions of the Royal Society B: Biological Sciences* 365, 3161–3176 (2010).

15. Dunn, P. O. *et al.* Extensive regional variation in the phenology of insects and their response to temperature across North America. *Ecology* 104, e4036 (2023).

16. Gutiérrez, D. & Wilson, R. J. Intra- and interspecific variation in the responses of insect phenology to climate. *Journal of Animal Ecology* 90, 248–259 (2021).

17. Ekholm, A., Tack, A. J. M., Bolmgren, K. & Roslin, T. The forgotten season: the impact of autumn phenology on a specialist insect herbivore community on oak. *Ecological Entomology* 44, 425–435 (2019).

18. Roslin, T. *et al.* Phenological shifts of abiotic events, producers and consumers across a continent. *Nat. Clim. Chang.* 11, 241–248 (2021).

19. Schleuning, M. *et al.* Ecological networks are more sensitive to plant than to animal extinction under climate change. *Nat Commun* 7, 13965 (2016).

20. Ren, Y. *et al.* Quantitative identification of yellow rust in winter wheat with a new spectral index: Development and validation using simulated and experimental data. *International Journal of Applied Earth Observation and Geoinformation* 102, 102384 (2021).

21. Kharouba, H. M., Vellend, M., Sarfraz, R. M. & Myers, J. H. The effects of experimental warming on the timing of a plant–insect herbivore interaction. *Journal of Animal Ecology* 84, 785–796 (2015).

22. Renner, S. S. & Zohner, C. M. Climate Change and Phenological Mismatch in Trophic Interactions Among Plants, Insects, and Vertebrates. *Annual Review of Ecology, Evolution, and Systematics* 49, 165–182 (2018).

23. Hegland, S. J., Nielsen, A., Lázaro, A., Bjerknes, A.-L. & Totland, Ø. How does climate warming affect

plant-pollinator interactions? *Ecology Letters* 12, 184–195 (2009).

24. Burkle, L. A., Marlin, J. C. & Knight, T. M. Plant-Pollinator Interactions over 120 Years: Loss of Species, Co-Occurrence, and Function. *Science* 339, 1611–1615 (2013).
25. Bell, J. R., Blumgart, D. & Shortall, C. R. Are insects declining and at what rate? An analysis of standardised, systematic catches of aphid and moth abundances across Great Britain. *Insect Conservation and Diversity* 13, 115–126 (2020).
26. Memmott, J., Craze, P. G., Waser, N. M. & Price, M. V. Global warming and the disruption of plant–pollinator interactions. *Ecology Letters* 10, 710–717 (2007).
27. Gallai, N., Salles, J.-M., Settele, J. & Vaissière, B. E. Economic valuation of the vulnerability of world agriculture confronted with pollinator decline. *Ecological Economics* 68, 810–821 (2009).
28. Parmesan, C. Influences of species, latitudes and methodologies on estimates of phenological response to global warming. *Global Change Biology* 13, 1860–1872 (2007).
29. Thackeray, S. J. *et al.* Phenological sensitivity to climate across taxa and trophic levels. *Nature* 535, 241–245 (2016).
30. van Asch, M., Salis, L., Holleman, L. J. M., van Lith, B. & Visser, M. E. Evolutionary response of the egg hatching date of a herbivorous insect under climate change. *Nature Clim Change* 3, 244–248 (2013).
31. Lemoine, N. P., Doublet, D., Salminen, J.-P., Burkepile, D. E. & Parker, J. D. Responses of plant phenology, growth, defense, and reproduction to interactive effects of warming and insect herbivory. *Ecology* 98, 1817–1828 (2017).
32. Fuentealba, A., Pureswaran, D., Bauce, É. & Despland, E. How does synchrony with host plant affect the performance of an outbreaking insect defoliator? *Oecologia* 184, 847–857 (2017).
33. Uelmen, J. A. *et al.* Effects of winter temperatures, spring degree-day accumulation, and insect population source on phenological synchrony between forest tent caterpillar and host trees. *Forest Ecology and Management* 362, 241–250 (2016).
34. Piao, S. *et al.* Plant phenology and global climate change: Current progresses and challenges. *Global Change Biology* 25, 1922–1940 (2019).
35. Samplonius, J. M. *et al.* Strengthening the evidence base for temperature-mediated phenological asynchrony and its impacts. *Nat Ecol Evol* 5, 155–164 (2021).
36. Jin, H. *et al.* New satellite-based estimates show significant trends in spring phenology and complex sensitivities to temperature and precipitation at northern European latitudes. *Int J Biometeorol* 63, 763–775

(2019).

37. Ge, Q., Wang, H., Rutishauser, T. & Dai, J. Phenological response to climate change in China: a meta-analysis. *Global Change Biology* 21, 265–274 (2015).
38. Thomsen, P. F. *et al.* Resource specialists lead local insect community turnover associated with temperature – analysis of an 18-year full-seasonal record of moths and beetles. *Journal of Animal Ecology* 85, 251–261 (2016).
39. Halsch, C. A. *et al.* Insects and recent climate change. *PNAS* 118, (2021).
40. Weaver, S. A. & Mallinger, R. E. A specialist bee and its host plants experience phenological shifts at different rates in response to climate change. *Ecology* 103, e3658 (2022).
41. Gao, M. *et al.* Three-dimensional change in temperature sensitivity of northern vegetation phenology. *Global Change Biology* 26, 5189–5201 (2020).
42. Gérard, M., Vanderplanck, M., Wood, T. & Michez, D. Global warming and plant–pollinator mismatches. *Emerging Topics in Life Sciences* 4, 77–86 (2020).
43. O'Neill, B. F. *et al.* Climatic change is advancing the phenology of moth species in Ireland. *Entomologia Experimentalis et Applicata* 143, 74–88 (2012).
44. Kharouba, H. M., Paquette, S. R., Kerr, J. T. & Vellend, M. Predicting the sensitivity of butterfly phenology to temperature over the past century. *Global Change Biology* 20, 504–514 (2014).
45. Chmura, H. E. *et al.* The mechanisms of phenology: the patterns and processes of phenological shifts. *Ecological Monographs* 89, e01337 (2019).
46. Kharouba, H. M., Lewthwaite, J. M. M., Guralnick, R., Kerr, J. T. & Vellend, M. Using insect natural history collections to study global change impacts: challenges and opportunities. *Philosophical Transactions of the Royal Society B: Biological Sciences* 374, 20170405 (2018).
47. Davis, C. L., Guralnick, R. P. & Zipkin, E. F. Challenges and opportunities for using natural history collections to estimate insect population trends. *Journal of Animal Ecology* 92, 237–249 (2023).
48. Van ASCH, M., Van TIENDEREN, P. H., Holleman, L. J. M. & Visser, M. E. Predicting adaptation of phenology in response to climate change, an insect herbivore example. *Global Change Biology* 13, 1596–1604 (2007).
49. Michielini, J. P., Dopman, E. B. & Crone, E. E. Changes in flight period predict trends in abundance of Massachusetts butterflies. *Ecology Letters* 24, 249–257 (2021).
50. Davies, W. J. Multiple temperature effects on phenology and body size in wild butterflies predict a complex

response to climate change. *Ecology* 100, e02612 (2019).

51. Thébault, E. & Fontaine, C. Stability of Ecological Communities and the Architecture of Mutualistic and Trophic Networks. *Science* 329, 853–856 (2010).
52. Tucker, C. J. *et al.* An extended AVHRR 8-km NDVI dataset compatible with MODIS and SPOT vegetation NDVI data. *International Journal of Remote Sensing* 26, 4485–4498 (2005).
53. Dong, L., Wu, C., Wang, X. & Zhao, N. Satellite observed delaying effects of increased winds on spring green-up dates. *Remote Sensing of Environment* 284, 113363 (2023).
54. Zhang, X. Reconstruction of a complete global time series of daily vegetation index trajectory from long-term AVHRR data. *Remote Sensing of Environment* 156, 457–472 (2015).
55. Chen, J. *et al.* A simple method for reconstructing a high-quality NDVI time-series data set based on the Savitzky–Golay filter. *Remote Sensing of Environment* 91, 332–344 (2004).
56. White, M. A. *et al.* Intercomparison, interpretation, and assessment of spring phenology in North America estimated from remote sensing for 1982–2006. *Global Change Biology* 15, 2335–2359 (2009).
57. Zhang, X. *et al.* Monitoring vegetation phenology using MODIS. *Remote Sensing of Environment* 84, 471–475 (2003).
58. Gonsamo, A., Chen, J. M., Price, D. T., Kurz, W. A. & Wu, C. Land surface phenology from optical satellite measurement and CO2 eddy covariance technique. *Journal of Geophysical Research: Biogeosciences* 117, (2012).
59. Altermatt, F. Climatic warming increases voltinism in European butterflies and moths. *Proceedings of the Royal Society B: Biological Sciences* 277, 1281–1287 (2009).
60. Nail, K. R., Stenoien, C. & Oberhauser, K. S. Immature Monarch Survival: Effects of Site Characteristics, Density, and Time. *Annals of the Entomological Society of America* 108, 680–690 (2015).
61. Wäckers, F. L., Romeis, J. & van Rijn, P. Nectar and Pollen Feeding by Insect Herbivores and Implications for Multitrophic Interactions. *Annual Review of Entomology* 52, 301–323 (2007).
62. Jacobsen, D. J. & Raguso, R. A. Lingering Effects of Herbivory and Plant Defenses on Pollinators. *Current Biology* 28, R1164–R1169 (2018).
63. Misra, G., Buras, A. & Menzel, A. Effects of Different Methods on the Comparison between Land Surface and Ground Phenology—A Methodological Case Study from South-Western Germany. *Remote Sensing* 8, 753 (2016).
64. Pedregosa, F. *et al.* Scikit-learn: Machine Learning in Python. *Journal of Machine Learning Research* 12,

2825–2830 (2011).

65. Yuan, C. & Yang, H. Research on K-Value Selection Method of K-Means Clustering Algorithm. *J* 2, 226–235 (2019).

66. Vitasse, Y. *et al.* Phenological and elevational shifts of plants, animals and fungi under climate change in the European Alps. *Biological Reviews* 96, 1816–1835 (2021).

67. Cornes, R. C., van der Schrier, G., van den Besselaar, E. J. M. & Jones, P. D. An Ensemble Version of the E-OBS Temperature and Precipitation Data Sets. *Journal of Geophysical Research: Atmospheres* 123, 9391–9409 (2018).

68. Wang, H. *et al.* Overestimation of the effect of climatic warming on spring phenology due to misrepresentation of chilling. *Nat Commun* 11, 4945 (2020).

69. Classen, A. T., Hart, S. C., Whitman, T. G., Cobb, N. S. & Koch, G. W. Insect Infestations Linked to Shifts in Microclimate. *Soil Science Society of America Journal* 69, 2049–2057 (2005).

70. Muñoz-Sabater, J. *et al.* ERA5-Land: a state-of-the-art global reanalysis dataset for land applications. *Earth System Science Data* 13, 4349–4383 (2021).

71. Castex, V., Beniston, M., Calanca, P., Fleury, D. & Moreau, J. Pest management under climate change: The importance of understanding tritrophic relations. *Science of The Total Environment* 616–617, 397–407 (2018).

72. Shen, M., Piao, S., Cong, N., Zhang, G. & Jassens, I. A. Precipitation impacts on vegetation spring phenology on the Tibetan Plateau. *Global Change Biology* 21, 3647–3656 (2015).

73. Liu, Q. *et al.* Modeling leaf senescence of deciduous tree species in Europe. *Global Change Biology* 26, 4104–4118 (2020).

74. Wu, C. *et al.* Increased drought effects on the phenology of autumn leaf senescence. *Nat. Clim. Chang.* 12, 943–949 (2022).

75. Hua, H. *et al.* Pine caterpillar occurrence modeling using satellite spring phenology and meteorological variables. *Environ. Res. Lett.* 17, 104046 (2022).

76. Gu, H. *et al.* Warming-induced increase in carbon uptake is linked to earlier spring phenology in temperate and boreal forests. *Nat Commun* 13, 3698 (2022).

From disturbances to nonlinear fitness and back

Shripad Tuljapurkar[1], Harman Jaggi[1], Samuel J. L. Gascoigne[2], Wenyun Zuo[1], Maja Kajin[2,3], and Roberto Salguero-Gómez[2]

[1]Stanford University, Department of Biology, CA, 94305, USA
[2]University of Oxford, Department of Biology, South Parks Road, Oxford OX1 3RB, UK
[3]University of Ljubljana, Department of Biology, Večna pot 111, 1000 Ljubljana, Slovenia

October 25, 2023

Abstract

A fundamental goal of Ecology is to predict how natural populations respond to disturbances. Accordingly, the last decades have witnessed key theoretical developments in stochastic demography and transient dynamics. However, both areas, have to date been largely disconnected. Here, we introduce an expression for the second derivatives of population growth rate with respect to demographic rates (*e.g.* survival-dependent state transitions and reproduction) with direct links to transient dynamics. We use this connection to develop a new mathematical framework showing how transient responses to pulse disturbances lead to a quantitative description of press disturbances. Second-derivatives of population growth rate with respect to said demographic rates are valuable as they quantify the degree of nonlinear selection acting on demographic rates and how environments shape the long-term performance of populations. Whilst valuable, previous methods to quantify second-order derivatives have heavily relied on vector calculus- potentially obscuring important demographic processes connected to second-order derivatives. Here we offer an intuitive method using perturbation theory and our approach is valid for any discrete-time, st(age)-based structured population model. Importantly, our new method implicates an intimate relationship between the nonlinear selection pressures acting on demographic rates with the emergent transient dynamics of populations over time. We showcase these relationships through mathematical proofs, connecting to Cohen's cumulative distance, and identifying a strong relationship between generation time across 439 unique plant and animal species (2690 population models). As such, this new method represents a valuable tool for population ecologists, comparative demographers, and conservation biologists to understand and protect structured populations in a changing world.

Introduction

The transient dynamics of structured systems (*e.g.*, populations, communities) are the system's responses following a pulse disturbance (Yang et al. 2008; Jentsch and White 2019). A pulse disturbance (such as an acute epidemic, fast invasion, or extreme, short weather event like a fire or hurricane) may perturb the system away from its stable state if it fails to resist the disturbance. As such transients are the dynamics that occur as the system returns back to the previous -or new- stable state (White et al. 2013; Tao et al. 2021). In contrast a press disturbance is a persistent change (e.g. global warming, river pollution) that alters the stable state itself in a more gradual manner (Donohue et al. 2016; Inamine et al. 2022). Though much attention has been paid both theoretically (Yang et al. 2008; Hastings 2001) and experimentally (Amor et al. 2020) to understand the responses of natural systems to pulse disturbances, not much theory or actual experimentation exists for their cousins: press disturbances (Inamine et al. 2022). Stage-structure population models represent a unique opportunity to marry both due to their temporal nature. These models treat time as a discrete entity, as the system is tracked every time unit, rather than continuously. As such, from the perspective of stage-structured models, a press disturbance can be viewed simply as a continuing series of pulses. Here, we focus on the consequences of that equivalence for natural populations by developing and applying new theory that explicitly links transient and stochastic population dynamics.

Here, we focus on populations structured by discrete stages (*e.g.*, age, size) and examined on discrete time: matrix population models (MPMs; (Caswell 2001b)). Under stationarity conditions, the population whose dynamics is described by a given MPM is at equilibrium, whereby the distribution of individuals in each of the states is defined by the stable structure distribution (hereafter SSD), a vector $\mathbf{u}_0$ and whose dynamics are guided by an exponential, fixed rate of growth, the population growth rate λ_0. A pulse disturbance that results in the deviation of the population vector from the SSD (*e.g.*, trophy hunting targets preferentially large/adult individuals (Traill et al. 2014), drought affects primarily juveniles in plant populations (Refsland and Fraterrigo 2018) will result in a transient dynamic as the population structure returns to the original -or a new (Capdevila et al. 2020)- SSD, as shown in the left panel of Fig 1. The pulse (*i.e.*, one-time) disturbance produces a change in population structure, and that change decays over time as the population structure returns to the SSD (indicated in the figure by vector $\mathbf{u}_0$).

In contrast, the effect of a press (*i.e.*, continued) disturbance can be thought of as the accumulation of the effect of repeated pulse disturbances, past and present, in a discrete time modelling framework. As illustrated in the right panel of Fig 1, the population structure reflects the current pulse disturbance, plus the decaying remnants of previous pulse disturbances. The cumulative result is to push population structure away from the original SSD to a new SSD (indicated in the figure by vector $\mathbf{u}_0'$).

We use this connection to develop a new mathematical framework showing how transient responses to pulse disturbances lead to a quantitative description of press disturbances. Press disturbances result in a linear change in the SSD but a nonlinear change in the population growth rate. Our analysis focuses on small disturbances and yields new expressions for the first derivatives of the SSD and the second derivatives of population growth rate with respect to demographic rates.

Some general insights into the nonlinearity of fitness have come from Cohen's seminal work on matrices and matrix products (Cohen 1981; Cohen 1979a; Cohen 1979b; Cohen 1980) and have been used for instance by Drake (2005). Other insights are due to Caswell, who has long argued for the importance of second derivatives and developed methods for their computation (Caswell 1996, 2001b; Shyu and Caswell 2014), with more recent work by (McCarthy et al. 2008; Stott 2016). The most powerful computational method to date (Shyu and Caswell 2014) uses matrix-vector calculus and does not require non-dominant eigenvalues and eigenvectors, which are difficult to compute stably in general (Demmel 1986). Our approach is different from earlier work, both conceptually and mathematically.

In the next section, we describe the (known) effects of pulse disturbances in terms of transient dynamics. We use these results to show how the effect of a press disturbance on the SSD is obtained by analyzing a continued series of pulses in a discrete-time modelling framework. The same approach yields the effect of a press disturbance on the stable reproductive value. We illustrate these changes for an a stage-structured matrix population model for *Phaseolus lunatus* (commonly, Lima bean) from the COMADRE database (Salguero-Gómez et al. 2015). In the subsequent section, we turn to fitness as the long-run growth rate. There, we describe how the linear effect of a press disturbance on growth rate, the well known sensitivity (*i.e.*, first derivative), can be quantified. We use that simple approach to derive new expressions for the second derivatives of population growth rate. We illustrate these developments using MPM for *Phaseolus lunatus*. Then, we explain three useful aspects of the unexpected connection between the structure of transients and the nonlinearity of population-level fitness, thereby connecting our results to previous work by Cohen (1977) and more recently byJiang et al. (2022).

We close with a discussion of the multiple implications of our analyses: the novelty of the intimate connection we reveal between nonlinearity of the population growth rate with the transient dynamic response to a pulse; the fundamental role of local convexity/concavity in thinking about constraints in life histories, and about stabilizing/disruptive selection; the relationship between these results and the norm of response of life history strategies to fluctuating environments and disturbance regimes; the relevance of our current approach and results to the analysis of stochastic matrix population models; the relationship between what we do here and second-order perturbation theory (Stott 2016); the many implications of the linkage between our conceptual approach and linear response theory. And finally, the uses of our approach in studying the effect of disturbances in other ecological settings.

Pulse Disturbances and Transients

MPMs

We use matrix population models (MPMs) for structured populations in discrete time and in a constant environment. In this setting, the population is represented by a vector $\mathbf{n}(t)$ at time t, and a population projection matrix $\mathbf{B}$. The elements (b_{ij}) of said matrix represent the per-capita contributions of individuals in state j at t_0 to the realization of individuals in state i at t_1. These elements may incorporate one or more vital rates (*e.g.*, fertility is often the product of survival and fecundity), are ≥ 0 and so matrix $\mathbf{B}$ is non-negative; we assume that $\mathbf{B}$ is primitive (and so irreducible; *i.e.*, the life cycle graph defined by $\mathbf{B}$ contains the necessary information to describe pathways from all stages to all other stages). Then, this matrix has a dominant eigenvalue λ_0 with its corresponding right and left eigenvectors $\mathbf{u}_0, \mathbf{v}_0$ (Caswell 2001b). We normalize both vectors (*i.e.*, multiply by a suitable constant) so that the scalar product is $(\mathbf{v}_0, \mathbf{u}_0) = \mathbf{v}_0^T\,\mathbf{u}_0 = 1$. The superscript T indicates a transpose.

The stable stage distribution (SSD) is the vector $\mathbf{u}_0$, and the stable reproductive value vector is $\mathbf{v}_0$. We put these vectors together in a matrix

$$\mathbf{Q}_0 = \mathbf{u}_0\,\mathbf{v}_0^T, \tag{1}$$

Then the original population matrix can be written as a sum

$$\mathbf{B} = \lambda_0\,(\mathbf{Q}_0 + \mathbf{Q}_1), \tag{2}$$

$$\text{where } \mathbf{Q}_1 = \frac{1}{\lambda_0}\,(\mathbf{B} - \lambda_0\,\mathbf{Q}_0) \text{ is just the difference.} \tag{3}$$

Starting with an initial population vector $\mathbf{n}(0)$ and following the population over time using the MPM yields the customary result (see Appendix 1 for details) that

$$\frac{\mathbf{n}(t)}{\lambda_0^t} = \frac{\mathbf{B}^t}{\lambda_0^t}\mathbf{n}(0) = \left(\mathbf{Q}_0 + \mathbf{Q}_1^t\right)\,\mathbf{n}(0) \to \mathbf{Q}_0\,\mathbf{n}(0) = \left(\mathbf{v}_0^T\,\mathbf{n}(0)\right)\,\mathbf{u}_0, \tag{4}$$

so the population structure converges to the SSD and the growth rate does so to λ_0.

Effects of a Single Pulse Disturbance

The result of a pulse disturbance acting on a stable population is to change the population structure from the SSD to a sum of the SSD plus an added vector $\mathbf{u}_\perp$ that is perpendicular to the SSD. That additional 'perpendicularity' is precisely what sets the population away from its stationary equilibrium. Thus, after a pulse disturbance, the population vector is proportional to

$$\mathbf{u}_0 + \mathbf{u}_\perp.$$

Over the next time interval, if we assume constant environments and lack of density dependence, the demographic processes defined by the original matrix $\mathbf{B}$ act on the population again (otherwise $\mathbf{B}$ will change, and with it a new SSD will emerge). The part of the population structure that is the SSD will not change, so only the second term above will differ. This $\mathbf{u}_\perp$ is not affected by $\mathbf{Q}_0$ (as may be seen from equation (3), also the Appendix A.1). The net result is that, under these conditions, the new population structure will be proportional to

$$\mathbf{u}_0 + \mathbf{Q}_1\,\mathbf{u}_\perp.$$

This change is illustrated by the left panel in Fig 2. As time proceeds, the perpendicular component of the SSD ($\mathbf{u}_0$) shrinks and the population eventually returns to the SSD $\mathbf{u}_0$ (as shown in figure 2). The changes in the population structure are simply the transients,

$$\mathbf{u}_\perp, \mathbf{Q}_1\,\mathbf{u}_\perp, \mathbf{Q}_1^2\,\mathbf{u}_\perp, \mathbf{Q}_1^3\,\mathbf{u}_\perp, \ldots$$

and these eventually disappear as the population returns to the SSD. The convergence is illustrated by the bottom picture C in the left panel of Fig 2.

Press Disturbance as the Accumulation of Pulse Disturbances

Now let us turn to a press disturbance, in which the population matrix $\mathbf{B}$ is perturbed for all time, meaning that one or more demographic processes is permanently changed, so the MPM matrix $\mathbf{B}$ is changed to $\mathbf{B}+\mathbf{D}$ where the change is $\mathbf{D}$. For instance, if only one demographic process, say b_{23}, changes, then d_{23} is the only nonzero element of matrix $\mathbf{D}$. We visualize a one-off perturbation differently, as the same pulse disturbance at every time.

The right panel of Fig 2 shows how the effect of this press disturbance can alternatively be seen as the effect of a continued series of pulses of the same intensity and effect. The immediate result of a small pulse at time t_0 is that the population structure changes from the original SSD $\mathbf{u}_0$ (at time t_0) to the sum $\mathbf{u}_0 + \mathbf{z}^*$ in the next time step t_1, where (as detailed in the Appendix) the change is

$$\mathbf{z}^* = (\mathbf{I} - \mathbf{Q}_0)\,\frac{\mathbf{D}}{\lambda_0}\,\mathbf{u}_0. \tag{5}$$

Note that $\mathbf{z}^*$ is perpendicular to the SSD. If the perturbed structure was parallel to the SSD, then the new structure would be a multiple of the SSD, and by definition -when normalised to add up to 1- would result in the very SSD vector. Over the subsequent time interval, from time t_1 to time t_2, this initial change is acted on by the population matrix and becomes

$$\mathbf{Q}_1\,1z^*. \tag{6}$$

However, at t_2 there is also a new pulse, which produces a new change of size $\mathbf{z}^*$. Noe that at t_1 there is also a new pulse, which produces a new change of size $\mathbf{z}^*$ at t_2. So, as shown in the right panel of Fig 2, at time 2 the new population structure is the sum

$$\mathbf{u}_0 + \mathbf{z}^* + \mathbf{Q}_1\,\mathbf{z}^*.$$

Continuing in this way (as in Fig 2), the effect of a press disturbance is the continued sum of its effects through discrete time

$$\mathbf{z}^* + \mathbf{Q}_1\,\mathbf{z}^* + \mathbf{Q}_1^2\,\mathbf{z}^* + \ldots.$$

This overall effect can be summed as a geometric series, so the new SSD is

$$\mathbf{u}_0' = \mathbf{u}_0 + (\mathbf{I} - \mathbf{Q}_1)^{-1}\,\mathbf{z}^*. \tag{7}$$

The process of convergence from the old to the new SSD is illustrated in the bottom right panel F of Fig 2).

Effects of a Press via a New Matrix

The preceding discussion about the effect of a press disturbance reveals the form of the resulting new SSD. Remember that the press changes the population matrix $\mathbf{B}$ to $\mathbf{B} + \mathbf{D}$, where the changes in all elements are small. We combine equation (5) and equation (7) in a particular way. First define the matrix

$$\mathbf{J}_0 = \frac{1}{\lambda_0}(\mathbf{I} - \mathbf{Q}_1)^{-1}\,(\mathbf{I} - \mathbf{Q}_0). \tag{8}$$

Then the new SSD produced by the press (as shown by (5 – 7)) is

$$\mathbf{u}_0 + \mathbf{Z},\ \text{where } \mathbf{Z} = \mathbf{J}_0\,\mathbf{D}\,\mathbf{u}_0. \tag{9}$$

As shown more formally in the Appendix 2, equation (9) is correct only to first order, meaning that the change we have obtained is the linear change (equivalently, the first derivative) of the SSD.

A precisely analogous argument can be made for the stable reproductive value. As a result of a small press disturbance, the stable reproductive value changes from $\mathbf{v}_0$ to

$$\mathbf{v}_0 + \mathbf{Y},\ \text{where } \mathbf{Y}^T = \mathbf{v}_0^T\,\mathbf{D}\,\mathbf{J}_0. \tag{10}$$

These changes in the SSD and stable reproductive value are key to the analyses below.

Example: Pulse and Press Disturbance for *Phaseolus lunatus* MPM

We use MPM for *Phaseolus lunatus* (COMPADRE database) to compare Pulse and Press disturbance as shown in Figure 3. For the pulse, we perturb Stage 1 of the SSD $\mathbf{u}_0$ and track the trajectory of the stage. As shown in top-left panel of Figure 3, after 10 time steps Stage 1 damps to the original

SSD $\mathbf{u}_0$ (dotted black line). Note that despite we only perturbed Stage 1, the transient effects can be observed in other stages as shown in the top-right panel of 3.

For the Press disturbance, we perturb elements (1,5) and (6,5) of the original MPM (increase by 80%). We again track the dynamics of Stage 1 of the original SSD ($\mathbf{u}_0$) and find Stage 1 converges to a new stable stage distribution, shown in dashed black line in the bottom-left panel of Figure 3.

Nonlinearity in Fitness

In our analyses of structured populations, the fitness of a life history is the long run growth rate λ_0 determined by the elements of matrix $\mathbf{B}$. To quantify the contributions of elements of $\mathbf{B}$ on λ_0, we can calculate the first-order impact (*i.e.*, sensitivities) of population growth rate as a function of these matrix elements ($\lambda_0(b_{pq})$). However, fitness can also vary as a function of pairs of matrix elements ($\lambda_0(b_{pq}, b_{kl})$, where $(p, q), (k, l)$ are row-column indices). Here, we explore nonlinearity in terms of the slope (first derivative) and curvature (second derivative) of these functions.

In this section, we show analyzing derivatives is the same thing as analyzing the effect of a press disturbance. For example, say we want to analyze the functional dependence of varying the matrix element b_{pq} on $\lambda_0(b_{pq})$. To do so, create a press disturbance that permanently changes only the pq element of the population projection matrix, with a new value say $(b_{pq} + d)$. In matrix terms, we change to a new population projection matrix $(\mathbf{B} + \mathbf{D})$ where only the (p, q) element of $\mathbf{D}$ is nonzero and equals d; all other elements of $\mathbf{D}$ equal zero. We provide an intuitive approach to evaluate the slope (first derivative) and the curvature (second derivative) of the function. Our work overcomes the limitation that responses of population dynamics to a change in vital rates are assumed linear (Hodgson and Townley 2004), but may not be as highlighted in Stott (2016).

Simple Approach to Slope *aka* Sensitivity

We begin with a simple method of finding the slope, the first derivative, of population growth rate with respect to pq, $\lambda_0(b_{pq})$, which is of course familiar as the sensitivity (Caswell 2001b),

$$s_{pq} = \frac{\partial \lambda_0}{\partial b_{pq}}. \tag{11}$$

We now describe a simple approach to compute the slopes. To explain, we start with a stationary stable population, in which the fraction of individuals in stage q is u_{0q}, the qth component of the SSD. In the next time interval, these individuals may transition to new states or stay in the same state (or die). To each final living state p, the initial fraction in state q contributes the amount $b_{pq}\, u_{0q}$. We weight this contribution by the final state's reproductive value v_{0p}, and identify $(v_{0p}\, b_{pq}\, u_{0q})$ as the weighted contribution of the $p \leftarrow q$ transition. The sum of these contributions over all initial and final states is λ_0 (as it should).

To apply the approach (discussed above) to a single element in the transition matrix, suppose that we change the transition rate for the $p \leftarrow q$ transition from (b_{pq}) to $(b_{pq} + d)$, by adding some small d. Then (following the logic of the previous paragraph) the change in stable growth rate is the product of three terms:

a) the additional per-capita rate for that transition, *i.e.*, d;

b) the fraction of population that is subject to this change, *i.e.*, u_{0q};

c) the relative weight of ending in the final state q, *i.e.*, v_{0p}.

The product is: $d\, v_{0p}\, u_{0q}$. Dividing this change by d, we conclude that the first derivative of population growth rate to a disturbance of the $p \leftarrow q$ transition is

$$\frac{\partial \lambda_0}{\partial b_{pq}} = v_{0p}\, u_{0q} = s_{pq}. \tag{12}$$

So our simple method indeed yields the standard result (Caswell 2001b).

Using the new approach: Second derivatives

Just as press disturbances can impart small changes on individual, press disturbances can also shift co-varying vital rates (*e.g.*, early-life vs. late-life reproduction). Interestingly, the disturbance of two vital rates can also be used to quantify the second derivatives of population growth rate. For ease of exposition, say we create a press disturbance and change the pq and kl matrix elements to $b_{pq} + d$ and $b_{kl} + f$. We assume that d, f are small but we want to consider nonlinear changes, so we also include terms in $d^2, f\, d, f^2$.

Fig 4 illustrates two distinct ways of carrying out the above press disturbance, which must lead to the same overall change in fitness.

Say we use the first route, A to B and then B to D. In the change from A to B, our simple argument above shows that the change in fitness is the product

$$f\, v_0(k)\, u_0(l). \tag{13}$$

Now we want to make the change from B to D. But at B, equation (9) shows that (see Appendix for details) the SSD has already changed to $(\mathbf{u}_0 + f\, \mathbf{Z}_1)$ with

$$\mathbf{Z}_1 = u_{0l} \begin{pmatrix} J_{0,1k} \\ J_{0,2k} \\ \vdots \end{pmatrix}. \tag{14}$$

Also at B, equation (10) shows that the stable reproductive value has also already changed to $(\mathbf{v}_0 + f\, \mathbf{Y}_1)$ with

$$\mathbf{Y}_1^T = v_{0k} \begin{pmatrix} J_{0,l1} & J_{0,l2} & \dots \end{pmatrix}. \tag{15}$$

Now we are ready to use our approach to say that in the transition B to D, the fitness changes by the product of

a) the stable proportion in stage q, which equation (14) shows is $(u_{0q} + f Z_1(q))$,

b) the change in the rate, d,

c) the stable reproductive value in stage p, which equation (15) shows is $(v_{0p} + f Y_1(p))$.

The product of these terms (ignore terms higher than quadratic, see Figure 4 for more) has to be added to the change (equation (13)) to get the total change in growth rate A to B to D,

$$f\, v_0(k)\, u_0(l) + d\, v_0(p)\, u_0(q) + f\, d\, \left(u_{0q}\, Y_1(p) + v_{0,p} Z_1(q)\right). \tag{16}$$

Using (14 – 15) the total change is the sum

$$\begin{aligned} \text{Linear change} &= f\, v_0(k)\, u_0(l) + d\, v_0(p)\, u_0(q), \\ &+ \\ \text{Nonlinear change} &= f\, d\, \left(u_{0q}\, v_{0k}\, J_{0,lp} + u_{0,l}\, v_{0,p}\, J_{0,qk}\right). \end{aligned} \tag{17}$$

We conclude that the nonlinearity is revealed by making two press disturbances. As shown in Fig 4, we could alternatively go from A to C and then C to D. That process involves distinct changes to the SSD and reproductive value. But we get the same final result as in equation (17). We can think about these changes in terms of the second derivatives of fitness (as explained further in the Appendix) to find

$$\frac{\partial^2 \lambda_0}{\partial b_{pq} \partial b_{kl}} = \left[s_{pl}\, J_{0,qk} + s_{kq}\, J_{0,lp}\right], \tag{18}$$

where we have used the sensitivities (equation (11)). Note that our expression for the second derivative is symmetric with respect to an exchange of the elements b_{pq}, b_{kl} (as it should be).

The curvature of fitness as measured by the second derivatives in equation (18) depends on the matrix $\mathbf{J}_0$. Consequently any analysis of second derivatives will provide detailed information about $\mathbf{J}_0$. The next section describes the multiple connections between $\mathbf{J}_0$ and transient dynamics. A computationally useful version of (18) uses Kronecker products (see Appendix A.33). We provide a detailed example to calculate second-derivatives using our perturbation approach for *Phaseolus lunatus* in Appendix A.5 and Figure A.1. The matrix for second-derivatives is depicted in Figure A.2. We also compute the second derivatives to show that our method yields the same result as the one in Shyu and Caswell (2014) (see Appendix A.6).

Transients and Nonlinearity

The previous section identifies the central role of the matrix $\mathbf{J}_0$ in defining the nonlinear response to a pulse disturbance and thus the second derivatives of fitness. Repeating the definition from equation (8),

$$\mathbf{J}_0 = \frac{1}{\lambda_0}(\mathbf{I}-\mathbf{Q}_1)^{-1}(\mathbf{I}-\mathbf{Q}_0).$$

Since matrix $\mathbf{Q}_1$ shapes the transient dynamics after a pulse, those transient dynamics also shape $\mathbf{J}_0$. The connection revealed between transients and nonlinearity of the dominant eigenvalue is unexpected and intimate. In this section we further illuminate this connection by three new results connecting $\mathbf{J}_0$ to transients.

Matrix $\mathbf{J}_0$ and cumulative distance to stability

An important metric to assess the difference between an observed stage distribution and the stable SSD is the cumulative distance to stability (Cohen 1979a). Several studies (Williams et al. 2011; White et al. 2013) have employed this metric. Here we point out that the matrix $\mathbf{J}_0$ actually determines the cumulative distance to stability.

As we know, any non-stable initial population distribution at time $t = 0$ converges towards the SSD. Following Cohen (1979a), at each later time t, the “distance” from stability is measured by summing the elements of the difference vector $f(t) = \lambda_0^{-t}\,\mathbf{n}(t) - \mathbf{Q}_0\,\mathbf{n}(0)$. Convergence means that this distance is decreasing, so the cumulative vector $F(t) = \sum_{m=0}^{(t-1)} f(m)$ should have a limit. For an initial population vector $\mathbf{n}(0)$ Cohen showed this limit to be

$$\lim_{t\to\infty} F(t) = \left[\left(\mathbf{I} + \mathbf{Q}_0 - \frac{\mathbf{B}}{\lambda_0}\right)^{-1} - \mathbf{Q}_0\right]\mathbf{n}(0). \tag{19}$$

We find that Cohen’s cumulative distance is just

$$\lim_{t\to\infty} F(t) = \mathbf{J}_0\,\mathbf{n}(0), \tag{20}$$

as shown in the Appendix. Thus $\mathbf{J}_0$ is directly related to the asymptotic cumulative distance to stability.

Structure of $\mathbf{J}_0$ for population matrices with distinct eigenvalues

When the matrix population model $\mathbf{B}$ has distinct eigenvalues (and linearly independent eigenvectors), we can write the spectral decomposition of $\mathbf{B}$ (Good 1969) as: $\mathbf{B} = \lambda_0\,\mathbf{u}_0\,\mathbf{v}_0^{\dagger} + \lambda_1\,\mathbf{u}_1\,\mathbf{v}_1^{\dagger} + \lambda_2\,\mathbf{u}_2\,\mathbf{v}_2^{\dagger} + \cdots = \sum_{j=0}\lambda_j\,e^{\mathbf{i}\omega_j}\,\mathbf{u}_j\,\mathbf{v}_j^{\dagger}$, where $\mathbf{u}_j$ and $\mathbf{v}_j$ are right and left eigenvectors of $\mathbf{B}$. In this case, we write the higher eigenvalues (maybe complex) as $\lambda_j = e^{(r_j + \mathbf{i}\omega_j)}$ for $j \geq 1$ and write the eigenvalue ratio as:

$$\frac{\lambda_j}{\lambda_0} = \frac{e^{(r_j + \mathbf{i}\omega_j)}}{e^{r_0}} = \tau_j \, e^{\mathbf{i}\omega_j}$$

where $\tau_j = e^{r_j - r_0}$ and $\tau_j < 1$; the τ_j are the inverse damping ratios Caswell (2001a). The spectral decomposition for $\mathbf{B}$, and the definition equation (1) show that

$$\mathbf{Q}_1 = \sum_{j \geq 1} \tau_j \, e^{\mathbf{i}\omega_j} \, \mathbf{u}_j \, \mathbf{v}_j^{\dagger}. \tag{21}$$

We can now write an explicit expression for $\mathbf{J}_0$ (details in Appendix) as

$$\mathbf{J}_0 = \sum_{j \geq 1} \frac{\mathbf{u}_j \, \mathbf{v}_j^{\dagger}}{(1 - \tau_j \, e^{\mathbf{i}\omega_j})}. \tag{22}$$

This is a spectral decomposition of $\mathbf{J}_0$ (excluding the eigenvector $\mathbf{u}_0$ for which the eigenvalue is 0). Thus the vectors $\mathbf{u}_j$, $\mathbf{v}_j$ are right, left eigenvectors of $\mathbf{J}_0$ corresponding to eigenvalue $\left(1 - \tau_j \, e^{\mathbf{i}\omega_j}\right)^{-1}$. One consequence is that the dominant eigenvalue of $\mathbf{J}_0$ depends on the damping ratio τ_1.

Matrix $\mathbf{J}_0$ and Asymptotics of Transients

The preceding discussion implies that the dominant eigenvalue of $\mathbf{J}_0$ is a quantitative measure of the asymptotic convergence of transients. Previous studies have shown that life history significantly influences transient dynamics of a population (Haridas and Tuljapurkar 2007).

Jiang et al. (2022) found a strong correlation between transients (using damping time) with generation time (T_c), a key life history trait (Gaillard et al. 2005). This finding led us to hypothesize that the dominant eigenvalue of $\mathbf{J}_0$ is also correlated with life history traits. To examine this hypothesis, we analyzed 439 unique age and stage- structured species (after correcting for phylogenetic inertia) using the COMADRE Animal Matrix Database (Salguero-Gómez et al. 2016), the COMPADRE Plant Matrix Database (Salguero-Gómez et al. 2015), and previously published mammalian database in Jiang et al. (2022). As shown in Figure 5, we find that the dominant eigenvalue of $\mathbf{J}_0$ is indeed strongly correlated with generation time T_c on the log-log scale (Figure 5).

Thus the higher (subdominant) eigenvalues and eigenvectors of $\mathbf{B}$ completely determine our matrices $\mathbf{Q}_1$ and $\mathbf{J}_0$. Of course, the relationships in this subsection are of little computational use if there are repeated eigenvalues, or if we cannot compute the eigenvalues accurately. But even then, the powers of $\mathbf{Q}_1$ and thus the matrix $\mathbf{J}_0$ describe the transient dynamics of the population matrix. This connection is described by Cohen (1979a) using a cumulative distance measure, and we now show that is directly given by our matrix $\mathbf{J}_0$.

Discussion

Population ecology has, over recent decades, acquired a sizeable arsenal of tools to approximate and quantify how natural populations respond to environmental stochasticity (Roughgarden 1975; Doak et al. 1994; Medeiros et al. 2023). In parallel, the field has also made important progress in the understanding of how natural populations respond to one-off (*i.e.*, pulse) disturbances (Jentsch and White 2019). However, natural populations are rarely exposed to a single disturbance that fades fast enough (or where there is enough time) for the population to go back to stationary equilibrium. Here, we propose a novel approach to examine how natural populations respond to press disturbances. This approach is based on known results about pulse disturbances and transients to analyze press disturbances and nonlinear responses of population growth rate to demographic rate perturbations. Our results reveal an intimate -and unexpected- connection between the nonlinearity of population growth rate to vital rates, and transient dynamics. These findings provide valuable insights into the ways populations respond to disturbance regimes, with multiple implications for ecological modelling, ecological forecasting, and comparative demography.

A key contribution of this study is the introduction of a new approach for calculating the second derivatives of long-term population growth rates with respect to their underlying vital rates in st(age)-structured populations (*e.g* matrix population models, Caswell (2001b) and Ellner et al. (2016)). This approach, which is both intuitive and powerful, enables researchers to explore the impact of linear and nonlinear selection on vital rates such as survival, growth, and reproduction. Our approach unlocks a deeper understanding of the factors influencing population dynamics. Indeed, the second derivative of population growth rate with respect to all vital rates that constitute an MPM provides information of important evolutionary implications (Doak et al. 1994; Brodie et al. 1995; Vasseur and Fox 2007; Shyu and Caswell 2014). Namely, these second derivatives inform on: (1) whether a function (in our case, the average fitness of individuals in the population) changes linearly as vital rates are perturbed (*e.g.*, Caswell (2001b)); 2) if nonlinear, whether fitness follows a concave (negative self-second derivative) or convex (positive self-second derivative) function for a specific vital rate (*e.g.*, Caswell (2001b)); and (3) if the second derivative of fitness with respect to vital rates is positive for observed life histories, then the examined value corresponds to a local minimum, and *vice versa* if the second derivative of fitness is negative at a critical point, then that critical point corresponds to a local maximum (Brodie et al. 1995). Here, statement (3) is of particular evolutionary and ecological importance, because it provides valuable insights into the stability of populations. Indeed, this way of thinking about the dynamics of a population in a stochastic environment enables us to conclude - based on a given second derivative value - whether fitness will increase as vital rates are perturbed or not. In other words, if a local maximum is evidenced, then further disturbances of a given (or all) vital rate(s) will inevitably only lead to the decrease in fitness. This information is particularly valuable when examining population forecasts of species to climate extremes (Thibault and Brown 2008), and selection for optimal life history strategies for a given environment (Tuljapurkar et al. 2009). As such, we argue that our second derivative approach is particularly valuable for active research in human demography (*e.g.*, McLeod and Day (2019)), population ecology (*e.g.*, Feng et al. (2022)), and comparative biology (*e.g.*, Compagnoni et al. (2021)). We emphasize the applicability of second-order perturbation theory, such as Kato's theory (Kato 2013), in describing the nonlinear response in structured populations. This line of work opens up possibilities for using this method in multiple contexts, such as community composition and nonlinear multi-species interactions (Bender et al. 1984; Collins et al. 2020), broadening the scope of its application.

Our findings reveal a robust link between the matrix $\mathbf{J}_0$ and short-term population dynamics in the aftermath of a perturbation. When a pulse disturbance perturbs the vital rates of a st(age)-structured population, the resulting nonlinear response in fitness can be quantified through the second-order derivative of the population growth rate. Here, we have formally defined the second derivative of the population growth rate in terms of the matrix $\mathbf{J}_0$ (See appendix). This formalization establishes a clear association between the nonlinear response in fitness and transient dynamics. These transient dynamics, stemming from a pulse disturbance, are characterized by the matrix Q_1, which is a constituent element in the $\mathbf{J}_0$ equation (7), and consequently, it shapes $\mathbf{J}_0$. This interconnection gives rise to second-order fitness derivatives that exhibit nonlinear selection pressures, displaying concavity when the self-second derivative is negative and convexity when positive (Levine et al. 2022), with these effects being influenced by the transient phases in the population's dynamic trajectory.

In the realm of community ecology, it has been demonstrated that the interplay between pulse and press disturbances can lead to intricate, nonlinear interactions within ecological communities (Inamine et al. 2022). Pulse disturbances afford opportunities for select species during transient phases, while press disturbances can induce nonlinear, often unpredictable shifts in species performance over time. These interactions cascade through the community, affecting species composition and abundance in ways that defy straightforward predictions offered by linear population dynamics models. Our approaches, explicitly linking transient dynamics to well-established approaches to quantify stochastic demographics, coupled with the ability of st(age)-structured models to incorporate intra- and inter-specific effects (*e.g.*, Kayal et al. (2018) and Adler et al. (2012)) offer unique opportunities to integrate responses of natural systems across levels of biological organisation: from individuals, to populations, to full communities. This integration is a primary need in the field of ecological resilience (Capdevila et al. 2021).

Our findings also suggest a parallel in the context of population dynamics. The co-occurrence of press and pulse disturbances is a plausible scenario, particularly in light of increasing environmental stochasticity. Conceptually, the mechanics of press disturbances can be understood as an amalgamation of multiple, back-to-back pulse disturbances. Given that a single pulse disturbance, along with the ensuing transient behavior, indirectly impacts the nonlinearity of fitness responses, we posit that long-term press disturbances, along with the associated transients dislocating populations from their original stable state, will yield a more intricate and nonlinear response in fitness. In this study, we have elucidated the mathematical framework underpinning the connection between transients and nonlinearity in fitness. This connection helps in understanding transient dynamics and resilience metrics in structured populations, offering new avenues for exploration in population ecology and comparative demography.

An important area for future investigation in this regard is the link between the environmental response of vital rates and the environmental response of fitness. Specifically, the examination of environment-vital rate reaction norms in natural populations holds potential for further research in understanding the causes of trait variance in populations over time and the plasticity of life history processes in response to environmental changes (Klingenberg 2019). Our results point to new directions to examine population responses in stochastic environments. To see why, note that way a population fares in a stochastic environment can be viewed in terms of a sequence of unequal pulses, and their cummulative effects (as shown in Figure 1). So for example, we can examine how shifts in mean, variance, and temporal autocorrelation may impact a population's ability to persist (Drake 2005; Vasseur and Fox 2007). We highlight the need for further research on the relationships between first-order and second-order derivatives of population growth rate with respect to vital rates as an yet unexplored area offering exciting opportunities for the field of ecological forecast, has hinted at by Shyu and Caswell (2014). In summary, the theoretical developments presented here, together with the findings that a tight connection exists between transient dynamics and stochastic dynamics open up new avenues in the study of structured demography. We argue that the potential implications are wide-ranging, and include the fields of formal demography, population ecology, and comparative demography. The insights into the connections between nonlinearity, transients, and selection pressures are expected to have a significant impact on future research in these areas, providing valuable tools for understanding and managing population dynamics in a changing world.

References

Adler, Peter B, Harmony J Dalgleish, and Stephen P Ellner (2012). “Forecasting plant community impacts of climate variability and change: when do competitive interactions matter?” *Journal of Ecology* 100.2, pp. 478–487.

Amor, DR, C Ratzke, and J Gore (2020). *Transient invaders can induce shifts between alternative stable states of microbial communities. Sci Adv 6: eaay8676.*

Bender, Edward A, Ted J Case, and Michael E Gilpin (1984). “Perturbation experiments in community ecology: theory and practice”. *Ecology* 65.1, pp. 1–13.

Brodie, Edmund D, Allen J Moore, and Fredric J Janzen (1995). “Visualizing and quantifying natural selection”. *Trends in Ecology & Evolution* 10.8, pp. 313–318.

Capdevila, Pol, Iain Stott, Maria Beger, and Roberto Salguero-Gómez (2020). “Towards a comparative framework of demographic resilience”. *Trends in Ecology & Evolution* 35.9, pp. 776–786.

Capdevila, Pol et al. (2021). *Reconciling resilience across ecological systems, species and subdisciplines.*

Caswell, H. (2001a). *Matrix population models: construction, analysis and interpretation.* 2nd. Sunderland, Mass.: Sinauer associates, Sunderland, Mass.

Caswell, Hal (1996). “Second derivatives of population growth rate: calculation and applications”. *Ecology*, pp. 870–879.

— (2001b). *Matrix Population Models: Construction, Analysis, and Interpretation.* 2nd. Sinauer Associates Inc., Sunderland, MA.

Cohen, J.E. (1977). “Ergodicity of age structure in populations with Markovian vital rates, III: finite-state moments and growth rate; an illustration”. *Advances in Applied Probability*, pp. 462–475.

— (1979a). “The cumulative distance from an observed to a stable age structure”. *SIAM Journal on Applied Mathematics* 36.1, pp. 169–175.

— (1980). “Convexity properties of products of random nonnegative matrices”. *Proceedings of the National Academy of Sciences* 77.7, pp. 3749–3752.

Cohen, Joel E (1981). “Convexity of the dominant eigenvalue of an essentially nonnegative matrix”. *Proceedings of the American Mathematical Society* 81.4, pp. 657–658.

— (1979b). “Random evolutions and the spectral radius of a non-negative matrix”. *Mathematical Proceedings of the Cambridge Philosophical Society* 86.2, pp. 345–350. DOI: `10.1017/S0305004100056164`.

Collins, Scott L et al. (2020). “Press–pulse interactions and long-term community dynamics in a Chihuahuan Desert grassland”. *Journal of Vegetation Science* 31.5, pp. 722–732.

Compagnoni, Aldo et al. (2021). “Herbaceous perennial plants with short generation time have stronger responses to climate anomalies than those with longer generation time”. *Nature Communications* 12.1, p. 1824.

Demmel, James Weldon (1986). “Computing stable eigendecompositions of matrices”. *Linear Algebra and its Applications* 79, pp. 163–193.

Doak, Daniel, Peter Kareiva, and Brad Klepetka (1994). “Modeling population viability for the desert tortoise in the western Mojave Desert”. *Ecological Applications* 4.3, pp. 446–460.

Donohue, Ian et al. (2016). “Navigating the complexity of ecological stability”. *Ecology letters* 19.9, pp. 1172–1185.

Drake, J.M. (2005). “Population effects of increased climate variation”. *Proceedings of The Royal Society B* 272.1574, p. 1823.

Ellner, Stephen P, Dylan Z Childs, Mark Rees, et al. (2016). “Data-driven modelling of structured populations”. *A practical guide to the Integral Projection Model. Cham: Springer.*

Feng, Tao, Hongjuan Zhou, Zhipeng Qiu, and Yun Kang (2022). “Impacts of demographic and environmental stochasticity on population dynamics with cooperative effects”. *Mathematical Biosciences* 353, p. 108910.

Gaillard, J.M. et al. (2005). “Generation Time: A Reliable Metric to Measure Life-History Variation among Mammalian Populations”. *American Naturalist* 166.1, pp. 119–123.

Good, Irving John (1969). “Some applications of the singular decomposition of a matrix”. *Technometrics* 11.4, pp. 823–831.

Haridas, CV and Shripad Tuljapurkar (2007). “Time, transients and elasticity”. *Ecology Letters* 10.12, pp. 1143–1153.

Hastings, Alan (2001). “Transient dynamics and persistence of ecological systems”. *Ecology Letters* 4.3, pp. 215–220.

Hodgson, David J and Stuart Townley (2004). “Methodological insight: linking management changes to population dynamic responses: the transfer function of a projection matrix perturbation”. *Journal of Applied Ecology* 41.6, pp. 1155–1161.

Horvitz, Carol C and Douglas W Schemske (1995). “Spatiotemporal variation in demographic transitions of a tropical understory herb: projection matrix analysis”. *Ecological monographs* 65.2, pp. 155–192.

Inamine, Hidetoshi et al. (2022). “Pulse and Press Disturbances Have Different Effects on Transient Community Dynamics”. *The American Naturalist* 200.4, pp. 571–583.

Jentsch, Anke and Peter White (2019). “A theory of pulse dynamics and disturbance in ecology”. *Ecology* 100.7, e02734.

Jiang, Sha et al. (2022). “Reproductive dispersion and damping time scale with life-history speed”. *Ecology Letters* 25.9, pp. 1999–2008.

Karlin, S. and H.M. Taylor (1975). *A first course in stochastic processes.* Academic Press.

Kato, Tosio (1976). *Perturbation theory for linear operators.* Vol. 132. Springer Science & Business Media.

— (2013). *Perturbation theory for linear operators.* Vol. 132. Springer Science & Business Media.

Kayal, Mohsen et al. (2018). “Predicting coral community recovery using multi-species population dynamics models”. *Ecology Letters* 21.12, pp. 1790–1799.

Klingenberg, Christian Peter (2019). “Phenotypic plasticity, developmental instability, and robustness: The concepts and how they are connected”. *Frontiers in Ecology and Evolution* 7, p. 56.

Levine, Jacob I, Jonathan M Levine, Theo Gibbs, and Stephen W Pacala (2022). “Competition for water and species coexistence in phenologically structured annual plant communities”. *Ecology letters* 25.5, pp. 1110–1125.

McCarthy, Dominic, Stuart Townley, and Dave Hodgson (2008). “On second order sensitivity for stage-based population projection matrix models”. *Theoretical Population Biology* 74.1, pp. 68–73.

McLeod, David V and Troy Day (2019). “Social evolution under demographic stochasticity”. *PLoS computational biology* 15.2, e1006739.

Medeiros, Lucas P et al. (2023). “Ranking species based on sensitivity to perturbations under non-equilibrium community dynamics”. *Ecology Letters* 26.1, pp. 170–183.

Refsland, Tyler and Jennifer Fraterrigo (2018). “Fire increases drought vulnerability of Quercus alba juveniles by altering forest microclimate and nitrogen availability”. *Functional Ecology* 32.10, pp. 2298–2309.

Roughgarden, Jonathan (1975). “A simple model for population dynamics in stochastic environments”. *The American Naturalist* 109.970, pp. 713–736.

Salguero-Gómez, Roberto et al. (2015). “The compadre P lant M atrix D atabase: an open online repository for plant demography”. *Journal of Ecology* 103.1, pp. 202–218.

Salguero-Gómez, Roberto et al. (2016). “COMADRE: a global data base of animal demography”. *Journal of Animal Ecology* 85.2, pp. 371–384.

Shyu, Esther and Hal Caswell (2014). “Calculating second derivatives of population growth rates for ecology and evolution”. *Methods in Ecology and Evolution* 5.5, pp. 473–482.

Stott, Iain (2016). “Perturbation analysis of transient population dynamics using matrix projection models”. *Methods in Ecology and Evolution* 7.6, pp. 666–678.

Tao, Yun et al. (2021). “Transient disease dynamics across ecological scales”. *Theoretical Ecology* 14.4, pp. 625–640.

Thibault, Katherine M and James H Brown (2008). “Impact of an extreme climatic event on community assembly”. *Proceedings of the National Academy of Sciences* 105.9, pp. 3410–3415.

Traill, Lochran W, Susanne Schindler, and Tim Coulson (2014). “Demography, not inheritance, drives phenotypic change in hunted bighorn sheep”. *Proceedings of the National Academy of Sciences* 111.36, pp. 13223–13228.

Tuljapurkar, Shripad, Jean-Michel Gaillard, and Tim Coulson (2009). “From stochastic environments to life histories and back”. *Philosophical Transactions of the Royal Society B: Biological Sciences* 364.1523, pp. 1499–1509.

Vasseur, David A and Jeremy W Fox (2007). “Environmental fluctuations can stabilize food web dynamics by increasing synchrony”. *Ecology Letters* 10.11, pp. 1066–1074.

White, J Wilson et al. (2013). “Transient responses of fished populations to marine reserve establishment”. *Conservation Letters* 6.3, pp. 180–191.

Williams, Jennifer L et al. (2011). “Distance to stable stage distribution in plant populations and implications for near-term population projections”. *Journal of ecology* 99.5, pp. 1171–1178.

Yang, Louie H, Justin L Bastow, Kenneth O Spence, and Amber N Wright (2008). “What can we learn from resource pulses”. *Ecology* 89.3, pp. 621–634.

Figures

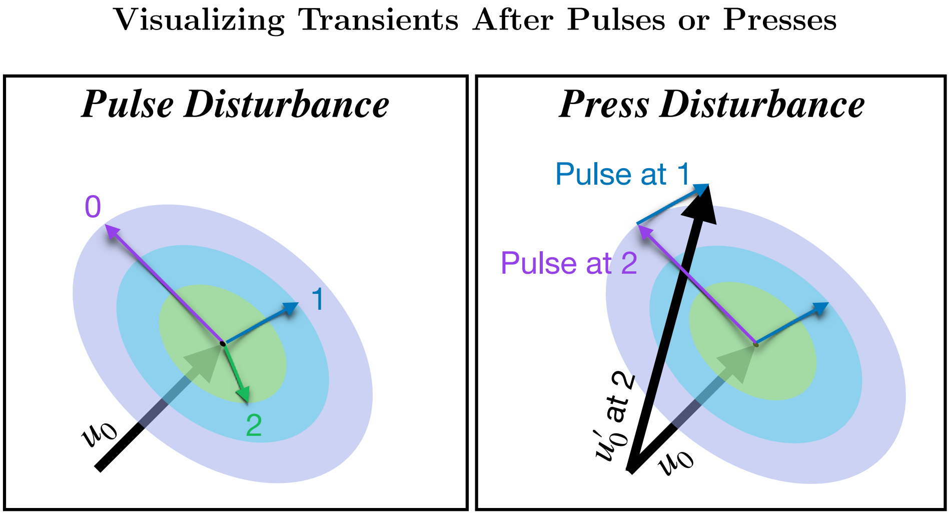

Figure 1: The left panel illustrates transient dynamics of a structured population after a pulse (one-time) disturbance. At time t_0, the purple arrow depicts pulse disturbance. After one time step, at time t_1, the pulse decays showing subsequent rotation and shrinkage of deviations from the SSD $\mathbf{u}_0$ (blue arrow), and then at time t_2 (green arrow), *etc.*. Note that eventually, the structure converges to original stable structure $\mathbf{u}_0$. In the right panel, results of a press (permanent) disturbance are illustrated as the sum of the effects of the current (at time t_2) pulse, and the decaying effects of past pulses (blue arrow at time t_1). In the case of press disturbance (to matrix elements), the convergence is to a new stable structure $\mathbf{u}_0'$ as shown in the right panel.

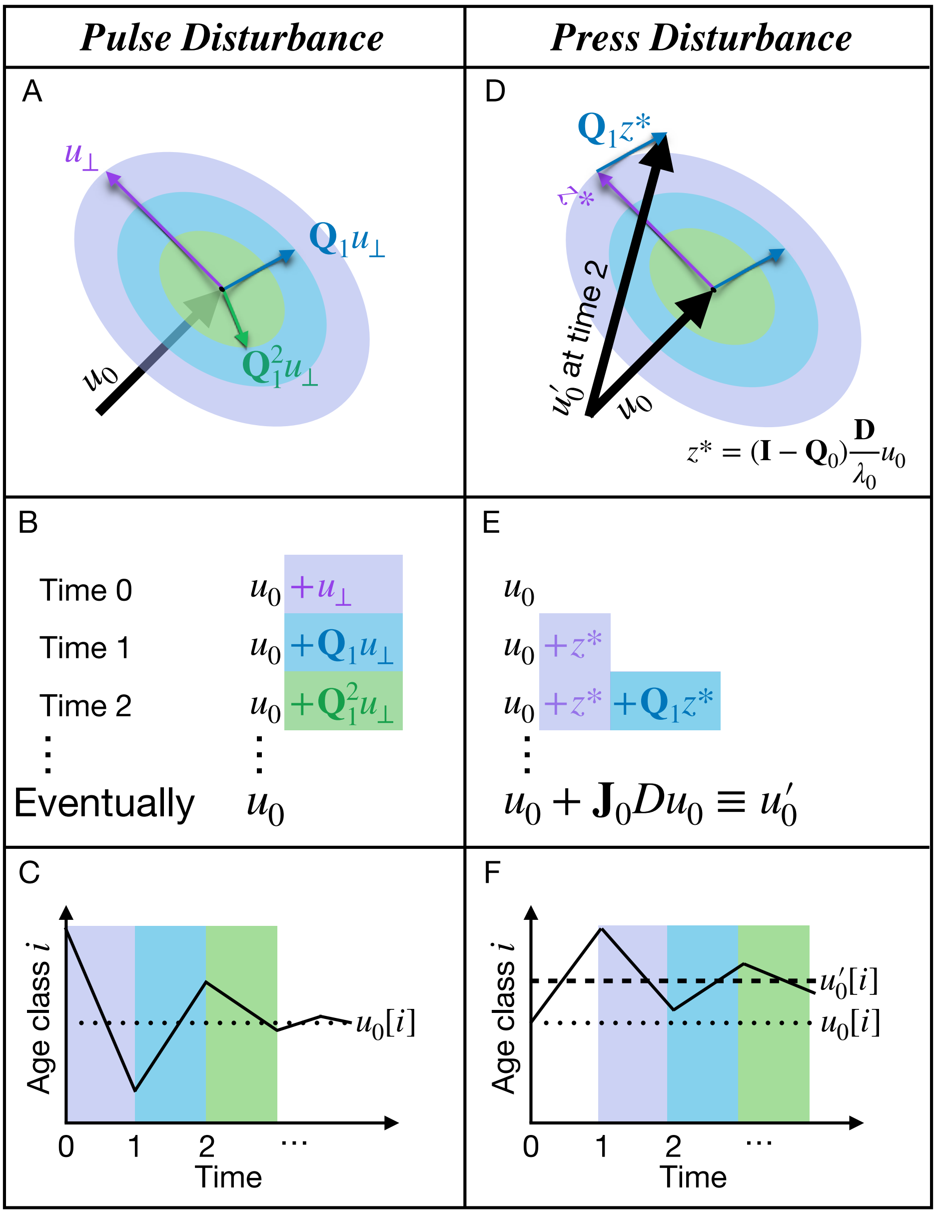

Figure 2: Left panel: A, transient dynamics after a pulse (one-time) pulse at t_0, showing subsequent (at t_1 and t_2) rotation and shrinkage of deviations from the SSD $\mathbf{u}_0$; B, explicit form of transient contribution to structure, with eventual return to SSD; C, decaying transients in one component of the population structure. Right panel: D, result of a press (permanent) disturbance, as a sum of the effect of the current (at t_2) pulse, and the decaying effects of past pulses at times t_1 and t_0 (only two are shown); E, explicit form of population structure, with eventual convergence to the new SSD; F, accumulation of changes in the SSD over time.

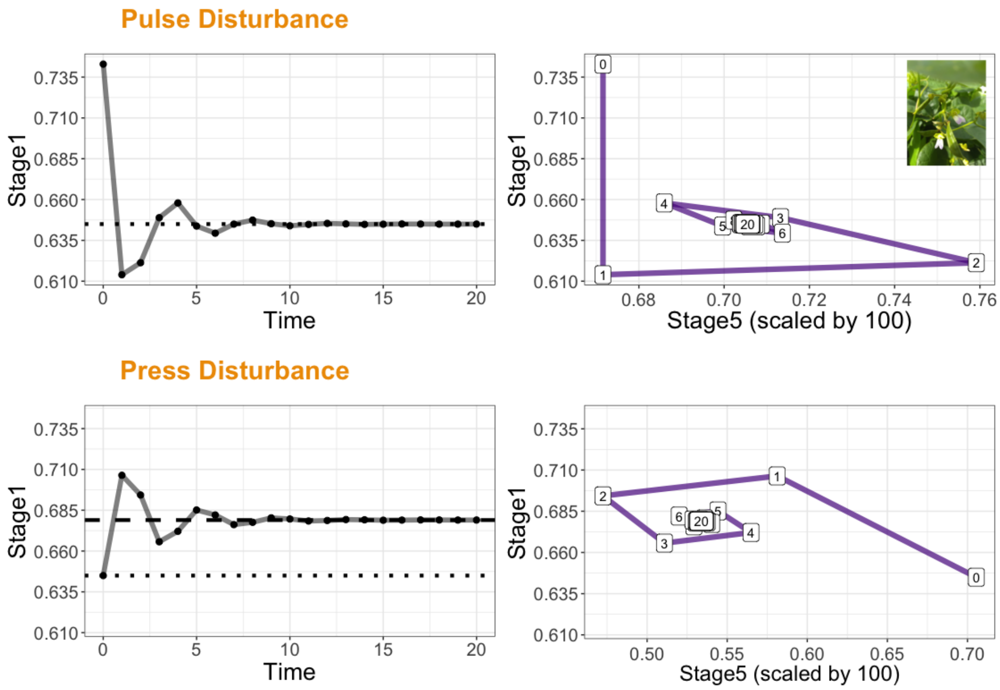

Figure 3: Pulse and Press disturbances for *Phaseolus lunatus*. The top two panels follow transient dynamics in Stage 1 after a pulse disturbance to the Stable Stage Distribution ($\mathbf{u}_0$) (Stage 1 perturbed). On the top-left panel, Stage 1 converges to SSD (depicted by the dotted black line). On the top-right panel, we examine the transient dynamics by considering two stages. We follow the convergence to SSD with Stage 5 on the x-axis and Stage 1 on the y-axis. The bottom two panels follow transient dynamics in Stage 1 after a press disturbance to two elements of the transition matrix (with 6 stages). We perturb (1,5) and (5,6) elements of the MP and follow the convergence to SSD for Stage 1. As shown in bottom-left panel, Stage 1 is perturbed from its SSD (depicted by dotted black line) and converges to a new SSD (depicted by the dashed black line) following a press disturbance. On the bottom-right panel, we examine the transient dynamics by considering two stages, Stage 1 on the y-axis and Stage 5 on the x-axis. Picture credit for *Phaseolus lunatus*: iNaturalist

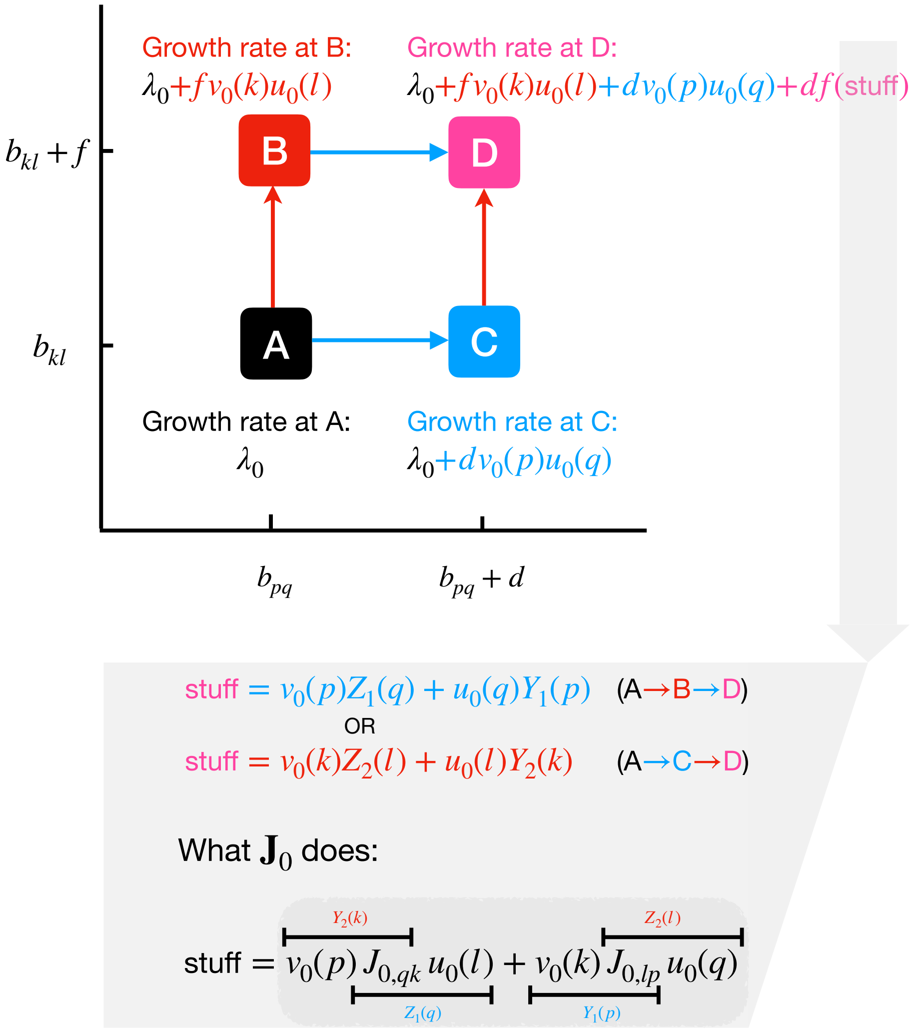

Figure 4: Computing the second derivatives of fitness with respect to projection matrix elements. The horizontal and vertical axes indicate rates for the two demographic transitions, (p, q) and (k, l). Point A indicates the starting values, where the fitness is λ_0, SSD is $\mathbf{u}_0$ and stable reproductive value is $\mathbf{v}_0$. A press disturbance of both demographic rates ends at point D. We consider two possible routes. First route: go from A to B by changing only the demographic rate for the $k \leftarrow l$ transition (*i.e.*, b_{pq} is unchanged but b_{kl} becomes $b_{kl} + f$. At B the new stable population is, say, $\mathbf{u}_0 + f\mathbf{Z}_1$ and the new reproductive value is, say, $\mathbf{v}_0 + f\mathbf{Y}_1$. Next go from B to D, by changing only b_{pq} by an amount d. Second route: starting at A, go from A to C by perturbing the $p \leftarrow q$ transition rate by an amount d. At C the new stable population is, say, $\mathbf{u}_0 + d\,\mathbf{Z}_2$ and the new reproductive value is, say, $\mathbf{v}_0 + d\,\mathbf{Y}_2$. Next, go from C to D by changing only b_{kl} by an amount f.

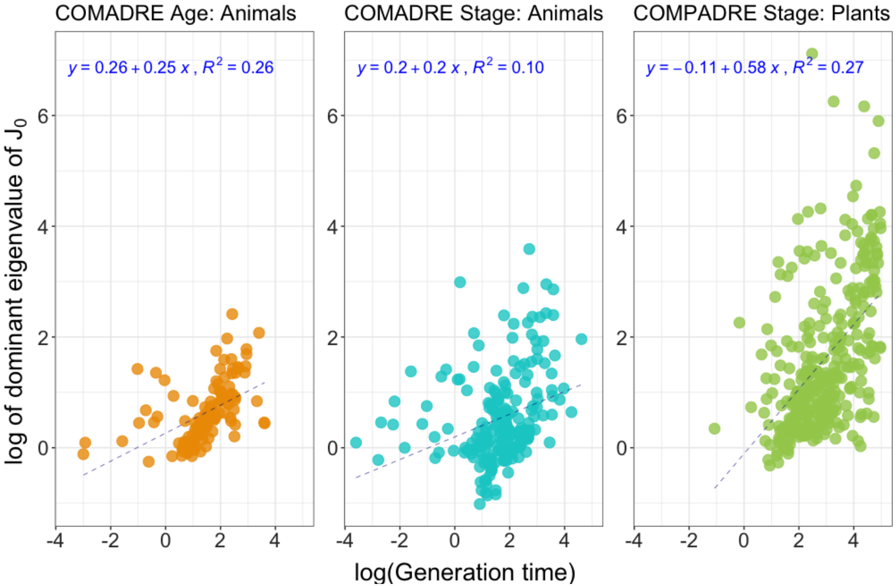

Figure 5: This figure examines the relationship between generation time (T_c) and the dominant eigenvalue of $\mathbf{J}_0$ based on phylogenetic generalized least squares. The y-axis corresponds to log of the dominant eigenvalue of $\mathbf{J}_0$ and the x-axis corresponds to log of generation time T_c. Each panel corresponds to a database: COMADRE age-structured matrices, COMADRE stage-structured matrices, COMPADRE stage-structured matrices. The correlation between dominant eigenvalue of $\mathbf{J}_0$ and T_c is consistently positive across all databases.

nature communications

Article

https://doi.org/10.1038/s41467-024-44768-4

Meta-analysis shows no consistent evidence for senescence in ejaculate traits across animals

Received: 13 July 2023

Accepted: 4 January 2024

Krish Sanghvi[1,4] ✉, **Regina Vega-Trejo**[1,4] ✉, **Shinichi Nakagawa**[2], **Samuel J. L. Gascoigne**[1], **Sheri L. Johnson**[3], **Roberto Salguero-Gómez**[1], **Tommaso Pizzari**[1] ✉ & **Irem Sepil**[1] ✉

Male reproductive traits such as ejaculate size and quality, are expected to decline with advancing age due to senescence. It is however unclear whether this expectation is upheld across taxa. We perform a meta-analysis on 379 studies, to quantify the effects of advancing male age on ejaculate traits across 157 species of non-human animals. Contrary to predictions, we find no consistent pattern of age-dependent changes in ejaculate traits. This result partly reflects methodological limitations, such as studies sampling a low proportion of adult lifespan, or the inability of meta-analytical approaches to document non-linear ageing trajectories of ejaculate traits; which could potentially lead to an underestimation of senescence. Yet, we find taxon-specific differences in patterns of ejaculate senescence. For instance, older males produce less motile and slower sperm in ray-finned fishes, but larger ejaculates in insects, compared to younger males. Notably, lab rodents show senescence in most ejaculate traits measured. Our study challenges the notion of universal reproductive senescence, highlighting the need for controlled methodologies and a more nuanced understanding of reproductive senescence, cognisant of taxon-specific biology, experimental design, selection pressures, and life-history.

Senescence is the age-dependent irreversible deterioration of organismal function that leads to an increased risk of intrinsic mortality[1] and a decline in reproductive output[2] with advancing age. While senescence has been reported in some taxa[3], it is unclear whether senescence is a general outcome of ageing[4–8]. Senescence is driven by a variety of proximate mechanisms, from excessive biosynthesis in late-life (hyperfunction theory[9]) and age-dependent deterioration of cellular repair[10], to the accumulation of mutations[11], oxidative damage[12], and telomere attrition[13]. From an evolutionary perspective, senescence is commonly hypothesized to be the result of relaxed selection against deleterious mutations in older organisms, as first proposed by Medawar's 'mutation accumulation theory'[14]. Other evolutionary explanations for senescence include selection for alleles, which increase performance early in life but convey net costs later in life ('antagonistic pleiotropy'[15]), and trade-offs between investment in survival versus reproduction ('disposable soma'[16]). In contrast, some animals show an absence of reproductive senescence[4]. Negligible senescence is predicted in animals with indeterminate growth, like some fish[17,18], where individuals continue to grow post-maturity, thus improving their ability to reproduce throughout their lives due to age-dependent

---

[1]Department of Biology, University of Oxford, Oxford, UK. [2]Evolution and Ecology Research Centre, School of Biological, Earth and Environmental Sciences, University of New South Wales, Sydney, Australia. [3]Department of Zoology, University of Otago, Dunedin, New Zealand. [4]These authors contributed equally: Krish Sanghvi, Regina Vega-Trejo. ✉e-mail: krishsangvi2007@gmail.com; regina.vegatrejo@bms.ox.ac.uk; tommaso.pizzari@biology.ox.ac.uk; irem.sepil@biology.ox.ac.uk

increases in gonad size[8,17]. The ability of some animals to maintain cellular repair and sustain homeostasis in reproductive tissues throughout life might also lead to negligible senescence[19].

Reproductive senescence (i.e., the age-dependent decline in reproductive success) has been relatively well documented in females[20,21]. Yet, patterns, causes, and consequences of male reproductive senescence are less understood[22]. Understanding male reproductive senescence is crucial for several reasons. Males typically face intense intra-sexual competition. Thus, age-dependent changes in male ejaculate traits can drive variation in male reproductive success[23,24], affecting sperm competition, cryptic female choice[25], and generating potential for sexual conflict[26–28]. Additionally, sperm are potentially more vulnerable to organismal ageing than eggs[10,29] because male germlines have higher rates of cell divisions and mutation accumulation[30,31] but poorer DNA repair machinery[12,32] than female germlines. Such deterioration in the male germline can severely impact offspring phenotypes via paternal age effects, thus having important consequences for organismal health (reviewed in[33]).

Current evidence for senescence in male ejaculate traits is inconclusive. Several studies show that older males have lower ejaculate quantities[34] and poorer sperm quality[35–37] than younger males. However, other studies have reported improvements[38–41], or no significant changes in ejaculate traits with advancing male age[42–45]. The heterogeneity in these reported effects might be caused by various biological and methodological factors that modulate the effects of advancing male age on ejaculate traits[35,46] (Tables 1 and 2). A meta-analytical approach is thus crucial to understand the influence of these 'moderators' (Tables 1 and 2) and to investigate the general effects of advancing male age on ejaculate traits. Yet, no study has done this systematically for non-human animals (see[35] for humans; [18] for a review in fish; [47] for effects of male age on seminal fluid).

Here, we conduct a meta-analysis to address three aims. First, we test whether advancing male age affects ejaculate traits across non-human animals (aim 1). Although reproductive senescence is not a ubiquitous outcome of ageing, it is commonly predicted to occur by classical theories of ageing. We thus predict that senescence in ejaculate traits will be observed commonly across species (see Tables 1 and 2 for predictions as to how different ejaculate traits might be affected differently). Second, we investigate the role of biological and methodological moderators (see Tables 1 and 2 for the possible influence of each) in modulating the effects of male age on ejaculate traits (aim 2). Third, we quantify how advancing male age affects reproductive outcomes, such as male fertilisation success and fecundity. Here, we also test whether the effects of advancing male age on ejaculate traits differ from those on reproductive outcomes (aim 3). We find no consistent evidence for senescence in ejaculate traits overall; however, we find taxonomic class- and trait-specific patterns. We also find that studies sampling higher proportions of species' lifespans show stronger evidence for senescence. Overall, we suggest methodological improvements and provide novel hypotheses for studying senescence. The research gaps highlighted by us will be key in aiding our understanding of male reproductive senescence.

Results

Using a systematic review, we identified 379 studies with relevant data on how advancing male age affects ejaculate traits (Supplementary Fig. 1). From these studies, we obtained 1814 effect sizes across 157 species of non-human animals. We then created a meta-analytical model, using Zr (Fischer's z-transformed correlation coefficient) as our effect size, to understand the overall effects of advancing male age on ejaculate traits. For all our meta-analytical models, we included effect size, cohort, study, species, and phylogenetic relatedness as random effects. From the included studies, we further collected data on various biological and methodological variables (moderators) to test their independent and additive influence on patterns of ageing in ejaculate traits, using meta-regressions. Importantly, for four over-represented taxonomic classes (Mammalia, Insecta, Aves, Actinopterygii), we further conducted four separate meta-regressions to investigate the extent of senescence in ejaculate traits. Some studies also contained additional data on age-dependent changes in reproductive outcomes (e.g. fertilisation success, reproductive output, offspring traits). For these studies, we compared the effects of advancing male age on ejaculate traits and reproductive outcomes. Furthermore, we conducted several analyses to test for different forms of publication biases. Finally, we also conducted two sensitivity analyses to test whether

Table 1 | Possible influence of different biological moderators on male reproductive senescence at the level of ejaculate traits

Biological moderators	Possible influence
Taxon-specific effects*	Phylogenetic history and taxa-specific biology (e.g. ecosystems, niches, metabolic rates, mating systems, mode of thermoregulation, degree of parental care) could influence how male age affects ejaculate traits[4,59].
Ejaculate traits*	Evidence for reproductive senescence can depend on the specific trait measured[61]. This can be due to trade-offs between different ejaculate traits[60] or different traits being under varying selection pressures[62].
Degree of sperm competition*	Species with increased levels of sperm competition have evolved increased investment in competitive ejaculate traits such as sperm number and velocity[95], which may reduce the rate of senescence in these traits[42]. However, high levels of sperm competition may also lead males to produce large, high-quality ejaculates early in life but exacerbate senescence in ejaculate traits at older ages[96].
Life-history strategies and mortality risk	Life-history strategies of animals and the pace of life of individuals determine the rate and onset of reproductive senescence[48]. Life-history strategies are affected by mortality risk in populations. For instance, animals may invest more in early-life reproduction when age-dependent mortality risk is high[97] and thus show higher reproductive senescence rates than animals facing lower age-dependent mortality risk[98]. Organisms that evolve in environments with high extrinsic mortality might show faster rates of senescence when old due to deleterious late-life expressed alleles not being selected against[15].
Seminal fluid changes	Levels of antioxidants in seminal fluid[47] and abundance of seminal fluid proteins can change as males age[66], independent of changes in sperm. These age-dependent changes in the seminal fluid can affect sperm phenotype over and above the direct effects of male age on sperm[47].
Ontogeny of secondary sexual traits	The ontogeny of secondary sexual traits can influence the evolution of male reproductive senescence rates[27]. For instance, in species where male traits such as weapons or ornaments improve with age, males are hypothesised to evolve lower rates of reproductive senescence, compared to species where these traits do not improve with age[40,51]
Parental care	Species with parental care might have evolved to allocate more energy/resources to caring for offspring and investing in current reproductive opportunities at the cost of reduced allocation to future reproduction. This could accelerate reproductive senescence in species with parental care[2].

Moderators marked with an asterisk were included in our meta-analysis because there were sufficient data across studies.

Table 2 | Possible influence of different methodological moderators on male reproductive senescence at the level of ejaculate traits

Methodological moderators	Possible influence
Proportion lifespan sampled*	A higher proportion of lifespan sampled will increase the probability of detecting reproductive senescence, as the onset of senescence usually occurs late in life[4,18,35,47].
Ejaculate collection method*	If males have control over ejaculation during ejaculate collection (e.g. natural mating or mating with dummy females), males might have the opportunity to strategically adjust ejaculate phenotypes[99]. This could cause age-independent changes in ejaculate traits, reducing the detectability of senescence. Additionally, when males have control over ejaculation, studies might obtain a smaller proportion of the sperm reserves available to a male, which may not be representative of a male's whole-ejaculate phenotype, compared to studies that use invasive methods to obtain ejaculates (e.g. dissection).
Population type*	Reproductive senescence rates can differ between males in captive versus wild populations[68,100]. Additionally, some domesticated animals are often culled prior to reaching ages where senescence can be detected[101]. Other domesticated animals have undergone generations of artificial selection for unusual life histories (e.g. extremely short generation time in broiler chicken[102]. These factors could lead to patterns of senescence differing between domesticated and wild animals.
Cross-sectional versus longitudinal sampling*	A cross-sectional sampling of males makes reproductive senescence harder to detect, especially if low-quality males selectively disappear[55,56]. Cross-sectional studies might thus underestimate male reproductive senescence, compared to the longitudinal sampling of the same males at different ages[103].
Manipulations*	Manipulated environments that are outside of what healthy organisms typically experience, such as environments with stressful conditions, can exacerbate reproductive senescence[104]. Thus, males exposed to manipulations such as thermal stress, poor diet, or toxins could be more likely to show reproductive senescence than males not subjected to these stressors. Other manipulations, such as experimental inbreeding[105] or selection for deleterious mutations[106], may exacerbate reproductive senescence.
Mating history	High mating rates can exacerbate male reproductive senescence[23]. In studies where male mating history is not controlled for, old males often have more matings than young males. These studies might thus show stronger evidence for senescence in ejaculate traits. On the other hand, low mating rates (e.g. virgins) might cause old males to accumulate sperm for longer durations, thus producing larger ejaculates than young males[66].
Post-meiotic sperm storage	Temporal changes in sperm traits can also occur due to post-meiotic storage of mature sperm in males before ejaculation and in females following mating[54]. The duration of sexual rest in males can influence the amount of post-meiotic damage to sperm, such that for a given age, males with shorter sexual rest (e.g. high mating rate) will incur lower post-meiotic sperm damage[54]. Further, deleterious effects of post-meiotic sperm storage may be exacerbated in old males if old males are less able to repair post-meiotic cellular damage in sperm[54].

Moderators marked with an asterisk were included in our meta-analysis because there were sufficient data across studies.

evidence for senescence was sensitive to the proportion of lifespan of the associated species a study sampled and the aims of the study.

Aim 1: Effects of advancing male age on ejaculate traits

We found no general effect of advancing male age on ejaculate traits (mean [95% confidence interval (CI)]: −0.006 [−0.486 to 0.474], $z = -0.025$, $P = 0.978$, Fig. 1A). Heterogeneity in our dataset was high ($I^2 = 95\%$), with 40% attributed to true differences between studies, 19% to differences between effect sizes, 0% to between-species differences, and 0.6% to differences between cohorts. Notably, phylogenetic relatedness (Supplementary Fig. 2) explained 35.4% of heterogeneity, suggesting a phylogenetic signal on male reproductive senescence.

Aim 2: Role of biological and methodological moderators

We did not find a significant general effect of advancing male age on ejaculate traits in our full model (which included all moderators with data for >75% of effect sizes; mean [95% CI]: −0.197 [−1.496 to 1.103]). However, the included moderators explained a significant proportion of the total heterogeneity in our data ($R^2 = 12.17\%$, $Q_M = 99.606$, $Q_E = 15299.075$, $P < 0.001$, DF = 36).

We did not find evidence for age-dependent changes in ejaculates in any taxonomic class (Fig. 1B for four major classes, Supplementary Fig. 3 for all classes), except in Malacostraca (which showed improvement with advancing male age), when effects were averaged across all ejaculate traits. However, taxonomic class explained a significant proportion of heterogeneity ($R^2 = 8.26\%$, $Q_M = 26.082$, $P = 0.025$, DF = 14). Similarly, when averaged across all taxa, we did not find evidence for advancing male age to affect any individual ejaculate trait significantly. Yet, the ejaculate trait explained a small but significant proportion of heterogeneity ($R^2 = 1.72\%$; $Q_M = 51.287$; $P < 0.001$, DF = 13, Fig. 2A).

We detected taxonomic class-specific effects of advancing male age on individual ejaculate traits. For insects (Insecta, $k = 258$), ejaculate size, quantity of sperm (corrected for body or testis size), number of sperm, and sperm viability, improved with advancing male age (Fig. 2B). For ray-finned fish (Actinopterygii, $k = 174$), sperm motility and velocity decreased, whereas ejaculate size increased, with advancing male age (Supplementary Fig. 4A). However, we found no significant effect of advancing male age on individual ejaculate traits in birds (Aves, $k = 318$; Supplementary Fig. 4B) or mammals (Mammalia, $k = 990$; Supplementary Fig. 4C).

We also observed species-specific effects of advancing male age on individual ejaculate traits. For lab rodents, *Rattus norvegicus* and *Mus musculus* ($k = 373$, combined), most traits (i.e. sperm viability, number, motility, per cent of sperm with morphological defects, sperm concentration, sperm mitochondrial function, sperm DNA and oxidative damage) showed senescence (Fig. 2C; Supplementary Fig. 5A). For bulls (*Bos taurus*, $k = 173$), ejaculate size increased with advancing male age (Supplementary Fig. 5B). For *Gallus spp.* (domestic chicken and red junglefowl combined, $k = 183$), number of sperm and ejaculate size showed senescence (Supplementary Fig. 5C; see Fig. 3 for a summary of all taxa- and species-specific effects). The male gonadosomatic index of a species (GSI: i.e. the ratio of testes to body mass, used as a proxy for the degree of sperm competition) did not modulate how advancing male age affected ejaculate traits ($R^2 = 0.26\%$, $Q_M = 0.786$, $P = 0.375$, DF = 1, Supplementary Fig. 6). Finally, using linear mixed-effects models, we detected some evidence for a quadratic effect of advancing male age on the per cent of morphologically normal sperm, viable sperm, and motile sperm (Supplementary Fig. 7).

Studies sampling a higher proportion of the maximum adult lifespan of a species provided stronger evidence for senescence in ejaculate traits ($R^2_{\text{all}} = 0.57\%$, $Q_M = 4.838$, $P = 0.028$, DF = 1, Fig. 4A; see Supplementary Fig. 8 for distribution of lifespans sampled across

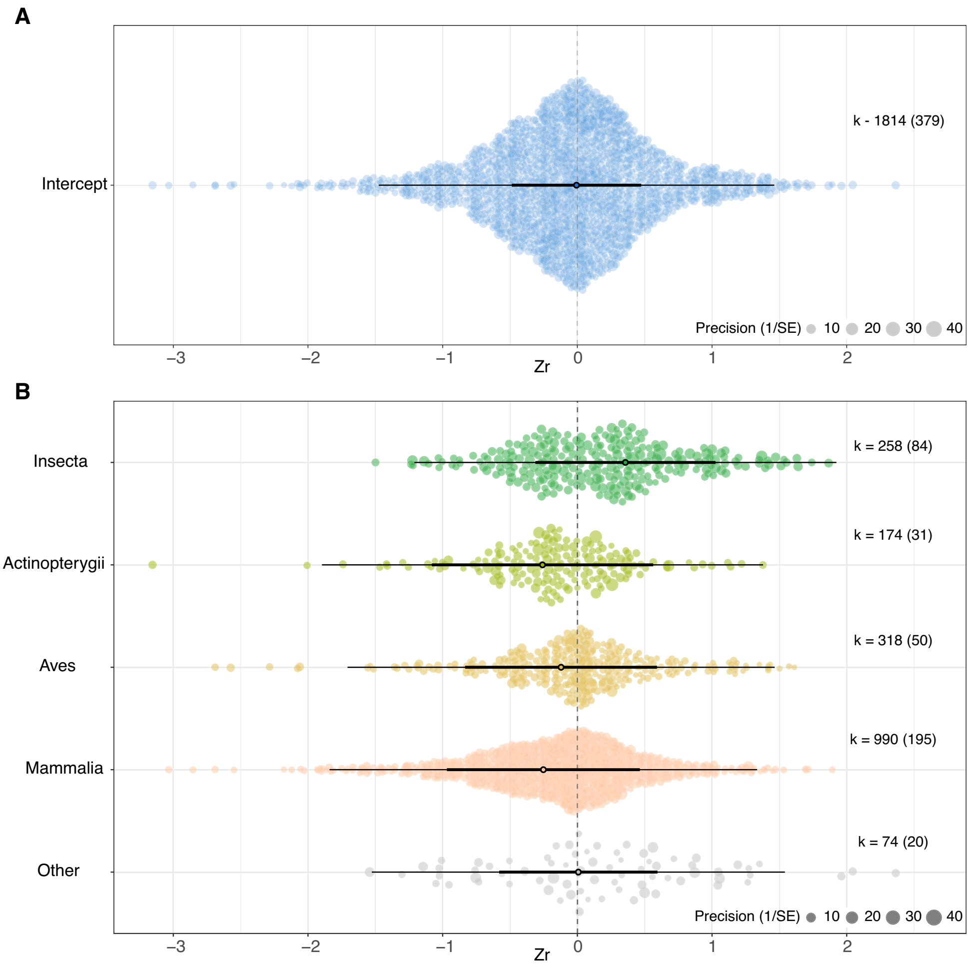

Fig. 1 | No consistent evidence for senescence in ejaculate traits, irrespective of taxonomic class. A Meta-analytical model of the overall effect of advancing male age on ejaculate traits. **B** Effect of advancing male age on ejaculate traits for each taxonomic class (note that animal classes with less than 25 effect sizes were grouped together in 'Other'). The size of each data point represents the precision of the effect size (1/SE). The *x*-axis represents values of effect sizes as Fisher's z-transformed correlation coefficient (Zr), while the *y*-axis shows the density distribution of effect sizes. The position of the overall effect is shown by the dark circle, with negative values depicting senescence in ejaculate traits and positive values showing improvement in ejaculate traits with advancing male age. Bold error bars (95% CI) show whether overall effect size is significantly different from zero (i.e. not overlapping zero), while light error bars show the 95% prediction interval (PI) of effect sizes, and black dot shows mean effect size. Sample sizes reported as: *k* = number of effect sizes (in brackets: number of studies). Source data is provided as a source data file.

taxa). This result was supported mainly in captive and lab populations, but not wild and domestic populations ($R^2_{\text{captive}} = 32.43\%$, $R^2_{\text{lab}} = 1.24\%$, $R^2_{\text{wild}} = 0.52\%$, $R^2_{\text{domestic}} = 0.36\%$; Fig. 4B–E). The stage of an organism's ontogeny (Supplementary Fig. 9) at which it was sampled significantly influenced the evidence for senescence. Specifically, studies that sampled a higher youngest or oldest age of the associated species (as a proportion of a species' maximum adult lifespan) reported stronger evidence for senescence in ejaculate traits (youngest: $P = 0.032$, $R^2_{\text{all}} = 0.64\%$, Supplementary Fig. 10; oldest: $P = 0.009$, $R^2_{\text{all}} = 0.97\%$, Supplementary Fig. 11). We did not find evidence for reproductive senescence in ejaculate traits, irrespective of the method used to collect ejaculates from males (e.g. electroejaculation, dissection, natural matings). However, ejaculate collection method explained significant heterogeneity in the data ($R^2 = 1.36\%$; $Q_M = 7.52$, $P = 0.023$, DF = 2, Supplementary Fig. 12). Population type ($R^2 = 1.12\%$; $Q_M = 2.724$, $P = 0.605$, DF = 4, Supplementary Fig. 13) or male sampling method (i.e. longitudinal or cross-sectional; $R^2 = 0.08\%$, $Q_M = 0.639$, $P = 0.887$, DF = 3, Supplementary Fig. 14), did not modulate the effect of advancing male age on ejaculate traits. We also tested whether males who experienced unnatural manipulations (i.e. conditions outside of their typical range, compared to a well-defined control in the study) showed more senescence than males who did not undergo unnatural manipulations. We detected no senescence or improvement in ejaculate traits irrespective of whether males underwent unnatural manipulations (e.g. heat stress) or not ($R^2 = 0\%$, $Q_M = 0.021$, $P = 0.989$, DF = 2, Supplementary Fig. 15A, B), or found significant differences in effects sizes between manipulated and unmanipulated males ($P = 0.885$).

Aim 3: Effects of advancing male age on reproductive outcomes

We found that male reproductive outcomes (i.e. measures of male fertilisation success, reproductive output, or offspring quality) did not improve or decline with advancing male age overall (Supplementary

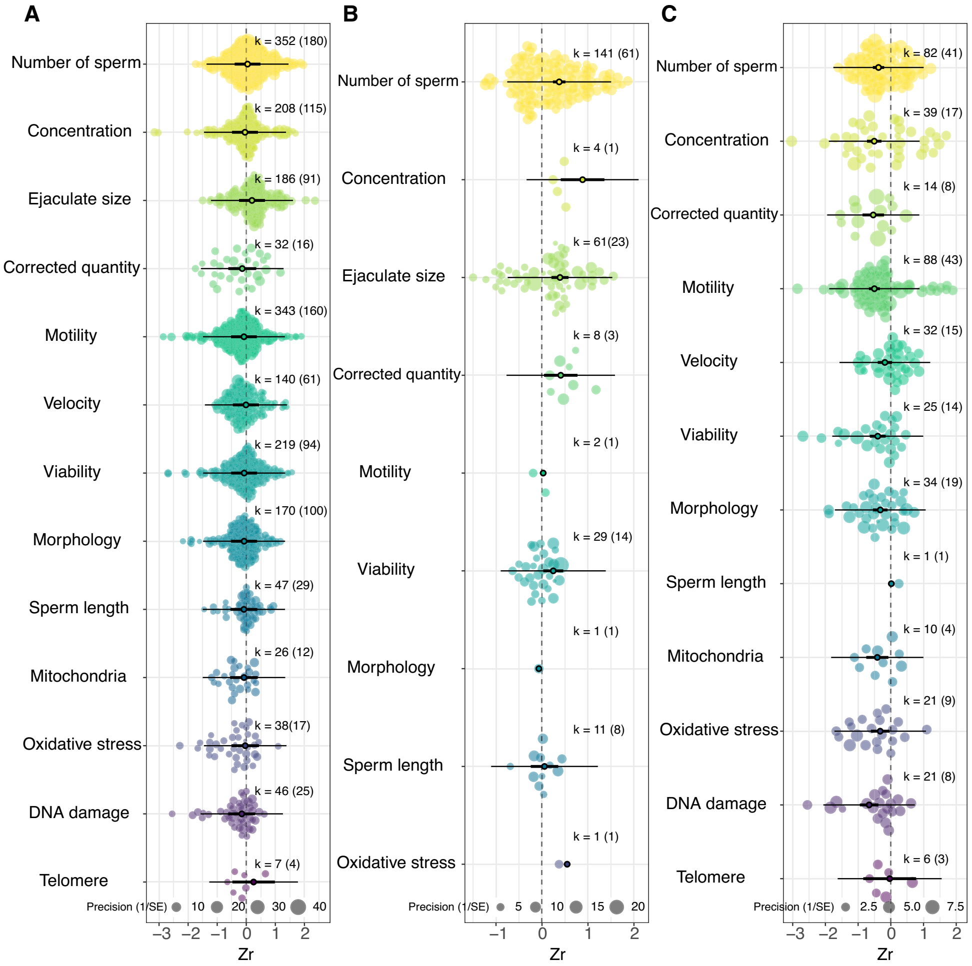

Fig. 2 | No consistent evidence for senescence in ejaculate traits when all taxa were considered, but some ejaculate traits improve with advancing age (in insects), while other traits decline (in lab rodents). A Effect of advancing male age on individual ejaculate traits across all 157 species in the dataset. **B** Effect of advancing male age on individual ejaculate traits in the class- Insecta. **C** Effect of advancing male age on individual ejaculate traits for the two most over-represented species combined (lab rodents): *Mus musculus* and *Rattus norvegicus*. The size of each data point represents the precision of the effect size (1/SE). The *x*-axis represents values of effect sizes as Fisher's z-transformed correlation coefficient (Zr), while the *y*-axis shows the density distribution of effect sizes. The position of the overall effect is shown by the dark circle, with negative values depicting senescence in ejaculate traits and positive values showing improvement in ejaculate traits with advancing male age. Sample sizes reported as: k = number of effect sizes (in brackets: number of studies). Bold error bars (95% CI) show whether overall effect size is significantly different from zero (i.e. not overlapping zero), while light error bars show the 95% PI of effect sizes, and black dot shows mean effect sizes. Note that error bars are not provided for traits with a number of effect sizes less than 3. Source data is provided as a source data file.

Fig. 16A). However, reproductive outcomes were less likely to deteriorate with advancing male age, than ejaculate traits ($R^2 = 1.76\%$, $Q_M = 9.783$, P = 0.002, DF = 1; Supplementary Fig. 16B).

Publication bias

We found no statistical evidence for publication bias, except for a time-lag bias, with more recent studies being more likely to show senescence in ejaculate traits (Supplementary Fig. 17, 18, 19).

Other sensitivity analyses

We found no significant evidence for senescence in ejaculate traits, even when restricting the analysis to studies that sampled more than 10% of the maximum adult lifespan of the species (mean [95% confidence interval (C.I.)]: −0.020 [−0.549 to 0.509], $z = -0.075$, $P = 0.940$, Supplementary Fig. 20). Results from our taxonomic class-specific models, which again only included studies that sampled >10% of maximum adult lifespan, were qualitatively similar to results from models that included all studies (Supplementary Fig. 21).

We additionally objectively categorised study aims as explicitly interested in senescence (i.e. studies using "ageing", "ageing", "senescence", "senescent", or "senescing" in their abstracts or titles, $N = 101$ studies) or not ($N = 273$ studies). We did not find significant evidence for overall senescence in ejaculate traits, even when we only analysed studies whose aims were categorised as interested in senescence (mean [95% confidence interval (CI)]: −0.294 [−0.760 to 0.172], $z = -1.238$, $P = 0.216$, Supplementary Fig. 22). Study aims however, explained a significant proportion of heterogeneity in effect sizes ($R^2 = 5.08\%$, $Q_M = 36.287$, $P < 0.001$, DF = 2; Supplementary Fig. 22). Furthermore, studies that were interested in senescence sampled a higher proportion of maximum adult lifespan of the associated species

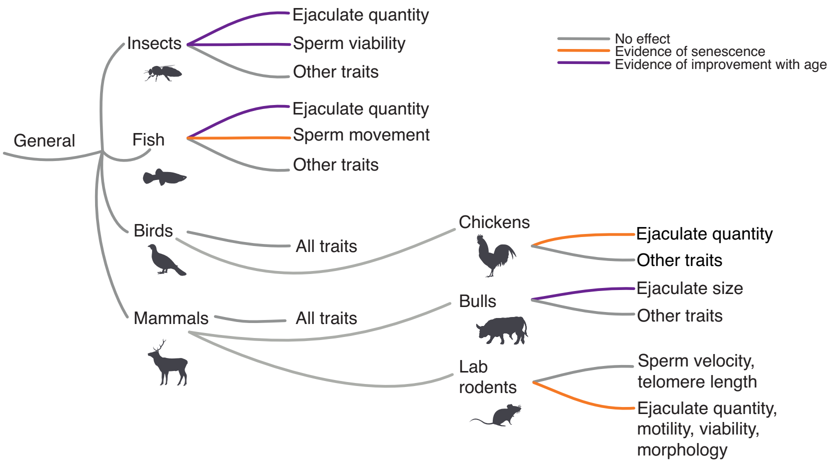

Fig. 3 | Specific ejaculate traits and taxonomy interacted to affect the evidence for senescence. Summary of results for how advancing male age affects different ejaculate traits across various taxa in our meta-analysis. "Chickens" refers to domestic chickens and red junglefowl combined. Species icons from PhyloPics, with artist credits and copyright: Kamil S. Jaron (CC0 1.0), Emma Moffett (CC0 1.0), T. Michael Keesey (PDM 1.0), Steven Traver (CC0 1.0), Georgios Lyras (CC0 1.0). Only traits with >3 effect sizes are included in the summary.

(34%) than studies not interested in senescence (20%, Supplementary Fig. 23).

Discussion

Senescence is central to our understanding of ecology[48], evolution[48], life history[16], and society[49]. Senescence in male ejaculate traits can influence sexual selection[50,51], sexual conflict[26,36], and offspring health[13]. We thus cannot fully understand organismal biology without understanding the evidence for, and consequences of, male reproductive senescence at the level of ejaculates. Our meta-analysis reviews the effects of advancing male age on ejaculate traits across animals in order to test for senescence and highlights key gaps in knowledge that will facilitate a better understanding of ageing.

Contrary to expectations, we detected no consistent evidence for senescence in ejaculate traits across studies (aim 1). Our results contrast those of a meta-analysis in humans[35], which found senescence across most ejaculate traits in men. These differences in results possibly reflect stronger selection pressures in non-human animals to maintain sperm function across all ages compared to men. In our dataset, the phylogenetically closest relative to humans were rodents (exemplified by lab rodents), which, like humans[35], showed evidence for senescence in most ejaculate traits. Current human longevity is much higher than what it was just a few centuries ago[52]. Such recent increases in human longevity could lead to men living much beyond the age at which sperm function can be maintained, leading to greater senescence in the ejaculates of men compared to other animals.

We suggest several potential non-mutually exclusive reasons for the lack of senescence in our meta-analysis. While we discovered that increasing the proportion of lifespan sampled by a study yielded greater evidence for senescence (also shown by[18,35,47]), studies in our meta-analysis tended to sample a low proportion of maximum adult lifespan (median = ~25%, Supplementary Fig. 9), which could have underestimated senescence. Another reason could be that many of the studies included in our analysis were not explicitly testing for senescence. To account for this, we conducted an analysis only on studies that were explicitly interested in senescence. These studies sampled a higher proportion of the lifespan of the associated species yet did not provide evidence for senescence in ejaculate traits overall. However, a reason for this lack of evidence could be that study aims are difficult to quantify, and our classification of aims might have excluded relevant studies. Curvilinear patterns of ageing could also have led us to underestimate senescence. This is because age-dependent changes in ejaculate traits were analysed as a linear function (effect sizes). However, ageing is often curvilinear[4,53]. Our test of quadratic effects showed some evidence in support of this. Thus, if ejaculate traits improve from early to mid-adult life (i.e. maturation) and deteriorate (i.e. senesce) later in life, the positive part of the function would be disproportionately represented against the negative part of the function[54]. Our results overall highlight the need for meta-analysts to develop techniques to calculate and analyse non-linear effect sizes to investigate such patterns.

Selective disappearance of poor-quality males with increasing age could also underestimate senescence[55,56]. Comparing means of age groups in longitudinal studies (like in our meta-analysis) can only account for selective disappearance if all individuals are sampled at all ages, which was rarely done across studies. To account for selective disappearance in cases where not all males survive to be sampled at all ages, we would need to analyse individual-level longitudinal data [rarely reported] for each male in each study rather than comparing the means of different age groups[57]. Age-dependent improvement or negligible senescence in ejaculate traits could also reflect a true biological pattern, with senescence not being an inevitable outcome of ageing for many ejaculate traits and species[4,58]. For instance, taxa with indeterminate growth or slow life histories might show negligible senescence[8,17].

We suggest corollary methodological improvements for more rigorous testing of male reproductive senescence. Specifically, studies could sample higher proportions of a male's maximum lifespan and report survival curves of the studied populations; test for curvilinear effects of age by measuring at least three age cohorts in early-, mid-, and late-adult life; separate confounding effects of male mating history and age by comparing virgin versus frequently mated old and young males; test for selective disappearance by sampling males longitudinally and report individual-level data for each male; be explicit about which theories of ageing are being tested and their corollary predictions; and sample equal number of males in all age classes. Overall, we conclude that senescence is likely occurring in the taxon-specific ejaculate traits where we found supporting evidence. However, we could have underestimated the extent of senescence where

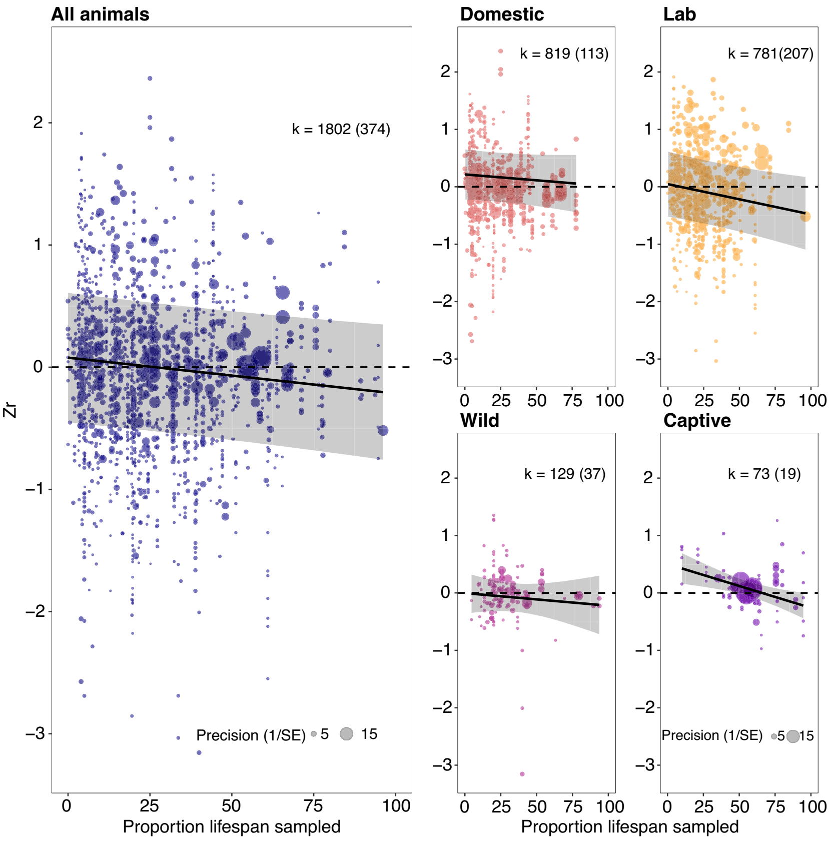

Fig. 4 | Increasing the proportion of the maximum adult lifespan sampled increased the likelihood of finding senescence. Effect of proportion of maximum adult lifespan sampled (*x*-axis) on the effect size i.e. Fisher's z transformed r (*y*-axis) across the entire dataset (**A**), and broken down for domestic (**B**), laboratory (**C**), wild (**D**), and captive animals (**E**). The size of each data point represents the precision of the effect size (1/SE). The dark line with shaded bars represents the overall effect of lifespan sampled on effect sizes and its 95% CI, respectively, and the black line shows the mean regression line. Negative values depict senescence in ejaculate traits with advancing age, while positive values show improvement in ejaculate traits with advancing male age. Sample sizes reported as: *k* = number of effect sizes (in brackets: number of studies). Source data is provided as a source data file.

supporting evidence was lacking due to some aforementioned limitations.

Some biological and methodological moderators were important in explaining the observed heterogeneity in effect sizes (aim 2). However, as the effects of these moderators were tested individually, our results could possibly be explained by other moderators not simultaneously included in the analysis. Thus, our results should only be treated as hypothesis-generating rather than evidence of causation. Taxonomic class and ejaculate trait explained a significant proportion of heterogeneity. This heterogeneity could be attributed to differences in ecologies, niches, behaviours, life-history strategies, metabolisms, and evolutionary histories of animals[4,59]. Heterogeneity explained by ejaculate traits could be due to covariances between different ejaculate traits[60]; some traits being more sensitive to age-dependent deterioration than others[61]; or different traits being under varying selection pressures[62]. Additionally, some ejaculate traits are more likely to influence fertilisation success than others[60]. It is thus possible for traits that are more important determinants of fertilisation success to evolve slower rates of senescence than less important traits[63], which future studies could test.

We discovered some taxonomic class-specific evidence for age-dependent changes in individual ejaculate traits. Insects showed an increase in all sperm and ejaculate quantity traits. This increase could be associated with their mating status, as most studies (>75%) on insects in our meta-analysis kept males as virgins. Specifically, in species with life-long spermatogenesis and low rates of sperm loss (such as some insects[64,65]), low mating rates can result in old males accumulating more sperm and producing larger ejaculates than young males[66]. Ray-finned fish (Actinopterygii) showed evidence for senescence in sperm velocity and motility but also age-dependent increases in ejaculate size. This result could be due to old males producing larger ejaculates to compensate for senescence in sperm performance. Increases in fish ejaculate size could also reflect the effects of continuous post-maturity growth in many fish species[17,18,67], leading to older males having larger gonads. We did not find consistent evidence for senescence in ejaculate traits in mammals or birds.

We detected several species-specific patterns of senescence. Specifically, most ejaculate traits in lab rodents (*Mus musculus* and *Rattus norvegicus* combined) showed senescence, even when only control/wild-type genetic strains were analysed (e.g. C57 for mice, Brown Norway and Sprague Dawley for rats). This could be due to studies on lab rodents usually having equal sample sizes of males in each age cohort, thus possibly limiting bias towards weighting of the positive part (early- to mid-life) of the curvilinear ageing function. Consistent evidence for senescence in lab rodents could also be associated with senescence being exacerbated in lab-adapted populations[68]. For a more nuanced understanding of such traits by taxon interactions, we suggest that future studies account for age-dependent changes in body and testes size (as covariates), test for post-meiotic senescence of sperm during storage in males, record whether studied species exhibit continuous spermatogenesis and sperm reabsorption; and measure multiple ejaculate traits simultaneously (i.e. sperm quantity and performance/viability), because sperm quantity versus performance traits might be affected by age in different ways.

Extending the proportion of the maximum adult lifespan sampled increased the evidence for senescence in ejaculate traits for a species. This result suggests that the onset of reproductive senescence usually occurs late in life[4,69], and senescence will more likely be detected if studies sample a larger proportion of lifespan. However, this may be biased by the population sampled, as this association was strong in captive and lab animals but not in wild and domestic animals. We did not find evidence for senescence at any level of other methodological moderators (aim 2). This result could be due to the effects of methodological moderators being taxon-specific or being revealed only under interactions with other methodological or biological moderators. The lack of an effect of study methodologies might also be explained by moderators that we did not include in our analyses (Table 2).

We detected no consistent evidence for overall improvement or senescence in reproductive outcomes of males (i.e. measures of fertilisation success, egg/offspring number/viability/quality; aim 3). Our meta-analysis used data on reproductive outcomes only from studies that also measured ejaculate traits, which possibly represents a biased subset of studies on ageing of reproductive outcomes. However, we found that reproductive outcomes were less likely to exhibit age-dependent deterioration than ejaculate traits. This difference could be due to not all ejaculate traits being key determinants of reproductive success (e.g. fertilisation success[70]), and deterioration in some ejaculate traits having little consequence for a male's reproductive outcome[71]. Lower rates of age-dependent declines in male reproductive outcomes could also be due to female-driven effects (e.g. cryptic female choice, reproductive compensation), which might provide a buffer against low-quality ejaculates of old males. For instance, females might be able to eject poor-quality sperm via cryptic female choice[72], or females mated to older males might compensate by investing more resources into provisioning[73]. Additionally, viability selection in old males could purge low-quality male genotypes, leading to old males having higher means and lower variances for reproductive outcomes than young males[46,74]. These results suggest that age-dependent changes in ejaculate traits may not accurately reflect changes in reproductive outcomes. We emphasize that studies should ideally measure ejaculate traits, male reproductive success, and offspring phenotypes to elucidate the fitness consequences of advancing male age.

Methods

We followed the PRISMA-EcoEvo guidelines for our meta-analysis[75] and conducted statistical analyses in R[76] v 4.1.2. Supplementary figures 1-24) and Supplementary notes 1-12) are provided in the "Supplementary Information" file. Data, model outputs, metadata, code, PRISMA checklist, and pre-registration have all been deposited at OSF (https://osf.io/dk8sq/).

Search protocol

We conducted a literature search using search strings on SCOPUS and Web of Science on 21st January and 27th March 2021, respectively (see Supplementary Notes 1 for specific search strings). In addition, we conducted a backward and forward search using seven relevant papers related to the topic of our meta-analysis[11,13,22,24,43,54,77]. We additionally conducted a search for unpublished research using the Bielefeld Academy Search Engine[78]. Finally, we contacted 56 researchers who study the ecology and evolution of male reproductive senescence to ask for unpublished data. Our search resulted in a total of 9412 unique abstracts from published sources and 271 abstracts from unpublished sources (PRISMA diagram: Supplementary Fig. 1). We screened these abstracts in Rayyan[79] and abstrackr[80] using pre-defined selection criteria (see below). We ensured that the screening process was highly repeatable (Supplementary Notes 2).

Inclusion criteria

For a study to be included in our analysis, some selection criteria had to be fulfilled during the abstract and full-text screening stages. When screening abstracts, the study had to be a research article (not a review, meta-analysis, or case study) on non-human animals written in English and quantifying ejaculate traits in males of different ages. When screening full-texts, the study needed to contain data on the effects of male age on ejaculate traits, non-overlapping age groups of males, and appropriate data for calculation of effect sizes. We only included studies where at least two age groups of adult males could be compared (see Supplementary Notes 3 for our definition of "adults"). We deemed a total of 379 studies (374 from published and five from unpublished sources) appropriate for data extraction based on our selection criteria and included them in our meta-analysis (PRISMA diagram in Supplementary Fig. 1). These studies represented 157 species.

Data collection

To quantify the evidence for or against male reproductive senescence (aim 1), we collected data on means, standard deviations (SD) or standard errors (SE), the number of males in each age group, and the number of unique males in the study, wherever reported (see Supplementary Notes 4 for formulae used to calculate SD). If we could not obtain means and SD/SE, we noted the "test statistic" (e.g. t from t-tests or R^2 values) reported in the study from which effect sizes can be easily obtained. We ensured that the data extraction process was highly repeatable (Supplementary Notes 2).

To understand how biological moderators affect patterns of senescence (aim 2), we recorded information on various biological variables from the 379 studies included in the meta-analysis. We recorded the species and taxonomic class of the study organism, and the ejaculate traits measured in the study (see Supplementary Notes 5 for definitions of each trait). The ejaculate traits were either measures of sperm/ejaculate quantity (e.g. sperm concentration, sperm number, and ejaculate volume), sperm performance (e.g. sperm motility, velocity, viability), or intra-cellular measures of sperm quality (e.g. oxidative stress in sperm, DNA damage to sperm, sperm telomere length). Finally, we recorded the gonadosomatic index (GSI, i.e. the ratio of testis mass to body mass, as a proxy for sperm competition[81,82]) for each species, wherever possible (see Supplementary Notes 6; metadata on OSF https://osf.io/dk8sq/).

To understand how methodological moderators affect patterns of senescence in ejaculate traits (aim 2), we collected data on various methodological variables from included studies (see Supplementary Notes 7). Initially, we recorded the maximum lifespan (male-specific whenever possible or species-specific when male-specific data were not available) and age at adulthood of the species studied (see Supplementary Notes 6). Data on maximum lifespan and age at adulthood, as well as sources of these data, can be found at OSF (https://osf.io/dk8sq/). We then calculated the proportion of maximum adult lifespan sampled for a species in each study (converted to years). Some of the data on maximum adult lifespans (especially for vertebrates) were obtained from large databases/datasets (that often only reported species-level lifespans without reporting the sex of the measured individuals). Thus, these data may not always accurately reflect the maximum male lifespans of the specific populations included in our meta-analysis.

We also recorded the method of sperm extraction (e.g. electro-ejaculation, natural mating); population type (whether males belonged to wild, domestic, captive or laboratory populations (see Supplementary Notes 8 for definitions)); method for measuring male age (i.e. whether male age was known directly or indirectly estimated from a measure of phenotype); whether the ejaculate was stored in cold conditions (<5 °C, irrespective of the duration of storage) before analysis of sperm performance; and whether the study was experimental or not[18]. In some studies, males underwent "unnatural manipulations" (see Supplementary Notes 9 for detailed definitions). Here, we also recorded whether the data were obtained from males that underwent these "unnatural" manipulations (i.e. males that experienced conditions outside of their typical range that were compared to a well-defined control in the study) or from males that were used as controls in the same study.

We investigated whether advancing male age affects male reproductive outcomes (aim 3) and whether the effects of male age on reproductive outcomes (see Supplementary Notes 5 for definitions) differ from those on ejaculate traits. For this, we collected data on how advancing male age affects male fertilisation success, the number of eggs produced by the mated females, the number of offspring produced by the mated females, egg viability and hatchability; offspring viability, offspring developmental rate and offspring body condition, whenever available in a study (53 studies in total).

Calculating effect sizes

We used Fisher's *z*-transformed correlation coefficient (Zr) as the effect size in our meta-analysis[83]. Each effect size was calculated from either standardised mean differences (when two age groups were compared), simulations (when multiple age groups were compared), or test statistics (see Supplementary Notes 10 for formulae used). Effect sizes from these three calculation methods were not significantly different from each other (Supplementary Notes 10; Supplementary Fig. 24); thus, all effect sizes, irrespective of their calculation methods, were analysed together in our models. We corrected all calculated effect sizes (Zr) by a multiplier to obtain the final effect sizes to be used in the analyses (see Supplementary Notes 10) so that negative effect sizes indicated senescence, while positive effect sizes indicated improvement in ejaculate traits with advancing male age.

Data analysis

We first created a meta-analytical model (i.e. null model) to test for the general overall effect of advancing male age on ejaculate traits (aim 1), using the rma.mv function in the metafor package[84]. We included the effect size (Zr) as our response variable in the null model and random effects of: effect size ID (which represents the residual within-study variance), cohort ID, study ID, and species name to control for non-independence of effect sizes[85]. We also added a correlation matrix quantifying the phylogenetic relatedness of species in our dataset to control for non-independence arising due to shared phylogenetic history and test for a phylogenetic signal[86]. The phylogenetic tree (Supplementary Fig. 2) was built using the packages ape[87] and rotl[88], which use data from the OpenTreeOfLife[89]. We quantified the total heterogeneity[90] not due to sampling error as I^2, which can range from 0–100. We quantified partial heterogeneity explained by each random effect using the function i2_ml from the orchard package[91].

We created meta-regressions to investigate how moderators modulated the effects of advancing male age on ejaculate traits (aim 2). In all meta-regressions, we included the same random effects and phylogenetic matrix as in our null model and effect size (Zr) as our response variable. We first conducted a meta-regression with all moderators for which data were available for >75% of effect sizes and studies ("full" model). This full model was used to estimate the proportion of heterogeneity explained by moderators[92] while accounting for the confounding effects of other moderators. The full model included moderators of taxonomic class, ejaculate trait, proportion of maximum adult lifespan sampled, whether or not males had control over ejaculation, population type, sampling method of males, method of age estimation, whether or not a study was experimental, and whether or not males underwent "unnatural" manipulations. We then built several meta-regressions to explore individually the effects of each methodological and biological moderator (see Tables 1 and 2, Supplementary Notes 7, most of which had been pre-registered at OSF: https://osf.io/dk8sq/). Here, we also tested how the youngest and oldest ages sampled of the associated species (as a proportion of the maximum lifespan of the species) affected the evidence for senescence. We further tested the influence of the gonadosomatic index of species (GSI), which was not included in the full model, as it only had data for <75% of studies and was not pre-registered.

For each meta-regression model, we calculated the total heterogeneity (Q_M) and the proportion of total heterogeneity explained by moderators (marginal R^2), with the function r2_ml using the orchard package[91]. *P* values ($\alpha = 0.05$) indicate whether the heterogeneity explained was significant or not[90]. We created models without an intercept to test whether each level of a moderator showed evidence for senescence or improvement in ejaculate traits with age. However, for moderators with two levels, we were additionally interested in comparing effect sizes in one level to those in the other level. In such cases, we created a model with one level of the moderator as the intercept (here, a P value expressed whether one level of the moderator was different from the other level).

Taxonomic classes of Insecta, Actinopterygii, Aves, and Mammalia were over-represented classes in our dataset, each with >150 effect sizes from >30 studies (Supplementary Fig. 2). We thus created four separate meta-regressions for each class, with ejaculate trait as a moderator. Moreover, four species: lab mice (*Mus musculus*), lab rats (*Rattus norvegicus*), chicken/red junglefowl (*Gallus spp.*), and bulls (*Bos taurus*) were over-represented in our dataset (each species had >150 effect sizes across >20 studies; Supplementary Fig. 2). For these species, we created separate meta-regression models with ejaculate trait as a moderator.

Shapes of reproductive ageing are often curvilinear, characterised by an initial period of maturation, where performance increases from early- to mid-adult life and subsequently decreases (i.e. senescence) in late-adult life[4,53]. To test whether the effects of male age on ejaculate traits were curvilinear, we used linear mixed-effects models[93] (Supplementary Notes 11). These analyses were limited to traits which were measured on the same scale and units across studies/taxa.

We also used data from studies that measured age-dependent changes in both ejaculate traits and reproductive outcomes. Then, we ran a meta-regression using a type of trait (reproductive outcome or ejaculate trait) as a moderator (aim 3).

Publication bias

We conducted a sensitivity analysis of our null model by replacing the random effects terms of cohort and effect size ID with a variance–covariance matrix[94]. We also performed various publication bias tests[94] (funnel plot, trim and fill multi-level meta-regression, and selection model; Supplementary Notes 12). These analyses were done to test for biased sampling of effect sizes in our study based on their precision, magnitude, publication year, and sample size.

Other sensitivity analysis

We conducted two additional sensitivity analyses. First, we accounted for the low proportions of maximum adult lifespans sampled by studies in our meta-analysis. Here, we re-ran our null model and models for the taxonomic classes of Insecta, Mammalia, Aves, and Actinopterygii, only using data from studies that sampled >10% of the maximum adult lifespan of the species. Second, we classified study aims as being explicitly interested in senescence or not. Studies that mentioned “ageing”, “ageing”, “senescence”, “senescent”, or “senescing” in their abstracts or titles were classified as explicitly interested in senescence. We then created a meta-regression with the study aim (i.e. interested in senescence or not) as our moderator to test whether studies that were interested in senescence showed senescence in ejaculate traits overall.

Reporting summary

Further information on research design is available in the Nature Portfolio Reporting Summary linked to this article.

Data availability

The data generated in this study have been deposited in the Open Science Framework database (https://osf.io/dk8sq/) with the following https://doi.org/10.17605/OSF.IO/DK8SQ. The data are available without any restricted access. The raw data are available under the file name “raw_data.csv”. The processed data are available under the file name “spermFinalAllData.csv”. The data used to produce the manuscript figures are provided in the Source Data file. Source data are provided in this paper.

Code availability

All associated code can be found at the Open Science framework database (https://osf.io/dk8sq/) with the following https://doi.org/10.17605/OSF.IO/DK8SQ.

References

1. Reinke, B. A. et al. Diverse aging rates in ectothermic tetrapods provide insights for the evolution of aging and longevity. *Science* **376**, 1459–1466 (2022).
2. Lemaître, J.-F. & Gaillard, J.-M. Reproductive senescence: new perspectives in the wild: reproductive senescence in the wild. *Biol. Rev.* **92**, 2182–2199 (2017).
3. Nussey, D. H., Froy, H., Lemaitre, J.-F., Gaillard, J.-M. & Austad, S. N. Senescence in natural populations of animals: Widespread evidence and its implications for bio-gerontology. *Ageing Res. Rev.* **12**, 214–225 (2013).
4. Jones, O. R. et al. Diversity of ageing across the tree of life. *Nature* **505**, 169–173 (2014).
5. Jones, O. R. & Vaupel, J. W. Senescence is not inevitable. *Biogerontology* **18**, 965–971 (2017).
6. Monaghan, P., Charmantier, A., Nussey, D. H. & Ricklefs, R. E. The evolutionary ecology of senescence. *Funct. Ecol.* **22**, 371–378 (2008).
7. Roper, M., Capdevila, P. & Salguero-Gómez, R. Senescence: why and where selection gradients might not decline with age. *Proc. R. Soc. B.* **288**, 20210851 (2021).
8. Vaupel, J., Baudisch, A., Dölling, M., A. Roach, D. & Gampe, J. The case for negative senescence. *Theor. Popul. Biol.* **65**, 339–351 (2004).
9. Blagosklonny, M. V. The hyperfunction theory of aging: three common misconceptions. *Oncoscience* **8**, 103–107 (2021).
10. Paul, C. & Robaire, B. Ageing of the male germ line. *Nat. Rev. Urol.* **10**, 227–234 (2013).
11. Radwan, J. Male age, germline mutations and the benefits of polyandry: germline mutations, ageing and polyandry. *Ecol. Lett.* **6**, 581–586 (2003).
12. Mannucci, A. et al. The impact of oxidative stress in male infertility. *Front. Mol. Biosci.* **8**, 799294 (2022).
13. Monaghan, P. & Metcalfe, N. B. The deteriorating soma and the indispensable germline: gamete senescence and offspring fitness. *Proc. R. Soc. B.* **286**, 20192187 (2019).
14. Medawar, P. *An Unsolved Problem of Biology*. (1952).
15. Williams, P. D. & Day, T. Antagonistic pleiotropy, mortality source interactions, and the evolutionary theory of senescence. *Evolution* **57**, 1478–1488 (2003).
16. Rose, M. & Charlesworth, B. A test of evolutionary theories of senescence. *Nature* **287**, 141–142 (1980).
17. Purchase, C. F. et al. A synthesis of senescence predictions for indeterminate growth, and support from multiple tests in wild lake trout. *Proc. R. Soc. B.* **289**, 20212146 (2022).
18. Vrtílek, M., Žák, J. & Reichard, M. Evidence for reproductive senescence across ray-finned fishes: a review. *Front. Ecol. Evol.* **10**, 982915 (2022).
19. Bodnar, A. G. Cellular and molecular mechanisms of negligible senescence: insight from the sea urchin. *Invertebr. Reprod. Dev.* **59**, 23–27 (2015).
20. Archer, R., Paniw, M., Vega-Trejo, R. & Sepil, I. A sex skew in life-history research: the problem of missing males Proc. R. Soc. *Proc. R. Soc. B* **289** 20221117 (2022).
21. Lemaître, J.-F., Ronget, V. & Gaillard, J.-M. Female reproductive senescence across mammals: a high diversity of patterns modulated by life history and mating traits. *Mechan. Ageing Dev.* **192**, 111377 (2020).
22. Fricke, C. & Koppik, M. Male reproductive ageing: a tale of the whole ejaculate. *Reproduction* **158**, R219–R229 (2019).
23. Aich, U., Head, M. L., Fox, R. J. & Jennions, M. D. Male age alone predicts paternity success under sperm competition when effects of age and past mating effort are experimentally separated. *Proc. R. Soc. B.* **288**, 20210979 (2021).
24. Gasparini, C., Marino, I. A. M., Boschetto, C. & Pilastro, A. Effect of male age on sperm traits and sperm competition success in the guppy (*Poecilia reticulata*). *J. Evolut. Biol.* **23**, 124–135 (2010).
25. Jones, A. G. The evolution of alternative cryptic female choice strategies in age-structured populations. *Evolution* **56**, 2530–2536 (2002).
26. Adler, M. I. & Bonduriansky, R. Sexual conflict, life span, and aging. *Cold Spring Harb. Perspect. Biol.* **6**, a017566–a017566 (2014).
27. Bonduriansky, R., Maklakov, A., Zajitschek, F. & Brooks, R. Sexual selection, sexual conflict and the evolution of ageing and life span. *Funct. Ecol.* **22**, 443–453 (2008).
28. Parker, G. A. Sexual conflict over mating and fertilization: an overview. *Philos. Trans. R. Soc. B* **361**, 235–259 (2006).
29. Bronikowski, A. M. et al. Sex-specific aging in animals: perspective and future directions. *Aging Cell* **21** (2022).
30. Bergeron, L. A. et al. Evolution of the germline mutation rate across vertebrates. *Nature* https://doi.org/10.1038/s41586-023-05752-y (2023).
31. Crow, J. F. The origins, patterns and implications of human spontaneous mutation. *Nat. Rev. Genet.* **1**, 40–47 (2000).
32. Reinhardt, K. & Turnell, B. Sperm ageing: a complex business. *Funct. Ecol.* **33**, 1188–1189 (2019).
33. Sharma, R. et al. Effects of increased paternal age on sperm quality, reproductive outcome and associated epigenetic risks to offspring. *Reprod. Biol. Endocrinol.* **13**, 35 (2015).
34. Cornwallis, C. K., Dean, R. & Pizzari, T. Sex-specific patterns of aging in sexual ornaments and gametes. *Am. Nat.* **184**, E66–E78 (2014).
35. Johnson, S. L., Dunleavy, J., Gemmell, N. J. & Nakagawa, S. Consistent age-dependent declines in human semen quality: a systematic review and meta-analysis. *Ageing Res. Rev.* **19**, 22–33 (2015).

36. Dean, R. et al. Male reproductive senescence causes potential for sexual conflict over mating. *Curr. Biol.* **20**, 1192–1196 (2010).
37. Gasparini, C., Devigili, A. & Pilastro, A. Sexual selection and ageing: interplay between pre- and post-copulatory traits senescence in the guppy. *Proc. R. Soc. B.* **286**, 20182873 (2019).
38. Decanini, D. P., Wong, B. B. M. & Dowling, D. K. Context-dependent expression of sperm quality in the fruitfly. *Biol. Lett.* **9**, 20130736 (2013).
39. Girndt, A. et al. Male age and its association with reproductive traits in captive and wild house sparrows. *J. Evol. Biol.* **32**, 1432–1443 (2019).
40. Lifjeld, J. T. et al. When older males sire more offspring—increased attractiveness or higher fertility? *Behav. Ecol. Sociobiol.* **76**, 61 (2022).
41. Wedell, N. & Ritchie, M. G. Male age, mating status and nuptial gift quality in a bushcricket. *Anim. Behav.* **67**, 1059–1065 (2004).
42. Delbarco-Trillo, J., Tourmente, M., Varea-Sánchez, M. & Roldan, E. R. S. Is male reproductive senescence minimized in Mus species with high levels of sperm competition? *Biol. J. Linn. Soc.* **123**, 463–470 (2018).
43. Vega-Trejo, R., Fox, R. J., Iglesias-Carrasco, M., Head, M. L. & Jennions, M. D. The effects of male age, sperm age and mating history on ejaculate senescence. *Funct. Ecol.* **33**, 1267–1279 (2019).
44. Mickova, K. et al. Age-related changes in sperm traits and evidence for ageing costs of sperm production in a sexually promiscuous passerine. *Front. Ecol. Evolut.* **11** (2023).
45. Sandfoss, M. R., Reichling, S. & Roberts, B. M. Sperm morphology and forward motility are indicators of reproductive success and are not age- or condition-dependent in a captive breeding population of endangered snake. *PLoS ONE* **18**, e0282845 (2023).
46. Johnson, S. L. & Gemmell, N. J. Are old males still good males and can females tell the difference?: Do hidden advantages of mating with old males off-set costs related to fertility, or are we missing something else? *Bioessays* **34**, 609–619 (2012).
47. Fricke, C. et al. Timeless or tainted? The effects of male ageing on seminal fluid. *Front. Ecol. Evol.* **11**, 1066022 (2023).
48. Healy, K., Ezard, T. H. G., Jones, O. R., Salguero-Gómez, R. & Buckley, Y. M. Animal life history is shaped by the pace of life and the distribution of age-specific mortality and reproduction. *Nat. Ecol. Evol.* **3**, 1217–1224 (2019).
49. Kirkwood, T. B. L. The origins of human ageing. *Philos. Trans. R. Soc. Lond. B* **352**, 1765–1772 (1997).
50. Promislow, D. Mate choice, sexual conflict, and evolution of senescence. *Behav. Genet.* **33**, 191–201 (2003).
51. Archer, C. R. & Hunt, J. Understanding the link between sexual selection, sexual conflict and aging using crickets as a model. *Exp. Gerontol.* **71**, 4–13 (2015).
52. Oeppen, J. & Vaupel, J. W. Broken limits to life expectancy. *Science* **296**, 1029–1031 (2002).
53. Baudisch, A. & Stott, I. A pace and shape perspective on fertility. *Methods Ecol. Evol.* **10**, 1941–1951 (2019).
54. Pizzari, T., Dean, R., Pacey, A., Moore, H. & Bonsall, M. B. The evolutionary ecology of pre- and post-meiotic sperm senescence. *Trends Ecol. Evolut.* **23**, 131–140 (2008).
55. Hämäläinen, A. et al. Senescence or selective disappearance? Age trajectories of body mass in wild and captive populations of a small-bodied primate. *Proc. R. Soc. B.* **281**, 20140830 (2014).
56. Sanghvi, K., Iglesias-Carrasco, M., Zajitschek, F., Kruuk, L. E. B. & Head, M. L. Effects of developmental and adult environments on ageing. *Evolution* **76**, 1868–1882 (2022).
57. van de Pol, M. & Verhulst, S. Age-dependent traits: a new statistical model to separate within- and between-individual effects. *Am. Nat.* **167**, 766–773 (2006).
58. Finch, C. E. Update on slow aging and negligible senescence—a mini-review. *Gerontology* **55**, 307–313 (2009).
59. Jones, O. R. et al. Senescence rates are determined by ranking on the fast-slow life-history continuum. *Ecol. Lett.* **11**, 664–673 (2008).
60. Snook, R. Sperm in competition: not playing by the numbers. *Trends in Ecology &. Evolution* **20**, 46–53 (2005).
61. Naciri, M., Aars, J., Blanchet, M.-A., Gimenez, O. & Cubaynes, S. Reproductive senescence in polar bears in a variable environment. *Front. Ecol. Evol.* **10**, 920481 (2022).
62. Schluter, D., Price, T. & Rowe, L. Conflicting selection pressures and life history trade-offs. *Proc. R. Soc. Lond. B* **246**, 11–17 (1991).
63. Moorad, J. A. & Ravindran, S. Natural selection and the evolution of asynchronous aging. *Am. Nat.* **199**, 551–563 (2022).
64. Kehl, T., Karl, I. & Fischer, K. Old-male paternity advantage is a function of accumulating sperm and last-male precedence in a butterfly. *Mol. Ecol.* **22**, 4289–4297 (2013).
65. Reinhardt, K., Naylor, R. & Siva-Jothy, M. T. Male mating rate is constrained by seminal fluid availability in bedbugs, *Cimex lectularius*. *PLoS ONE* **6**, e22082 (2011).
66. Sepil, I. et al. Male reproductive aging arises via multifaceted mating-dependent sperm and seminal proteome declines, but is postponable in *Drosophila*. *Proc. Natl Acad. Sci. USA* **117**, 17094–17103 (2020).
67. Patnaik, B. K., Mahapatro, N. & Jena, B. S. Ageing in fishes. *Gerontology* **40**, 113–132 (1994).
68. Zajitschek, F., Zajitschek, S. & Bonduriansky, R. Senescence in wild insects: key questions and challenges. *Funct. Ecol.* **34**, 26–37 (2020).
69. Gaillard, J. & Lemaître, J. An integrative view of senescence in nature. *Funct. Ecol.* **34**, 4–16 (2020).
70. Smith, C. C. Opposing effects of sperm viability and velocity on the outcome of sperm competition. *Behav. Ecol.* **23**, 820–826 (2012).
71. Gage, M. J. G. et al. Spermatozoal traits and sperm competition in atlantic salmon. *Curr. Biol.* **14**, 44–47 (2004).
72. Wagner, R. H., Helfenstein, F. & Danchin, E. Female choice of young sperm in a genetically monogamous bird. *Proc. R. Soc. Lond. B* **271** (2004).
73. Harris, W. E. & Uller, T. Reproductive investment when mate quality varies: differential allocation versus reproductive compensation. *Philos. Trans. R. Soc. B* **364**, 1039–1048 (2009).
74. Brooks, R. Can older males deliver the good genes?. *Trends Ecol. Evolut.* **16**, 308–313 (2001).
75. O'Dea, R. E. et al. Preferred reporting items for systematic reviews and meta-analyses in ecology and evolutionary biology: a PRISMA extension. *Biol. Rev.* **96**, 1695–1722 (2021).
76. R Development Core Team. R: a language and environment for statistical computing. (R Foundation for Statistical Computing, Vienna, 2022).
77. Jones, T. M. & Elgar, M. A. The role of male age, sperm age and mating history on fecundity and fertilization success in the hide beetle. *Proc. R. Soc. Lond. B* **271**, 1311–1318 (2004).
78. Pieper, D. & Summann, F. Bielefeld Academic Search Engine (BASE): an end-user oriented institutional repository search service. *Libr. Hi Tech.* **24**, 614–619 (2006).
79. Ouzzani, M., Hammady, H., Fedorowicz, Z. & Elmagarmid, A. Rayyan—a web and mobile app for systematic reviews. *Syst. Rev.* **5**, 210 (2016).
80. Rathbone, J., Hoffmann, T. & Glasziou, P. Faster title and abstract screening? Evaluating Abstrackr, a semi-automated online screening program for systematic reviewers. *Syst. Rev.* **4**, 80 (2015).
81. Polanin, J. R. & Snilstveit, B. Converting between effect sizes. *Campbell Syst. Rev.* **12**, 1–13 (2016).

82. Parker, G. A., Ramm, S. A., Lehtonen, J. & Henshaw, J. M. The evolution of gonad expenditure and gonadosomatic index (GSI) in male and female broadcast-spawning invertebrates: GSI in broadcast spawning invertertebrates. *Biol. Rev.* **93**, 693–753 (2018).
83. Nakagawa, S. & Cuthill, I. C. Effect size, confidence interval and statistical significance: a practical guide for biologists. *Biol. Rev.* **82**, 591–605 (2007).
84. Viechtbauer, W. Conducting Meta-Analyses in *R* with the **metafor** Package. *J. Stat. Soft.* **36** (2010).
85. Noble, D. W. A., Lagisz, M., O'dea, R. E. & Nakagawa, S. Nonindependence and sensitivity analyses in ecological and evolutionary meta-analyses. *Mol. Ecol.* **26**, 2410–2425 (2017).
86. Cinar, O., Nakagawa, S. & Viechtbauer, W. Phylogenetic multilevel meta-analysis: a simulation study on the importance of modelling the phylogeny. *Methods Ecol. Evol.* **13**, 383–395 (2022).
87. Paradis, E., Claude, J. & Strimmer, K. APE: analyses of phylogenetics and evolution in R language. *Bioinformatics* **20**, 289–290 (2004).
88. Michonneau, F., Brown, J. W. & Winter, D. J. rotl: an R package to interact with the Open Tree of Life data. *Methods. Ecol. Evol.* **7**, 1476–1481 (2016).
89. Hinchliff, C. E. et al. Synthesis of phylogeny and taxonomy into a comprehensive tree of life. *Proc. Natl Acad. Sci. USA* **112**, 12764–12769 (2015).
90. Higgins, J. P. T. & Thompson, S. G. Quantifying heterogeneity in a meta-analysis. *Stat. Med.* **21**, 1539–1558 (2002).
91. Nakagawa, S. et al. orchaRd: An R package for drawing 'orchard'plots (and 'caterpillars' plots) from meta-analyses and meta-regressions with categorical moderators. Preprint at *EcoEvoRxiv* https://doi.org/10.32942/X2QC7K (2020).
92. Senior, A. M. et al. Heterogeneity in ecological and evolutionary meta-analyses: its magnitude and implications. *Ecology* **97**, 3293–3299 (2016).
93. Bates, D., Mächler, M., Bolker, B. & Walker, S. Fitting Linear Mixed-Effects Models using lme4. https://doi.org/10.48550/ARXIV.1406.5823 (2014)
94. Nakagawa, S. et al. Methods for testing publication bias in ecological and evolutionary meta-analyses. *Methods Ecol. Evol.* **13**, 4–21 (2022).
95. Lüpold, S., de Boer, R. A., Evans, J. P., Tomkins, J. L. & Fitzpatrick, J. L. How sperm competition shapes the evolution of testes and sperm: a meta-analysis. *Philos. Trans. R. Soc. B* **375**, 20200064 (2020).
96. Lemaître, J.-F. et al. Early-late life trade-offs and the evolution of ageing in the wild. *Proc. R. Soc. B* **282**, 20150209 (2015).
97. Hechinger, R. F. Mortality affects adaptive allocation to growth and reproduction: field evidence from a guild of body snatchers. *BMC Evol. Biol.* **10**, 136 (2010).
98. Reznick, D. N., Bryant, M. J., Roff, D., Ghalambor, C. K. & Ghalambor, D. E. Effect of extrinsic mortality on the evolution of senescence in guppies. *Nature* **431**, 1095–1099 (2004).
99. Kelly, C. D. & Jennions, M. D. Sexual selection and sperm quantity: meta-analyses of strategic ejaculation. *Biol. Rev.* **86**, 863–884 (2011).
100. Reichard, M. Evolutionary ecology of aging: time to reconcile field and laboratory research. *Ecol. Evol.* **6**, 2988–3000 (2016).
101. Wondatir Workie, Z., Gibson, J. P. & van der Werf, J. H. J. Analysis of culling reasons and age at culling in Australian dairy cattle. *Anim. Prod. Sci.* **61**, 680 (2021).
102. Bennett, C. E. et al. The broiler chicken as a signal of a human reconfigured biosphere. *R. Soc. Open Sci.* **5**, 180325 (2018).
103. Nussey, D. H., Coulson, T., Festa-Bianchet, M. & Gaillard, J.-M. Measuring senescence in wild animal populations: towards a longitudinal approach. *Funct. Ecol.* **22**, 393–406 (2008).
104. Cooper, E. B. & Kruuk, L. E. B. Ageing with a silver-spoon: A meta-analysis of the effect of developmental environment on senescence. *Evolut. Lett.* **2**, 460–471 (2018).
105. Keller, L. F., Reid, J. M. & Arcese, P. Testing evolutionary models of senescence in a natural population: age and inbreeding effects on fitness components in song sparrows. *Proc. R. Soc. B.* **275**, 597–604 (2008).
106. Yousefzadeh, M. J. et al. Mouse models of accelerated cellular senescence. *Methods Mol. Biol.* **1896**, 203–230 (2019).

Acknowledgements

We are extremely grateful to all the researchers who provided us with unpublished/missing data and life tables for various species, without whom our meta-analysis would not be possible: Abdallah Assiri, Adolfo Cordero, Adrienne Crosier, Alberto Velando, Alfonso Bolarin, Aline Malawey, Alistair Senior, Anders Pape Moller, Anil Kumar, Antje Girndt, Ashley Watt, Asim Orem, Bradley Metz, Bryan Neff, Budhan Pukazhenthi, Charles Fox, Chris Friesen, Chris Weldon, Christine Miller, Christophe Bressac, Claudia Fricke, Claudio Maia, Claus Wedekind, Clelia Gasparini, Clint McDonald, Craig Packer, Daniel Sasson, Davnah Payne, Diana Perez Staples Folger, Martha Reyez Hernandez, Distl Ottmar, Elena Zambrano, Emily "Becky" Cramer, Emily Duval, Erin MacCartney, Felipe Martinez, Fumio Hayashi, Gabriele Sorci, Gerard Wilkinson, Gerlind Lehmann, Gregor Majdic, Hasan Sevgili, Heriberto Martinez, Ilie Racotta, Ioannis Tsakmakidis, Jan Lifjeld, Jane Hurst, Janice Bailey, Maurice Clotilde, Jesus Dorado, Jurgen Heinze, Karen Lockyear, Karolina Stasiak, Katarzyna Kotarska, Kathrin Langen, Klaus Reinhardt, Leandro Miranda, Leslie Curren, Linda Penfold, Maira Brito, Malgorzata Kruczek, Manasi Kanuga, Marion Mehlis, Mark Elgar, Martin Brinkworth, Martin Schulze, Maud Bonato, Megan Head, Melissah Rowe, Michael Greenfield, Michael Ritchie, Michele Di Iorio, Michelle Helinski, Milos Krist, Moira O'Bryan, Muhammed Ines Inanc, Naomi Pierce, Nicolaia Iaffaldano, Nikos Papadopolous, Nikron Thongtip, Nils Cordes, Nucharin Songsasen, Megan Brown, Pablo Bermejo Alvares, Paco Garcia Gonzales, Panos Milonas, Patricia Diogo, Paul Joseph, Philip Downing, Priscilla Ramos, Rakesh Seth, Stuart Reynolds, Rebecca Dean, Sachiko Koyama, Satoshi Hiroyoshi, Silvia Cerolini, Sina Metzler, Stanislaw Kondrack, Stefan Luepold, Steven Ramm, Stuart Meyers, Theo Bakker, Tobias Kehl, Triin Hallap, Ulrike Luderer, Upama Aich, Wael Farag, Wei Shi, Wen Liao, Xiaoxu Li, Yasaman Alavi, Yih Fwu Lin, and Yingmei Zhang. We are also thankful to Milan Vrtilek, Rose O'Dea, Kevin Foster, Ana Silva, and Ellie Bath for their helpful comments and suggestions, as well as members of the Biology of Sperm Conference, 2023, for constructive criticism. Finally, we thank Neil Gemmell who supported preliminary meta-analytic investigations conducted by SJ and SN. KS was supported by an SSE Rosemary Grant award. R.V.T. and T.P. were supported by a BBSRC Standard Grant (BB/V001256/1). S.N. was supported by an Australian Research Council (ARC) Discovery Project Grant (DP210100812). S.J. was supported by a Royal Society of New Zealand Grant. R.S.G. was supported by a NERC Independent Research Fellowship (NE/M018458/1). I.S. was supported by a Biotechnology and Biological Sciences Research Council (BBSRC) Fellowship (BB/T008881/1), a Royal Society Dorothy Hodgkin Fellowship (DHF\R1\211084), and a Wellcome Institutional Strategic Support Fund, University of Oxford (BRR00060).

Author contributions

K.S., R.V.T., T.P., and I.S. designed the study. K.S., S.G., and R.V.T. screened the studies. S.N. and S.J. provided extra studies. R.S.G. suggested methods to standardise age. K.S. extracted data. R.V.T. checked for repeatability of data extraction. R.V.T., S.N., S.J., and K.S. wrote the code and analysed the data. K.S., R.V.T., and I.S. wrote the first draft of the paper. All authors contributed in the critical assessment of the paper and subsequent revisions.

Competing interests
The authors declare no competing interests.

Additional information
Supplementary information The online version contains supplementary material available at https://doi.org/10.1038/s41467-024-44768-4.

Correspondence and requests for materials should be addressed to Krish Sanghvi, Regina Vega-Trejo, Tommaso Pizzari or Irem Sepil.

Peer review information *Nature Communications* thanks Victor Ronget and the other anonymous reviewer(s) for their contribution to the peer review of this work. A peer review file is available.

References

Acasuso-Rivero, C., Murren, C. J., Schlichting, C. D., & Steiner, U. K. (2019). Adaptive phenotypic plasticity for life-history and less fitness-related traits. *Proceedings of the Royal Society B*, *286*. https://doi.org/10.1098/rspb.2019.0653

Adler, M. I., & Bonduriansky, R. (2014). Why do the well-fed appear to die young?: A new evolutionary hypothesis for the effect of dietary restriction on lifespan. *BioEssays*, *36*, 439–450. https://doi.org/10.1002/bies.201300165

Altmann, J., & Alberts, S. C. (2005). Growth rates in a wild primate population: Ecological influences and maternal effects. *Behavioral Ecology & Sociobiology*, *57*, 490–501. https://doi.org/10.1007/s00265-004-0870-x

Alves, A. N., Sgrò, C. M., Piper, M. D., & Mirth, C. K. (2022). Target of rapamycin drives unequal responses to essential amino acid depletion for egg laying in Drosophila melanogaster. *Frontiers in Cell & Developmental Biology*, *10*. https://doi.org/10.3389/fcell.2022.822685

Andersson, M. (2017). Helping relatives survive and reproduce: Inclusive fitness and reproductive value in brood parasitism. *The American Naturalist*, *189*, 138–152. https://doi.org/10.1086/689991

Andrews, R. M. (1976). Growth rate in island and mainland anoline lizards. *American Society of Ichthyologists & Herpetologists*, *1976*, 477–482. https://www.jstor.org/stable/1443362

Arthreya, K. B., & Karlin, S. (1971). On branching processes with random environments: I: Extinction probabilities. *The Annals of Mathematical Statistics*, *42*, 1499–1520. https://www.jstor.org/stable/2240275

Bahlai, C. A., White, E. R., Perrone, J. D., Cusser, S., & Whitney, K. S. (2021). The broken window: An algorithm for quantifying and characterizing misleading trajectories in ecological processes. *Ecological Informatics*, *64*. https://doi.org/10.1016/j.ecoinf.2021.101336

Barraquand, F., & Yoccoz, N. G. (2013). When can environmental variability benefit population growth? Counterintuitive effects of nonlinearities in vital rates. *Theoretical Population Biology*, *89*, 1–11. https://doi.org/10.1016/j.tpb.2013.07.002

Barton, N. H., & Etheridge, A. M. (2011). The relation between reproductive value and genetic contribution. *Genetics*, *188*, 953–973. https://doi.org/10.1534/genetics.111.127555

Bassar, R. D., Heatherly, T., Marshall, M. C., Thomas, S. A., Flecker, A. S., & Reznick, D. N. (2015). Population size-structure-dependent fitness and ecosystem consequences in Trinidadian guppies. *Journal of Animal Ecology*, *84*, 955–968. https://doi.org/10.1111/1365-2656.12353

Bathiany, S., Dakos, V., Scheffer, M., & Lenton, T. M. (2018). Climate models predict increasing temperature variability in poor countries. *Science Advances*, *4*, 1–11. https://doi.org/10.1126/sciadv.aar5809

Benard, M. F., & McCauley, S. J. (2008). Integrating across life-history stages: Consequences of natal habitat effects on dispersal. *The American Naturalist*, *171*, 553–567. https://doi.org/10.1086/587072

Bernard, C., Santos, G. S., Deere, J. A., Rodriguez-Caro, R., Capdevila, P., Kusch, E., Gascoigne, S. J. L., Jackson, J., & Salguero-Gómez, R. (2023). Mosaic - A unified trait database to complement structured population models. *Scientific Data*, *10*. https://doi.org/10.1038/s41597-023-02070-w

Bielby, J., Mace, G. M., Bininda-Emonds, O. R. P., Cardillo, M., Gittleman, J. L., Jones, K. E., Orme, C. D. L., & Purvis, A. (2007). The fast-slow continuum in mammalian life history: An empirical reevaluation. *The American Naturalist*, *169*, 748–757. https://doi.org/10.1086/516847

Bingemer, J., Hohberg, K., & Schill, R. O. (2016). First detailed observations on tardigrade mating behaviour and some aspects of the life history of Isohypsibius dastychi Pilato, Bertolani & Binda 1982 (Tardigrada, Isohypsibiidae). *Zoological Journal of the Linnean Society*, *178*, 856–862. https://doi.org/10.1111/zoj.12435

Bjørkvoll, E., Grøtan, V., Aanes, S., Sæther, B. E., Engen, S., & Aanes, R. (2012). Stochastic population dynamics and life-history variation in marine fish species. *The American Naturalist*, *180*, 372–387. https://doi.org/10.1086/666983

Blagosklonny, M. V. (2006). Aging and immortality: Quasi-programmed senescence and its pharmacologic inhibition. *Cell Cycle*, *5*, 2087–2102. https://doi.org/10.4161/cc.5.18.3288

Blagosklonny, M. V. (2021). The hyperfunction theory of aging: Three common misconceptions. *Oncoscience*, *8*, 103–107. https://doi.org/10.18632/oncoscience.545

Bocedi, G., Palmer, S. C., Malchow, A. K., Zurell, D., Watts, K., & Travis, J. M. (2021). Rangeshifter 2.0: An extended and enhanced platform for modelling spatial eco-evolutionary dynamics and species' responses to environmental changes. *Ecography*, *44*, 1453–1462. https://doi.org/10.1111/ecog.05687

Bogert, C. M. (1949). Thermoregulation in reptiles, a factor in evolution. *Evolution*, *3*, 195–211. https://doi.org/10.1111/j.1558-5646.1949.tb00021.x

Bonsall, M. B., & Klug, H. (2011). The evolution of parental care in stochastic environments. *Journal of Evolutionary Biology*, *24*, 645–655. https://doi.org/10.1111/j.1420-9101.2010.02203.x

Bonte, D., Dyck, H. V., Bullock, J. M., Coulon, A., Delgado, M., Gibbs, M., Lehouck, V., Matthysen, E., Mustin, K., Saastamoinen, M., Schtickzelle, N., Stevens, V. M., Vandewoestijne, S., Baguette, M., Barton, K., Benton, T. G., Chaput-Bardy, A., Clobert, J., Dytham, C., … Travis, J. M. (2012). Costs of dispersal. *Biological Reviews*, *87*, 290–312. https://doi.org/10.1111/j.1469-185X.2011.00201.x

Borges, J. L. (1999). *On exactitude in science*. Penguin.

Boyce, M. S., Haridas, C. V., Lee, C. T., Boggs, C. L., Bruna, E. M., Coulson, T., Doak, D., Drake, J. M., Gaillard, J. M., Horvitz, C. C., Kalisz, S., Kendall, B. E., Knight, T., Mastrandrea, M., Menges, E. S., Morris, W. F., Pfister, C. A., & Tuljapurkar, S. D. (2006). Demography in an increasingly variable world. *Trends in Ecology & Evolution*, *21*, 141–148. https://doi.org/10.1016/j.tree.2005.11.018

Brodie, E. D., Moore, A., & Janzen, F. (1995). Visualizing and quantifying natural selection. *Trends in Ecology & Evolution*, *10*, 313–318. https://doi.org/10.1016/S0169-5347(00)89117-X

Bruijning, M., Metcalf, C. J. E., Jongejans, E., & Ayroles, J. F. (2020). The evolution of variance control. *Trends in Ecology & Evolution*, *35*, 22–33. https://doi.org/10.1016/j.tree.2019.08.005

Bull, J. C., & Bonsall, M. B. (2008). Overcompensatory population dynamic responses to environmental stochasticity. *Journal of Animal Ecology*, *77*, 1296–1305. https://doi.org/10.1111/j

Bull, J. C., Pickup, N. J., Pickett, B., Hassell, M. P., & Bonsall, M. B. (2007). Metapopulation extinction risk is increased by environmental stochasticity and assemblage complexity. *Proceedings of the Royal Society B*, *274*, 87–96. https://doi.org/10.1098/rspb.2006.3691

Burton, O. J., Phillips, B. L., & Travis, J. M. (2010). Trade-offs and the evolution of life-histories during range expansion. *Ecology Letters*, *13*, 1210–1220. https://doi.org/10.1111/j.1461-0248.2010.01505.x

Cam, E., Aubry, L. M., & Authier, M. (2016). The conundrum of heterogeneities in life history studies. *Trends in Ecology & Evolution*, *31*, 872–886. https://doi.org/10.1016/j.tree.2016.08.002

Campos, F. A., Morris, W. F., Alberts, S. C., Altmann, J., Brockman, D. K., Cords, M., Pusey, A., Stoinski, T. S., Strier, K. B., & Fedigan, L. M. (2017). Does climate variability influence the demography of wild primates? Evidence from long-term life-history data in seven species. *Global Change Biology*, *23*, 4907–4921. https://doi.org/10.1111/gcb.13754

Capdevila, P., Beger, M., Blomberg, S. P., Hereu, B., Linares, C., & Salguero-Gómez, R. (2020a). Longevity, body dimension and reproductive mode drive differences in aquatic versus terrestrial life-history strategies. *Functional Ecology*, *34*, 1613–1625. https://doi.org/10.1111/1365-2435.13604

Capdevila, P., Stott, I., Beger, M., & Salguero-Gómez, R. (2020b). Towards a comparative framework of demographic resilience. *Trends in Ecology & Evolution*, *35*, 776–786. https://doi.org/10.1016/j.tree.2020.05.001

Capdevila, P., Stott, I., Cant, J., Beger, M., Rowlands, G., Grace, M., & Salguero-Gómez, R. (2022). Life history mediates the trade-offs among different components of demographic resilience. *Ecology Letters*, *25*, 1566–1579. https://doi.org/10.1111/ele.14004

Careau, V., Réale, D., Humphries, M. M., & Thomas, D. W. (2010). The pace of life under artificial selection: Personality, energy expenditure, and longevity are correlated in domestic dogs. *The American Naturalist*, *175*, 753–758. https://doi.org/10.1086/652435

Carslake, D., Townley, S., & Hodgson, D. J. (2008). Nonlinearity in eigenvalue-perturbation curves of simulated population projection matrices. *Theoretical Population Biology*, *73*, 498–505. https://doi.org/10.1016/j.tpb.2008.03.004

Caswell, H. (1978). A general formula for the sensitivity of population growth rate to changes in life history parameters. *Theoretical Population Biology*, *14*, 215–230. https://doi.org/10.1016/0040-5809(78)90025-4

Caswell, H. (1996a). Analysis of life table response experiments ii. Alternative parameterizations for size- and stage-structured models. *Ecological Modelling*, *88*, 73–82. https://doi.org/10.1016/0304-3800(95)00070-4

Caswell, H. (1996b). Second derivatives of population growth rate: Calculation and applications. *Ecology*, *77*, 870–879. https://doi.org/10.2307/2265507

Caswell, H. (2001). *Matrix population models: Construction, analysis, and interpretation* (2nd edition). Sinauer.

Caswell, H. (2007). Sensitivity analysis of transient population dynamics. *Ecology Letters*, *10*, 1–15. https://doi.org/10.1111/j.1461-0248.2006.01001.x

Caswell, H. (2009). Stage, age and individual stochasticity in demography. *Oikos*, *118*, 1763–1782. https://doi.org/10.1111/j.1600-0706.2009.17620.x

Caswell, H. (2010). Life table response experiment analysis of the stochastic growth rate. *Journal of Ecology*, *98*, 324–333. https://doi.org/10.1111/j.1365-2745.2009.01627.x

Caswell, H. (2019a). The formal demography of kinship: A matrix formulation. *Demographic Research*, *41*, 679–712. https://doi.org/10.4054/DemRes.2019.41.24

Caswell, H. (2019b). *Sensitivity analysis: Matrix methods in demography and ecology*. Springer Nature.

Caswell, H. (2020). The formal demography of kinship ii: Multistate models, parity, and sibship. *Demographic Research*, *42*, 109–114. https://doi.org/10.4054/DemRes.2020.42.38

Caswell, H., & Salguero-Gómez, R. (2013). Age, stage and senescence in plants. *Journal of Ecology*, *101*, 585–595. https://doi.org/10.1111/1365-2745.12088

Cecco, G. J. D., & Gouhier, T. C. (2018). Increased spatial and temporal autocorrelation of temperature under climate change. *Scientific Reports*, *8*, 1–9. https://doi.org/10.1038/s41598-018-33217-0

Chang, C.-C., Moiron, M., Sánchez-Tójar, A., Niemelä, P. T., & Laskowski, K. L. (2024). What is the meta-analytic evidence for life-history trade-offs at the genetic level? *Ecology Letters*, *27*. https://doi.org/10.1111/ele.14354

Charlesworth, B. (1994). *Evolution in age-structured populations* (Vol. 2). Cambridge University Press.

Charnov, E. L. (1993). *Life history invariants: Some explorations of symmetry in evolutionary ecology*. Oxford University Press.

Che-Castaldo, J., Jones, O. R., Kendall, B. E., Burns, J. H., Childs, D. Z., Ezard, T. H., Hernandez-Yanez, H., Hodgson, D. J., Jongejans, E., Knight, T., Merow, C., Ramula, S., Stott, I., Vindenes, Y., Yokomizo, H., & Salguero-Gómez, R. (2020). Comments to “Persistent problems in the construction of matrix population models”. *Ecological Modelling*, *416*, 1–3. https://doi.org/10.1016/j.ecolmodel.2019.108913

Cheverud, J. M. (1988). A comparison of genetic and phenotypic correlations. *Evolution*, *42*, 958. https://doi.org/10.2307/2408911

Chi, H., & Liu, H. (1985). Two new methods for the study of insect population ecology. *Bulletin of the Institute of Zoology, Academia Sinica*, *24*, 225–240.

Childs, D. Z., Coulson, T. N., Pemberton, J. M., Clutton-Brock, T. H., & Rees, M. (2011). Predicting trait values and measuring selection in complex life histories: Reproductive allocation decisions in Soay sheep. *Ecology Letters*, *14*, 985–992. https://doi.org/10.1111/j.1461-0248.2011.01657.x

Childs, D. Z., Sheldon, B. C., & Rees, M. (2016). The evolution of labile traits in sex- and age-structured populations. *Journal of Animal Ecology*, *85*, 329–342. https://doi.org/10.1111/1365-2656.12483

Clutton-Brock, T. H., & Pemberton, J. M. (2004). *Soay sheep: Dynamics and selection in an island population*. Cambridge University Press.

Cochran, M. E., & Ellner, S. (1992). Simple methods for calculating age-based life history parameters for stage-structured populations. *Ecological Monographs*, *62*, 345–364. https://doi.org/10.2307/2937115

Colchero, F., Eckardt, W., & Stoinski, T. (2021). Evidence of demographic buffering in an endangered great ape: Social buffering on immature survival and the role of refined sex-age classes on population growth rate. *Journal of Animal Ecology*, *90*, 1701–1713. https://doi.org/10.1111/1365-2656.13486

Colchero, F., Jones, O. R., Conde, D. A., Hodgson, D., Zajitschek, F., Schmidt, B. R., Malo, A. F., Alberts, S. C., Becker, P. H., Bouwhuis, S., Bronikowski, A. M., Vleeschouwer, K. M. D., Delahay, R. J., Dummermuth, S., Fernández-Duque, E., Frisenvænge, J., Hesselsøe, M., Larson, S., Lemaître, J. F., … Gaillard, J. M. (2019). The diversity of population responses to environmental change. *Ecology Letters*, *22*, 342–353. https://doi.org/10.1111/ele.13195

Cole, L. C. (1954). The population consequences of life history phenomena. *The Quarterly Review of Biology*, *29*, 103–137. https://doi.org/10.1086/400074

Compagnoni, A., Bibian, A. J., Ochocki, B. M., Rogers, H. S., Schultz, E. L., Sneck, M. E., Elderd, B. D., Iler, A. M., Inouye, D. W., Jacquemyn, H., & Miller, T. E. (2016). The effect of demographic correlations on the stochastic population dynamics of perennial plants. *Ecological Monographs*, *86*, 480–494. https://doi.org/10.1002/ecm.1228

Compagnoni, A., Evers, S., & Knight, T. (2024). Spatial replication can best advance our understanding of population responses to climate. *Ecography*, *2024*. https://doi.org/10.1111/ecog.06833

Compagnoni, A., Levin, S., Childs, D. Z., Harpole, S., Paniw, M., Römer, G., Burns, J. H., Che-Castaldo, J., Rüger, N., Kunstler, G., Bennett, J. M., Archer, C. R., Jones, O. R., Salguero-Gómez, R., & Knight, T. M. (2021). Herbaceous perennial plants with short generation time have stronger responses to climate anomalies than those with longer generation time. *Nature Communications*, *12*, 1–8. https://doi.org/10.1038/s41467-021-21977-9

Conquet, E., Ozgul, A., Blumstein, D. T., Armitage, K. B., Oli, M. K., Martin, J. G., Clutton-Brock, T. H., & Paniw, M. (2023). Demographic consequences of changes in environmental periodicity. *Ecology*, *104*. https://doi.org/10.1002/ecy.3894

Coulson, T., Catchpole, E. A., Albon, S. D., Morgan, B. J., Pemberton, J. M., Clutton-Brock, T. H., Crawley, M. J., & Grenfell, B. T. (2001). Age, sex, density, winter weather, and population crashes in Soay sheep. *Science*, *292*, 1528–1531. https://doi.org/10.1126/science.292.5521.1528

Coulson, T. (2021). Environmental perturbations and transitions between ecological and evolutionary equilibria: An eco-evolutionary feedback framework. *Peer Community Journal*, *1*. https://doi.org/10.24072/pci

Coulson, T., Potter, T., & Felmy, A. (2021). Predicting evolution over multiple generations in deteriorating environments using evolutionarily explicit integral projection models. *Evolutionary Applications*, *14*, 2490–2501. https://doi.org/10.1111/eva.13272

Crean, A. J., & Bonduriansky, R. (2014). What is a paternal effect? *Trends in Ecology & Evolution*, *29*, 554–559. https://doi.org/10.1016/j.tree.2014.07.009

Crouse, D. T., Crowder, L. B., & Caswell, H. (1987). A stage-based population model for loggerhead sea turtles and implications for conservation. *Ecology*, *68*, 1412–1423. https://doi.org/10.2307/1939225

Cubaynes, S., Brandell, E. E., Stahler, D. R., Smith, D. W., Almberg, E. S., Schindler, S., Wayne, R. K., Dobson, A. P., vonHoldt, B. M., MacNulty, D. R., Cross, P. C., Hudson, P. J., & Coulson, T. (2022). Disease outbreaks select for mate choice and coat color in wolves. *Science*, *378*. https://doi.org/10.1126/science.abi8745

Cushing, J. M., Constantino, R. F., Dennis, B., Desharnais, R., & Henson, S. M. (2003). *Chaos in ecology: Experimental nonlinear dynamics*. Elsevier.

Dalgleish, H. J., Koons, D. N., & Adler, P. B. (2010). Can life-history traits predict the response of forb populations to changes in climate variability? *Journal of Ecology*, *98*, 209–217. https://doi.org/10.1111/j.1365-2745.2009.01585.x

Darimont, C. T., & Child, K. R. (2014). What enables size-selective trophy hunting of wildlife? *PLoS ONE*, *9*. https://doi.org/10.1371/journal.pone.0103487

Davidson, P. L., Nadolski, E. M., & Moczek, A. P. (2023). Gene regulatory networks underlying the development and evolution of plasticity in horned beetles. *Current Opinion in Insect Science*, 101114. https://doi.org/10.1016/j.cois.2023.101114

De Jong, G., & Van Noordwijk, A. J. (1992). Acquisition and allocation of resources: Genetic (co)variances, selection, and life histories. *The American Naturalist*, *139*, 749–770. https://doi.org/10.1086/285356

De Kroon, H., Van Groenendael, J., & Ehrlén, J. (2000). Elasticities: A review of methods and model limitations. *Ecology*, *81*, 607–618. https://doi.org/10.1890/0012-9658(2000)081[0607:EAROMA]2.0.CO;2

De Roos, A. M. (1997). A gentle introduction to physiologically structured population models. Springer US.

De Roos, A. M. (2021). Dynamic population stage structure due to juvenile – adult asymmetry stabilizes complex ecological communities. *Proceedings of the National Academy of Sciences*, *118*. https://doi.org/10.1073/pnas.2023709118/-/DCSupplemental.y

De Roos, A. M., Metz, J. A. J., Evers, E., & Leipoldt, A. (1990). A size dependent predator-prey interaction: Who pursues whom? *Journal of Mathematical Biology*, *28*, 609–643. https://doi.org/10.1007/BF00160229

De Vries, C., & Caswell, H. (2019). Stage-structured evolutionary demography: Linking life histories, population genetics, and ecological dynamics. *The American Naturalist*, *193*, 545–559. https://doi.org/10.1086/701857

Dey, S., Proulx, S. R., & Teotónio, H. (2016). Adaptation to temporally fluctuating environments by the evolution of maternal effects. *PLoS Biology*, *14*. https://doi.org/10.1371/journal.pbio.1002388

Doak, D. F., Morris, W. F., Pfister, C., Kendall, B. E., & Bruna, E. M. (2005). Correctly estimating how environmental stochasticity influences fitness and population growth. *The American Naturalist*, *166*, E14–E21. https://doi.org/10.1086/430642

Doak, D. F., Waddle, E., Langendorf, R. E., Louthan, A. M., Chardon, N. I., Dibner, R. R., Keinath, D. A., Lombardi, E., Steenbock, C., Shriver, R. K., Linares, C., Garcia, M. B., Funk, W. C., Fitzpatrick, S. W., Morris, W. F., & Peterson, M. L. (2021). A critical comparison of integral projection and matrix projection models for demographic analysis. *Ecological Monographs*, *91*. https://doi.org/10.1002/ecm.1447

Doherty, P. F., Schreiber, E. A., Nichols, J. D., Hines, J. E., Link, W. A., Schenk, G. A., & Schreiber, R. W. (2004). Testing life history predictions in a long-lived seabird: A population matrix approach with improved parameter estimation. *Oikos*, *105*, 606–618. https://doi.org/10.1111/j.0030-1299.2004.13119.x

Drake, J. M. (2005). Population effects of increased climate variation. *Proceedings of the Royal Society B*, *272*, 1823–1827. https://doi.org/10.1098/rspb.2005.3148

Dupont, L., Thierry, M., Zinger, L., Legrand, D., & Jacob, S. (2023). Beyond reaction norms: The temporal dynamics of phenotypic plasticity. *Trends in Ecology & Evolution*. https://doi.org/10.1016/j.tree.2023.08.014

Easterling, M. R., Ellner, S. P., & Dixon, P. M. (2000). Size-specific sensitivity: Applying a new structured population model. *Ecology*, *81*, 694–708. https://doi.org/10.1890/0012-9658(2000)081[0694:SSSAAN]2.0.CO;2

Ebert, T. A. (1999). Populations methods in demography. *Methods & Demography*.

Ellner, S. P., Childs, D. Z., & Rees, M. (2016). *Data-driven modelling of structured populations*.

Emlen, D. J., & Nijhout, H. F. (2001). Hormonal control of male horn length dimorphism in Onthophagus taurus (Coleoptera: Scarabaeidae): A second critical period of sensitivity to juvenile hormone. *Journal of Insect Physiology*. https://doi.org/10.1016/S0022-1910(01)00084-1

Emlen, D. J. (1997). Alternative reproductive tactics and male-dimorphism in the horned beetle Onthophagus acuminatus (Coleoptera: Scarabaeidae). *Bevioral Ecology & Sociobiology*, *41*, 335–341. https://doi.org/10.1007/s002650050393

Endo, N., & Eltahir, E. A. (2018). Modelling and observing the role of wind in anopheles population dynamics around a reservoir. *Malaria Journal*, *17*. https://doi.org/10.1186/s12936-018-2197-5

Engen, S., Bakke, Ø., & Islam, A. (1998). Demographic and environmental stochasticity-concepts and definitions. *Biometrics*, *54*, 840–846. https://doi.org/10.2307/2533838

Enríquez, P. J. V., Daalen, S. V., & Caswell, H. (2022). Individual stochasticity in the life history strategies of animals and plants. *PLoS ONE*, *17*. https://doi.org/10.1371/journal.pone.0273407

Evans, M. E., & Holsinger, K. E. (2012). Estimating covariation between vital rates: A simulation study of connected vs. separate generalized linear mixed models (glmms). *Theoretical Population Biology*, *82*, 299–306. https://doi.org/10.1016/j.tpb.2012.02.003

Evers, S. M., Knight, T. M., & Compagnoni, A. (2023). The inclusion of immediate and lagged climate responses amplifies the effect of climate autocorrelation on long-term growth rate of populations. *Journal of Ecology*, 1–12. https://doi.org/10.1111/1365-2745.14155

Ezard, T. H., Bullock, J. M., Dalgleish, H. J., Millon, A., Pelletier, F., Ozgul, A., & Koons, D. N. (2010). Matrix models for a changeable world: The importance of transient dynamics in population management. *Journal of Applied Ecology*, *47*, 515–523. https://doi.org/10.1111/j.1365-2664.2010.01801.x

Fabian, D. K., Kapun, M., Nolte, V., Kofler, R., Schmidt, P. S., Schlötterer, C., & Flatt, T. (2012). Genome-wide patterns of latitudinal differentiation among populations of Drosophila melanogaster from North America. *Molecular Ecology*, *21*, 4748–4769. https://doi.org/10.1111/j.1365-294X.2012.05731.x

Fanson, B. G., Fanson, K. V., & Taylor, P. W. (2012). Cost of reproduction in the Queensland fruit fly: Y-model versus lethal protein hypothesis. *Proceedings of the Royal Society B*, *279*, 4893–4900. https://doi.org/10.1098/rspb.2012.2033

Fay, R., Authier, M., Hamel, S., Jenouvrier, S., van de Pol, M., Cam, E., Gaillard, J. M., Yoccoz, N. G., Acker, P., Allen, A., Aubry, L. M., Bonenfant, C., Caswell, H., Coste, C. F., Larue, B., Le Coeur, C., Gamelon, M., Macdonald, K. R., Moiron, M., … Sæther, B. E. (2022a). Quantifying fixed individual heterogeneity in demographic parameters: Performance of correlated random effects for Bernoulli variables. *Methods in Ecology & Evolution*, *13*, 91–104. https://doi.org/10.1111/2041-210X.13728

Fay, R., Hamel, S., Van De Pol, M., Gaillard, J. M., Yoccoz, N. G., Acker, P., Authier, M., Larue, B., Le Coeur, C., Macdonald, K. R., Nicol-Harper, A., Barbraud, C., Bonenfant, C., Van Vuren, D. H., Cam, E., Delord, K., Gamelon, M., Moiron, M., Pelletier, F., … Sæther, B.-E. (2022b). Temporal correlations among demographic parameters are ubiquitous but highly variable across species. *Ecology Letters*. https://doi.org/10.1111/ele.14026

Ferreira, M. S., Kajin, M., Vieira, M. V., Zangrandi, P. L., Cerqueira, R., & Gentile, R. (2013). Life history of a neotropical marsupial: Evaluating potential contributions of survival and reproduction to population growth rate. *Mammalian Biology*, *78*, 406–411. https://doi.org/10.1016/j.mambio.2013.03.002

Foley, P. (1994). Predicting extinction times from environmental stochasticity and carrying capacity. *Conservation Biology*, *8*, 124–137. https://doi.org/10.1046/j.1523-1739.1994.08010124.x

Forsythe, A. B., Day, T., & Nelson, W. A. (2021). Demystifying individual heterogeneity. *Ecology Letters*, *24*, 2282–2297. https://doi.org/10.1111/ele.13843

Francis, T. B., Abbott, K. C., Cuddington, K., Gellner, G., Hastings, A., Lai, Y. C., Morozov, A., Petrovskii, S., & Zeeman, M. L. (2021). Management implications of long transients in ecological systems. *Nature Ecology & Evolution*, *5*, 285–294. https://doi.org/10.1038/s41559-020-01365-0

Franco, M., & Silvertown, J. (2004). A comparative demography of plants based upon elasticities of vital rates. *Ecology*, *85*, 531–538. https://doi.org/10.1890/02-0651

Gaillard, J. M., & Yoccoz, N. G. (2003). Temporal variation in survival of mammals: A case of environmental canalization? *Ecology*, *84*, 3294–3306. https://doi.org/10.1890/02-0409

Gaillard, J.-M., Festa-Bianchet, M., & Yoccoz, N. G. (1998). Population dynamics of large herbivores: Variable recruitment with constant adult survival. *Trends in Ecology & Evolution*, *13*, 249–251. https://doi.org/10.1016/S0169-5347(97)01237-8

Gaillard, J.-M., Yoccoz, N. G., Lebreton, J.-D., Bonenfant, C., Devillard, S., Loison, A., Pontier, D., & Allaine, D. (2005). Generation time: A reliable metric to measure life-history variation among mammalian populations. *The American Naturalist*, *166*. https://doi.org/10.1086/430330

Gamelon, M., Touzot, L., Baubet, É., Cachelou, J., Focardi, S., Franzetti, B., Nivois, É., Veylit, L., & Sæther, B. E. (2021). Effects of pulsed resources on the dynamics of seed consumer populations: A comparative demographic study in wild boar. *Ecosphere*, *12*. https://doi.org/10.1002/ecs2.3395

Gascoigne, S. J. L., Kajin, M., & Salguero-Gómez, R. (2023a). Criteria for buffering in ecological modeling. *Trends in Ecology & Evolution*. https://doi.org/10.1016/j.tree.2023.11.006

Gascoigne, S. J. L., Kajin, M., Tuljapurkar, S., Santos, G. S., Steiner, U. K., Vinton, A. C., Jaggi, H., Sepil, I., & Salguero-Gómez, R. (2023b). Structured demographic buffering: A framework to explore the environment drivers and demographic mechanisms underlying demographic buffering. *bioRxiv*. https://doi.org/10.1101/2023.07.20.549848

Gascoigne, S. J. L., Nalukwago, D. I. U., & Barbosa, F. (2022). Larval density, sex, and allocation hierarchy affect life history trait covariances in a bean beetle. *The American Naturalist*, *199*, 291–301. https://doi.org/10.5061/dryad.z08kprrdk

Gascoigne, S. J. L., Rolph, S., Sankey, D., Nidadavolu, N., Pičman, A. S. S., Hernández, C. M., Philpott, M. E., Salam, A., Bernard, C., Fenollosa, E., Lee, Y. J., McLean, J., Perera, S. H. A., Spacey, O. G., Kajin, M., Vinton, A. C., Archer, C. R., Burns, J. H., Buss, D. L., … Salguero-Gómez, R. (2023c). A standard protocol to report discrete stage-structured demographic information. *Methods in Ecology & Evolution*. https://doi.org/10.1111/2041-210X.14164

Gerber, N., & Kokko, H. (2018). Abandoning the ship using sex, dispersal or dormancy: Multiple escape routes from challenging conditions. *Philosophical Transactions of the Royal Society B*, *373*. https://doi.org/10.1098/rstb.2017.0424

Giannakou, M. E., & Partridge, L. (2007). Role of insulin-like signalling in Drosophila lifespan. *Trends in Biochemical Sciences*, *32*, 180–188. https://doi.org/10.1016/j.tibs.2007.02.007

Gillespie, J. H. (1977). Natural selection for variances in offspring numbers: A new evolutionary principle. *The American Naturalist*, *111*, 1010–1014.

Grafen, A. (1999). Formal darwinism, the individual-as-maximizing-agent analogy and bet-hedging. *Proceedings of the Royal Society B*, *266*, 799–803. https://doi.org/10.1098/rspb.1999.0708

Grafen, A. (2006). A theory of Fisher's reproductive value. *Journal of Mathematical Biology*, *53*, 15–60. https://doi.org/10.1007/s00285-006-0376-4

Grant, A., & Benton, T. G. (2000). Elasticity analysis for density-dependent populations in stochastic environments. *Ecology*, *81*, 680–693. https://doi.org/10.1890/0012-9658(2000)081[0680:EAFDDP]2.0.CO;2

Greaney, M. (2016). *Back blast*. Berkley Books.

Green, W. C. H., & Rothstein, A. (1991). Trade-offs between growth and reproduction in female bison. *Oecologia*, *86*, 521–527. https://doi.org/10.1007/BF00318318

Gremer, J. R., Crone, E. E., & Lesica, P. (2012). Are dormant plants hedging their bets? Demographic consequences of prolonged dormancy in variable environments. *The American Naturalist*, *179*, 315–327. https://doi.org/10.5061/dryad.nh1r171j

Grether, G. F., Millie, D. F., Bryant, M. J., Reznick, D. N., & Mayea, W. (2001). Rain forest canopy cover, resource availability, and life history evolution in guppies. *Ecology*, *82*, 1546–1559. https://doi.org/10.1890/0012-9658(2001)082[1546:RFCCRA]2.0.CO;2

Griffith, A. B. (2017). Perturbation approaches for integral projection models. *Oikos*, *126*, 1675–1686. https://doi.org/10.1111/oik.04458

Groot, C., & Margolis, L. (1991). *Pacific salmon life histories*. UBC Press.

Halley, J. M. (1996). Ecology, evolution and 1/f-noise. *Trends in Ecology & Evolution*, *11*, 33–37. https://doi.org/10.1016/0169-5347(96)81067-6

Halley, J. M., & Inchausti, P. (2004). The increasing importance of 1/f-noises as models of ecological variability. *Fluctuation & Noise Letters*, *4*. https://doi.org/10.1142/S0219477504001884

Halofsky, J. E., Peterson, D. L., & Harvey, B. J. (2020). Changing wildfire, changing forests: The effects of climate change on fire regimes and vegetation in the Pacific Northwest, USA. *Fire Ecology*, *16*. https://doi.org/10.1186/s42408-019-0062-8

Hansen, B. B., Gamelon, M., Albon, S. D., Lee, A. M., Stien, A., Irvine, R. J., Sæther, B. E., Loe, L. E., Ropstad, E., Veiberg, V., & Grøtan, V. (2019). More frequent extreme climate events stabilize reindeer population dynamics. *Nature Communications*, *10*, 1616. https://doi.org/10.1038/s41467-019-09332-5

Haridas, C. V., & Tuljapurkar, S. (2005). Elasticities in variable environments: Properties and implications. *The American Naturalist*, *166*, 481–495. https://doi.org/10.1086/444444

Hastings, A. (2001). Transient dynamics and persistence of ecological systems. *Ecology Letters*, *4*, 215–220. https://doi.org/10.1046/j.1461-0248.2001.00220.x

Hastings, A., Abbott, K. C., Cuddington, K., Francis, T., Gellner, G., Lai, Y. C., Morozov, A., Petrovskii, S., Scranton, K., & Zeeman, M. L. (2018). Transient phenomena in ecology. *Science*, *361*. https://doi.org/10.1126/science.aat6412

Haussmann, M. F., & Vleck, C. M. (2002). Telomere length provides a new technique for aging animals. *Oecologia*, *130*, 325–328. https://doi.org/10.1007/s00442-001-0827-y

He, Z., Webster, S., & He, S. Y. (2022). Growth–defense trade-offs in plants. *Current Biology*, *32*, R634–R639. https://doi.org/10.1016/j.cub.2022.04.070

Healy, K., Ezard, T. H., Jones, O. R., Salguero-Gómez, R., & Buckley, Y. M. (2019). Animal life history is shaped by the pace of life and the distribution of age-specific mortality and reproduction. *Nature Ecology & Evolution*, *3*, 1217–1224. https://doi.org/10.1038/s41559-019-0938-7

Healy, K., McNally, L., Ruxton, G. D., Cooper, N., & Jackson, A. L. (2013). Metabolic rate and body size are linked with perception of temporal information. *Animal Behaviour*, *86*, 685–696. https://doi.org/10.1016/j.anbehav.2013.06.018

Heft, D. E., & Walton, W. E. (2008). Effects of the El Niño-Southern Oscillation (ENSO) cycle on mosquito populations in southern California. *Journal of Vector Ecology*, *33*, 17–29. https://doi.org/10.3376/1081

Heidinger, B. J., Blount, J. D., Boner, W., Griffiths, K., Metcalfe, N. B., & Monaghan, P. (2012). Telomere length in early life predicts lifespan. *Proceedings of the National Academy of Sciences*, *109*, 1743–1748. https://doi.org/10.1073/pnas.1113306109

Henriques, C. M., & Ferreira, M. G. (2012). Consequences of telomere shortening during lifespan. *Current Opinion in Cell Biology*, *24*, 804–808. https://doi.org/10.1016/j.ceb.2012.09.007

Heppell, S. S. (1998). Application of life-history theory and population model analysis to turtle conservation. *Copeia*, *2*, 367–375. https://doi.org/10.2307/1447430

Hernández, C. M., Ellner, S. P., Adler, P. B., Hooker, G., & Snyder, R. E. (2023). An exact version of life table response experiment analysis, and the R package exactLTRE. *Methods in Ecology & Evolution*, *14*, 939–951. https://doi.org/10.1111/2041-210X.14065

Hernández, C. M., Ellner, S. P., Snyder, R. E., & Hooker, G. (2024). The natural history of luck: A synthesis study of structured population models. *Ecology Letters*, *27*. https://doi.org/10.1111/ele.14390

Higgins, S. I., Pickett, S. T., & Bond, W. J. (2000). Predicting extinction risks for plants: Environmental stochasticity can save declining populations. *Trends in Ecology & Evolution*. https://doi.org/10.1016/S0169-5347(00)01993-5

Hilde, C. H., Gamelon, M., Sæther, B. E., Gaillard, J. M., Yoccoz, N. G., & Pélabon, C. (2020). The demographic buffering hypothesis: Evidence and challenges. *Trends in Ecology & Evolution*, *35*, 523–538. https://doi.org/10.1016/j.tree.2020.02.004

Hoffmann, A. A., & Bridle, J. (2022). Plasticity and the costs of incorrect responses. *Trends in Ecology & Evolution*. https://doi.org/10.1016/j.tree.2022.11.012

Holmes, E. E., & York, A. E. (2003). Using age structure to detect impacts on threatened populations: A case study with steller sea lions. *Conservation Biology*, *17*, 1794–1806. https://doi.org/10.1111/j.1523-1739.2003.00191.x

Hopkins, B. R., Sepil, I., Thézénas, M.-L., Craig, J. F., Miller, T., Charles, P. D., Fischer, R., Kessler, B. M., Bretman, A., Pizzari, T., & Wigby, S. (2019). Divergent allocation of sperm and the seminal proteome along a competition gradient in Drosophila melanogaster. *Proceedings of the National Academy of Sciences*, *116*, 17925–17933. https://doi.org/10.5287/bodleian:zBdPnBZNB

Houde, A. E. (1994). Effect of artificial selection on male colour patterns on mating preference of female guppies. *Proceedings of the Royal Society B*, *256*, 125–130. https://doi.org/10.1098/rspb.1994.0059

Huang, Y., Wu, C., Huang, W., Liu, Y., Qi, M., Bai, J., Dong, Y., Gascoigne, S. J. L., Ciais, P., Peñuelas, J., & Salguero-Gómez, R. (2023). Climate change has desynchronized insect and vegetation phenologies across europe. *bioRxiv*. https://doi.org/10.1101/2023.12.11.571152

Hughes, K. A., Rodd, F. H., & Reznick, D. N. (2005). Genetic and environmental effects on secondary sex traits in guppies (Poecilia reticulata). *Journal of Evolutionary Biology*, *18*, 35–45. https://doi.org/10.1111/j.1420-9101.2004.00806.x

Iglesias-Carrasco, M., Head, M. L., Jennions, M. D., & Cabido, C. (2016). Condition-dependent trade-offs between sexual traits, body condition and immunity: The effect of novel habitats. *BMC Evolutionary Biology*, *16*. https://doi.org/10.1186/s12862-016-0706-0

Ivanov, D. K., Escott-Price, V., Ziehm, M., Magwire, M. M., Mackay, T. F., Partridge, L., & Thornton, J. M. (2015). Longevity GWAS using the Drosophila genetic reference panel. *Journals of Gerontology - Series A Biological Sciences and Medical Sciences*, *70*, 1470–1478. https://doi.org/10.1093/gerona/glv047

Jackson, J., Childs, D. Z., Mar, K. U., Htut, W., & Lummaa, V. (2019). Long-term trends in wild-capture and population dynamics point to an uncertain future for captive elephants. *Proceedings of the Royal Society B*, *286*, 20182810. https://doi.org/10.1098/rspb.2018.2810

Jackson, J., Le Coeur, C., & Jones, O. (2022). Life-history predicts global population responses to the weather in the terrestrial mammals. *eLife*, *11*. https://doi.org/10.1101/2021.04.22.440896

Jacquemyn, H., Brys, R., & Jongejans, E. (2010). Seed limitation restricts population growth in shaded populations of a perennial woodland orchid. *Ecology*, *91*, 119–129. https://doi.org/10.1890/08-2321.1

Jaggi, H., Steinsaltz, D., & Tuljapurkar, S. (2023). Migration in uncertain times. *bioRxiv*. https://doi.org/10.1101/2023.04.23.537980

Jäkäläniemi, A., Ramula, S., & Tuomi, J. (2013). Variability of important vital rates challenges the demographic buffering hypothesis. *Evolutionary Ecology*, *27*, 533–545. https://doi.org/10.1007/s10682-012-9606-y

James, A. C., Azevedo, R. B. R., & Partridge, L. (1997). Genetic and environmental responses to temperature of Drosophila melanogaster from a latitudinal cline. *Genetics*, *146*, 881–890. https://academic.oup.com/genetics/article/146/3/881/6053954

Jasilioniene, A., Jdanov, D. A., Sobotka, T., Andreev, E. M., Zeman, K., & Shkolnikov, V. M. (2015). *Methods protocol for the human fertility database*. http://www.humanfertility.org/Docs/methods.pdf

Jean, W. H., & Helms, B. P. (1983). Geometric mean approximations. *The Journal of Financial & Quantitative Analysis*, *18*, 287–293. https://doi.org/10.2307/2330720

Jelbert, K., Buss, D., McDonald, J., Townley, S., Franco, M., Stott, I., Jones, O., Salguero-Gómez, R., Buckley, Y., Knight, T., Silk, M., Sargent, F., Rolph, S., Wilson, P., & Hodgson, D. (2019). Demographic amplification is a predictor of invasiveness among plants. *Nature Communications*, *10*. https://doi.org/10.1038/s41467-019-13556-w

Jenouvrier, S., Long, M. C., Coste, C. F., Holland, M., Gamelon, M., Yoccoz, N. G., & Sæther, B. E. (2022). Detecting climate signals in populations across life histories. *Global Change Biology*, *28*, 2236–2258. https://doi.org/10.1111/gcb.16041

Jensen, A. L. (2000). Sex and age structured matrix model applied to harvesting a white tailed deer population. *Ecological Modelling*, *128*, 245–249. https://doi.org/10.1016/S0304-3800(00)00198-8

Jensen, J. L. (1906). Sur les fonctions convexes et les inégalités entre les valeurs moyennes. *Acta Mathematica*. https://doi.org/10.1007/BF02418571

Jimenez, A. G. (2016). Physiological underpinnings in life-history trade-offs in man's most popular selection experiment: The dog. *Journal of Comparative Physiology B: Biochemical, Systemic, and Environmental Physiology*, *186*, 813–827. https://doi.org/10.1007/s00360-016-1002-4

Jones, J. H. (2007). Demogr: A package for the construction and analysis of age-structured demographic models in R. *Journal of Statistical Software*, *22*. http://www.jstatsoft.org/

Jones, J. H. (2011). Primates and the evolution of long, slow life histories. *Current Biology*, *21*. https://doi.org/10.1016/j.cub.2011.08.025

Jones, O. R., Barks, P., Stott, I., James, T. D., Levin, S., Petry, W. K., Capdevila, P., Che-Castaldo, J., Jackson, J., Römer, G., Schuette, C., Thomas, C. C., & Salguero-Gómez, R. (2022). Rcompadre and Rage—Two R packages to facilitate the use of the COMPADRE and COMADRE databases and calculation of life-history traits from matrix population models. *Methods in Ecology & Evolution*, *13*, 770–781. https://doi.org/10.1111/2041-210X.13792

Jones, O. R., Scheuerlein, A., Salguero-Gómez, R., Camarda, C. G., Schaible, R., Casper, B. B., Dahlgren, J. P., Ehrlén, J., García, M. B., Menges, E. S., Quintana-Ascencio, P. F., Caswell, H., Baudisch, A., & Vaupel, J. W. (2014). Diversity of ageing across the tree of life. *Nature*, *505*, 169–173. https://doi.org/10.1038/nature12789

Jongejans, E., de Kroon, H., Tuljapurkar, S., & Shea, K. (2010). Plant populations track rather than buffer climate fluctuations. *Ecology Letters*, *13*, 736–743. https://doi.org/10.1111/j.1461-0248.2010.01470.x

Jouvet, L., Rodríguez-Rojas, A., & Steiner, U. K. (2018). Demographic variability and heterogeneity among individuals within and among clonal bacteria strains. *Oikos*, *127*, 728–737. https://doi.org/10.1111/oik.04292

Kapali, G. P., Callier, V., Gascoigne, S. J. L., Harrison, J. F., & Shingleton, A. W. (2022). The steroid hormone ecdysone regulates growth rate in response to oxygen availability. *Scientific Reports*, 1–10. https://doi.org/10.1038/s41598-022-08563-9

Karasov, T. L., Chae, E., Herman, J. J., & Bergelson, J. (2017). Mechanisms to mitigate the trade-off between growth and defense. *Plant Cell*, *29*, 666–680. https://doi.org/10.1105/tpc.16.00931

Kendall, B. E., Fujiwara, M., Diaz-Lopez, J., Schneider, S., Voigt, J., & Wiesner, S. (2019). Persistent problems in the construction of matrix population models. *Ecological Modelling*, *406*, 33–43. https://doi.org/10.1016/j.ecolmodel.2019.03.011

Kilpimaa, J., Alatalo, R. V., & Siitari, H. (2004). Trade-offs between sexual advertisement and immune function in the pied flycatcher (Ficedula hypoleuca). *Proceedings of the Royal Society B*, *271*, 245–250. https://doi.org/10.1098/rspb.2003.2568

King, J. G., & Hadfield, J. D. (2019). The evolution of phenotypic plasticity when environments fluctuate in time and space. *Evolution Letters*, *3*, 15–27. https://doi.org/10.1002/evl3.100

Kleon, A. (2012). *Steal like an artist*. Workman Publishing Company.

Klinkhamer, P. G. L., & Jong, T. J. D. (1983). Is it profitable for biennials to life longer than two years? *Ecological Modelling*, *20*, 223–232. https://doi.org/10.1016/0304-3800(83)90008-X

Knutson, T. R., McBride, J. L., Chan, J., Emanuel, K., Holland, G., Landsea, C., Held, I., Kossin, J. P., Srivastava, A. K., & Sugi, M. (2010). Tropical cyclones and climate change. *Nature Geoscience*, *3*, 157–163. https://doi.org/10.1038/ngeo779

Komonen, A., Grapputo, A., Kaitala, V., Kotiaho, J. S., & Päivinen, J. (2004). The role of niche breadth, resource availability and range position on the life history of butterflies. *Oikos*, *105*, 41–54. https://doi.org/10.1111/j.0030-1299.2004.12958.x

Koons, D. N., Metcalf, C. J. E., & Tuljapurkar, S. (2008). Evolution of delayed reproduction in uncertain environments: A life-history perspective. *The American Naturalist*, *172*, 797–805. https://doi.org/10.1086/592867

Koons, D. N., Pavard, S., Baudisch, A., & Metcalf, C. J. E. (2009). Is life-history buffering or lability adaptive in stochastic environments? *Oikos*, *118*, 972–980. https://doi.org/10.1111/j.1600-0706.2009.16399.x

Korn, R. (1997). *Optimal portfolios: Stochastic models for optimal investment and risk management in continuous time*. World scientific.

Kubrak, O. I., Nylin, S., Flatt, T., Nässel, D. R., & Leimar, O. (2017). Adaptation to fluctuating environments in a selection experiment with Drosophila melanogaster. *Ecology & Evolution*, *7*, 3796–3807. https://doi.org/10.1002/ece3.2965

Kvalnes, T., Sæther, B. E., Engen, S., & Roulin, A. (2022). Density-dependent selection and the maintenance of colour polymorphism in barn owls. *Proceedings of the Royal Society B*, *289*. https://doi.org/10.1098/rspb.2022.0296

Lamberton, D., & Lapeyre, B. (2011). *Introduction to stochastic calculus applied to finance*. CRC Press.

Lande, R., Sæther, B. E., & Engen, S. (1997). Threshold harvesting for sustainability of fluctuating resources. *Ecology*, *78*, 1341–1350. https://doi.org/10.1890/0012-9658(1997)078[1341:THFSOF]2.0.CO;2

Lawler, R. R., Caswell, H., Richard, A. F., Ratsirarson, J., Dewar, R. E., & Schwartz, M. (2009). Demography of Verreaux's sifaka in a stochastic rainfall environment. *Oecologia*, *161*, 491–504. https://doi.org/10.1007/s00442-009-1382-1

Lefkovitch, L. P. (1965). The study of population growth in organisms grouped by stages. *Biometrics*, *21*, 1–18. https://doi.org/10.2307/2528348

Lemaître, J. F., Berger, V., Bonenfant, C., Douhard, M., Gamelon, M., Plard, F., & Gaillard, J. M. (2015). Early-late life trade-offs and the evolution of ageing in the wild. *Proceedings of the Royal Society B*, *282*. https://doi.org/10.1098/rspb.2015.0209

Lennartsson, T., & Oostermeijer, J. G. B. (2001). Demographic variation and population viability in Gentianella campestris: Effects of grassland management and environmental stochasticity. *Journal of Ecology*, *89*, 451–463. https://doi.org/10.1046/j.1365-2745.2001.00566.x

Leslie, P. H. (1945). On the use of matrices in certain population. *Biometrika*, *33*, 183–212. https://doi.org/10.2307/2332297

Le Coeur, C., Yoccoz, N. G., Salguero-Gómez, R., & Vindenes, Y. (2022). Life history adaptations to fluctuating environments: Combined effects of demographic buffering and lability. *Ecology Letters*, *25*, 2107–2119. https://doi.org/10.1111/ele.14071

Levin, S. C., Evers, S., Potter, T., Guerrero, M. P., Childs, D. Z., Compagnoni, A., Knight, T. M., & Salguero-Gómez, R. (2022). Rpadrino: An R package to access and use PADRINO , an open access database of Integral Projection Models. *Methods in Ecology & Evolution*, *2022*, 1–7. https://doi.org/10.1111/2041-210x.13910

Lewis, S. C., & King, A. D. (2017). Evolution of mean, variance and extremes in 21st century temperatures. *Weather and Climate Extremes*, *15*, 1–10. https://doi.org/10.1016/j.wace.2016.11.002

Li, S. L., & Ramula, S. (2015). Demographic strategies of plant invaders in temporally varying environments. *Population Ecology*, *57*, 373–380. https://doi.org/10.1007/s10144-015-0479-0

Lind, M. I., Ravindran, S., Sekajova, Z., Carlsson, H., Hinas, A., & Maklakov, A. A. (2019). Experimentally reduced insulin/IGF-1 signaling in adulthood extends lifespan of parents and improves Darwinian fitness of their offspring. *Evolution Letters*, *3*, 207–216. https://doi.org/10.1002/evl3.108

Long, T. (1970). Genetic effects of fluctuating temperature in populations of Drosophila melanogaster. *Genetics*, *66*, 401. https://doi.org/10.1093/genetics/66.2.401

López-Otín, C., Blasco, M. A., Partridge, L., Serrano, M., & Kroemer, G. (2013). The hallmarks of aging. *Cell*, *153*, 1194. https://doi.org/10.1016/j.cell.2013.05.039

Lustenhouwer, N., Moerman, F., Altermatt, F., Bassar, R. D., Bocedi, G., Bonte, D., Dey, S., Fronhofer, E. A., da Rocha, É. G., Giometto, A., Lancaster, L. T., Prather, R. B., Saastamoinen, M., Travis, J. M., Urquhart, C. A., Weiss-Lehman, C., Williams, J. L., Börger, L., & Berger, D. (2023). Experimental evolution of dispersal: Unifying theory, experiments and natural systems. *Journal of Animal Ecology*, *92*, 1113–1123. https://doi.org/10.1111/1365-2656.13930

MacArthur, R. H. (1960). Review of population studies: Animal ecology and demography. Cold Spring Harbor symposia on quantitative biology vol. xxii. *Quarterly Review of Biology*, 82–83.

MacArthur, R. H., & Wilson, E. O. (1967). *The theory of island biogeography*. Princeton University Press.

Mack, R. N. (2000). Cultivation fosters plant naturalization by reducing environmental stochasticity. *Biological Invasions*, *2*, 111–122. https://doi.org/10.1023/A:1010088422771

Maldonado-Chaparro, A. A., Blumstein, D. T., Armitage, K. B., & Childs, D. Z. (2018). Transient LTRE analysis reveals the demographic and trait-mediated processes that buffer population growth. *Ecology Letters*, *21*, 1693–1703. https://doi.org/10.1111/ele.13148

Marques, G. M., Augustine, S., Lika, K., Pecquerie, L., Domingos, T., & Kooijman, S. A. (2018). The AmP project: Comparing species on the basis of dynamic energy budget parameters. *PLoS Computational Biology*. https://doi.org/10.1371/journal.pcbi.1006100

Marshall, K. E., & Sinclair, B. J. (2010). Repeated stress exposure results in a survival-reproduction trade-off in Drosophila melanogaster. *Proceedings of the Royal Society B*, *277*, 963–969. https://doi.org/10.1098/rspb.2009.1807

Masson-Delmotte, V., Zhai, P., Pirani, A., Connors, S. L., Péan, C., Berger, S., Caud, N., Chen, Y., Goldfarb, L., Gomis, M. I., Huang, M., Leitzell, K., Lonnoy, E., Matthews, J., Maycock, T. K., Waterfield, T., Yelekçi, O., Yu, R., & Zhou, B. (2021). Ipcc: Climate change 2021: The physical science basis. *Cambridge University Press. In Press.*

May, R. M. (1973). Stability in randomly fluctuating versus deterministic environments. *The American Naturalist*, *107*, 621–650. https://doi.org/10.1086/282863

May, R. M. (1976). Simple mathematical models with very complicated dynamics. *Nature*, *261*, 459–467.

McDonald, J. M., Ghosh, S. M., Gascoigne, S. J., & Shingleton, A. W. (2018). Plasticity through canalization: The contrasting effect of temperature on trait size and growth in Drosophila. *Frontiers in Cell & Developmental Biology*, *6*. https://doi.org/10.3389/fcell.2018.00156

McDonald, J. M., Nabili, P., Thorsen, L., Jeon, S., & Shingleton, A. W. (2021). Sex-specific plasticity and the nutritional geometry of insulin-signaling gene expression in Drosophila melanogaster. *EvoDevo*, *12*, 1–17. https://doi.org/10.1186/s13227-021-00175-0

McDonald, J. L., Franco, M., Townley, S., Ezard, T. H., Jelbert, K., & Hodgson, D. J. (2017). Divergent demographic strategies of plants in variable environments. *Nature Ecology & Evolution*, *1*, 0029. https://doi.org/10.1038/s41559-016-0029

McDonald, J. L., Stott, I., Townley, S., & Hodgson, D. J. (2016). Transients drive the demographic dynamics of plant populations in variable environments. *Journal of Ecology*, *104*, 306–314. https://doi.org/10.1111/1365-2745.12528

McPeek, M. A. (2004). The growth/predation risk trade-off: So what is the mechanism? *The American Naturalist*, *163*. https://doi.org/10.1086/382755

Melbourne, B. A., & Hastings, A. (2008). Extinction risk depends strongly on factors contributing to stochasticity. *Nature*, *454*, 100–103. https://doi.org/10.1038/nature06922

Merow, C., Bois, S. T., Allen, J. M., Xie, Y., & Silander, J. A. (2017). Climate change both facilitates and inhibits invasive plant ranges in New England. *Proceedings of the National Academy of Sciences*, *114*, E3276–E3284. https://doi.org/10.1073/pnas.1609633114

Metcalf, C. J. E. (2016). Invisible trade-offs: Van Noordwijk and de Jong and life-history evolution. *The American Naturalist*, *187*, 3–5. https://doi.org/10.1086/685487

Milles, A., Banitz, T., Bielcik, M., Frank, K., Gallagher, C. A., Jeltsch, F., Jepsen, J. U., Oro, D., Radchuk, V., & Grimm, V. (2023a). Local buffer mechanisms for population persistence. *Trends in Ecology & Evolution*, *38*, 1051–1059. https://doi.org/10.1016/j.tree.2023.06.006

Milles, A., Bielcik, M., Banitz, T., Gallagher, C. A., Jeltsch, F., Jepsen, J. U., Oro, D., Radchuk, V., & Grimm, V. (2023b). Defining ecological buffer mechanisms should consider diverse approaches. *Trends in Ecology & Evolution*. https://doi.org/10.1016/j.tree.2023.12.008

Milner, J. M., Elston, D. A., & Albon, S. D. (1999). Estimating the contributions of population density and climatic fluctuations to interannual variation in survival of Soay sheep, 1235–1247. https://doi.org/10.1046/j.1365-2656.1999.00366.x

Møller, A. P. (2006). Sociality, age at first reproduction and senescence: Comparative analyses of birds. *Journal of Evolutionary Biology*, *19*, 682–689. https://doi.org/10.1111/j.1420-9101.2005.01065.x

Møller, A. P., & Thornhill, R. (1998). Male parental care, differential parental investment by females and sexual selection. *Animal Behaviour*, *55*, 1507–1515.

Morozov, A., Abbott, K., Cuddington, K., Francis, T., Gellner, G., Hastings, A., Lai, Y. C., Petrovskii, S., Scranton, K., & Zeeman, M. L. (2020). Long transients in ecology: Theory and applications. *Physics of life reviews*, *32*, 1–40. https://doi.org/10.1016/j.plrev.2019.09.004

Morris, W. F., Altmann, J., Brockman, D. K., Cords, M., Fedigan, L. M., Pusey, A. E., Stoinski, T. S., Bronikowski, A. M., Alberts, S. C., & Strier, K. B. (2011). Low demographic variability in wild primate populations: Fitness impacts of variation, covariation, and serial correlation in vital rates. *The American Naturalist*, *177*, 14–28. https://doi.org/10.5061/dryad.1985

Morris, W. F., & Doak, D. F. (2002). *Quantitative conservation biology: Theory & practice of population viability analysis*. Sinauer.

Morris, W. F., & Doak, D. F. (2004). Buffering of life histories against environmental stochasticity: Accounting for a spurious correlation between the variabilities of vital rates and their contributions to fitness. *The American Naturalist*, *163*, 579–590. https://doi.org/10.1086/382550

Morris, W. F., Pfister, C. A., Tuljapurkar, S., Haridas, C. V., Boggs, C. L., Boyce, M. S., Bruna, E. M., Church, D. R., Coulson, T., Doak, D. F., Forsyth, S., Gaillard, J. M., Horvitz, C. C., Kalisz, S., Kendall, B. E., Knight, T. M., Lee, C. T., & Menges, E. S. (2008). Longevity can buffer plant and animal populations against changing climatic variability. *Ecology*, *89*, 19–25. http://www.esajournals.org/doi/pdf/10.1890/07-0774.1

Nagwani, A. K., Kaczmarek, Ł., & Kmita, H. (2022). Applicable life-history and molecular traits for studying the effects of anhydrobiosis on aging in tardigrades. *Diversity*, *14*. https://doi.org/10.3390/d14080664

Neubert, M. G., & Caswell, H. (1997). Alternatives to resilience for measuring the responses of ecological systems to perturbations. *Ecology*, *78*, 653–665. https://doi.org/10.1890/0012-9658(1997)078[0653:ATRFMT]2.0.CO;2

Newton, I., & Rothery, P. (1997). Senescence and reproductive value in sparrowhawks. *Ecology*, *78*, 1000–1008. https://doi.org/10.1890/0012-9658(1997)078[1000:SARVIS]2.0.CO;2

Ni, K., Spiess, A. N., Schuppe, H. C., & Steger, K. (2016). The impact of sperm protamine deficiency and sperm DNA damage on human male fertility: A systematic review and meta-analysis. *Andrology*, *4*, 789–799. https://doi.org/10.1111/andr.12216

Nielsen, J., Hedeholm, R. B., Heinemeier, J., Bushnell, P. G., Christiansen, J. S., Olsen, J., Ramsey, C. B., Brill, R. W., Simon, M., Steffensen, K. F., & Steffensen, J. F. (2016). Eye lens radiocarbon reveals centuries of longevity in the Greenland shark (Somniosus microcephalus). *Science*, *353*, 702–704. https://doi.org/10.1126/science.aaf3617

Nisbet, R. M., Muller, E. B., Lika, K., & Kooijman, S. A. L. M. (2000). From molecules to ecosystems through dynamic energy budget models. *Journal of Animal Ecology*, *69*, 913–926. https://www.jstor.org/stable/2647153

Noda, I. (1960). The emergence of winged viviparous female in aphid VI. Difference in the rate of development between the winged and the unwinged forms. *Japanese Journal of Ecology*, *10*, 97–102. https://doi.org/10.18960/seitai.10.3_97

Nussey, D. H., Wilson, A. J., Morris, A., Pemberton, J., Clutton-Brock, T., & Kruuk, L. E. (2008). Testing for genetic trade-offs between early- and late-life reproduction in a wild red deer population. *Proceedings of the Royal Society B*, *275*, 745–750. https://doi.org/10.1098/rspb.2007.0986

Oli, M. K., & Dobson, F. S. (2003). The relative importance of life-history variables to population growth rate in mammals: Cole's prediction revisited. *The American Naturalist*, *161*, 422–440. https://doi.org/10.1086/367591

Orzack, S. H. (1985). Population dynamics in variable environments. V. The genetics of homeostasis revisited. *The American Naturalist*, *125*, 550–572. https://www.jstor.org/stable/2461273

Orzack, S. H., & Tuljapurkar, S. (1989). Population dynamics in variable environments. VII. The demography and evolution of iteroparity. *The American Naturalist*, *133*, 901–923. https://doi.org/10.1086/284959

Ovaskainen, O., & Hanski, I. (2002). Transient dynamics in metapopulation response to perturbation. *Theoretical Population Biology*, *61*, 285–295. https://doi.org/10.1006/tpbi.2002.1586

Overgaard, J., Hoffmann, A. A., & Kristensen, T. N. (2011). Assessing population and environmental effects on thermal resistance in Drosophila melanogaster using ecologically relevant assays. *Journal of Thermal Biology*, *36*, 409–416. https://doi.org/10.1016/j.jtherbio.2011.07.005

Ozgul, A., Fichtel, C., Paniw, M., & Kappeler, P. M. (2023). Destabilizing effect of climate change on the persistence of a short-lived primate. *Proceedings of the National Academy of Sciences*, *120*. https://doi.org/10.1073/pnas.2214244120

Paniw, M., James, T. D., Archer, C. R., Römer, G., Levin, S., Compagnoni, A., Che-Castaldo, J., Bennett, J. M., Mooney, A., Childs, D. Z., Ozgul, A., Jones, O. R., Burns, J. H., Beckerman, A. P., Patwary, A., Sanchez-Gassen, N., Knight, T. M., & Salguero-Gómez, R. (2021). The myriad of complex demographic responses of terrestrial mammals to climate change and gaps of knowledge: A global analysis. *Journal of Animal Ecology*, *90*, 1398–1407. https://doi.org/10.1111/1365-2656.13467

Paniw, M., Maag, N., Cozzi, G., Clutton-Brock, T., & Ozgul, A. (2019). Life history responses of meerkats to seasonal changes in extreme environments. *Science*, *363*, 631–635. https://doi.org/10.1126/science.aau5905

Paniw, M., Ozgul, A., & Salguero-Gómez, R. (2018). Interactive life-history traits predict sensitivity of plants and animals to temporal autocorrelation. *Ecology Letters*, *21*, 275–286. https://doi.org/10.1111/ele.12892

Paris, J. R., Whiting, J. R., Daniel, M. J., Obiol, J. F., Parsons, P. J., van der Zee, M. J., Wheat, C. W., Hughes, K. A., & Fraser, B. A. (2022). A large and diverse autosomal haplotype is associated with sex-linked colour polymorphism in the guppy. *Nature Communications*, *13*. https://doi.org/10.1038/s41467-022-28895-4

Park, J. S. (2019). Cyclical environments drive variation in life-history strategies: A general theory of cyclical phenology. *Proceedings of the Royal Society B*, *286*. https://doi.org/10.1098/rspb.2019.0214

Park, J. S., & Post, E. (2022). Seasonal timing on a cyclical earth: Towards a theoretical framework for the evolution of phenology. *PLoS Biology*, *20*. https://doi.org/10.1371/journal.pbio.3001952

Park, J. S., & Wootton, J. T. (2021). Slower environmental cycles maintain greater life-history variation within populations. *Ecology Letters*, *24*, 2452–2463. https://doi.org/10.1111/ele.13867

Parker, N. F., & Shingleton, A. W. (2011). The coordination of growth among Drosophila organs in response to localized growth-perturbation. *Developmental Biology*. https://doi.org/10.1016/j.ydbio.2011.07.002

Pearl, R. (1925). *The biology of population growth*. Alfred A. Knopf.

Pélabon, C., Hilde, C. H., Einum, S., & Gamelon, M. (2020). On the use of the coefficient of variation to quantify and compare trait variation. *Evolution Letters*, *4*, 180–188. https://doi.org/10.1002/evl3.171

Petchey, O. L. (2000). Environmental colour affects aspects of single-species population dynamics. *Proceedings of the Royal Society B*, *267*, 747–754. https://doi.org/10.1098/rspb.2000.1066

Petchey, O. L., Gonzalez, A., & Wilson, H. B. (1997). Effects on population persistence: The interaction between environmental noise colour, intraspecific competition and space. *Proceedings of the Royal Society B*, *264*, 1841–1847.

Peters, A., Delhey, K., Denk, A. G., & Kempenaers, B. (2004). Trade-offs between immune investment and sexual signaling in male mallards. *The American Naturalist*, *164*, 51–59.

Petersen, A., Robertson, G. J., Thorstensen, S., & Mallory, M. L. (2020). Annual survival of arctic terns in western iceland. *Polar Biology*, *43*, 1843–1849. https://doi.org/10.1007/s00300-020-02749-5

Pfister, C. A. (1998). Patterns of variance in stage-structured populations: Evolutionary predictions and ecological implications. *Proceedings of the National Academy of Sciences*, *95*, 213–218. https://doi.org/10.1073/pnas.95.1.213

Philippi, T., & Seger, J. (1989). Hedging one's evolutionary bets, revisited. *Trends in Ecology & Evolution*, *4*, 41–44.

Pick, J. (2023). Why should we quantify fitness in terms of the number of zygotes and not recruits? *8th Meeting of the Evolutionary Demography Society*.

Post, E. (2019). *Time in ecology: A theoretical framework*. Princeton University Press.

Potter, T., Arendt, J., Bassar, R. D., Watson, B., Bentzen, P., Travis, J., & Reznick, D. N. (2023). Female preference for rare males is maintained by indirect selection in trinidadian guppies. *Science*, *380*, 309–312. https://doi.org/10.1126/science.ade5671

Raventós, J., Mújica, E., González, E., Bonet, A., & Ortega-Larrocea, M. P. (2021). The effects of hurricanes on the stochastic population growth of the endemic epiphytic orchid Broughtonia cubensis living in Cuba. *Population Ecology*, *63*, 302–312. https://doi.org/10.1002/1438-390X.12098

Reed, A. W., & Slade, N. A. (2012). Buffering and plasticity in vital rates of oldfield rodents. *Journal of Animal Ecology*, *81*, 953–959. https://doi.org/10.1111/j.1365-2656.2012.01976.x

Rees, M., & Ellner, S. P. (2009). Integral projection models for populations in temporally varying environments. *Ecological Monographs*, *79*, 575–594. https://doi.org/10.1890/08-1474.1

Regan, J. C., Froy, H., Walling, C. A., Moatt, J. P., & Nussey, D. H. (2020). Dietary restriction and insulin-like signalling pathways as adaptive plasticity: A synthesis and re-evaluation. *Functional Ecology*, *34*, 107–128. https://doi.org/10.1111/1365-2435.13418

Reisen, W. K., Cayan, D., Tyree, M., Barker, C. M., Eldridge, B., & Dettinger, M. (2008). Impact of climate variation on mosquito abundance in California. *Journal of Vector Ecology*, *33*, 89–98. https://doi.org/10.3376/1081-1710(2008)33[89:iocvom]2.0.co;2

Revell, L. J. (2009). Size-correction and principal components for interspecific comparative studies. *Evolution*, *63*, 3258–3268. https://doi.org/10.1111/j.1558-5646.2009.00804.x

Revell, L. J. (2012). Phytools: An R package for phylogenetic comparative biology (and other things). *Methods in Ecology & Evolution*, *3*, 217–223. https://doi.org/10.1111/j.2041-210X.2011.00169.x

Roberts, W. A. (2002). Are animals stuck in time? *Psychological Bulletin*, *128*, 473–489. https://doi.org/10.1037/0033-2909.128.3.473

Rodríguez-Caro, R. C., Graciá, E., Blomberg, S. P., Cayuela, H., Grace, M., Carmona, C. P., Pérez-Mendoza, H. A., Giménez, A., & Salguero-Gómez, R. (2023). Anthropogenic impacts on threatened species erode functional diversity in chelonians and crocodilians. *Nature Communications*, *14*. https://doi.org/10.1038/s41467-023-37089-5

Rodríguez-Caro, R. C., Capdevila, P., Graciá, E., Barbosa, J. M., Giménez, A., & Salguero-Gómez, R. (2021). The limits of demographic buffering in coping with environmental variation. *Oikos*, *130*, 1346–1358. https://doi.org/10.1111/oik.08343

Roerdink, J. B. T. M. (1988). The biennial life strategy in a random environment. *Journal of Mathematical Biology*, *26*, 199–215. https://doi.org/10.1007/BF00277733

Roerdink, J. B. T. M. (1989). The biennial life strategy in a random environment supplement. *Journal of Mathematical Biology*, *27*, 309–319. https://doi.org/10.1007/BF00275814

Roff, D. A. (2002). *Life history evolution*. Sinauer.

Roff, D. A., & Fairbairn, D. J. (2007). The evolution of trade-offs: Where are we? *Journal of Evolutionary Biology*, *20*, 433–447. https://doi.org/10.1111/j.1420-9101.2006.01255.x

Romeijn, J., & Smallegange, I. M. (2022). Exploring how the fast-slow pace of life continuum and cell size structure microorganism life history variation. *bioRxiv*. https://doi.org/10.1101/2022.11.28.517963

Rootes, W. L., Chabreck, R. H., Wright, V. L., Brown, B. W., & Hess, T. J. (1991). Growth rates of American alligators in estuarine and palustrine wetlands in Louisiana. *Estuaries*, *14*, 489–494. https://doi.org/10.2307/1352272

Roper, M., Capdevila, P., & Salguero-Gómez, R. (2021). Senescence: Why and where selection gradients might not decline with age. *Proceedings of the Royal Society B*, *288*. https://doi.org/10.1098/rspb.2021.0851

Roper, M., Green, J. P., Salguero-Gómez, R., & Bonsall, M. B. (2023). Inclusive fitness forces of selection in an age-structured population. *Communications Biology*, *6*. https://doi.org/10.1038/s42003-023-05260-9

Rose, F. (1948). Orchis purpurea huds. *Journal of Ecology*, *36*, 366–377. https://doi.org/10.2307/2256683

Rotella, J. J., Link, W. A., Chambert, T., Stauffer, G. E., & Garrott, R. A. (2012). Evaluating the demographic buffering hypothesis with vital rates estimated for Weddell seals from 30 years of mark-recapture data. *Journal of Animal Ecology*, *81*, 162–173. https://doi.org/10.1111/j.1365-2656.2011.01902.x

Roth, G., & Caswell, H. (2016). Hyperstate matrix models: Extending demographic state spaces to higher dimensions. *Methods in Ecology & Evolution*, *7*, 1438–1450. https://doi.org/10.1111/2041-210X.12622

Sæther, B. E. (1997). Environmental stochasticity and population dynamics of large herbivores: A search for mechanisms. *Trends in Ecology & Evolution*, *7*, 143–149.

Sæther, B. E., Coulson, T., Grøtan, V., Engen, S., Altwegg, R., Armitage, K. B., Barbraud, C., Becker, P. H., Blumstein, D. T., Dobson, F. S., Festa-Bianchet, M., Gaillard, J. M., Jenkins, A., Jones, C., Nicoll, M. A., Norris, K., Oli, M. K., Ozgul, A., & Weimerskirch, H. (2013). How life history influences population dynamics in fluctuating environments. *The American Naturalist*, *182*, 743–759. https://doi.org/10.1086/673497

Sæther, B. E., Engen, S., Islam, A., McCleery, R., & Perrins, C. (1998). Environmental stochasticity and extinction risk in a population of a small songbird, the great tit. *The American Naturalist*, *151*, 441–450. https://doi.org/10.1086/286131

Salguero-Gómez, R. (2021). Commentary on the life history special issue: The fast-slow continuum is not the end-game of life history evolution, human or otherwise. *Evolution & Human Behavior*, *42*, 281–283. https://doi.org/10.1016/j.evolhumbehav.2021.03.005

Salguero-Gómez, R., Jackson, J., & Gascoigne, S. J. L. (2021). Four key challenges in the open-data revolution. *Journal of Animal Ecology*, *90*, 2000–2004. https://doi.org/10.1111/1365-2656.13567

Salguero-Gómez, R., Jones, O. R., Archer, C. R., Bein, C., de Buhr, H., Farack, C., Gottschalk, F., Hartmann, A., Henning, A., Hoppe, G., Römer, G., Ruoff, T., Sommer, V., Wille, J., Voigt, J., Zeh, S., Vieregg, D., Buckley, Y. M., Che-Castaldo, J., … Vaupel, J. W. (2016a). COMADRE: A global data base of animal demography. *Journal of Animal Ecology*, *85*, 371–384. https://doi.org/10.1111/1365-2656.12482

Salguero-Gómez, R., Jones, O. R., Archer, C. R., Buckley, Y. M., Che-Castaldo, J., Caswell, H., Hodgson, D., Scheuerlein, A., Conde, D. A., Brinks, E., de Buhr, H., Farack, C., Gottschalk, F., Hartmann, A., Henning, A., Hoppe, G., Römer, G., Runge, J., Ruoff, T., … Vaupel, J. W. (2015). The COMPADRE plant matrix database: An open online repository for plant demography. *Journal of Ecology*, *103*, 202–218. https://doi.org/10.1111/1365-2745.12334

Salguero-Gómez, R., Jones, O. R., Jongejans, E., Blomberg, S. P., Hodgson, D. J., Mbeau-Ache, C., Zuidema, P. A., Kroon, H. D., & Buckley, Y. M. (2016b). Fast–slow continuum and reproductive strategies structure plant life-history variation worldwide. *Proceedings of the National Academy of Sciences*, *113*, 230–235. https://doi.org/10.1073/pnas.1717717114

Sanghvi, K., Iglesias-Carrasco, M., Zajitschek, F., Kruuk, L. E., & Head, M. L. (2022). Effects of developmental and adult environments on ageing. *Evolution*, *76*, 1868–1882. https://doi.org/10.1111/evo.14567

Sanghvi, K., Vega-Trejo, R., Nakagawa, S., Gascoigne, S. J. L., Johnson, S. L., Salguero-Gómez, R., Pizzari, T., & Sepil, I. (2024). Meta-analysis shows no consistent evidence for senescence in ejaculate traits across animals. *Nature Communications*, *15*. https://doi.org/10.1038/s41467-024-44768-4

Sanghvi, K., Zajitschek, F., Iglesias-Carrasco, M., & Head, M. L. (2021). Sex- and trait-specific silver-spoon effects of developmental environments, on ageing. *Evolutionary Ecology*, *35*, 367–385. https://doi.org/10.1007/s10682-021-10115-y

Santos, G. S., Gascoigne, S. J. L., Dias, A. T., Kajin, M., & Salguero-Gómez, R. (2023). A unified framework to identify demographic buffering in natural populations. *bioRxiv*, 1–31. https://doi.org/10.1101/2023.07.03.547528

Schroderus, E., Jokinen, I., Koivula, M., Koskela, E., Mappes, T., Mills, S. C., Oksanen, T. A., & Poikonen, T. (2010). Intra-and intersexual trade-offs between testosterone and immune system: Implications for sexual and sexually antagonistic selection. *The American Naturalist*, *176*. https://doi.org/10.1086/656264

Sepil, I., Hopkins, B. R., Dean, R., Bath, E., Friedman, S., Swanson, B., Ostridge, H. J., Harper, L., Buehner, N. A., Wolfner, M. F., Konietzny, R., Thézénas, M. L., Sandham, E., Charles, P. D., Fischer, R., Steinhauer, J., Kessler, B. M., & Wigby, S. (2020). Male reproductive aging arises via multifaceted mating-dependent sperm and seminal proteome declines, but is postponable in Drosophila. *Proceedings of the National Academy of Sciences*, *117*, 17094–17103. https://doi.org/10.1073/pnas.2009053117

Shefferson, R. P., Jacquemyn, H., Kull, T., & Hutchings, M. J. (2020). The demography of terrestrial orchids: Life history, population dynamics and conservation. *Botanical Journal of the Linnean Society*, *192*, 315–332. https://doi.org/10.1093/botlinnean/boz084

Shen, S. S., Gurung, A. B., Oh, H. S., Shu, T., & Easterling, D. R. (2011). The twentieth century contiguous us temperature changes indicated by daily data and higher statistical moments. *Climatic Change*, *109*, 287–317. https://doi.org/10.1007/s10584-011-0033-9

Sheth, S. N., & Angert, A. L. (2018). Demographic compensation does not rescue populations at a trailing range edge. *Proceedings of the National Academy of Sciences*, *115*, 2413–2418. https://doi.org/10.1073/pnas.1715899115

Shingleton, A. W., Das, J., Vinicius, L., & Stern, D. L. (2005). The temporal requirements for insulin signaling during development in Drosophila. *PLoS Biology*, *3*, 1607–1617. https://doi.org/10.1371/journal.pbio.0030289

Shingleton, A. W., Frankino, W. A., Flatt, T., Nijhout, H. F., & Emlen, D. J. (2007). Size and shape: The developmental regulation of static allometry in insects. *BioEssays*, *29*, 536–548. https://doi.org/10.1002/bies.20584

Shreve, S. (2005). *Stochastic calculus for finance I: The binomial asset pricing model*. Springer Science & Business Media.

Shyu, E., & Caswell, H. (2014). Calculating second derivatives of population growth rates for ecology and evolution. *Methods in Ecology & Evolution*, *5*, 473–482. https://doi.org/10.1111/2041-210X.12179

Simmonds, E. G., & Jones, O. R. (2024). Uncertainty propagation in matrix population models: Gaps, importance and guidelines. *Methods in Ecology & Evolution*, *15*, 427–438. https://doi.org/10.1111/2041-210X.14276

Simmons, L. W., & Emlen, D. J. (2006). Evolutionary trade-off between weapons and testes. *Proceedings of the National Academy of Sciences*, *103*, 16346–16351. https://doi.org/10.1073/pnas.0603474103

Skinner, M. K. (2016). Epigenetic transgenerational inheritance. *Nature Reviews Endocrinology*, *12*, 68. https://doi.org/10.1038/nrendo.2015.206

Smallegange, I. M., Caswell, H., Toorians, M. E., & de Roos, A. M. (2017). Mechanistic description of population dynamics using dynamic energy budget theory incorporated into integral projection models. *Methods in Ecology & Evolution*. https://doi.org/10.1111/2041-210X.12675

Smallegange, I. M., Deere, J. A., & Coulson, T. (2014). Correlative changes in life-history variables in response to environmental change in a model organism. *The American Naturalist*, *183*, 784–797. https://doi.org/10.1086/675817

Smith, J. M. (1983). Models of evolution. *Proceedings of the Royal Society B*, *219*, 315–325. https://www.jstor.org/stable/35853

Snell-Rood, E. C. (2013). An overview of the evolutionary causes and consequences of behavioural plasticity. *Animal Behaviour*, *85*, 1004–1011. https://doi.org/10.1016/j.anbehav.2012.12.031

Snell-Rood, E. C., & Moczek, A. P. (2012). Insulin signaling as a mechanism underlying developmental plasticity: The role of FOXO in a nutritional polyphenism. *PLoS ONE*, *7*. https://doi.org/10.1371/journal.pone.0034857

Snyder, R. E., & Ellner, S. P. (2018). Pluck or luck: Does trait variation or chance drive variation in lifetime reproductive success? *The American Naturalist*, *191*, E90–E107. https://doi.org/10.1086/696125

Snyder, R. E., & Ellner, S. P. (2022). Snared in an evil time: How age-dependent environmental and demographic variability contribute to variance in lifetime outcomes. *The American Naturalist*, *200*, E124–E140. https://doi.org/10.1086/720411

Starrfelt, J., & Kokko, H. (2012). Bet-hedging-a triple trade-off between means, variances and correlations. *Biological Reviews*, *87*, 742–755. https://doi.org/10.1111/j.1469-185X.2012.00225.x

Stearns, S. C. (1989). Trade-offs in life-history evolution. *Functional Ecology*, *3*, 259–268. https://doi.org/10.2307/2389364

Stearns, S. (1992). *The evolution of life histories*. Oxford University Press.

Stearns, S. C. (1983). The influence of size and phylogeny on patterns of covariation among life-history traits in the mammals. *Oikos*, *41*, 173–187. https://doi.org/10.2307/3544261

Stearns, S. C., & Medzhitov, R. (2015). *Evolutionary medicine*. Oxford University Press.

Steiner, U. K., Tuljapurkar, S., & Coulson, T. (2014). Generation time, net reproductive rate, and growth in stage-age-structured populations. *The American Naturalist*, *183*. https://doi.org/10.5061/dryad.3m5fc

Steiner, U. K., Tuljapurkar, S., & Roach, D. A. (2021). Quantifying the effect of genetic, environmental and individual demographic stochastic variability for population dynamics in Plantago lanceolata. *Scientific Reports*, *11*. https://doi.org/10.1038/s41598-021-02468-9

Steiner, U. K., & Tuljapurkar, S. (2012). Neutral theory for life histories and individual variability in fitness components. *Proceedings of the National Academy of Sciences*, *109*, 4684–4689. https://doi.org/10.1073/pnas.1018096109

Steiner, U. K., & Tuljapurkar, S. (2023). Adaption, neutrality and life-course diversity. *Ecology Letters*, *26*, 540–548. https://doi.org/10.1111/ele.14174

Stott, I., Hodgson, D. J., & Townley, S. (2012). Beyond sensitivity: Nonlinear perturbation analysis of transient dynamics. *Methods in Ecology & Evolution*, *3*, 673–684. https://doi.org/10.1111/j.2041-210X.2012.00199.x

Stott, I., Salguero-Gómez, R., Jones, O., Ezard, T., Gaillard, J.-M., Gamelon, M., Hodgson, D., Lachish, S., Lebreton, J.-D., & Simmonds, E. G. (2023). Beyond the fast-slow continuum of life histories. *Authorea*. https://doi.org/10.22541/au.169029175.51225048/v1

Stott, I., Townley, S., & Hodgson, D. J. (2011). A framework for studying transient dynamics of population projection matrix models. *Ecology Letters*, *14*, 959–970. https://doi.org/10.1111/j.1461-0248.2011.01659.x

Sultan, S. E., & Spencer, H. G. (2002). Metapopulation structure favors plasticity over local adaptation. *The American Naturalist*, *160*, 271–283. http://www.journals.uchicago.edu/t-and-c

Sutherland, W. J., Freckleton, R. P., Godfray, H. C. J., Beissinger, S. R., Benton, T., Cameron, D. D., Carmel, Y., Coomes, D. A., Coulson, T., Emmerson, M. C., Hails, R. S., Hays, G. C., Hodgson, D. J., Hutchings, M. J., Johnson, D., Jones, J. P., Keeling, M. J., Kokko, H., Kunin, W. E., … Wiegand, T. (2013). Identification of 100 fundamental ecological questions. *Journal of Ecology*, *101*, 58–67. https://doi.org/10.1111/1365-2745.12025

Takada, T., Kawai, Y., & Salguero-Gómez, R. (2018). A cautionary note on elasticity analyses in a ternary plot using randomly generated population matrices. *Population Ecology*, *60*, 37–47. https://doi.org/10.1007/s10144-018-0619-4

Travis, J. M. J., Mynard, P., & Bocedi, G. (2021). Evolution of reduced dormancy during range expansions. *bioRxiv*. https://doi.org/10.1101/2021.10.11.463894

Trenberth, K. E. (2011). Changes in precipitation with climate change. *Climate Research*, *47*, 123–138. https://doi.org/10.3354/cr00953

Tuljapurkar, S., & Lee, R. (1997). Demographic uncertainty and the stable equivalent population. *Mathematical & Computer Modelling*, *26*, 39–56. https://doi.org/10.1016/S0895-7177(97)00168-4

Tuljapurkar, S. (1982). Population dynamics in variable environments. iii. Evolutionary dynamics of r-selection. *Theoretical Population Biology*, *21*, 141–165. https://doi.org/10.1016/0040-5809(82)90010-7

Tuljapurkar, S. (1989). An uncertain life: Demography in random environments. *Theoretical Population Biology*, *35*, 227–294. https://doi.org/10.1016/0040-5809(89)90001-4

Tuljapurkar, S. (1990). *Population dynamics in variable environments*. Springer-Verlag.

Tuljapurkar, S. (2023). From the past into the future. *8th Meeting of the Evolutionary Demography Society*.

Tuljapurkar, S., Gaillard, J. M., & Coulson, T. (2009a). From stochastic environments to life histories and back. *Philosophical Transactions of the Royal Society B*, *364*, 1499–1509. https://doi.org/10.1098/rstb.2009.0021

Tuljapurkar, S., & Haridas, C. V. (2006). Temporal autocorrelation and stochastic population growth. *Ecology Letters*, *9*, 327–337. https://doi.org/10.1111/j.1461-0248.2006.00881.x

Tuljapurkar, S., Horvitz, C. C., & Pascarella, J. B. (2003). The many growth rates and elasticities of populations in random environments. *The American Naturalist*, *162*. https://doi.org/10.1086/378648

Tuljapurkar, S., & Istock, C. (1993). Environmental uncertainty and variable diapause. *Theoretical Population Biology*, *43*, 251–280. https://doi.org/10.1006/tpbi.1993.1011

Tuljapurkar, S., Jaggi, H., Gascoigne, S. J. L., Zuo, W., Kajin, M., & Salguero-Gómez, R. (2023). From disturbances to nonlinear fitness and back. *bioRxiv*. https://doi.org/10.1101/2023.10.20.563360

Tuljapurkar, S., Steiner, U. K., & Orzack, S. H. (2009b). Dynamic heterogeneity in life histories. *Ecology Letters*, *12*, 93–106. https://doi.org/10.1111/j.1461-0248.2008.01262.x

Tuomi, J., Crone, E. E., Gremer, J. R., Jäkäläniemi, A., Lesica, P., Pedersen, B., & Ramula, S. (2013). Prolonged dormancy interacts with senescence for two perennial herbs. *Journal of Ecology*, *101*, 566–576. https://doi.org/10.1111/1365-2745.12086

Urban, M. C. (2015). Accelerating extinction risk from climate change. *Science*, *348*, 571–573. https://doi.org/10.1126/science.aaa4984

Urquhart-Cronish, M., Angert, A. L., Otto, S. P., & MacPherson, A. (2024). Density-dependent selection during range expansion affects expansion load in life history traits. *The American Naturalist*, *203*, 382–392. https://doi.org/10.1086/728599

Van Daalen, S. F., & Caswell, H. (2017). Lifetime reproductive output: Individual stochasticity, variance, and sensitivity analysis. *Theoretical Ecology*, *10*, 355–374. https://doi.org/10.1007/s12080-017-0335-2

Van Daalen, S. F., & Caswell, H. (2020). Variance as a life history outcome: Sensitivity analysis of the contributions of stochasticity and heterogeneity. *Ecological Modelling*, *417*. https://doi.org/10.1016/j.ecolmodel.2019.108856

Van De Crommenacker, J., Hammers, M., Dugdale, H. L., Burke, T. A., Komdeur, J., & Richardson, D. S. (2022). Early-life conditions impact juvenile telomere length, but do not predict later life-history strategies or fitness in a wild vertebrate. *Ecology and Evolution*, *12*. https://doi.org/10.1002/ece3.8971

Van De Walle, J., Fay, R., Gaillard, J. M., Pelletier, F., Hamel, S., Gamelon, M., Barbraud, C., Blanchet, F. G., Blumstein, D. T., Charmantier, A., Delord, K., Larue, B., Martin, J., Mills, J. A., Milot, E., Mayer, F. M., Rotella, J., Sæther, B. E., Teplitsky, C., … Jenouvrier, S. (2023). Individual life histories: Neither slow nor fast, just diverse. *Proceedings of the Royal Society B*, *290*. https://doi.org/10.1098/rspb.2023.0511

Van Noordwijk, A. . J. ., & De Jong, G. (1986). Acquisition and allocation of resources: Their influence on variation in life history tactics. *The American Naturalist*, *128*, 137–142. https://doi.org/10.1086/284547

Van Petegem, K. H. P., Boeye, J., Stoks, R., & Bonte, D. (2016). Spatial selection and local adaptation jointly shape life-history evolution during range expansion. *The American Naturalist*, *188*, 485–498. https://doi.org/10.5061/dryad.n0c67

Van Tienderen, P. H. (2000). Elasticities and the link between demographic and evolutionary dynamics. *Ecology*, *81*, 666–679. https://doi.org/10.1890/0012-9658(2000)081[0666:EATLBD]2.0.CO;2

Van Valen, L. (1973). A new evolutionary law. *Evolutionary theory*, *1*. https://www.mn.uio.no/cees/english/services/van-valen/evolutionary-theory/volume-1/vol-1-no-1-pages-1-30-l-van-valen-a-new-evolutionary-law.pdf

Vasseur, D. A., DeLong, J. P., Gilbert, B., Greig, H. S., Harley, C. D., McCann, K. S., Savage, V., Tunney, T. D., & O'Connor, M. I. (2014). Increased temperature variation poses a greater risk to species than climate warming. *Proceedings of the Royal Society B*, *281*. https://doi.org/10.1098/rspb.2013.2612

Vázquez, D. P., Gianoli, E., Morris, W. F., & Bozinovic, F. (2017). Ecological and evolutionary impacts of changing climatic variability. *Biological Reviews*, *92*, 22–42. https://doi.org/10.1111/brv.12216

Veit, W., Gascoigne, S. J. L., & Salguero-Gómez, R. (2023). Evolution, complexity, and life history theory. *Authorea*. https://doi.org/10.22541/au.167770655.56360178/v1

Verhulst, S., Tinbergen, J. M., & Daan, S. (1997). Multiple breeding in the Great Tit. A trade-off between successive reproductive attempts? *Functional Ecology*, *11*, 714–722. https://doi.org/10.1046/j.1365-2435.1997.00145.x

Vinton, A. C., Gascoigne, S. J. L., Sepil, I., & Salguero-Gómez, R. (2022). Plasticity's role in adaptive evolution depends on environmental change components. *Trends in Ecology & Evolution*, *37*, 1067–1078. https://doi.org/10.1016/j.tree.2022.08.008

Vinton, A. C., Gascoigne, S. J. L., Sepil, I., & Salguero-Gómez, R. (2023). The importance of spatial and temporal structure in determining the interplay between plasticity and evolution. *Trends in Ecology & Evolution*, *38*, 221–223. https://doi.org/10.1016/j.tree.2022.12.009

Vitalis, R., Rousset, F., Kobayashi, Y., Olivieri, I., & Gandon, S. (2013). The joint evolution of dispersal and dormancy in a metapopulation with local extinctions and kin competition. *Evolution*, *67*, 1676–1691. https://doi.org/10.1111/evo.12069

Von Takach Dukai, B., Lindenmayer, D. B., & Banks, S. C. (2018). Environmental influences on growth and reproductive maturation of a keystone forest tree: Implications for obligate seeder susceptibility to frequent fire. *Forest Ecology & Management*, *411*, 108–119. https://doi.org/10.1016/j.foreco.2018.01.014

Wang, H. Y., Shen, S. F., Chen, Y. S., Kiang, Y. K., & Heino, M. (2020). Life histories determine divergent population trends for fishes under climate warming. *Nature Communications*, *11*. https://doi.org/10.1038/s41467-020-17937-4

Wang, J., Yang, X., Santos, G. S., Ning, H., Li, T., Zhao, W., Si, X., Lu, S., & Li, S. (2023). Flexible demographic strategies promote the population persistence of a pioneer conifer tree (Pinus massoniana) in ecological restoration. *Forest Ecology & Management*, *529*, 120727. https://doi.org/10.1016/j.foreco.2022.120727

West-Eberhard, M. J. (2003). *Developmental plasticity and evolution*. Oxford University Press.

Westerband, A. C., & Horvitz, C. C. (2017). Photosynthetic rates influence the population dynamics of understory herbs in stochastic light environments. *Ecology*, *98*, 370–381. https://doi.org/10.1002/ecy.1664

Westneat, D. F., Walters, A., McCarthy, T. M., Hatch, M. I., & Hein, W. K. (2000). Alternative mechanisms of nonindependent mate choice. *Animal Behaviour*, *59*, 467–476. https://doi.org/10.1006/anbe.1999.1341

White, J. W., Botsford, L. W., Hastings, A., Baskett, M. L., Kaplan, D. M., & Barnett, L. A. (2013). Transient responses of fished populations to marine reserve establishment. *Conservation Letters*, *6*, 180–191. https://doi.org/10.1111/j.1755-263X.2012.00295.x

Wieczynski, D. J., Turner, P. E., & Vasseur, D. A. (2018). Temporally autocorrelated environmental fluctuations inhibit the evolution of stress tolerance. *The American Naturalist*, *191*, E195–E207. https://doi.org/10.1086/697200

Wiener, P., & Tuljapurkar, S. (1994). Migration in variable environments: Exploring life-history evolution using structured population models. *Journal of Theoretical Biology*, *166*, 75–90. https://doi.org/10.1006/jtbi.1994.1006

Wigby, S., Brown, N. C., Allen, S. E., Misra, S., Sitnik, J. L., Sepil, I., Clark, A. G., & Wolfner, M. F. (2020). The Drosophila seminal proteome and its role in postcopulatory sexual selection: Drosophila seminal fluid proteins. *Philosophical Transactions of the Royal Society B*, *375*. https://doi.org/10.1098/rstb.2020.0072

Wilbur, H. M., Tinkle, D. W., & Collins, J. P. (1974). Environmental certainty, trophic level, and resource availability in life history evolution. *The American Naturalist*, *108*, 805–817. https://doi.org/10.1086/282956

Wilmoth, J. R., Andreev, K., Jdanov, D., & Glei, D. A. (2021). Methods protocol for the human mortality database, 1–80. https://www.mortality.org/File/GetDocument/Public/Docs/MethodsProtocolV6.pdf

Wilson, A. J., Réale, D., Clements, M. N., Morrissey, M. M., Postma, E., Walling, C. A., Kruuk, L. E., & Nussey, D. H. (2010). An ecologist's guide to the animal model. *Journal of Animal Ecology*, *79*, 13–26. https://doi.org/10.1111/j.1365-2656.2009.01639.x

Wong, G. K., & Jim, C. Y. (2017). Urban-microclimate effect on vector mosquito abundance of tropical green roofs. *Building and Environment*, *112*, 63–76. https://doi.org/10.1016/j.buildenv.2016.11.028

Wood, A., Gascoigne, S. J. L., Gambetta, G. A., Jeffers, E., & Coulson, T. (2023). Seasonal weather impacts wine quality in Bordeaux. *iScience*. https://doi.org/10.1016/j.isci.2023.107954

Woodman, J. P., Cole, E. F., Firth, J. A., Perrins, C. M., & Sheldon, B. C. (2023). Disentangling the causes of age-assortative mating in bird populations with contrasting life-history strategies. *Journal of Animal Ecology*, *92*, 979–990. https://doi.org/10.1111/1365-2656.13851

Xue, B., & Leibler, S. (2018). Benefits of phenotypic plasticity for population growth in varying environments. *Proceedings of the National Academy of Sciences*, *115*, 12745–12750. https://doi.org/10.1073/pnas.1813447115

Zentall, T. R. (2005). Animals may not be stuck in time. *Learning & Motivation*, *36*, 208–225. https://doi.org/10.1016/j.lmot.2005.03.001

Zera, A. J., & Harshman, L. G. (2001). The physiology of life history trade-offs in animals. *Annual Review of Ecological Systems*, *32*, 95–126. https://digitalcommons.unl.edu/bioscizera/15

Zera, A. J., & Zhao, Z. (2006). Intermediary metabolism and life-history trade-offs: Differential metabolism of amino acids underlies the dispersal-reproduction trade-off in a wing-polymorphic cricket. *The American Naturalist*. https://doi.org/10.1086/503578